STATISTICAL ANALYSIS OF TURBIDITE CYCLES IN SUBMARINE FAN SUCCESSIONS

CHENGSHENG CHEN

INFORMATION TO USERS

This manuscript has been reproduced from the microfilm master. UMI films the text directly from the original or copy submitted. Thus, some thesis and dissertation copies are in typewriter face, while others may be from any type of computer printer.

The quality of this reproduction is dependent upon the quality of the copy submitted. Broken or indistinct print, colored or poor quality illustrations and photographs, print bleedthrough, substandard margins, and improper alignment can adversely affect reproduction.

In the unlikely event that the author did not send UMI a complete manuscript and there are missing pages, these will be noted. Also, if unauthorized copyright material had to be removed, a note will indicate the deletion.

Oversize materials (e.g., maps, drawings, charts) are reproduced by sectioning the original, beginning at the upper left-hand corner and continuing from left to right in equal sections with small overlaps. Each original is also photographed in one exposure and is included in reduced form at the back of the book.

Photographs included in the original manuscript have been reproduced xerographically in this copy. Higher quality 6" x 9" black and white photographic prints are available for any photographs or illustrations appearing in this copy for an additional charge. Contact UMI directly to order.

UMI

A Bell & Howell Information Company
300 North Zeeb Road, Ann Arbor MI 48106-1346 USA
313/761-4700 800/521-0600

STATISTICAL ANALYSIS OF TURBIDITE CYCLES IN SUBMARINE FAN SUCCESSIONS

By

Chengsheng Chen, M.Sc.

A thesis submitted to the School of Graduate Studies
in partial fulfilment of the requirements
for the degree of
Doctor of Philosophy

Department of Earth Sciences
Memorial University of Newfoundland

April 1997

St. John's Newfoundland

Abstract

To statistically test and evaluate the significance of asymmetric upward thickening and thinning trends and other cyclic patterns in turbidite successions, twenty-eight bed-by-bed sections with a wide coverage in geological time, tectonic settings, facies characteristics, and depositional environments were measured and described. First, 286 sandstone packets were selected from the 28 turbidite sections through statistically based segmentation. Then, these packets were examined by three powerful correlation tests (Kendall's, Spearman's, and Pearson's correlation tests) and four tests for randomness. Only 34 (11.9%) of the sandstone packets pass tests designed to identify asymmetry at the 10% significance level. Monte Carlo simulation and the binomial probability analysis indicate that the number of asymmetric sequences identified in the original set of turbidite sandstone packets is indistinguishable from the number which can be produced by random processes.

Eighty-six sandstone packets were tested for upward coarsening and fining trends. It was found that as many as 50% of sandstone packets from coarse-grained channel fills fine or coarsen upward. Upward fining sequences dominate, which is interpreted as the result of channel filling or the stacking of onlapping deposits at a channel mouth.

The Hurst statistic provides a measure of long-term persistence. Sixteen (84.2%) of 19 turbidite sections show the Hurst phenomenon, i.e., irregular and non-periodic clustering of high and low values of bed-thickness, grain-size, and sandstone percentage. This clustering is related to vertical changes of sedimentary facies caused by

lateral shifting of environments on the fan surface. The strength of the clustering, inferred from Hurst K values, might be useful as an index to distinguish submarine fan environments: channel-levee complexes tend to have strong clustering; lobe-interlobe deposits tend to display moderate clustering; and basin-floor sheet sand systems tend to have weak clustering.

Combining facies characteristics observed in the field with the statistical results provides some criteria for the identification of submarine fan environments, and yields four preliminary fan models. (1) Type 1 sandy fans typically form in forearc basins, are fed by littoral sources or fan deltas, and are characterized by very coarse (pebbly sandy) sediments. Both channel and lobe deposits are well developed. A significant number of upward fining sequences can be found in channel deposits. Channel-interchannel complexes, particularly channel-levee complexes, display strong clustering of bed-thickness, grain-size and other parameters. (2) Type 2 sandy fans mainly form in forearc basins but also in foreland basins, and are fed by littoral sources or small rivers. The basic features of this model are similar to those of model 1, but pebbly sediments are absent or rare, and upward fining sequences lack significance. (3) Type 1 muddy fans tend to form in passive margins, foreland basins or foredeeps, and are fed by a large river delta. They are typically characterized by nested sandy bodies of channel and crevasse-splay-lobe deposits in very well-developed muddy levee deposits, which causes strong clustering of bed-thickness, grain-size and other parameters. Channels might gradually die out without a sandy lobe at the end. (4) Type 2 muddy fans form in

the same tectonic settings as model 3, but sediments are mainly derived from failure at the shelf break, resulting in well-developed megaturbidite beds with thick mud caps. The large, muddy turbidity currents responsible for these beds are usually unchannelized and efficiently transport sandy sediments to form wide spread basin-floor sand sheets.

Acknowledgements

My greatest appreciation is extended to my thesis supervisor, Prof. R. N. Hiscott, for suggesting this project, giving advice, editing text, and providing financial support. The supervisory committee members, Prof. J. D. Harper and Prof. A. F. King, are thanked for their advice, and for criticism of the second draft of the thesis.

I would like to acknowledge the Graduate Fellowship that I received from the School of Graduate Studies of Memorial University and financial support for the field work from EXXON Company (Houston).

Prof. F. Ricci Lucchi at University of Bologna, Italy, is greatly appreciated for his hospitality and help, and for guiding me to turbidite sections during field studies in the northern Italian Apennines. I am particularly indebted to Dr. Jinlu Lin and Dr. Yulong Cui at the Department of Geology, University of California, Davis, for their help and enthusiasm during my field work in the Great Valley, California. They helped me to look for turbidite sections, drove me to and from the field and campgrounds, and continuously sent food to my campsite. Without their help, I cannot imagine how I could have completed the field work. The thesis examiners, Prof. C. W. Harper Jr. at University of Oklahoma, Prof. J. W. F. Waldron at Saint Mary's University, and Prof. C. Hurich at Memorial University, are thanked for their critical comments and constructive suggestions on the manuscript.

I am grateful for the friendship, advice, and assistance that I received from the staff, H. Lu, and my fellow students, S. Awadallah and A. Mahgoub, at Memorial University.

Particularly, S. Awadallah spent one month living in a tent at a campground in the Gaspé Peninsula, Quebec, and there measured several turbidite sections for this thesis in poor weather. He also generously provided the author with a computer program for plotting the sections measured in the Gaspé Peninsula.

I would also like to thank my family for their support. My mother, Fengying Zhang, provided a great deal of encouragement and understanding during my studies. Most importantly, my wife, Jianguo Guan, and my son, Peiyi, provided love, friendship, patience, and inspiration that made this whole effort possible. I dedicate this dissertation to Jianguo, for her constant love and encouragement.

TABLE OF CONTENTS

APPENDICES

List of Figures

List of Tables

Chapter 1

INTRODUCTION

1.1 Problems in the Study of Deep-Marine Turbidite Cycles

Deep-marine sandy turbidite systems, particularly submarine fans, constitute major hydrocarbon reservoirs throughout the world (Weimer and Link, 1991). Consequently, a clear understanding of their geometry, cyclic patterns, facies and facies associations, reservoir quality, transportational and depositional processes, and other controls is critical for exploring these deposits effectively. To satisfy this need, deep-marine turbidites have been the focus of considerable study (e.g. Mutti and Ricci Lucchi, 1972; Middleton and Bouma, 1973; Whitaker, 1976; Stanley and Kelling, 1978; Walker, 1978; Tillman and Ali, 1982; Nelson and Nilsen, 1984; Bouma et al., 1985; Mutti and Normark, 1987, 1991; Pickering et al., 1989, 1995; Normark and Piper, 1991; Mutti, 1992; Clark and Pickering, 1996). Studies of modern and ancient turbidite systems have yielded many key concepts leading to a better understanding of their characteristics and depositional processes. At the same time, however, many puzzles and problems have surfaced that need further study (see Bouma, 1983/1984; Bouma et al., 1985; the unpublished documents of ComFan II, 1988).

One of these puzzles revolves around the recognition of cyclicity in submarine fan

systems. Many researchers, following the hypothesis of Mutti and Ricci Lucchi (1972) and Ricci Lucchi (1975), have claimed that turbidites deposited in channels of submarine fans are characterized by cycles of upward thinning and fining, while those deposited on submarine fan lobes display cyclic thickening and coarsening. These putative upward thinning and thickening sequences have been subjectively recognized in the field or from graphic columns and pictorial logs (e.g. Ricci Lucchi, 1975; Ingersoll, 1981). The genetic significance of these subjectively identified sequences is questionable, because randomly selected values of bed thickness and/or grain size can generate a number of asymmetric sequences that rival, in quality, those claimed from some field studies (Hiscott, 1981). Further, some published examples of asymmetric sequences can be reinterpreted to have completely opposite asymmetry by selecting different positions for the bases of the sequences (Walker, 1984, p.183). Even though the validity of some published vertical trends has been repeatedly challenged (e.g. Martini et al., 1978; Hiscott, 1981; Walker, 1984; Heller and Dickinson,1985; Pickering et al., 1989; Anderton, 1995), only a few publications outlining statistical tests for such sequences have thus far appeared (Martini et al., 1978; Heller and Dickinson, 1985; Waldron, 1987; Lowey, 1992; Murray et al., 1996). It is my belief that no convincing statistical demonstrations supporting or refuting the hypothesis of common asymmetric cycles have been published because inappropriate test methods and/or too flexible testing standards have been used.

Because a simple statistical procedure for recognition of asymmetric trends of bed thickness or grain size has not been available, some rather presumed asymmetric

sequences have been used to underpin the more popular submarine fan models (e.g. Mutti and Ricci Lucchi, 1972; Walker, 1978; Shanmugam and Moiola, 1988). These highly simplified and hypothetical models have been widely and sometimes uncritically applied as a means to identify ancient submarine fan channel and lobe deposits, respectively (Fig. 1.1). This uncritical application has led to a common misunderstanding of cyclic patterns of turbidites, depositional processes on submarine fans, and the degree of facies predictability in turbidite systems. A clear remedy to this generic problem in turbidite studies would be the development of a practical statistical procedure and powerful statistical methods to reevaluate and verify the importance and significance of asymmetric sequences. Only then can the genesis of such sequences be properly evaluated.

If statistically discernible asymmetyric sequences lack significance in submarine fan successions, then are there (1) other cyclic patterns of bed-thickness and/or other properties, or (2) other criteria for identification of submarine fan environments? These are important questions which this thesis will address. The development of submarine fan systems has been widely considered, particularly in the realm of sequence stratigraphy, to be controlled by periodic eustatic sea-level changes and pulses in source-area tectonics, such that submarine fan successions should show long-term cyclic patterns. To date, however, most work on long-term turbidite cycles has been restricted to a qualitative analysis of cycle controls (e.g. Shanmugam and Moiola, 1982; Stow et al., 1985; Mutti, 1985, 1992; Pickering et al., 1989; Weimer, 1989; Vail et al., 1991). It is hard to find a

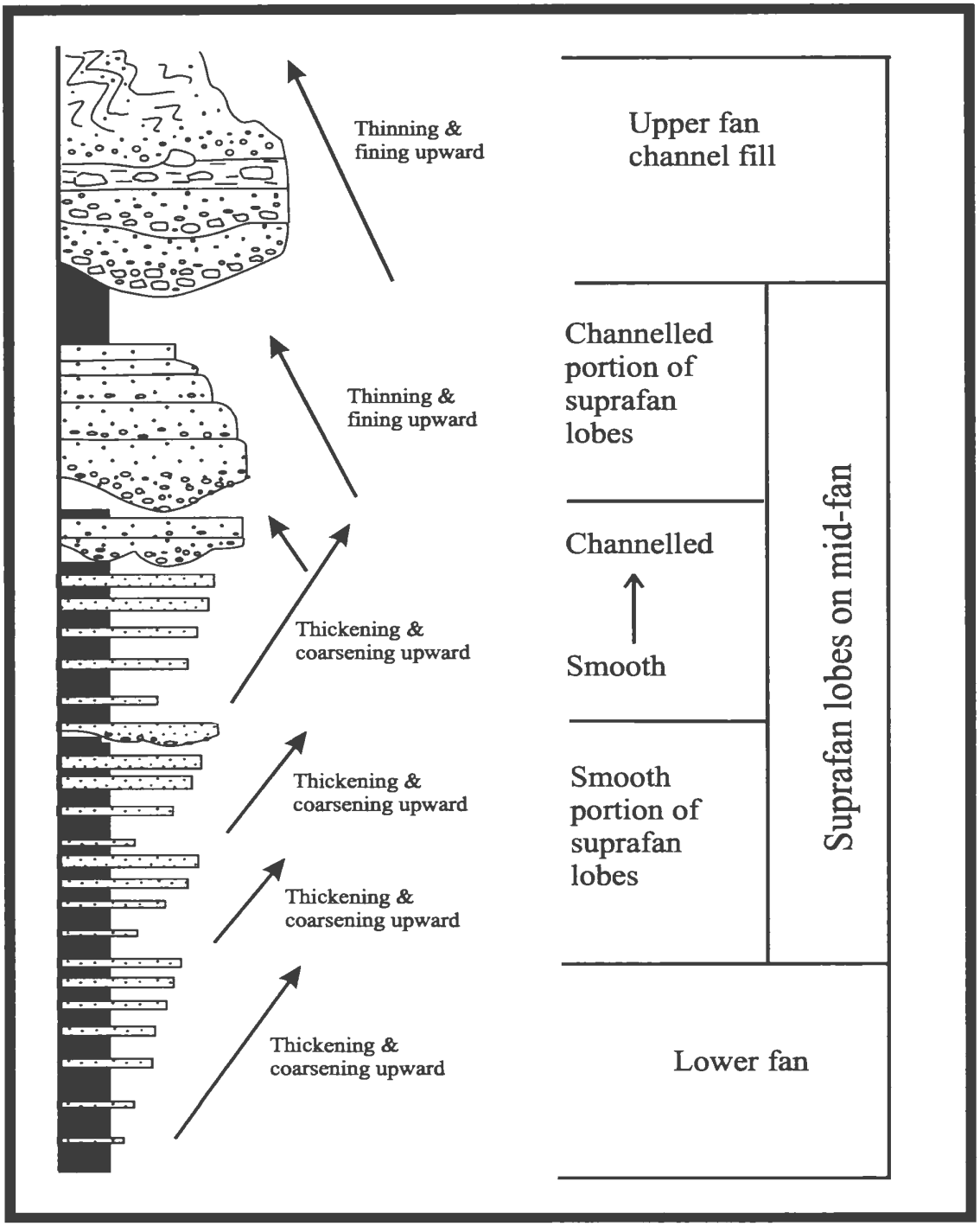

Fig.1.1 Hypothetical submarine fan model from Walker (1978) showing upward thickening and coarsening (negative) cycles in the lower and mid-fan lobes, and upward thinning and fining (positive) cycles in the mid- to upper fan channels. Even though it was proposed almost 20 years ago, this and similar models are still in use recently (e.g. Mutti, 1992; and Stow et al., 1996), and the basic concept of asymmetric cycles as valid tools to interpret turbidite successions is widely used (e. g. many papers in Weimer et al., 1994).

case study that statistically or quantitatively investigates long-term cyclic patterns of any turbidite attributes, such as bed thickness, grain size, sand/mud ratio and structures. Long-term turbidite cycles, if they exist, would be potentially useful for paleoenvironmental and perhaps tectonic reconstructions.

1.2 Scope and Purpose of the Thesis

This thesis is an investigation of upward thinning and thickening sequences and cyclic patterns of turbidites in submarine fan systems. The main objectives are:

(1) to discover a suitable statistical procedure to test for the presence and significance of upward thinning and thickening sequences in independently confirmed deposits of channels and unchannelized lobes, respectively, in order to establish whether such sequences truly are a useful criterion for recognition of these depositional settings;

(2) to examine other possible cyclic patterns in turbidite successions to rely on where asymmetric cycles are rare;

(3) to theoretically reevaluate the origins of any statistically confirmed turbidite cycles in order to gain a better understanding of depositional processes of deep-marine turbidites;

(4) to develop new criteria for the recognition of deep-marine turbidite environments, and therefore provide input into the development of submarine fan models.

1.3 Database and General Methodology

Eleven turbidite sections (Table 1.1a), with a total thickness of 1831 m and 5173 beds, were measured bed-by-bed by the author in the Italian Apennines (Ricci Lucchi, 1975), the California Great Valley (Ingersoll, 1981), and with the assistance of S. Awadallah the Gaspé Peninsula of Quebec (Hiscott et al., 1986; Strong and Walker, 1981). The localities where sections were measured show either a channel-filling geometry or an unchannelized lobe geometry. Sections in the Italian Apennines were included because they formed the basis of Ricci Lucchi's (1975) hypothesis that asymmetric sequences correspond to submarine fan channel and lobe deposits. Sections in the California Great Valley were claimed, by Ingersoll (1981), to consist of unambiguous asymmetric cycles (Fig. 1.2). Sections in the Gaspé Peninsula of Quebec convinced Hiscott (1980) that upward thinning and thickening sequences are not common.

All beds recognizable at outcrops, mostly thicker than 1 cm, were measured and described separately. Sandstone and siltstone beds that were too thin to be described separately were merged into mud beds. Data collected from the field include bed thickness, sandstone thickness, thickness of individual Bouma divisions, basal and upper grain size of sandy beds (pebble, granule, coarse-grained, medium-grained, and fine-grained sand, and silt), sedimentary structures, morphology of bed base and top, presence/absence of amalgamation, paleocurrent direction, lateral continuity at the outcrop scale, and vertical organization of grain size and structures.

In addition to sections measured by the author and by S. Awadallah, several bed-by-

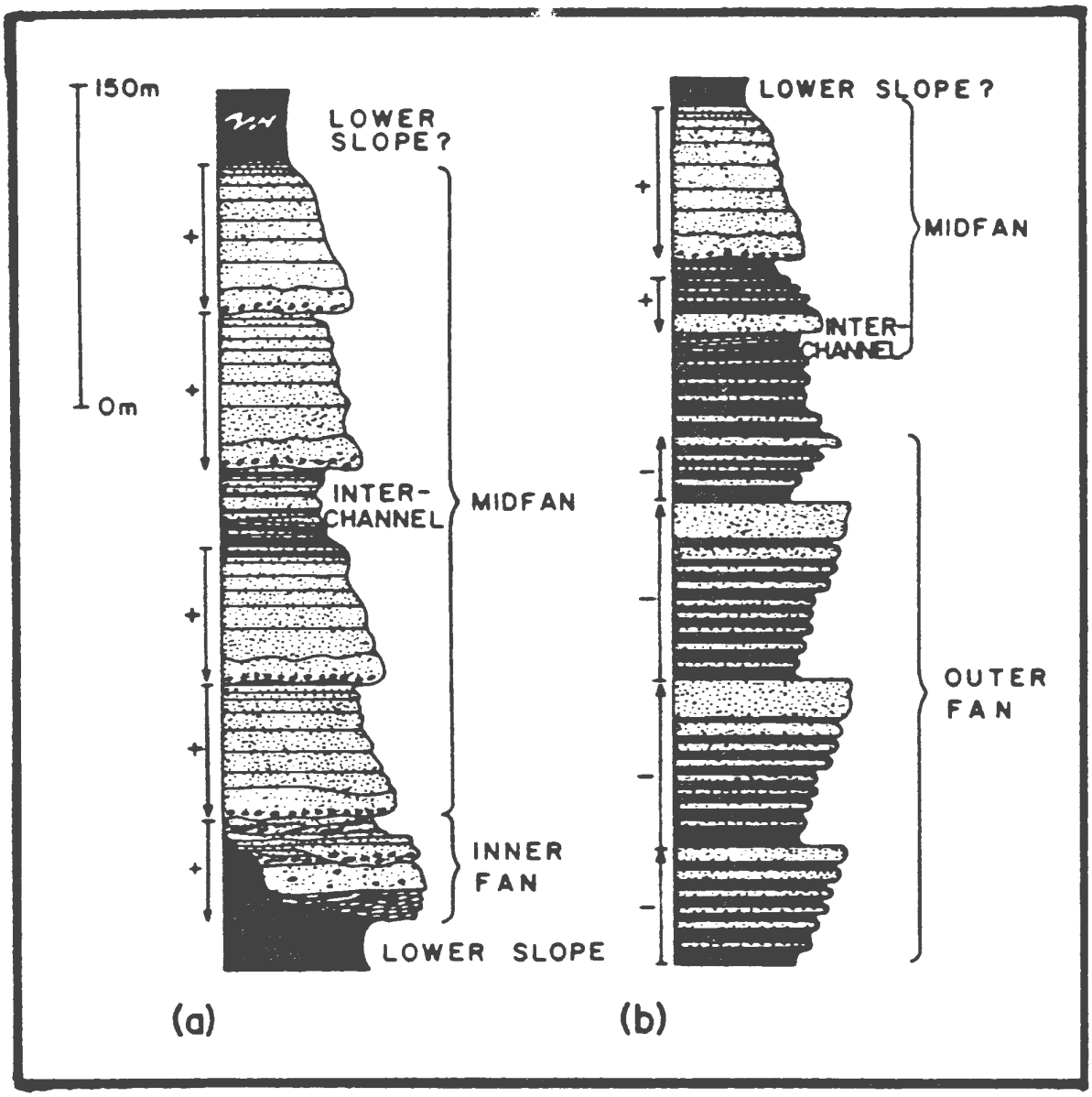

Fig. 1.2 Idealized asymmetric sequences in the Great Valley Group, California, from Ingersoll (1978). Section (a) represents Ingersoll's interpretation of the Venado Formation at Monticello Dam. The entire section was measured for this thesis. Section (b) represents the Sites Formation at Cache Creek. The section measured for the thesis at this location lies within the outer fan portion as interpreted by Ingersoll.

Table 1.1a: List of turbidite sections measured for this thesis

Location		Unit	Proposed Environments	Number of Sections	Thickness (m)	Number of beds	Measurer or reference
ITALY	Santerno Valley	Miocene Marnoso arenacea	Lobes & basin plain sand sheets (Ricci Lucchi, 1975; Cattaneo and Ricci Lucchi, 1995)	4	445.27	738	the author
	Savio Valley		Channel fill (Ricci Lucchi, 1975)	2	49.48	75	the author
CALIFORNIA	Monticello Dam	Upper Cretaceous Venado Formation	Channel fill (Ingersoll, 1978)	1	383.7	379	the author
	Cache Creek	Upper Cretaceous Sites Formation	Lobes (Ingersoll, 1978)	1	277.99	565	the author
QUEBEC	Cap Ste-Anne	Lower Ordovician Tourelle Formation	Lobes (Hiscott, 1980)	2	222.3	523	S. Awadallah
	Petite Vallée	Middle Ordovician Cloridorme Formation	Lobes (Hiscott et al., 1986)	1	452.45	2893	S. Awadallah
TOTAL				11	1831.19	5173	

Table 1.1b: List of turbidite sections obtained from the research of other individuals

Location	Unit	Proposed Environments	Number of Sections	Thickness (m)	Number of beds	Measurer or reference
Barbados	Eocene Scotland Formation	Channel fill (Larue & Speed, 1982)	2	109.68	183	R.N. Hiscott
ODP Sites 931, 944, 946	Amazon Fan	Lobes related to channel bifurcation (Pirmez et al., 1996)	3	335.08	485	Pirmez et al.
Gulf Islands, British Columbia	Upper Cretaceous Nanaimo Group	Channel fill (England & Hiscott, 1992)	7	572.94	560	R.N. Hiscott
Northern Norway Nålneset	Upper Precambrian Kongsfjord Formation	Channel-lobe transition zone (Drinkwater, 1995)	3	247.98	825	N.J. Drinkwater
Arkansas DeGray Lake	Pennsylvanian Jackfork Group	Crevass-splay lobes and levee (Bouma et al., 1995)	2	212.89	2514	M.B. DeVries
TOTAL			17	1478.57	4567	

bed datasets were obtained from colleagues, the thesis supervisor, and other sources. These have a total thickness of 1478.57 m and 4567 beds (Table 1.1b). All data gathered from the sections in Table 1.1 were entered into a spreadsheet program to permit statistical analysis. Data from sections in Table 1.1a form Appendix I.

A number of statistical techniques were used to analyze turbidite cycles in this study. First, the split-moving window (Webster, 1980) and the maximum likelihood estimation (Radhakrishnan et al., 1991) techniques were applied to divide turbidite sections into segments of different statistical character so that sandy segments (i.e., "packets" or clusters) could be selected for further statistical tests for asymmetric and other trends. Second, seven non-parametric and parametric methods, including the most powerful tests for trends ---- Kendall's, Spearman's, and Pearson's correlation tests ---- were employed to examine asymmetric upward thinning and thickening trends and other non-random patterns. Third, a Monte Carlo simulation technique was used to generate randomly shuffled sequences and to compare statistical results of tests for trends and tests for randomness from original sandstone packets with results from randomly shuffled sequences. By using Monte Carlo simulation plus the binomial probability analysis, the significance of the asymmetric sequences and other non-random sequences recognized in a selected section could be numerically estimated. Finally, Hurst's statistical technique was introduced to test for long-term persistence, or cycles, in the turbidite successions. Except for Kendall's, Spearman's, and Pearson's correlation tests, which were used by Lowey (1992) and except for the turning point test and the median crossing test which are

similar to the runs tests and the signs of differences test used by Heller and Dickinson (1985), Waldron (1987), and Murray et al. (1996), many statistical methods used in this study have not been used before in turbidite research; i.e., the split-moving window and the maximum likelihood estimation techniques, two tests for randomness (the rank difference test, and the length-of-runs test), and the Hurst test.

1.4 Terminology

Upward thinning and thickening sequences are defined as asymmetric vertical trends of bed thickness within a sand-rich bed cluster. Such trends are determined by a bed-by-bed comparison of individual bed thicknesses. They are, therefore, phenomena related to the "short-term persistence" of bed thickness. Upward fining and coarsening sequences have the same definition as upward thinning and thickening sequences, but they are asymmetric vertical trends of grain size, on a bed-by-bed basis.

Cycles are presumed to be defined by some repeated periodic structure to a "time series" of turbidite attributes. They, at a larger scale, reflect the "long-term persistence" of order, in the terminology of statistics. The repeated appearance of sand-rich bed clusters or packets in a turbidite succession is assumed to be an example of such long-term cyclicity, regardless of whether there are any asymmetric trends within these bed clusters. A turbidite succession may comprise different cyclic components; that is, different scale cycles.

In description of turbidite sections, the term "packet" or "cluster" is used in this thesis.

A packet (or cluster) is defined as a group of beds with similar facies characteristics, and records deposition in a particular environment or subenvironment (e.g. Sullwold, 1960; Ojakangas, 1968; Corbett, 1972; Nilsen and Simoni, 1973; Hiscott, 1980; Pickering et al., 1989). A sandstone packet may be either the fill of a single channel or the deposit of a lobe, whereas a thin bedded siltstone-mudstone packet may represent deposits of a levee or an interchannel or interlobe environment. The base and top boundaries of a packet are assumed herein to be marked by either a sharp change (i.e. a step or discontinuity) or a gradual change of bed-thickness and/or grain-size. Figure 1.3 presents a graphic overview of definitions of a "layer", a "bed", a "couplet", and a "packet" used in this thesis.

The term "lobe" has been given a variety of different meanings (e.g. Shanmugam and Moiola, 1991), and still has no single clear definition (Mutti, 1992). In this thesis, a lobe is defined to be an overall equant to elongate sandy body in a submarine fan system, deposited at or near the mouth of a channel where turbidity currents become progressively unchannelized or unconfined, and having transitional lateral and distal margins.

Megaturbidites (Ref., Normark, et al., 1993; Porebski et al., 1991; Bouma, 1987; Hiscott and Pickering, 1984) are unusually thick turbidite beds, consisting of a thick or thin sand layer which may show evidence for flow reflections or deflections, and a very thick, structureless, and largely ungraded mud cap. They are laterally extensive and cover a significant part of the basin of deposition. A megaturbidite bed is deposited by one single turbidity current event. The great area extent of megaturbidites suggests that

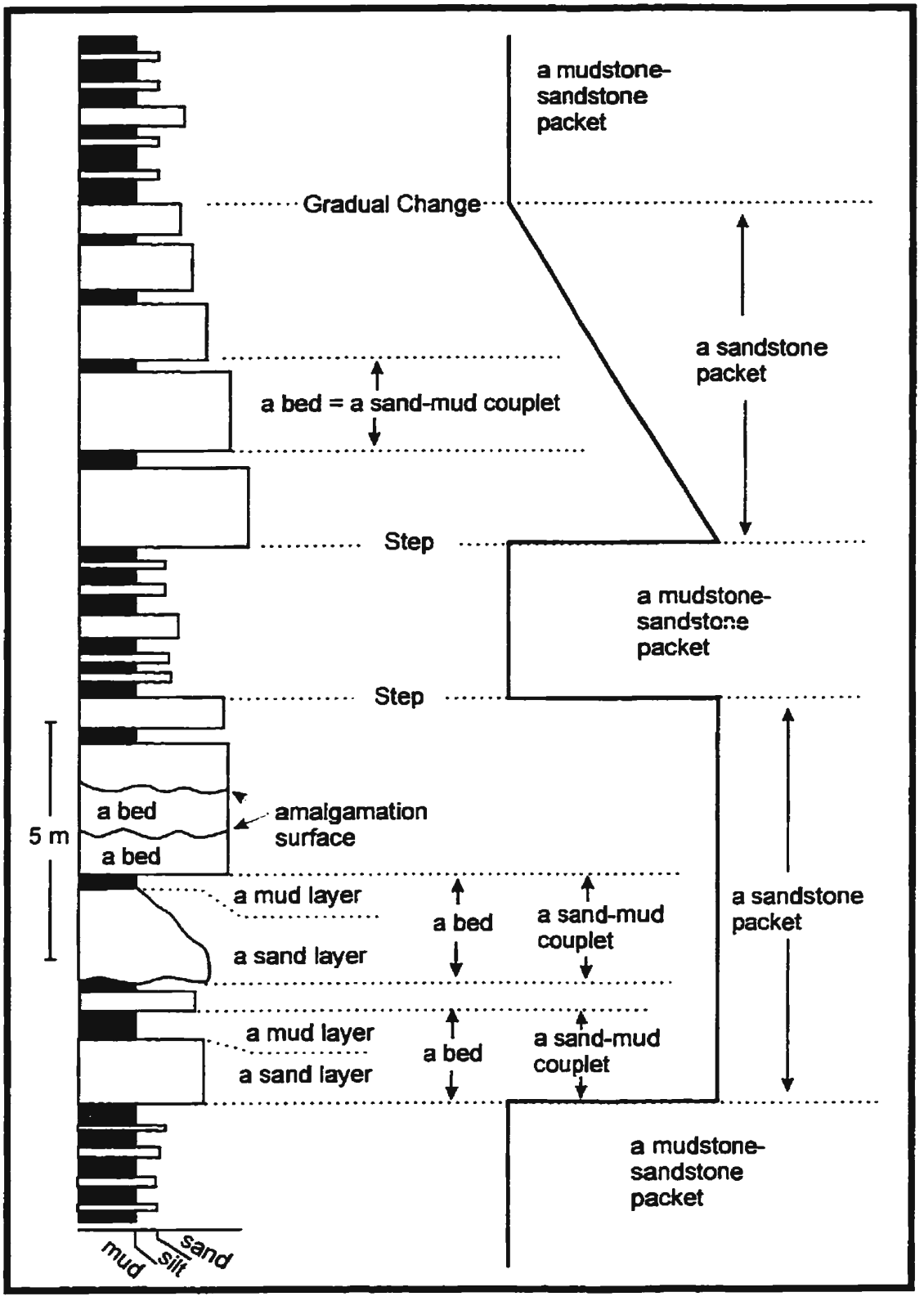

Fig. 1.3 Schematic view of definitions of a "layer", "bed", "couplet", and "packet".

they are formed by muddy turbidity currents with a large volume caused by catastrophic events, particularly shelf margin failures. Such large currents are believed not to be confined to the channel network on submarine fans within the same basin of deposition.

1.5 Organization of the Thesis

The thesis consists of four parts:

(1) Chapter 2 describes the general geology of the turbidite sections. Regional geological settings, general sedimentary characteristics, and lithofacies logs of the bed-by-bed sections are presented.

(2) Chapters 3 and 4 establish a statistical procedure to test for asymmetric upward thinning and thickening sequences. The statistical results are presented in Chapter 4.

(3) Chapter 5 introduces the Hurst statistical technique to test for long-term persistence, or cycles, of turbidite properties. A discussion of the importance of turbidite cycles in submarine fan successions is presented.

(4) Chapter 6 is an integrative analysis of facies characteristics and statistical results from the studied sections. New criteria for the identification of fan environments and preliminary fan models are presented.

Chapter 2

GEOLOGY OF TURBIDITE SECTIONS SELECTED FOR STATISTICAL ANALYSIS

2.1 Introduction

The general geological characteristics of turbidite sections selected for statistical analysis in this study are first outlined. Since upward thinning and thickening sequences have been proposed as a key criterion for identification of submarine fan channel and lobe deposits, respectively, turbidite sections which show a geometry of either channel-filling or unchannelized lobe deposits are intentionally selected.

Due to the large database, the description of individual sections in this chapter is brief and is focused on: (1) regional geological settings, and (2) general sedimentary characteristics. The description of the latter will be based on the plotted lithofacies logs. Detailed facies description is beyond the scope of this study.

Each field section will be provisionally interpreted in this chapter, based on features noted in the field and not on statistically based criteria. Statistical results (Chapter 4) will be used to modify or sharpen these interpretations.

2.2 California, Great Valley Sections

2.2.1 Geological Setting and Location of Measured Sections

Two bed-by-bed turbidite sections were measured on the western side of the Sacramento Valley, California, in the Upper Cretaceous Venado and Sites formations (Kirby, 1943) of the Great Valley Group, along Putah Creek and Cache Creek, respectively (Fig. 2.1).

The Great Valley Group is a succession of deep-water sedimentary rocks deposited in a roughly N-S trending forearc basin, called the Great Valley basin (Dickinson and Seeley, 1979; Ingersoll, 1982). This basin developed between a continental-margin magmatic arc, represented by the present Sierra Nevada to the east, and the associated trench, represented by the Franciscan Complex to the west. The sedimentation rate in the axis of this forearc basin was very high: during Late Jurassic to Late Cretaceous time, about 15,000 m of deep-water mudstone, sandstone, and fine conglomerate were deposited (Ingersoll, 1981). Sediments were derived from volcanic, plutonic, and metamorphic rocks in the magmatic arc to the east and north (Dickinson, 1971; Dickinson and Seeley, 1979; Dickinson et al., 1982).

The Great Valley Group forms a relatively uncomplicated east-dipping homocline (Ojakangas, 1968). Kirby (1943) defined six formations in the Upper Cretaceous part of the Great Valley Group in the Sacramento Valley, from base upward, the Venado, Yolo, Sites, Funks, Guinda, and Forbes formations. Ingersoll (1983, 1990) divided the Great Valley Group into five lithostratigraphic units ranging from Tithonian to Campanian in

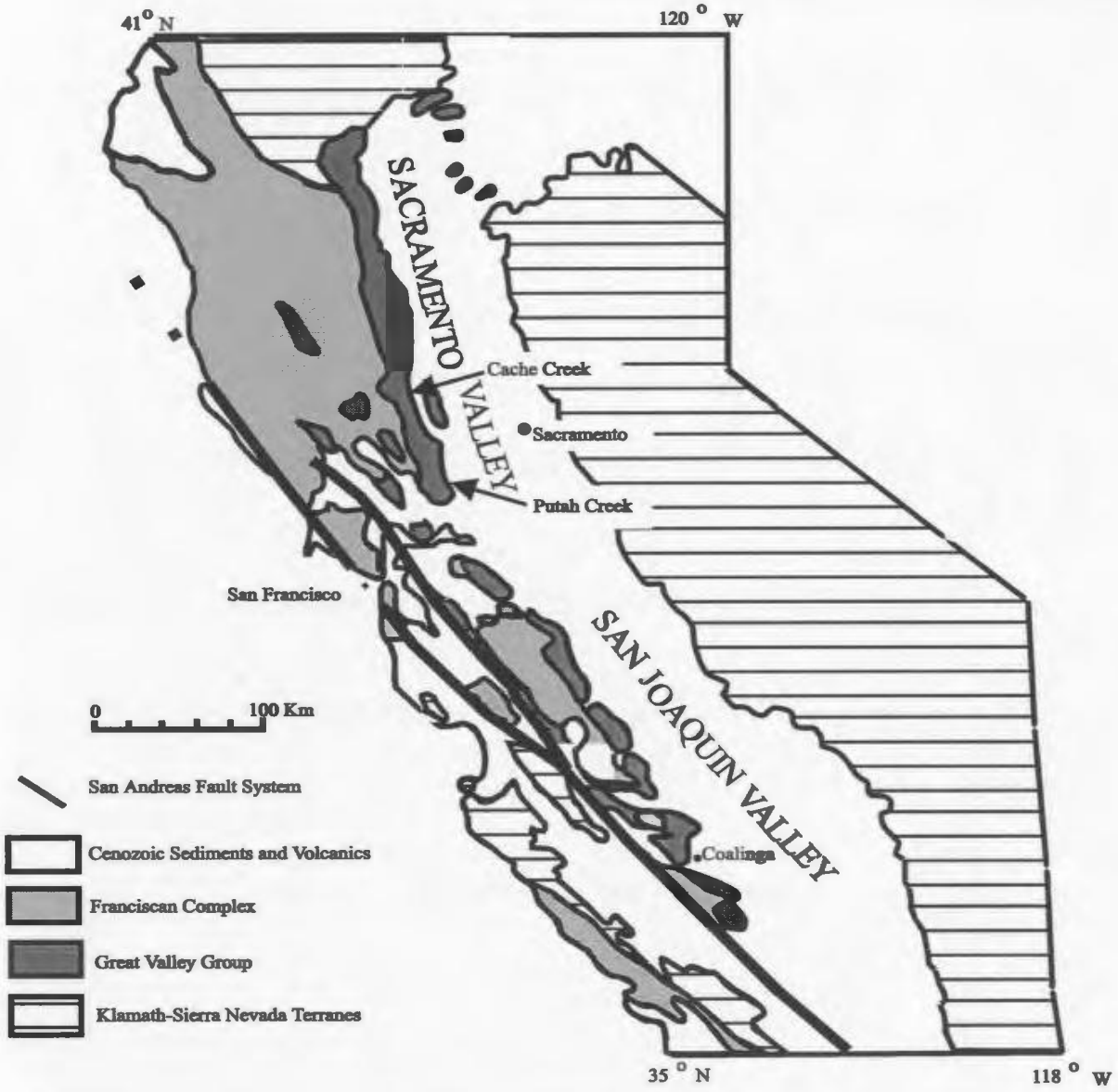

Fig. 2.1 Index map showing locations of the Putah Creek (Monticello Dam) section and the Cache Creek section, Great Valley Group. This map also shows principal components of the Late Mesozoic arc-trench system. The Sierra Nevada terranes represent the Late Mesozoic magmatic arc, and the Franciscan assemblage represents the accretionary prism developed landward of the Mesozoic trench.The Great Valley Group comprises forearc basin deposits (redrawn from Ingersoll, 1978).

age: the Stony Creek, Lodoga, Boxer, Cortina, and Rumsey formations. The Venado and Sites formations of Kirby (1943) are included in the Cortina Formation of Ingersoll. A turbidite origin for the Venado and the Sites sandstones was proposed by Ojakangas (1968) and Ingersoll et al. (1977).

2.2.2 Putah Creek Monticello Dam Section (Venado Formation)

2.2.2.1 Description

The Venado Formation is completely exposed along the road cut of California Route 128 beside Putah Creek where it is crossed by the Monticello Dam (Fig. 2.2). It is 383.5 m thick at this site, and is mainly composed of thick beds of sandstone, pebbly sandstone, and conglomerate. The lower part of the formation occupies a channel, ~4 km wide, cutting into the Boxer Shale. The upper sandstone units extend laterally for more than 10 km, burying the channel (Ghosh and Lowe, in press). The Venado Formation at this site was interpreted by Ingersoll (1978, 1981) as inner and mid fan channel deposits, and the underlying Boxer Shale and overlying Yolo Shale as lower-slope deposits.

This section through the Venado Formation was chosen and measured not only because of its excellent exposure but also because of the report by Ingersoll (1978, 1981) that it is characterized by very well developed upward thinning and fining cycles (Fig. 1.2). Figures 2.3b-c show the lithofacies logs of this section; detailed section measurements are in Appendix I. In addition to being partly a channel fill, the Venado Formation at this locality has the following characteristics.

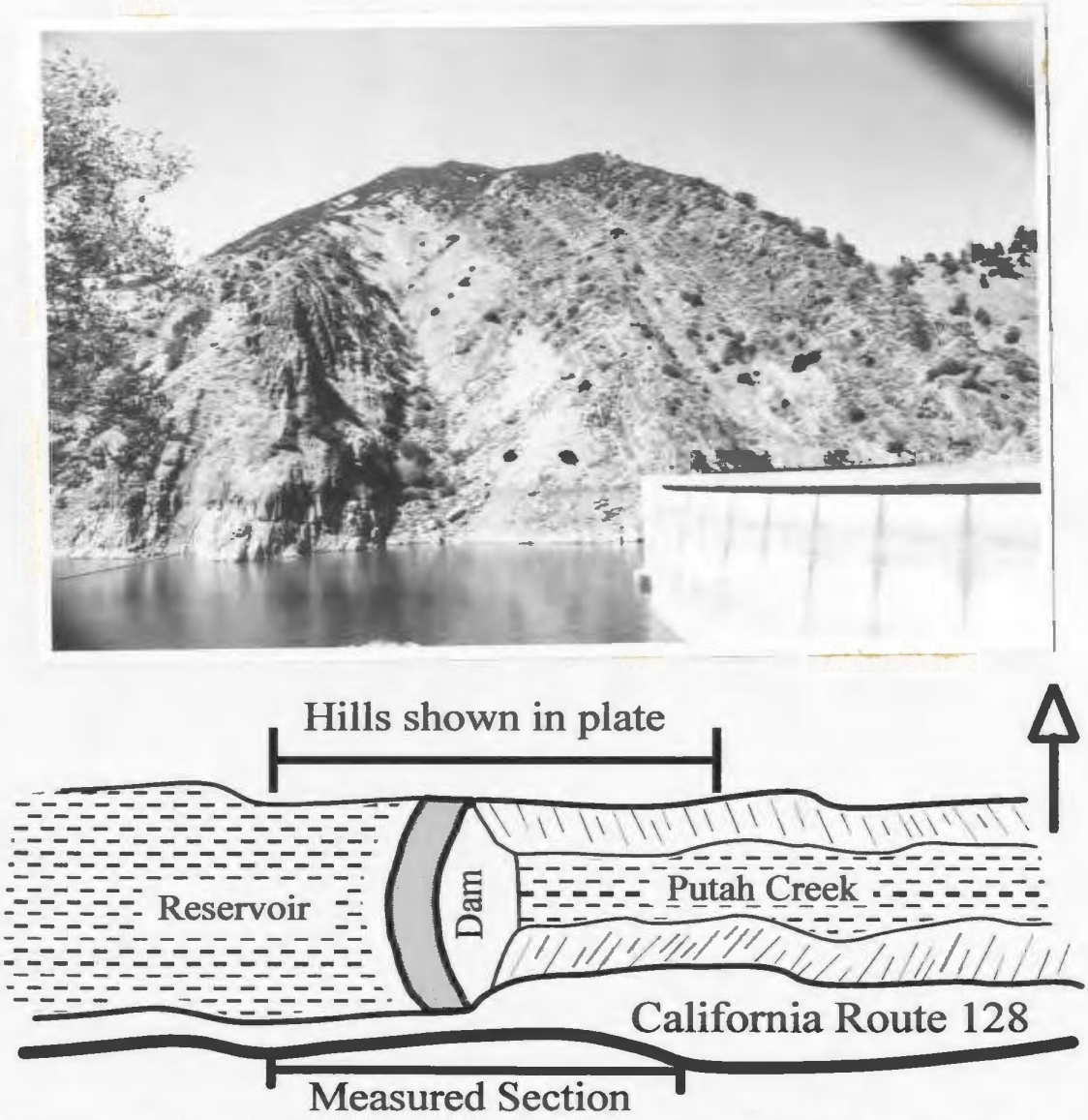

Fig. 2.2 View, looking north, of the Venado Formation at Monticello Dam, Putah Creek, Great Valley, California. Upsection is to the right. The less photogenic measured section, from where the photograph was taken, is at the south side of the dam.

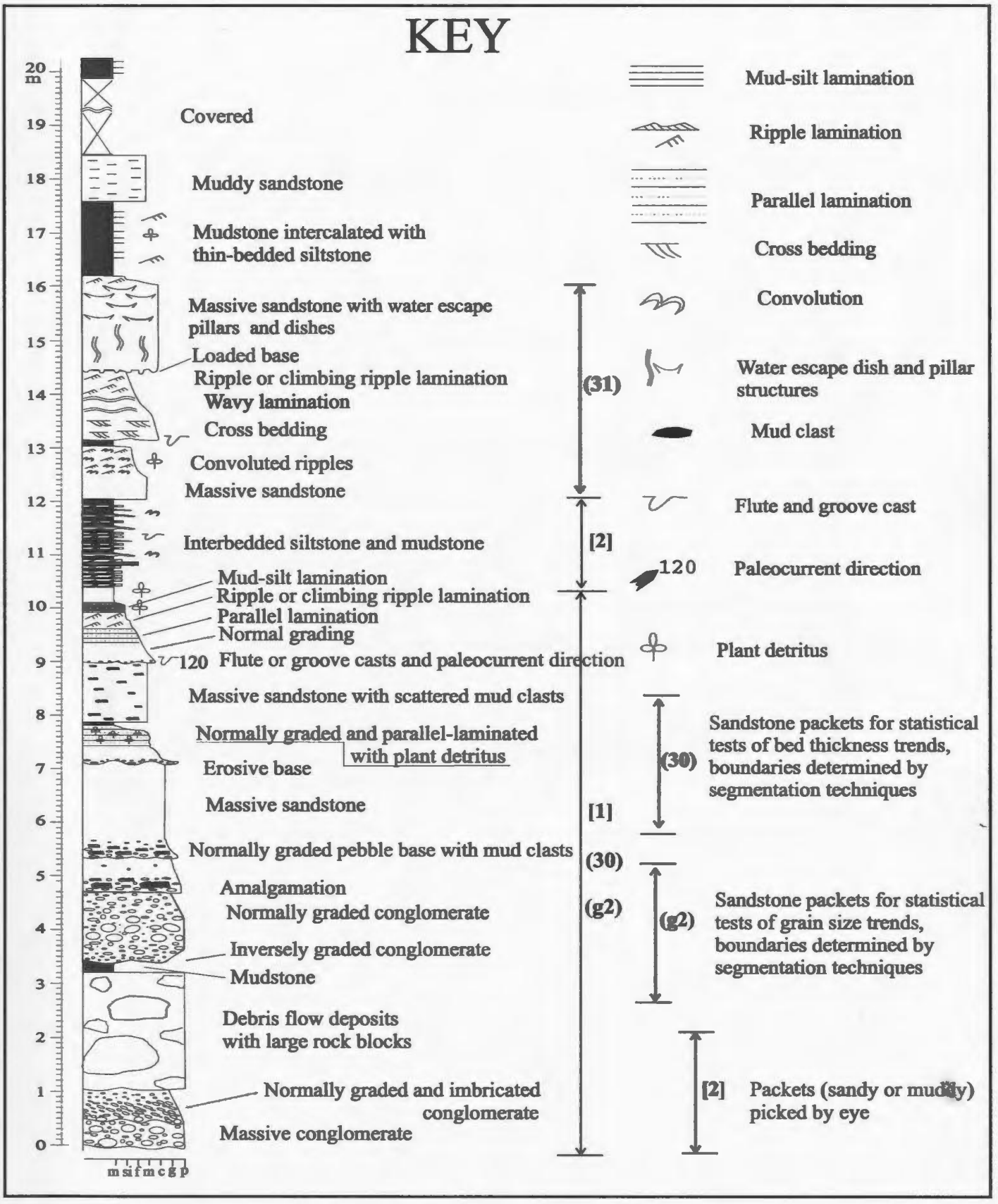

Fig. 2.3a Key for lithofacies logs of turbidite sections measured in California and in Italy.

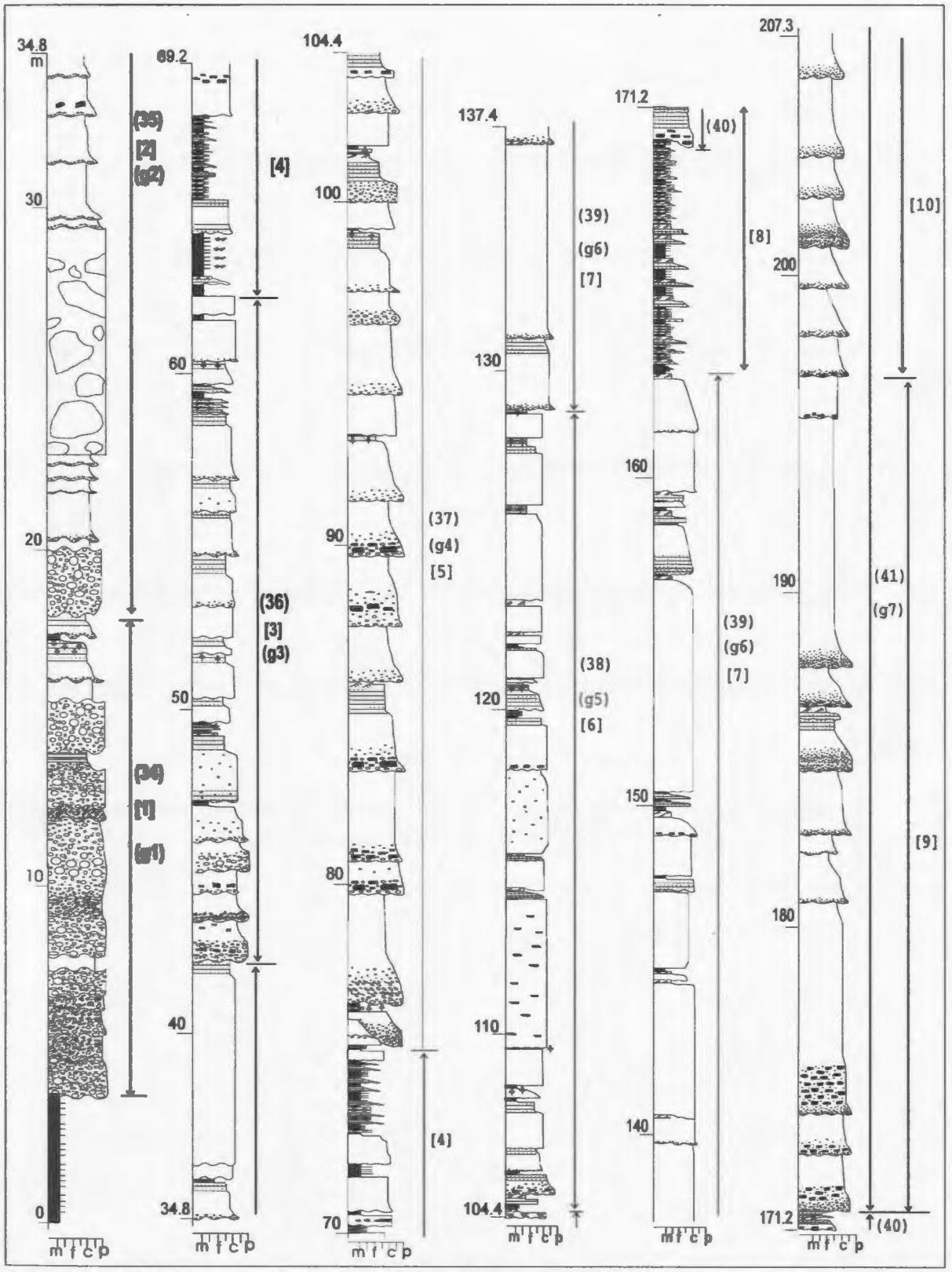

Fig. 2.3b The measured section of the Venado Formation at Monticello Dam, Putah Creek, along the road cut of California Route 128 (continued next page).

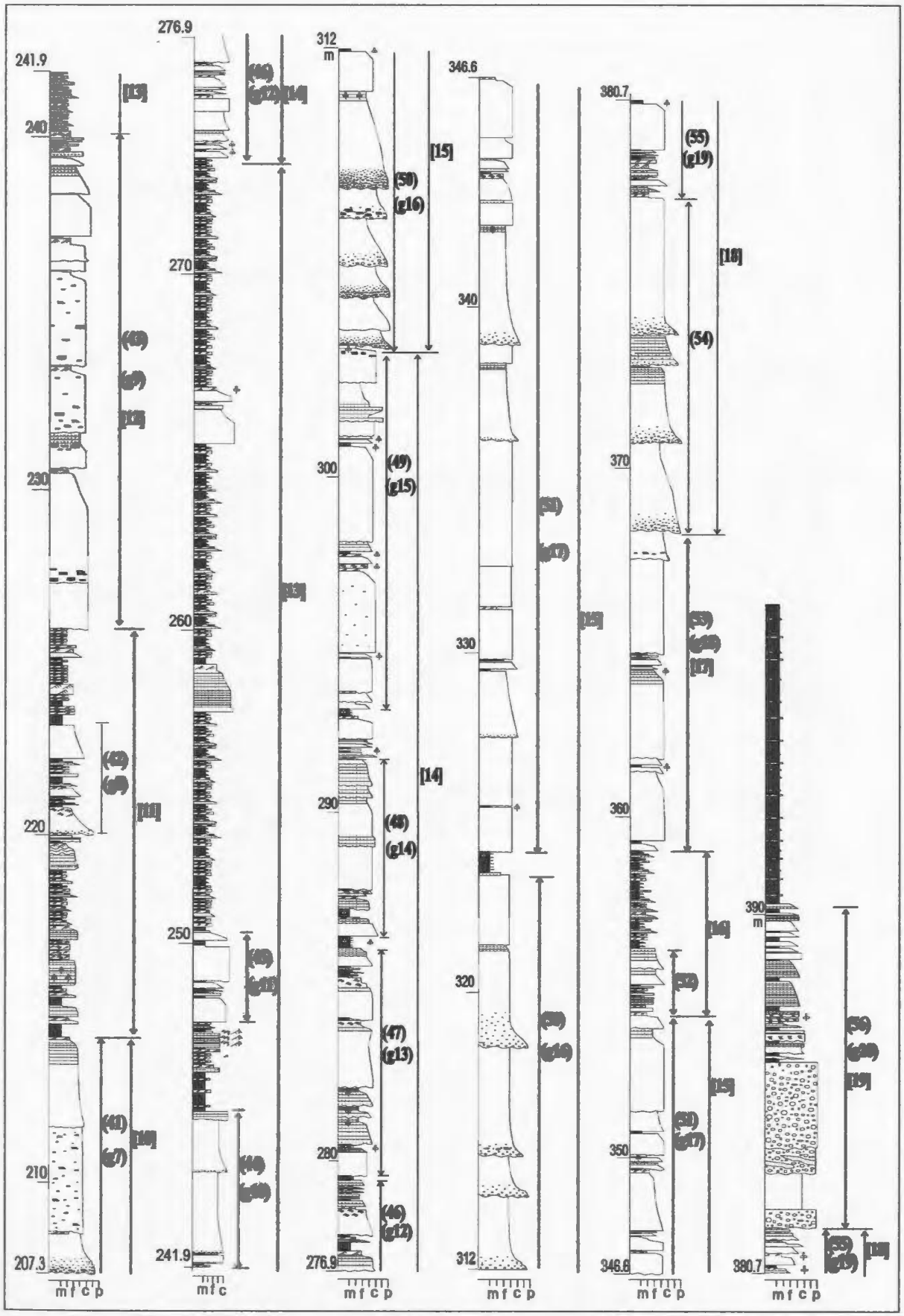

Fig. 2.3c The measured section of the Venado Formation at Monticello Dam, Putah Creek, along the road cut of California Roate 128 (end).

(1) The section comprises 8% conglomerate, 32.2% pebbly sandstone, 43.2% sandstone, and 16.6% interbedded siltstone and mudstone. For the whole section, the mudstone/(conglomerate + sandstone + siltstone) ratio is 1:13.5.

(2) Both coarse and fine beds are segregated into packets (e.g. Fig. 2.3c, 226-240 m and 259-265 m, Fig. 2.4).

(3) The percentage of sandstone plus conglomerate in sandstone and conglomerate packets is very high, from 97% to 100%; even in packets of interbedded siltstone and mudstone, the percentage of siltstone is still high, from 50% to 70%.

(4) Amalgamation is common, as irregular erosive bases to conglomerate, pebbly sandstone or sandstone beds, with pebbles and mud clasts concentrated along the erosive bases (Fig. 2.5).

(5) Bouma division T_a (= division S_3 of Lowe, 1982) dominates pebbly sandstone and sandstone beds. Most pebbly sandstone beds have a normally graded base, and upward become massive (i.e. structureless). Most sandstone beds are massive and ungraded (Fig. 2.5). As a result of strong amalgamation, bed tops (including Bouma divisions T_b, T_c and T_{c-d}), if they were originally deposited, are not preserved in most pebbly sandstone beds. Thin T_b and/or T_c divisions are preserved as caps on many sandstone beds. Some sandstone beds consist mainly of the T_b division.

Fig. 2.4 Thin-bedded siltstone and mudstone beds in a siltstone-mudstone packet at 265-274 m, figure 2.3c. Top is to the left. Note the two intercalated, thicker sandstone beds; the upper one is 43 cm thick. The Venado Formation at the Monticello Dam section, California.

Fig. 2.5 Amalgamated, very thick-bedded, coarse-grained, massive (ungraded) sandstone with mud clasts concentrated along erosive bases. The Venado Formation at the Monticello Dam section, California. Top is to the left. Bedding is nearly vertical.

Nineteen coarse-grained and fine-grained packets were recognized in the field (Fig. 2.3b-c, numeric codes [1] to [19]). Packets [4], [8], [11], [13], and [16] are interbedded thin siltstone and mudstone, with a few intercalated beds of medium to thick sandstone. Ripple laminations are very well developed in siltstone beds. These packets have a siltstone/mudstone ratio larger than 1:1.

Packets [6], [12], [14], and [17] are mainly composed of sandstone beds. Since amalgamation in these packets is not very strong, many beds have a parallel base and a preserved T_c and/or T_{d-e} top. Most mud clasts are smaller than 10 cm and scattered throughout the host sandstone bed. Parallel lamination (T_b) is well developed in packet [14].

Packets [1], [2], [3], [5], [7], [9], [10], [15], [18], and [19] appear to fine upward based on the field observation. The lower part of each packet is strongly amalgamated conglomerate or pebbly sandstone beds, passing upward into sandstone beds. The basal bed of each packet has an irregular erosive lower contact or incises down into the underlying bed(s). Some of these amalgamated, upward fining packets are accompanied by an upward decrease in amalgamation, which is indicated either by an upward increase in preservation of T_b or T_c and T_{d-e} division(s), or by an upward decrease in the number of large mud clasts. Upward fining is not accompanied by upward thinning trends of the quality implied by Ingersoll (1978).

2.2.2.2 Interpretation

Based on coarse texture, strong amalgamation, ubiquitous basal erosion, and the map-scale distribution of the Venado Formation, a channel setting is inferred for at least packets [1] to [5], and possibly [1] to [10]. Intervening mud/silt-rich packets [4] and [8] may be overbank (levee) deposits. They resemble the basal parts of channel-levees cored on Amazon Fan (Flood, Piper, Klaus et al., 1995).

In an active channel or "nest" of stacked channels (e.g. Clark and Pickering, 1996, p183, 206), both erosional and depositional phases may alternate. Backfilling of channels can lead to infilling of the lower part of a channel by a channel-mouth lobe (e.g. Normark et al., in press). Subsequent rejuvenation of the channel can erode and incise downward into the previous channel or lobe deposits. Because coarse sediments are deposited in the axial area or talweg of a channel (e.g., Watson, 1981; Hein and Walker, 1982), and finer sediments at the mouth of the channel, cycles of incision and backfilling might produce upward fining cycles (but not necessary upward thinning trends). This hypothesis is summarized in Figure 2.6. The cycles produced by these processes are here termed "incision-backfill cycles". Except for packet [19], which is possibly an abandoned channel fill (cf. ODP Site 934, Flood, Piper, Klaus et al., 1995), packets [1], [2], [3], [5], [7], [9], [10], [15] and [18] are interpreted as incision-backfill cycles. Note that if cycles of basinward channel incision and backfilling are frequent and irregular events, well organized upward fining cycles might not be expected.

Using the procedures of architectural element analysis proposed by Clark and

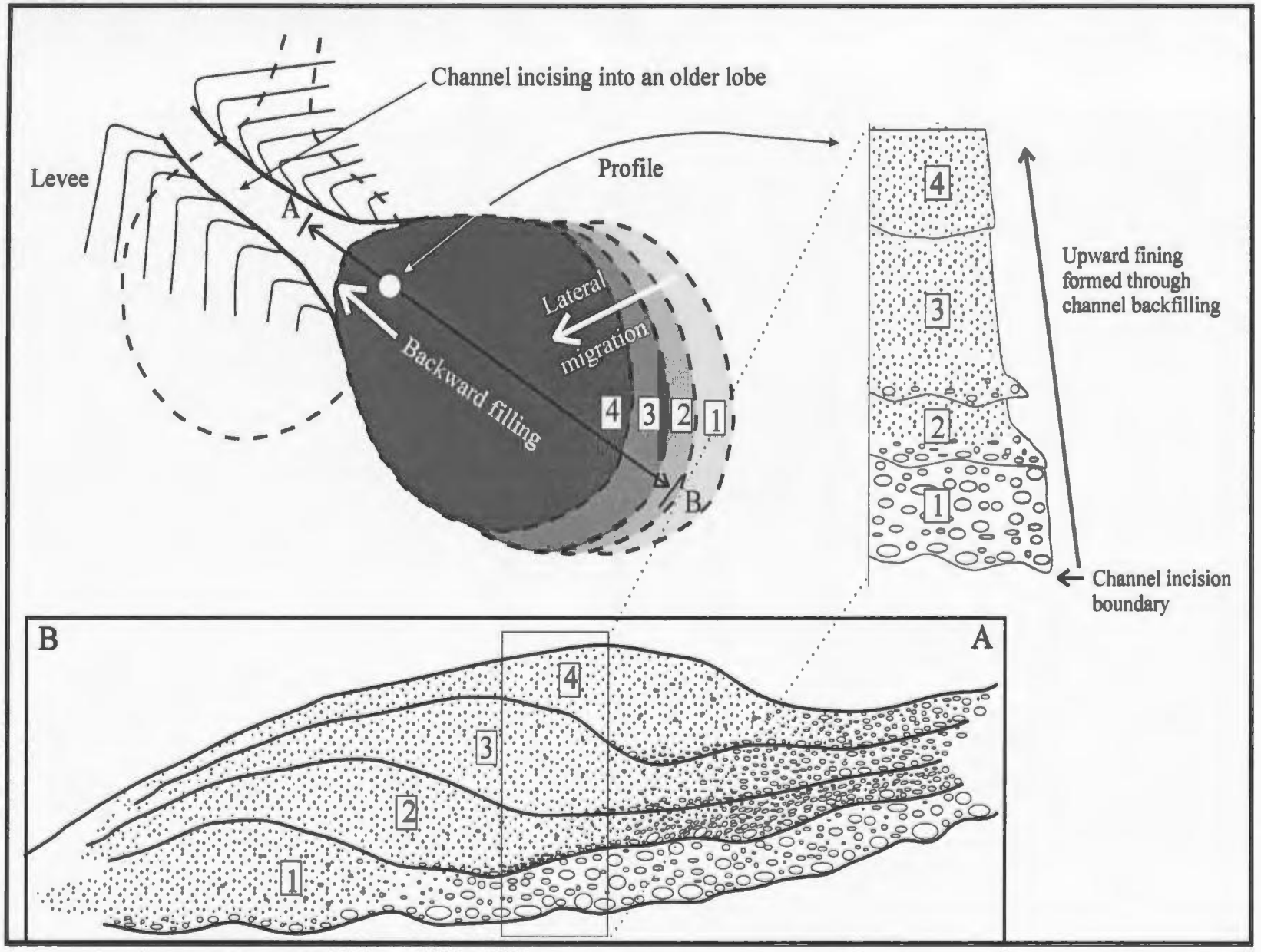

Fig. 2.6 Schematic model to show channel incision and backfilling.

Pickering (1996), the base of packet [1] and the top of packet [19], i.e. the base and top of the Venado Formation, are fourth-order bounding surfaces, which define the whole Venado channel and/or lobe system. Inside the formation, boundaries of coarse and fine packets are third-order bounding surfaces, defining nested offset stacked channels and/or lobes similar to channel stacking patterns 9 or 8 in figures 9.2 and 9.8 of Clark and Pickering (1996, p. 183, 187). Clark and Pickering (1996, chapter 9 and 10) associated such patterns of nested, offset, stacked channels with erosional channels in which deposits are characterized by coarse-grained fills associated with highly concentrated sediment gravity flows, a high sand/mud ratio, deep scours, and poorly developed levees.

The 19 coarse and fine packets can be combined into six higher-rank cycles, each capped by a mud-rich packet (Fig. 2.3b-c):

[1] [2] [3] ---> [4]

[5] [6] [7] ---> [8]

[9] [10] ---> [11]

[12] ---> [13]

[14] [15] ---> [16]

[17] [18] [19] ---> Yolo Shale

Packets [12], [14] and [17], at the base of the upper three of these higher-order cycles, have a relatively fine texture, rather weak amalgamation and well-preserved bed tops ---- characteristics of unchannelized lobes (Mutti and Normark, 1987; Reading and Richards, 1994). If the interpretation of the mud/silt-rich packets as levees is correct, then each of

these three higher-order cycles may represent the following sequence of events: (a) establishment of a sandy lobe on top of an older levee flank as landward channel switching provides a new sand source, (b) advance of a leveed channel over the lobe, (c) stacked incision-backfill cycles, (d) channel abandonment by landward avulsion or canyon switching, so that coarse-grained sediments are overlain by levee deposits or slope shales (e.g. Yolo Shale). In this model, then the upper part of the Venado Formation at the Monticello Dam represents the vertical superposition of three unchannelized through channelized lobe successions. The lower part of the Formation represents extended deposition in a large erosional channel, as advocated by Ghosh and Lowe (in press).

2.2.3 Cache Creek Section (the Sites Formation)

2.2.3.1 Description

The Sites Formation is a sandstone-dominated unit, about 789 m thick along Cache Creek (Murray, 1992). Both the underlying Yolo Shale and the overlying Funks Shale (Kirby, 1943) represent lower slope deposits succeeded by basin plain deposits (Ingersoll, 1981). The measured 359 m-long section is in the lower part of the Sites Formation (Fig. 2.7a-b). Ingersoll (1978, 1981) claimed that this part of the Sites Formation is characterized by upward thickening cycles representing lobe deposits. Murray et al. (1996) measured the same section, but concluded from a 'runs analysis' that the section is *not* composed of a succession of upward thickening and coarsening cycles. The section

shows the following facies characteristics.

(1) The section consists of 85% sandstone and 15% mudstone (mudstone/[sandstone + siltstone] = 1:5.6). Medium to coarse grained sand dominates, but granules and pebbles are not present.

(2) Graded or massive Bouma division T_a forms 90% of all sandstone in this section. Many sandstone beds are composed of a thick T_a division and a thin T_c and/or T_{d-c} top. T_b divisions (parallel lamination) are well developed in a few beds.

(3) Amalgamation is quite strong at the lower part of this section (Fig. 2.7a, 16 -- 125 m). Mud clasts are absent in these amalgamated beds. In contrast, amalgamation is uncommon in the middle and upper part of the section, where many beds have a non-erosive, parallel base or a weakly erosive, slightly wavy base (Fig. 2.8). Bouma divisions T_c and T_{d-c} are present in many of these beds. A few beds contain mud clasts, but most are less than 10 cm long, scattered in the bed or 'floating' in the upper part of the bed.

(4) As shown in the field or in figures 2.7a-b, it is apparent that sandstone beds are bundled into packets which are separated by contrasting intervals or packets of mudstone interbedded with thin and ripple-laminated siltstones.

The section is *not* characterized by simple upward thickening and coarsening cycles as was proposed by Ingersoll (1978, 1981). This section provides a good illustration of the ambiguity that can creep into subjective cycle recognition (Walker, 1984). By selecting different possible starting points in the section, both upward thickening and

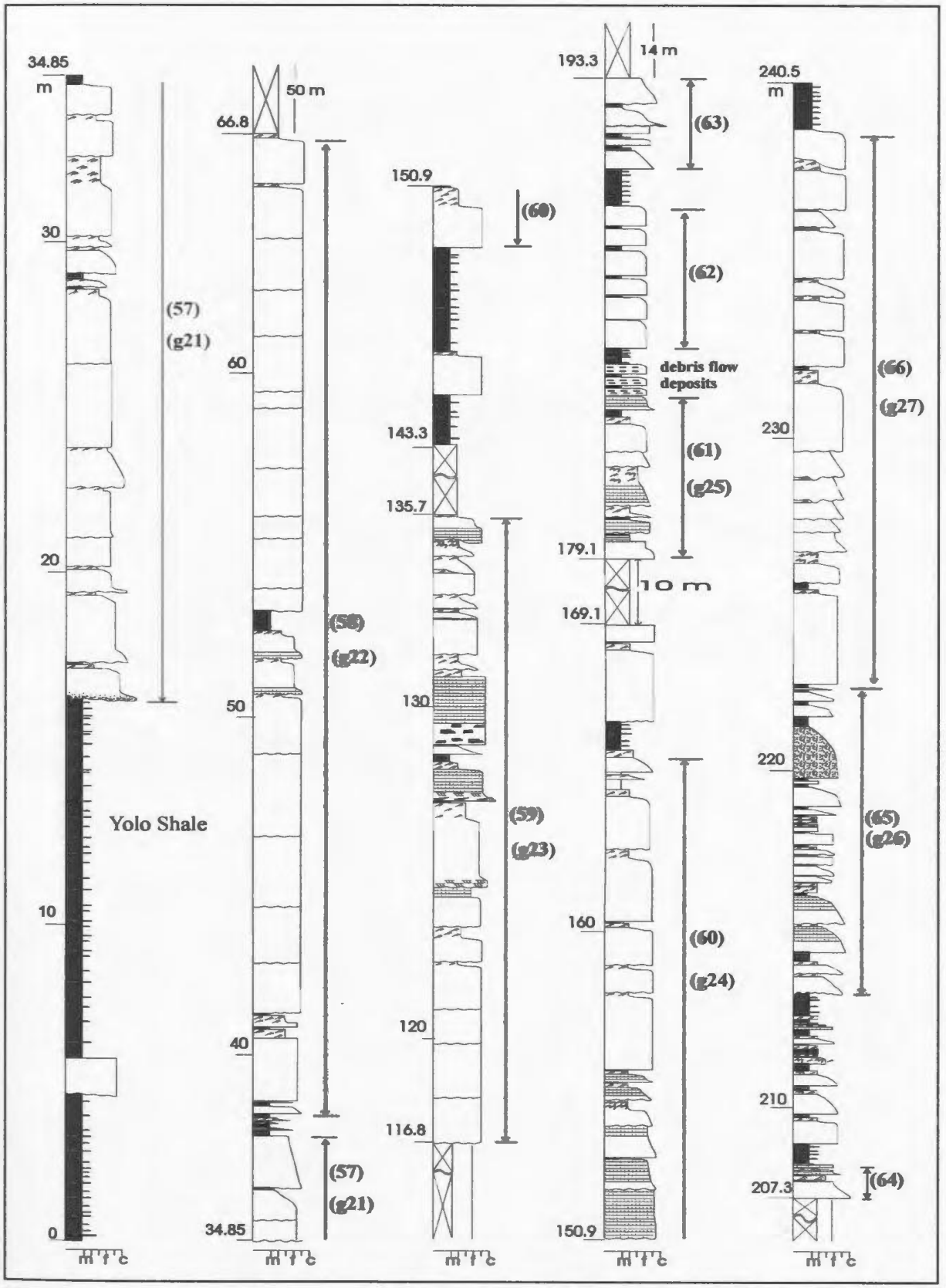

Fig. 2.7a The Measured section of the Sites Formation of the Great Valley Group at Cache Creek, California (continued next page). See Figure 2.3a for key.

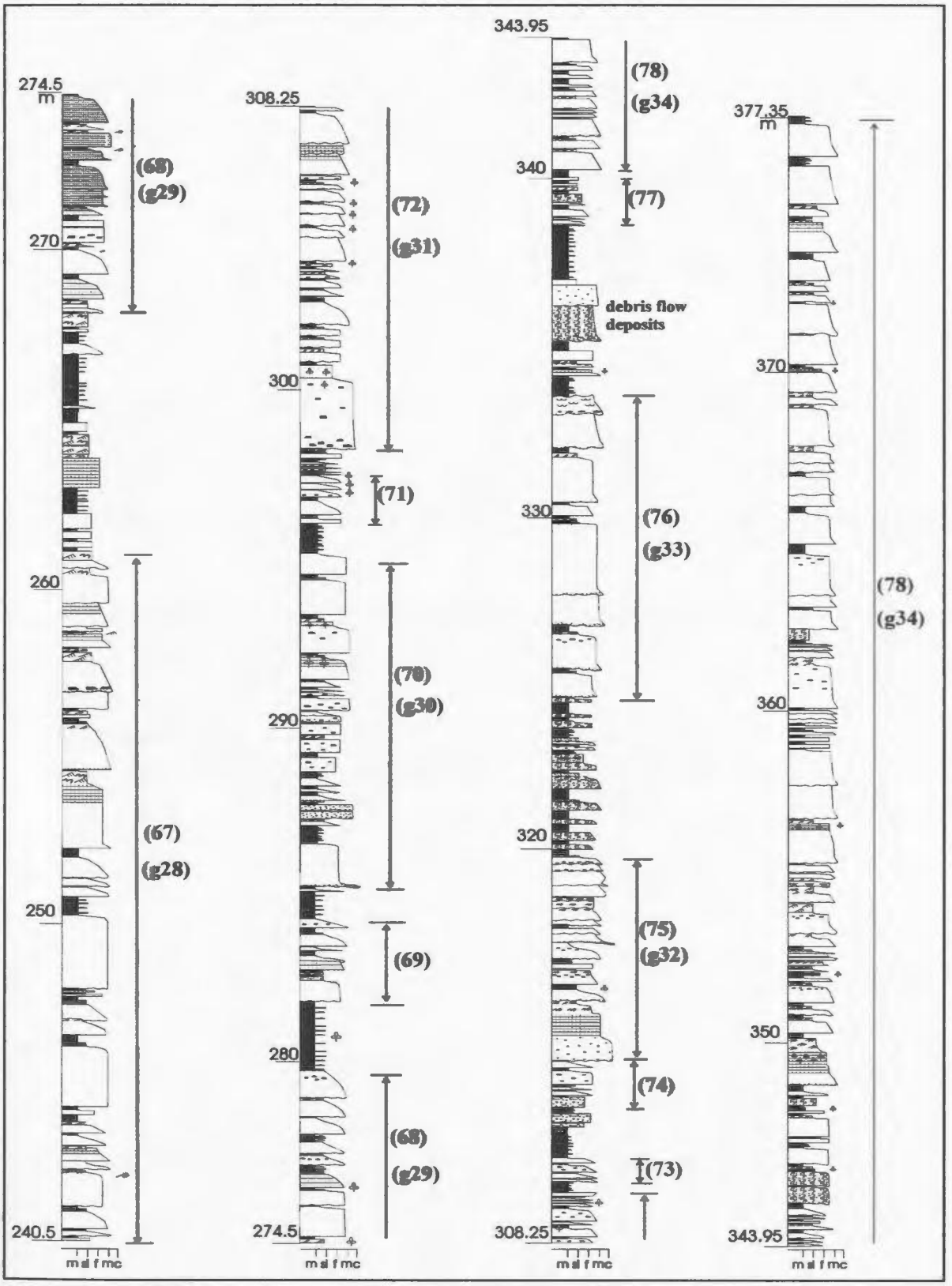

Fig. 2.7b The measured section of the Sites Formation of the Great Valley Group at Cache Creek, California (end). See Figure 2.3a for key.

Fig. 2.8 Thick-bedded, medium- to coarse-grained sandstone beds with a parallel base and top at 229-236 m, Figure 2.7a. The Sites Formation at the Cache Creek section, California. Top is to the right. Note the back-pack for scale.

upward thinning sequences can be proposed involving the same beds (e.g. 295 ---> 300 m versus 298 ---> 303 m). Objective statistical criteria (chapters 3 and 4) can help remove such ambiguity.

2.2.3.2 Interpretation

Although lateral tracing of the sandstone beds is not possible in the Cache Creek area, the facies and bed thickness are like those widely accepted to be indicative of submarine fan lobes (e. g. Reading and Richards, 1994; Mutti and Normark, 1987; Shanmugam, 1991). Such lobes can form beyond channels or in broad interchannel lows (e.g. high-amplitude reflection packets of Flood et al., 1991; Pirmez et al., in press). The mudstone and siltstone packets, with a siltstone/mudstone ratio ranging from 1:12 to 3:10 , are interpreted as inter-lobe muds, distal levee deposits (cf. Pirmez et al., in press), or muds deposited when sediment supply was reduced by external factors (e.g. sea-level rise).

2.3 Northern Apennines Sections, Italy

2.3.1 Geological Setting and Location of Measured Sections

The middle to upper Miocene Marnoso arenacea is composed of deep water sandstone and mudstone with local thickness in excess of 3000 m (Ricci Lucchi, 1986). It accumulated in a NNW-SSE elongated foredeep, which lay between the northeastern Adriatic foreland and the Apennine thrust belt to the southwest, and which extended as far north as the Alpine orogenic chain to the northwest (Fig. 2.9). The Alpine chain and

the Adriatic foreland constitute the major sediment source and the Apennines thrust belt the minor sediment source to the basin (Ricci Lucchi, 1986).

The Marnoso arenacea is very well exposed in the area between the Santerno Valley and the Savio Valley and had been studied in detail by Mutti and Ricci Lucchi (1972, 1975), Ricci Lucchi (1975, 1981, 1984, 1986), and others. The hypothesis that upward thinning and fining sequences and upward thickening and coarsening sequences can be used to infer depositional setting (channel *versus* lobe) (Mutti and Ricci Lucchi, 1972; Ricci Lucchi, 1975) is based mainly on field observations in the Marnoso arenacea. In order to statistically test for asymmetric sequences, six bed-by-bed sections (Table 1.1) were measured in the Santerno and Savio Valleys (Fig. 2.10).

2.3.2 Santerno Valley Sections

2.3.2.1 Description

Sections measured along the Santerno Valley consist of turbidite sandstone and siltstone, turbidite mudstone, turbidite carbonate mudstone, and hemipelagic mudstone (F. Ricci Lucchi, personal communication in the field, 1995). Since the hemipelagic mudstone is mainly composed of carbonate components, it is hard to distinguish from turbidite carbonate mudstone. It is also hard to separate the hemipelagic mudstone from the turbidite mudstone even though the turbidite mud in these sections is darker than the hemipelagic mud, because the turbidite mud commonly passes gradually upward into the hemipelagic mud. Therefore, only one mudstone facies was recognized during section

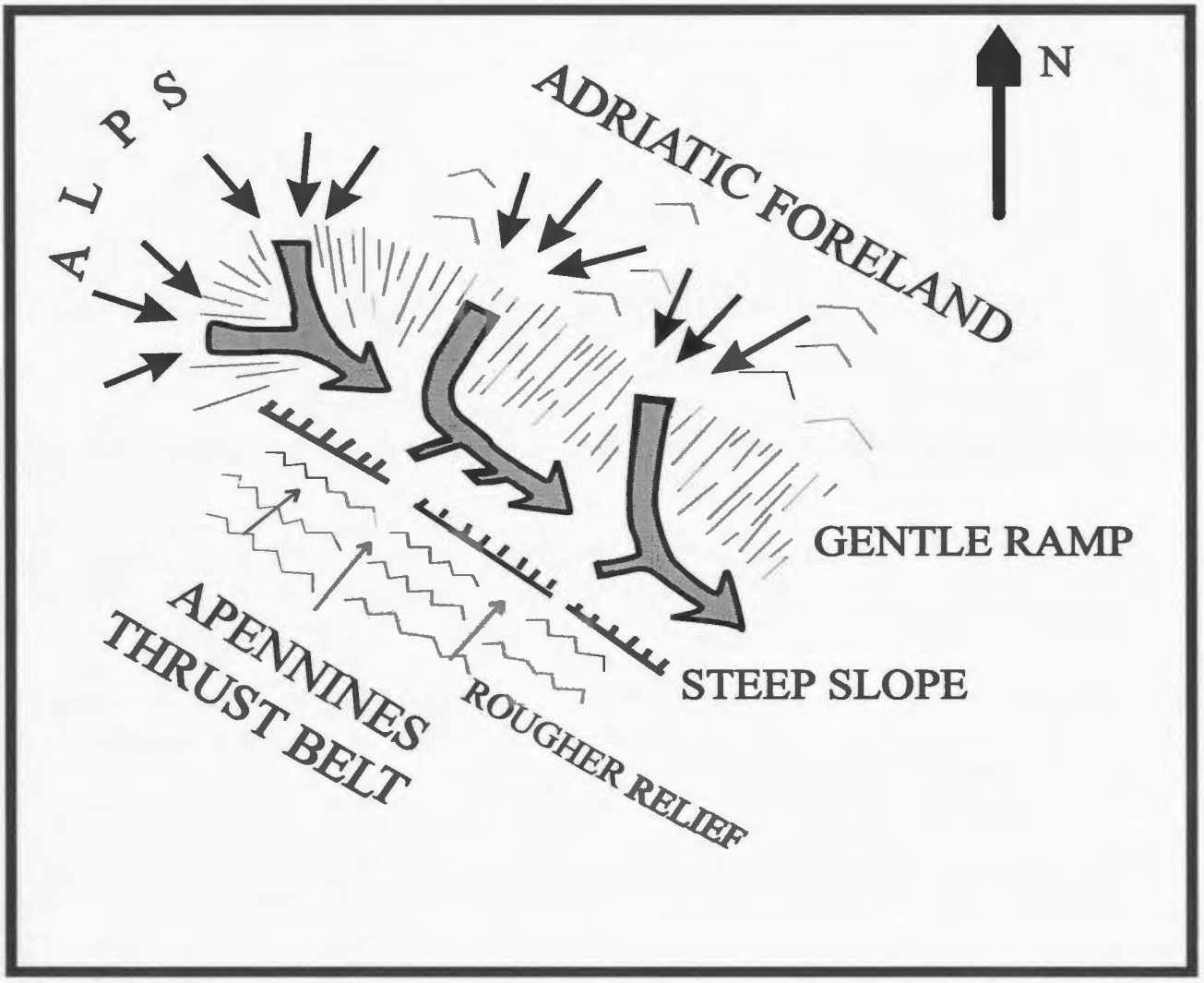

Fig. 2.9 Schematic diagram showing dispersal pattern in an idealized Apenninic foredeep. The Alpine chain and Adriatic foreland acted as the major sediment source, and the Apennines thrust belt as a minor source to the basin (after Ricci Lucchi, 1986).

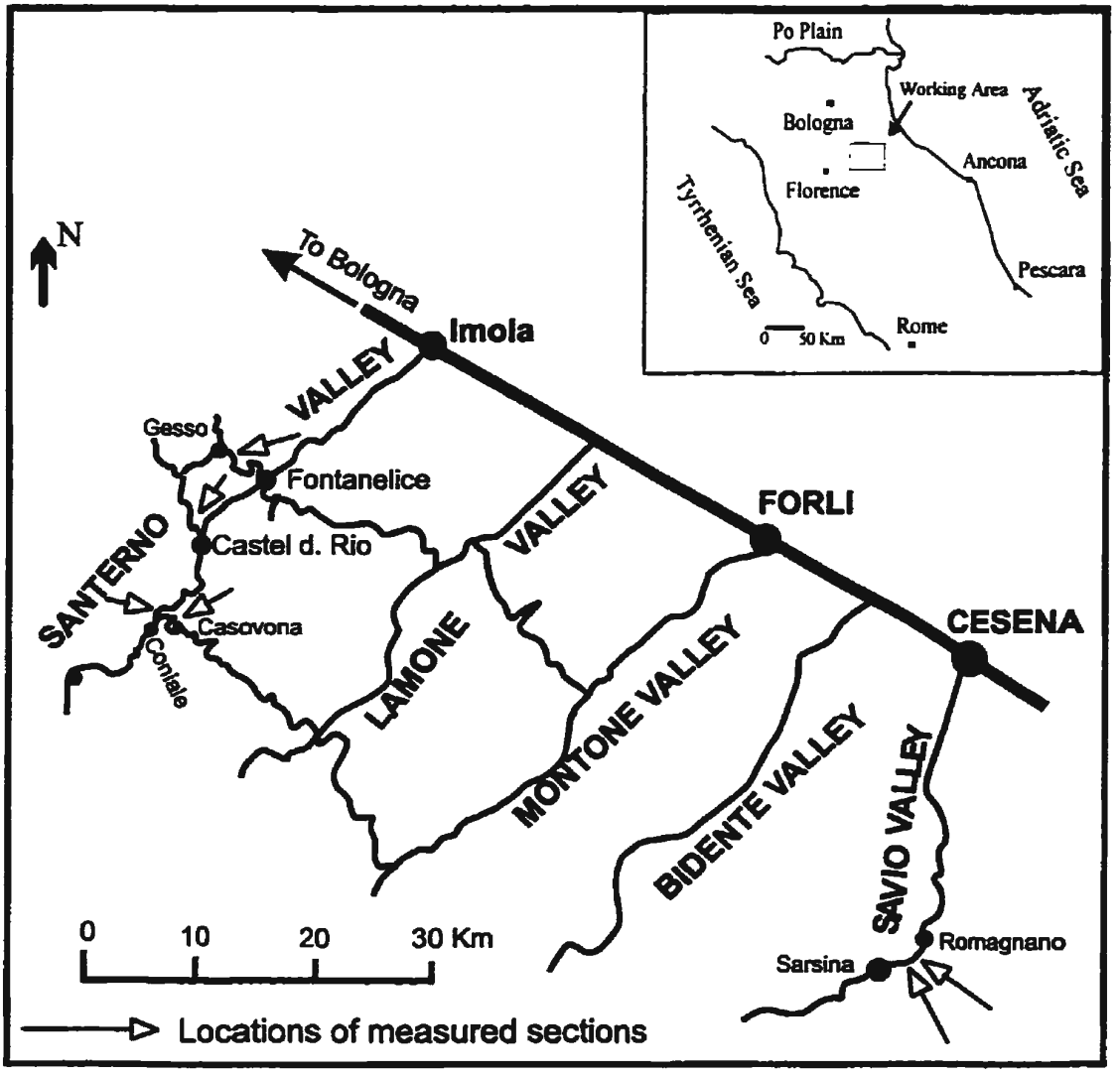

Fig. 2.10 Rail line (bold), roads, selected communities, and locations of measured sections in the Santerno, Lamone, Montone, Bidente and Savio valleys, northern Apennines, Italy.

measurement. These sections share the following facies characteristics.

(1) Mudstone/sandstone ratio ranges from 1.2:1 to 1:2.4 (Fig. 2.11, 2.12a-b and 2.13).

(2) Sandstone beds are medium to fine grained and contain an average of 30% mud matrix.

(3) Bouma divisions T_b, T_c and T_{d-e} are particularly well developed (Fig. 2.11, 2.12a-b and 2.13). Many beds lack a T_a division or have only a thin T_a base, being instead dominated by a T_b division and a thick uppermost T_c division. Most thin to medium siltstone beds contain ripple laminations (T_c). The T_c divisions in most beds are strongly convoluted.

(4) Several basin-wide megaturbidite beds, each composed of a thick sandy base and a very thick muddy cap, were recognized by Ricci Lucchi and Valmori (1980). For example, the Contessa bed of Ricci Lucchi and Valmori (1980) at the Coniale section consists of a 24 cm-thick normally graded coarse to medium grained sand (T_a), a 240 cm-thick parallel laminated division of medium to fine grained sand (T_b), a 80 cm-thick division of climbing ripples in very fine sand and silt (T_c), 50 cm of silt with parallel laminae (T_d), and a homogeneous mud cap (T_e) as thick as 495 cm (Fig. 2.13). This bed was deposited by a single turbidity current.

(5) Most sandstone beds cluster into packets (Fig. 2.11, 2.12, 2.13, 2.14, 2.15).

(6) Amalgamation characterizes only a few sand beds. Most sand beds have a parallel base and a preserved T_{d-e} top, which indicates that basal erosion was minor or absent.

(7) The parallelism and lateral continuity of sandstone beds are impressive in these

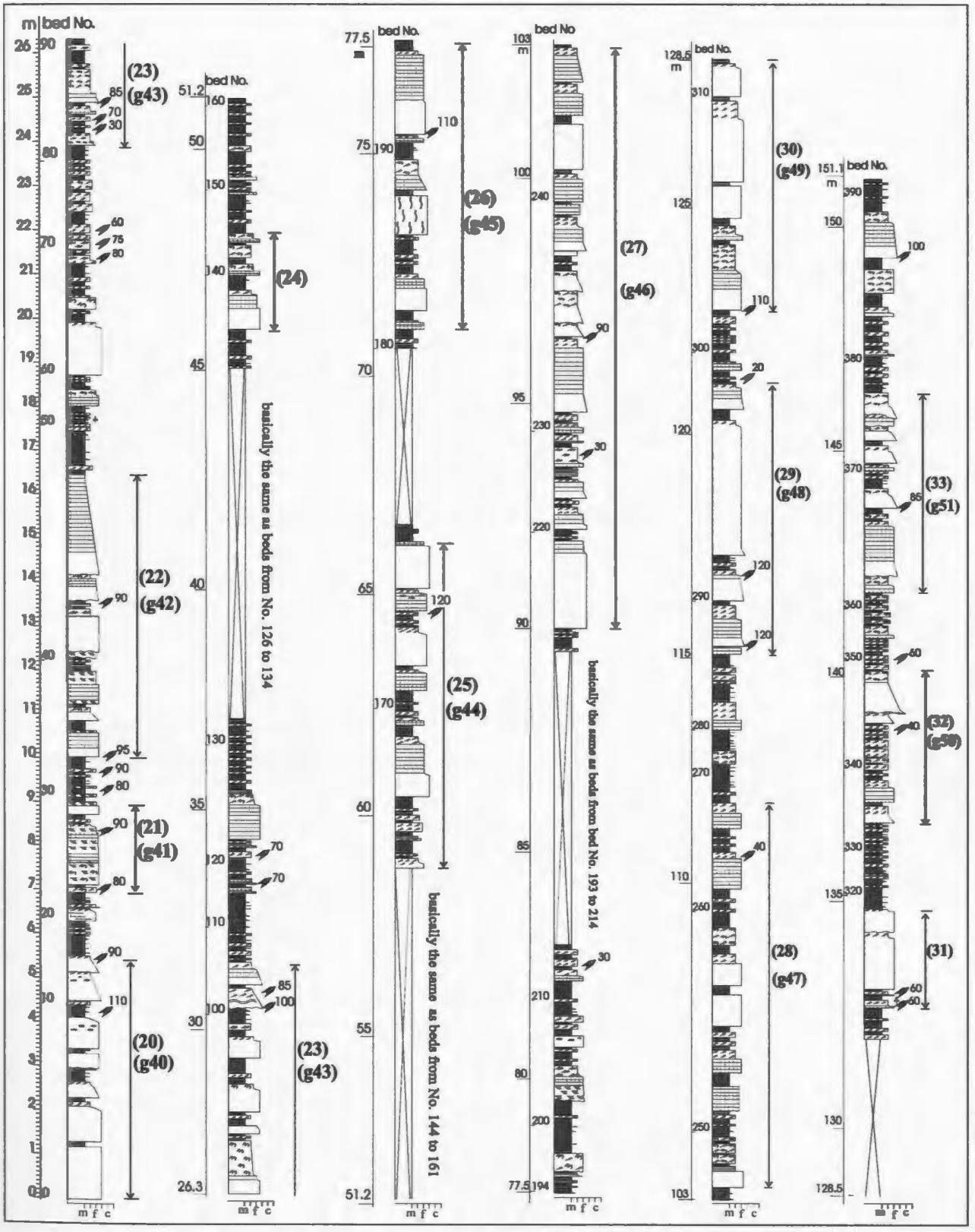

Fig. 2.11 Lithofacies log of Castel del Rio measured section, Santerno Valley, North Italian Apennines. See Figure 2.3a for key.

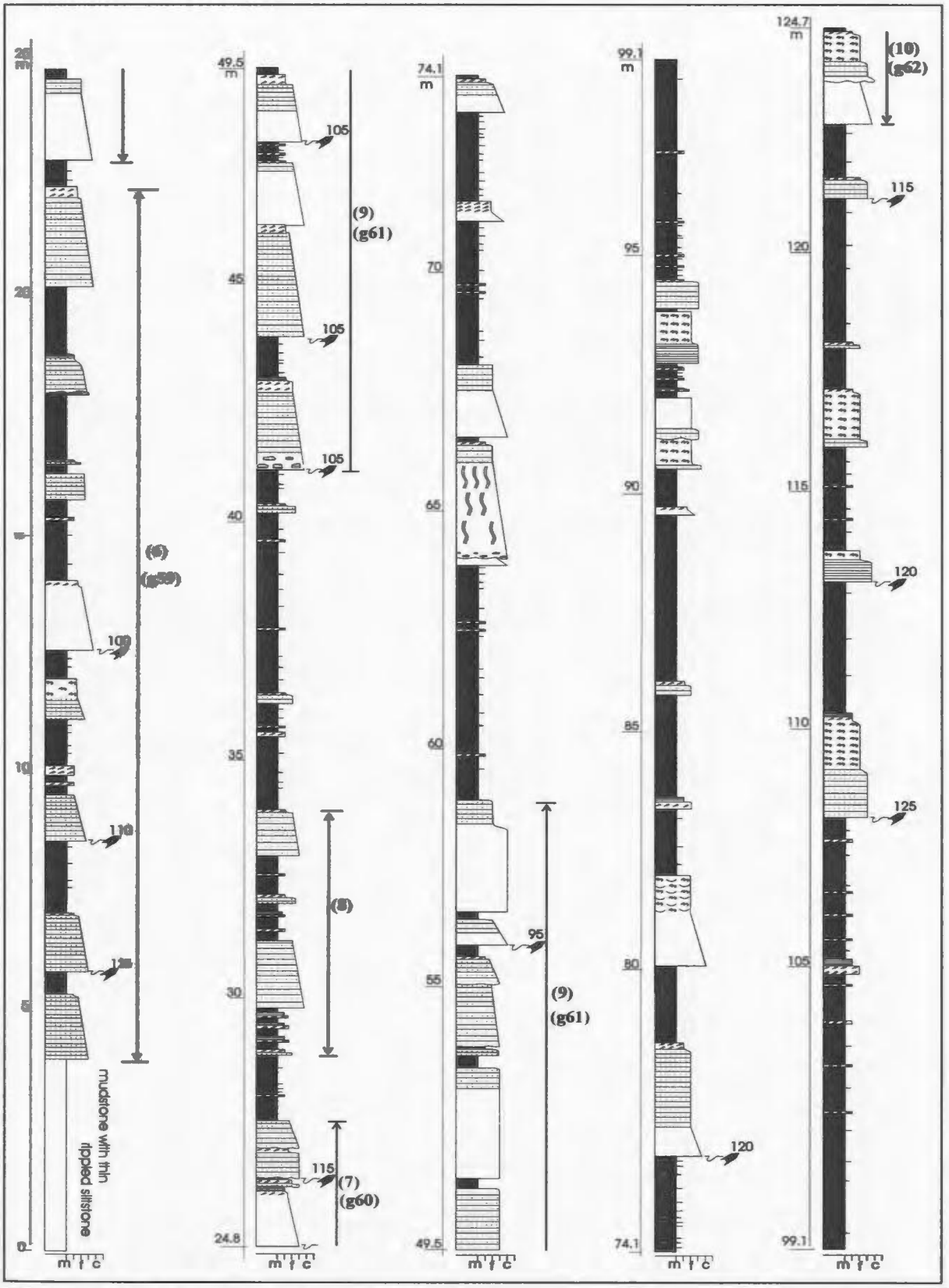

Fig. 2.12a Lithofacies log of Casovona measured section, Santerno Valley, northern Italian Apennines (continued next page). See Figure 2.3a for key.

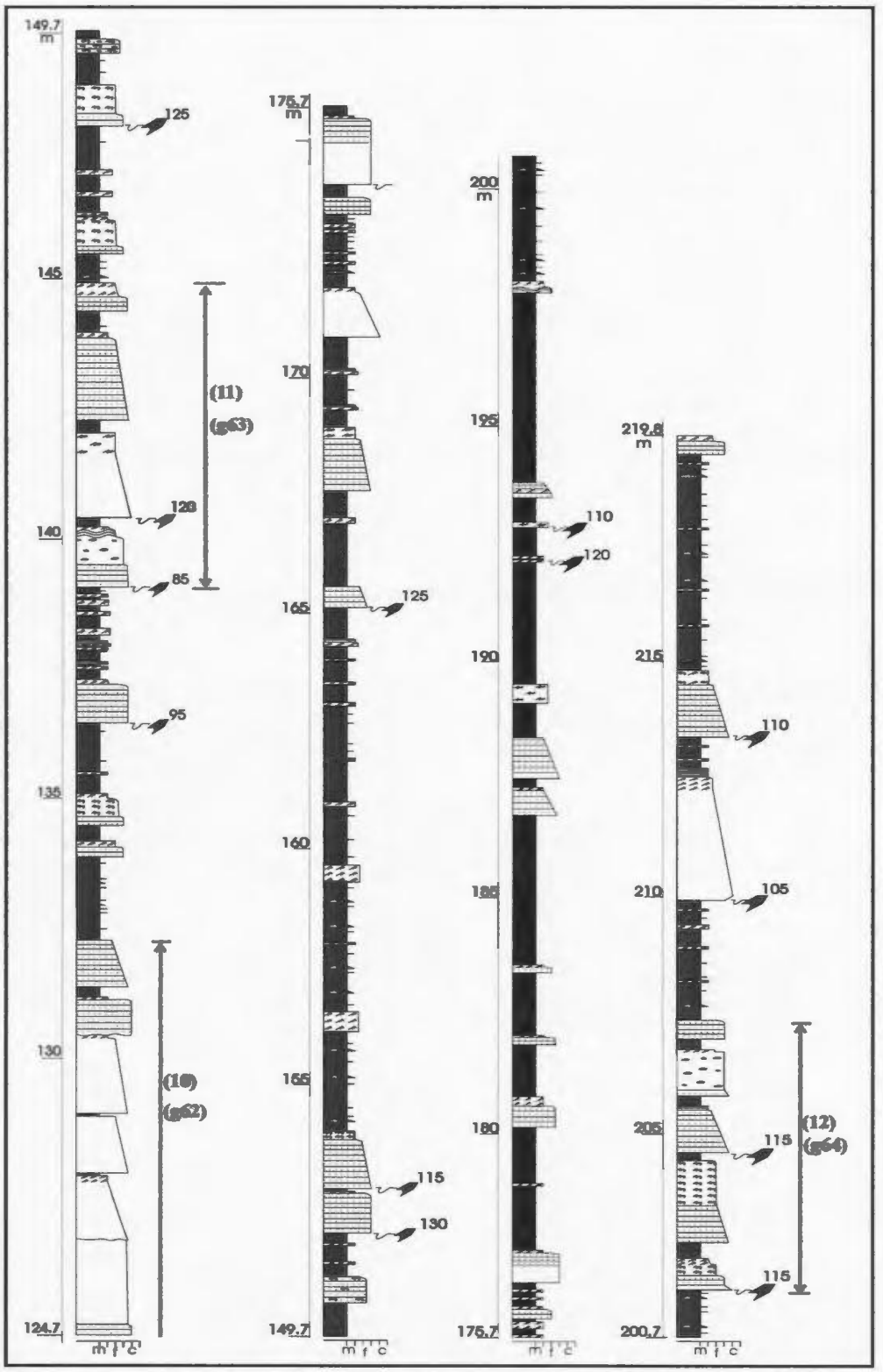

Fig. 2.12b Lithofacies log of Casovona measured section, Santerno Valley, northern Italian Apennines (end). See Figure 2.3a for key.

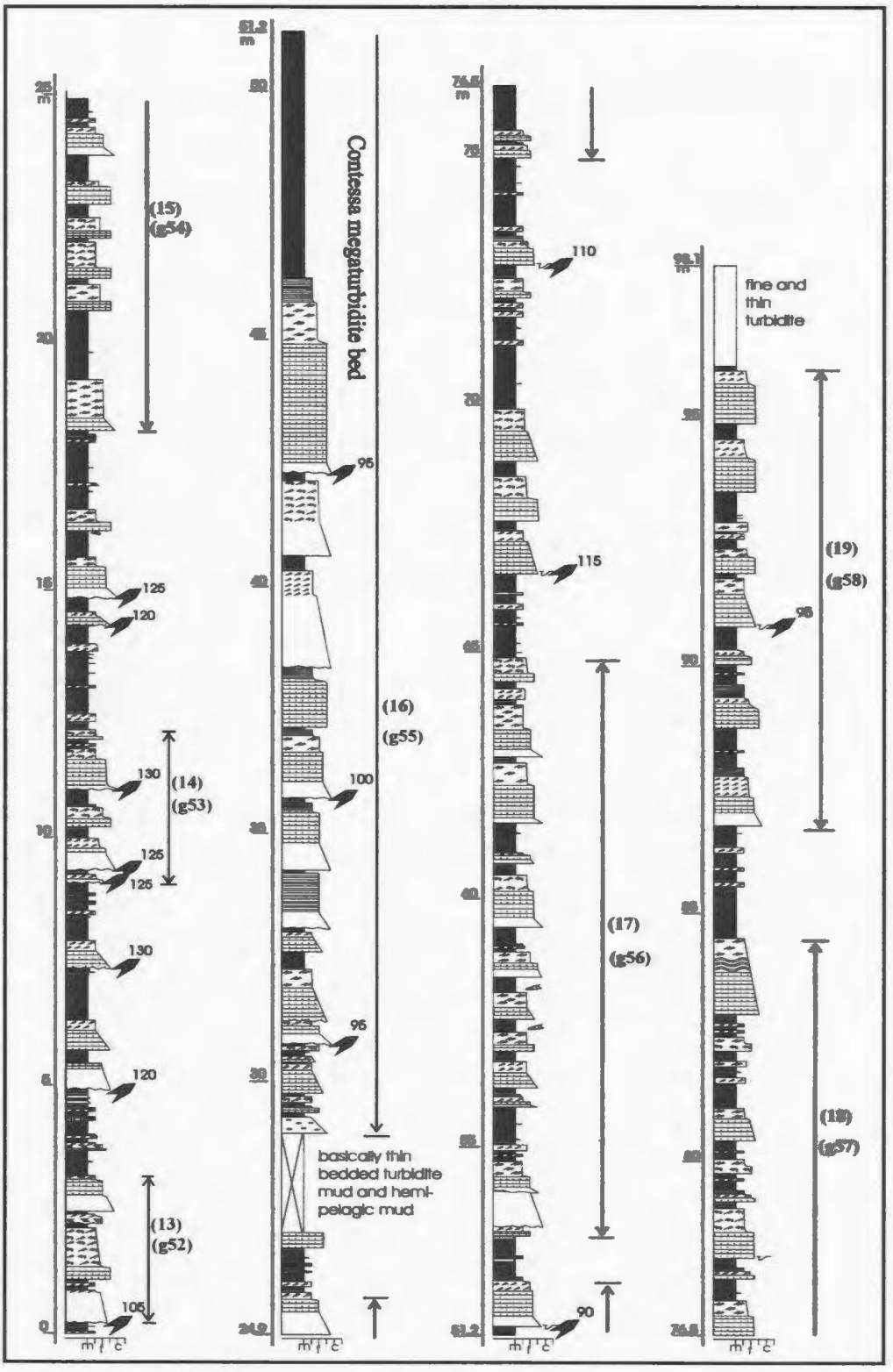

Fig. 2.13 Lithofacies log of Coniale measured section, Santerno Valley, northern Italian Apennines. See Figure 2.3a for key.

Fig. 2.14 View of the Marnoso arenacea turbidites in a cliff (Santerno Valley) near the Coniale section (Fig. 2.13). The thicker sandstone beds are grouped into packets. The thickest bed at the cliff top is the Contessa megaturbidite (Fig. 2.13).

Fig. 2.15 A sandstone bed packet (packet (9), Figure 2.12a) overlying a mudstone-siltstone bed packet. The Marnoso arenacea at the Casovona section, Santerno Valley, Italy.

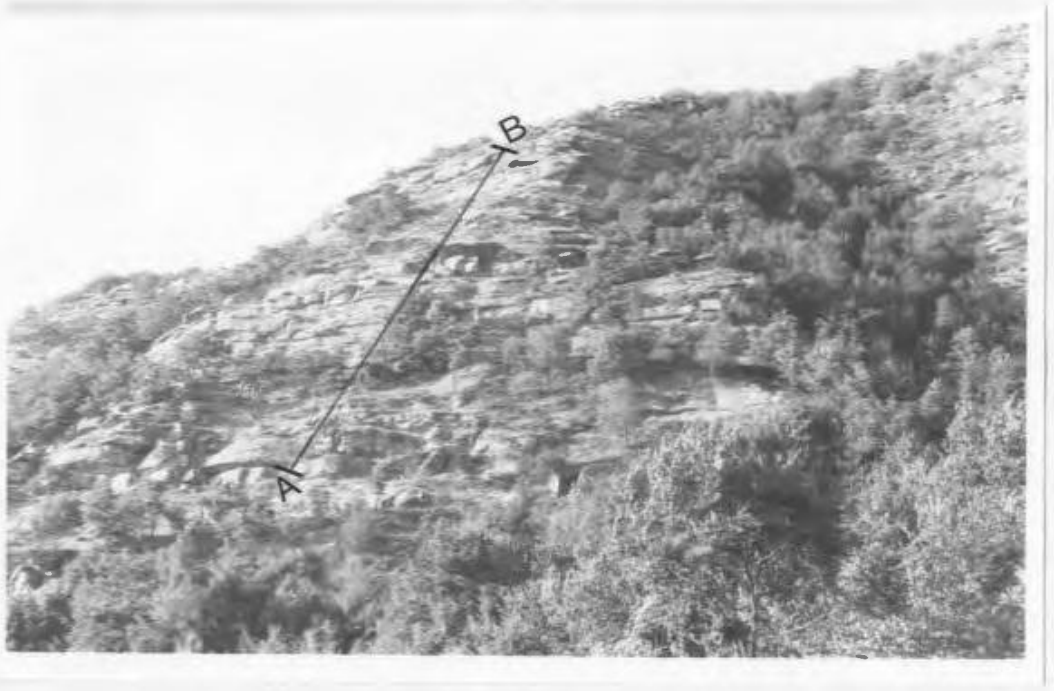

Fig. 2.16 View of the Casovona section, the Santerno Valley to the left. The section was measured along line AB, with a total of stratigraphic thickness of 219.8 m (Fig. 2.12). Along this mountain side, 3 km lateral correlation of turbidite sandstone beds had been accomplished by Cattaneo and Ricci Lucchi (1995).

sections. According to Ricci Lucchi and Valmori (1980), about 50% of megaturbidite-like beds can be traced for over 60 km. Cattaneo and Ricci Lucchi (1995) demonstrated good lateral continuity of sandstone packets along a mountain side near Casovona (Fig. 2.16).

2.3.2.2 Interpretation

The abundance of fines in the suspended load of turbidity currents enhanced their mobility so that sand was deposited over a large area (Mutti, 1979, 1985). Slow flow deceleration of these "efficient" currents permitted traction transport to produce lamination of Bouma divisions T_b, T_c and T_d. Facies characteristics, clustering of coarse and fine deposits, and the lateral continuity of sand beds are consistent with deposition on submarine fan lobes (Ricci Lucchi, 1975, 1981,1984, 1986; cf. Reading and Richards, 1994; Mutti and Normark, 1987; Shanmugam and Moiola, 1991). Based on the good continuity of most sandstone beds for 3 km near Casovona, Cattaneo and Ricci Lucchi (1995) reinterpreted those sandstone packets as basin plain sand sheets.

2.3.3 Savio Valley Sections

2.3.3.1 Description

Two short sections were measured in the cliff at Romagnano, above and below an inaccessible gap of a few tens of meters. The Romagnano section B (Fig. 2.17) is exactly the same section described by Ricci Lucchi (1975) in his figure 24 as upward thinning

cycles formed in channels. The essential features of the Romagnano sections are:

(1) most sandstone beds are amalgamated (Fig. 2.18), and mud clasts can be seen lying directly on some amalgamation surfaces;

(2) water-escape structures (dishes and pillars) are well developed in some thick sandstone beds (Fig. 2.19);

(3) both Bouma divisions T_a and T_b are common (in contrast to sections in the Santerno Valley in which T_a divisions are not important);

(4) the sand body has a flat erosional base which can be traced for a long distance (Ricci Lucchi (1981), cutting down into an underlying mudstone intercalated with very thin siltstone beds, and is overlain by similar mudstone;

(5) the mudstone/sandstone ratio is 1:63.2 for section A above the 10 m point, and 1:3.2 for section B below the 31 m point.

2.3.3.2 Interpretation

Lateral tracing for the geometry of these sandstone packets is not possible at the outcrop. However, the facies are very similar to channel fills that are very well exposed in the Santerno Valley (Fig. 2.20). Large-scale correlation in the Savio Valley area confirms that the sand body has a channel-filling geometry (Fig. 2.21).

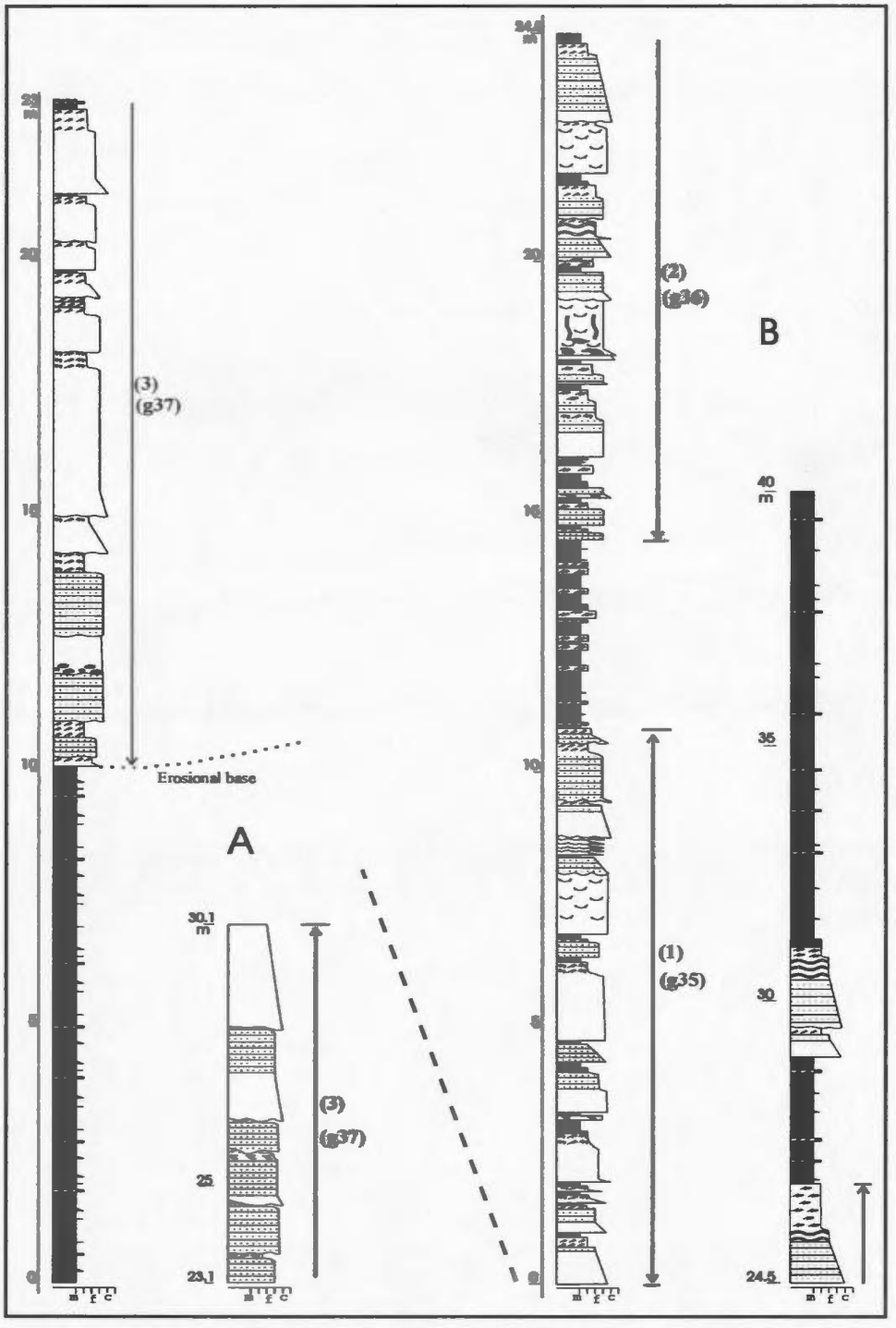

Fig. 2.17 Lithofacies logs of Romagnano measured sections A and B, Savio Valley, northern Italian Apennines. A few tens of meters between A and B could not be measured. See Figure 2.3a for key.

Fig. 2.18 Amalgamated turbidite beds of the Marnoso arenacea at 20-21 m of the Romagnano section B (Fig. 2.17), Savio Valley, Italy.

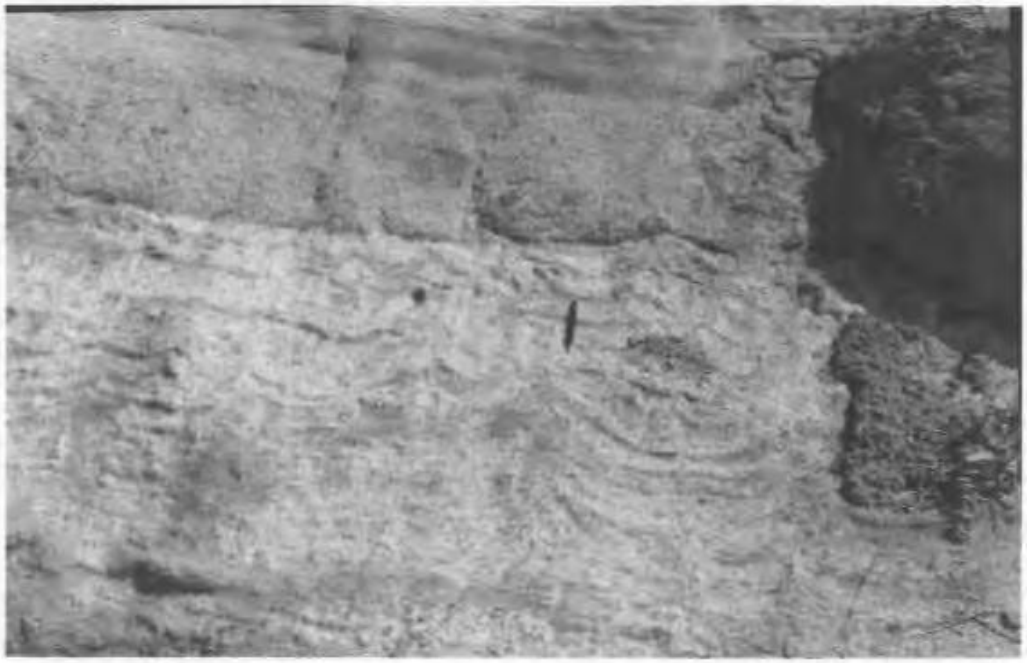

Fig. 2.19 Water escape dish and pillar structure in a very thick sandstone bed at 18 m of the Romagnano section B (Fig. 2.17).

Fig. 2.20 View of channel fill of Marnoso arenacea turbidites at the Santerno Valley, Italy. Note the pinch-out geometry of channel deposits at the right side. The visible part of the channel in this photograph is about 2.2 km wide and 60 m in depth (Ricci Lucchi, 1981).

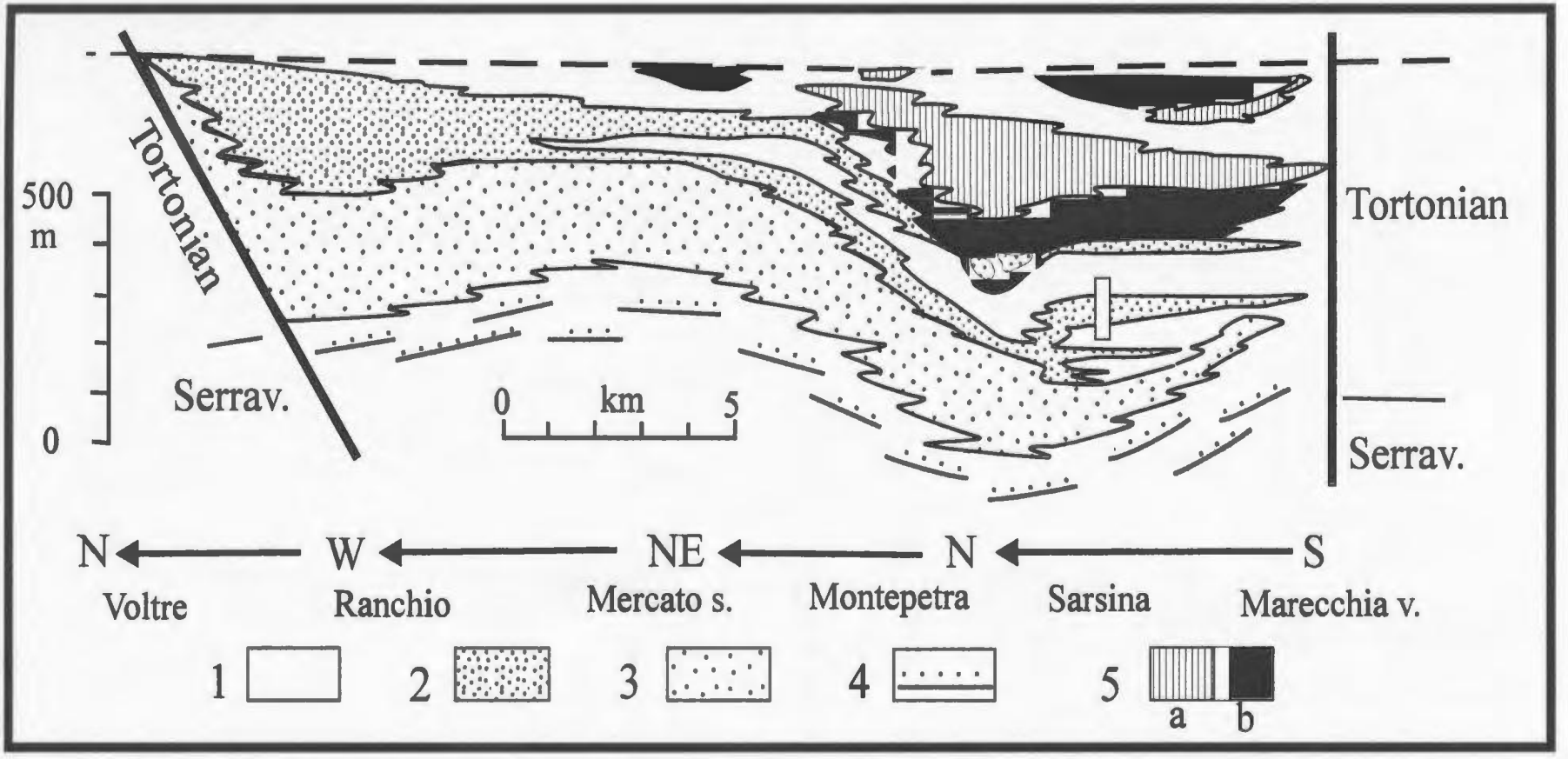

Fig. 2.21 Cross section of the upper Marnoso arenacea in the Savio Valley area, northern Italian Apennines. 1: slope and fine-grained facies of receding fans, 2: channelized sandstones and conglomerates, 3: outer fan deposits, 4: basin plain association, 5: chaotic bodies (a: intrabasinal, b: extrabasinal). Redrawn from Ricci Lucchi (1973). The white bar in the Sarsina section indicates the approximate location of the Romagnano section measured for this thesis.

2.4 Quebec, Gaspé Peninsula Sections

2.4.1 Geological Setting

The Lower Ordovician Tourelle Formation and the Middle Ordovician Cloridorme Formation are mainly composed of turbidite mudstone and sandstone and are very well exposed along the coastline of the Gaspé Peninsula. The Tourelle and Cloridorme formations were deposited in the Ordovician foreland basin (Fig. 2.22) which developed between the eastern continental margin of Laurentia (North America) and an offshore belt of volcanic arcs and accretionary complexes during the Taconic Orogeny (Quinlan and Beaumont, 1984; Hiscott et al., 1986). Small subbasins were developed along the inner steep slope of the basin in depressions between thrust sheets. The Tourelle Formation has been interpreted as several overlapping, small and sand-rich submarine fans that were confined to these slope basins (Hiscott et al., 1986; Hiscott and DeVries, 1995). The Cloridorme Formation, in contrast, was deposited on the floor of the foreland basin and, where sandy, has been interpreted as lobe deposits (Hiscott et al., 1986).

Two turbidite sections were measured in the Tourelle Formation at Cap Ste-Anne, and one section in the Cloridorme Formation at Petite-Vallée.

2.4.2 Cap Ste-Anne Sections (Tourelle Formation)

2.4.2.1 Description

The Tourelle Formation is about 300-500 m thick (Hiscott, 1977). Two measured sections at Cap Ste-Anne overlap stratigraphically, and are 280 m apart. These are the

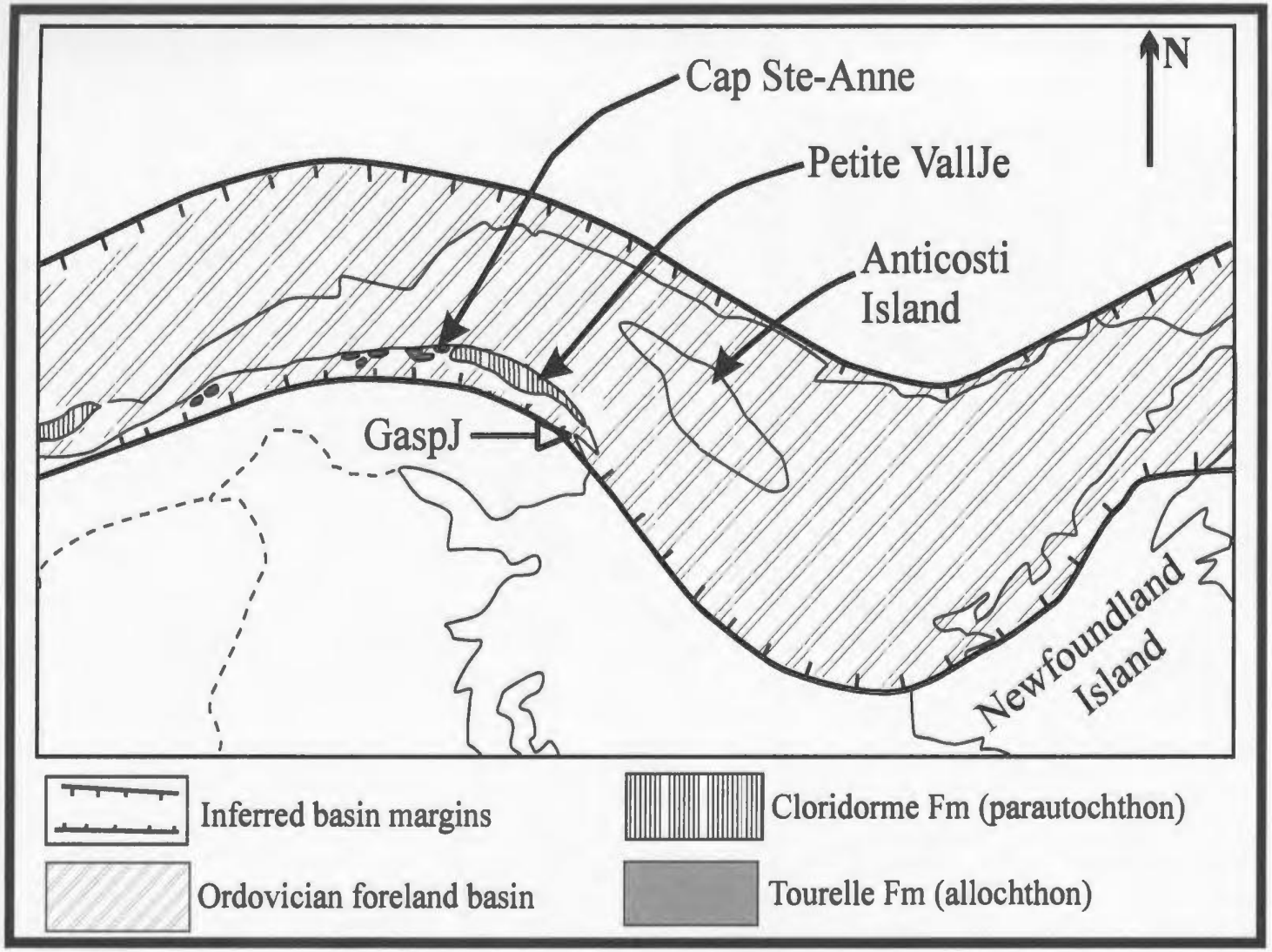

Fig. 2.22 Index map showing locations of Cap Ste-Anne section (Tourelle Formation) and Petite VallJe section (Cloridorme Formation). This map also shows the approximate extent of the Ordovician foreland basin (from Hiscott et al., 1986).

same as sections B and F of Hiscott and DeVries (1995). The top bed of section 1 correlates with the basal bed of section 2. The total measured thickness is 233 m. The major characteristics of these sections are as follows.

(1) This part of the Tourelle Formation belongs to facies association 3 of Hiscott (1980), composed of sandstone packets which alternate with interbedded mudstone and siltstone packets (Fig. 2.23).

(2) The mudstone/sandstone ratio for these sections is overall 1:2.5.

(3) Sandstone packets range from 8 to 30 m thick, and consist of medium to coarse grained sandstone.

(4) Most sandstone layers in these packets are thickly bedded and amalgamated along wavy erosive bases.

(5) Normally graded Bouma T_a divisions dominate, whereas a rippled T_c division only forms a thin veneer at the top of most beds. Due to amalgamation, T_{d-e} divisions, if they had been originally deposited, are only preserved in a few beds. Parallel laminated T_b is not well developed in these sandstone beds.

(6) Many sandstone beds at nearby similar outcrops can be traced with little thickness variation over distances approaching or exceeding 1 km (Hiscott and DeVries, 1995).

(7) Interbedded mudstone and siltstone intervals are 10 to 50 m thick, with siltstone/mudstone ratios of about 1:4 to 1:2. Most siltstone beds are thinner than 10 cm. Ripple lamination is very well developed in siltstone beds.

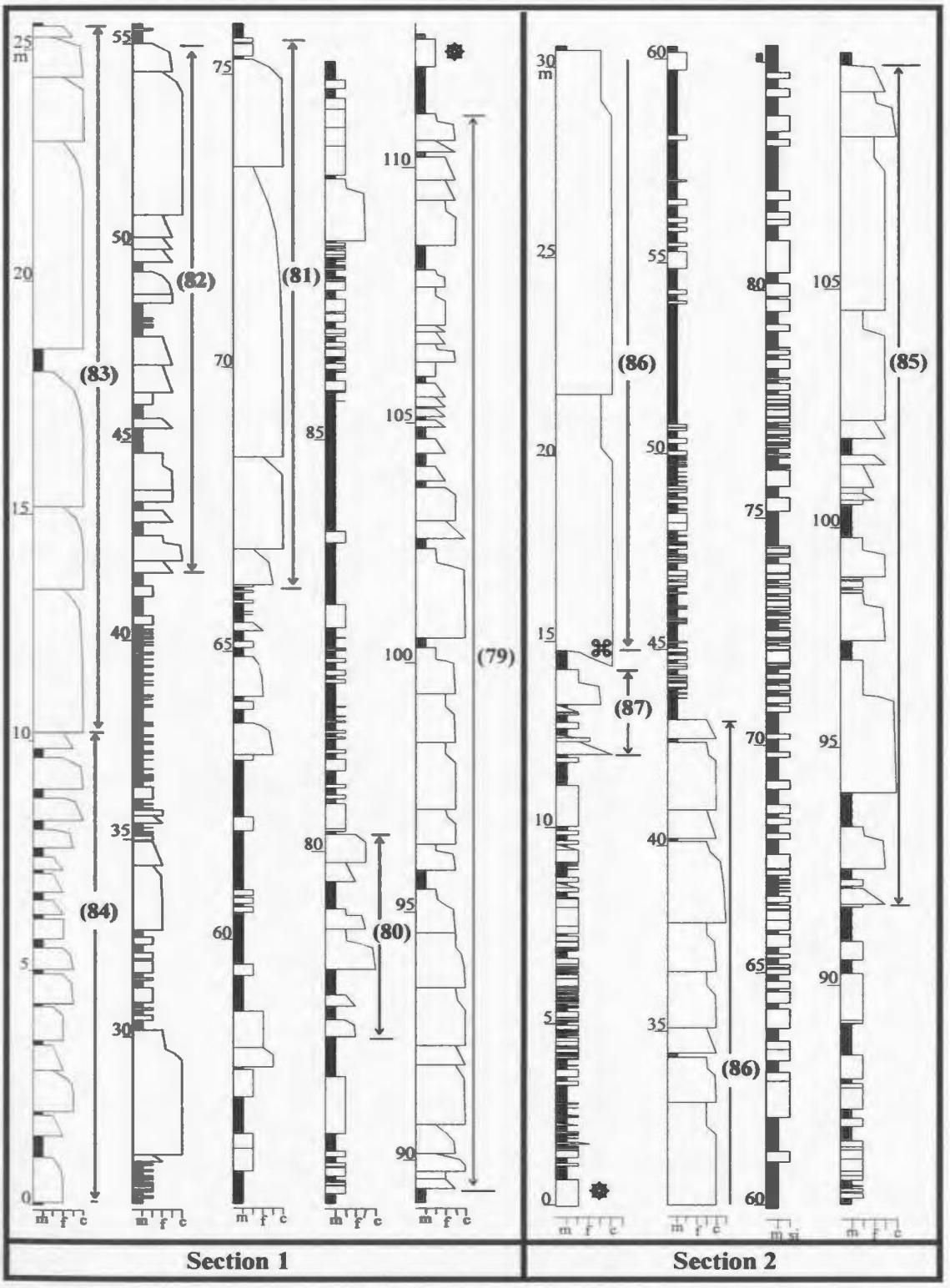

Fig. 2.23 Lithofacies logs of Cap Ste-Anne measured sections (Tourelle Formation), Gaspé, Quebec. ❁ = same bed; ⌘ = scoured base (9 m deeper erosion about 250 m west of section 2). Internal structures in sandstone layers are not shown.

2.4.2.2 Interpretation

The relatively high siltstone/mudstone ratio in fine-grained packets might suggest that these are levee deposits. The good lateral continuity of sandstone packets and limited erosion suggest lobe deposits, perhaps near channel mouths to explain an association with levees and local scouring (Hiscott and DeVries, 1995; cf. Normark, Piper and Hiscott, in press). This agrees with the interpretation of the Tourelle Formation as mid-fan lobe deposits proposed by Hiscott (1980).

2.4.3 Petite-Vallée Section (Cloridorme Formation)

2.4.3.1 Description

The Petite-Vallée member of the Cloridorme Formation is 835 m thick (Hiscott et al., 1986). The section measured for this thesis is immediately east of the river mouth at Petite-Vallée, and is 452 m thick. The section has following characteristics:

(1) It consists of 50.2% sandstone and siltstone and 49.8% mudstone (Mudstone/[sandstone + siltstone] = 1:1.01).

(2) Beds are clearly grouped into sandstone packets and mudstone-siltstone intervals (Fig. 2.24a-c).

(3) Most sandstone packets consist of more than 90% sandstone and less than 10% mudstone. Sandstone is typically fine to medium grained. Most sandstone beds are 10 to 50 cm thick, but a few exceed 1 m. Normally graded T_a, parallel laminated T_b, and rippled T_c Bouma divisions are well developed in many beds.

(4) Although amalgamation is common in most sandstone packets, most amalgamated beds still retain part of their upper T_c division. Beds have a parallel base or a slightly wavy base. Large basal scours have not been found at outcrop.

(5) Mud clasts were found in some beds, commonly floating in sand matrix.

(6) The lateral continuity of sandstone packets in this section is unknown because lateral tracing is impossible. Good continuity is inferred, however, from a similar and directly overlying part of the same formation in which sandstone packets can be traced laterally along the paleocurrent direction for more than 3 km (Enos, 1969).

(7) Mudstone-siltstone intervals are mudstone-dominated, and contain about 5% to 30% siltstone laminae, rarely with intercalated thin sandstone beds. Mudstone is parallel laminated. Most siltstone layers are less than 3 cm thick, and ripple-laminated.

2.4.3.2 Interpretation

The sandstone packets are interpreted as sand-rich lobe deposits. Mudstone-siltstone intervals are interpreted as interlobe deposits, or muddy drapes deposited during inactive periods of lobe sedimentation. Pickering and Hiscott (1985) and Hiscott et al. (1986) suggest that the lobes of the Petite-Vallée member constitute a basin-floor sheet sand system, analogous to the Marnoso arenacea (Cattaneo and Ricci Lucchi, 1995).

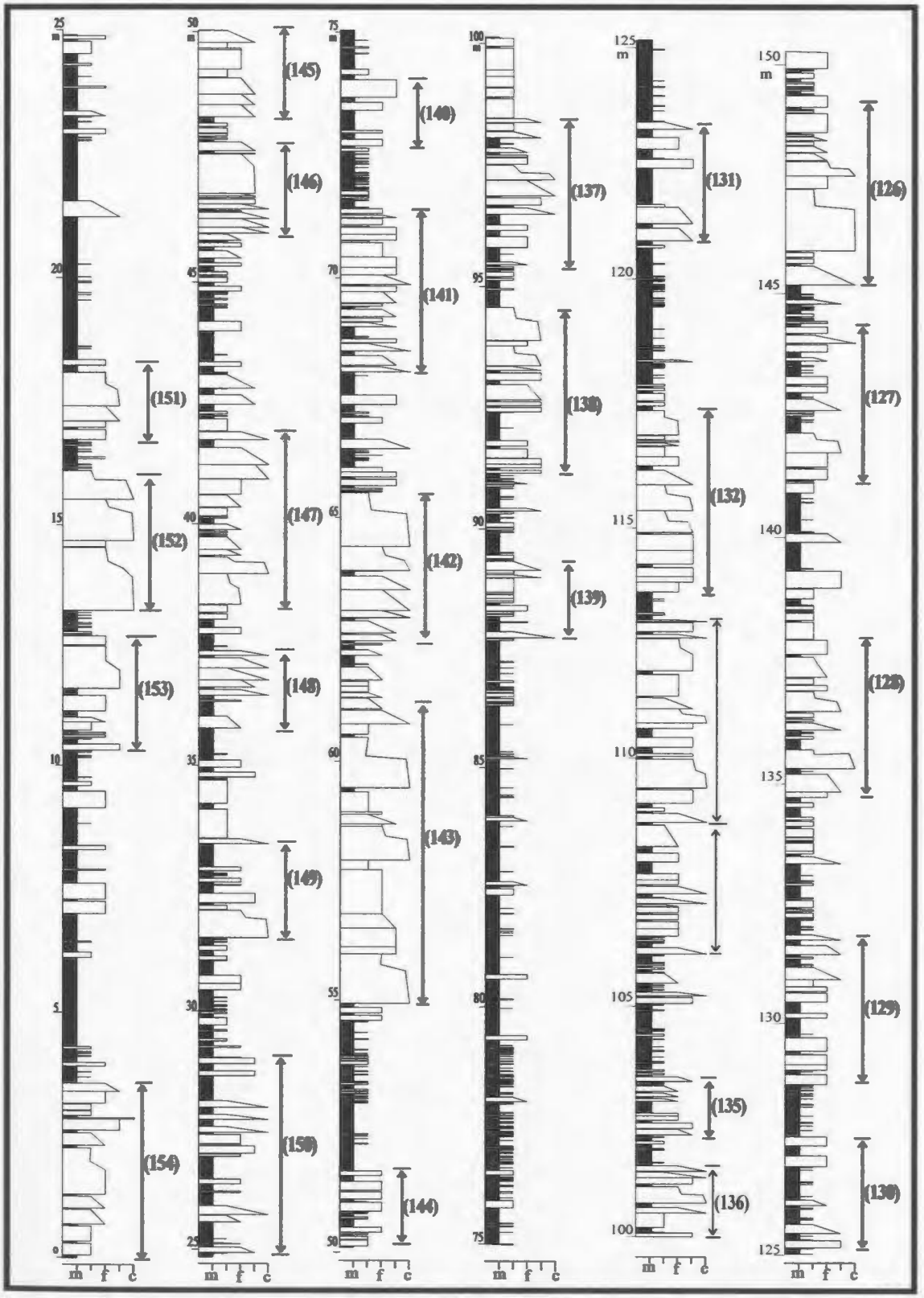

Fig. 2.24a Lithofacies log of Petite-Vallée measured section (Cloridorme Formation), Gaspé, Quebec (continued next two pages). Internal structures in sandstone layers are not shown.

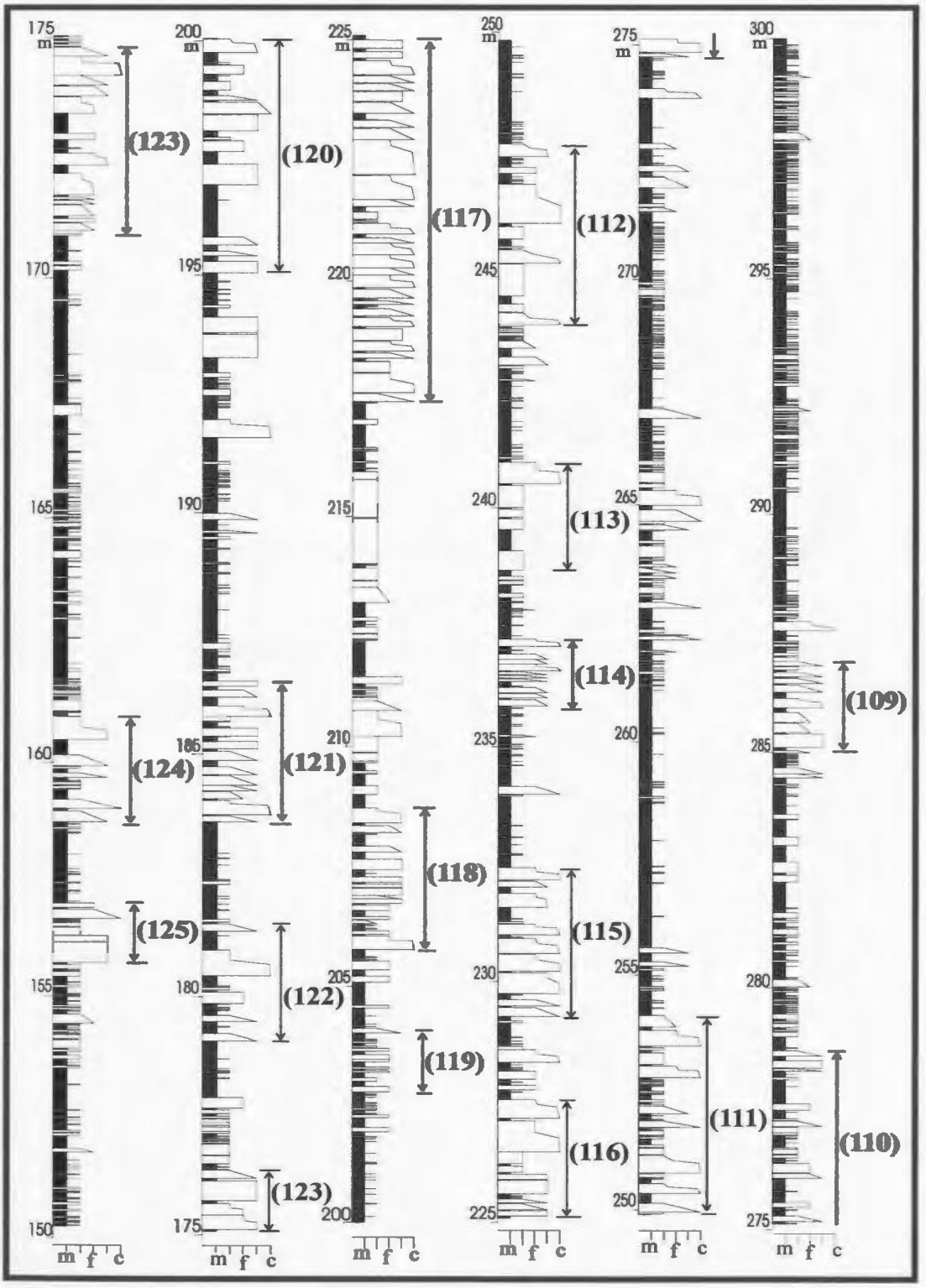

Fig. 2.24b Lithofacies log of Petite-Vallée measured section (Cloridorme Formation), Gaspé, Quebec (continued next page). Internal structures in sandstone layers are not shown.

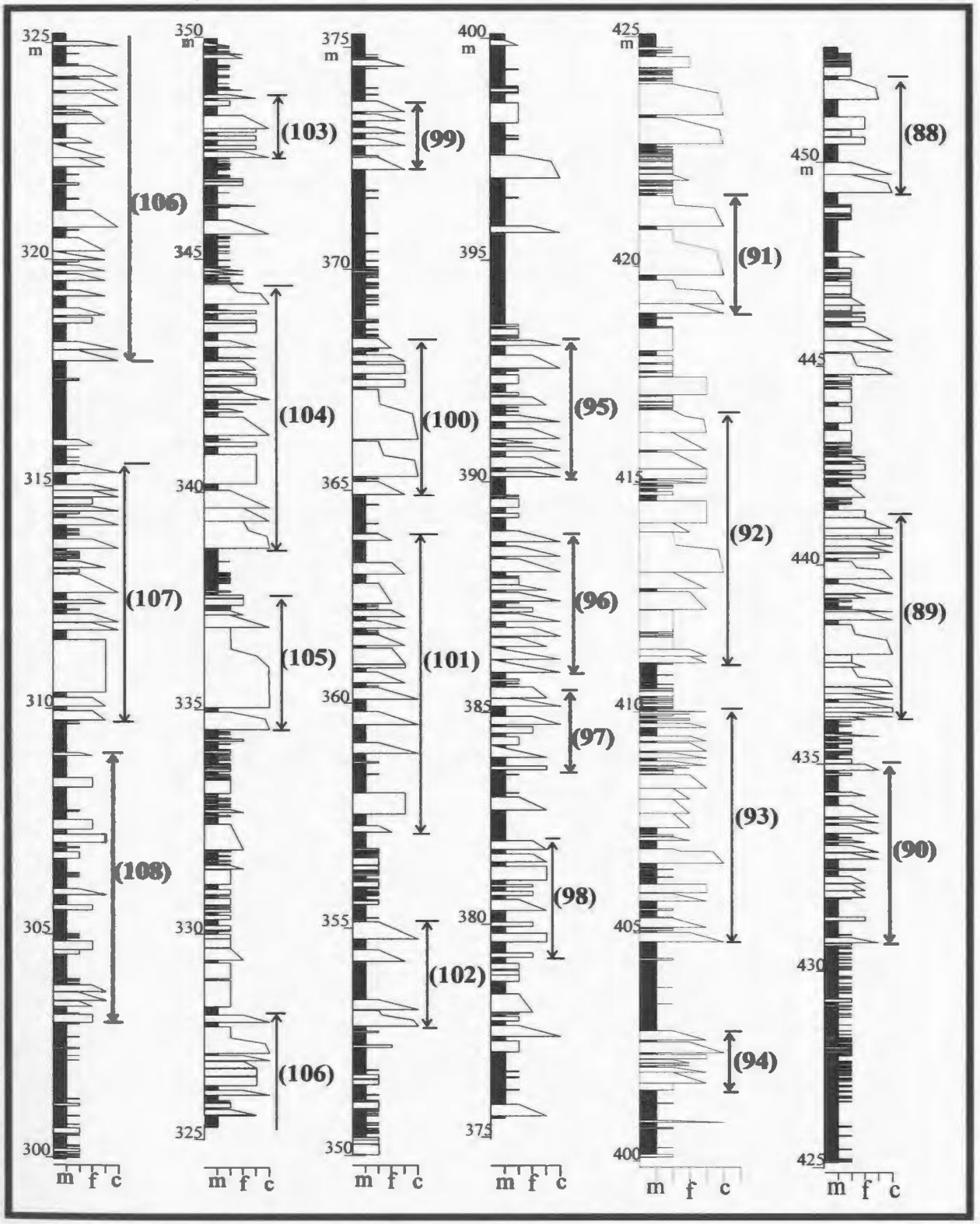

Fig. 2.24c Lithofacies log of Petite-Vallée measured section (Cloridorme Formation), Gaspé, Quebec (end). Internal structures in sandstone layers are not shown.

2.5 Pleistocene Amazon Fan Sections

2.5.1 Introduction

The Amazon Fan is the third largest modern submarine fan (Fig. 2.25). It extends downslope from the shelf break off northeast Brazil for more than 700 km to depths in excess of 4700 m, and has been fed throughout the Pleistocene by the Amazon river (Damuth and Flood, 1985). The middle fan is defined as the part of the fan where the channel talweg is at a higher elevation than the adjacent interchannel areas. Such high-standing channels are particularly susceptible to avulsion (Pirmez, 1994). High-Amplitude Reflection Packets (HARPs) underlie and interfinger with laterally shingled muddy channel-levee complexes of the middle fan. These HARP units are sand rich (Pirmez et al., in press; Hiscott et al., in press). Formation MicroScanner (FMS) images obtained during ODP Leg 155 enabled a complete bed-by-bed lithologic section to be derived at sites 931, 935, 936, 944, and 946. Three of these sections, from sites 931, 944, and 946 (Pirmez et al., in press), have been incorporated into the database used for this thesis.

2.5.2 Sedimentary Characteristics of the Selected Sections

Since this study aims to test for asymmetric trends of bed thickness in sand-rich packets, the selected sections at sites 931, 944 and 946 are confined to the sandy HARP units. These are characterized by grouping or clustering of sandy beds and mud-silt beds (Fig. 2.26a-b). Mud/sand ratio is 1.01:1 at Site 931, 1.42:1 at Site 944, and 1:5.9 at Site

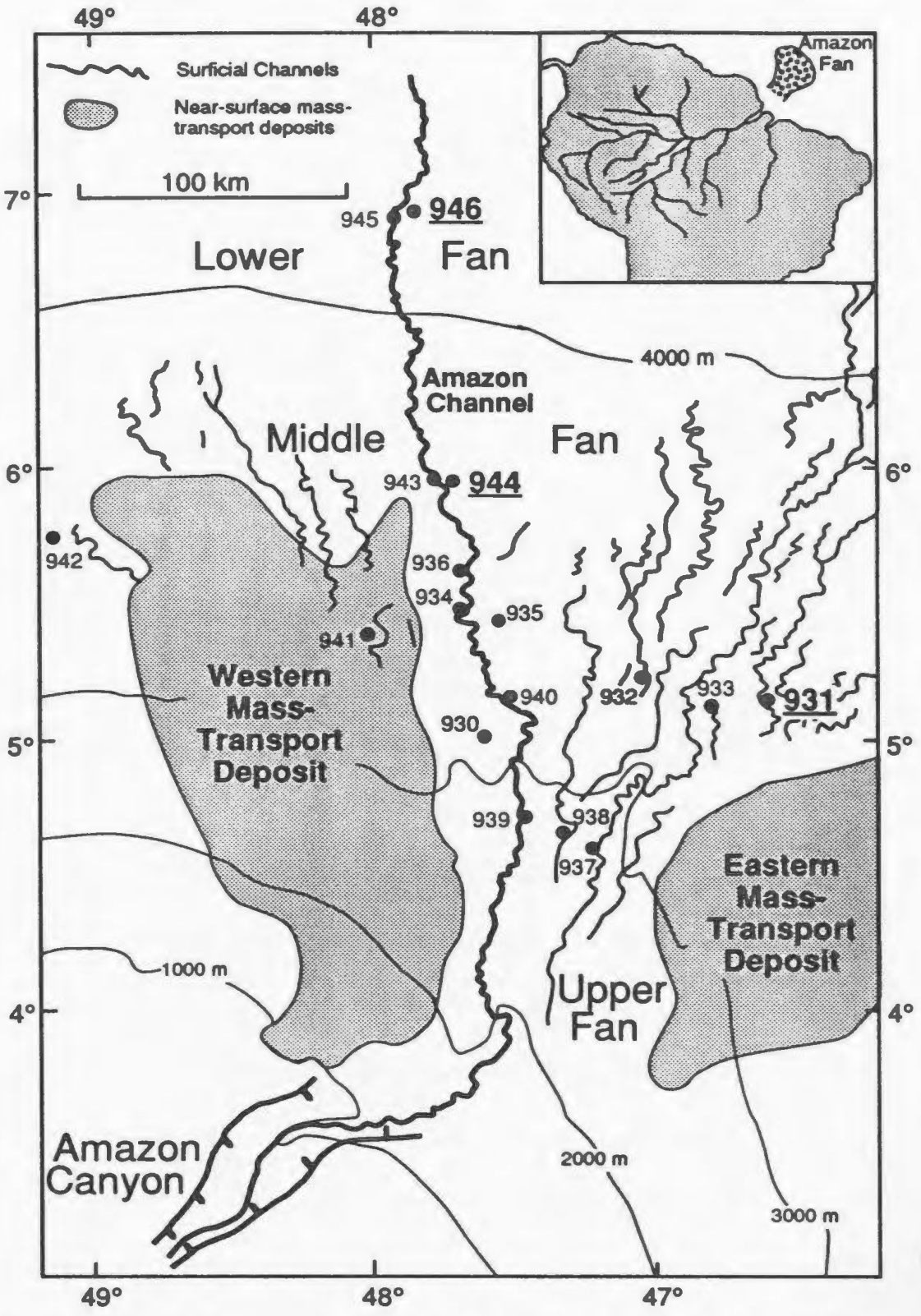

Fig. 2.25 Locations of Amazon Fan and ODP sites 931, 944 and 946 treated in this thesis (from Flood et al., 1995). Amazon channel is the most recently active channel on this fan. The Western Mass-Transport Deposit partly to completely buries abandoned channels for some distance downslope of Site 941.

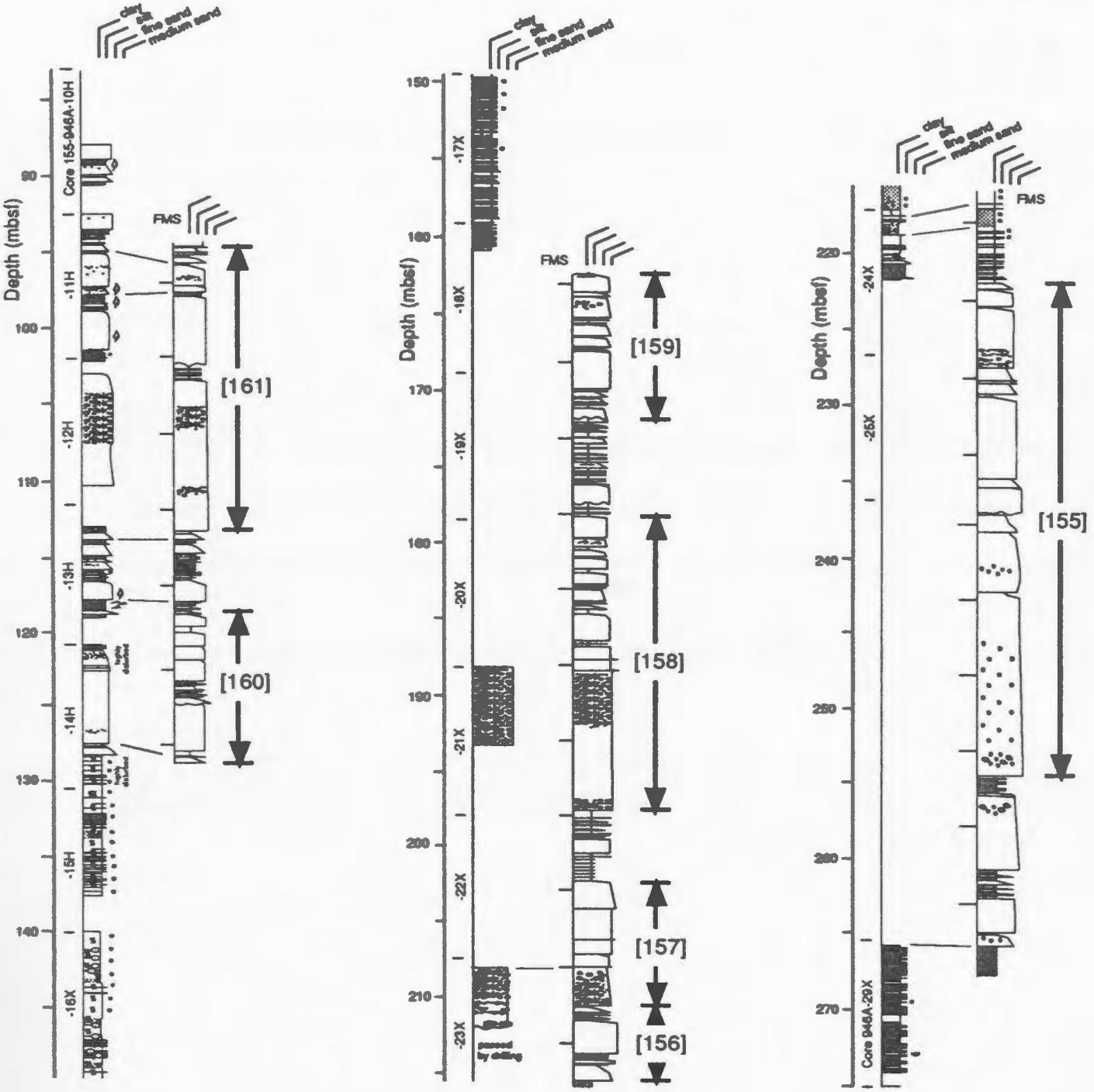

Fig. 2.26a. FMS-derived section from ODP Hole 946A on the Amazon Fan. Recovered cores are shown on the left side for comparison. Depth (mbsf) represents meters below sea floor. From Pirmez et al. (in press). See Figure 2.3a for key to packet numbering.

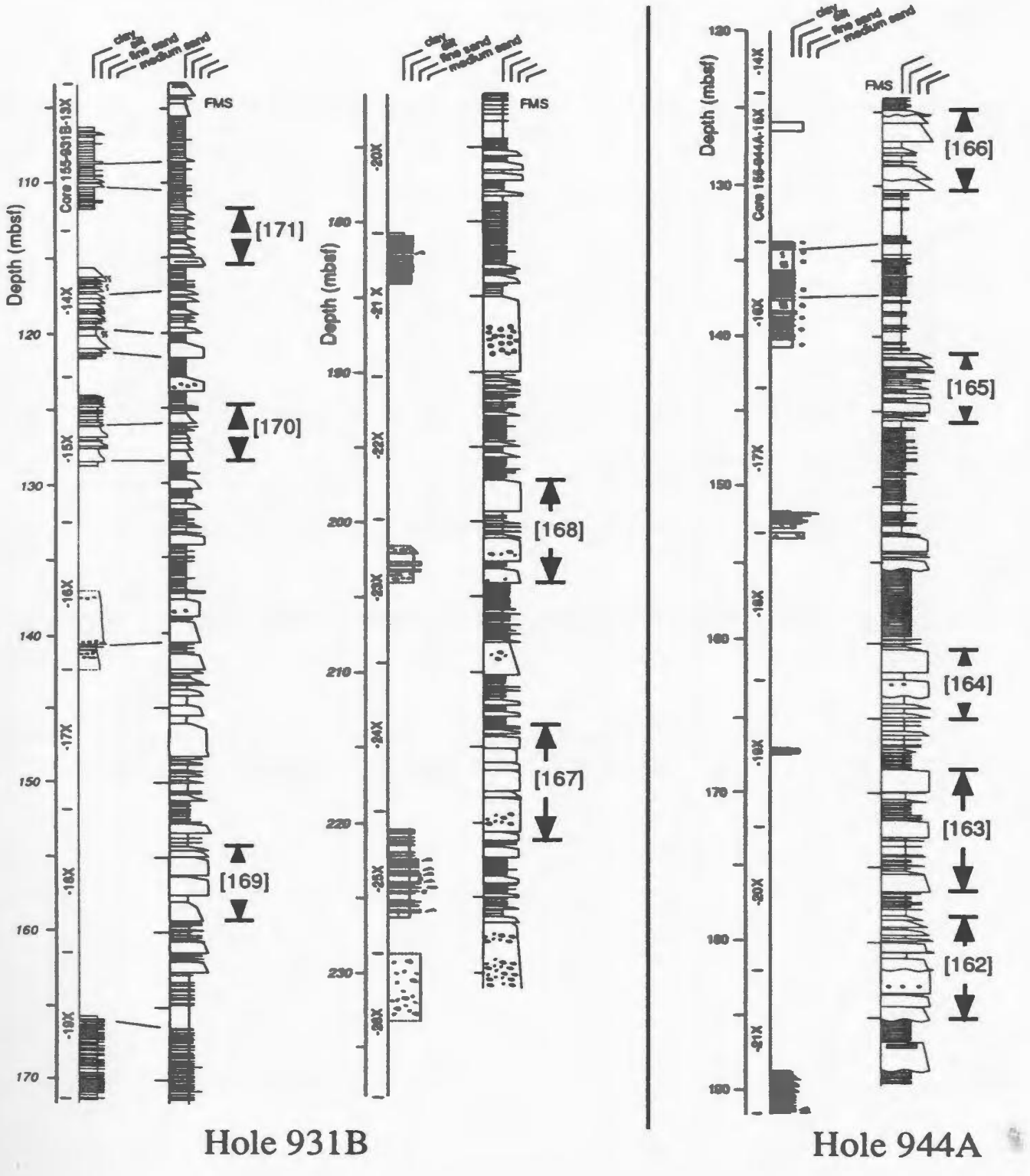

Fig. 2.26b. FMS-derived sections from ODP Holes 931B and 944A on the Amazon Fan (Pirmez et al. in press). Recovered cores are shown on the left side for comparison. See Figure 2.3a for key to packet numbering.

946.

Sand packets 2.2-32.6 m thick contain five to twenty-one sand beds ranging in thickness from 2 cm to 11.7 m. The following characteristics stand out.

(1) Almost all sand beds thicker than about 1 m contain mud clasts in variable concentration (Pirmez et al., in press), and FMS images from several very thick sand beds also show the presence of mud clasts.

(2) Fine to medium sand dominates. Coarser grains are locally present, as suggested by core recovery, geophysical logs and FMS images.

(3) FMS images suggest that sand beds commonly have sharp bases, whereas graded, rather sharp tops are common.

(4) Amalgamation is well developed in many sand packets, but there are still many sand beds, particularly thin to medium beds, that preserve their fine tops.

(5) Many sand packets have a sheet-like shape, extending laterally for several kilometers to several tens of kilometers (Pirmez et al., in press), and individual sand beds can be correlated between sites 945 and 946, proving good lateral continuity (see figure 29 on page 686 of Flood, Piper, Klaus et al., 1995).

Mud-silt intervals 1.1-25.2 m thick mainly consist of interbedded silt laminae and clay laminae, and sometimes contain intercalated beds of silt and/or sand. Boundaries between sand packets and mud-silt intervals are commonly sharp in wireline logs (gamma-ray, resistivity, neutron porosity, velocity and density).

High resolution seismic data suggest that the sheet-like HARPs are formed, in detail, of subtly lenticular sand bodies deposited in very shallow depressions on the top of a broadly lobe-like feature.

2.5.3 Interpretation

The shingled stacks of interchannel "lobes" are believed to form after channel bifurcation or avulsion on the middle fan. Channel entrenchment upfan of the avulsion point provides sand to the lobe, and then a newly established leveed channel progrades over the lobe (Hiscott et al., 1997; Pirmez et al., in press). The thin bedded mud-silt intervals are interpreted as distal overbank deposits. Alternating sand packets and mud-silt intervals apparently formed by a single avulsion event suggest pulses of channel entrenchment near the avulsion point as the system returns to an equilibrium (graded) profile.

The widespread sheet-like sand packets of Amazon Fan are indistinguishable in facies and sand content from those seen in ancient successions of, for example, the Tourelle Formation (Fig. 2.23) and the Marnoso arenacea (Fig. 2.11, 2.12a-b, 2.13). This suggests that periodic supply of sand to interchannel depressions following avulsions also needs to be considered for some turbidite successions even in foreland basins.

2.6 Barbados Sections

Quartzose turbidites, assigned to the Scotland Formation of uncertain but probable

early Tertiary age (Speed and Larue, 1982) or early to middle Eocene age (Pudsey and Reading, 1982; Kasper and Larue, 1986), have been incorporated into the Barbados Ridge accretionary complex between the northwestern Lesser Antilles magmatic arc and the South American craton. Due to the complex history of the Caribbean-South American plate boundary and poor age control. the limits of the turbidite basin and sediment source remain highly speculative. It has been assumed that these sediments were derived from the South American craton and deposited on its northern margin (Dickey, 1980; Velbel, 1980; Pudsey and Reading, 1982; Westbrook, 1982). However, based on petrographic analysis and regional paleogeographic analysis, a depositional model of a foredeep and a multiple source (including orogenic and cratonic terraces) was proposed by Kasper and Larue (1986). Despite such contrasting tectonic models, all authors reached unanimity on the view that the terrigenous turbidites of Barbados were originally deposited in a delta-fed, radial deep-sea fan system. Larue (1985) claimed that upward thinning and thickening sequences are common in these turbidite successions, and took them as a major criterion for determination of fan environments.

Two short turbidite sections were measured by Dr. R.N. Hiscott in the Upper Scotland Formation, one, with cumulative bed thickness of 49 m, in unit of tc4 of Larue and Speed (1983) at the Chalky Mount, and the other, with cumulative bed thickness of 69 m, at the Breedy's Brick Factory section of Larue (1985). Both tc4 and Breedy's Brick Factory sections were interpreted as channelized successions (Larue and Speed, 1983; Larue, 1985). They show a clustering of coarse thick beds and fine thin beds. Amalgamation is

well developed in thick sandstone packets, and most sandstone beds have an erosive base. According to internal structures and grain size, these sandstone packets can be divided into two groups. Group 1 is characterized by pebble-based, thick and coarse sandstone beds with predominantly massive or normally graded T_a divisions and commonly containing mud clasts in the lower portion of the beds. Sandstone beds of group 2 do not have pebble bases and contain more tractional structures including parallel lamination, cross bedding, and ripple lamination.

The sandstone packets in these two sections are similar in facies characteristics to those in the upper portion of the Monticello Dam section, California (Fig. 2.3b-c). Group 1 is believed to be channel deposits and group 2 unchannelized lobe deposits at channel mouth.

2.7 British Columbia Sections

Seven short turbidite sections in the Upper Cretaceous Nanaimo Group were measured bed-by-bed by Dr. R.N. Hiscott in the Georgia Basin, southwestern British Columbia. The Nanaimo Group was deposited in an elongate forearc basin, one of a series of sedimentary basins developed on the Pacific margin of North America during the Late Cretaceous (Dickinson, 1976; England, 1990). Paleocurrent data show that sediments were transported from the eastern arc area toward the west and northwest and into the basin (England, 1990). With thicknesses of 25.8 to 210.6 m, these sections are too short to analyse for cyclicity, but the marked channel filling geometry of sandstone and

conglomerate bodies identified through regional mapping (figure 4 of England and Hiscott, 1992; England, 1990) makes these sections important for characterization of channel deposits. The Georgia Basin has the same tectonic origin as the Great Valley basin of California, which makes it possible to compare major controls, especially tectonics, on these two turbidite systems (see Chapter 6).

The major characteristics of these sections are as follows. (1) Thick and coarse-grained beds and thin and fine-grained beds are bundled into packets. (2) Packets of thick and coarse-grained beds comprise mainly pebble conglomerate and coarse sandstone, rarely medium and fine sandstone; that is, sediments are very coarse. (3) Erosion is widespread beneath conglomerate and sandstone beds. Some scours cut up to 10 m or more into underlying strata, and amalgamation is very strong (see figures 8 and 10 of England and Hiscott, 1992). (4) Due to basal erosion, most conglomerate and sandstone beds are head cut-off, displaying only massive or normally graded divisions. (5) Some beds quickly pinch out laterally. (6) Mud clasts with variable sizes occur in many conglomerate and sandstone beds. (7) Load casts and water-escape structures (dishes and pillars) are well developed in some beds. (8) Intervals of fines, mainly composed of interbedded fine sandstone/siltstone and mudstone, are very thin in these short sections, ranging from 0.3 to 8.4 m, and most of these intervals have a high percentage of sandstone and siltstone, higher than 50%. However, long sections of interbedded mudstones and siltstones (the Northumberland and Mayne formations) have been measured in this area and interpreted as major levee units by England and Hiscott (1992).

The lenticular geometry and above features strongly suggest that the conglomerate and sandstone packets fill channels. These conglomerate and sandstone packets are very similar to channel deposits in the Monticello Dam section of the Venado Formation.

2.8 Northern Norway Sections

The deep-water deposits of the Upper Precambrian Kongsfjord Formation, Northern Norway, accumulated on a passive continental margin (Drinkwater et al., 1996). Three bed-by-bed turbidite logs of the lowermost part of the formation at the Nålneset section, with a total bed thickness of 248 m, were provided to the author by N.J. Drinkwater. Lateral correlation along the 3 km-long Nålneset section shows a continuous, sheet-like geometry of turbidite sandstone packets (figure 39.4 of Drinkwater, 1995). Internally, these packets are characterized by well developed parallel and cross stratification, climbing ripples, abundant liquefaction and dewatering structures, and high sand:shale ratios. Sediments are dominantly medium to very coarse grained. Amalgamation is common, but any form of large-scale channelling is absent. All these features favour deposition in an environment where turbidity currents became unconfined and sheet-flows became prevalent, resulting in rapid deposition of sandy sediments, with erosion limited to localized scouring. Drinkwater (1995) suggests accumulation at a channel-lobe transition.

2.9 Arkansas, DeGray Lake Sections

The Pennsylvanian Jackfork Group around Degray Lake, Arkansas, is dominated by turbidites in a submarine fan setting (Morris, 1974, 1977; Lock and Fisco, 1979; Morris et al., 1979; Moiola and Shanmugam, 1984; Breckon, 1988; DeVries and Bouma, 1992; Mutti, 1992; Bouma et al., 1995). These rocks accumulated in a remnant ocean basin (Graham et al., 1975) or a foreland basin (Thomas, 1985; McConnell, 1989). The Jackfork Group has been described by Moiola and Shanmugam (1984) as a longitudinal submarine fan system which prograded westward. Sediments were derived mainly from the east and partly from the craton to the north and island arc to the south (Briggs and Cline, 1967; Morris, 1974).

Two sections with bed thickness of 213 m at the DeGray Dam spillway, east and west respectively, were measured bed-by-bed and provided to the author by M. DeVries, EXXON Corporation. In the two sections, thick sandy beds and thin mud/silt beds are clearly separated into packets (DeVries and Bouma, 1992). There are two types of sandstone packet: (1) sheet-like packets characterized by well-developed massive divisions (T_a) and amalgamation, and mud clasts in thick beds; (2) packets with poor lateral continuity of many sandstone beds, and better developed Bouma sequences. The thin-bedded mud/silt packets have a sandstone/shale ratio about 0.5:1, a clear contrast to ratios of 1.2:1 to 4.4:1 for sandstone packets. Ripple laminae are the typical feature of thin beds of siltstone and fine sandstone in these packets. Based on the vertical organization of the sections and lateral continuity, Bouma et al. (1995) interpreted type 1

sandstone packets as crevasse-splay lobe deposits, type 2 as overbank deposits at levee crests, and the thin-bedded packets as distal levee deposits.

2.10 Summary

The twenty-eight bed-by-bed turbidite sections which provide the foundation for this thesis represent diverse variations in geological time, tectonic setting, and facies characteristics. Tectonic settings range from forearc basins and foreland basins to passive continental margins. Sand-rich and mud-rich fan systems are included. Facies characteristics, as well as the lateral continuity of sand bodies, indicate that these turbidite successions include channel-fills, overbank levee deposits, sheet-like sand bodies of unchannelized lobes, and interlobe muddy deposits. Hence, this study should yield widely applicable results concerning statistical tests for asymmetric trends in bed-thickness and grain size in submarine fan channel and lobe deposits. The datasets can also be examined for other cyclic patterns. More importantly, it may be possible to obtain new criteria for identification of subenvironments in fan systems by comparing results of the statistical tests examined here and sedimentary features of these representative turbidite successions (see Chapter 6).

Chapter 3

PROCEDURES AND METHODS TO STATISTICALLY TEST FOR ASYMMETRIC TRENDS

3.1 Introduction

Only five substantive publications have appeared outlining statistical tests for bed-thickness cycles in turbidite successions (Martini et al., 1978; Heller and Dickinson, 1985; Waldron, 1987; Lowey, 1992; and Murray et al., 1996). Studies are not only few, but the results of these studies do not agree with one other. For example, Lowey (1992) claimed that asymmetric sequences in the Dezadeash Formation, Yukon, were both common and statistically convincing. In contrast, Murray et al. (1996) found no compelling evidence for such trends in the Sites Formation, Great Valley, California. As a result, two important questions have arisen: (1) are the methods and/or procedures used by previous workers appropriate for testing for asymmetric trends; (2) are asymmetric sequences really well-developed and statistically convincing in some turbidite sections but not in others? To deal with these two questions, one must first look into the previously proposed methods and testing procedures, then try to find the most powerful methods and effective procedures.

3.1.1 Previously Proposed Techniques

Among the five published studies, two used runs tests (Heller and Dickinson, 1985; Murray et al., 1996). For runs testing, symbols +, -, and 0 represent, respectively, a single bed thicker than, thinner than, and equal in thickness to the next bed. For testing for asymmetric trends, a run is defined as a sequence of identical symbols (e.g. +, -) preceded and followed by a different symbol. When counting runs, symbol 0 is neutral and is merged into an adjacent + or - run, or can occur within such a run.

The runs test is based on the hypothesis that, if upward thinning and/or thickening trends are present, the number of runs will tend to be small. Otherwise, for a random sequence, the number of runs will usually be larger. However, this method is very sensitive to noise in the data; it even fails to recognize an overall upward thinning or thickening trend with superimposed noise in the form of very thin and/or thick beds. In order to overcome this shortcoming, Heller and Dickinson (1985) used a moving average technique to smooth the data. Smoothing methods with variable vigour have been applied by Lowey (1992), and Murray et al. (1996). A moving average technique can filter noise out from basic signals, and therefore can improve the runs test to some extent. However, successive values in a smoothed time series are not independent. Thus, this technique introduces two other related problems: (1) Edgington's test cannot be used to test the hypothesis of randomness for an averaged sequence (Waldron, 1986); (2) it may create spurious upward thinning and thickening sequences (Fig. 3.1).

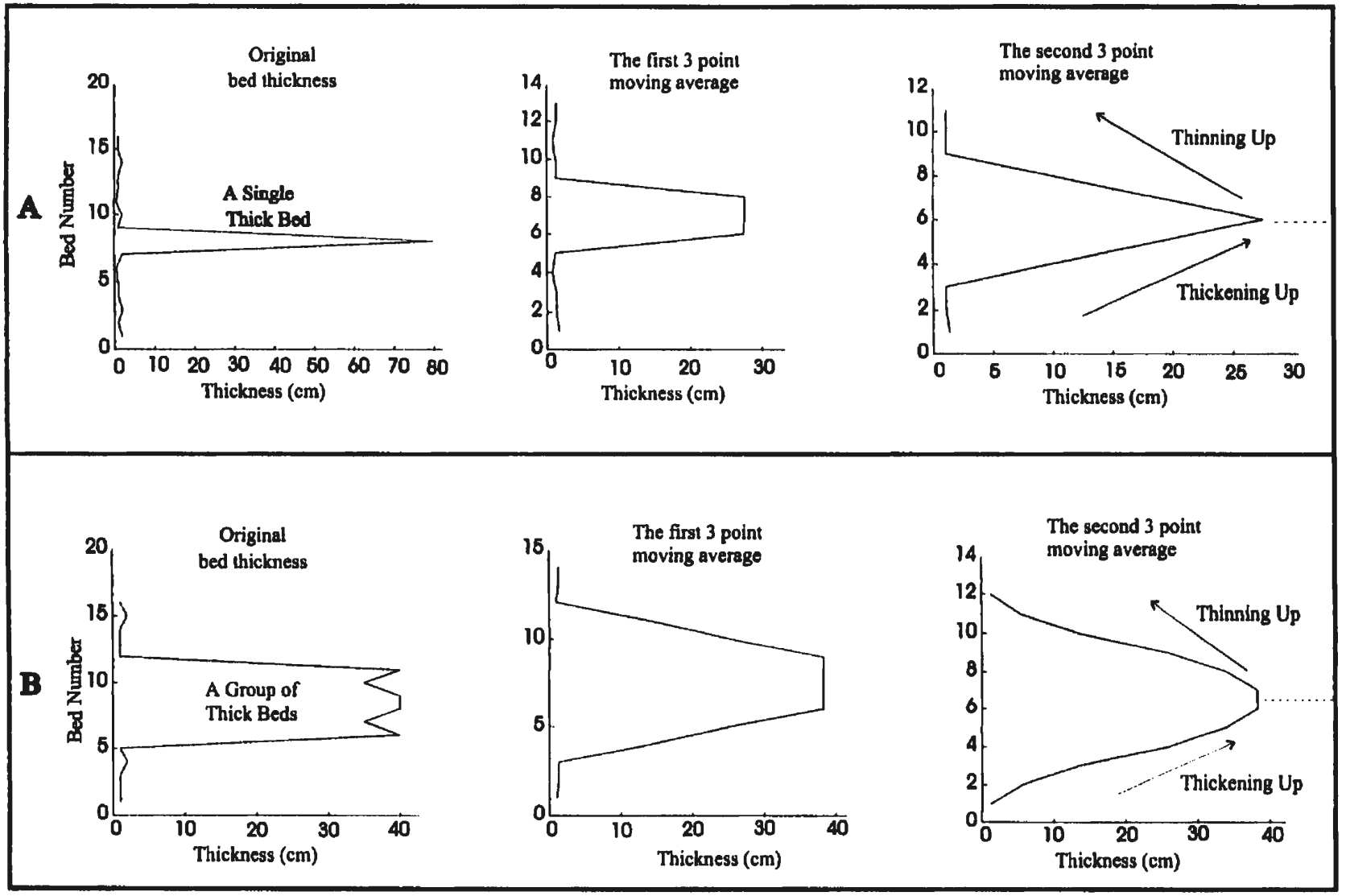

Fig. 3.1 Symmetrical sequences (or paired asymmetrical sequences) created by using moving average techniques.

Murray et al. (1996) tested asymmetric trends in a section by using Monte Carlo simulation to compare the number of runs for his measured section and randomly shuffled sequences. The imperfection in their analysis is clear. First, they took the whole measured section of 399 beds, not individual sandstone packets, as a testing unit, such that if asymmetric sequences exist in the section, they still need to be subjectively selected. Therefore, it not an objective test procedure. Secondly, according to the runs about the median test, the section is characterized by clusters of thin and thick beds (i.e., packets). However, Murray et al. (1996) based their estimation of the significance of asymmetric trends in the section on a comparison of the number of runs up and runs down in the original section and in sequences randomly shuffled from that section. Without question, the number of runs up and runs down must be less in an original sequence with clusters of thin and thick beds than in sequences randomly shuffled from the original sequence, because the clustering of thin and thick beds has the potential to reduce the number of runs. The conclusions of Murray et al. (1996), therefore, are suspect.

Waldron (1987) proposed to use the signs of differences test (Moore and Wallis, 1943) to statistically identify asymmetric upward thinning and thickening trends. This test allows a smoothed sequence to be evaluated, setting one of the two problems caused by using the moving average technique. However, the application of tests for the number of runs (Edgington's test) still remains unsettled. In the signs of differences test, the rejection of the null hypothesis is based on the total number of negative changes in bed

thickness (i.e. bed x+1 is thinner than bed x) in a sequence of known length. Therefore, this test has an inherent weakness in that it fails to handle sequences with a mixture of upward thinning and thickening trends, because alternating increases and decreases in bed thickness cancel each other in computation (Lowey, 1992).

Fourier analysis has been used to identify asymmetric cycles of bed-thickness in turbidites by Martini et al. (1978). Information concerning the asymmetric cycles was contained in the phase angles associated with the periodic components. This method is futile both because it still requires a subjective judgement of the significance of trends revealed, and because most, if not all, turbidite sections do not have well-defined periodic cycles in bed thickness (Waldron, 1987). Fourier analysis is an inappropriate procedure if the time series is only quasi-periodic (Davis, 1986).

Lowey (1992) introduced several statistical techniques to test for asymmetric sequences in a turbidite section in Yukon, Canada. He advocated correlation methods (Spearman's rank correlation, Kendall's rank correlation, and Pearson's correlation) and the least squares method. The utility and power of these methods is confirmed by the results of this thesis. Unfortunately, Lowey (1992) picked 40 megasequences (sandstone packets with a range from 7 to 88 beds and from 3 m to 70 m thick) by eye, and then used Fourier analysis to confirm the selection of these 40 megasequences. His analysis is questionable because Fourier analysis cannot detect such irregular periodic cycles (Davis, 1986). More serious is Lowey's selection of a level of significance $\alpha = 32\%$ to test his 40 megasequences, resulting in his conclusion that fifteen thicken upward and ten thin

upward. According to the definition of Type I error, the probability, P, of rejecting the null hypothesis when it is true equals the significance level, α, of the test:

$$P(U>C)_{\mu=\mu_0}=\alpha$$

Where U = testing statistic value for a sample; C = critical value of the test; μ = the mean of a population from which the sample was drawn; μ_0 = random population mean. Therefore, 13 out of the twenty-five asymmetric sequences identified by Lowey (1992) might be attributed to Type I error. According to the calculation of the normal approximation to the binomial distribution (Kreyszig, 1967, p. 775; Simpson et al., 1960, p. 137), the cumulative binomial probability of rejecting the null hypothesis 15 or more times in 40 trials at the 0.32 significance level when the null hypothesis is true equals 0.28, and 16 or more times in 40 trials is 0.18. Thus, at least 16 (not 13) of the 25 asymmetric sequences might be random. In addition, the asymmetry is not consistent, so useful conclusions cannot be drawn about organization of bed thicknesses.

This literature review suggests that statistical tests for asymmetric sequences are still at a very preliminary stage. No convincing results have been achieved because inappropriate test methods and/or unreasonable testing standards had been used. Moreover, all the previous tests were only based on a very limited database; i.e., based on a single section (Lowey, 1992; Murray et al., 1996) or several very short sections of less than 100 m (e.g. Martini et al., 1978; Waldron, 1987). Quite clearly, a reasonable procedure for statistically testing for asymmetric trends in turbidite successions must

instead be based on powerful methods and on a large database.

3.1.2 Test Procedures in This Study

This study was designed to develop a reliable and objective statistical procedure to test for asymmetric trends in turbidite sandstone packets. The approach follows six steps:

1) assessment and selection of statistical methods;
2) estimation of the power of the selected methods in testing for asymmetric trends and other patterns, in order to see which methods are the most powerful;
3) determination of the lower limit of sample size that can effectively be tested by the selected methods;
4) statistical segmentation of turbidite sections into sandstone and mudstone packets in order to select sandstone packets for further tests for asymmetric trends. This avoids subjectively selecting sandstone packets;
5) application of the selected statistical methods to the sandstone packets picked through step 4;
6) estimation of the significance of asymmetric trends in turbidite successions by using a Monte Carlo simulation technique.

3.2 Statistical Methods

A series of measured bed thicknesses can be viewed as a time series in which bed number (counted from the base or from the top of a section) is taken as event number.

Such a time series can be analyzed mathematically for trend, cycles and randomness. Many statistical techniques have been developed to test for randomness and trends, but not all of those techniques can be applied to any time series because some techniques require a relatively large sample and were originally designed only to test for randomness *versus* some regular cyclic patterns (e.g. autocorrelation test, cumulative periodogram test [Box and Jenkins, 1970], and Wald-Wolfowitz [1943] test). Some techniques of time-series analysis can deal with unequal time steps, as in a turbidite succession, but the absolute age of each event, or step, must be known (Miller and Kahn, 1962, p. 346). Instead, it is simpler to use bed number as an analogue for time steps of equal duration, and to use conventional approaches to analysis of the data.

For evaluating the null hypothesis of randomness there is no single method sufficiently powerful that it can give a definitive conclusion. A more reliable result can be derived from simultaneously using several methods (Srikanthan et al., 1983). In preparing to test for asymmetric trends in turbidite successions, some restrictions must be appreciated: (1) according to the definition and interpretation of turbidite asymmetric sequences of Mutti and Ricci Lucchi (1972), statistical tests must be based on bed-by-bed thickness changes; hence, these are short-term-persistence tests; (2) the number of beds comprising most turbidite sandstone packets is not large enough to meet the requirement of some methods; and (3) cycles of bed thickness, if they exist, cannot be expected to have a fixed periodicity, so that some tests cannot be used.

After researching a variety of statistical methods with the above restrictions in mind,

three widely known yet powerful methods were selected to test for asymmetric trends in turbidite sandstone packets of submarine fan systems. They are Kendall's rank correlation test, Spearman's rank correlation test, and Pearson's correlation test. Four tests for randomness were also evaluated in order to check other possible non-random patterns: the rank difference test, turning points test, median crossing test, and length-of-runs test.

3.2.1 Trend Tests

1) Kendall's Rank Correlation Test (Kendall's τ)

In Kendall's τ test (Kendall, 1969, 1976, Kendall and Gibbons, 1990), the rank (in bed thickness) of each bed is compared with the rank of all overlying beds within the sequence. A negative score (the target bed is thicker than an overlying bed) or a positive score (the target bed is thinner than an overlying bed) is obtained for each comparison. Kendall's τ is calculated by:

$$\tau = \frac{p - Q}{n(n-1)/2}$$

or, if ties exist, by:

$$\tau = \frac{p - Q}{\sqrt{p + Q + Ex}\sqrt{p + Q + Ey}}$$

Where p is the total number of positive scores, Q the total number of negative scores, and n the number of beds or sample size. Ey is the sum of "extra y": when the rank of bed-

thickness (the x variable) of a bed is tied with that of an overlying bed, an "extra *y*" is counted. *Ex* is the sum of "extra *x*"; for this study, *Ex* = 0, because bed numbers (the y variable) cannot be tied. τ varies from -1 to +1, with consistent thickening upward giving $\tau = +1$, and consistent thinning upward giving $\tau = -1$. No asymmetric trend gives $\tau = 0$. τ is approximately normally distributed with:

$$\text{mean} = \mu_\tau = 0$$

and

$$\text{Standard deviation} = \sigma_\tau = \sqrt{\frac{2(2n+5)}{9n(n-1)}}$$

That is,

$$Z = \frac{\tau - \mu_\tau}{\sigma_\tau} = \frac{\tau}{\sqrt{\frac{2(2n+5)}{9n(n-1)}}}$$

is approximately normally distributed with zero mean and unit variance. For a random succession of bed thicknesses and for sample size as small as 4, τ approximates a normal distribution (Table 3.1). The null hypothesis of no trends can be evaluated at any appropriate significance level. In this study, the test is two-tailed, for example, if a test is undertaken at the significance level $\alpha = 10\%$, and if the Z value falls into the 5% area under the distribution curve either at the right or left tail, then the null hypothesis is

rejected.

Table 3.1 Probabilities of Kendall's τ under the null hypothesis (H_0) for n = 4 (from Daniel, 1978).

Value of τ	Frequency of occurrence under H_0	Probability of occurrence under H_0
-1	1	1/24
-.67	3	3/24
-.33	5	5/24
0	6	6/24
.33	5	5/24
.67	3	3/24
1.0	1	1/24

2) Spearman's Rank Correlation Test (Spearman's ρ)

In calculating Spearman's ρ (Siegel, 1956; Kendall, 1969; Daniel, 1978; Press et al., 1986; Rock, 1988; Kendall and Gibbons, 1990), $R(x_i)$ is defined as the rank of x_i among the other x's, with $R(x_i) = 1$ if x_i is the smallest observed value of x. $R(y_i)$ is similarly defined as the rank of y_i among the other y's. If ties occur among the x's or y's, each tied value is assigned the mean of the rank positions for which it is tied. For this study, the variable y, bed number, is ranked in increasing order from bottom to top: 1, 2, 3, 4 ...; and the variable x, bed thickness, is replaced by its rank in the sequence. When there are no ties, Spearman's rank correlation coefficient ρ is defined by:

$$\rho = 1 - \frac{6\Sigma d_i^2}{n^3 - n}$$

Where

$$\Sigma d_i^2 = \sum_{i=1}^{n} [R(x_i) - R(y_i)]^2$$

and n = sample size. When ties are present, then the test statistic is slightly more complicated

$$\rho = \frac{\Sigma x^2 + \Sigma y^2 - \Sigma d_i^2}{2\sqrt{\Sigma x^2 \Sigma y^2}}$$

Where

$$\Sigma x^2 = \frac{n^3 - n}{12} - \Sigma T_x$$

and

$$\Sigma y^2 = \frac{n^3 - n}{12} - \Sigma T_y$$

$$T = \frac{m^3 - m}{12}$$

m = the number of observations tied at a given rank. All summations are from 1 to n. As for Kendall's τ, ρ ranges from -1 to +1, with ρ = 1 when bed-thickness (x) and bed number (y) have identical rankings (a perfect upward thickening sequence), and ρ = -1

when the two series of values have reversed directions of increasing rank (a perfect upward thinning sequence). The significance of ρ is tested by computing:

$$t=\rho\sqrt{\frac{n-2}{1-\rho^2}}$$

which is distributed approximately as a student's t distribution with n - 2 degrees of freedom. To test for both asymmetric upward thinning and thickening trends, a two-tailed test is preferred.

3) Pearson's Correlation Test (Pearson's γ)

Pearson's γ is a measurement of the linear relationship between two variables, x and y (Hoel, 1971; Downie and Heath, 1983; Press et al., 1986). It is given by the formula:

$$\gamma=\frac{n\Sigma xy-(\Sigma x)(\Sigma y)}{\sqrt{[n\Sigma x^2-(\Sigma x)^2][n\Sigma y^2-(\Sigma y)^2]}}$$

In calculating γ, y (bed number) and x (bed thickness) are actual values, instead of their rank. The value of γ varies from +1 through 0 to -1, with γ = 1 indicating a perfect direct correlation between the two variables (in the case of this study, a perfect upward thickening sequence), γ = -1 a perfect inverse linear correlation between the two variables (a perfect upward thinning sequence), and γ = 0 no linear correlation (a random sequence).

In computing the significance of γ, the follow statistic is used:

$$t=\gamma\sqrt{\frac{n-2}{1-\gamma^2}}$$

which is distributed approximately as a student's t distribution with n - 2 degrees of freedom (Press, 1986). The test is two-tailed.

In many statistical text books, Pearson's correlation test and the Least Squares analysis are discussed separately. The Pearson's coefficient arises as an efficient unbiased estimate of covariance for the bivariate normal distribution. The least-squares coefficient is based on the least-property and is estimated by fitting a straight line to data (Dixon and Massey, 1957). Even though these two methods are conceptually different, their coefficients are equal when used to analyse the linear correlation between two variables, as shown below.

In computing the least squares coefficient *S* (Davis, 1973, 1986), the equation of the least squares line is:

$$\hat{Y}=b_0+b_1x \qquad (1)$$

with

$$b_0=\bar{y}-b_1\bar{x} \qquad (2)$$

$$b_1=\frac{\Sigma xy-(\Sigma x)(\Sigma y)/n}{\Sigma x^2-(\Sigma x)^2/n} \qquad (3)$$

By substituting equation (2) into equation (1), we find that:

$$\hat{Y}=\bar{y}-b_1\bar{x}+b_1x$$

or

$$\hat{Y}-\bar{y}=b_1(x-\bar{x}) \qquad (4)$$

Replacing b_1 according to equation (3) gives:

$$\hat{Y}-\bar{y}=(x-\bar{x})\frac{\Sigma xy-(\Sigma x)(\Sigma y)/n}{\Sigma x^2-(\Sigma x)^2/n}$$

Squaring and taking sums gives:

$$\Sigma(\hat{Y}-\bar{y})^2=\Sigma(x-\bar{x})^2\frac{[\Sigma xy-(\Sigma x)(\Sigma y)/n]^2}{[\Sigma x^2-(\Sigma x)^2/n]^2}$$

Noting that

$$\Sigma(x-\bar{x})^2=\Sigma x^2-(\Sigma x)^2/n$$

allows simplification to:

$$\Sigma(\hat{Y}-\bar{y})^2=\frac{[\Sigma xy-(\Sigma x)(\Sigma y)/n]^2}{\Sigma x^2-(\Sigma x)^2/n} \qquad (5)$$

The least squares coefficient S is defined as:

$$S=\sqrt{\frac{\Sigma(\hat{Y}-\bar{y})^2}{\Sigma(y-\bar{y})^2}} \qquad (6)$$

Now, recall that Pearson's γ is defined as:

$$\gamma=\frac{n\Sigma xy-(\Sigma x)(\Sigma y)}{\sqrt{[n\Sigma x^2-(\Sigma x)^2][n\Sigma y^2-(\Sigma y)^2]}}$$

Squaring and dividing numerator and denominator of the right hand side of this equation by n^2 gives:

$$\gamma^2=\frac{[\Sigma xy-(\Sigma x)(\Sigma y)/n]^2}{[\Sigma x^2-(\Sigma x)^2/n][\Sigma y^2-(\Sigma y)^2/n]} \qquad (7)$$

Noting that

$$[\Sigma y^2-(\Sigma y)^2/n]=\Sigma(y-\bar{y})^2$$

and using equation (5) allows equation (7) to be transformed into:

$$\gamma^2=\frac{\Sigma(\hat{Y}-\bar{y})^2}{\Sigma(y-\bar{y})^2} \qquad (8)$$

Equation (8) is identical to equation (6), with $\gamma^2 = S^2$. Therefore, Pearson's γ = least squares coefficient *S*. Possibly without knowing this, Lowey (1992) used both Pearson's

correlation and least squares methods to test for asymmetric sequences. From Tables 5 and 6 of Lowey (1992), it can be seen that the test statistics for these two methods are identical, except for his megasequence 11 and 14, where there appear to be typographical errors.

3.2.2 Tests for Randomness

1) Rank difference test (Meacham, 1968)

Bed thickness is replaced by its rank (R_i) in a sandstone packet, with the thinnest bed being assigned rank one (R_1).

The R statistic is calculated by:

$$R = \sum_{i=2}^{n} |R_i - R_{i-1}|$$

Where n = the number of beds, and R = sum of the absolute values of the rank differences between successive beds in a single sequence or sandstone packet. For a random succession of bed thicknesses, R is normally distributed with:

$$\text{mean} = \mu_R = (n+1)(n-1)/3$$

and

$$\text{Standard deviation} = \sigma_R = \sqrt{(n-2)(n+1)(4n-7)/90}$$

A Z statistic is computed as follows:

$$Z_R = \frac{R - \mu_R}{\sigma_R}$$

If Z_R lies within a certain confidence interval, then the null hypothesis that the sequence results from a random process cannot be rejected at the corresponding significance level, α. For example, if we test a sequence of bed thicknesses at $\alpha = 0.1$, and if the value of Z_R falls within the central 90% of a standard normal distribution, then the null hypothesis is accepted. The same approach is used for the Turning Points test and Median Crossing test, below.

2) Turning Points Test (Kendall, 1976)

Bed thickness values, x_i, in a sequence are replaced by 1 if $x_{i-1} < x_i > x_{i+1}$ or $x_{i-1} > x_i < x_{i-1}$, otherwise by 0. A single 1 represents a turning point. The number of turning points, TP, is approximately normally distributed with:

$$\text{mean} = \mu_T = 2(n-2)/3$$

and

$$\text{Standard deviation} = \sigma_T = \sqrt{(16n - 29)/90}$$

The Z statistic is calculated by:

$$Z_T = \frac{TP - \mu_T}{\sigma_T}$$

If $|TP - \mu_T|$ is sufficiently large at a selected significance level, then the null hypothesis

that the sequence is generated by a purely random process would be rejected, where Z_T is assumed to be an observation from a standard normal distribution. Because the number of turning points in a sequence is always one less than the number of runs up and down, this method is conceptually identical to the runs-up-and-down test.

3) Median Crossing Test (Fisz, 1963)

The median crossing test (Fisz, 1963) is based on a binary series. For bed thicknesses, x_i, if $x_i<\bar{x}$ (median), x_i is assigned a value of 0; if $x_i>\bar{x}$, x_i is replaced by the value 1. If $x_i=\bar{x}$, no value is assigned to x_i (i.e. this bed is ignored because it neither larger or smaller than the median), and n is reduced by 1. If the original sequence has been generated by a purely random process, then M, the total number of times either 0 is followed by 1 or 1 is followed by 0, is approximately normally distributed with:

$$\text{mean} = \mu_M = (n-1)/2$$

and

$$\text{Standard deviation} = \sigma_M = \sqrt{(n-1)/4}$$

The Z statistic is:

$$Z_M = \frac{M-\mu_M}{\sigma_M}$$

If Z_M lies within a selected confidence interval, then the hypothesis that the sequence

resulted from a random process cannot be rejected at that significant level, α. This test is actually similar to the runs-about-median method (Wald-Wolfowit, 1943), because M is always one less than the number of runs on either side of the median.

4) Length-of-Runs Test (Gold test, 1929)

A run length, s, is defined as the number of consecutive beds either all above or all below the median value of bed thickness. If M_s denotes the total number of runs of length s, then for a random process the expected value of M_s is:

$$E(M_s)=(n+3-s)/2^{s+1}$$

and the sum:

$$L=\sum_{s=1}^{s'}[M_s-E(M_s)]^2/E(M_s)$$

is distributed as chi-square with (s'-1) degrees of freedom, where s' is the maximum run length in the sequence. This is a one-tailed test. If L falls below a pre-selected critical value (determined by the significance level, α), then the hypothesis of randomness cannot be rejected at that significance level.

3.3 Power Estimation and Sample Size Analysis

3.3.1 Experiments on the Power of the Seven Methods

The power of a test is statistically defined as the probability of rejecting a false null hypothesis, denoted by 1 - β (β = Type II error = probability of accepting the null hypothesis when it is not true). In this section, "power" is evaluated by assessing the relative capability of a test to recognize asymmetric or other orderly trends when they are present.

In order to evaluate the power of the seven methods in testing for asymmetric and other trends, several artificial sequences were generated and tested (Fig. 3.2a-b). These sequences encompass most possible patterns of bed thickness in turbidite sandstone packets; i.e., simple asymmetric trends (sequences 1. 2, 3); asymmetric trends with superimposed noise (sequences 4, 5, 6, 7 and 8), symmetric trends (sequence 9), step-wise sequences (sequence 10), grouping of thick and thin beds (sequence 11), and random distributions (sequences 12, 13, 14, 15 and 16). In this thesis, "noise" is defined as very thin and/or very thick beds superimposed on an overall trend of bed thicknesses. It can also be random positive or negative deviations from an otherwise smooth trend or pattern.

Throughout this chapter, if a sequence passes a test at, say, $\alpha \leq 10\%$, it will be stated that the null hypothesis is rejected, or that the sequence passes the test. Otherwise, if the α value for the sequence exceeds, say, 10%, it will be stated that the null hypothesis cannot be rejected.

Sequences 1 and 2 are idealized upward thinning and thickening sequences. They

Figure 3.2a and 3.2b showing results of experiments on the power of the seven statistical techniques in testing for asymmetric trends and other possible trends. Sequences 1 to 11 were artificially generated: sequences 1 and 2 show near perfect asymmetric trends, sequences 3 to 8 have overall asymmetric trends but with "noise" in the form of very thick and/or very thin beds, sequence 9 displays a symmetric pattern, sequence 10 a step-wise pattern, and sequence 11 the pattern of grouped thin and thick beds. Sequences 12 to 16 were formed through a random-shuffle-program (Appendix II-2). τ, ρ and γ represent Kendall's, Spearman's and Pearson's correlation coefficients, respectively. ZT, ZR, Zm and FL are test statistics for the Turning Point Test, Rank Difference Test, Median Crossing Test, and Length-of-Runs Test. $\alpha\tau$, $\alpha\rho$, $\alpha\gamma$, αT, αR, αm, and αL are the significance levels at which the null hypothesis of no preferred order would be rejected by each test. For example, with significance level $\alpha = 0.05$, sequence 5 would fail the null hypothesis for Kendall's τ test ($\alpha\tau = 0.045$), but would accept the null hypothesis for all other tests (all αx values > 0.05).

No.	Thk (cm)
1	97
2	83
3	80
4	74
5	69
6	50
7	43
8	39
9	24
10	20
11	13
12	4

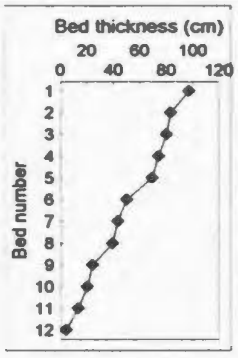

SEQUENCE:1

τ = -1.000
ατ = 0.000
ρ = -1.000
αρ = 0.000
γ = -0.994
αγ = 0.000
ZT = -4.954
αT = 0.000
ZR = -4.765
αR = 0.000
Zm = -2.714
αm = 0.007
FL = 59.334
αL = 0.000

No.	Thk (cm)
1	90
2	72
3	78
4	64
5	63
6	42
7	59
8	37
9	42
10	18
11	30
12	9

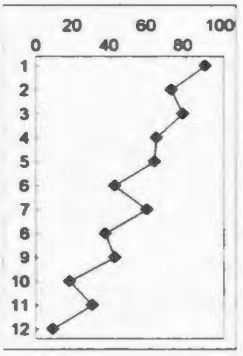

SEQ: 3

τ = -0.870
ατ = 0.000
ρ = -0.974
αρ = 0.000
γ = -0.949
αγ = 0.000
ZT = 0.991
αT = 0.322
ZR = -3.205
αR = 0.001
Zm = -1.508
αm = 0.132
FL = 25.118
αL = 0.000

No.	Thk (cm)
1	64
2	53
3	42
4	64
5	42
6	1
7	95
8	27
9	16
10	25
11	16
12	100
13	12
14	2

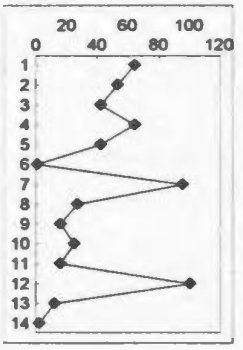

SEQ: 5

τ = -0.402
ατ = 0.045
ρ = -0.477
αρ = 0.085
γ = -0.340
αγ = 0.235
ZT = 0.000
αT = 1.000
ZR = -0.202
αR = 0.840
Zm = -0.832
αm = 0.405
FL = 5.922
αL = 0.205

No.	Thk (cm)
1	48
2	56
3	40
4	40
5	7
6	38
7	27
8	1
9	7
10	30
11	16
12	14
13	16
14	18
15	4

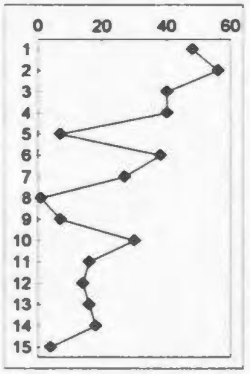

SEQ: 7

τ = -0.502
ατ = 0.009
ρ = -0.676
αρ = 0.006
γ = -0.716
αγ = 0.003
ZT = -1.089
αT = 0.276
ZR = -1.687
αR = 0.092
Zm = -0.832
αm = 0.405
FL = 7.709
αL = 0.052

Bed No.	Thk (cm)
1	3
2	22
3	15
4	30
5	32
6	43
7	43
8	54
9	62
10	76
11	76
12	81
13	81

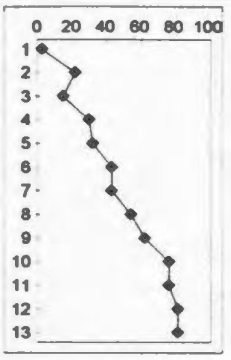

SEQ: 2

τ = 0.954
ατ = 0.000
ρ = 0.974
αρ = 0.000
γ = 0.984
αγ = 0.000
ZT = -3.782
αT = 0.000
ZR = -4.217
αR = 0.000
Zm = -2.530
αm = 0.011
FL = 21.556
αL = 0.001

1	2
2	20
3	9
4	17
5	90
6	25
7	36
8	24
9	43
10	50
11	1
12	63
13	68
14	61
15	69

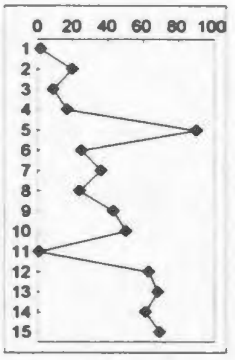

SEQ: 4

τ = 0.524
ατ = 0.006
ρ = 0.596
αρ = 0.019
γ = 0.573
αγ = 0.025
ZT = 0.871
αT = 0.384
ZR = -1.506
αR = 0.132
Zm = -0.832
αm = 0.405
FL = 7.709
αL = 0.052

1	2
2	90
3	1
4	30
5	35
6	30
7	46
8	80
9	3
10	47
11	50
12	47
13	63
14	10
15	45
16	66
17	70

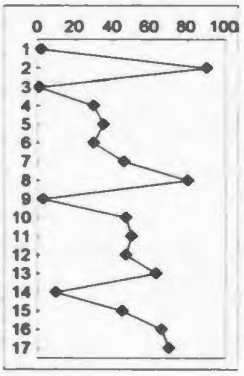

SEQ: 6

τ = 0.341
ατ = 0.056
ρ = 0.380
αρ = 0.133
γ = 0.308
αγ = 0.229
ZT = 0.000
αT = 1.000
ZR = 0.074
αR = 0.941
Zm = -0.258
αm = 0.796
FL = 5.709
αL = 0.127

1	2
2	13
3	1
4	2
5	16
6	24
7	3
8	10
9	27
10	20
11	30
12	1
13	5
14	1
15	35
16	39
17	34
18	2
19	1
20	40
21	30

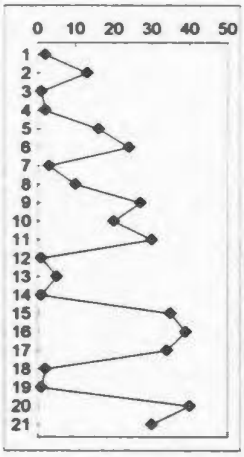

SEQ: 8

τ = 0.273
ατ = 0.083
ρ = 0.316
αρ = 0.162
γ = 0.413
αγ = 0.062
ZT = 0.180
αT = 0.857
ZR = -1.040
αR = 0.298
Zm = -1.147
αm = 0.251
FL = 11.821
αL = 0.003

Fig.3.2a

No.	Thk (cm)
1	3
2	6
3	14
4	27
5	21
6	38
7	39
8	46
9	43
10	67
11	70
12	42
13	40
14	31
15	38
16	7
17	20
18	34
19	18
20	12
21	4
22	5

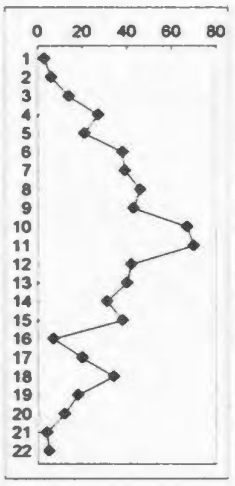

SEQ: 9

τ = -0.113
ατ = 0.462
ρ = -0.153
αρ = 0.497
γ = -0.134
αγ = 0.552
ZT = -1.760
αT = 0.078
ZR = -4.669
αR = 0.000
Zm = -2.837
αm = 0.005
FL = 143.27
αL = 0.000

No.	Thk (cm)
1	2
2	77
3	50
4	44
5	15
6	22
7	18
8	10
9	51
10	66
11	87
12	84
13	50
14	68
15	15
16	26
17	20

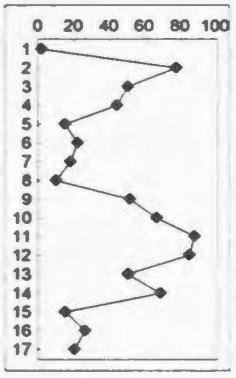

SEQ: 11

τ = 0.089
ατ = 0.618
ρ = 0.151
αρ = 0.563
γ = 0.097
αγ = 0.711
ZT = -0.609
αT = 0.543
ZR = -1.405
αR = 0.160
Zm = -1.807
αm = 0.071
FL = 11.640
αL = 0.040

No.	Thk (cm)
1	22
2	76
3	32
4	15
5	76
6	62
7	81
8	43
9	54
10	30
11	81
12	43
13	3

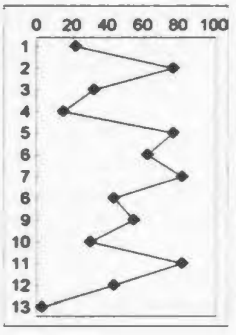

SEQ: 13

τ = -0.039
ατ = 0.852
ρ = -0.040
αρ = 0.896
γ = -0.082
αγ = 0.791
ZT = 1.182
αT = 0.237
ZR = 0.456
αR = 0.649
Zm = 0.632
αm = 0.527
FL = 2.592
αL = 0.459

No.	Thk (cm)
1	69
2	36
3	25
4	20
5	61
6	50
7	43
8	68
9	1
10	24
11	9
12	90
13	63
14	17
15	2

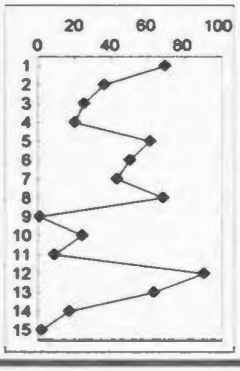

SEQ: 15

τ = -0.219
ατ = 0.255
ρ = -0.296
αρ = 0.283
γ = -0.211
αγ = 0.449
ZT = -0.435
αT = 0.663
ZR = -0.783
αR = 0.434
Zm = -0.832
αm = 0.405
FL = 3.713
αL = 0.294

Bed No.	Thk (cm)
1	2
2	65
3	53
4	40
5	65
6	56
7	68
8	6
9	12
10	10
11	5
12	12
13	9

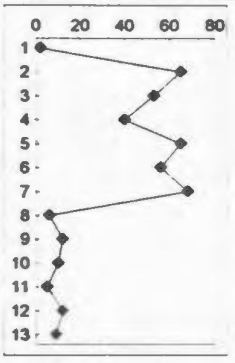

SEQ: 10

τ = -0.260
ατ = 0.216
ρ = -0.351
αρ = 0.240
γ = -0.527
αγ = 0.065
ZT = 1.182
αT = 0.237
ZR = -1.026
αR = 0.305
Zm = -1.897
αm = 0.058
FL = 16.671
αL = 0.005

1	20
2	43
3	83
4	39
5	24
6	74
7	4
8	50
9	13
10	80
11	69
12	97

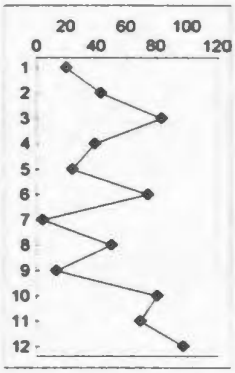

SEQ: 12

τ = 0.242
ατ = 0.273
ρ = 0.336
αρ = 0.286
γ = 0.385
αγ = 0.216
ZT = 0.991
αT = 0.322
ZR = 0.693
αR = 0.488
Zm = 0.905
αm = 0.366
FL = 0.813
αL = 0.666

1	78
2	18
3	63
4	37
5	42
6	90
7	42
8	64
9	72
10	30
11	59
12	9

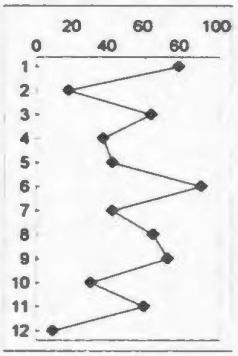

SEQ: 14

τ = -0.137
ατ = 0.534
ρ = -0.240
αρ = 0.452
γ = -0.218
αγ = 0.495
ZT = 0.991
αT = 0.322
ZR = 1.083
αR = 0.279
Zm = 2.111
αm = 0.035
FL = 5.872
αL = 0.015

1	5
2	30
3	1
4	40
5	27
6	1
7	2
8	10
9	3
10	1
11	34
12	13
13	30
14	2
15	24
16	2
17	1
18	39
19	20
20	16
21	35

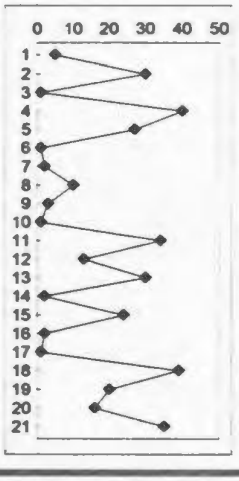

SEQ: 16

τ = 0.107
ατ = 0.496
ρ = 0.139
αρ = 0.549
γ = 0.166
αγ = 0.473
ZT = 0.722
αT = 0.470
ZR = 0.917
αR = 0.359
Zm = -0.229
αm = 0.819
FL = 3.323
αL = 0.505

Fig.3.2b

passed all four tests for randomness and the three trend tests (i.e. the null hypotheses of randomness and no trends were both rejected) at higher than the 95% confidence level ($\alpha < 0.05$). The high correlation between bed number and bed thickness indicated by the three correlation tests confirms the asymmetric trends.

Sequences 3 and 4 have fluctuating thicknesses but clear upward thinning or thickening trends. Sequence 4 contains noise from one thick and one thin bed. The upward thickening (sequence 4) and thinning (sequence 3) trends are confirmed by all three correlation tests (Fig. 3.3 A, B). The turning points test and the median crossing test failed to reject the null hypothesis for sequence 3, and three tests (the turning points test, rank differences test, and median crossing test) could not reject the null hypothesis for sequence 4 at a widely employed significance level of $\alpha = 10\%$.

Sequences 5, 6, 7 and 8 are more complicated, having an overall upward thinning or thickening trend with superimposed noise in the form of both thick beds and thin beds. Data for sequences 5 and 6 are relatively scattered, and sequence 6 contains more noise than sequence 5. Pearson's linear correlation test failed to detect the overall trends in these two sequences (Fig. 3.3 C, D). Data for sequences 7 and 8 are not as scattered as those of sequences 5 and 6, but sequence 8 contains a large number of interspersed very thin beds (Note: when viewed from a distance in the field, such very thin beds can easily be ignored during subjective cycle assessment). Sequences 7 and 8, but not 5 and 6, maintain sufficient correlation to pass Pearson's test (Fig. 3.3 E, F). Sequences 6 and 8, due to a large amount of noise, are only able to pass Spearman's rank correlation test at the

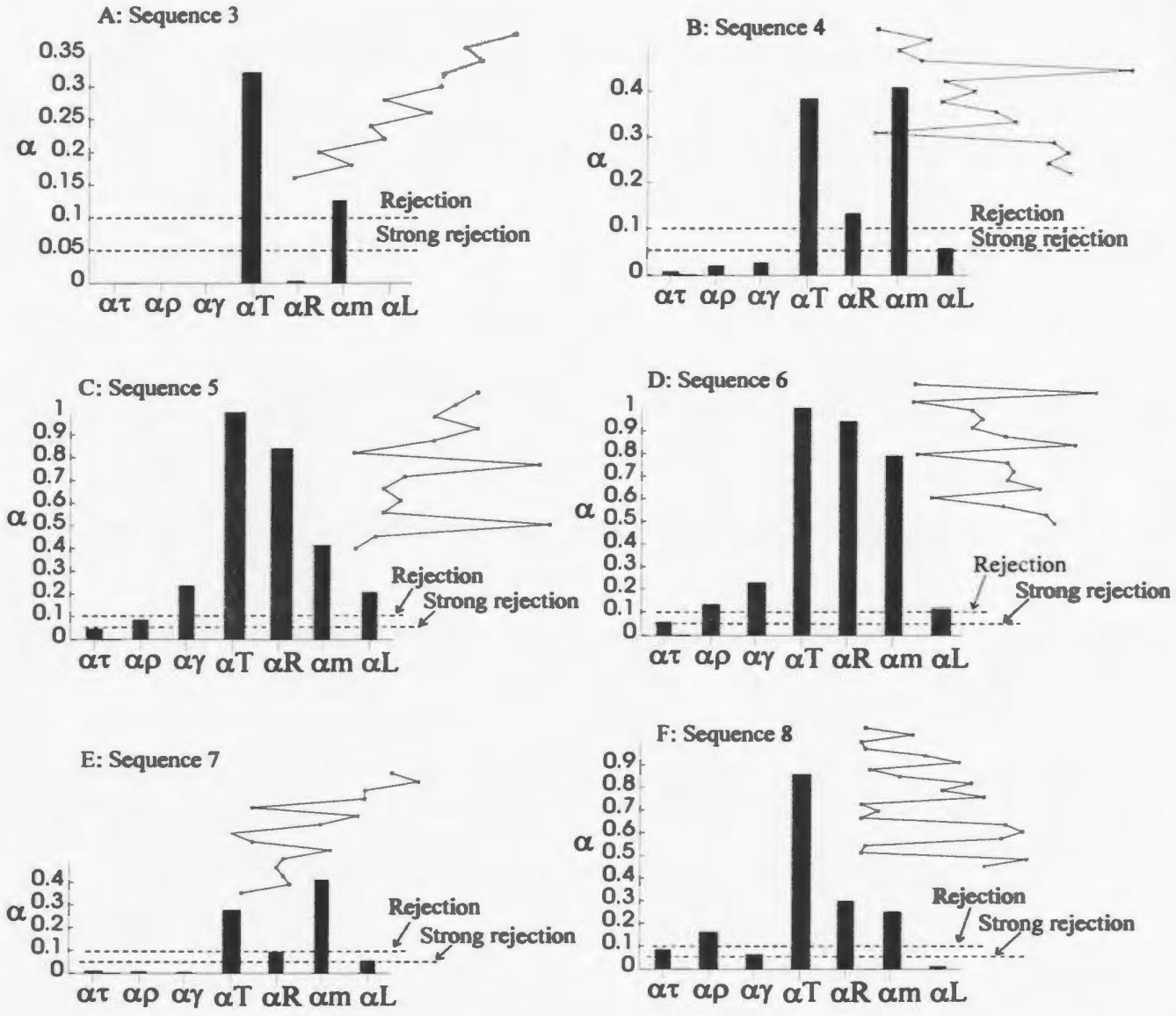

Fig. 3.3 Significance levels at which sequences 3 to 16 in Figures 3.2a-b would pass the seven tests. α = significance level; $\alpha\tau$, $\alpha\rho$, $\alpha\gamma$, αT, αR, αm, and αL represent significance levels at which a sequence would pass Kendall's τ, Spearman's ρ, Pearson's γ, the turning point, the rank difference, the median crossing, and the length-of-runs tests, respectively. Note that if a sequence passed a test at $\alpha = 0.05$, the null hypothesis was strongly rejected; if at $\alpha > 0.1$, then the null hypothesis was accepted. The bed-thickness pattern for each sequence is shown without scales to facilitate comparison with Figure 3.2.

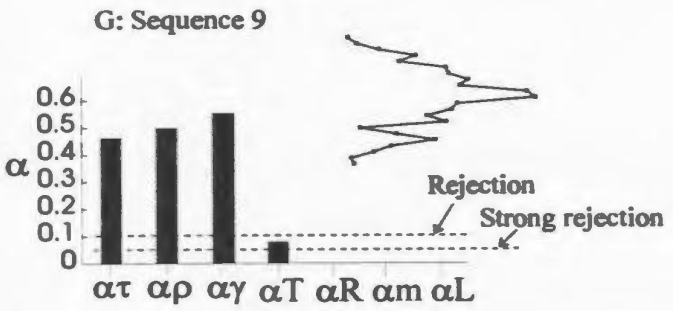
G: Sequence 9
α
0.6
0.5
0.4
0.3
0.2
0.1
0
Rejection
Strong rejection
ατ αρ αγ αT αR αm αL

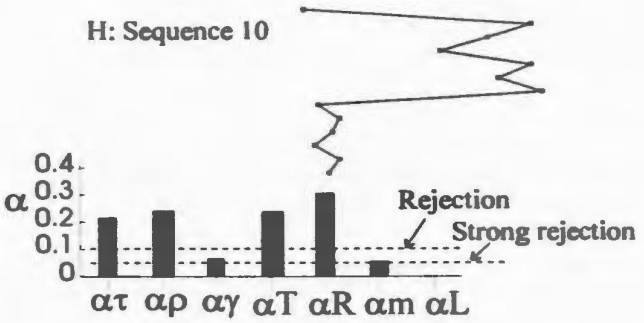
H: Sequence 10
α
0.4
0.3
0.2
0.1
0
Rejection
Strong rejection
ατ αρ αγ αT αR αm αL

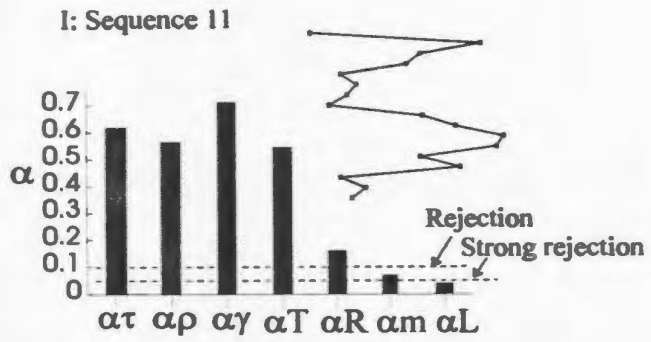
I: Sequence 11
α
0.7
0.6
0.5
0.4
0.3
0.2
0.1
0
Rejection
Strong rejection
ατ αρ αγ αT αR αm αL

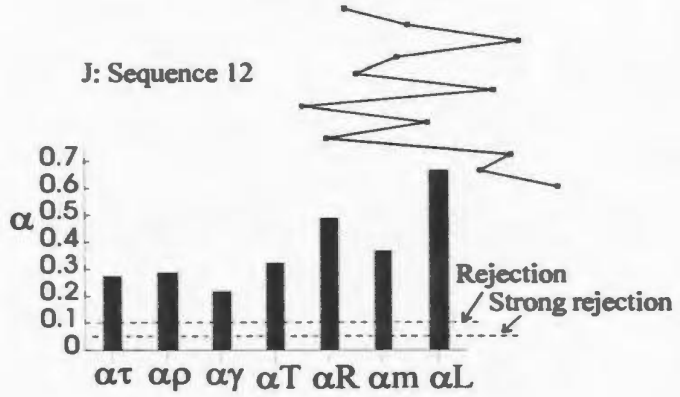
J: Sequence 12
α
0.7
0.6
0.5
0.4
0.3
0.2
0.1
0
Rejection
Strong rejection
ατ αρ αγ αT αR αm αL

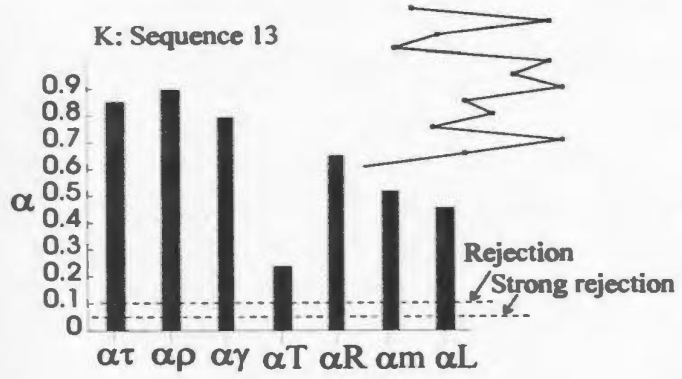
K: Sequence 13
α
0.9
0.8
0.7
0.6
0.5
0.4
0.3
0.2
0.1
0
Rejection
Strong rejection
ατ αρ αγ αT αR αm αL

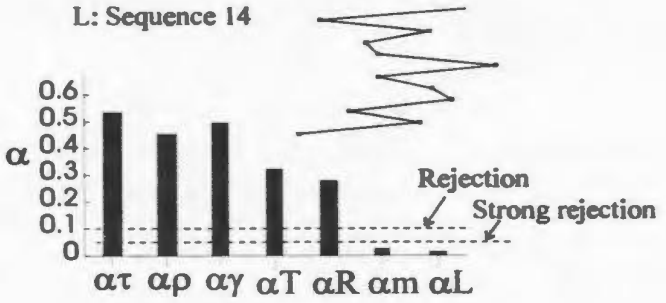
L: Sequence 14
α
0.6
0.5
0.4
0.3
0.2
0.1
0
Rejection
Strong rejection
ατ αρ αγ αT αR αm αL

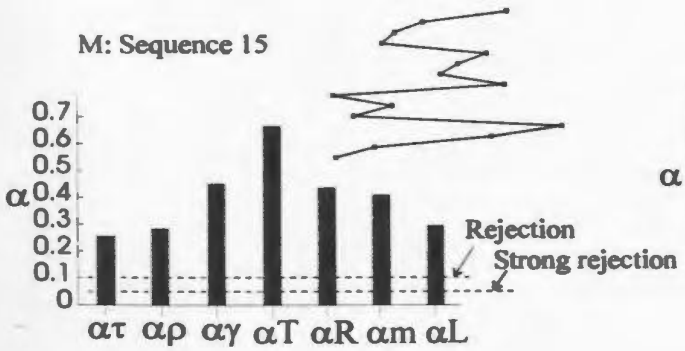
M: Sequence 15
α
0.7
0.6
0.5
0.4
0.3
0.2
0.1
0
Rejection
Strong rejection
ατ αρ αγ αT αR αm αL

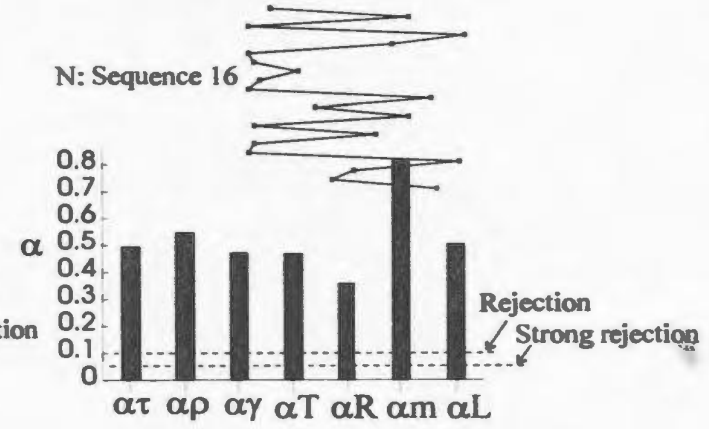
N: Sequence 16
α
0.8
0.7
0.6
0.5
0.4
0.3
0.2
0.1
0
Rejection
Strong rejection
ατ αρ αγ αT αR αm αL

relatively high significance levels of $\alpha = 13.3\%$ and $\alpha = 16.2\%$, respectively (Fig. 3.3 D, F). Kendall's rank correlation test, in contrast, successfully identified the asymmetric trends in sequences 5 through 8 (Fig. 3.3). Considering tests for randomness, the null hypothesis could not be rejected by the turning points test and the median crossing test for sequences 5 through 8. For sequence 7, the null hypothesis was rejected by the rank differences test and the length-of-runs test because data in this sequence are not very scattered. Sequence 8 was recognized as non-random by the length-of-runs test (rejecting the null hypothesis), which may be simply due to the high-frequency spectral pattern (i.e., grouping) rather than the overall upward thickening trend (see also Appendix III).

Sequence 9 has a symmetric trend. All three correlation tests predictably fail to identify this type of trend. However, the null hypothesis of randomness was rejected by all four tests for randomness (Fig. 3.3 G).

For sequence 10 with its step-wise pattern (Pickering et al., 1989, p. 85), the null hypothesis of no trend could not be rejected by Kendall's and Spearman's correlation tests, but was rejected by Pearson's linear correlation test. For this case, the null hypothesis of randomness was rejected by the median crossing test and the length-of-runs test (Fig. 3.3 H).

In sequence 11, thick and thin beds are grouped separately. For this case, only the median crossing test and the length-of-runs test rejected the null hypothesis (Fig. 3.3 I).

Sequences 12, 13, 14, 15, and 16 were generated by a random-shuffle program (Appendix II-2). Figures 3.3 J-N show the significance levels at which these sequences

would be able to pass the seven tests, respectively. For all five sequences, the three correlation tests accepted the null hypothesis of no asymmetric trends ($\alpha >> 10\%$). The null hypothesis of randomness for all these sequences, except for sequence 14, was accepted by all four tests for randomness. Sequence 14 fluctuates rapidly, which makes a large number of runs, yet it passed the median crossing test and the length-of-runs test. This indicates that not only a low, but also a large number of runs in a sequence can cause rejection of the null hypothesis.

3.3.2 Sample Size (n) Analysis

At the inception of this study, it was envisaged that the number of beds forming a sandstone packet would need to be at least ten before statistical tests could be applied. Below some minimum sample size, there is a higher probability that random variation can form an asymmetric sequence. In order to objectively determine the smallest number of beds which can be selected for testing for asymmetric trends, the following experiment was undertaken. For each sample size from $n = 3$ to $n = 15$, two hundred randomly shuffled sequences were generated by means of a random-shuffle program (RANSHUF, Appendix II-2) and tested for asymmetric and other trends or randomness by using the computer program ASYMRAN.FOR (Appendix II-1). Then, for every sample size and for each testing method, the percentage of sequences which passed the test (by rejecting the null hypothesis for that test) at significance levels $\alpha = 5\%$ and 10% was calculated and plotted (Tables 3.2 and 3.3, Figs. 3.4 and 3.5). Except for the median crossing test and the

Table 3.2 Percentages of 200 randomly shuffled sequences (for sample sizes 3 to 15) for which the null hypothesis was rejected at the 5% significance level. N/AV = not available (i.e., no sequence passed the relevant test at this significance level).

Sample size	Kendall's Correlation	Spearman's Correlation	Pearson's Correlation	Turning Point	Rank Difference	Median Crossing	Length-of-Runs
3	N/AV	34	N/AV	N/AV	N/AV	N/Av	N/AV
4	7.5	8	8	9	15	N/AV	64
5	7	8	3.5	2	2.5	N/AV	31
6	5	5	3	8	3.5	12	23
7	5.5	4	5.5	2.5	5	9	19.5
8	7	7.5	7.5	9.5	6	3	13
9	4	6.5	3	5	6.5	5.5	18.5
10	6	6	6.5	4.5	5	3	19.5
11	5	4.5	6	3.5	6.5	6	14
12	4	5	4	7	3	4.5	8.5
13	6.5	8.5	6.5	9	4	10.5	20
14	4	4	6	9.5	2	1.5	27
15	4.5	4	4.5	4.5	5.5	3	24.5

Note: N/AV = not available; for example, when n = 3, a sequence even with its three values successively increasing or decreasing could only pass Kendall's test at a significance level larger than 5%.

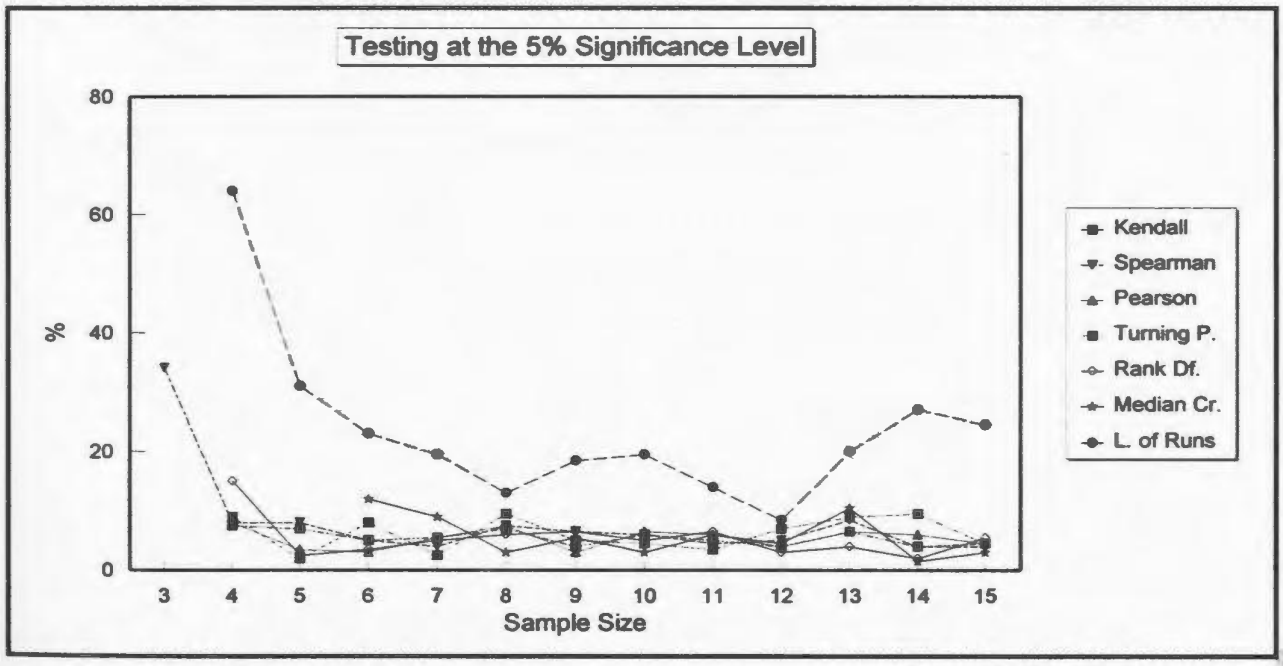

Fig. 3.4 Graph of data in Table 3.2, indicating that when sample size n > 4, the percentages of sequences rejected at the 5% significance level from a set of randomly shuffled sequences are basically stable for Kendall's, Spearman's and Pearson's correlation tests, and the turning point and rank difference tests.

Table 3.3 Percentages of 200 randomly shuffled sequences (for sample sizes 3 to 15) for which the null hypothesis was rejected at the 10% significance level.

Sample Length	Kendall's Correlation	Spearm's Correlation	Pearsn's Correlation	Turning Point	Rank Difference	Median Crossing	Length of Runs
3	N/AV	34	34	N/AV	N/AV	N/AV	N/AV
4	9	9	12	11	15.5	26.5	64
5	9	10	9.5	9	11	31	62
6	12.5	10	9	9	9.5	12	23
7	12.5	9.5	10	11	12.5	9	19.5
8	11.5	10	10	9.5	12	13	36.5
9	11	9.5	11	5	11	17	29.5
10	9	10.5	10.5	7.5	11	14.5	38
11	10	9	9.5	3.5	12	6	19.5
12	10	7	9	14	7	4.5	43
13	10	10	11	13.5	13.5	10.5	33
14	10.5	11.5	10	9.5	10.5	7.5	36
15	10.5	11.5	13.5	10	9	9.5	32

Note: N/AV = not available; for example, when n = 3, a sequence even with its three values successively increasing or decreasing could only pass Kendall's test at a significance level larger than 5%.

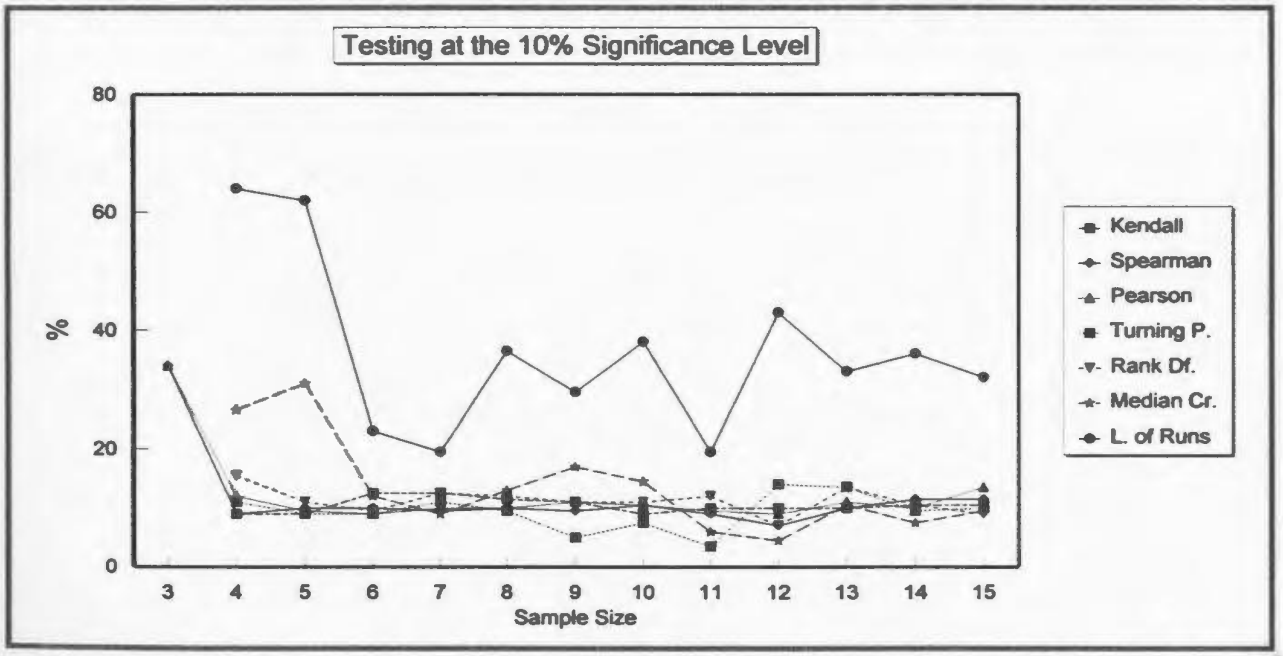

Fig. 3.5 Graph of data in Table 3.3, indicating that when sample size n > 4, the percentages of sequences rejected at the 10% significance level from a set of randomly shuffled sequence are stable for Kendall's, Spearman's and Pearson's correlation tests, and the turning point and rank difference tests.

length-of-runs test, the percentages overall remain stable for $n \geq 6$ at the 5% significance level and for $n \geq 4$ at the 10% significance level (Figs. 3.4 and 3.5).

For the median crossing test, a larger n is required to maintain an overall stable percentage ($n \geq 8$ at $\alpha = 5\%$, $n \geq 6$ at $\alpha = 10\%$). For the length-of-runs test, no conclusions about a minimum acceptable sample size can be drawn from this experiment. A serious problem with this test is the very high percentages of rejection for random sequences (Fig. 3.4, 3.5).

An evaluation of numbers of permutations may also help constrain the minimum sample size required for tests of asymmetric trends. When n = 3 (three different values), there are only [3!] (i.e., 3 "factorial" = $3 \times 2 \times 1$) arrangements, and two out of the six arrangements, i.e. 33.3%, will show upward increasing and decreasing trends (compare with n = 3 values for Spearman's and Pearson's tests, Tables 3.2 and 3.3). When n = 4, there are 24 different arrangements, of which two (8%) have four values consistently increasing or decreasing (consistent with n = 4 values of 8% and 9% for Kendall's and Spearman's tests, Tables 3.2 and 3.3). Beyond n = 5, the number of rejections of the null hypothesis for random sequences closely approximates the significance level, α, as it should. Exception is the length-of-runs test, which reports non-random behavior in far too many randomly shuffled sequences than can be considered acceptable (i.e. for more than α). Consequently, this test is deemed unreliable even for n = 15.

Instead of a minimum of ten beds (Pickering et al., 1989, p.84), the results of the experiment outlined above suggest that bed clusters of more than 6 beds can be tested for

asymmetric trends by the three correlation tests at the 5% significance level. When tests use a 10% significance level, as in this thesis (Chapter 4), packets with $n \geq 4$ can be successfully tested.

3.3.3 Power and Dependability of the tests

Based on the above experiments, the relative power of the seven statistical techniques in testing for asymmetric and other trends, and randomness, can be estimated as follows.

1) For testing for asymmetric upward thinning and thickening trends, all three correlation tests are powerful. Most powerful is Kendall's rank correlation test, followed by Spearman's rank correlation test, and finally Pearson's linear correlation test. Kendall's rank correlation test identified all overall upward thickening or thinning trends (i.e. sequences 1 through 8 in Fig. 3.2a) at higher than the 90% confidence level. Because the calculation of τ compares each field value (e.g. bed-thickness) with all succeeding values in a sequence (Harper, in press), this test does not succumb to even a large amount of noise. Spearman's rank correlation test is slightly sensitive to noise, and Pearson's linear correlation test is particularly affected by noise in the form of very thick and very thin beds which make a significant deviation (or residual) from the regression line (e.g., sequences 5 and 6 in Fig. 3.2a and Fig. 3.3). The high power of the three correlation tests has been confirmed by the sample size analysis; that is, for randomly shuffled sequences, the number of rejections of the null hypothesis by these three tests closely approximates the significance level, α, when $n \geq 4$ (Tables 3.2, 3.3, Figs. 3.4, 3.5).

Note that the three correlation tests are not entirely independent, but are highly correlated statistics (Kendall and Gibbons, 1990). However, inconsistent results from these tests occur for some cases. For example, $\tau = -1$, $\rho = -1$, $\gamma = -0.62$ for the following case (Dr. Charles Harper, 1997, per. comm.):

Bed Number:	1	2	3	4	5	6	7	8	9	10	11
Bed Thickness (cm)	1000	218.8	66.9	26.5	12.9	7.3	4.7	3.4	2.6	2.1	1.8

The null hypothesis of no trend is not rejected by Pearson's correlation test because the correlation is not linear (also see sequences 5 and 6 in Fig. 3.3). Because there are Daniels' and Durbin-Stuart inequalities between τ and ρ and because the relationship of these two coefficients is not a simple one (Kendall and Gibbons, 1990), the null hypothesis of no rank correlation between any two variables may, in a few cases, be rejected by only one of Kendall's and Spearman's tests at a given α, say $\alpha = 0.1$, (e.g., sequences 109, 162, 173, and 194 in Appendix III). Accordingly, all three correlation tests are employed in this study, and criteria are proposed to deal with cases for which the three methods do not give consistent results (see Chapter 4).

Although all three correlation methods tolerate noisy data and successfully detect asymmetric trends, most previous researchers, except Lowey (1992), have used low power methods like runs tests, the signs of differences test, and spectral tests to search for asymmetric sequences in turbidite successions (e.g. Martini et al., 1978; Heller and Dickinson, 1985; Waldron, 1987; Murray et al., 1996). This may be simply because in

almost all statistics and time-series books, runs and spectral tests are put in the category of trend analysis, whereas the three correlation tests introduced in this chapter are instead proposed for assessing the association or correlation between two variables. In fact, testing for asymmetric upward thinning and thickening sequences in turbidite successions is in essence an examination of the correlation between two variables, bed number and bed thickness.

2) The four tests for randomness are not so informative as the three correlation tests. There are two serious problems with these four tests. (a) Even though, for random sequences, the number of rejections of the null hypothesis by the turning point test and the rank difference test is close to α when $n \geq 5$, and by the median crossing test when $n \geq 8$ (Tables 3.2, 3.3), these three tests failed to recognize many trends with superimposed noise from thin and thick beds (Fig. 3.2a). (b) The length-of-runs test successfully rejected the null hypothesis of randomness at $\alpha < 10\%$ for sequences 1, 2, 3, 4, 7 and 8 in Figure 3.2a. However, rejections of the null hypothesis by this test when applied to random sequences are too many, i.e. much higher than α (Table 3.2, 3.3). This requires that if a sequence passes this test, it still needs further checking.

3) The three correlation tests usually fail to identify symmetric trends, step-wise patterns (Pickering et al., 1989, p.85), and clustering of thin and/or thick beds. For such patterns, the null hypothesis is more likely to be rejected by two or more of the four tests for randomness (Fig. 3.3 G, H and I).

Based on the results from synthetic sequences (Fig. 3.2, 3.3) and from sample size

analysis (Table 3.2, 3.3), the remainder of this thesis will use the three correlation methods to test for asymmetric trends and the four tests for randomness to check other patterns of bed thickness in naturally occurring turbidite sandstone packets. A computer program named ASYMRAN.FOR has been written for this purpose (Appendix II-1).

3.4 Selection of Sandstone Packets

Asymmetric upward thinning and thickening sequences, as originally defined by Mutti and Ricci Lucchi (1972), are vertical trends in bed thickness within individual sandstone packets in turbidite sections. Hence, sandstone packets must be picked out from the section first, instead of taking a whole section as a testing unit (e.g. Murray et al., 1996). To date, no statistical techniques to select sandstone packets from turbidite sections have been published. This thesis introduces the Split-Moving Window (Webster, 1973, 1980) and Maximum Likelihood Estimation (Radhakrishnan et al., 1991) methods to split turbidite sections into segments with different means and variances. The more sandy segments can, in this way, be selected for statistical tests for asymmetric and other trends. This avoids subjectively selecting sandstone packets for further testing (e.g. Lowey, 1992). Note that the segmentation undertaken is based on the assumption that sharply bounded segments or bed packets with different means and variances of bed thickness, grain size, and/or other measurements reflect different facies associations, and therefore represent different depositional environments in submarine fan systems (see the definition of packets in Chapter 1). Any attempt to recognize trends

that bridge segments with contrasting properties would violate the assumptions: (i) that all observations come from a single population; and (ii) that successive observations are independent.

3.4.1 Split-Moving Window (Webster, 1973, 1980)

The split-moving window method was designed to segment multivariate one-dimensional spatial series. This technique splits a section (or sequence) by means of viewing the section through a window which is moved along the section in a stepwise fashion (i.e., one observation or one bed every time) from one end to the other. At each position of the moving window, the exposed part of the section is split about its midpoint and either Mahalanobis D^2 or squared Euclidean distance (E^2) is computed between the two halves. D^2 is given by:

$$D^2=[\bar{X}_1-\bar{X}_2]'W^{-1}[\bar{X}_1-\bar{X}_2]$$

Where $\bar{X}_1$ and $\bar{X}_2$ are the mean vectors of the observed variates in the two halves of the moving window, respectively; $[\bar{X}_1-\bar{X}_2]'$ is the transpose of matrix $[\bar{X}_1-\bar{X}_2]$. W is the pooled within-halves variance-covariance matrix, and W^{-1} the inverse matrix of W. In matrix W, each element is the average value of the corresponding elements in the variance-covariance matrices of the two halves. In this study, only two variables, bed-thickness and grain-size, were used to split turbidite sections into sandstone packets and mudstone-siltstone packets. Thus, W is a 2 × 2 matrix: a_{11} is the pooled variance of bed-

thickness, a_{22} the pooled variance of grain-size, and a_{12} and a_{21} are pooled covariances of these two variables.

E^2 is more simple:

$$E^2=[\bar{X}_1-\bar{X}_2]'[\bar{X}_1-\bar{X}_2]$$

The peak values of D^2 or E^2 indicate an obvious difference of means of the two halves of a moving window, and therefore they represent segment boundaries.

To split turbidite sections into sandstone segments and mudstone-siltstone segments, two variates, bed thickness and grain size, were used. The two variates were first standardized to conform to standard normal distributions. The computation was done using the Fortran program published by Webster (1980). In this program, the width of moving windows is user-defined. Too wide a window causes some boundaries to be lost, whereas too narrow a window allows noise in the data to produce unacceptable peak values (boundaries) within some segments. In order to reliably select sandstone packets with 4 or more beds for further tests for trends and randomness, a moving window of 10 data points was found by trial and error to give best results (see Appendix I, and lithologic columns in Chapter 2). The 10-point window size is used throughout this thesis. For this window size, four thicker sand beds will form 80% of a half window at one slide position, and will result in a large difference in parameter mean values in the two parts of the moving window. More than four successive thicker sand beds will result in even larger differences, whereas a single thick sand bed will not produce a large

difference in 5-point means from one part of the window to the other part. Clearly, the individual data values must be obtained on a bed-by-bed base, not at regular vertical spacings as in well-log data. With fixed vertical sampling intervals, an unusually thick sand bed would contribute > 4 sequential values, and would lead to the immediate definition of a packet boundary.

Figure 3.6 represents an example of the segmentation of turbidite sections by the split-moving window technique. Overall, the section is successfully segmented into thick and thin sand packets and silt-mud packets. The boundaries determined by this technique is generally coincident with steps or discontinuities of bed-thickness and grain-size in the lithofacies logs. Note that the noise of a single and the other two thick sand beds intercalated in the silt-mud interval at around 30 m point of figure 3.6 does not significantly affect the segmentation. However, peak values of D^2 or E^2, sometimes, may occur within what appears to be a single segment. This is, in many cases, caused by several thin siltstone beds intercalated in sandstone segments (e.g., at the 48 m point of Figure 3.6). Rarely, variates change so gradually that a boundary cannot be determined by this technique (Webster, 1980). In these ambiguous circumstances, the determination of segment boundaries was assisted by the maximum likelihood estimation (below) and the subjective definition of packet boundaries (Chapter 1).

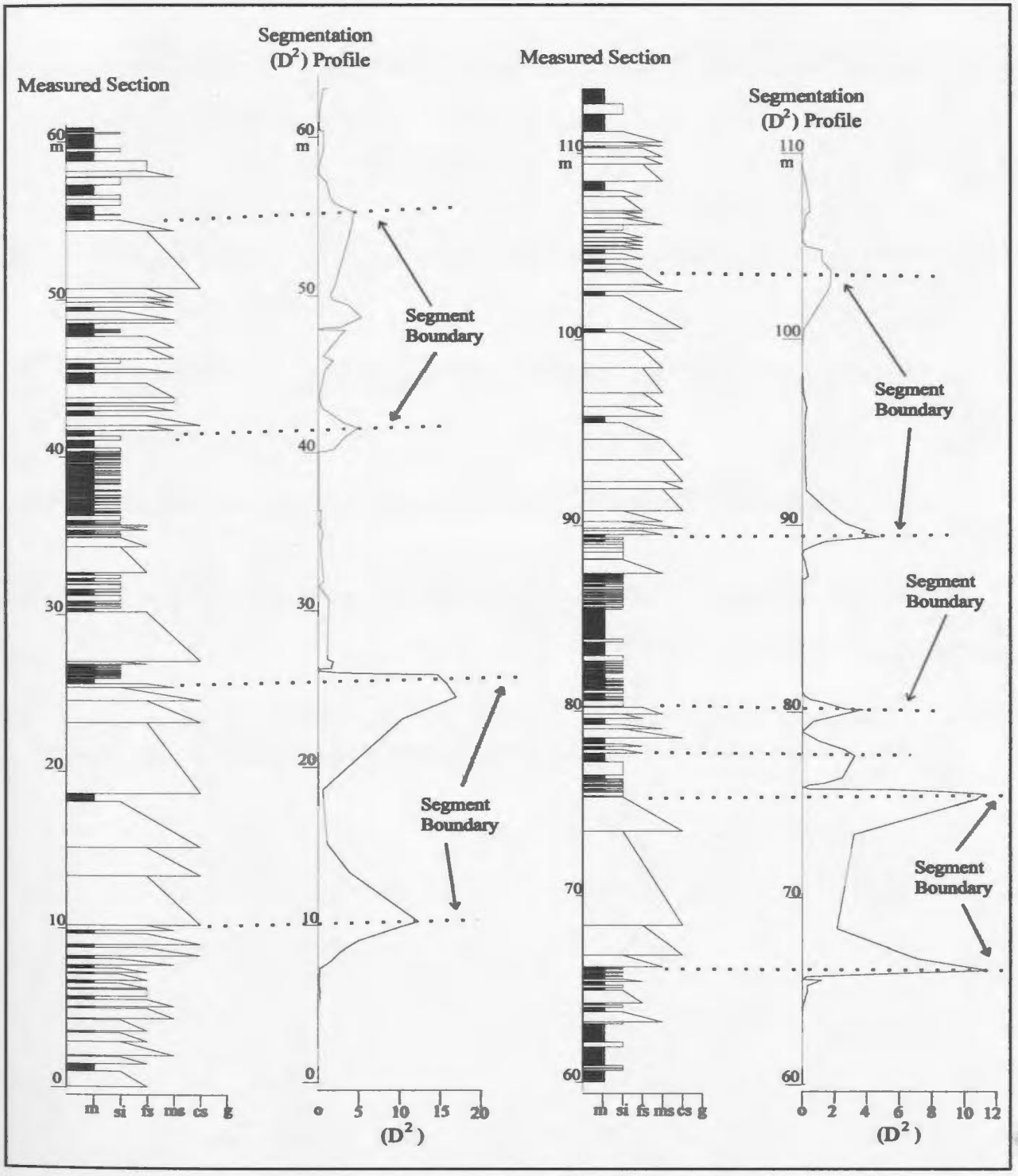

Fig. 3.6 An example of sequence segmentation from the Cap Ste-Anne section, Tourelle Formation, Gaspé Peninsula, Quebec. The turbidite section is segmented into thick-bedded and thin-bedded sand packets and shale-silt intervals using the split-moving window technique (Webster, 1980). The Peak values of D^2 indicate packet boundaries.

3.4.2 Maximum Likelihood Estimation (Radhakrishnan et al., 1991)

This technique was developed to segment univariate well-log data. The locations of segment boundaries are estimated by maximizing the likelihood function for a series of values of a selected variate. For the details of computation of this method, see Radhakrishnan et al (1991). In this study, series of sand bed thicknesses and grain size at the base of sand beds were treated separately by using the Fortran program of Radhakrishnan et al (1991). Although many boundaries detected by this method match those determined by the split-moving window technique, results seem less definitive. Specifically, (1) many more boundaries were determined, (2) some important boundaries that have been determined by the split-moving window method and that display a clear step or discontinuity in bed-thickness and/or grain-size in lithologic columns could not be detected, and (3) many calculated boundaries were two or three beds above or below those determined by the split-moving window technique and/or steps in facies characteristics. These shortcomings are attributed to the use of moving average in the calculation and the use of only a single variable in determining segment boundaries. Appendix I shows the segmenting results of this technique.

Because the apparent confidence with which boundaries can be selected is lower than with the split-moving window technique, the maximum-likelihood estimation is only utilised for segmentation where the split-moving window technique gives ambiguous results.

3.4.3 Results of Segmentation of Turbidite Sections

All turbidite sections involved in this study were split into segments with different means and variances using a combination of the split-moving window and maximum-likelihood estimation techniques. Segment boundaries determined by these statistical methods were checked by placing them beside the corresponding lithologic columns, in order to see if they coincide with packet boundaries defined in the field (Chapter 1). In this way, apparently spurious boundaries within segments with little facies variation were removed and some boundaries were adjusted slightly.

A total of 286 sandstone packets (segments), each with at least 4 beds having different values of bed thickness, were identified and selected for tests for asymmetric and other trends. Fifty-nine (10.3%) of the 572 boundaries of the 286 sandstone packets do not display a clear peak value of D^2 of the split-moving window. They, therefore, were determined either by the maximum likelihood estimation method or subjectively by using facies boundaries in the forms of steps or gradual changes (Fig. 1.3). All of these sandstone packets are marked on the corresponding lithologic columns in Chapter 2 and in Appendix I.

3.5 Summary

In order to effectively and objectively evaluate the significance of asymmetric sequences in turbidite successions, four issues have been investigated: (1) selecting methods for testing for asymmetric trends and randomness, (2) evaluating the power of

the selected methods, (3) determining minimum sample size for the tests (minimum number of beds in a sandstone packet), (4) selecting methods to statistically recognize sand-bed packets in turbidite sections (segmentation of sections).

This chapter shows:

1) Kendall's rank correlation test, Spearman's rank correlation test, and Pearson's linear correlation test are all powerful for testing for asymmetric trends. Kendall's test is the most powerful. Four tests for randomness (turning points test, rank differences test, median crossing test, length-of-runs test) are not very powerful and should only be used to check for other possible patterns in turbidite sandstone packets (Chapter 4).

2) Sandstone packets with at least four beds having different values of bed-thickness or grain-size can be tested for asymmetric trends using the three correlation methods.

3) Turbidite sections involved in this study were statistically segmented, and a total of 286 sandstone packets (or segments) were selected. For the segmentation of turbidite sections into sand-bed packets and silt-mud bed intervals, the split-moving window technique is preferred (see Fig. 3.6). Two subjective decisions are still required: (1) a selection of window width, and (2) a cross-check of segment boundaries with the field facies columns to identify problems and perhaps reassign some boundaries. The window width of 10 points is recommended for sand packet recognition leading to analysis of short-term cyclicity. For long-term cycles, a wider window would be required. Anyone who uses these methods must accept that statistical segmentation is a strong guide, but cannot unambiguously identify every boundary in complex natural successions.

However, these procedures are much more objective and reproducible than the simple decision on packet boundaries by visual inspection of graphic columns or field weathering profiles.

Chapter 4

STATISTICAL RESULTS OF TESTS FOR ASYMMETRIC TRENDS

4.1 Introduction

Three questions this study intends to answer are: (1) do most submarine-fan turbidite successions contain statistically demonstrable asymmetric upward thickening and thinning or upward coarsening and fining trends, or other short-term patterns in bed thickness and/or grain-size, such as step-wise pattern (Pickering et al., 1989); (2) can those trends be used to recognize environments; and (3) are asymmetric trends better developed in some turbidite sections than in others? This chapter aims to answer these questions.

The statistical tests applied to bed-thickness series in this study use the thicknesses of the sandy divisions of beds (including minor conglomerate, sandstone, and siltstone). Other researchers have used the same procedure (e.g. Mutti and Ricci Lucchi, 1972; Ricci Lucchi, 1975; Lowey, 1992) because it is difficult to impossible in most turbidite sections to separate Bouma divisions d and e of a sand-mud or silt-mud couplet from (a) a younger mud turbidite, or (b) muddy sediments deposited by other processes (e.g., hemipelagic and/or pelagic sediments).

4.2 Tests for Trends and Randomness

4.2.1 Tests Using the Bed Thicknesses of Sandstone Packets

The 286 sandstone packets which were statistically selected from 28 turbidite sections (Table 1.1) were tested for trends and randomness using the Fortran-77 program ASYMRAN.FOR (Appendix II-1). In all cases, the stratigraphic variable is bed number, not height in the sections (Hiscott, 1981). The 286 sandstone packets were plotted with bed thickness versus bed number and are shown in Appendix III. The significance levels at which the null hypothesis of randomness or no trend was rejected for each test, together with bed thickness data, are attached. The details of the results of these tests are given in Appendix IV-1.

Table 4.1 shows the number of sequences for which the null hypothesis of individual tests was rejected at various significance levels. A significance level $\alpha \leq 10\%$ is preferred, this being the maximum value generally used in statistical analyses of natural phenomena. At this significance level, the three correlation tests are able to recognize asymmetric trends with or without superimposed noise (Fig. 3.2a-b, Figs. 4.1, 4.2). Only one in ten sequences generated by random processes should pass each test at this significance level (Type I error).

Based on the experiment in power estimation of the employed tests and on reviewing the 286 plots of bed number versus bed thickness (Appendix III), a sandstone packet is considered as an asymmetric sequence if any of the following statements are true: (1) the null hypothesis was rejected for all three correlation tests at $\alpha \leq 10\%$ (Fig. 4.1, sequences

1, 2, 3, and 4); (2) the null hypothesis was rejected for Kendall's rank correlation test at $\alpha \leq 10\%$ and one of Spearman's and Pearson's correlation tests at $\alpha \leq 15\%$ (Fig. 4.1, sequence 5); (3) the null hypothesis was rejected for Kendall's test at $\alpha \leq 15\%$ and for Spearman's test at $\alpha \leq 10\%$ (Fig. 4.1, sequence 6). Since Pearson's correlation test is not as powerful as Kendall's and Spearman's tests, a sequence is not deemed to be asymmetric if it passed Pearson's test at $\alpha \leq 10\%$, but did not pass the other two correlation tests at $\alpha \leq 10\%$ or close to 10% level (Fig. 4.2, sequence 5).

Sequences in Figure 4.1, selected from the 286 analyzed sandstone packets, are examples of asymmetric sequences recognized by the three correlation tests using the criteria outlined above. Figure 4.2 shows examples from this same set of 286 packets of non-asymmetric or random sequences; these could only pass the three correlation tests at significance levels in the range 10% to 32%. Using $\alpha \leq 32\%$, as Lowey (1992) did, one would falsely attribute order to many random sequences, i.e., Type I error is unacceptable large.

The number and percentage of sequences for which the null hypothesis of one or more tests was rejected at $\alpha \leq 10\%$ are listed in Table 4.2. Only 34 out of 286 sandstone packets (11.9%) possess asymmetric trends using the above criteria. Note that for $\alpha =$ 10%, samples from a population of random bed-thickness series should pass such statistical tests 10% of the time (Type I error).

The binomial probability of exactly x successes in n random trials is given by

Table 4.1 The number and percentage of sequences passing individual tests for bed thickness trends at different significance levels (total sequences = 286)

Significance Level	Kendall's correlation		Spearman's correlation		Pearson's correlation		Turning Points		Rank Difference		Median Crossing		Length-of-Runs	
	n	%	n	%	n	%	n	%	n	%	n	%	n	%
< 5%	18	6.3%	19	6.6%	20	7%	24	8.4%	26	9.1%	18	6.3%	73	25.5%
< 10%	33	11.5%	30	10.5%	31	10.8%	46	16.1%	41	14.3%	47	16.4%	108	37.8%
< 15%	48	16.8%	44	15.4%	51	17.8%	59	20.6%	63	22.0%	52	18.2%	127	44.4%
< 20%	70	24.5%	65	22.7%	65	22.7%	91	31.8%	76	26.6%	66	23.1%	138	48.3%
< 25%	78	27.3%	74	25.9%	79	27.6%	98	34.3%	94	32.9%	67	23.4%	164	57.3%
< 30%	87	30.4%	88	30.8%	100	35.0%	112	39.2%	104	36.4%	86	30.1%	173	60.5%
< 35%	101	35.3%	102	35.7%	109	38.1%	125	43.7%	124	43.4%	98	34.3%	193	67.5%
< 40%	112	39.2%	122	42.7%	118	41.3%	126	44.1%	130	45.5%	108	37.8%	205	71.7%
< 45%	128	44.8%	133	46.5%	131	45.8%	149	52.1%	141	49.3%	131	45.8%	208	72.7%
< 50%	145	50.7%	138	48.3%	147	51.4%	160	55.9%	157	54.9%	139	48.6%	224	78.3%
< 55%	160	55.9%	152	53.1%	164	57.3%	166	58.0%	187	65.4%	144	50.3%	236	82.5%
< 60%	179	62.6%	167	58.4%	176	61.5%	189	66.1%	196	68.5%	182	63.6%	242	84.6%
< 65%	198	69.2%	194	67.8%	188	65.7%	199	69.6%	208	72.7%	183	64.0%	246	86.0%
< 70%	212	74.1%	204	71.3%	204	71.3%	211	73.8%	216	75.5%	210	73.4%	248	86.7%
< 75%	221	77.3%	222	77.6%	216	75.5%	223	78.0%	232	81.1%	239	83.6%	268	93.7%
< 80%	230	80.4%	239	83.6%	226	79.0%	236	82.5%	241	84.3%	262	91.6%	276	96.5%
< 85%	240	83.9%	247	86.4%	244	85.3%	252	88.1%	245	85.7%	277	96.9%	279	97.6%
< 90%	253	88.5%	267	93.4%	261	91.3%	257	89.9%	257	89.9%	280	97.9%	284	99.3%
< 95%	266	93%	277	96.9%	271	94.8%	258	90.2%	266	93.0%	280	97.9%	285	99.7%
< 100%	286	100%	286	100%	286	100%	286	100%	286	100%	286	100%	286	100%

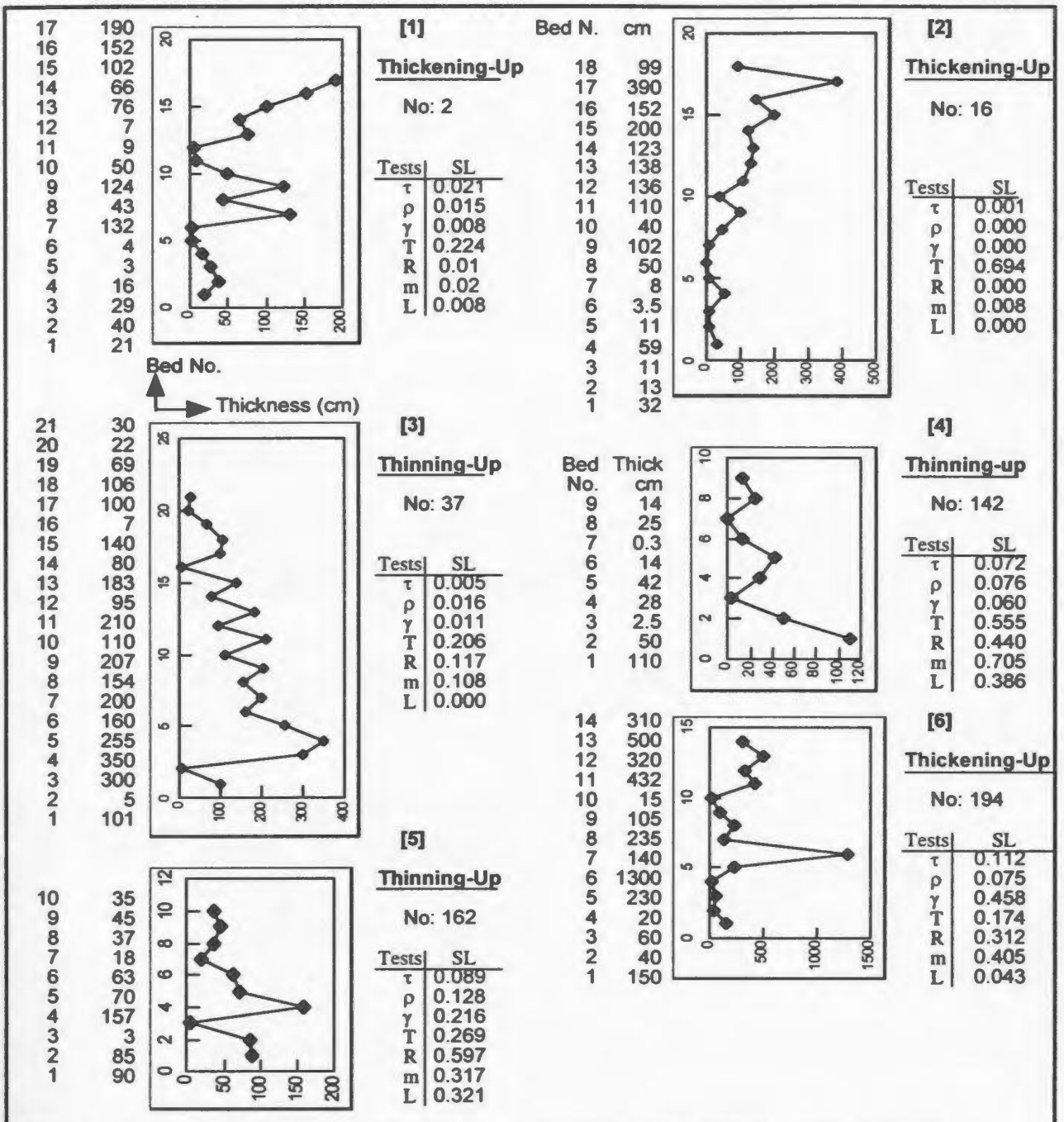

Tests τ, ρ, γ, T, R, m, and L represent Kendall's, Spearman's and Pearson's correlation tests, turning point test, rank difference test, median crossing test, and length-of-runs test, respectively. SL = significance levels at which a sequence passed individual tests.

Fig. 4.1 Examples of asymmetric sequences statistically identified from the 286 analyzed sandstone packets. Note: sequences [1], [2], [3], and [4] passed all three correlation tests at the significance level (SL) < 10%. Sequence [5] passed Kendall's correlation test at SL < 10%, Spearman's correlation test at SL < 15%, and Pearson's correlation test at SL = 21.6%. Sequence [6] passed Spearman's test at SL < 10%, and Kendall's test at SL < 15%, but Pearson's test at SL = 45.8%.

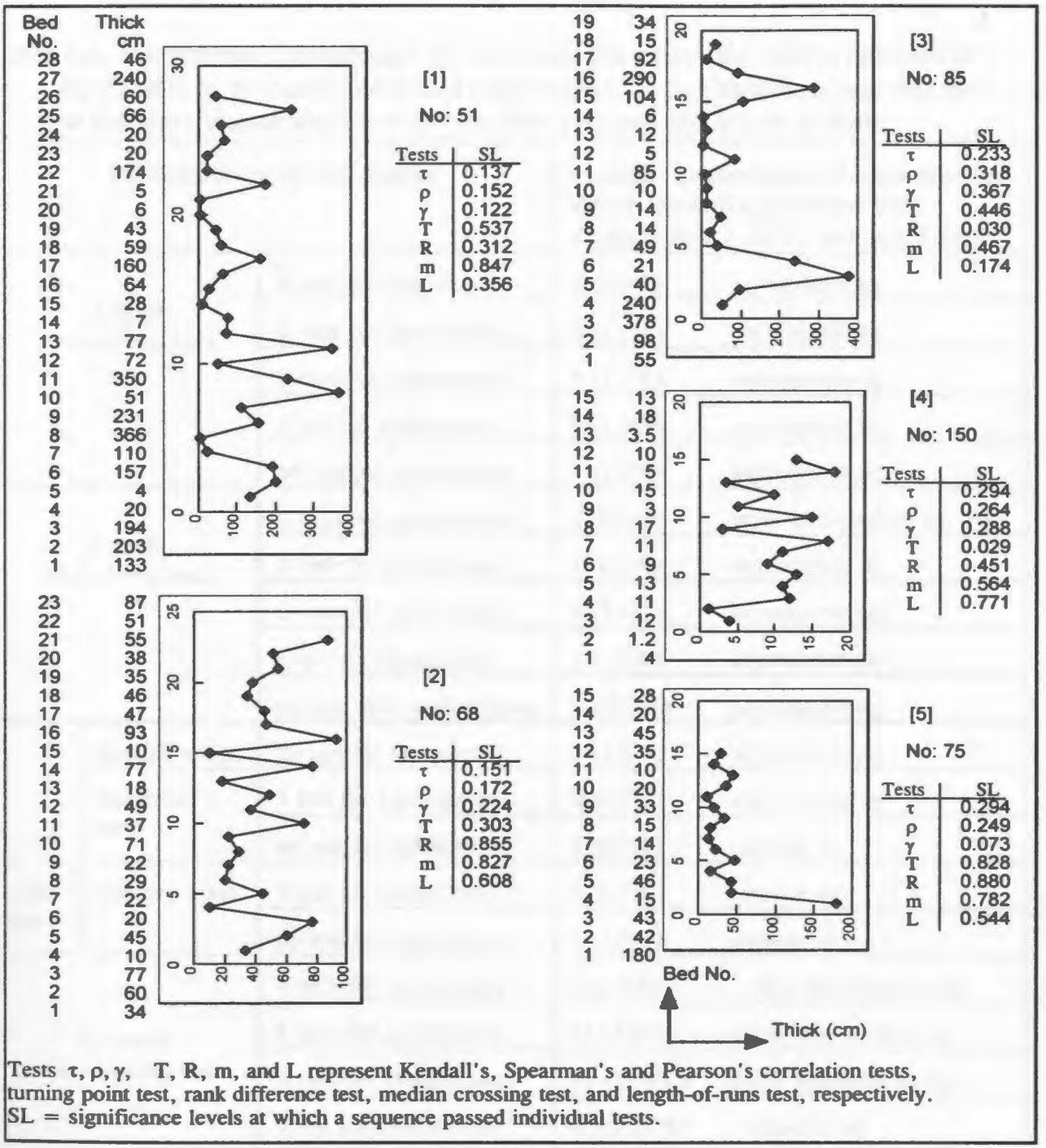

Fig. 4.2 Examples of sequences, selected from the 286 analyzed sandstone packets, that passed three or two correlation tests (Kendall's, Spearman's and Pearson's correlation tests) at significance levels between 10% and 32%. Using a test significance level of SL = 10%, none of these sequences can be considered to be asymmetric (i.e. the null hypothesis of no trend cannot be rejected). Sequence [5] does not show an asymmetric trend, but it passed Pearson's test at SL < 10%. This indicates that Pearson's test is not as powerful as Kendall's and Spearman's correlation tests.

Table 4.2 The number (percentage) of sequences for which the null hypothesis of no trend (i.e., no correlation) and randomness for bed-thickness was rejected at the significance level α = 10% in 286 analysed sandstone packets

Combinations of tests passed			Number (percentage) of sequences for which the null hypotheses were rejected at $\alpha \leq 10\%$, and conclusion
3 trend (correlation) tests		4 tests for randomness	2 (0.7%) asymmetric sq.
		3 tests for randomness	4 (1.4%) asymmetric sq.
		2 tests for randomness	5 (1.7%) asymmetric sq.
		1 test for randomness	5 (1.7%) asymmetric sq.
		no test for randomness	4 (1.4%) asymmetric sq.
2 trend (correlation) tests		3 tests for randomness	1 (0.3%) other non-random sq. ***
		3 tests for randomness	1 (0.3%) asymmetric sq.
		2 tests for randomness	3 (1.0%) asymmetric sq.
		1 test for randomness	3 (1.0%) asymmetric sq.
		no test for randomness	2 (0.7%) asymmetric sq.
1 trend test	Kendall's test	no test for randomness	3 (1.0%) asymmetric sq. *
	Spearman's test	1 test for randomness	2 (0.7%) asymmetric sq. **
		no test for randomness	1 (0.3%) random sq. ***
	Pearson's test	1 test for randomness	2 (0.7%) random sq.
		no test for randomness	3 (1.0%) random sq.
No trend (no correlation) tests		4 tests for randomness	3 (1.0%) other non-random sq.
		3 tests for randomness	11 (3.8%) other non-random sq.
		2 tests for randomness	39 (13.6%) other non-random sq.
		1 test for randomness	62 (21.7%) random sq.
		no test for randomness	130 (45.5%) random sq.
Total 34 (11.9%) asymmetric sq. recognized in 286 sst. packets			

Note: *--passed at least one of the other two trend tests at a significance level $\alpha < 15\%$
**--passed Kendall's correlation test at $\alpha < 15\%$
***--could only passed Kendall's correlation test at $\alpha > 15\%$

$$f(x) = \frac{n!}{x!(n-x)!} p^{x}(1-p)^{n-x} \quad \text{..... (Eqn. 4.1)}$$

where p is the probability of success in a single trial. When n is large and p is small, $f(x)$ becomes a very tedious quantity to calculate. In this situation, the binomial distribution can be approximated by the normal distribution (Kreyszig, 1967, p. 775; Simpson, 1960, p. 137); that is,

$$f(x) \sim f^{*}(x) \qquad (x = 0, 1, 2, ..., n),$$

where

$$f^{*}(x) = \frac{1}{\sqrt{2\pi}\sqrt{npq}} e^{-z^{2}/2} \quad \text{..... (Eqn. 4.2)}$$

and

$$q = 1 - p, \qquad Z = \frac{x - np}{\sqrt{npq}}$$

When $n = 30$, $p = 0.1$, the approximation of $f(x)$ by $f^{*}(x)$, as given below, is quite good.

x = number of successes	0	1	2	3	4	5	6
$f(x)$	0.0459	0.1158	0.2018	0.2428	0.2017	0.1158	0.0459
$f^{*}(x)$	0.0424	0.1413	0.2277	0.2361	0.1771	0.1023	0.0474

At the 10% significance level, the cumulative binomial probability of rejecting the null hypothesis of non-correlation between two variables, 33 or more times (Kendall's test, Table 4.1) in 286 trials, when it is true equals 0.22 (calculated using Eqn 4.2); 30 or more times (Spearman's test, Table 4.1) is 0.43; and 31 or more times (Pearson's test, Table 4.1) is 0.35. These probabilities are sufficiently high to suggest that the number

of asymmetric sequences identified by the three correlation tests in the 286 sandstone packets can easily be attributed to random processes.

Table 4.3a-b shows the distribution and percentage of the 34 asymmetric sequences in different turbidite sections and/or locations. In addition, 15 of the 34 asymmetric sequences identified by the three correlation tests are non-random based on two or more tests for randomness (Table 4.2). However, the three correlation tests are sufficiently powerful that the less consistent tests for randomness (Fig. 3.2) are not given much weight in the confirmation of asymmetric trends. Instead, tests for randomness are only relied on to identify symmetrical or irregular trends. Note that a rejection of the null hypothesis of randomness only signals the probability of a trend, but cannot give any information about the nature of the trend. The character of the trend must then be subjectively determined by eye, from a plot of bed number against bed-thickness.

Because a single test for randomness may not give a definitive conclusion, only sequences for which the null hypothesis of two or more such tests is rejected at $\alpha \leq 10\%$ need to be checked for the existence of trends. Only 54 of 286 sandstone packets (18.9%) meet this condition (see Table 4.2), and have been checked. Of these, 23 sequences more or less show a wavy pattern or a grouping of thin and thick beds (Fig. 4.3, sequences [1] and [2]), 30 sequences fluctuate strongly (Fig. 4.3, sequences [3] and [4]), 1 sequence displays a symmetric trend (Fig. 4.3, sequence [5]).

Table 4.3a The number and percentage of asymmetric upward thinning and thickening sequences statistically identified (at a significance level $\alpha = 10\%$) in individual sections or locations

Location		Stratigraphy	Proposed Environments	No.of sections	Thick(m) (No. of beds)	No. of sst. packets	No. that thk up	No. that thin up	Asym (%)
ITALY	Santerno Valley	Miocene Marnoso-arenacea	Lobes & basin plain sand sheets (Ricci Lucchi, 1975)	4	445.27 (738)	30	2	0	9.1%
	Savio Valley		Channel fill (Ricci Lucchi, 1975)	2	49.48 (75)	3	1	0	
CALIFORNIA	Monticello Dam	Upper Cretaceous Venado Formation	Channel fill (Ingersoll, 1978)	1	383.7 (379)	23	1	3	17.4%
	Cache Creek	Upper Cretaceous Sites Formation	Lobes (Ingersoll, 1978)	1	277.99 (565)	22	1	2	13.6%
QUEBEC	Cap Ste-Anne	Lower Ordovician Tourelle Formation	Lobes (Hiscott, 1980)	2	222.3 (523)	9	0	2	22.2%
	Petite-Vallée	Upper Ordovician Cloridorme Formation	Lobes (Hiscott et al., 1986)	1	452.45 (2893)	67	3	4	10.5%

Continued ...

Table 4.3b The number and percentage of asymmetric upward thinning and thickening sequences statistically identified (at a significance level $\alpha = 10\%$) in individual sections or locations (end)

Location	Stratigraphy	Proposed Environments	No. of sections	Thick(m) (No. of beds)	No. of sst. packets	No. that thicken up	No. that thin up	Asym (%)
Amazon Fan	Modern	Lobes related to channel bifurcation (Pirmez et al., in press)	3	335.08 (485)	17	0	2	11.9%
Barbados	Tertiary	Channel fill (Larue & Speed, 1982)	2	109.68 (183)	10	0	2	20%
British Columbia	Upper Cretaceous Nanaimo Formation	Channel fill (England & Hiscott, 1992)	7	572.94 (560)	26	1	3	15.4%
Arkansas DeGray Lake	Pennsylvanian Jackfork Group	Crevasse-splay lobes & levee (Bouma et al., 1995)	2	212.89 (2514)	42	1	2	7.1%
Northern Norway, Nalneset	Upper Precambrian Kongsfjord Formation	Channel-lobe transition zone (Drinkwater, 1995)	3	247.98 (825)	37	2	2	10.8%
TOTAL			28	3309.77 (9740)	286	12	22	11.9%
Number and percentage expected from 286 samples of a random population for $\alpha = 10\%$						~14	~14	10%

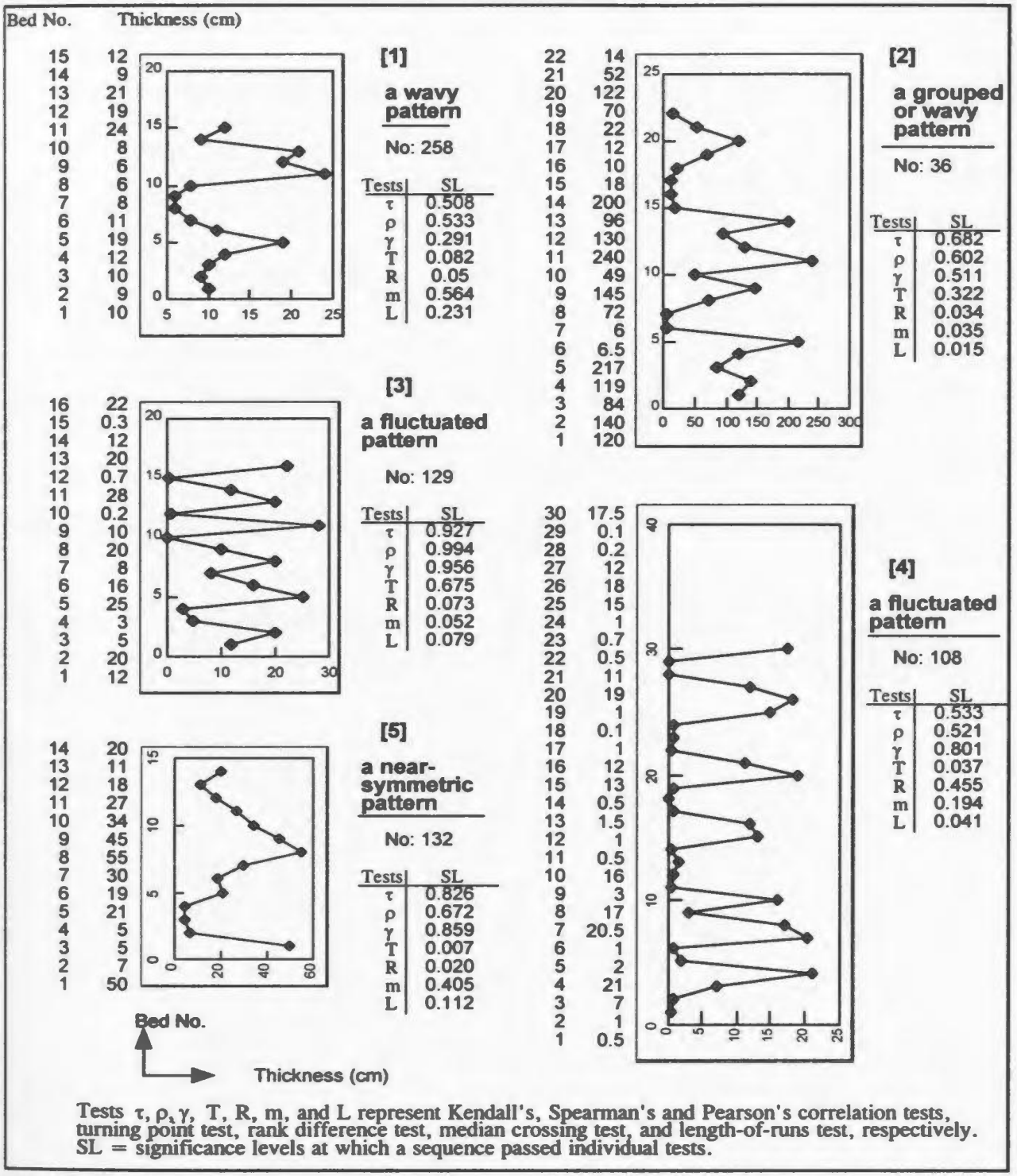

Fig. 4.3 Examples of sequences that show trends other than asymmetric trends, selected from the 286 analyzed sandstone packets. The significance level at which a sequence could pass individual tests is indicated.

4.2.2 Tests for Trends and Randomness Using Filtered Bed-Thickness Data

Field observation suggests that noise in the bed-thickness profile through most sandstone packets is caused by thin beds of siltstone. Even though the three correlation tests effectively ignore such noise and successfully identify any asymmetric trends, an experiment was undertaken to filter out the noise caused by thin bedded siltstone in sandstone packets by deleting data entries for siltstone beds thinner than 10 cm from the packets.

After removal of thin siltstone beds, the number of statistically identified sandstone packets is 280, because the bed number in six of the initial 286 packets decreased to less than four. The results of tests for randomness and trends on these 280 filtered packets differ little from results for the 286 unfiltered packets: 35 asymmetric sequences and 51 other non-random sequences were identified at a significance level of $\alpha = 10\%$ in these 280 sequences by running the program ASYMRAN.FOR (Table 4.4). This is only one asymmetric sequence more than, and only three other non-random sequences less than were previously recognized. Hence, filtering has no real effect on overall results or conclusions about asymmetric cycles and other patterns.

4.2.3 Trend Tests for Grain Size

Popular models of turbidite bed-thickness and grain-size cyclicity (Mutti and Ricci Lucchi, 1972; Ricci Lucchi, 1975; Walker, 1978, 1984) predict that an upward

Table 4.4 The number (percentage) of sequences for which the null hypothesis of no trend (i.e., no correlation) and randomness for bed-thicknesses was rejected at the significance level $\alpha = 10\%$ in 280 thin-siltstone-filtered sandstone packets

Combinations of tests passed			Number (percentage) of sequences for which the null hypotheses were rejected at $\alpha \leq 10\%$, and conclusion
3 trend (correlation) tests		4 tests for randomness	1 (0.4%) asymmetric sq.
		3 tests for randomness	6 (2.1%) asymmetric sq.
		2 tests for randomness	6 (2.1%) asymmetric sq.
		1 test for randomness	6 (2.1%) asymmetric sq.
		no test for randomness	5 (1.8%) asymmetric sq.
2 trend (correlation) tests		3 tests for randomness	1 (0.4%) other non-random sq. ***
		3 tests for randomness	1 (0.4%) asymmetric sq.
		2 tests for randomness	2 (0.7%) asymmetric sq.
		1 test for randomness	4 (1.4) asymmetric sq.
		non test for randomness	1 (0.4%) asymmetric sq.
1 trend test	Kendall's test	no test for randomness	2 (0.7%) asymmetric sq. *
	Spearman's test	1 test for randomness	1 (0.4%) asymmetric sq. **
		no test for randomness	3 (1.1%) random sq. ***
	Pearson's test	3 tests for randomness	1 (0.4%) other non-random sq.
		1 test for randomness	1 (0.4%) random sq.
		no tests for randomness	3 (1.1%) random sq.
No trend (no correlation) tests		3 tests for randomness	12 (4.3%) other non-random sq.
		2 tests for randomness	37 (13.2%) other non-random sq.
		1 test for randomness	51 (18.2%) random sq.
		no test for randomness	136 (48.6%) random sq.
Total 35 (12.5%) asymmetric sq. recognized in 280 filtered sst. packets			

Note: *--passed at least one of the other two trend tests at the significant level $\alpha < 15\%$
**--passed Kendall's correlation test at $\alpha < 15\%$
***--could only pass Kendall's correlation test at $\alpha > 15\%$

increase or decrease in bed thickness would be accompanied by a parallel increase or decrease in grain size. In order to test grain-size trends, a grain-size "score" was calculated for each bed, based on the ϕ scale, where the score = $-4 \times$ (thickness proportion of pebble and granule divisions) $+ 0 \times$ (thickness proportion of coarse sand divisions) $+ 1.5 \times$ (thickness proportion of medium sand divisions) $+ 3 \times$ (thickness proportion of fine sand divisions) $+ 7 \times$ (thickness proportion of silt divisions). The numerical constants are mid-point ϕ sizes for each grain-size class recognized in the field. Hence, the grain-size score is an estimate of average grain-size for each bed. Values of this score could be calculated for the measured sections in California, Italy, Barbados, and British Columbia, because individual gravelly and sandy beds in these sections had been divided during field description into divisions according to grain size and structures (Appendix I). The grain-size scores of 86 sandstone packets at these localities were statistically tested for trends by using the Fortran-77 program ASYMRAN.FOR.

In packets of amalgamated beds, tied values of grain-size score are common. For a packet with some tied values, the null hypothesis of tests for randomness, especially the turning points test, median crossing test, and length-of-runs test, may be rejected because the tied values impose a grouped pattern on the data. In such cases, the tests for randomness of the grain-size scores give spurious results. The three correlation tests, however, do not lose their testing power for most packets with ties. For example, Kendall's correlation test can successfully test a sequence with 10 tied

values out of 17 data points (sequence C in Fig. 4.4); however, Spearman's and Pearson's correlation tests misidentified this example as an asymmetric sequence. As a rule of thumb, it is recommended that a sequence only be considered to coarsen or fine upward if it passes Kendall's test and at least one of the other two correlation tests at a significance level $\alpha \leq 10\%$. Based on this criterion, 25 (29%) of the 86 sandstone packets coarsen or fine upward (Table 4.5 and 4.6). Figure 4.4 shows examples of sequences so determined to have asymmetric trends in grain size. The detailed results of the tests are presented in Appendix IV-2.

Note that proportionally more sandstone packets show significant grain-size trends (Table 4.5) than bed-thickness trends (Table 4.1). Fourteen of these twenty-five asymmetric sequences in grain-size are not accompanied by a parallel trend in bed-thickness; one upward fining sequence shows an opposite trend in bed-thickness (upward thickening); and the remaining ten upward fining and coarsening sequences are consistent with upward thinning and thickening trends. These examples suggest that grain-size might not correlate positively (or at all) with bed-thickness in turbidite sandstone packets. To investigate this issue, plots of log values of grain-size (mm) against log values of bed-thicknesses (cm) for sandstone packets from California, Italy, Barbados, and British Columbia are presented in Figure 4.5. Note that in order to obtain $\log_{10}$ values for both bed thickness (cm) and grain size (mm), grain-size "scores" which are based on the ϕ scale were first converted back to equivalent millimeter values. The data show no visual linear correlation between these two variables. This is

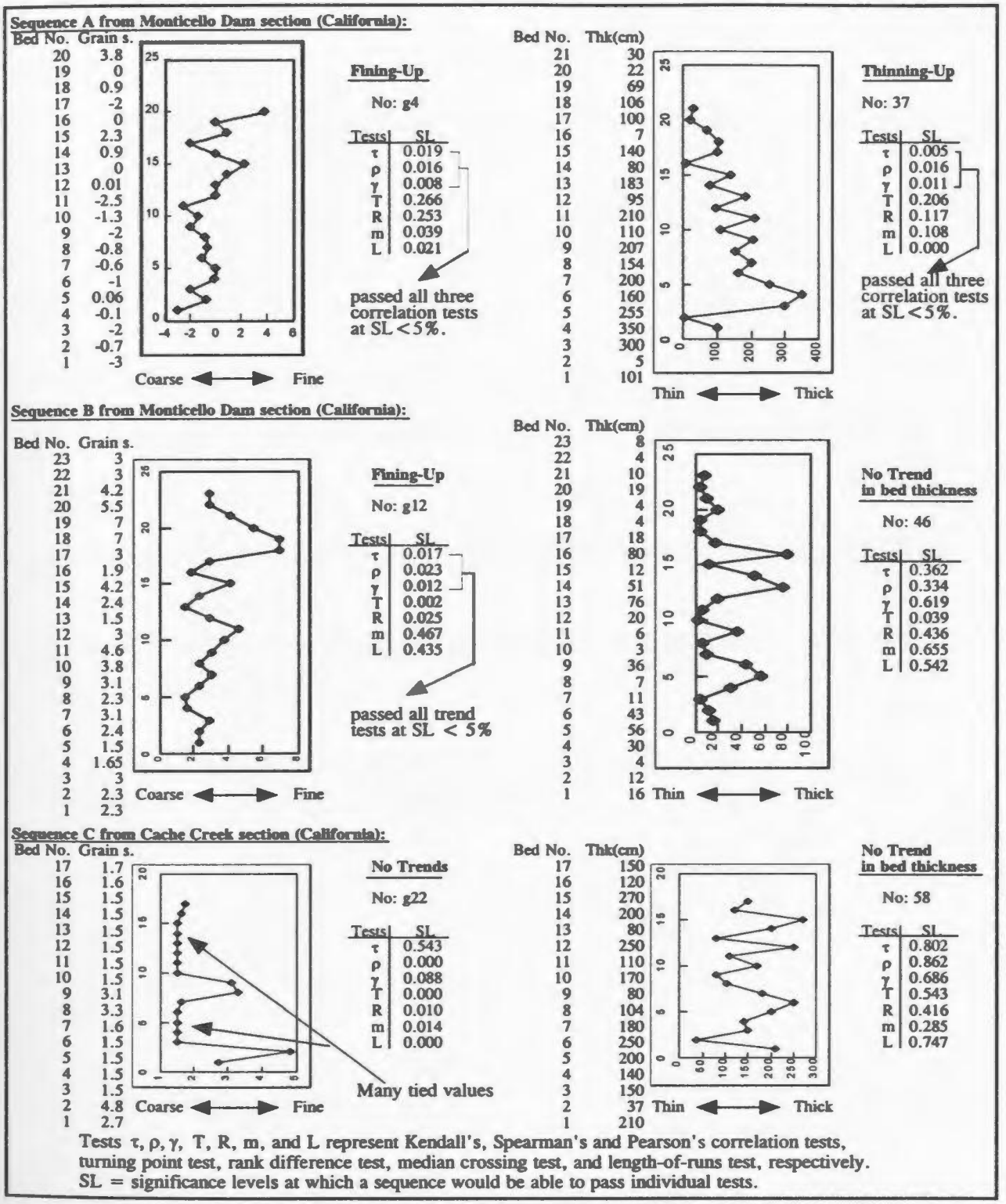

Fig. 4.4 Examples of grain-size trends, accompanied by the bed thickness profiles of the corresponding sandstone packets. Sequence A is an upward fining and thinning sequence; sequence B is an upward fining sequence without an asymmetric trend in bed thickness; sequence C, containing many tied values, could not pass Kendall's test (SL = 54.3%).

Table 4.5 The number and percentage of sequences that would pass individual tests for grain size trends at different significance levels (total sequences = 86)

Significance Level	Kendall's correlation		Spearman's correlation		Pearson's correlation		Turning Point		Rank Difference		Median Crossing		Length-of-Runs	
	n	%	n	%	n	%	n	%	n	%	n	%	n	%
< 5%	18	20.9%	20	23.3%	16	18.6%	24	27.9%	18	20.9%	13	15.1%	27	31.4%
< 10%	24	27.9%	25	29.1%	22	25.6%	35	40.7%	23	26.7%	22	25.6%	38	44.2%
< 15%	27	31.4%	31	36.0%	25	29.1%	38	44.2%	31	36.0%	25	29.1%	40	46.5%
< 20%	32	37.2%	35	40.7%	30	34.9%	44	51.2%	34	39.5%	33	38.4%	45	52.3%
< 25%	34	39.5%	40	46.5%	37	43.0%	46	53.5%	40	46.5%	34	39.5%	52	60.5%
< 30%	34	39.5%	44	51.2%	41	47.7%	51	59.3%	42	48.8%	37	43.0%	55	64.0%
< 35%	38	44.2%	47	54.7%	44	51.2%	53	61.6%	48	55.8%	42	48.8%	62	72.1%
< 40%	40	46.5%	50	58.1%	49	57.0%	53	61.6%	50	58.1%	44	51.2%	64	74.4%
< 45%	47	54.7%	52	60.5%	51	59.3%	56	65.1%	52	60.5%	45	52.3%	69	80.2%
< 50%	51	59.3%	52	60.5%	51	59.3%	57	66.3%	54	62.8%	49	57.0%	73	84.9%
< 55%	57	66.3%	53	61.6%	55	64.0%	58	67.4%	63	73.3%	51	59.3%	77	89.5%
< 60%	59	68.6%	57	66.3%	58	67.4%	62	72.1%	67	77.9%	60	69.8%	78	90.7%
< 65%	65	75.6%	62	72.1%	62	72.1%	65	75.6%	67	77.9%	60	69.8%	78	90.7%
< 70%	71	82.6%	65	75.6%	67	77.9%	70	81.4%	69	80.2%	69	80.2%	80	93.0%
< 75%	75	87.2%	69	80.2%	69	80.2%	74	86.0%	77	89.5%	76	88.4%	85	98.8%
< 80%	77	89.5%	72	83.7%	69	80.2%	77	89.5%	79	91.9%	83	96.5%	85	98.8%
< 85%	80	93.0%	79	91.9%	71	82.6%	80	93.0%	79	91.9%	84	97.7%	86	100%
< 90%	82	95.3%	80	93.0%	76	88.4%	80	93.0%	83	96.5%	84	97.7%	86	100%
< 95%	85	98.8%	82	95.3%	83	96.5%	80	93.0%	84	97.7%	84	97.7%	86	100%
< 100%	86	100.0%	86	100.0%	86	100.0%	86	100.0%	86	100.0%	86	100%	86	100%

Table 4.6 The number and percentage of sequences with asymmetric trends in grain size at different turbidite sections

Trends in Grain Size	Associated trends in bed thickness	Monticello Dam Section (California)	Cache Creek Section (California)	Sections of Northern Italian Apennines	Barbados Sections	British Columbia Sections
upward coarsening	upward thickening	0	1	2	0	0
	upward thinning	0	0	0	0	0
	no asymmetric trend	2	0	0	1	1
upward fining	upward thickening	1	0	0	0	0
	upward thinning	3	1	0	2	1
	no asymmetric trend	4	1	1	2	2
total number of sequences with asymmetric trends in grain size		10	3	3	5	4
number of tested sequences		20	14	30	10	12
% of sequences with grain-size trends		50.0%	21.4%	10.0%	50.0%	33.3%

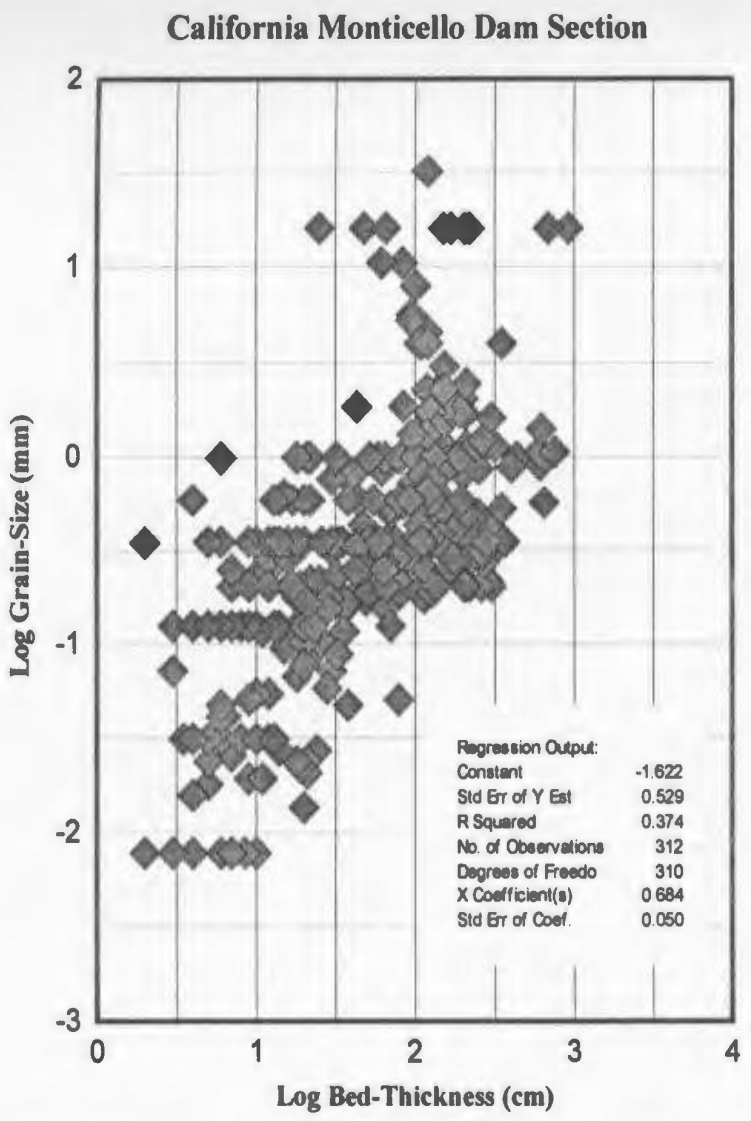

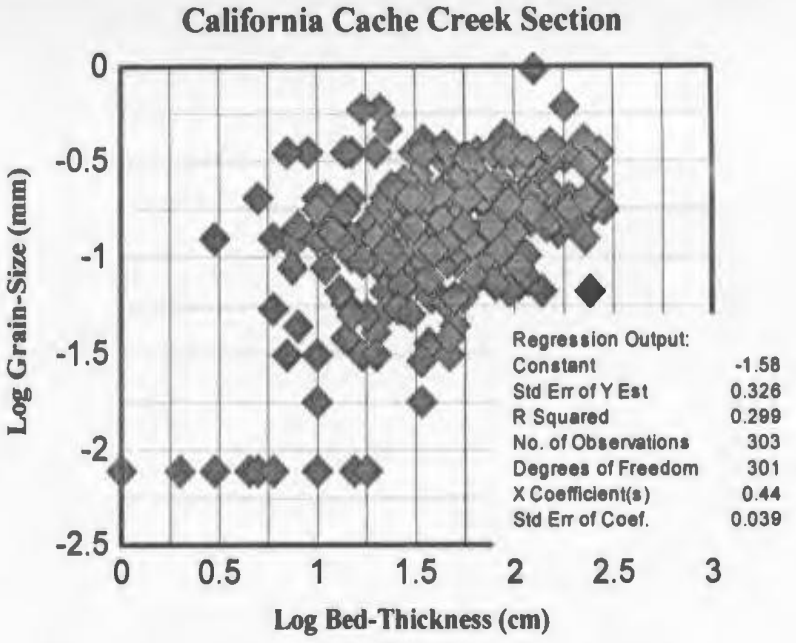

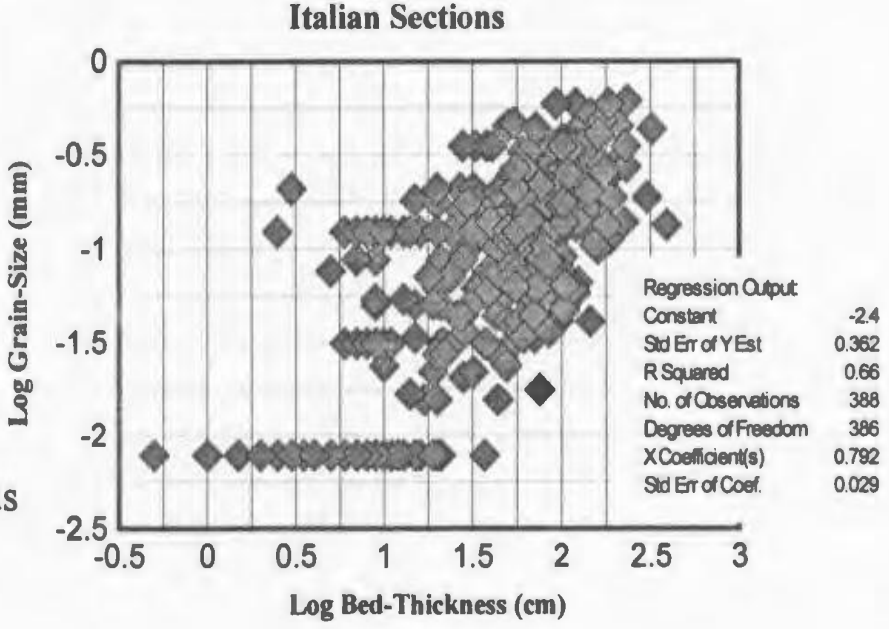

Fig. 4.5a Log values of bed thickness (cm) versus log values of grain size (mm), together with outputs of linear regression analysis.

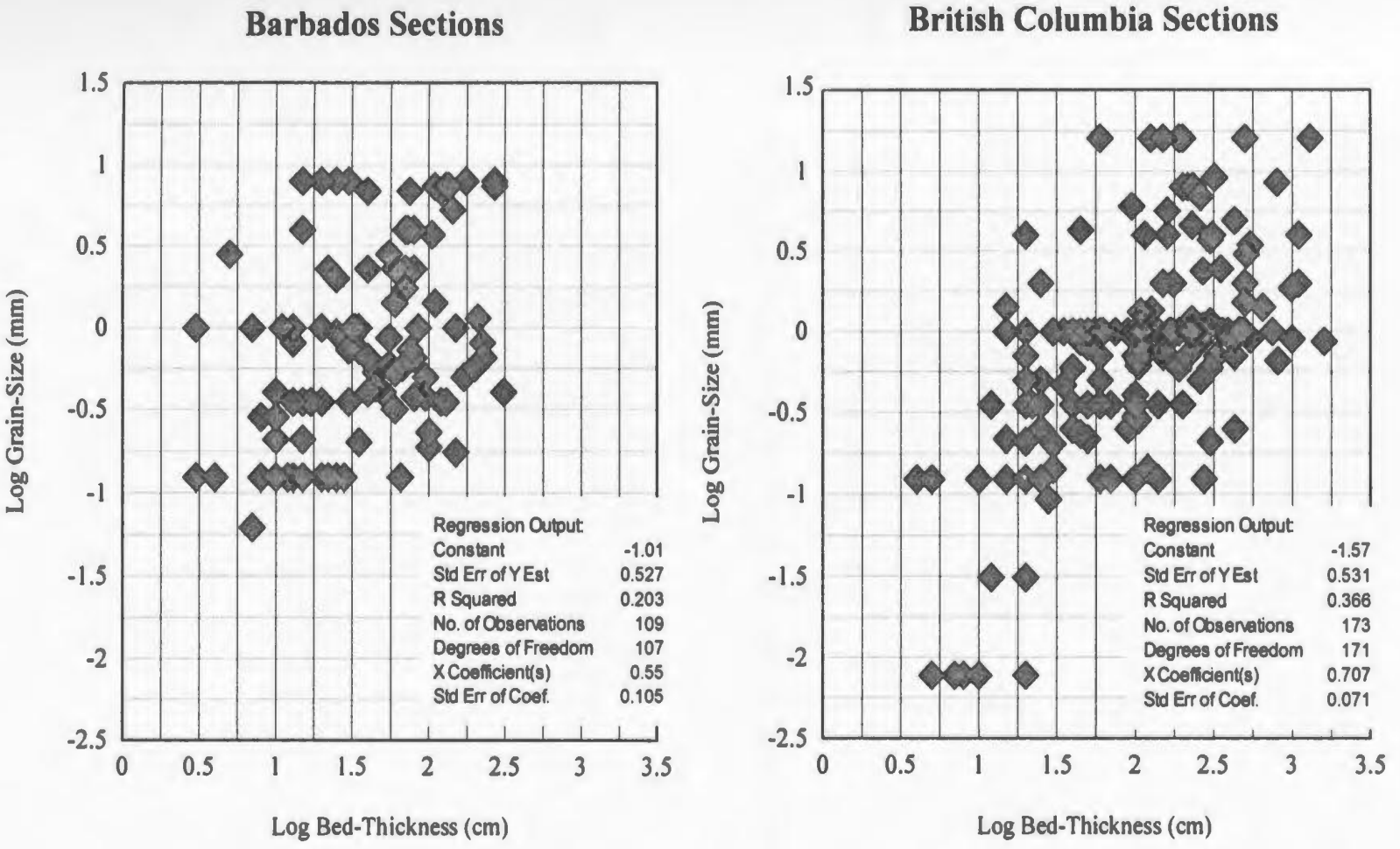

Fig. 4.5b Log values of bed thickness (cm) versus log values of grain size (mm), together with outputs of linear regression analysis.

consistent with the results of linear regression analysis, attached to Figure 4.5. A perfect linear correlation between two variables would result in a value of R^2 equal to 1. All, but the Italian sections, have R^2 values of 0.4 or less. The weak correlation (R^2 = 0.66) between bed-thickness and grain-size score in the Italian sections may be caused by abundant fine and thin beds contained in sandstone packets (see the data points of fine and thin beds at the upper part of the plot in Figure 4.5).

The geographic distribution of the 25 upward coarsening and fining sequences is very uneven (Table 4.6). For example, in the sections measured in the northern Italian Apennines, only 3 (10%) of 30 sandstone packets show grain-size trends, whereas 10 (50%) of 20 sandstone and conglomerate packets at the Monticello Dam, California, have upward fining or coarsening character. Eight of the latter fine upward and two coarsen upward.

4.2.4 Trend Tests for Sedimentary Structures

It was expected that some upward fining sequences would be accompanied by an upward increase in preservation of upper Bouma divisions. To test for such trends, a structure "score" was calculated for each bed, where the score = 0 × (thickness proportion of massive division, T_a) + 1.5 × (thickness proportion of graded division, T_a) + 3 × (thickness proportion of sandy parallel-laminated division, T_b) + 7 × (thickness proportion of rippled division, T_c) + 8.5 × (thickness proportion of silt-mud parallel-laminated division, T_{d-e}). Values of this score for 69 sandstone packets

from the measured sections in California, Italy, and Barbados were used to test for trends by using the Fortran-77 program ASYMRAN.FOR.

Eleven (15.9%) of the 69 sandstone packets are statistically recognized as structurally asymmetric sequences; six show upward increase in and five upward decrease in preservation of upper Bouma divisions (Table 4.7; Appendix IV-3). The results from tests for sedimentary structure trends demonstrate that many packets with asymmetric grain-size trends do not develop a parallel asymmetric structure trend. In the sections measured in California, Italy, and Barbados, only 7 of 21 asymmetric sequences in grain-size (Table 4.6) show a parallel asymmetric structure trend. In the eighteen sandstone and conglomerate packets selected from the Monticello Dam section, nine have asymmetric trends in grain-size (eight fine upward, one coarsens upward). Five of these nine sequences have parallel asymmetric structure trends. In these cases, it appears that the upward fining sequences, at least, are related to an upward decrease in erosion and therefore an upward increase in the preservation of upper Bouma divisions (e.g., sandstone packets (37), (43), and (51) in Fig. 2.3).

4.3 Frequency Distributions of Test Statistics

Many statistical tests are based on the assumption that random variables are normally distributed (Davis, 1986). For standard normal distributions, 68% of observations fall between +1 and -1 standard deviations of the mean, about 95% between +2 and -2 standard deviations, and more than 99% between +3 and -3

Table 4.7 The number and percentage of sequences with asymmetric trends in sedimentary structures at different turbidite sections

Trends in sedimentary structures	Associated trends in grain-size	Monticello Dam Section (California)	Cache Creek Section (California)	Sections of Northern Italian Apennines	Barbados Sections
upward increase in upper Bouma divisions	upward fining	4	1	0	1
	upward coarsening	0	0	0	0
	no asymmetric trend	0	0	0	0
upward decrease in upper Bouma divisions	upward fining	0	0	0	0
	upward coarsening	1	0	0	0
	no asymmetric trend	0	2	2	0
total number of sequences with asymmetric trends in sedimentary structures		5	3	2	1
number of tested sequences		18	14	28	9
% of sequences with asymmetric structure trends		27.7%	21.4%	7.0%	11.0%

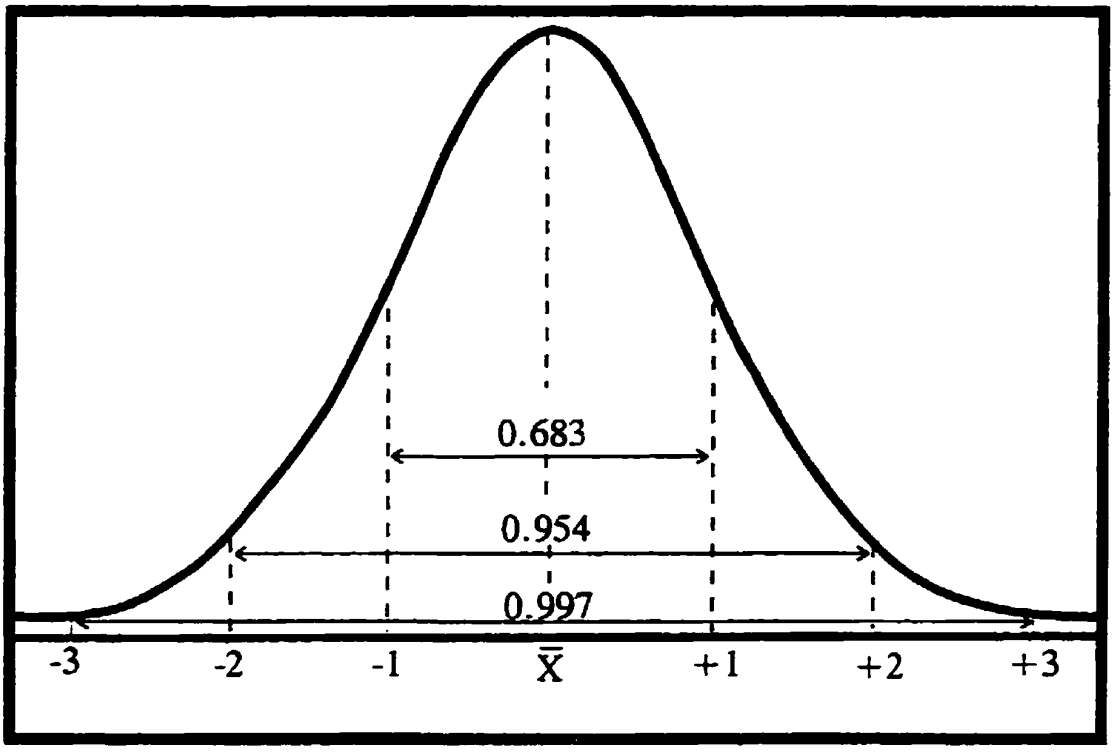

Fig. 4.6 Areas enclosed by increasing numbers of standard deviations for the standard normal distribution (from Davis, 1973).

standard deviations (Fig. 4.6).

The statistics of the three correlation tests and the three tests for randomness carried out on bed-thickness data from the 286 selected sandstone packets are distributed approximately normally (Fig. 4.7; Table 4.8). The mean and spread of values of the statistics for each correlation (trend) test is just what would be expected if a random process was controlling bed thickness. For the 286 tested sandstone packets, no more pass each test than can be ascribed to Type I error during testing of a randomly generated set of sequences. To strengthen this conclusion, the distributions of test statistics for 286 randomly shuffled sequences from the original 286 sandstone packets are presented in Figure 4.8 and Table 4.8. They are very similar to those of the original 286 sandstone packets (Fig. 4.7 and Table 4.8). For a random population, the normal distribution of τ, ρ and γ, with a mean = 0, has analytically been demonstrated by Kendall and Gibbons (1990, p. 60-70), Dixon and Massey (1957, p. 200), and Harper (in press).

4.4 Monte Carlo Simulation

The analytical calculation (using the cumulative binomial probability function Eqn. 4.2) of the probability of rejecting the null hypothesis in 286 random trials, and the frequency distributions of the statistics of the tests for the 286 sandstone packets (Fig. 4.7 and 4.8) suggest that even the 34 asymmetric upward thinning and thickening sequences (11.9% of total) may have been generated by random processes. Monte

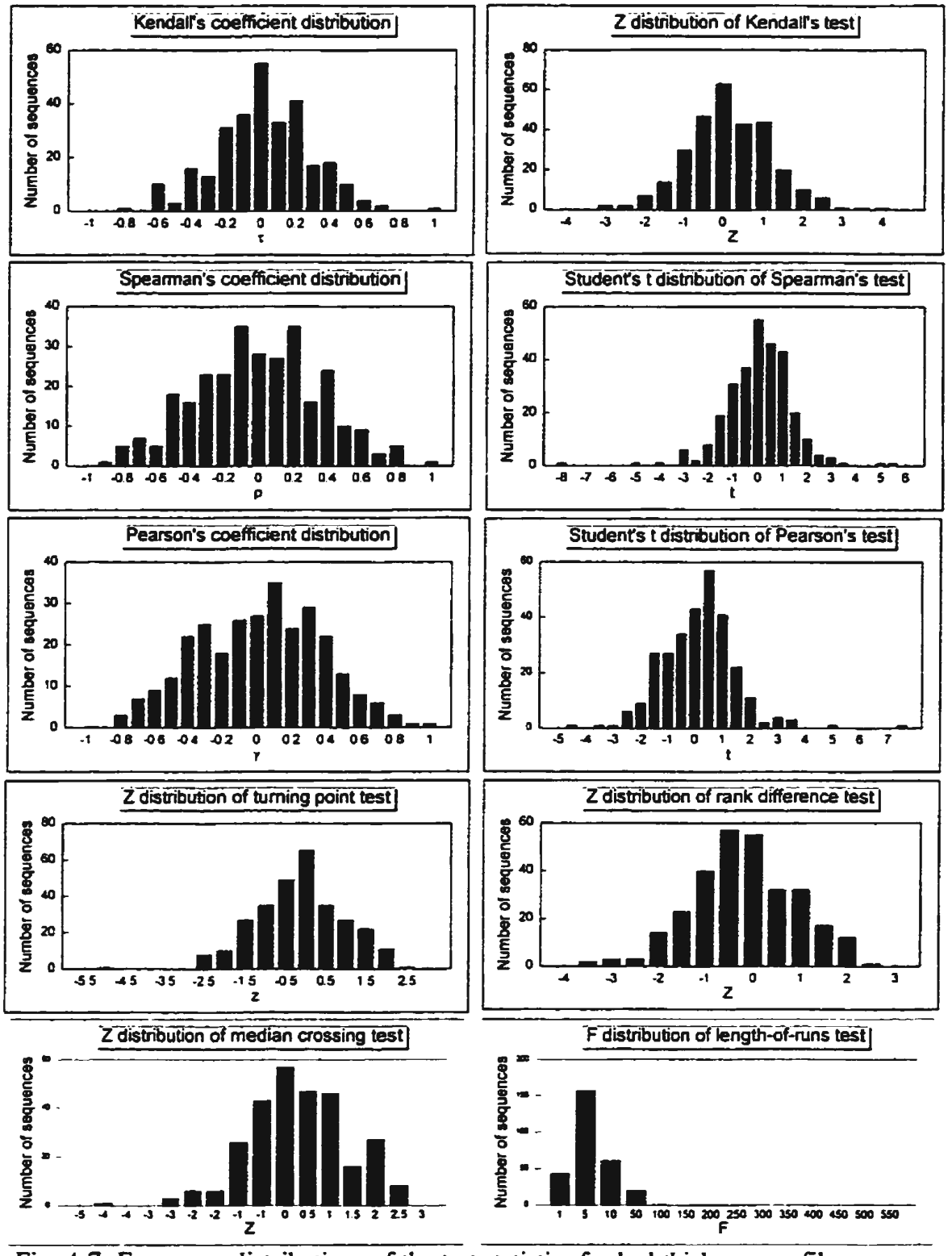

Fig. 4.7 Frequency distributions of the test statistics for bed-thickness profiles of 286 sandstone packets selected from turbidite sections involved in this study. The distribution parameters are shown in Table 4.8.

Table 4.8 Distribution characteristics of the test statistics for bed-thickness profiles of original and randomly shuffled sequences

286 original sandstone packets (sequences)									
Tests	Kendall's τ	Z test for τ	Spearman's ρ	t test for ρ	Pearson's γ	t test for γ	Z test for Turning Point	Z test for Rank Difference	Z test for Median Crossing
Mean	-0.0216	-0.08644	-0.04232	-0.17987	-0.03848	-0.12793	-0.37372	-0.40165	0.07435
Standard Deviation, s	0.276613	1.109875	0.363823	1.366208	0.36438	1.327592	1.115407	1.097964	1.06836
-1 s to +1 s	70.5%	70.8%	67.4%	77.0%	65.3%	74.2%	68.8%	68.0%	69.9%
-2 s to +2 s	93.5%	94.5%	95.5%	94.8%	96.6%	95.5%	95.9%	96.6%	94.8%
286 sequences generated through random shuffling of the 286 original sandstone packets									
Tests	Kendall's τ	Z test for τ	Spearman's ρ	t test for ρ	Pearson's γ	t test for γ	Z test for Turning Point	Z test for Rank Difference	Z test for Median Crossing
Mean	0.000739	0.020687	-0.01198	-0.02701	0.007402	-0.0339	-0.24387	-0.0119	0.36638
Standard Deviation, s	0.271235	0.958788	0.34875	1.172343	0.354415	1.83201	1.078663	0.915264	1.0248
-1 s to +1 s	74.2%	66.0 %	69.8%	75.6%	69.8%	89.3%	66.7%	65.3%	64.0%
-2 s to +2 s	92.3%	95.5%	94.5%	95.5%	94.9%	99.3%	97.3%	95.9%	98.6%

Note: the values in the row labelled -1 s to +1 s = the percentage of sequences falling into the area between -1 and +1 standard deviations and under the frequency curve; the values in the row labelled -2 s to +2 s have the same meaning but between -2 and +2 standard deviations.

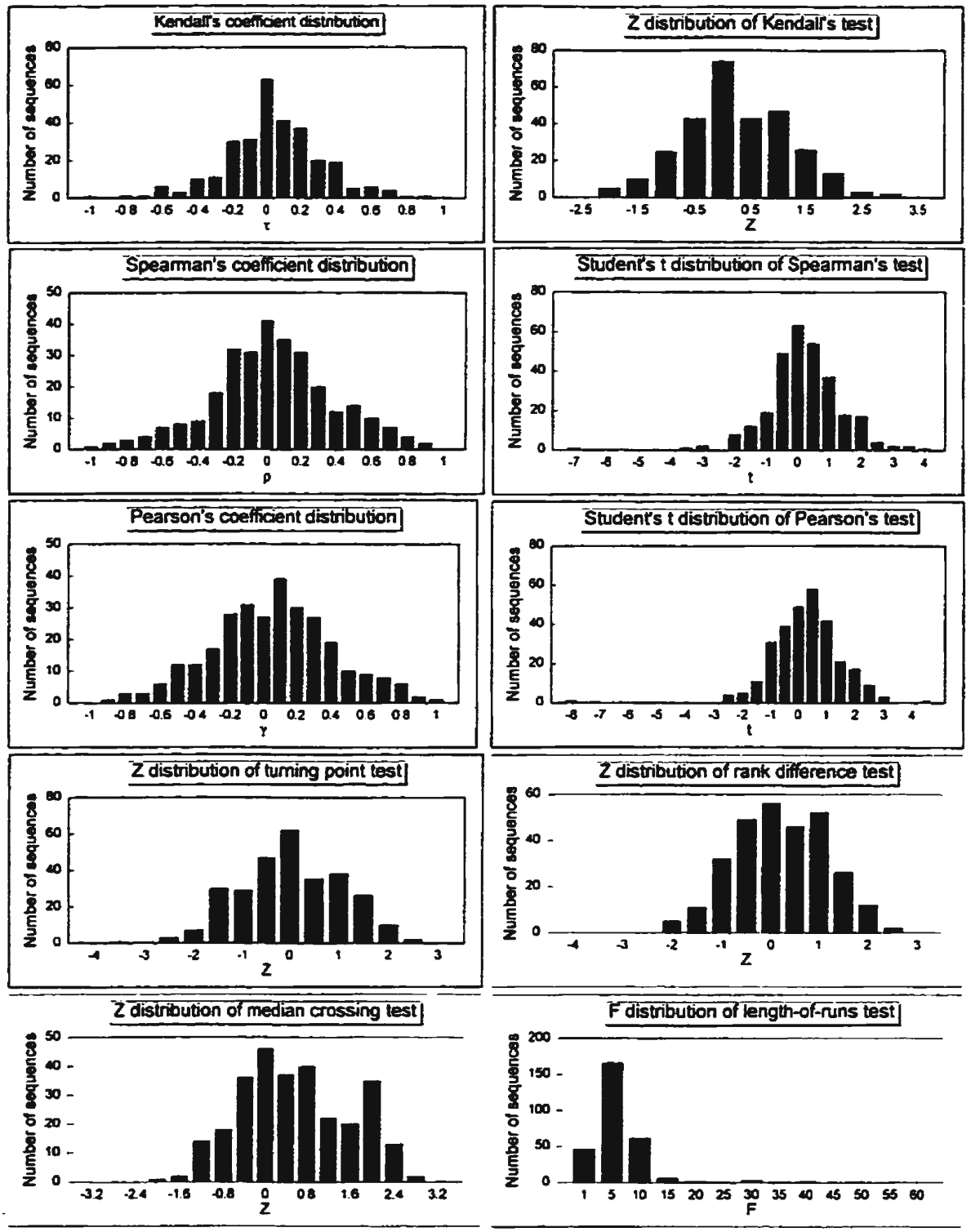

Fig. 4.8 Frequency distributions of the test statistics for bed-thickness profiles of 286 sequences generated by random shuffling of the 286 original sequences. The distribution parameters are shown in Table 4.8.

Carlo simulation can be used to compare the number of asymmetric sequences statistically identified from the original sandstone packets with the number expected in an equal number of randomly generated sequences.

In order to obtain a set of 286 random sequences, the bed thicknesses measured in each of the 286 original sandstone packets were randomized by sequentially shuffling them 20,000 times to generate one shuffled sequence. A Fortran-77 program, RANSHUF.FOR (Appendix II-2), with a default of 20,000 shuffles, was used for this operation, although a much smaller number of shuffles (e.g. 100 or 200) would probably have been sufficient. Then, the 286 randomly shuffled sequences were tested for asymmetric trends and randomness. The number of sequences for which the null hypothesis of individual tests was rejected at the significance levels $\alpha = 5\%$ and 10%, respectively, was counted. This process was repeated 100 times so that 100 sets of 286 randomly shuffled sequences were generated and tested. Consequently, the mean, maximum and minimum values of the number of sequences that passed individual tests at $\alpha = 5\%$ and 10% for the 100 sets of 286 randomly shuffled sequences were obtained.

In the following, pairs of percentages [n% and m%] relate to testing using α values of 5% and 10%, respectively. On average, random shuffles generate [5.7% and 10.8%] asymmetric sequences identified by Kendall's correlation test, [6.1% and 10.8%] by Spearman's correlation test, and [4.9% and 9.9%] by Pearson's correlation. The maximum percentages of asymmetric sequences in the 100 sets of 286 random

shuffles are [8.3% and 14.8%], recognized by Kendall's test, [9.6% and 14.8%] by Spearman's test, and [7.2% and 13.4%] by Pearson's test. The minimum percentages of asymmetric sequences are [2.1% and 5.8%] using Kendall's test, [2.4% and 6.9%] using Spearman's test, and [1.7% and 6.5%] using Pearson's test.

For the 286 original sandstone packets, 6.3%, 6.6% and 7% were identified as asymmetric sequences using $\alpha = 5\%$, and 11.5%, 10.5% and 10.8% as asymmetric sequences using $\alpha = 10\%$, for Kendall's, Spearman's and Pearson's correlation tests, respectively. All these values, except the percentage derived from Pearson's test using $\alpha = 5\%$, are very close to the corresponding average (mean) values for the 100 sets of 286 randomly shuffled sequences (Table 4.9 and Fig. 4.9). Hence, the number of asymmetric sequences identified in the original set of turbidite sandstone packets is almost identical to the number produced by random shuffling.

The number of non-random sequences detected in the original 286 sandstone packets by the four tests for randomness tends to be close to or slightly higher than the maximum values obtained from the randomly shuffled sequences (Table 4.9, Fig. 4.9).

4.5 Discussion

Based on the above statistical analysis, it is now possible to answer these questions: Are upward thinning and thickening cycles the dominant patterns in turbidite successions? Are such cycles numerous in some turbidite sections but not in others? The first question is directly related to general models of turbidite deposition in

Table 4.9 The percentages of sequences for which the null hypothesis of individual tests (using bed-thickness data) was rejected. Results are for both random sequences and the 286 sequences selected from field data.

	At the 5% Significance Level						
	Kendall's correlation test	Spearman's correlation test	Pearson's correlation test	Turning Point test	Rank Difference test	Median Crossing test	Length of Runs test
Random Sequences							
Minimum	2.1%	2.4%	1.7%	3.4%	2.8%	2.7%	23.0%
Mean	5.7%	6.1%	4.9%	7.1%	5.2%	4.6%	26.0%
Maximum	8.3%	9.6%	7.2%	8.3%	7.9%	7.4%	29.0%
Original Sequences	6.3%	6.6%	7%	8.4%	9.1%	6.3%	25.5%
	At the 10% Significance Level						
	Kendall's correlation test	Spearman's correlation test	Pearson's correlation test	Turning Point test	Rank Difference test	Median Crossing test	Length of Runs test
Random Sequences							
Minimum	5.8%	6.9%	6.5%	7.9%	5.8%	12.0%	28.3%
Mean	10.8%	10.8%	9.9%	11.6%	10.3%	16.0%	35.0%
Maximum	14.8%	14.8%	13.4%	14.4%	12.7%	19.0%	39.1%
Original Sequences	11.5%	10.5%	10.8%	16.1%	14.3%	16.4%	38.0%

Note: Minimum, mean and maximum values of percentages were derived from 100 sets of 286 sequences generated through random shuffling of the 286 original sequences

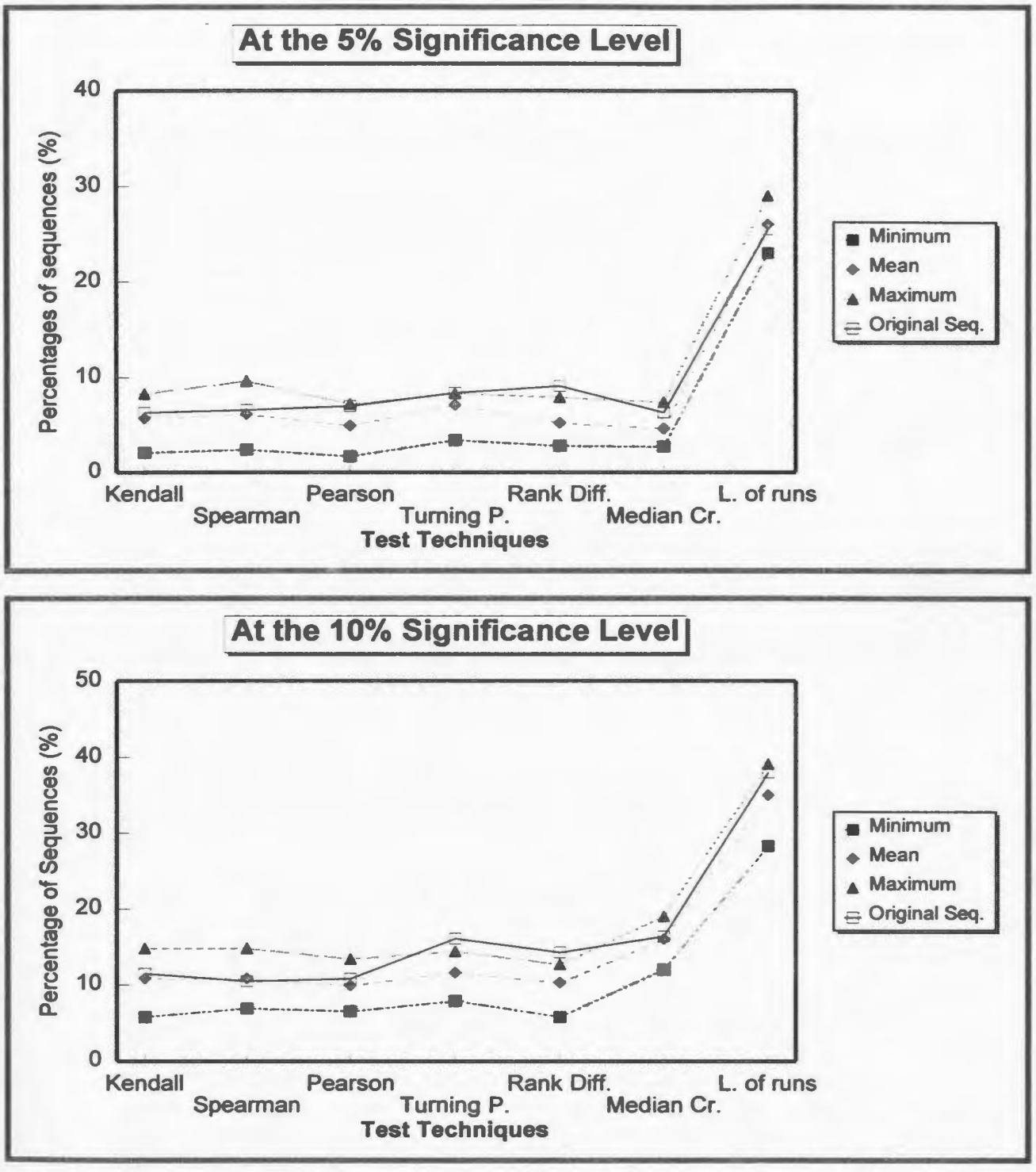

Fig. 4.9 Plots of the data in Table 4.9, giving a straightforward comparison between percentages of sequences for which the null hypothesis of individual tests was rejected in the 286 original sequences and in 100 sets of 286 sequences generated by random shuffling of the 286 original sequences. The minimum, mean and maximum percentages are from 100 sets of 286 random sequences.

submarine fans. The second must be answered with reference to case studies.

4.5.1 General analysis of asymmetric trends in bed thickness

The statistical analysis of this study is based on many turbidite sections from different areas of the world and from different stratigraphic units. These include sections on which Mutti and Ricci Lucchi (1972) and Ricci Lucchi (1975) based their hypothesis of asymmetric cycles, and sections that Ingersoll (1981) described as well organized upward thinning and thickening cycles. Hence, results discussed here have broad relevance to any evaluation of the importance of asymmetric cycles in turbidite successions.

Only 34 (11.9%) of the 286 sandstone packets selected from all the turbidite sections involved in this study are organized into statistically recognizable upward thinning and thickening sequences. Monte Carlo simulation (Fig. 4.9 and Table 4.9), the probability of rejecting the null hypothesis calculated as a cumulative binomial probability, and frequency distributions of the test statistics (Table 4.8, Figs. 4.7 and 4.8) all demonstrate that this percentage of asymmetric sequences is within the range that can be generated solely by random processes. These results strongly suggest that asymmetric cycles are not important in turbidite successions, and therefore cannot provide a criterion for identification of environments in submarine fan systems. It follows that models for submarine fans based on the widely publicized hypothesis of common asymmetric cycles (e.g. Mutti and Ricci Lucchi, 1972; Ricci Lucchi, 1975;

Walker, 1984; Shanmugam and Moiola, 1988; Mutti, 1992; Stow et al., 1996) should be reconsidered.

In the 34 statistically identified asymmetric sequences, the ratio of upward thinning to upward thickening sequences is 22:12 (1.83). If the odds are 50:50 for upward thinning versus upward thickening in a random population, the probability (calculated using Eqn. 4.2) of obtaining 22 or more upward thinning sequences out of a total of 34 is 0.06 which is marginally significant because for only one less, i.e. 21 or more times out of 34, the probability will become 0.11. However, the 22:12 result may still indicate the operation of some deterministic processes capable of generating a very small surplus of upward thinning sequences, superimposed on what are otherwise largely random events. This does not contradict the general conclusion that upward thinning and thickening cycles are not important in turbidite successions. It only means that a very limited number of upward thinning sequences may truly result from some organized and predictable processes. Candidate processes are discussed in the following section.

4.5.2 Case-by-Case Analysis of Asymmetric Cycles

The number (N) of sandstone packets selected from most turbidite sections or localities is not large (Table 4.3a-b). Due to the small sample (N), the results from Monte Carlo simulation (Table 4.9) cannot very effectively be applied to assess the significance of asymmetric sequences in individual turbidite successions or localities.

This problem can be remedied by calculating the cumulative binomial probability (Eqn. 4.1 if $n < 30$; Eqn. 4.2 if $n \geq 30$).

Sections in the Italian Apennines:

Thirty turbidite sandstone packets were statistically selected from four sections of the Miocene Marnoso arenacea, Santerno Valley (Table 4.3), which Ricci Lucchi (1975, 1978) interpreted as lobe deposits. Among them, only two packets were identified as upward thickening sequences using $\alpha = 10\%$ as limiting value (Note: all of the asymmetric sequences described in the rest of this chapter were statistically tested using this same limiting value). One of the two upward thickening sequences is accompanied by an upward coarsening trend (Fig. 4.10); the other is not.

Three additional sandstone packets were selected from two sections of the Marnoso arenacea, Savio Valley. These were considered as channel fills by Ricci Lucchi (1975). One of the three is statistically asymmetric: it thickens and coarsens upward, contrary to the hypothesis of Ricci Lucchi (1975). The other two packets show no order.

In the statistical tests for trends in grain size, another Marnoso arenacea sandstone packet fines upward but neither thins nor thickens upward (Table 4.6).

In summary, only three upward thickening sequences were statistically identified in the 33 selected sandstone packets, i.e. 9.1%. This is lower than the mean percentage of asymmetric sequences identified in the randomly shuffled sequences at the same significance level (Table 4.9). The probability of rejecting the null hypothesis 3 or

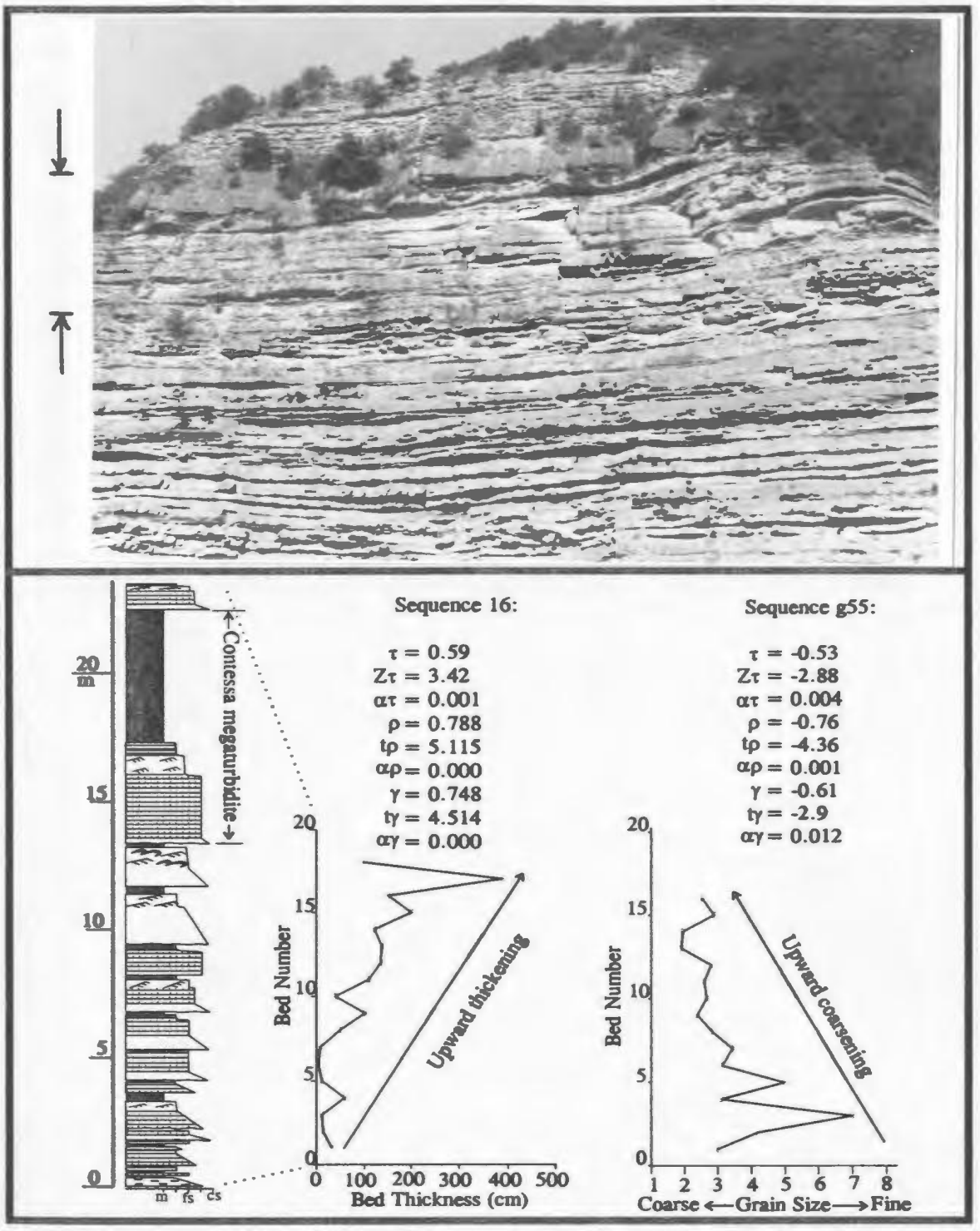

Fig. 4.10 An upward thickening and coarsening sequence in the Coniale section, Santerno Valley, Italy. The thickest sandstone bed (3.94 m) near the top of the photo is the Contessa megaturbidite of Ricci Lucchi and Valmori (1980). The interval shown in the column is indicated by arrows adjacent to the photograph. τ, ρ and γ represent Kendall's, Spearman's and Pearson's coefficients; Zτ, tρ and tγ are Z and t test values of these coefficients; ατ, αρ and αγ represent the significance level at which the sequence passed individual tests. The same variables are used in subsequent figures and tables in this chapter.

more times in 33 trials at $\alpha = 0.1$ when it is true is 0.69 (calculated using Eqn. 4.2). It is therefore concluded that asymmetric trends in bed thickness, as well as in grain size, are not important in these turbidite sections of the northern Italian Apennines.

Monticello Dam Section, Great Valley, California

Twenty-three packets of turbidite sandstone (including some conglomerate) were statistically selected from this part of the Upper Cretaceous Venado Formation, which Ingersoll (1981) interpreted as fan channel deposits (Fig. 1.2). Four asymmetric bed-thickness sequences (17.4%) were identified: three thin upward and one thickens upward. Under the null hypothesis, the probability of 4 or more successes in 23 trials at $\alpha = 0.1$ is 0.19 (calculated using Eqn. 4.1). So, it is not surprising to find 4 packets with asymmetric trends in the 23 sandstone packets.

Packets with asymmetric grain-size trends are more numerous at Monticello Dam. Eight upward fining and two upward coarsening sequences were statistically identified in 20 sandstone packets selected from this section (Table 4.6, Fig. 4.4). Since the tests are at a significance level $\alpha = 10\%$, only two of these asymmetric fining and coarsening sequences would have been expected if a random process was controlling grain-size (Type I error). Under the null hypothesis, the cumulative binomial probability of 3 or more successes in 20 trials is 0.13, and 4 or more successes in 20 trials is 0.043 (calculated using Eqn. 4.1). Thus, eight or seven of the ten asymmetric grain-size sequences might have been produced by some orderly processes.

In the bed-by-bed section (Figs. 2.3b-c), many beds have a pebbly base, many have their top missing, and amalgamation is common. In a single sandstone/conglomerate packet, either an upward decrease in the thickness of basal pebbly divisions or an upward increase in the preservation of upper Bouma divisions of individual beds may cause an upward decrease in the grain-size score and therefore upward fining. The latter is confirmed by the results of tests for trends in sedimentary structure scores (Table 4.7). Four of the eight upward fining sequences in this section show a parallel upward increase in the proportion of upper Bouma divisions; and one of the two upward coarsening sequences has a parallel upward decrease in the proportion of upper Bouma divisions.

The statistical results confirm the provisional interpretation of cyclic patterns at this locality (Chapter 2). Except for packet (g20), shown in Figures 2.3c and 4.11, which has been interpreted as a "channel-abandonment sequence", upward fining sequences (g4), (g6), (g16), and (g17) shown in lithofacies logs of Figures 2.3b-c might have resulted from (a) channel "incision and backfill" (see Chapter 2 for interpretation), (b) channel upward shallowing or gradual abandonment as a channel fills up, or (c) the stacking of onlapping deposits at a channel mouth. Channel backfilling, gradual abandonment, or onlapping at a channel mouth might cause a landward shift of coarse sedimentation and progressively less basal erosion, resulting in upward fining sequences (Fig. 2.6). These processes have been interpreted from observations of modern Hueneme and Dume submarine fans in the California

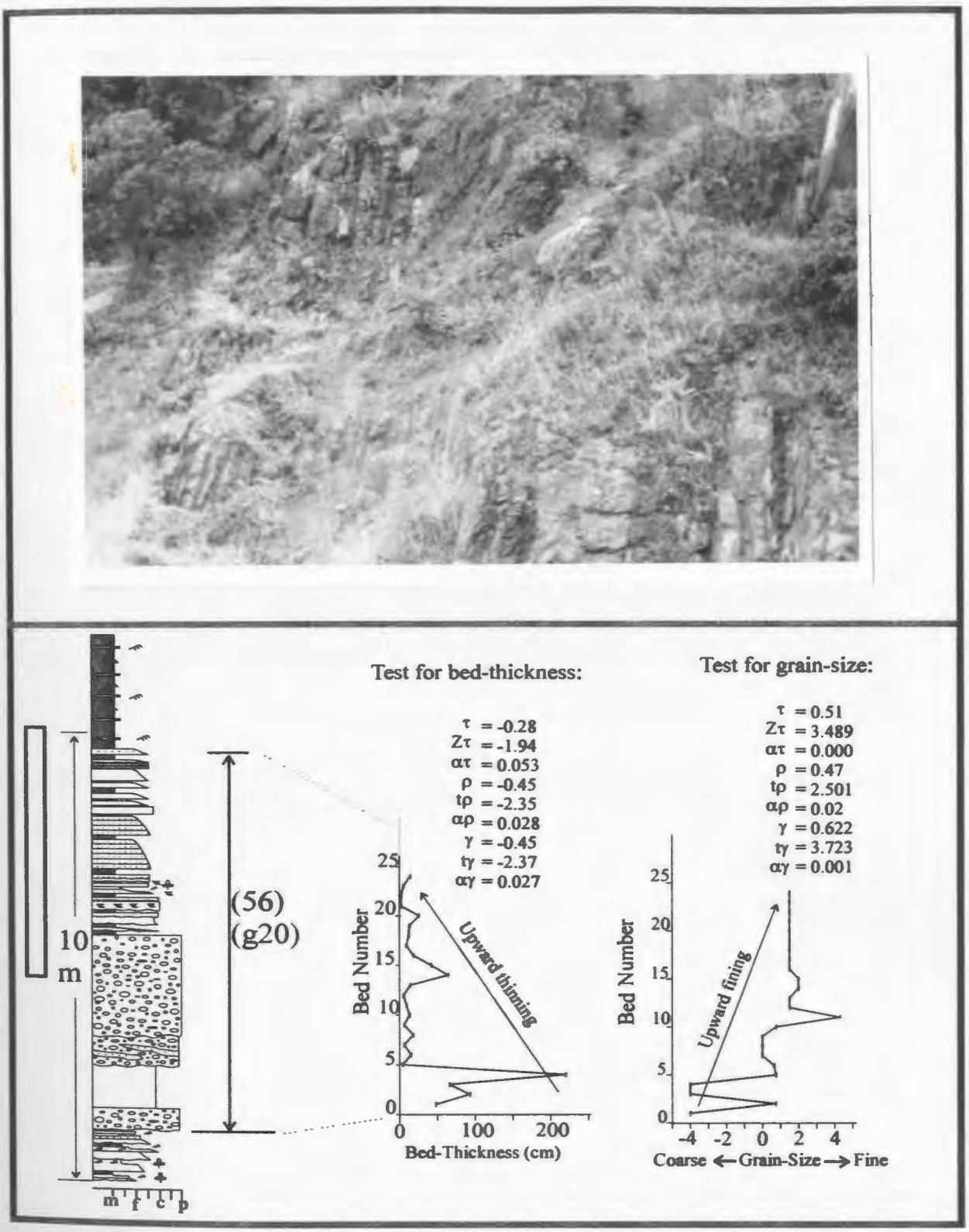

Fig. 4.11 An upward thinning and fining sequence statistically identified (at a significance level < 10%) in the Monticello Dam section, Great Valley, California. It is interpreted as the fill of an abandoned channel. In the photograph, the section top is to the left. The interval shown in the photograph is indicated by the white bar adjacent to the column.

Borderland (Normark et al, in press). Upward fining sequences (g5), (g9), and (g12), and upward coarsening sequences (g15) and (g19) might have been formed by "compensation" (Mutti and Sonnino, 1981) as lobes migrate and shingle against one another (Swart, 1990; Jordan et al., 1991; Bouma et al., 1995).

In summary, statistical testing shows that the Venado Formation at this locality is not characterized by a succession of upward thinning cycles as Ingersoll (1978, 1981) proposed. In contrast, upward fining sequences are statistically significant but not abundant. Such upward fining sequences might only be present in the coarsest central part of a channel, particularly in pebbly sand deposits at a channel-lobe transition zone. If sediments supplied to a fan system are fine-grained, such upward fining trends, if they exist, might be difficult to observe. Even though the lateral tracing required to accurately determine the geometry of every packet is impossible in the field, a pattern of nested, offset, stacked channels (Clark and Pickering, 1996) is inferred for the Venado channel system because the Venado channel deposits have the basic features of erosional channel deposits (see Chapter 2). The channel stacking pattern 9 or 8 of Clark and Pickering (1996) is possibly the best interpretation for incision-backfill cycles in the Venado Formation.

Cache Creek Section, Great Valley, California

Only two upward thinning sequences and one upward thickening sequence (13.6%) were identified in the 22 sandstone packets statistically selected from this section of the

Upper Cretaceous Sites Formation (Table 4.3), which Ingersoll (1978, 1981) interpreted as lobe deposits. In the tests for trends in grain size, only two upward fining sequences and one upward coarsening sequence were identified (Table 4.6). The upward coarsening sequence also thickens upward, and one upward fining sequence thins upward. Figure 4.12 shows the three upward thinning and/or fining sequences. Figure 4.13 shows the longest asymmetric sequence (79 beds) tested for this study. Its upward thickening and coarsening trends might have originated from random processes or lobe switching (compensation) or even lobe progradation (Mutti and Ricci Lucchi, 1972; Ricci Lucchi, 1975).

The percentage of asymmetric sequences in the section is little higher than the mean percentage for random sequences, but lower than the maximum (Table 4.8). However, the cumulative binomial probability of 3 or more successes in 22 trials at $\alpha = 0.1$ when the null hypothesis is true is 0.38 (calculated using Eqn. 4.1). Thus, there is no reason to suggest these asymmetric sequences were generated by any orderly process. The statistical results of this study contradict the proposal of Ingersoll (1978, 1981) that upward thickening and coarsening cycles characterize lobe deposits of the Cache Creek section (Fig. 1.2).

Sections in Gaspé Peninsula, Québec

Two sections of the Lower Ordovician Tourelle Formation, measured at Cap Ste-Anne, have been interpreted as lobe deposits (Hiscott, 1980; Hiscott and DeVries,

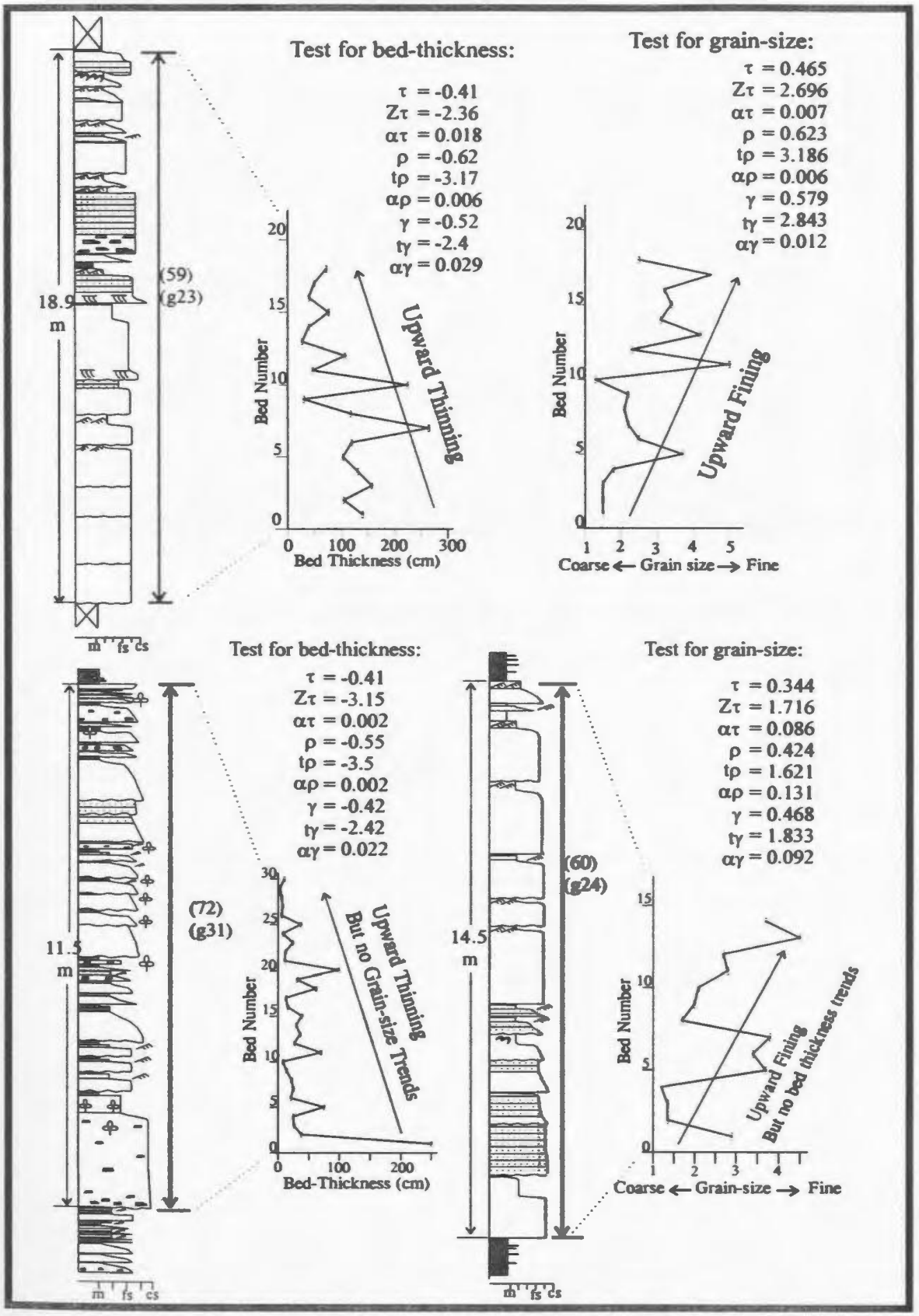

Fig. 4.12 Asymmetric sequences statistically identified in the Cache Creek measured section of the Sites Formation, Great Valley, California.

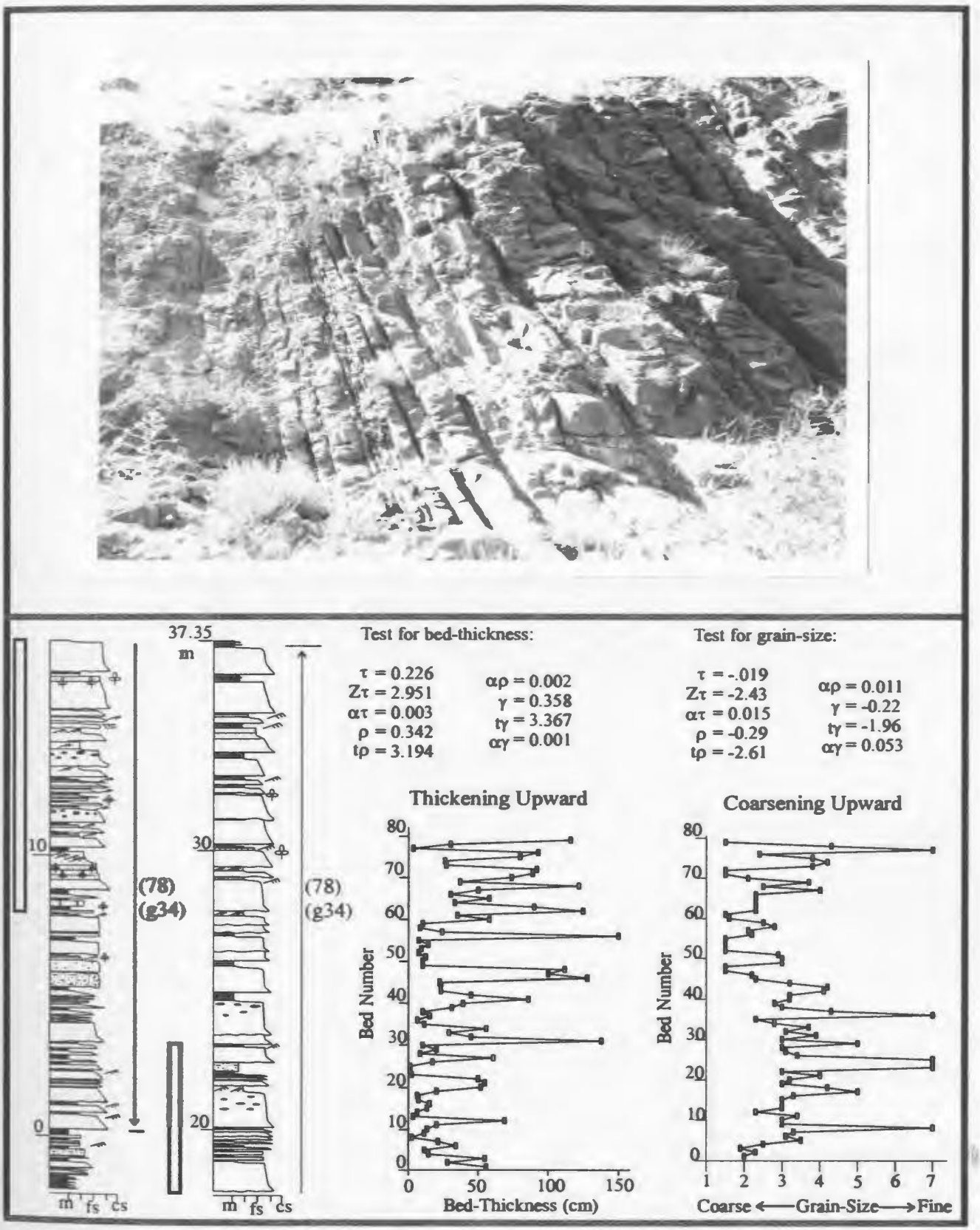

Fig. 4.13 A statistically identified upward thickening and coarsening sequence with 79 beds from the Cache Creek measured section, Great Valley, California. In the photo, the section top is to the right. The white bar beside the column identifies the interval shown in the photograph.

1995). Nine sandstone packets were statistically selected and tested. Two (22.2%) of these sandstone packets were identified as upward thinning sequences. The higher percentage of occurrence of asymmetric sequences in these sections could be attributed to the small sample size (9 packets). Under the null hypothesis, the cumulative binomial probability of 2 or more successes in 9 trials at $\alpha = 0.1$ is 0.23 (calculated using Eqn. 4.1). Therefore, there is no reason to suggest that these were not formed by random processes. The field view confirms this conclusion. The measured sections show that almost all beds in one of these two sequences are amalgamated (Fig. 2.23, sequence 83). Since erosion depth at each surface likely varies laterally, this upward thinning sequence could easily have been randomly generated.

Sixty-seven sandstone packets were statistically selected from a section in the Middle Ordovician Cloridorme Formation measured at Petite-Vallée. Only four upward thinning and three upward thickening sequences (i.e., 10.5% asymmetric sequences) were subsequently identified.

The percentage of asymmetric sequences in this section is almost the same as the mean percentage of asymmetric sequences identified in random sequences (Table 4.8). Although grain-size data in this section are inadequate for calculation of grain-size scores, the measured section (Fig. 2.24a-c) suggests no parallel trends, through the seven asymmetric sequences, in grain-size or in preservation of upper fine divisions of individual sand beds. The cumulative binomial probability of rejecting the null

hypothesis 7 or more times in 67 random trials at $\alpha = 0.1$ is 0.53 (calculated using Eqn. 4.2). Therefore, the seven asymmetric sequences in this section are considered to have been formed, at low probability (1 in 10), by random processes. The statistical results confirm that asymmetric sequences are not important in this part of the Cloridorme Formation.

Sections of the Modern Amazon Fan

Seventeen sandstone packets were selected from three sections constructed from Formation MicroScanner (FMS) images at ODP sites 931, 944, and 946 by Pirmez et al. (in press). These sandstone packets are in sheet-like HARPs (High Amplitude Reflection Packets) or lobes (Site 946). Internal seismic reflections locally form subdued lenses suggesting shallow channels (Hiscott et al., 1997; Flood, Piper, Klaus et al., 1995). Among these 17 sandstone packets, only two (11.8%) thin upward. These could have been formed by random bed-thickness variations because the cumulative binomial probability of 2 or more successes out of 17 random trials is 0.52 (calculated using Eqn. 4.1).

The statistical results reveal that sandstone packets in the sections selected from HARP units of the modern Amazon Fan are not characterized by preferred upward thinning and/or thickening patterns.

Sections in Barbados

The two sections measured in the Scotland Formation of Barbados are believed to be channel, levee and interchannel deposits (Larue and Speed, 1983; Larue, 1985; R.N. Hiscott, pers. comm., 1996). Ten sandstone packets were statistically selected from these sections. Two of these (20%) are statistically defined upward thinning sequences (Fig. 4.14). Five (50%) of the ten packets show asymmetric trends in grain-size; four fine upward, and one coarsens upward. One upward fining sequence has a parallel trend in both bed-thickness and the preservation of upper Bouma divisions, while another is only accompanied by an upward thinning trend. The remaining three asymmetric fining and coarsening sequences have no parallel trends in either bed-thickness or in the preservation of upper Bouma divisions.

Under the null hypothesis, the cumulative binomial probability of two or more successes in 10 trials at $\alpha = 0.1$ is 0.26 (calculated using Eqn. 4.1). Hence, the two asymmetric bed-thickness sequences identified in the ten packets can be attributed to a random process. However, the probability of rejecting the null hypothesis 5 or more times in 10 trials at $\alpha = 0.1$ when it is true is 0.0016. Thus, some of the five asymmetric sequences in grain size are probably not random, particularly the three upward fining sequences (packets 175, 177, and 178 in Appendix IV-2) which passed the three correlation tests at very low α levels (< 0.01). As at Monticello Dam, these upward fining sequences might be the product of some deterministic processes, such as channel incision and backfilling, or the stacking of onlapping deposits at a channel mouth.

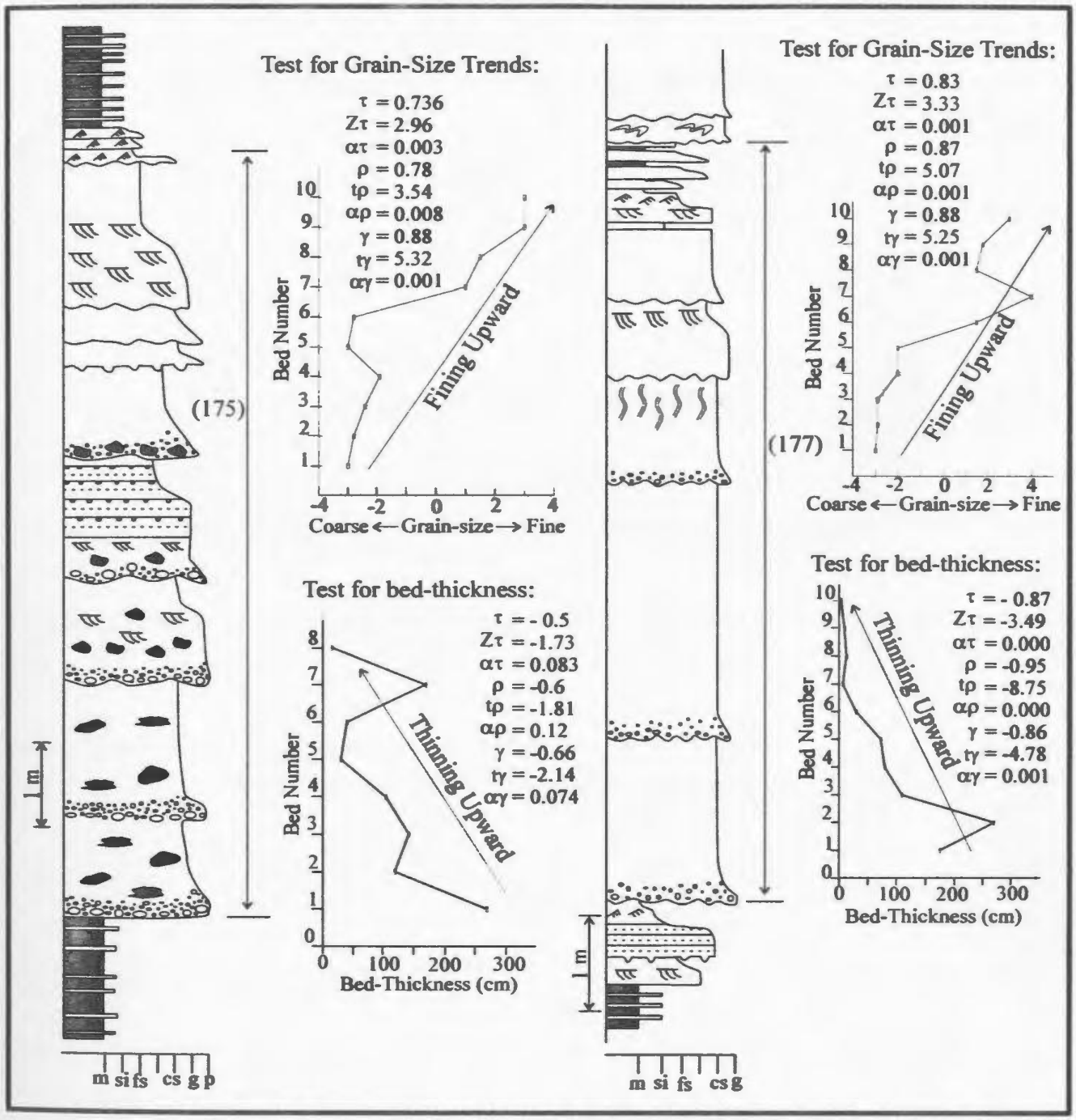

Fig. 4.14 Two upward thinning and fining sequences statistically identified from Barbados measured sections, accompanied by an upward increase in tractional structures. τ, ρ and γ represent Kendall's, Spearman's and Pearson's coefficients; Zτ, tρ and tγ are Z and t test values of these coefficients; ατ, αρ and αγ represent the significance levels at which these sequences would pass each of these tests. See Figure 2.3a for key.

Sections in Southwestern British Columbia

Three upward thinning and one upward thickening sequence (15.4%) were recognized statistically in 26 sandstone packets selected from seven short sections of the Upper Cretaceous Nanaimo Group in Southwestern British Columbia. These sandstones have been interpreted as channel fills (England and Hiscott, 1992). The percentage of asymmetric sequences in this section is slightly higher than the maximum percentage (14.8%) in the 100 sets of 286 randomly shuffled sequences (Table 4.8). However, the cumulative binomial probability of rejecting the null hypothesis 4 or more times in 26 random trials at $\alpha = 0.1$ equals 0.26 (calculated using Eqn. 4.1). Therefore, there is no reason to suggest that the four asymmetric sequences in bed thickness were not formed at random.

In tests for trends in grain-size, four (33.3%) of the 12 tested packets (data needed to calculate grain-size scores were not available for the remaining 14 packets) are inferred to have asymmetric trends; three fine upward and one coarsens upward. One of the three upward fining sequences thins upward; the other two have no parallel bed-thickness trends. Once again, the percentage occurrence of upward fining sequences is higher in these channel deposits than in randomly shuffled sequences. Under the null hypothesis, the probability of 4 or more successes in 12 random trials at $\alpha = 0.1$ is 0.026 (calculated using Eqn. 4.1). Therefore, some of the upward fining sequences identified in these sections could have been formed by orderly processes. Figure 4.15 shows three of these asymmetric sequences. Sequence 192 not only fines and thins upward but also shows an

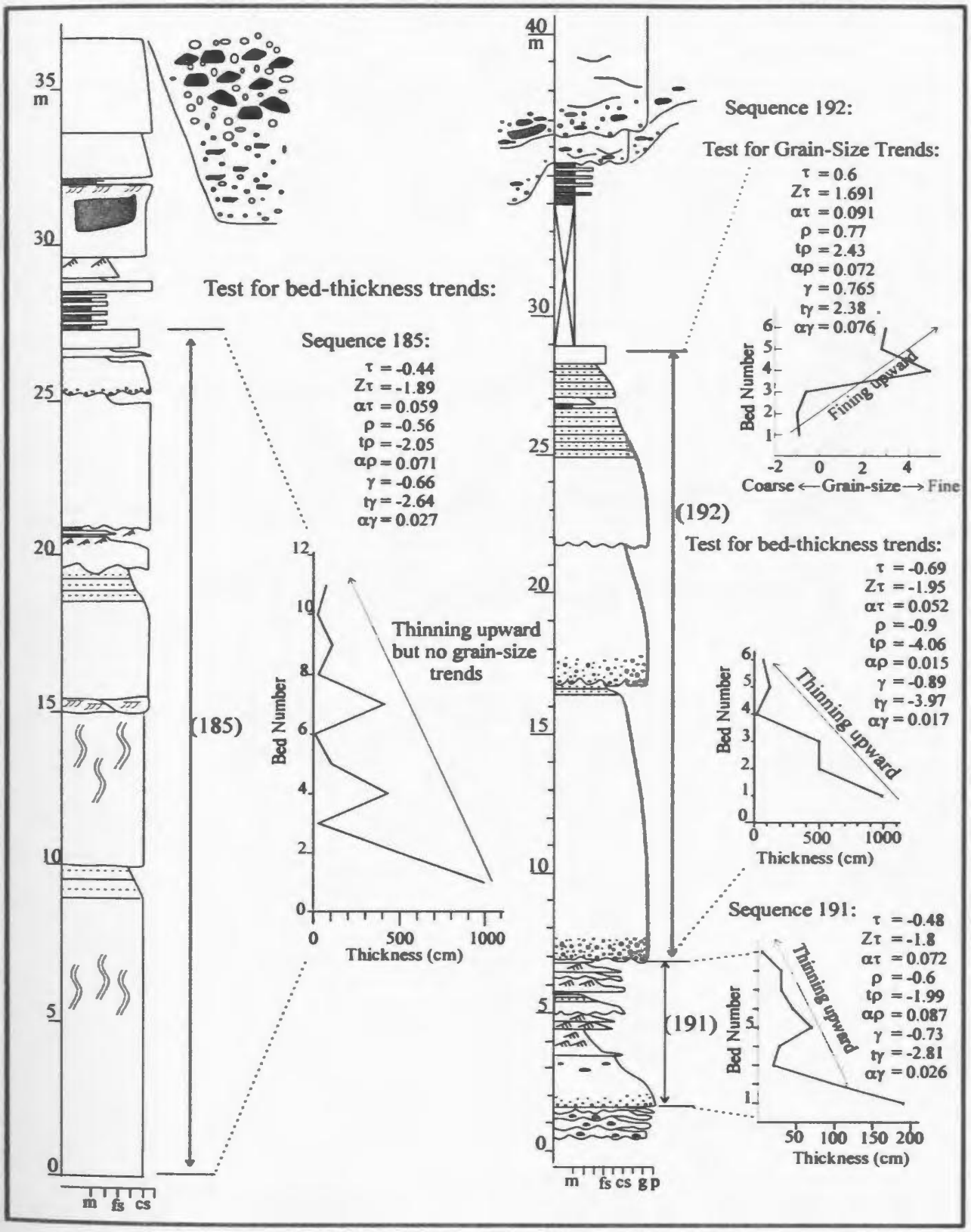

Fig. 4.15 Three upward thinning sequences from the Nanaimo Group, British Columbia. Sequence (192) is accompanied by an upward fining trend. All tests detailed here were passed at $\alpha < 10\%$. See Figure 2.3a for key.

upward increase in tractional structures; and both sequences 185 and 192 are overlain by interbedded shale and thin siltstone. These features are compatible with formation by processes proposed for the Monticello Dam section.

Sections in Arkansas

Forty-two sandstone packets were statistically selected from two sections of the Jackfork Group at the DeGray Spillway, Arkansas. These rocks have been interpreted as lobe and overbank levee deposits (Bouma et al., 1995). Two upward thinning and one upward thickening sequence were identified (7.1% of the sequences). This is close to the minimum percentage (about 6.4%) of asymmetric sequences expected in randomly generated sequences (Table 4.8). The probability of rejecting the null hypothesis 3 or more times in 42 random trials at $\alpha = 0.1$ is 0.82 (calculated using Eqn. 4.2). Hence, asymmetric trends are not important in sandstone packets of these sections.

Sections in Northern Norway

Two upward thinning and two upward thickening sequences (10.8%) were identified in 37 sandstone packets selected from three sections of the Kongsfjord Formation of Northern Norway. These outcrops are interpreted as lobe deposits (Drinkwater, 1995). The percentage of asymmetric sequences is almost the same as the mean percentage obtained from 100 sets of 286 randomly shuffled sequences. Under the null hypothesis, the probability of 4 or more successes in 37 trials at $\alpha = 0.1$ is 0.55 (calculated using

Eqn. 4.1). Therefore, upward thinning and thickening sequences are not significant in these sections.

Summary of Case Studies

The case studies answer the question posed at the beginning of this section: Are upward thinning and thickening sequences important in some turbidite successions but not in others? None of the turbidite units involved in this study are characterized by a significant number of upward thinning and thickening sequences.

Upward fining trends do occur in significant numbers in channel fills at Monticello Dam, in Barbados, and in British Columbia. These are interpreted to have been formed by channel incision and backfilling, or progressively upward unchannelizing, or the stacking of onlapping deposits at a channel mouth, and in a few cases by more rapid channel abandonment.

4.5.3 Analysis of Other Non-Random Trends in Bed Thickness

The number (54) of other non-random bed-thickness sequences in the selected sandstone packets is close to or a little higher than the maximum value obtained through the analysis of 100 sets of 286 randomly shuffled sequences (Table 4.9 and Fig. 4.9). Among the 54 non-random sequences, 30 sequences show a highly fluctuated pattern, and 23 sequences are characterized by alternate groups of thin beds and thick beds, or a wavy pattern (Fig. 4.3, examples [1] and [2]). Fifteen out of the thirty highly fluctuated

sequences have only 4 or 5 beds, and therefore cannot be evaluated with any confidence. The only consideration here is given to the longer sequences with grouped or wavy patterns. Some of these grouped sequences may have been generated by organized rather than random processes. Possible processes are lobe or channel switching, and intermittent unusually large failures forming large-volume turbidity currents. The switching of successive flow axes to the right or left of a topographic high produced by the thicker axial deposits of previous flows on a depositional lobe or channel mouth (i.e., compensation effects) has the potential to generate not only both upward thinning and thickening sequences (Swart, 1990; Jordan et al., 1991; Bouma et al., 1995), but also the grouped and wavy patterns. A simple alternation of sets of large and small turbidity currents related to changes in sediment supply in the source area can also produce a grouped pattern.

Sequences with grouped and wavy patterns, however, are not significant enough to be taken as an indicator for depositional processes and subenvironments in turbidite systems. The percentage of such sequences represented by the selected sandstone packets is still close to that in the randomly shuffled sequences, and the number of beds in most sandstone packets is too few to show such grouped and wavy patterns.

4.6 Summary

Only 11.9% upward thinning and thickening sequences (22 upward thinning and 12 upward thickening sequences) were identified by the three correlation tests at a

significance level α = 10% in the 286 selected sandstone packets. The analytical calculation of the cumulative binomial probability, Monte Carlo simulation, and the frequency distribution of statistics of the selected tests for the 286 sandstone packets all suggest that these 34 asymmetric bed-thickness sequences might have been generated by random bed-thickness changes.

The statistical results strongly argue that upward thinning and thickening sequences should not be used as indicators for subenvironments of submarine fans. Case studies further demonstrate that all turbidite sections involved in this study, whether channel deposits or lobe deposits, are not characterized by upward thinning and thickening cycles as Ricci Lucchi (1975) and many others have proposed.

Unlike vertical trends in bed thickness, upward fining sequences may be well developed in the coarse, particularly pebbly sand deposits of channels or the channel-lobe transition zone. The upward fining sequences are possibly formed by channel filling or backfilling, followed by channel switching.

Aside from asymmetric sequences, most other non-random bed-thickness sequences consist of high fluctuations and groupings of a few thin beds and thick beds, or a wavy pattern. The finding of this study indicates: 1) these patterns still need partly subjective identification, 2) most sandstone packets are not thick enough to show a clear fluctuated pattern or a grouped or wavy pattern, and 3) the limited number of these sequences in the selected sandstone packets cannot form a basis on which to discriminate turbidite environments.

In conclusion, even though some upward thinning and/or thickening sequences might have been produced by predictable sedimentary processes, such sequences are too few to have any significance at least in most turbidite successions, and therefore they cannot serve as criteria for identification of submarine fan environments.

Chapter 5

HURST TEST FOR LONG-TERM PERSISTENCE

5.1 Introduction

It has been statistically demonstrated in the previous chapter that submarine fan turbidite successions lack asymmetric bed-thickness trends. Then, do they display any other discernable cyclic organization of bed-thickness and/or other properties? This chapter aims to answer this question.

Murray et al. (1996) used a "runs about the median" technique to test whether thin and thick beds are grouped in the turbidite section measured at Cache Creek, Great Valley, California. They found that the number of runs (146) for the measured section was less than the average number of runs (193) from 100 randomly shuffled sequences. Therefore, they came to a conclusion that thick and thin beds are grouped into packets in the section. "Runs about the median" is a method that can be used for identification of grouped patterns in a time-series sequence. But when the test is applied to bed-by-bed comparisons with the median, it has inherent defects. First, many runs do not coincide one-for-one with thick- or thin-bedded packets; for example, where a thick-bedded sandstone packet contains a few beds thinner than the median so that it is divided into a number of runs. Second, a runs test is, as mentioned in chapter three, very sensitive to "noise" created by very thin or very thick beds. For example, if a section is composed of

overall thick- and thin-bedded packets which contain scattered unusually thin or thick beds, the number of runs about the median for the section may not be significantly different from that for a random sequence. Thus, a more powerful method is needed to test for cyclic organization of turbidite properties.

The Hurst test has been considered to be unique as a powerful test for clustering of low and high values in a time series, and has been widely applied in hydrology studies (e.g. Wallis and Matalas, 1970, 1971; Booy and Morgan, 1985). This thesis provides the first application of this method to turbidite studies.

5.2 Methodology

5.2.1 The Hurst Statistic

In the investigation of long-term storage in reservoirs for the utilization of the water of the river Nile, Hurst (1951, 1956) found the following proportionality:

$$R/S \sim N^h$$

where R is the range between minimum and maximum values on a plot of the cumulative departure from the mean ($\bar{X}$) of annual river discharge for N yearly observations. R is, therefore, defined to be the storage capacity required to maintain a constant outflow, which is equal to $\bar{X}$, over N years without shortage of water supply and without spillage from the reservoir. S is the sample standard deviation of the river discharge for the N observations. h denotes the Hurst coefficient, and is approximated by K with

$$K = \log (R/S)/\log (N/2)$$

For the details of the equation, see Hurst (1951, 1956) and Wallis and Matalas (1970, 1971). For purely random normal processes and large N, say several thousands of observations, Hurst (1951) and Feller (1951) independently found that $K = 0.5$. Nevertheless, after investigating many meteorologically related natural phenomena (e.g., rainfall, streamflow, stream and lake levels, tree rings, lake varves, atmospheric pressure and sunspots), Hurst noticed that K for these natural phenomena was approximately normally distributed, with a mean and standard deviation of 0.73 and 0.09, respectively. The tendency for such natural sequences to yield $K > 0.5$ (> 0.6 for finite value of N, see Wallis and Matalas, 1970) is referred to as the Hurst phenomenon (Wallis and Matalas, 1971).

The Hurst phenomenon has been attributed to (1) samples drawn from a marginal distribution, which here means a population that departs from a normal distribution, particularly caused by truncation of one tail of a normal distribution, (2) transience, i.e., a small sample N, and (3) serial dependence (Hurst, 1956; Wallis and Matalas, 1970). For the experiments of Hurst (1951, 1956), explanations (1) and (2) can be eliminated because most data sets of natural phenomena used by Hurst are Gaussian with sample size, N, ranging from several hundreds to thousands so as to avoid transience. Therefore, Hurst (1951, 1956) came to an important conclusion that the high K values are caused by serial dependence, expressed as a tendency for natural events to occur in irregular groups

in which high or low values preponderate. For example, the long series of levels of the river Nile recorded at Cairo shows that the overall high and low floods tend to be grouped together, much more so than if they were random events, but there is no obvious periodicity or other regularity. Hurst K is powerful for discovering such a long-term clustering of values (Hurst, 1956; Booy and Morgan 1985). So, it should be particularly useful for testing for cyclic clustering of turbidite properties.

It was found that for Gaussian independent sequences, the mean value of K is greater than 0.5. Hence, K is a biased estimator of h (expected to be 0.5) when N is finite (Mandelbrot and Wallis, 1969; Wallis and Matalas, 1970, 1971; Booy and Morgan, 1985). As a remedy, Mandelbrot and Wallis (1969) proposed H as an alternative estimator of h for small samples to eliminate transience as an explanation of the Hurst phenomenon. In the calculation of H, a procedure similar to the one used by Wallis and Matalas (1970) is adopted by this study. A series is divided repeatedly into j subseries of a specified length n such that the first subseries starts at observation 1, the second at observation $n/2$, the third at observation $2(n/2)$, and so on until the last subseries still has n observations. The specified values of n are shown in Table 5.1. For a given sequence with length N, n takes on all values shown in Table 5.1 that are less than or equal to N. If N is not equal to any value in Table 5.1, then set the last n = N. As an example, if N = 116, there will be 12 values of n to consider, 11 from Table 5.1 (20, 24, 30, ..., 100) and the last one = 116. For n = 30, the subseries for which calculations outlined below should be performed have start points and lengths of (1, 30), (15, 45), (30, 60), (45, 75), (60, 90),

(75, 105); in this case,

$j = 6$. $(R_n)/(S_n)_j$ is computed for each subseries by:

$$(R_n)_j/(S_n)_j = [Max\sum_{1}^{n}(x_i - \bar{x}) - Min\sum_{1}^{n}(x_i - \bar{x})]/(S_n)_j$$

where $(R_n)_j$ is the range of cumulative departures from the mean ($\bar{x}$) of a subseries with n observations of x_i (Fig. 5.1), and $(S_n)_j$ is the standard deviation of the subseries. Mean values of $(R_n)/(S_n)_j$ are then calculated for all values of $n \leq N$ (Table 5.1) by determining the mean of the $(R_n)/(S_n)_j$ values over the j subseries, denoted (R_n/S_n). If N = 234, for example, then 17 values of (R_n/S_n) (n = 20, 24, ..., 200, and 234) are obtained, which are then plotted against the corresponding values of n on logarithmic paper. The slope of the regression line for these data points is defined as H. Note that values in Table 5.1 are arbitrarily selected. Users can select their own values. The only purpose is to divide a sequence into subsequences with several lengths (n) and thus to obtain the slope (H) of a regression line.

Table 5.1 Specified Values of *n* for Computation of Hurst H

20 24 30 36 40 50 60 70 80 90 100 120 140 160 180 200 240
280 320 360 400 450 500 550 600 700 800 900 1000 1200 1400
1600 1800 2000 2400 3000

Figure 5.1 shows R, the range of cumulative departures from the mean, used for

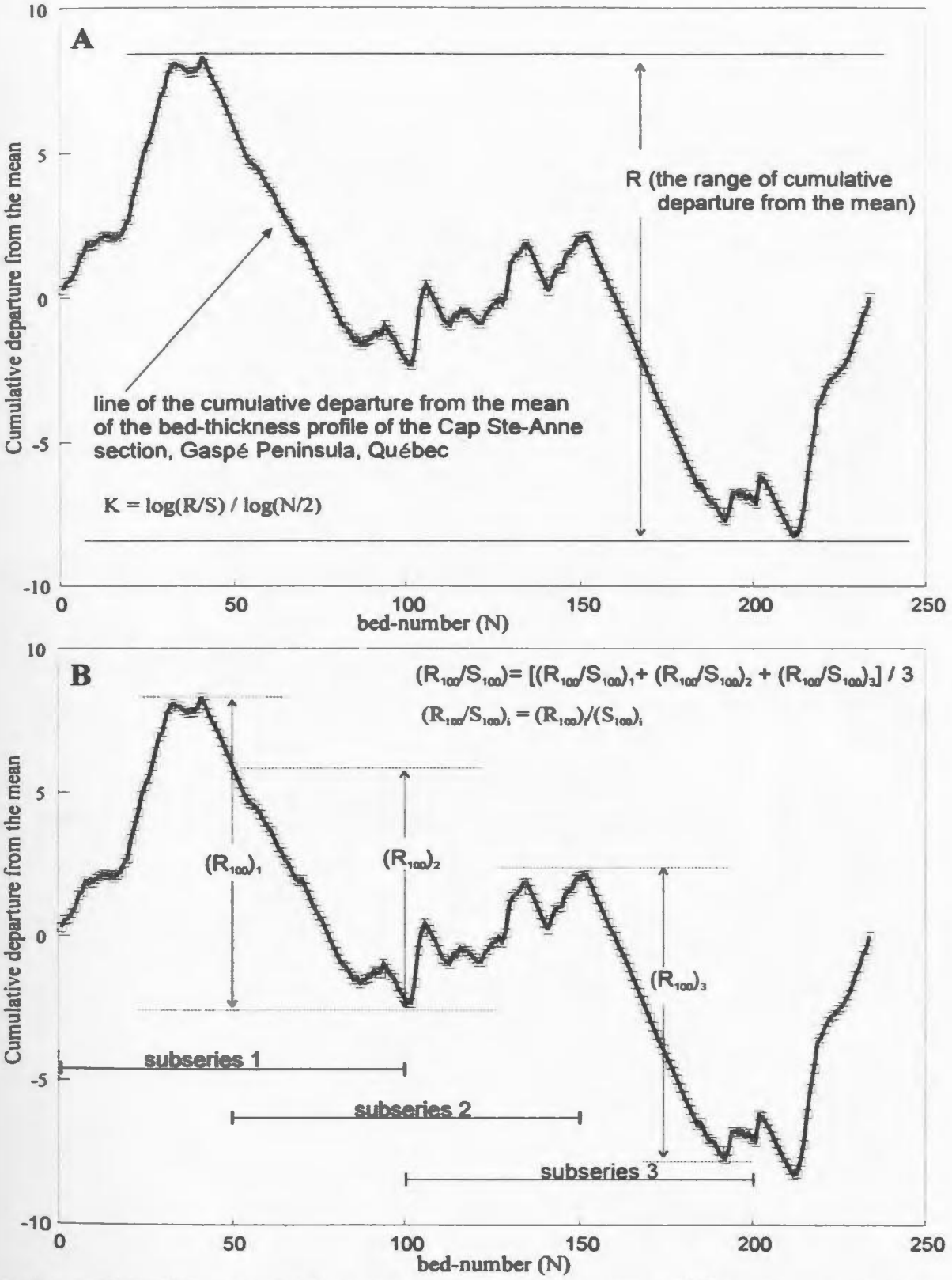

Fig. 5.1 A plot of the cumulative departure from the mean of the measurement, showing how to compute R of a whole sequence for calculating Hurst K (A), and how to calculate $(R_n)_j$ of subseries with n = 100 (B). For this example (N = 234), (R_{20}/S_{20}), (R_{24}/S_{24}) ... (R_{234}/S_{234}) should be computed in this way in order to obtain Hurst H.

calculating Hurst K, and shows how to compute (R_n/S_n) of subseries with length n, used for computing Hurst statistic H.

5.2.2 Reliability of Hurst K and H

An experiment was undertaken to confirm whether K or H is the preferred test statistic for "time-series" sequences of turbidite properties. The "time-series" sequence of bed-thicknesses of the Cache Creek section, California, was randomly shuffled to generate 300 random sequences; then values of Hurst K and H were calculated for both the original sequence and the 300 random sequences. This procedure was also applied to the sequences of grain-size scores and sandstone percentages of the same section.

Results are shown in Table 5.2. Note that K values obtained from the three original sequences are higher than the maximum values of K from their 300 random shuffles, but H values from the original sequences are smaller than the maximum values of H from random sequences.

For random sequences, the Hurst coefficient h is expected to be 0.5 when sample size N is large. The bed number (N) in the measured Cache Creek section is 599. The mean H value (around 0.55) is smaller than the mean K value (about 0.6) for each set of 300 randomly shuffled sequences (Table 5.2), confirming that H for shuffled sequences is closer in value to h than is K (Mandelbrot and Wallis, 1969; Wallis and Matalas, 1970, 1971; Booy and Morgan, 1985). However, when examining output files for tests using the Hurst H estimator, the following anomaly was discovered. The (R_n/S_n) values of most

Table 5.2 Results of the Hurst test for the Cache Creek section

	Original Sequence		300 Random Sequences					
			K Statistic			H Statistic		
	K	H	Max K	Mean $\bar{K}$	Min K	Max H	Mean $\bar{H}$	Min H
Bed-thickness	0.748	0.651	0.704	0.595	0.483	0.787	0.548	0.348
Grain-size score	0.778	0.689	0.704	0.592	0.479	0.734	0.543	0.358
Sandstone percentage	0.773	0.677	0.715	0.594	0.495	0.783	0.550	0.362

randomly shuffled sequences having a higher Hurst H than the original sequence are smaller than the corresponding (R_n/S_n) values of the original sequence (Fig. 5.2). Since the range of cumulative departure from the mean, R, is the most important parameter for the Hurst test, and K is directly proportional to R, K rather than H must be the preferred test statistic given that H and K give inconsistent results (Fig. 5.2). The bias inherent in using K as an estimator for the Hurst coefficient h can be remedied by using a Monte Carlo simulation technique for the calculation of significance levels for the tests (See the following section). Hence, K is adopted as the better statistic for the Hurst test for long-term persistence of turbidite characteristics, but only when used in parallel with Monte Carlo simulation. H is calculated in this study only for comparison.

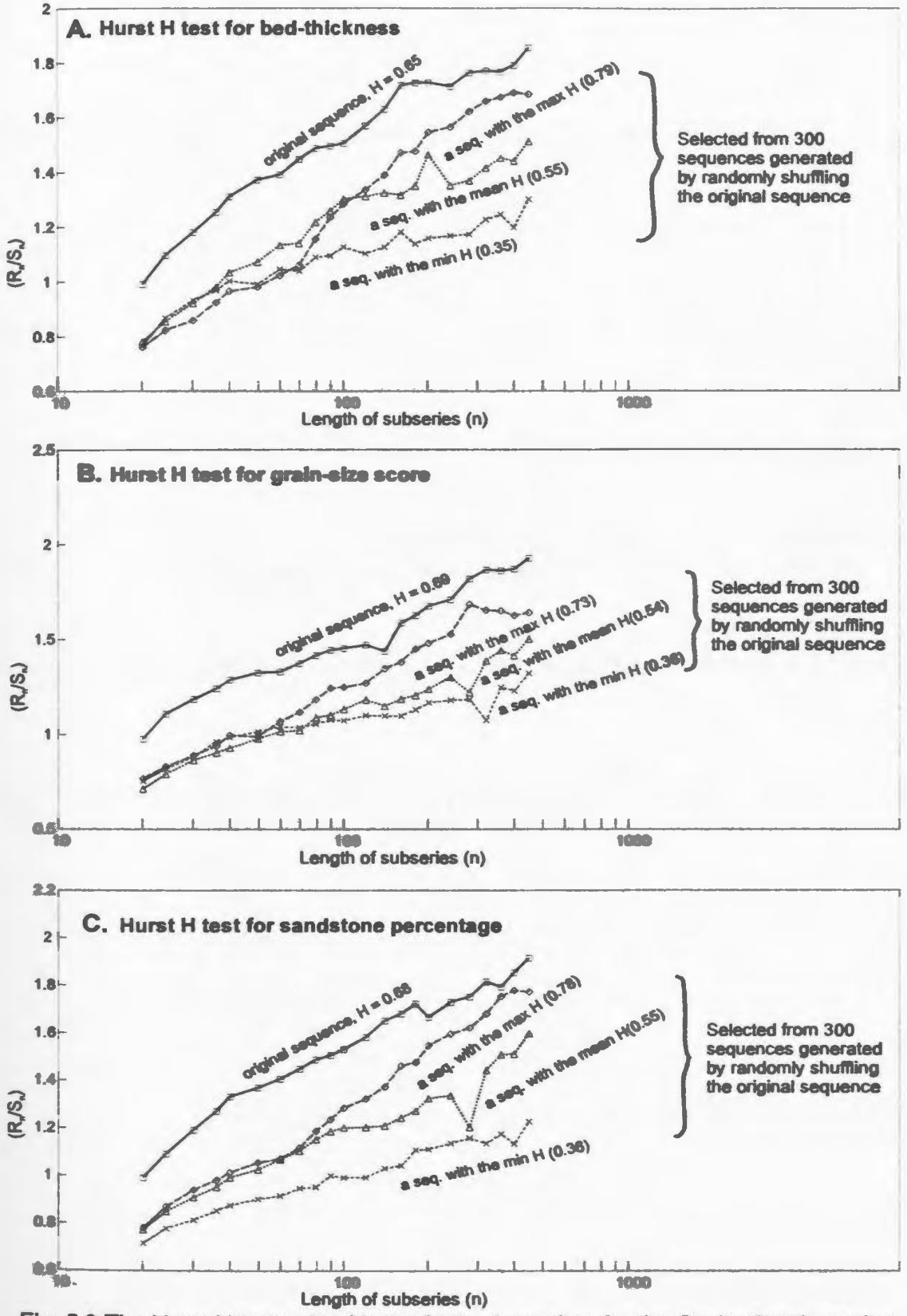

Fig. 5.2 The Hurst H test using Monte Carlo simulation, for the Cache Creek section, Great Valley, California. Note the higher values of (R_n/ S_n) for the original sequences even though their slope (H) is smaller than the maximum slope for the 300 randomly shuffled sequences.

5.2.3 Monte Carlo Simulation

Monte Carlo simulation, which randomly shuffles each original sequence to generate 300 random sequences, allows mean and standard deviation values of both Hurst K and H to be computed for the random sequences. The comparison of K and H values between original and randomly shuffled sequences eliminates any influence of deviations from the Gaussian distribution and transience (small N) as the explanations of the Hurst phenomenon. This technique also makes it unnecessary to worry about the biased estimation of the Hurst coefficient h by K and H. Thus, it provides an effective test for long-term persistence versus clustering in the studied turbidite successions.

A specified null hypothesis test, such as a Z test or a student t test, for Hurst K and H is not available. Monte Carlo simulation, however, provides a suitable approximate solution. The frequency distributions of K and H for a number of sets of 300 randomly shuffled turbidite sequences have been checked. When $N > 100$, the population of values of K very closely resembles a normal distribution with a standard deviation < 0.075; H has a normal distribution too, but with a standard deviation up to 0.128. These distribution characteristics permit the use of hypothesis tests for values of K and H calculated from the original turbidite sequences, analogous to the test described by Pfaffenberger and Patterson (1977, p 274-325). Here, the hypothesis for K is based on the assumption that, if the proportion of sequences with a $K \geq K_0$ (K_0 = the K value of an original turbidite sequence) in the 300 randomly shuffled sequences is smaller than a selected significance level, α (say, $\alpha = 10\%$ or 5%), then the hypothesis that the original

sequence and the 300 randomly shuffled sequences are drawn from the same population is rejected at that significance level, α. The null hypothesis and the alternative are then stated as:

$$H_0: P(K \geq K_0) \geq \alpha$$

$$H_a: P(K \geq K_0) < \alpha$$

This is one-tailed test. The hypothesis test for H is the same as that for K.

5.2.3 Test Procedure

The procedure for testing for cyclic clustering of properties of submarine fan turbidite successions consists of three steps. The first step is to compute Hurst K and H, the estimators of the Hurst coefficient h, for individual turbidite sections. The second step is Monte Carlo simulation for each section. The third step is to look for differences between the results for various field examples which might indicate that particular ranges of the Hurst K are indicative of particular submarine fan environments. A Fortran-77 program, HURST.FOR, has been written for step one and step two (Appendix II-3).

Three short turbidite sections measured in the northern Italian Apennines and six short sections from the Gulf Islands of British Columbia were not tested (small N). Nineteen sections with $N > 100$ were evaluated. Three bed-by-bed measurements were considered: (1) sandstone (including conglomerate and siltstone) thickness, (2) sandstone (conglomerate and siltstone) thickness percentage (i.e., sandstone versus mudstone in a bed), and (3) grain-size score.

Recall that the definition of "grain-size score" (Chapter 2) makes use of the ϕ scale of grain-size, and therefore is numerically inversely proportional to the actual grain-size. In the calculation of Hurst K and H , and for plotting of cumulative departures from the mean, some simple treatments for grain-size scores are needed. First, each value of grain-size score is multiplied by minus one (-1) so that the modified grain-size scores become numerically proportional to the actual grain-size (i.e., a coarser grain-size with a larger value), and therefore parallel to values of bed-thicknesses and sandstone percentages. Thus, a thick-bedded, coarse-grained and sandy bed cluster, or a thin-bedded, fine-grained and muddy bed cluster, would display an identical pattern in the plots of the cumulative departures from the mean of the three observations. Secondly, If there are negative values in a sequence of these modified grain-size scores, a positive number larger than the maximum absolute value of these negative scores is added to each observation of the sequence. By eliminating negative values, the sequence can then be transformed to log data that are required for computing Hurst K and H. One can also convert "grain-size scores" to the millimeter values beforehand, then simply use $\log_{10}$ values of grain size (mm) for the calculation of the Hurst K and H, and for plotting of cumulative departures from the mean. However, this manipulation does not produce different results from those obtained using grain-size scores.

5.3 Results

Table 5.3 presents the results of the Hurst test for the nineteen turbidite sections.

Table 5.3 The results of the Hurst test for the measurements of the nineteen turbidite sections

	K Statistics of 300 random sequences				Original Sequence			H Statistics of 300 random sequences				Original Sequence		
Sections	Max K	Mean $(\overline{K})$	Min K	STD DEV	K	No. of STD DEV from $\overline{K}$	α	Max H	Mean $(\overline{H})$	Min H	STD DEV	H	No. of STD DEV from $\overline{H}$	α
Cmont-b	0.678	0.581	0.488	0.036	0.874	8.078	< 0.3%	0.707	0.531	0.391	0.059	0.777	4.197	< 0.3%
Cmont-g	0.668	0.576	0.496	0.034	0.852	8.108	< 0.3%	0.682	0.523	0.373	0.056	0.728	3.634	< 0.3%
Cmont-s	0.678	0.578	0.487	0.034	0.825	7.248	< 0.3%	0.692	0.532	0.352	0.057	0.702	2.966	< 0.3%
Ccack-b	0.704	0.595	0.483	0.040	0.748	3.819	< 0.3%	0.787	0.548	0.348	0.077	0.651	1.335	8.7%
Ccack-g	0.704	0.592	0.479	0.037	0.778	4.969	< 0.3%	0.734	0.543	0.358	0.071	0.689	2.054	4.0%
Ccack-s	0.715	0.594	0.495	0.037	0.773	4.776	< 0.3%	0.783	0.550	0.362	0.073	0.677	1.738	4.3%
Qpet-b	0.652	0.573	0.495	0.032	0.774	6.358	< 0.3%	0.622	0.532	0.412	0.042	0.798	6.273	< 0.3%
Qpet-s	0.654	0.576	0.488	0.031	0.733	4.982	< 0.3%	0.656	0.535	0.407	0.045	0.688	3.422	< 0.3%
Qcsa1-b	0.712	0.601	0.465	0.047	0.852	5.306	< 0.3%	0.818	0.553	0.327	0.102	0.855	2.948	< 0.3%
Qcsa1-s	0.705	0.601	0.495	0.047	0.818	4.604	< 0.3%	0.811	0.557	0.313	0.105	0.860	2.884	< 0.3%
Qcsa2-b	0.751	0.598	0.474	0.048	0.755	3.254	< 0.3%	0.821	0.552	0.359	0.096	0.766	2.216	1.5%
Qcsa2-s	0.733	0.598	0.466	0.045	0.742	3.171	< 0.3%	0.821	0.553	0.280	0.092	0.831	3.011	< 0.3%
Itcast-b	0.715	0.593	0.490	0.040	0.668	1.896	2.3%	0.782	0.558	0.350	0.079	0.657	1.265	12.3%
Itcast-g	0.717	0.596	0.498	0.042	0.697	2.373	0.3%	0.816	0.552	0.336	0.075	0.659	1.419	7.7%
Itcast-s	0.708	0.594	0.488	0.040	0.684	2.231	1.0%	0.762	0.557	0.332	0.075	0.698	1.890	3.3%
Itconia-b	0.742	0.610	0.457	0.052	0.707	1.870	3.7%	0.881	0.563	0.089	0.119	0.754	1.602	6.3%
Itconia-g	0.752	0.611	0.474	0.053	0.747	2.592	0.3%	0.832	0.559	0.232	0.104	0.796	2.274	1.0%
Itconia-s	0.770	0.606	0.439	0.054	0.705	1.841	3.7%	0.945	0.567	0.317	0.110	0.674	0.966	17.3%
Itcaso-b	0.708	0.596	0.482	0.043	0.651	1.281	10.3%	0.790	0.565	0.287	0.077	0.581	0.198	45.3%
Itcaso-g	0.698	0.595	0.456	0.045	0.626	0.683	26.7%	0.736	0.552	0.360	0.074	0.560	0.106	46.7%
Itcaso-s	0.735	0.601	0.498	0.044	0.740	3.164	< 0.3%	0.747	0.558	0.315	0.076	0.706	1.955	1.7%
A931-b	0.723	0.607	0.494	0.048	0.62	0.16	42.0%	0.885	0.559	0.333	0.097	0.522	-0.375	64.3%
A931-s	0.715	0.61	0.479	0.049	0.67	1.257	12.0%	0.830	0.576	0.285	0.096	0.641	0.678	24.7%
A944-b	0.775	0.619	0.455	0.057	0.78	2.834	< 0.3%	0.881	0.581	0.221	0.122	0.726	1.190	13.0%
A944-s	0.752	0.608	0.456	0.056	0.73	2.21	1.67%	0.950	0.560	0.030	0.128	0.709	1.165	12.3%
A946-b	0.765	0.609	0.108	0.073	0.75	1.886	0.3%	0.937	0.567	0.182	0.116	0.799	2.007	3.0%
A946-s	0.778	0.613	0.469	0.057	0.79	3.123	< 0.3%	0.922	0.574	0.287	0.121	0.827	2.095	1.7%
Barb1-b	0.748	0.608	0.481	0.05	0.8	3.739	< 0.3%	0.954	0.568	0.337	0.100	0.741	1.736	4.0%
Barb1-s	0.722	0.605	0.491	0.05	0.75	2.986	< 0.3%	0.830	0.567	0.312	0.098	0.763	2.012	1.3%
Barb2-b	0.769	0.612	0.477	0.055	0.78	3.101	< 0.3%	0.880	0.574	0.282	0.116	0.807	2.008	2.0%
Barb2-s	0.747	0.611	0.462	0.052	0.76	2.947	< 0.3%	0.816	0.563	0.304	0.104	0.782	2.109	1.0%

...Continued

Table 5.3 The results of the Hurst test for the measurements of the nineteen turbidite sections

	K Statistics of 300 random sequences				Original Sequence			H Statistics of 300 random sequences				Original Sequence		
Sections	Max K	Mean ($\bar{K}$)	Min K	STD DEV	K	No. of STD DEV from $\bar{K}$	α	Max H	Mean ($\bar{H}$)	Min H	STD DEV	H	No. of STD DEV from $\bar{H}$	α
Brit-b	0.719	0.606	0.468	0.044	0.75	3.31	< 0.3%	0.739	0.561	0.284	0.085	0.583	0.260	39.7%
Brit-s	0.73	0.599	0.453	0.052	0.81	4.143	< 0.3%	0.864	0.562	0.305	0.094	0.727	1.748	2.7%
AkspE-b	0.666	0.582	0.497	0.036	0.81	8.746	< 0.3%	0.724	0.545	0.37	0.064	0.94	6.155	< 0.3%
AkspE-s	0.676	0.586	0.483	0.035	0.8	6.103	< 0.3%	0.72	0.54	0.358	0.062	0.88	5.555	< 0.3%
AkspW-b	0.695	0.58	0.499	0.033	0.8	6.616	< 0.3%	0.682	0.545	0.409	0.055	0.9	6.429	< 0.3%
AkspW-s	0.66	0.581	0.491	0.033	0.72	4.141	< 0.3%	0.697	0.536	0.4	0.057	0.83	5.102	< 0.3%
Nw12b	0.7	0.594	0.459	0.043	0.66	1.521	7.3%	0.745	0.553	0.314	0.072	0.609	0.786	20.3%
Nw15b	0.746	0.602	0.484	0.047	0.63	0.48	30.0%	0.917	0.562	0.353	0.091	0.627	0.715	23.3%
Nw16b	0.73	0.599	0.493	0.044	0.67	1.633	6.7%	0.804	0.560	0.374	0.082	0.620	0.733	21.0%

Note: b, g and s represent the data profiles of bed-thickness, grain-size and sandstone percentage, respectively.
Cmont, Ccack represent the Monticello Dam section and the Cache Creek section of the Great Valley, California;
Qpet, Qcsa1 and Qcsa2 are the Petite Vallée section and Cap Ste-Anne section of the Gaspé Peninsula, Quebec;
Itcast, Itconia and Itcaso represent the Castal de Rio section, the Coniale section, and the Casovona section measured in Santerno Valley of the northern Italian Apennines;
A931, A944 and A946 are the sections of ODP Sites 931, 944 and 946 on the Amazon Fan;
Barb1 and Barb2 are the two sections measured in Barbados;
Brit represents a section measured at the Gulf Island of British Columbia;
AkspE and AkspW represent the sections of the DeGray Dam spillway east and west, Arkansas;
Nw12, Nw15 and Nw16 are the sections at Nalneset, Northern Norway.

Results confirm that Hurst K and H vary with sample size N. Thus, K and H of the original sequence must be compared with those of random sequences having the same sample size. This is ensured by the Monte Carlo simulation technique which randomly shuffles each original sequence to generate 300 random sequences.

Table 5.3 shows that many profiles of the three types of bed-by-bed data pass the Hurst test for long-term persistence (i.e., the null hypothesis of no clustering is rejected). Note that many profiles attain a higher significance level when using H as the test criterion than using K (i.e., with K, the null hypothesis would be rejected more easily than with H). However, H is a less reliable statistic for the Hurst test than K, because H does not directly reflect R, the most important parameter for clustering (§5.2.2, Fig. 5.2).

5.3.1 Long-Term Clustering Cycles Revealed by the Hurst Phenomenon

For bed-thickness, grain-size score, and sandstone percentage in the ten sections measured in the Great Valley (California), in the Gaspé Peninsula (Québec), in Barbados, in the Gulf Islands (British Columbia), and in the DeGray Lake area (Arkansas), none of the 300 randomly shuffled sequences yielded a K value as large as the value for the original sequence. In Table 5.3, these sequences passed the Hurst K test at a significance level (α) < 0.3%. Two sections measured in the northern Italian Apennines and two sections from the Amazon Fan passed the Hurst K test at a significance level < 5% for all three data types. Two bed-thickness sequences from Northern Norway passed the test at the 10% significance level. In total, 16 (84.2%) of 19 turbidite sections passed the Hurst

K test with a significance level (α) $\leq$ 10%.

At the 10% significance level, the cumulative binomial probability of 4 or more successes in 19 random trials is 0.11, 5 or more successes is 0.035, and 16 or more successes is 0.0086 (calculated using Eqn. 4.1). The probability to obtain 5 or more successes in 19 random trials is a marginal value. Thus, at least 11 out of the 16 turbidite sections which passed the Hurst K test at the 10% significance level could not have been expected for random processes.

Under the null hypothesis, the odds of one or more section passing a test at the α/N level is less than or equal to α (Miller, 1981, p. 67-70; SAS Institute, 1990, p. 942-944; Harper, 1984, p. 5). Using the α/N (0.1/19 = 0.005) level for the Hurst K test, 12 of the 19 analyzed sections are significant (Table 5.3), passing the test at a significance level less 0.005. This coincides with the analytical calculation of the cumulative binomial probability.

Only three of the nineteen sections failed to pass the test (failed to cause rejection of the null hypothesis) at the 10% significance level. Of the three sections, the Casovona section measured in the Santerno Valley, northern Italian Apennines, passed the Hurst K test at a significance level (α) slightly higher than 10% (10.3%) for the bed-thickness profile, at α = 26.7% for the grain-size score profile, but at α < 0.3% for the sandstone percentage profile. The failure of the section at ODP Site 931, on the Amazon Fan, and sections 15 of Drinkwater (1995) to pass the Hurst K test may be simply because many thin beds were not measured or because these sections are not long enough to show long-

term vertical changes of sedimentary facies.

Considering all profiles based on the three types of field data (bed-thickness, grain-size score, and sandstone percentage), a total of forty profiles from the nineteen sections were tested for long-term persistence or clustering. Thirty-five (87.5%) of these profiles, each based on one of the bed-by-bed variables, pass the test at $\alpha < 10\%$. Thirty-three (82.5%) profiles pass the test at a significance level $\alpha < 5\%$.

Only cyclic clustering can account for the high values of Hurst K from these turbidite sections. The results from this study strongly suggest ($\alpha < 10\%$) that the three types of bed-by-bed data from many turbidite sections show a cyclic clustering pattern, i.e., they show the Hurst phenomenon.

5.3.2 Clustering Patterns

Figures 5.3 and 5.4 present the clustering patterns and the Hurst statistics of channel-levee deposits of the Monticello Dam section measured in the Great Valley. Plots of the cumulative departure from the mean (Fig. 5.3) provide a straightforward view of the clustering patterns. These plots are very similar to Fischer plots (Fischer, 1964).

Figures 5.5 and 5.6 provide an example of the clustering of the measurements of turbidites in submarine fan lobe environments, from the Cache Creek section in the Great Valley. The clustering of thin and thick beds in this section has been recognized by Murray et al. (1996) by means of a "run about the median" test. This characteristic is confirmed by the Hurst test. Note that the plots of the cumulative departure from the

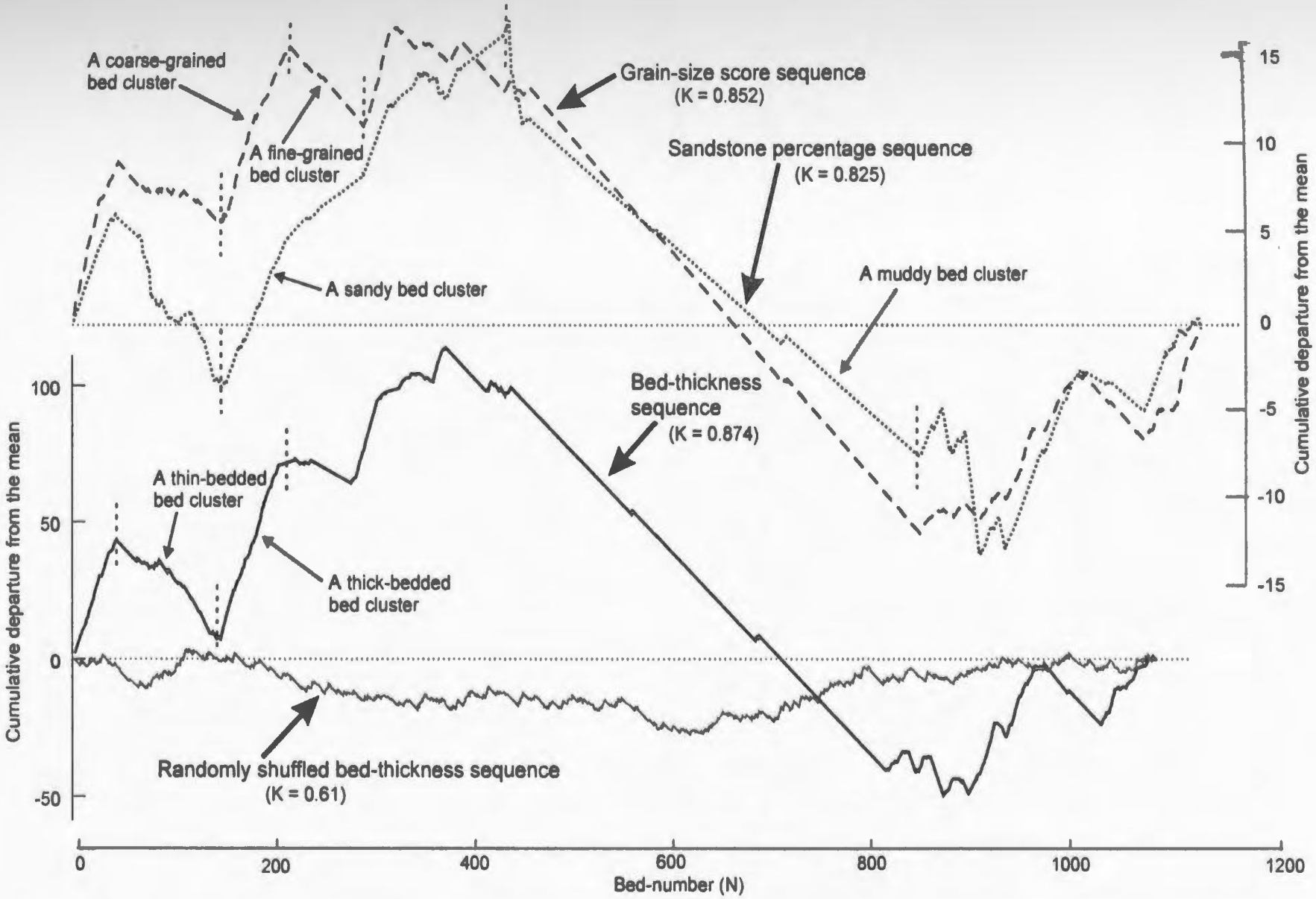

Fig. 5.3 Plots of the cumulative departure from the mean of bed-by-bed measurements at the Monticello Dam section, Great Valley, California, showing a distinct grouping pattern of low and high values. The same curve for a randomly shuffled bed-thickness sequence is plotted for comparison. In calculating the cumulative departure from the mean, log values of the field parameters have been used.

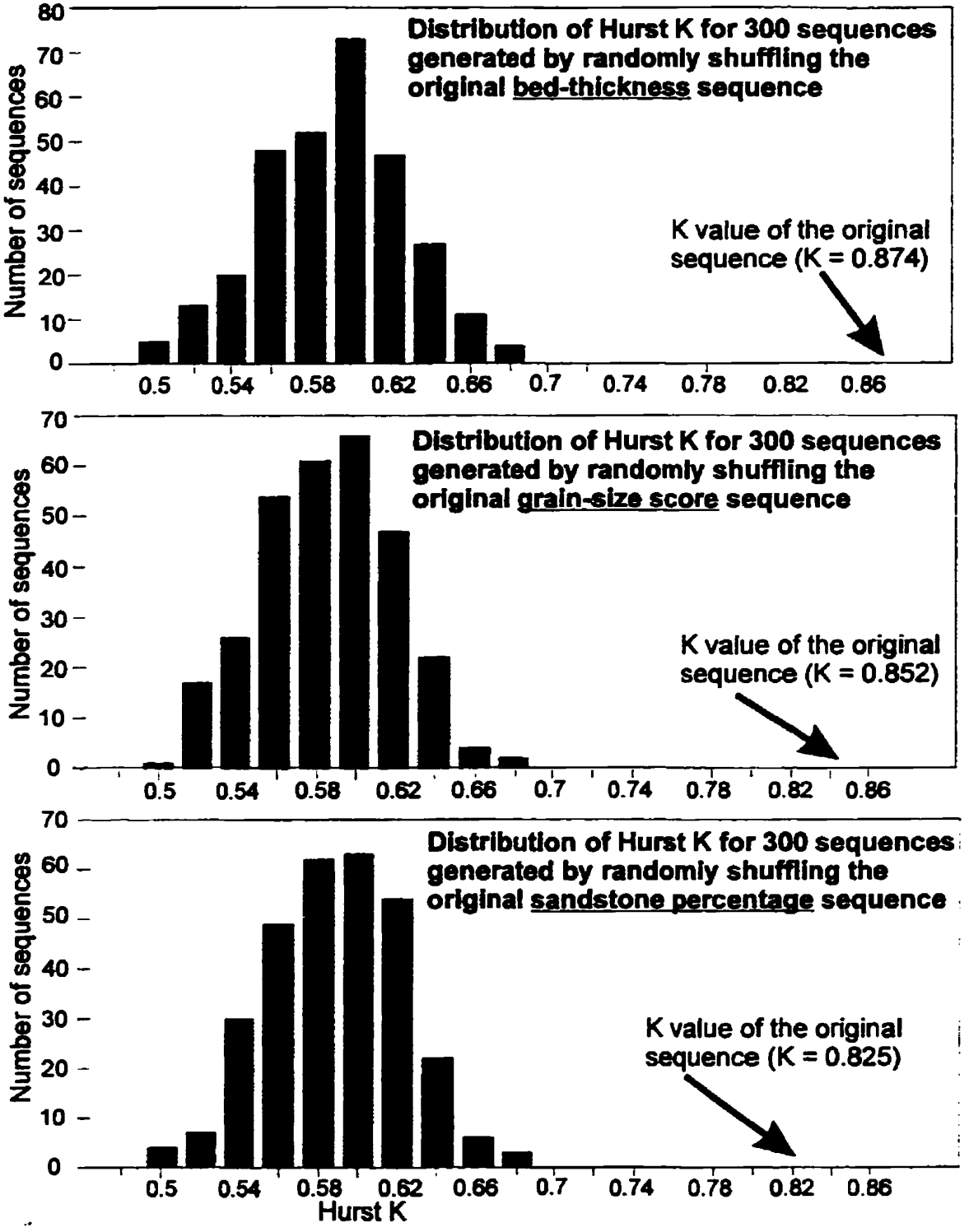

Fig. 5.4 Frequency distributions of the 300 sequences generated by randomly shuffling values for three field parameters at the Monticello Dam section, Great Valley, California. Note that the Hurst K values of the original sequences strongly deviate from the mean K of random sequences.

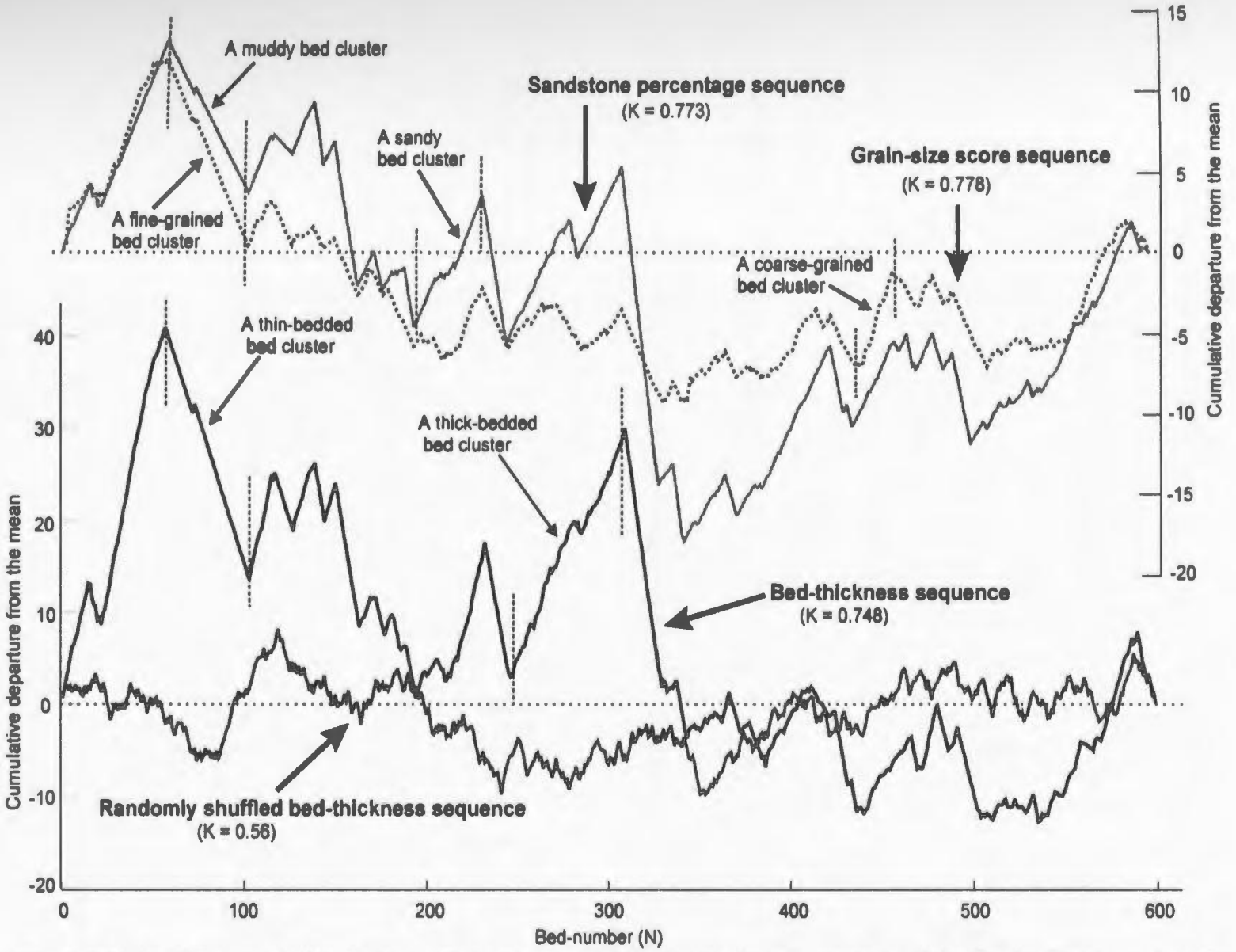

Fig. 5.5 Plots of the cumulative departure from the mean of bed-by-bed measurements of the Cache Creek section, Great Valley, California, showing a distinct grouping pattern of low and high values. The same curve for a randomly shuffled bed-thickness sequence is plotted for comparison. In calculating the cumulative departure from the mean, log values of the field parameters have been used. Note that the three types of bed-by-bed data show a consistent grouping pattern.

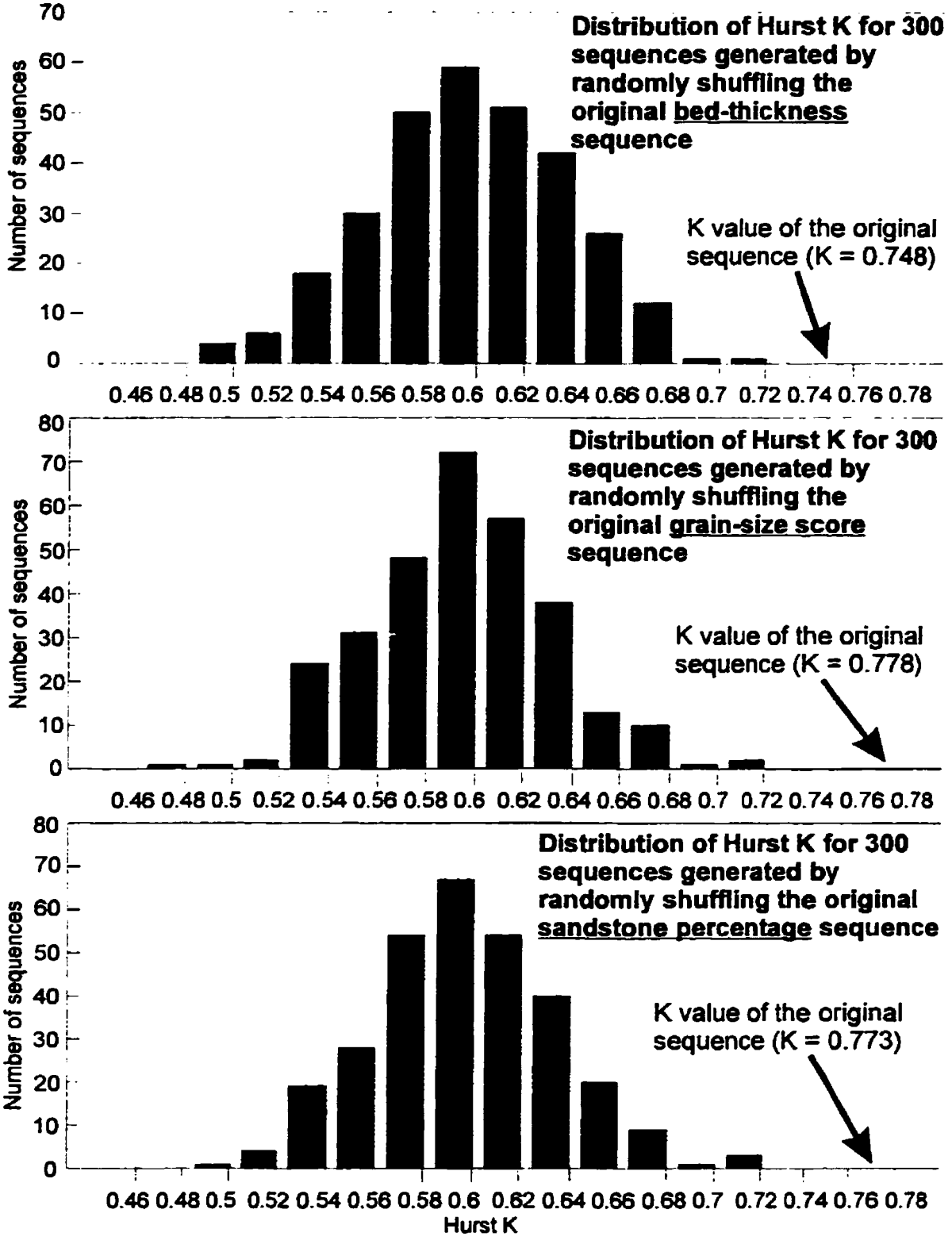

Fig. 5.6 Frequency distributions of the 300 sequences generated by randomly shuffling values for three field parameters at the Cache Creek section, Great Valley, California. Note that the Hurst K values of the original sequences strongly deviate from the mean K of random sequences.

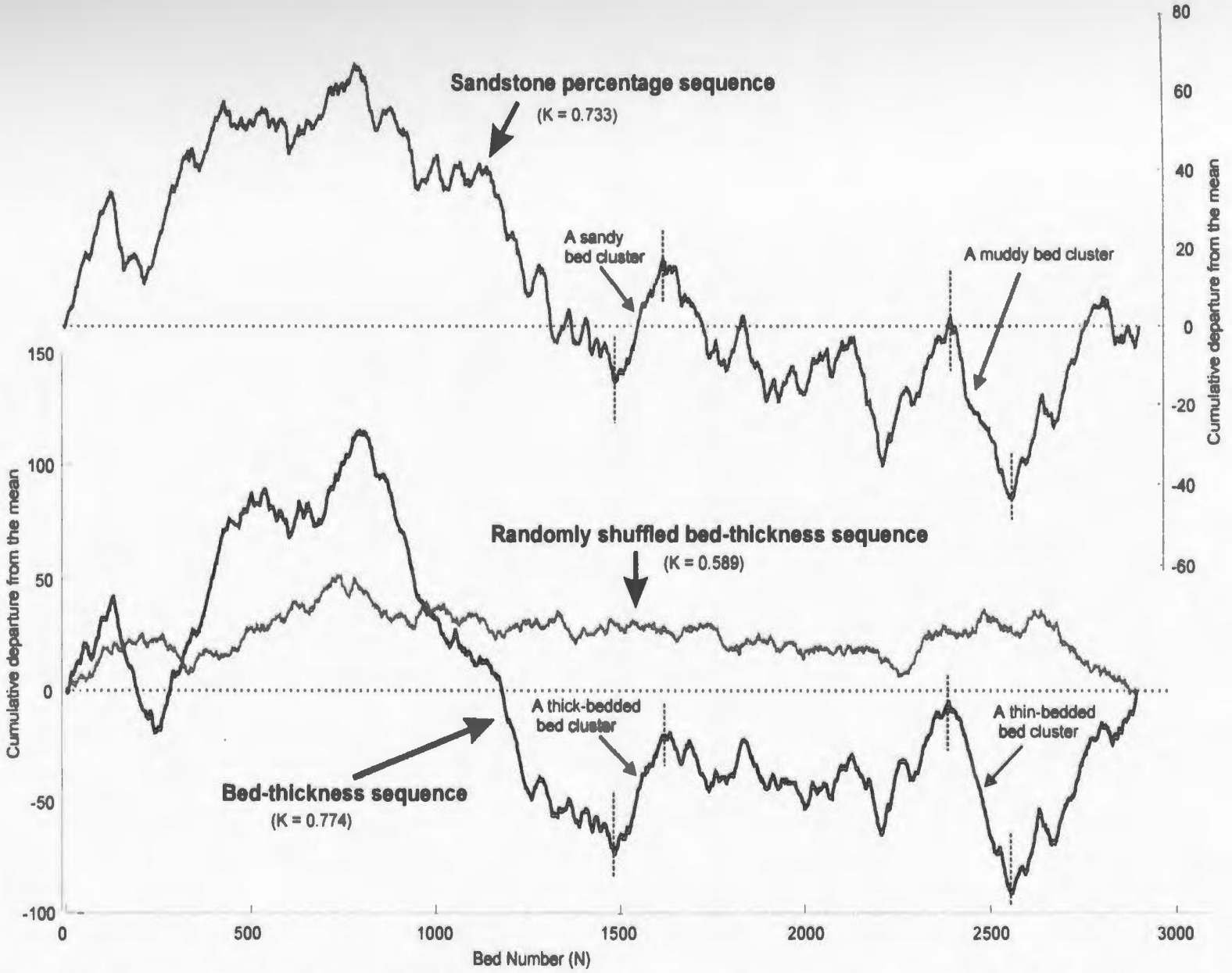

Fig. 5.7 Plots of the cumulative departure from the mean of bed-thicknesses and sandstone percentages for the Petite Vallée section, Gaspé Peninsula, Québec, showing a distinct irregular grouping pattern of low and high values. The same curve for a randomly shuffled bed-thickness sequence is plotted for comparison. In calculating the cumulative departure from the mean, log values of the field parameters have been used. Note that both sandstone percentage and bed-thickness have a consistent grouping pattern.

mean of the measurements (Fig. 5.5) much more clearly show this clustering than does the plot of bed-thickness versus bed number (Fig. 7 of Murray et al., 1996).

Figure 5.7 presents the clustering patterns of bed-thicknesses and sandstone percentages of the Petite Vallée section (Gaspé Peninsula), the longest section in this study, with 2893 beds.

It is important to find from Figures 5.3, 5.5 and 5.7 that the pattern of the cumulative departure from the mean is very similar for the three types of bed-by-bed data. This indicates that most thick-bedded bed clusters are also coarse-grained and sandy bed clusters, and most thin-bedded bed clusters coincide with fine-grained and muddy bed clusters. The alternate stacking of thin-bedded, fine-grained and muddy bed clusters and thick-bedded, coarse-grained and sandy bed clusters constitute a statistically significant facies organization in submarine fan systems.

5.3.3 Environmental Significance of the Hurst K

Hurst K is an estimator of the degree of clustering of thin and thick beds or low and high values of other measurements. The general clustering pattern of field variables in submarine fan systems is caused by vertical changes of facies and depositional environments. The thin-bedded, fine-grained and muddy bed clusters represent levee, channel margin or interchannel deposits in upper and middle fan regions, and interlobe or basin floor deposits in middle and outer fan lobe environments. The thick-bedded, coarse-grained and sandy bed clusters are associated with channel or crevasse-splay lobe

deposits (Bouma et al., 1995) in channel-levee complexes, and lobe deposits in middle and outer fan areas.

Use of the Hurst test indicates that both channel-levee deposits and lobe deposits in submarine fan systems show marked clustering for the three types of field data. Can the Hurst test further discriminate between submarine fan environments? This question is evaluated here only for those sections that are long enough to show an alternate stacking of clusters of one type or another. These sections must have been measured in detail, i. e., all beds thicker than 3 cm must have been measured, because the K value for a section in which all beds thicker than 3 cm have been measured would be different from that for the same section in which only beds thicker than 10 cm are measured. Ten sections from California, Italy, Quebec and Arkansas (Table 5.4) satisfy these requirements.

Both Hurst K for the field sections, and the number of standard deviations separating these values from the mean K values of the random sequences (Table 5.4) are used to distinguish depositional environments (Fig. 5.8). For the ten sections selected, the depositional environments are already reasonably well known from large-scale outcrop criteria (Table 1.1), so that the immediate aim is to see if similar environments share clustering characteristics. It is clear that the ten sections are well separated into three groups based mainly on the deviation from the mean K values (Fig. 5.8). Group 1 is characterized by a high K (strong clustering) and a large departure from the mean. It includes the Monticello Dam section of the Great Valley (California), which has been interpreted as channel-levee deposits (Ingersoll, 1978), and sections measured in the

Table 5.4 Hurst K and the number of the standard deviation from the mean $\bar{K}$ for ten turbidite sections

Sections	Depositional environments	Measurements	Hurst K	Deviation from $\bar{K}$
Monticello Dam, California	Channel-levee (Ingersoll, 1978)	Bed-thickness	0.874	8.078
		Grain-size score	0.852	8.108
		Sandstone %	0.825	7.248
DeGray Dam E, Arkansas	Levee and crevasse-splay lobes (Bouma et al., 1995)	Bed-thickness	0.81	8.746
		Sandstone %	0.8	6.103
DeGray Dam W, Arkansas		Bed-thickness	0.8	6.616
		Sandstone %	0.72	4.141
Cache Creek, California	Lobes (Ingersoll, 1978)	Bed-thickness	0.748	3.819
		Grain-size score	0.778	4.969
		Sandstone %	0.773	4.776
Petite Vallée, Québec	Lobes (Hiscott et al., 1986)	Bed-thickness	0.774	6.358
		Sandstone %	0.733	4.985
Cap Ste-Anne 1, Québec	Lobes (Hiscott ,1981)	Bed-thickness	0.852	5.306
		Sandstone %	0.818	4.604
Cap Ste-Anne 2, Québec		Bed-thickness	0.755	3.254
		Sandstone %	0.742	3.171
Castel del Rio, Italy	Lobe or basin-floor sheet sand systems (Ricci Lucchi, 1975; Cattaneo and Ricci Lucchi, 1995)	Bed-thickness	0.668	1.986
		Grain-size score	0.697	2.373
		Sandstone %	0.684	2.231
Coniale, Italy		Bed-thickness	0.707	1.87
		Grain-size score	0.747	2.592
		Sandstone %	0.705	1.841
Casovona, Italy		Bed-thickness	0.651	1.281
		Grain-size score	0.625	0.683
		Sandstone %	0.74	3.164

Note: The deviation from the mean ($\bar{K}$) for an original sequence is calculated by: $(K - \bar{K}) / S$; $\bar{K}$ and S (standard deviation) are computed from the frequency distribution of K values of the 300 sequences generated by randomly shuffling the original sequence.

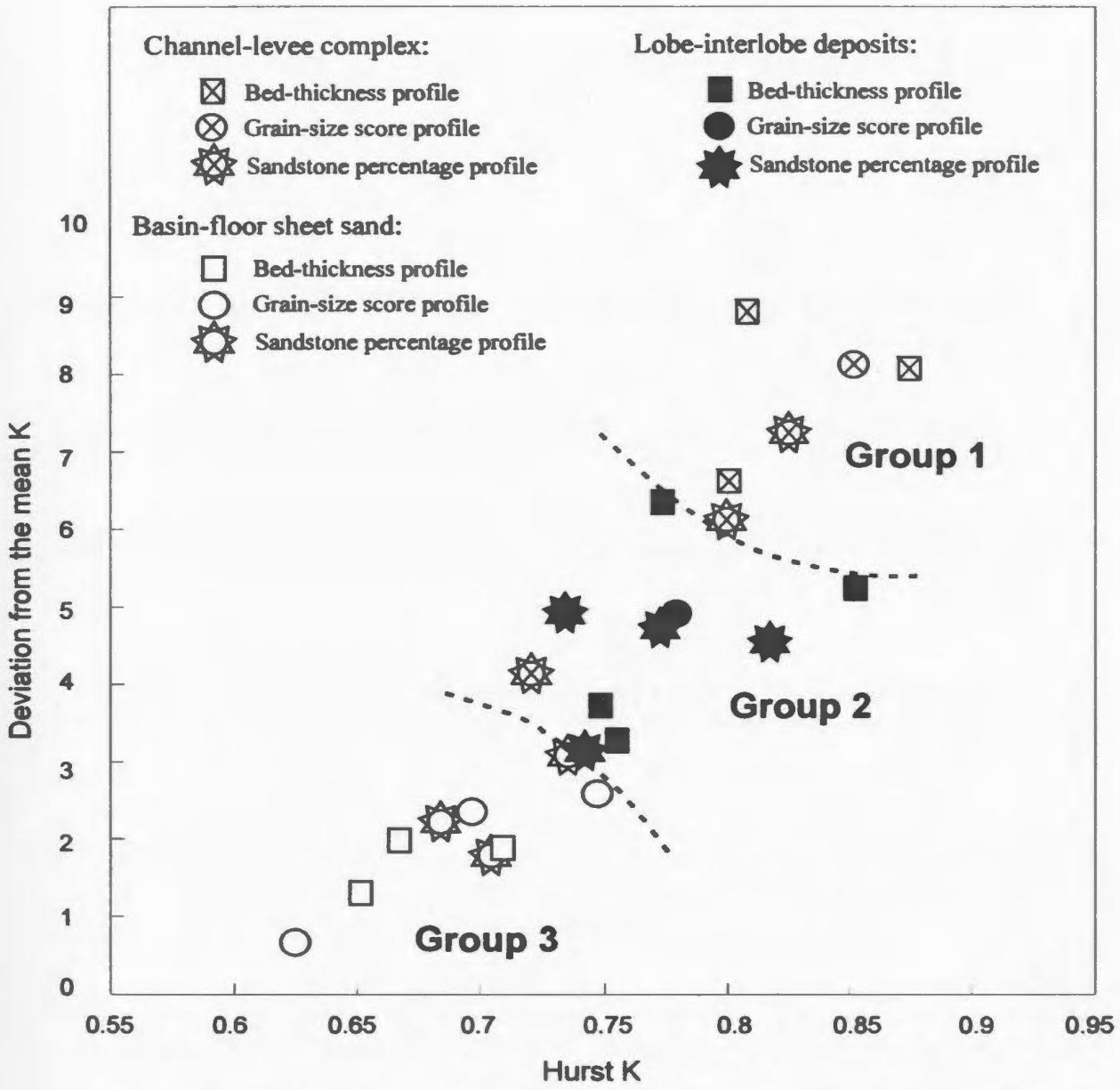

Fig. 5.8 A plot of data from Table 5.3. Data points from channel-levee deposits, lobe-interlobe deposits, and basin-floor sand systems can be separated into three groups.

DeGray Lake area (Arkansas), which have been interpreted as levee and crevasse-splay lobe deposits of channel-levee complexes (Bouma et al., 1995). Group 2 has a medium K and a moderate departure from the mean. It contains the Cache Creek section of the Great Valley and sections measured in the Gaspé Peninsula (Québec). All these sections have been interpreted as lobe deposits (Ingersoll, 1978; Hiscott, 1980; Hiscott et al., 1986; Murray et al., 1996). Group 3 has a lower K and a small departure from the mean. All three longer sections measured in the Santerno Valley of the northern Italian Apennines plot in this group. These deposits have been interpreted as a basin-floor sheet sand system (Cattaneo and Ricci Lucchi, 1995). Sections which contain both channel and lobe deposits span groups 1 and 2, depending on whether levee deposits are well developed or not. All three types of field data (bed-thickness, grain-size score, and sandstone percentage) give consistent results, so only one global plot is required. Due to the limited data points in Figure 5.8, future improvements are expected, perhaps by using well-logging data.

5.4 Orderly Cycles?

Submarine fan turbidite successions have been demonstrated to be characterized by cycles of thin-bedded bed clusters and thick-bedded bed clusters, believed to be associated with changes of depositional environments. The question is: are these cycles orderly or hierarchical.

Accentuated deposition on submarine fans has been widely considered to occur during

low stands of sea-level (e.g. Posamentier et al., 1988; Vail et al., 1991; Mutti, 1985, 1992; Normark et al., in press). At times of low sea-level, rivers may discharge hyperpycnal flows directly to submarine canyons to form turbidity currents which carry sediments well down to fan areas, and sediment failures at the shelf-break generate highly efficient turbidity currents which carry sand to fan environments. At times of high sea-level, many submarine fans are draped by more muddy sediments. Periodic changes of sea-level (Haq et al., 1987) might, then, produce orderly or hierarchical cycles of thick-sandy and thin-muddy turbidites in fan systems. In contrast, tectonically induced fluctuations in sediment supply, submarine canyon and fan channel switching, channel bifurcation and avulsion, lobe shifting, multiple sediment inputs, erosion of previous deposits by turbidity currents, and many other processes are believed to cause random shifting of subenvironments and sedimentary facies and to produce irregular and non-periodic depositional cycles. These processes can completely mask any record of orderly, periodic sea-level changes, if they exist.

Bed thicknesses of turbidites are not proportional to even short-term accumulation rates, so it is almost impossible to obtain accurate time spans for sandy bed clusters and muddy bed clusters in most submarine fan successions (ancient or modern). Therefore, unambiguous recognition of orderly or hierarchical depositional cycles in most submarine fan successions caused by periodic sea-level changes (e.g. Haq et al., 1987) is basically impossible, even though sea-level changes may have provided a primary control on the development of these fan systems (Normark et al., in press).

Drummond and Wilkinson (1996) demonstrated that natural bed-thickness populations plot as exponential frequency distributions without a modal class. The exponential frequency distribution of bed-thicknesses for turbidite sections has been confirmed by this study (Fig. 5.9) and by others (e.g. Hiscott et al., 1992; Rothman et al., 1994). Based on their assumption that each regularly recurring forcing mechanism should produce a single mode in a bed-thickness population, Drummond and Wilkinson (1996) argued that most natural sedimentary sections are not formed of hierarchical or orderly cycles.

What Drummond and Wilkinson (1996) demonstrated, however, is only that bed thicknesses in these natural populations do not concentrate to one or more modal class (e.g., beds largely 20-50 cm thick and 2-4 m thick, say, with few beds in between). This is only one type of organizational hierarchy. Another type of hierarchy might be clustering of thinner and thicker beds of a normal or exponential population into packets. This type of hierarchy was not evaluated by Drummond and Wilkinson (1996), but is easily tested using the Hurst statistic and associated tests. For these tests, a normal (or log-normal) bed-thickness population is not necessary. Further, the existence of a modal class does not imply the presence of orderly cycles. For example, Hurst (1951) tested 690 sequences of seventy-five different natural phenomena and found that they all had a normal or nearly normal frequency distribution, but that most exhibited an irregular grouping pattern, having a mean Hurst K value of 0.73 with a standard deviation of 0.092. This constitutes the basis for the recognition of the Hurst phenomenon ---- the tendency for natural events to occur in irregular or non-periodic groups in which high or

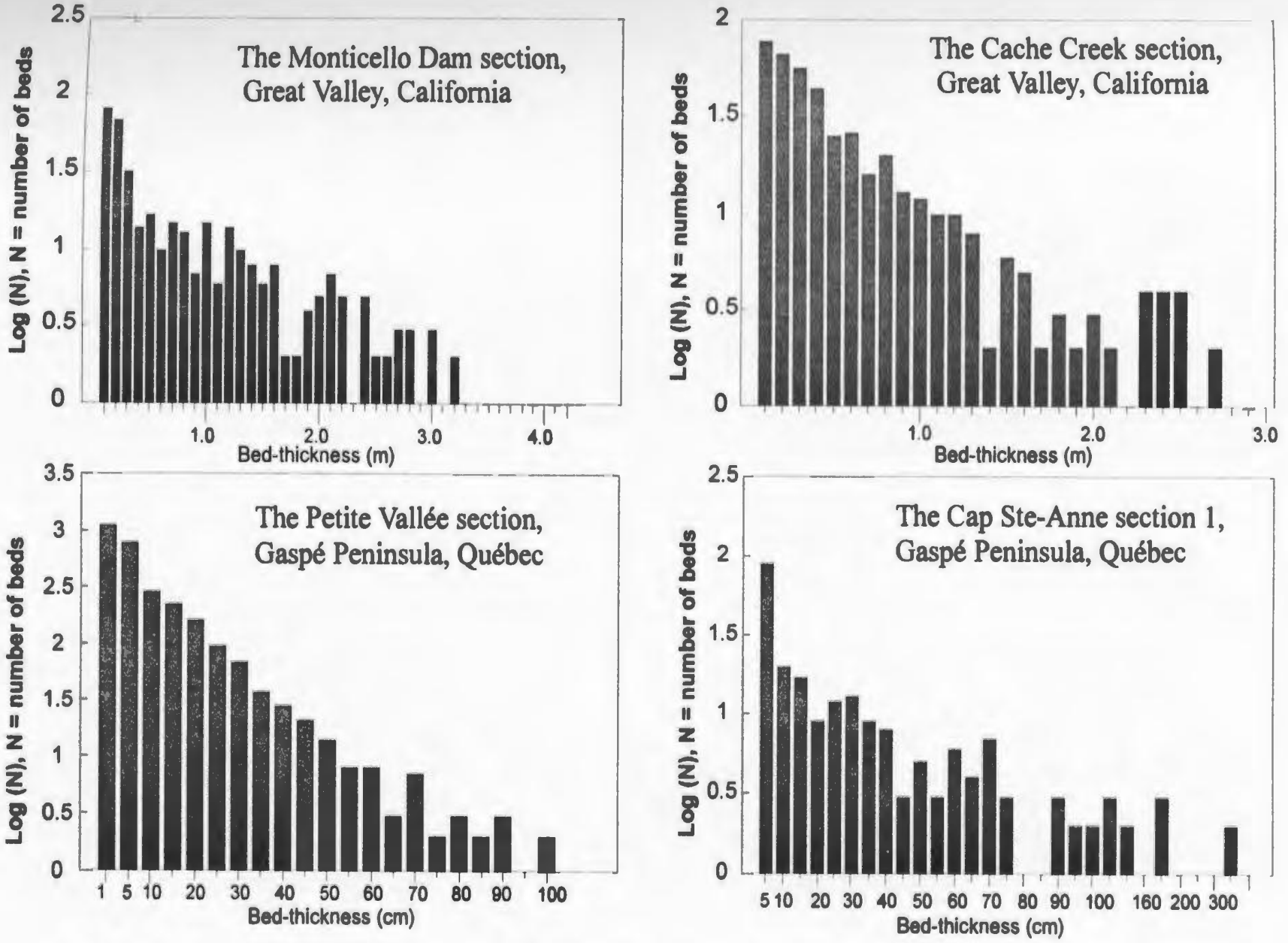

Fig. 5.9a Bed-thickness frequency distributions of the turbidite sections measured for this thesis. Each bar indicates the number of beds equal or thinner than the associated value but thicker than the value of its left bar.

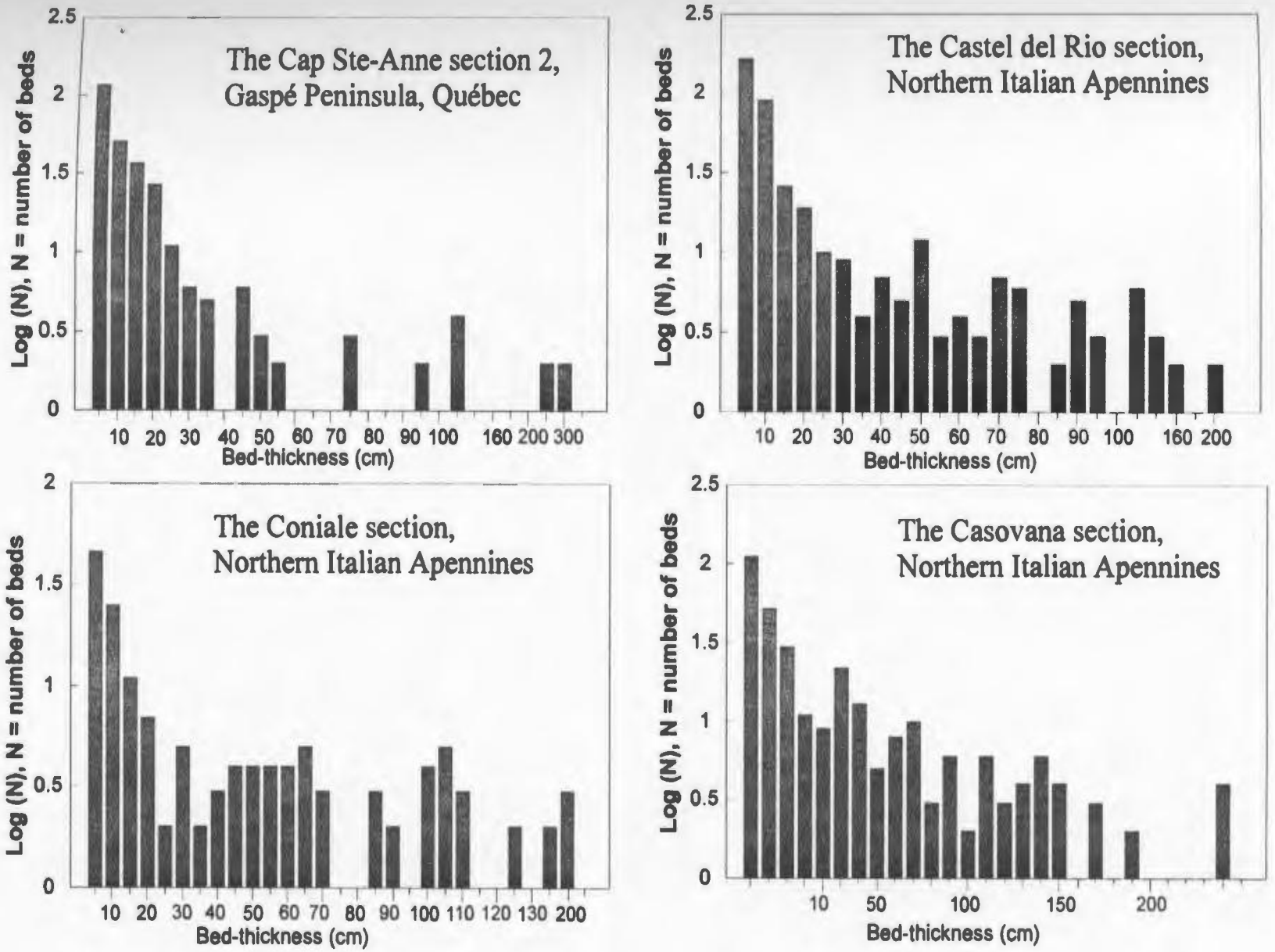

Fig. 5.9b Bed-thickness frequency distributions of the turbidite sections measured for this thesis. Each bar indicates the number of beds equal or thinner than the associated value but thicker than the value of its left bar.

low values predominate (Hurst, 1956). The high Hurst K values from the studied turbidite sections (Table 5.3) demonstrate that high and low values of field measurements are clustered together, but these clusters appear not to exhibit any statistically discernable periodicity or regularity (Figs. 5.3, 5.5, 5.7); this means submarine fan turbidite successions show the Hurst phenomenon.

Thicknesses of bed clusters cannot be transformed into time durations for reasons previously mentioned, so that a search for hierarchical cycles which might correspond to periodic sea-level or climatic changes is unwarranted even for a section like the Petite Vallée section in which erosion at bed bases is seldom enough to have removed the muddy top of the underlying couplet, or for any other section lacking independent absolute dates. At best, division of the time span for deposition by the number of clusters might yield an average frequency to compare with known frequencies for various orders of sea-level fluctuation. The clusters are so irregular in the sections involved in this study (Fig. 5.3, 5.5, 5.7), however, that this has not been attempted.

5.5 Summary

Using the Hurst test and a 10% significance level, Sixteen (84.2%) of nineteen turbidite sections show a grouping pattern of low and high values for the three field measurements of bed-thickness, grain-size score, and sandstone percentage.

Hurst K is an estimator of the degree of clustering of low and high values of measurements. Channel-levee complexes tend to have strong clustering, inferred from a

higher K value and its strong departure from the mean value of K for random sequences. Lobe-interlobe deposits have a medium K and a moderate departure from the mean value of K for random sequences. Basin floor sheet sand systems tend to have a lower K and a weaker departure from the mean value of K for random sequences.

Although the presence of orderly sea-level cycles in submarine fan deposits cannot be ruled out, many random processes might instead control the vertical stacking of turbidite facies, accounting for an irregular and non-periodic stacking of thin-fine-muddy bed clusters and thick-coarse-sandy bed clusters with no recognizable internal order. If such limited organization is a general feature of turbidite successions, then the best tool for environmental interpretation in cases where morphological elements cannot be mapped out in the field is believed to be the strength of clustering (Fig. 5.8). Although long ignored, facies associations or facies intervals (i.e. clustering of various facies) had been proposed as a qualitative indicator of submarine fan environments by many researchers (e.g. Haner, 1971; Walker and Mutti, 1973; Cleary and Conolly, 1974) several years before asymmetric cycles became popular. This thesis adds a quantitative dimension to its use. Enlightened by this study, one might investigate other standard methods of facies transition analysis (e.g., Markov Chain analysis, Harper, 1984) to evaluate clusterings produced by shifting depositional environments in turbidite systems.

Chapter 6

IMPLICATIONS AND CONCLUSIONS

6.1 Introduction

This study was designed: (1) to develop a reasonable statistical procedure to test for asymmetric sequences in turbidite successions, (2) to statistically search for other possible cyclic patterns, (3) to theoretically interpret statistically recognizable cycles, and (4) to develop new criteria for recognition of deep-marine turbidite environments. In previous chapters, the first three objectives have been addressed. With the statistical results and the facies measurements of various turbidite successions, it is now possible to deal with the last objective.

Before discussing new criteria for identification of subenvironments in submarine fan systems, the extent to which the statistical results of this study are applicable to well logs and to facilitating lateral correlations will be investigated. This approach is necessary because there are distinct differences between outcrop data and well-log data and because lateral correlation is particularly important for determination of the geometry of depositional bodies.

6.2 Applications to Well Logs

In well logging, data are obtained at fixed linear spacings, rather than bed-by-bed. These data reflect several formation characteristics, including fluid properties, mud

content, and organic content. Shales and muddy siltstones, for example, show higher gamma-ray values than sandstones, but a lower sound velocity, a lower electric resistivity and a lower porosity. One might expect an upward increase in the log responses which reflect mud content of a sandstone packet that fines upward, and *vice versa*. Such asymmetric trends, if present, should be statistically recognizable in well logs (e.g., McGovney and Radovich, 1985).

In the outcrops examined for this thesis, most sandstone packets which can be demonstrated statistically to have asymmetric grain-size trends consist mostly of amalgamated pebbly-sandstones and sandstones (Appendix IV-2, Fig. 2.3). These sandstone packets show no distinct vertical changes in mud content, and thus have blocky log signatures (cf. Hiscott and DeVries, 1995; Nilsen et al., 1994; Mahaffie, 1994).

It is well known that changes in facies associations, reflecting changes in depositional environments, should have a distinct response in well log data. The Hurst test procedures, outlined in Chapter 5, can readily be applied to well log data so as to assess depositional environments in a framework compatible with the results from outcrops (Fig. 5.8). Caution is needed, however, because the sampling at a fixed increment in well logging permits single very thick beds may create the Hurst effect. It is believed, however, that such effects are not likely significant when the Hurst method is applied to a long section. The technique significantly reduces the effects of noise and simplifies the identification of sandy and muddy intervals or bed clusters.

6.3 Applications to Lateral Correlation

Previous chapters show that submarine fan turbidite vertical successions are characterized by irregular clustering of thin-bedded, fine-grained and muddy beds, and thick-bedded, coarse-grained and sandy beds (Table 5.3). Due to this property, two techniques that have been applied to this study (e.g., Fig. 3.6 and Fig. 5.7) ---- the split-moving window and the plots of cumulative departures from the mean ---- are believed to have potential to assist the lateral correlation of facies units in submarine fan turbidite successions. The split-moving window (Webster, 1973, 1980) is a powerful technique to split turbidite sections into thick, coarse and sandy bed packets and thin, fine and muddy bed packets, even where variations are subtle (see Chapter 3). The plots of cumulative departures from the mean or from a certain value (users' choice) provide a global view of sandy and muddy bed clusters in a section (Fig. 5.3, 5.5 and 5.7). A combination of these two methods will successfully segment turbidite sections into sandy bed clusters and muddy bed clusters. These bed clusters can be used to assist the correlation, particularly, of unconfined lobe deposits, even where clustering is not well developed.

There is another advantage in using statistically based lateral correlations: the correlation lines enclosing packets may show the two-dimensional geometries of sediment bodies so as to provide a link to the morphological elements of submarine fan systems (Pickering et al., 1995).

6.4 Criteria for Identification of Fan Environments

A number of turbidite sections from a wide range of ages, basin tectonic settings, and known depositional environments have been involved in this study. Many of the sections have been measured in the field in great detail (Table 1.1). The upward thickening and thinning sequences which have been widely advertised as environmental indicators are not statistically significant in these turbidite sections (Table 4.9, Fig. 4.9). So, what criteria can be used for identification of depositional environments in submarine fan systems in cases where morphological elements cannot be mapped out in the field? Both facies characteristics observed in the field and the statistical results from this study yield some alternative criteria.

6.4.1 Facies Characteristics

The basic facies features of turbidite sections involved in this study have been outlined in Chapter 2. A summary follows.

Channel Deposits:

Turbidite sections with the geometry of channel fills include the Monticello Dam section in the Great Valley, seven sections in the Gulf Islands (British Columbia), two Barbados sections, and two sections in the Savio Valley (the northern Italian Apennines). These sections share many of the following features.

(1) Thick, sandy beds and thin, muddy beds are bundled into packets, representing channel deposits and levee or channel margin or interchannel deposits, respectively.

Thick and sandy bed packets show a wide range of grain sizes controlled by tectonic settings of basins and sediment sources. Channel deposits of the Monticello Dam section and sections in the Gulf Islands, which were deposited in forearc basins and derived from magmatic arcs (Dickinson and Seeley, 1979; Ingersoll, 1982; England, 1990), are coarse-grained, comprising mainly conglomerate, pebbly sandstone and coarse sandstone, rarely medium and fine sandstone. Percentages of sandstone and siltstone range from 40% to 70% in thin and muddy bed packets of levee or interchannel deposits associated with these coarse-grained channel complexes. In contrast, the channel deposits of Savio Valley sections and Barbados sections, which were interpreted to have been deposited in foreland basins or foredeeps (Ricci Lucchi, 1986; Kasper and Larue, 1986), consist mainly of fine- to coarse-grained sandstones and rare pebbly sandstones. Percentages of sandstone and siltstone range from 10% to 50% in thin and muddy bed packets of levee or interchannel deposits associated with these fine-grained channel complexes.

(2) Beds in thick and sandy bed packets are strongly amalgamated. Erosional basal contacts are widespread beneath conglomerate and sandstone beds. Mud clasts and pebbles are commonly concentrated along erosive bed-bases.

(3) Water-escape structures (dishes and pillars) are well developed in some thick sandstone beds.

(4) Bouma division T_a or division S_3 of Lowe (1982) dominates pebbly sandstone and sandstone. Most sandstone beds are massive (structureless), but most pebbly sandstone beds have a normally graded pebble base and upward become massive sandstone. Due to

ubiquitous strong basal erosion, most conglomerate and sandstone beds have truncated tops: Bouma divisions T_b, T_c and T_{d-e}, if they were originally deposited, are missing or only partly preserved.

Lobe Deposits:

Except for the 12 sections which fill channels and the sections measured in the Santerno Valley (the northern Italian Apennines), all other sections listed on Table 1.1 are interpreted as lobe deposits. General facies features of these sections are summarized as follows.

(1) Thick and sandy beds and thin and muddy beds are grouped together into packets. Sandy bed packets represent lobe deposits (e.g., the Cache Creek section, the Petite Vallée section), or crevasse-splay lobe deposits (Arkansas sections, Bouma et al., 1995), or interchannel lobe deposits (Amazon Fan sections, Pirmez et al., in press, and ?Cap Ste-Anne sections). Sandy bed packets consist of fine- to coarse-grained sandstone; pebbles and granules are practically absent in these sections. Muddy bed packets represent interlobe or levee deposits or deposits formed during periods of fan inactivity. Percentages of sandstone and siltstone in most of these thin and muddy bed packets are less than 30%.

(2) Even though amalgamation is not uncommon in sandy bed packets, most sandstone beds have a parallel or only slightly wavy base. Large basal scours are absent. Mud clasts are smaller (mostly less than 10 cm long), scattered in a sandy bed or

"floating" in the upper part of a bed, which suggests that mud clasts were mixed with sandy sediments and transported a certain distance down the fan from their point of origin before being deposited.

(3) In amalgamated sandstone bed packets, massive or normally graded Bouma division T_a dominates most sandstone beds, and a thin cap of upper divisions T_c and/or T_{d-e} is commonly preserved. Normally graded T_a, parallel laminated T_b, and rippled T_c are well developed in many unamalgamated beds.

Basin-Floor Sheet Sand Systems:

These include turbidite sections measured in the Santerno Valley of the northern Italian Apennines. They have the following facies characteristics.

(1) Sandstone beds tend to be grouped into packets. These beds consist of fine- to medium-grained sand. Muddy bed intervals are composed of thin-bedded and rippled siltstone, turbidite mudstone, and hemipelagic mudstone, intercalated with sandstone beds.

(2) Amalgamation is rare. Most sandstone beds have a parallel, non-erosive base and a well preserved T_{d-e} top. Small mud clasts only appear in a very few sandstone beds, "floating" in sand matrix.

(3) Sandstone commonly has a high content of mud matrix (30%).

(4) T_b, T_c, and T_{d-e} divisions dominate most sandstone beds. T_c divisions in most beds are strongly convoluted.

(5) Many thick sandstone beds have impressive lateral continuity, and can be traced over 60 km (Ricci Lucchi and Valmori, 1980). Most of the laterally continuous beds have unusually thick mudstone caps and have been described as megaturbidites (Ref. Normark et al., 1993; Bouma, 1987; Hiscott and Pickering, 1984).

6.4.2 Asymmetric Sequences

Results of the three powerful correlation tests, the Monte Carlo simulation technique, and the analytical calculation of the cumulative binomial probability have demonstrated the following relationships between asymmetric sequences and depositional environments in submarine fan systems.

(1) For channel deposits, the number of sandstone packets which show upward thickening and thinning trends is not significantly different from that for randomized profiles (Table 4.9, Fig. 4.9). More sandstone (to conglomeratic) packets show significant grain-size trends than bed-thickness trends, particularly upward fining trends in coarse channel fills (Table 4.5, and Table 4.6: the Monticello Dam section, Barbados sections, and British Columbia sections). This suggests that upward fining trends, if more common than expected for random events, might be an indicator of coarse channel deposits, supporting the hypothesis of Mutti and Ricci Lucchi (1972). Upward fining trends, if present, should also be statistically recognizable in well-logs.

(2) For lobe and basin-floor sheet sand deposits, there are no more sandstone packets showing asymmetric trends in bed thickness or in grain size than there are in random

sequences. Hence, asymmetric trends of neither bed thickness nor grain size can be used as indicators for assessing depositional environment.

6.4.3 Long-Term Clustering

The Hurst test has revealed the common existence of irregular clustering for three types of field data (bed thickness, grain size score, and sandstone percentage) in submarine fan turbidite successions (Table 5.3). The clustering of the three variables is genetically associated with the shifting of sedimentary facies in response to changes in depositional environments in fan systems. On the basis of limited data, the strength of clustering appears to be indicative of depositional environments (Fig. 5.8): (1) alternate stacking of channel and levee deposits would result in a high Hurst K and a strong departure from the mean value of K for random sequences; (2) lobe and interlobe deposits tend to have a medium K and a moderate departure from the mean value of K for random sequences; and (3) basin-floor sheet sand systems have a lower K and a weaker departure from the mean value of K for random sequences.

6.4.4 Summary of Criteria

Combining facies characteristics with statistical results gives criteria outlined in Table 6.1 for interpretation of depositional environments in submarine fan systems, particularly for cases where morphological elements cannot be mapped out in the field.

Table 6.1 Criteria for identification of submarine fan environments.

Upper Fan, Middle Fan Channel Deposits	1. Strong amalgamation and strong basal scour. 2. Mud clasts are concentrated on erosive bases. 3. The range of grain size can be very wide, from pebble (sometimes cobble) to fine sand. For a pebbly sandstone bed, pebbles are commonly concentrated on the bed base. 4. Most sandy beds are head cut-off (missing upper Bouma divisions) and consist only of T_a or S_3 divisions. 5. Thick to very thick beds are dominant. 6. For coarse channel fills, statistically discernible upward fining sequences can be developed. 7. Strong clustering of thick-bedded, coarse-grained and sandy beds and thin-bedded, fine-grained and muddy beds, inferred by a high Hurst K and a strong departure from the mean value of K for random sequences.
Lobe Deposits	1. Amalgamation is common, but large basal scours are rare; most sandy beds have a parallel or slightly wavy base. 2. Mud clasts are scattered in a sandy bed, or floating in the upper part of a bed, and usually less than 20 cm long. 3. Pebble and granule grades are largely absent. 4. Upper divisions T_c and/or T_{d-e} are commonly partly preserved although T_a dominates most sandy beds. 5. Most beds are thin- to thick-bedded. 6. Asymmetric bed-thickness or grain-size sequences lack any significance. 7. Moderate clustering of bed thickness, grain size and sandstone percentage for the classic lobe deposits, inferred by a medium Hurst K and a moderate departure from the mean value of K for random sequences; but strong clustering for crevasse-splay lobe deposits in leveed channel systems.
Basin-Floor Sheet Sand Systems	1. Rare amalgamation. Most sandstone beds have a parallel, non-erosive base and a well preserved T_{d-e} top. 2. Most sandstone beds are fine- to medium-grained, with a high content of mud matrix (up to 30% or more). 3. T_b, T_c, and T_{d-e} divisions dominate most sandstone beds. 4. Some very thick beds with unusually thick mudstone caps are so called "megaturbidites". 5. Asymmetric bed-thickness or grain-size sequences lack any significance. 6. A lower Hurst K than channel or lobe deposits and a weaker departure from the mean value of K for random sequences.

6.5 Fan Models

For the studied turbidite sections, the tectonic settings and depositional environments are already reasonably known from regional geology and from large-scale outcrop criteria (Table 1.1), so that the immediate aim is to see if submarine fans in similar tectonic settings share facies and statistical characteristics. Incorporating facies characteristics with tectonic settings of the studied turbidite sections provides the frameworks of what are believed to be four preliminary fan models (Fig. 6.1). These models are based on the assumption that tectonic setting and sediment supply are major controls on fan characteristics (e.g., Bouma et al., 1985; Shanmugam and Moiola, 1988; Pickering et al., 1989). Due to the limited data base in this thesis, further research will be needed to justify and/or expand this set of fan models.

(1) Model 1 fans (type 1 sandy fans) typically form in forearc basins, are fed by littoral sources or fan deltas, and are characterized by very coarse (pebble and sand) sediments. Both channel and lobe deposits are well developed. A significant number of upward fining sequences might be found in channel deposits. Channel-interchannel complexes, particularly channel-levee complexes, display strong clustering of bed-thickness, grain-size and other parameters.

(2) Model 2 fans (type 2 sandy fans) mainly form in forearc basins but also in foreland basins, and are fed by littoral sources or small rivers. The basic features of this model are similar to those of model 1, but sediments consist mainly of sand; pebbly sediments are absent or rare, and upward fining sequences lack significance.

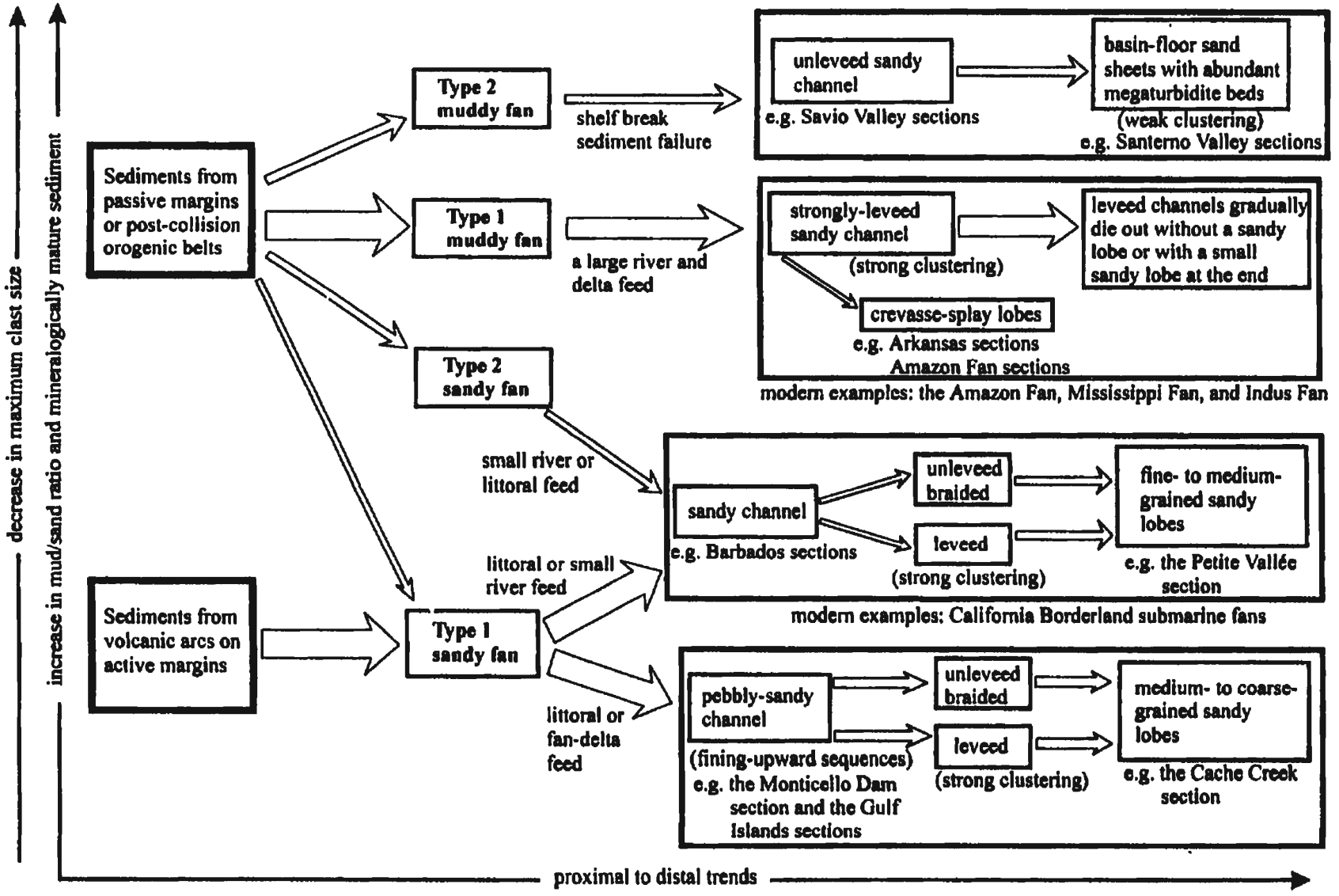

Fig. 6.1 Integrative fan models, based on the studied turbidite sections of the thesis. See Table 6.1 for facies characteristics.

(3) Model 3 fans (type 1 muddy fans) tend to form in passive margins, foreland basins or foredeeps, and are fed by large river deltas. They are typically characterized by nested sandy bodies of channel and crevasse-splay-lobe deposits encased within very well developed muddy levee deposits, which causes strong clustering of bed-thickness, grain-size and other parameters. Channels might gradually die out without an extensive sandy lobe at the end.

(4) Model 4 fans (type 2 muddy fans) form in the same tectonic settings as model 3, but sediments are mainly derived from failures at the shelf break, away from feeder channels of the fans, resulting in well-developed megaturbidite beds with thick mud caps. The large, muddy turbidity currents responsible for these beds are usually unchannelized and efficiently transport sandy sediments to form wide-spreaded basin-floor sand sheets.

6.6 Conclusions

This integrative analysis of turbidite cycles in submarine fan successions has taken many statistical approaches, with much new information gathered along the way. Since each chapter of this thesis already has a summary, only the major contributions of the thesis will be presented here.

1) A database containing twenty-eight turbidite sections which have been measured in great detail (this study and others) was built in order to deal with one of the most important genetic problems in turbidite studies; that is, whether submarine fan turbidite successions are characterized by asymmetric bed-thickness and/or grain-size trends, and whether these trends can serve as criteria for identification of depositional environments.

2) A statistical procedure has been developed for evaluating the significance of asymmetric sequences in turbidite successions. This procedure includes: (a) statistically segmenting turbidite sections into sandstone packets and mudstone-siltstone packets so that sandy packets can be objectively selected for further tests for asymmetric trends; (b) selecting powerful methods to test for asymmetric trends through experiments on power estimation; (c) performing experiments on sample size in order to determine a lower limit for the number of beds in a sandstone packet that can be used to test for asymmetric trends by the selected methods; and (d) using a Monte Carlo simulation technique and the analysis of the cumulative binomial probability to evaluate the significance of asymmetric sequences in turbidite sections.

3) This study has objectively and effectively evaluated the significance of statistically discernible asymmetric sequences in turbidite successions, and has demonstrated that the polarity of asymmetric sequences in sandstone packets cannot be used as criteria for identification of submarine fan environments, except that upward fining sequences occur more commonly than expected for the outcome of random processes in coarse-grained channel fills.

4) This study provides the first application of the powerful Hurst statistic to the study of turbidite cycles. The results from the Hurst test demonstrate that submarine fan turbidite successions are characterized by irregular, non-periodic cyclic clustering of low and high values of bed thickness, grain size and sandstone percentage. This clustering is related to the lateral shifting of sedimentary environments. The strength of clustering of

the three types of field data might be indicative of submarine fan environments (Fig. 5.8). The Hurst test for cyclic clustering and associated plots of cumulative departures from the mean of individual measurements can be applied to well logs and might assist short-distance lateral correlations.

5) Based on the facies features and statistical results for turbidite sections from known depositional environments and tectonic settings, integrative criteria for the identification of submarine fan environments and an initial set of fan models are proposed.

6.7 Future Work

It is hoped that this study will provide acceptable procedures for the consistent statistical analysis of turbidite cycles in submarine fan systems. An enormous benefit would ensue if journal publications never again claim to have identified fan environments based on subjective recognition of a few asymmetric cycles, with no statistical back-up. Through time, more data will be added to evaluate the preliminary conclusions and suggestions made in this thesis. Parallel studies of bed-thickness populations have recently become popular (Hiscott et al., 1992, 1993; Rothman et al., 1994; Pirmez et al., in press; Beattie and Dade, 1996). One element of this thesis research that may provide scope for further work is the application of the Hurst statistic to well logs in an effort to differentiate fan environments.

More upward fining sequences than upward coarsening sequences have been statistically identified in the turbidite sections of coarse-grained channel fills. However,

the number of sandstone packets selected from such sections and used to test for asymmetric trends is limited (Table 4.6). Data from more turbidite sections of channel fills of all types are required to extend the test for grain-size trends, because upward fining sequences, if they are truly common, should be genetically associated with some particular depositional processes, such as channel filling during progressive abandonment, or channel back-filling.

REFERENCES

Anderton, R., 1995, Sequences, cycles and other nonsense: are submarine fan models any use in reservoir geology? In, A.J. Hartley, and D.J. Prosser (editors), Characterization of deep marine clastic systems. Geological Society Special Publication No. 94, p.5-11.

Bachman, S.B., and Graham, S.A., 1985, La Jolla Fan, Pacific Ocean. In, A.H. Bouma, W.R. Normark, and N.E. Barnes (editors), Submarine fans and related turbidite systems. Springer-Verlag New York, p. 65-70.

Beattie, P.D. and Dade, W.B., 1996, Is scaling in turbidite deposition consistent with forcing by earthquakes? Journal of Sedimentary Research, v. 66, p. 909-915.

Booy, C. and Morgan, D.R., 1985, The effect of clustering of flood peaks on a flood risk analysis for the Red River. Can. J. Civ. Eng., v. 12, p.150-165.

Bouma, A.H., 1987, Megaturbidite: an acceptable term? Geo-Marine Letters, v. 7, p63-67.

Bouma, A.H. (editor), 1983/1984, COMFAN. Geo-Marine Letters, v. 3, p. 53-224.

Bouma, A.H., DeVries, M.B., and Cook, T.W., 1995, Correlation efficiency as a tool to better determine depositional subenvironments in submarine fans. Gulf Coast Association of Geological Societies Transactions, v. 45, p. 31-40.

Bouma, A.H., Normark, W.R. & Barnes, N.E. (editors), 1985, Submarine fans and related turbidite systems. Springer-Verlag New York, 351 p.

Bowen, A.J., Normark, W.R., and Piper, D.J.W., 1984, Modelling of turbidity currents on Navy submarine fan, California Continental Borderland. Sedimentology, v. 31, p. 169-185.

Box, G.E.P., and Jenkins, G.M., 1970, Time series analysis: Forecasting and control. Holden-Day, San Francisco, California, 409 p.

Breckon, C.E., 1988, Sedimentology and facies of the Pennsylvanian Jackford Group in the Caddo Valley and DeGray Quadrangles, clark County, Arkansas. M.Sc. Thesis, University of Tulsa, Tulsa, Oklahoma, 134 p.

Briggs, G., and Cline, L.M., 1967, Paleocurrents and source areas of late Paleozoic

sediments of the Ouachita Mountains, southeastern Oklahoma. Journal of Sedimentary Petrology, v. 37, p. 985-1000.

Cattaneo, A. and Ricci Lucchi, F., 1995, Long-distance correlation of sandy turbidites: a 2.5 km long cross-section of Marnoso arenacea, Santerno Valley, Northern Apennines. In, K.T. Pickering, R.N. Hiscott, N.H. Kenyon, F. Ricci Lucchi, and R.D.A. Smith (editors), Atlas of deep-water environments: Architectural style in turbidite systems. Chapman & Hall, London, p. 303-306.

Cherven, V.B., 1991, Architecture of the Winters submarine fan, Sacramento Basin, California. In, A.D. Miall and N. Tyler (editors), The three-dimensional facies architecture of terrigenous clastic sediments and its implications for hydrocarbon discovery and recovery. SEPM, Concepts in Sedimentology and Paleontology, v. 3, p. 296-309.

Clark, J.D., and Pickering, K.T., 1996, Submarine channels: processes and architecture. Vallis Press, London, 229 p.

Cleary, W.J., and Conolly, J.R., 1974, Hatteras deep-sea fan. Journal of Sedimentary Petrology, v. 44, p. 1140-1154.

Corbett, K.D., 1972, Features of thick-bedded sandstones in a proximal flysch sequence, Upper Cambrian, southwest Tasmania. Sedimentology, v. 19, p. 99-114.

Damuth, J.E., and Flood, R.D., 1985, Amazon Fan, Atlantic Ocean. In, A.H. Bouma, W.R. Normark, and N.E. Barnes (editors), Submarine fans and related turbidite systems. Springer-Verlag New York, p. 97-106.

Damuth, J.E., Flood, R.D., Kowsmann, R.O., Belderson, R.H., and Gorini, M.A., 1988, Anatomy and growth pattern of Amazon deep-sea fan as revealed by long-range side-scan sonar (GLORIA) and high-resolution seismic studies. AAPG, V. 72, p. 885-911.

Damuth, J.E., Kolla, V., Flood, R.D., Kowsmann, R.O., Monteiro, M.C., Gorino, M.A., Palma, J.J.C., and Belderson, R.H., 1983, Distributary channel meandering and bifurcation patterns of the Amazon deep-sea fan as revealed by long range Side-scan Sonar (GLORIA). Geology, v. 11, p. 94-98.

Daniel, W.W., 1978, Applied nonparametric statistics. Houghton Mifflin Company, Boston, 503 p.

Davis, J.C., 1973, Statistics and data analysis in geology. John Wiley & Sons, Inc, New York, 550 P.

Davis, J.C., 1986, Statistics and data analysis in geology, 2nd edition. John Wiley & Sons, New York, 646 p.

DeVries, M.B., and Bouma, A.H., 1992, Lateral correlation trends in bedded and massive turbidites, with an example from DeGray Lake, Arkansas. Gulf Coast Association of Geological Societies Transactions, v. 42, p. 789-791.

Dickey, P. A., 1980, Barbados as a fragment of South America ripped off by continental drift. Trans. Caribb. Geol. Conf., 9th, P. 51-52.

Dickinson. W.R., 1971, Clastic sedimentary sequences deposited in shelf, slope, and trough settings between magmatic arcs and associated trenches. Pacific Geology 3, p. 15-30.

Dickinson, W.R., 1976, Sedimentary basins developed during evolution of Mesozoic-Cenozoic arc-trench system in western North America. Canadian Journal of earth Sciences, v. 13, p. 1268-1287.

Dickinson, W.R., and Seely, D.S., 1979, Structure and stratigraphy of forearc regions. AAPG Bulletin, v. 63, p. 2-31.

Dickinson, W.R., Ingersoll, R.V., Cowan, D.S., Helmold, K.P., and Suczek, C.A., 1982, Provenance of Franciscan graywackes in coastal California. Geological Society of America Bulletin, v. 93, p. 95-107.

Dixon, W.J., and Massey, F., 1957, Introduction to statistical analysis. McGray-Hill, New York.

Downie, N.M., and Heath, R.W., 1983, Basic statistical methods. Harper & Row, Publishers, New York, 371 p.

Drinkwater, N.J., 1995, Sheet-like turbidite system: the Kongsfjord Formation, Finnmark, North Norway. In, K.T. Pickering, R.N. Hiscott, N.H. Kenyon, F. Ricci Lucchi, and R.D.A. Smith (editors), Atlas of deep water environments: architectural style in turbidite systems. Chapman & Hall, London, p. 267-274.

Drinkwater, N.J., Pickering, K.T., and Siedlecka, A., 1996, Deep-water fault-controlled sedimentation, Arctic Norway and Russia: response to Late Proterozoic rifting and the opening of the Iapetus Ocean. Journal of Geological Society, London, v. 153, p. 427-436.

Drummond, C.N., and Wilkinson, B.H., 1996, Stratal thickness frequencies and the prevalence of orderedness in stratigraphic sequences. The Journal of Geology, v. 104, p. 1-18.

England, T. D. J., 1990, Late Cretaceous to Paleocene Evolution of the Georgia basin, southwestern British Columbia. Ph.D. thesis, Memorial University of Newfoundland, St. John's, NFLD, Canada, 481 p.

England, T.D.J. and Hiscott, R.N., 1992. Lithostratigraphy and deep-water setting of the upper Nanaimo Group (Upper Cretaceous), outer Gulf Islands of southwestern British Columbia. Can. J. Earth Sci., v. 29, p. 579-595.

Enos, P., 1969, Cloridorme Formation, Middle Ordovician flysch, northern Gaspé Peninsula, Quebec. Geological Society of America Special Paper 117, 66 p.

Feller, W., 1951, The asymptotic distribution of the range of sums of independent random variables. Ann. Math. Statist., v. 22, p. 427-432.

Fichter, L.S. and Poché, D.J., 1993, Ancient environments and the interpretation of geologic history, 2nd edition. Maxwell Macmillan Canada, Inc., 269 p.

Fischer, A.G., 1964, The Lofer cyclothems of the Alpine Triassic. In, D.F. Merriam (editor), Symposium of cyclic sedimentation. Kansas Geological Survey Bulletin 169, p. 107-149.

Fisz, M., 1963, Probability theory and mathematical statistics. Wiley, New York, N.Y., 326 p.

Flood, R.D., Manley, P.L., Kowsmann, R.O., Appi, C.J., and Pirmez, C., 1991, Seismic facies and Late Quaternary growth of Amazon Submarine Fan. In, Weimer, P., and Link, M.H. (editors), Seismic facies and sedimentary processes of modern and ancient submarine fans. New York, Springer-Verlag, p. 415-433.

Flood, R.D., Piper, D.J.W., Klaus, A., et al., 1995, Proceedings of the Ocean Drilling Program, initial reports, 155. College Station, TX (Ocean Drilling Program), 1233 p.

Ghosh, B., and Lowe, D.R., in press, Architectural element analysis of deep-water clastic sedimentary sequences: An example from the Cretaceous Venado sandstone member, Sacramento Valley, California. Journal of Sedimentary Research.

Gold, E., 1929, Notes on the frequency of occurrence of sequence in a series of events of two types. Q.J.R. Meteorol. Soc., v. 55, p. 307-309.

Graham, S.A., Dickinson, W.R., and Ingersoll, R.V., 1975, Himalayan-Bengal model for flysch dispersal in the Appalachian-Ouachita System. Geological Society of America Bulletin, v. 86, p. 273-286.

Haner, B.E., 1971, Morphology and sediments of Redondo submarine fan, southern California. Geol. Soc. America Bull., v. 82, p. 2413-2432.

Haq, B.U., Hardenbol, J., and Vail, P.R., 1987, Chronology of fluctuating sea levels since the Triassic. Science, v. 235, p. 1156-1166.

Harper, Jr. C.W., in press, Thickening and/or thinning upward patterns in sequences of strata: tests of significance. Sedimentology.

Harper, Jr. C.W., 1984a, Improved methods of facies sequence analysis. In, R.G. Walker (editor), Facies Models, Second edition. Geoscience Canada Reprint Series 1, p. 11-13.

Harper, Jr. C.W., 1984b, A Fortran IV program for comparing rank algorithms in quantitative biostratigraphy. Computers and Geosciences, v. 10, p. 3-29.

Hein, F.J., and Walker, R. G., 1982, The Cambro-Ordovician Cap Enrage Formation, Quebec, Canada: conglomeratic deposits of a braided submarine channel with terraces. Sedimentology, v. 29, p. 309-329.

Heller, P.L., and Dickinson, W.R., 1985, Submarine ramp facies model for delta-fed, sand-rich turbidite systems. AAPG, v. 69, p. 960-976.

Hiscott, R.N., 1977, Sedimentology and regional implications of deep-water sandstones of the Tourelle Formation, Ordovician, Quebec. Ph.D. thesis, McMaster University, 542 p.

Hiscott, R.N., 1980, Depositional framework of sandy mid-fan complexes of Tourelle Formation, Ordovician, Quebec. AAPG, v. 64, p. 1052-1077.

Hiscott, R.N., 1981, Deep-sea fan deposit in the Macigno Formation (Middle-Upper Oligocene) of the Gordana Valley, Northern Apennines, Italy--Discussion. J. Sed. Petrol., v. 51, p. 1015-1023.

Hiscott, R.N., Colella, A., Pezard, P., Lovell, M.A., and Malinverno, A., 1992, Sedimentology of deep water volcaniclastics, Oligocene, Izu-Bonin forearc basin, based on formation microscanner images. In, B. Taylor, K. Fujioka et al., (editors),

Proceedings of the Ocean Drilling Program, Scientific Results, v. 126, p. 75-96.

Hiscott, R.N., Colella, A., Pezard, P., Lovell, M.A., and Malinverno, A., 1993, Basin plain turbidite succession of the Oligocene Izu-Bonin intraoceanic forearc basin. Marine and Petroleum Geology, v. 10, p. 450-466.

Hiscott, R.N., and DeVries, M., 1995, Internal characteristics of sandbodies of the Ordovician Tourelle Formation, Quebec, Canada. In K.T. Pickering, R.N. Hiscott, N.H. Kenyon, F. Ricci Lucchi, and R.D.A. Smith (editors), Atlas of deep water environments: architectural style in turbidite systems. Chapman & Hall, London, p. 207-211.

Hiscott, R.N., Pirmez, C., and Flood, R.D., 1997, Amazon submarine fan drilling: a big step forward for deep-sea fan models. Geoscience Canada, v. 24, p. 13-24.

Hiscott, R.N, and Pickering, K.T., 1984, Reflected turbidity currents on an Ordovician basin floor, Canadian Appalachians. Nature, v. 311, p. 143-145.

Hiscott, R.N., Pickering, K.T., and Beeden, D.R., 1986, Progressive filling of a confined Middle Ordovician foreland basin associated with the Taconic Orogeny, Quebec, Canada. International Association of Sedimentologists, Special Publications No. 8, p. 309-325.

Hiscott, R.N., Pirmez, C., and Flood, R.D., in press, Amazon submarine fan drilling: a giant step forward for fan models. In, R.D. Flood, D.J.W. Piper, A. Klaus et al. (editors), Proceedings of the Ocean Drilling Program, Scientific Report volume 155. Ocean Drilling Program, College Station, TX.

Hoel, P.G., 1971, Introduction to mathematical statistics, 4th edition. John Wiley & Sons, Inc., New York, 409 p.

Hurst, H.E., 1951. Long term storage capacity of reservoirs. Trans. Am. Soc. Civ. Engrs., v. 116, p. 770-808.

Hurst, H.E., 1956. Methods of using long-term storage in reservoirs. Proceedings of the Institution of Civil Engineers Part I, v. 5, p. 519-590.

Ingersoll, R.V., 1978, Submarine fan facies of the Upper Cretaceous Great Valley sequence, northern and central California. Sed. Geol., v. 21, p. 205-230.

Ingersoll, R.V., 1981, Petrofacies, lithofacies, submarine-fan facies of the Great Valley Group (sequence). In, S.A. Graham (editor), Field Guild to the Mesozoic-Cenozoic

Convergent margin of Northern California, Pacific Section AAPG, v. 50, p. 59-69.

Ingersoll, R.V., 1982, Initiation and evolution of the Great Valley forearc basin of northern and central California, U.S.A. In, J.K. Legget (editor), Trench-Forearc Geology: Sedimentation and Tectonics on Modern and Ancient Active Plate Margins. Geological Society Special Publication No. 10, Blackwell Scientific, Oxford, p. 459-667.

Ingersoll, R.V., 1983, Petrofacies and provenance of late Mesozoic forearc basin, northern and central California. AAPG Bulletin, v. 67, p. 1125-1142.

Ingersoll, R.V., 1990, Nomenclature of upper Mesozoic strata of the Sacramento Valley of California; review and recommendations. In R.V. Ingersoll and T.H. Nilsen (editors), Sacramento valley symposium and guidebook. Pacific Section, Society of Economic Paleontologists and Mineralogists, Field Trip Guidebook, v. 65, p. 1-3.

Ingersoll, R.V, Rich, E.I., and Dickinson, W.R., 1977, Field guide: Great Valley Sequences, Sacramento Valley. Geological Society of America, Cordilleran Section, Annual Meeting, Guidebook, No. 8, 72 p.

Jordan, D.W., Lowe, D.R., Slatt, R.M., Stone, C.G., D'Agostino, A., Scheihing, M.H., and Gillespie, R.H., 1991, Scales of geological heterogeneity of Pennsylvanian Jackfork Group, Ouachita Mountains, Arkansas: Application to field development and exploration for deep-water sandstones. Guidebook, Dallas Geological Society Field Trip No.3, 147 p.

Kasper, D. C. and Larue, D. K., 1986, Paleogeographic and tectonic implications of quartzose sandstones of Barbados. Tectonics, v. 5, No. 6, p. 837-854.

Kendall, M.G., 1969, Rank correlation methods. Charles Griffin & Co. Ltd., London, p.1-9.

Kendall, M.G., 1976. Time series, 2nd edition. Hafner Press (Macmillan Publishing Co. Inc.), New York, p. 21-28.

Kendall, M.G., and Gibbons, J.D., 1990, Rank correlation methods, Fifth edition. Oxford University Press, New York, 260 p.

Kirby, J.M., 1943, Upper Cretaceous stratigraphy of west side of Sacramento Valley, south of Willows, Glenn County, California. AAPG Bulletin, v. 27, p. 279-305.

Kreyszig, E., 1967, Advanced engineering mathematics, Second edition. John Wiley and

Sons Inc., New York, 898 p.

Larue, D. K., 1985, Quartzose turbidites of the accretionary complex of Barbados, II: Variations in bedding styles, facies and sequence. Sedimentary Geology, v. 42, p. 217-253.

Larue, D. K. and Speed, R. C., 1983, Quartzose turbidites of the accretionary complex of Barbados, I: Chalky Mount Succession. Jour. of Sedimentary Petrology, v. 53, p. 1337-1352.

Lock, B.E., and Fisco, J.R., 1979, Outer deep-sea fan depositional lobe sequence from the Jackford Group of southern Arkansas (abs.). Gulf Coast Association of Geological Societies Transactions, v.29, p. 281.

Lowe, D.R., 1982. Sediment gravity flows: II. depositional models with special reference to the deposits of high-density turbidity currents. J. Sed. Petrol., v.52, p. 279-297.

Lowey, G.W., 1992. Variation in bed thickness in a turbidite succession, Dezadeash Formation (Jurassic-Cretaceous), Yukon, Canada: evidence of thinning-upward and thickening-upward cycles. Sed. Geol., v. 78, p. 217-232.

Mahaffie, M.J., 1994, Reservoir classification for turbidite intervals at the Mars Discovery Mississippi Canyon 807, Gulf of Mexico. In, Weimer, P., Bouma, A.H., and Perkins, B.f. (editors), Submarine fans and turbidite systems: Sequence stratigraphy, reservoir architecture and production characteristics, Gulf of Mexico and International. Gulf Coast Section, SEPMF, Fifteen Annual Research Conference (1994), p. 233-244.

Mandelbrot, B.B., and Wallis J.R., 1969, Computer experiments with fractional Gaussian noises, Part 1, Averages and variances. Water Resour. Res., v. 5, p. 228-241.

Manley, P.L., and Flood, R.D., 1988, Cyclic sediment deposition within Amazon Deep-Sea Fan. AAPG Bulletin, v. 72, p. 912-925.

Martini, I.P., Sagri, M., and Doveton, J.H., 1978, Lithologic transition and bed thickness periodicities in turbidite successions of the Antola Formation, Northern Apennines, Italy. Sedimentology, v. 25, p. 603-623.

McConnell, D.A., 1989, Determination of offset across the northern margin of the Wichita uplift, southwest Oklahoma. Geological Society of America Bulletin, v. 101, p. 1317-1332.

McGovney, J.E., and Radovich, B.J., 1985, Seismic stratigraphy and facies of the Frigg Fan complex. In, O.R. Berg and D.G. Woolverton (editors), Seismic stratigraphy II: An integrated approach. AAPG Memoir 39, p. 139-154.

Meacham, I., 1968, Correlation in sequential data -- three simple indicators. Civil Engineering Transactions, The Institution of Engineers, Australia, CE10(2), p. 225-228.

Middleton, G.V., and Bouma, A.H. (editors), 1973, Turbidites and deep-water sedimentation. Pacific Section Soc. Econ. Paleontol. Mineral., Los Angeles, Calif., 157 p.

Miller, R.G., 1981, Simultaneous statistical inference. Springer-Verlag, New York, 299 p.

Miller, R. L., and Kahn, J.S., 1962, Statistical analysis in the geological sciences. Wiley, New York.

Moiola, R.J., and Shanmugam, G., 1984, Submarine fan sedimentation, Ouachita Mountains, Arkansas and Oklahoma. Gulf Coast Association of Geological Societies Transactions, v. 34, p. 175-182.

Moore, G.H., and Wallis, W.A., 1943, Time series tests based on signs of differences. J. Am. Statist. Assoc., v. 38, p. 153-164.

Morris, R.C., 1974, Carboniferous rocks of the Ouachita Mountains, Arkansas: a study of facies patterns along the unstable slope and axis of a flysch trough. In, G. Briggs, (editor), Carboniferous of the southeastern United States. Geological Society of America Special Paper 148, p. 241-279.

Morris, R.C., 1977, Flysch facies of the Ouachita trough--with examples from the Spillway at the DeGray Dam, Arkansas. Symposium on the Geology of the Ouachita Mountains, Arkansas Geological Commission, v. 1, p. 158-169.

Morris, R.C., Proctor, K.E., and Koch, M.R., 1979, Petrology and diagenesis of deep-water sandstones, Ouachita Mountains, Arkansas and Oklahoma. In, P.A. Scholle and P.R. Schluger (editors), Aspects of diagenesis. SEPM Special Publication 26, p. 263-279.

Morton, R.A., 1991, Contrasting styles of Late Neogene deep-water sandstone deposition, offshore Texas. In, A.D. Miall and N. Tyler (editors), The three-dimensional facies architecture of terrigenous clastic sediments and its implications for hydrocarbon discovery and recovery. SEPM, Concepts in Sedimentology and

Paleontology, v. 3, p. 288-295.

Murray, C.J., 1992, Geostatistical application in petroleum geology and sedimentary geology Ph.D. dissertation, Stanford University, 301 p.

Murray, C.J., Lowe, D.R., Graham, S.A., Martinez, P.A., Zeng, J., Carroll, A.R., Cox, R., Hendrix, M., Heubeck, C., Miller, D., Moxon, I.W., Sobel, E., Wendebourg, J., Williams, T., 1996, Statistical analysis of bed-thickness patterns in a turbidite section from the Great Valley Sequence, Cache Creek, northern California. Journal of Sedimentary Research, Section A, v. 66, p. 900-908.

Mutti, E., 1979, Turbidites et cones sous-marins profonds. In, P. Homewood (editor), Sedimentation detritique (fluviatile, littorale et marine). Institut Geologique, University Fribourg, Switzerland, p. 353-419.

Mutti, E., 1985, Turbidite systems and their relations to depositional sequences. In, G.G. Zuffa (editor), Provenance of arenites. NATO Advanced Scientific Inst., p. 65-94.

Mutti, E., 1992, Turbidite sandstones. Milan, Italy, Agip Special Publication, 275 p.

Mutti, E., and Ghibaudo, G., 1972, Un esempio di torbiditi di conoide sottomarina esterna: le Arenarie di San Salvatore (Formazione di Bobbio, Miocene) nell' Appennino di Piacenza. Mem. Acc. Sci. Torino Classe Sci. Fis. Nat. Ser. 4, no. 16, 40 p.

Mutti, E., and Normark, W.R., 1987, Comparing examples of modern and ancient turbidite systems: problems and concepts. In, Leggett, J.K., and Zuffa, G.G. (editors), Marine clastic sedimentology. Graham and Trotman, London, p. 1-37.

Mutti, E., and Normark, W.R., 1991, An integrated approach to the study of turbidite systems. In, Weimer, P., and Link, M.H. (editors), Seismic facies and sedimentary processes of modern and ancient submarine fans. New York, Springer-Verlag, p. 75-106.

Mutti, E., and Ricci Lucchi, F., 1972, Le torbidite dell' Apennino Setlentrionale: introduzione all' analisi di facies. Mem. Soc. Geol. Intal. 11, p.161-199: (1978, English translation by T.H. Nilsen, Int. Geol. Rev., v. 20, p. 125-166).

Mutti, E., and Sonnino, M., 1981, Compensation cycles: A diagnostic feature of sandstone lobes (abst.). International Association of Sedimentologists, 2nd European Meeting, Bologna, p. 120-123.

Nelson, C.H., and Nilsen, T.H., 1984, Modern and ancient deep-sea fan sedimentation. Soc. Econ. Paleontol. Mineral., Short Course, 14, 404 p.

Nilsen, T.H., 1980, Modern and ancient submarine fans: discussion of papers by R.G. Walker and W.R. Normark. AAPG, v. 64, p. 1094-1101.

Nilsen, T.H., Imperato, D.P., and Moor, D.W., 1994, Reservoir geometry and architecture of productive Upper Cretaceous mud-rich and sand-rich submarine fan systems, Sacramento Basin, California. In, Weimer, P., Bouma, A.H., and Perkins, B.f. (editors), Submarine fans and turbidite systems: Sequence stratigraphy, reservoir architecture and production characteristics, Gulf of Mexico and International: Gulf Coast Section, SEPMF, Fifteen Annual Research Conference (1994), p. 269-280.

Nilsen, T.H., and Simoni, T.R., 1973, Deep-sea fan paleocurrent patterns of the Eocene Butano Sandstone, Santa Cruz Mountains, California. U.S. Geol. Survey Jour. Res., v. 1, p. 439-452.

Normark, W.R., 1970, Growth patterns of deep-sea fans. AAPG, v. 54, p. 2170-2195.

Normark, W.R., 1978, Fan valleys, channels, and depositional lobes on modern submarine fans: characters for recognition of sandy turbidite environments. AAPG, v. 62, p. 912-931.

Normark, W.R., and Piper, D.J.W., 1991, Initiation processes and flow evolution of turbidity currents: Implications for depositional record. In, From Shoreline to Abyss, SEPM Special Publication No. 46, p. 207-230.

Normark, W.R., Piper, D.J.W., and Hess, G.R., 1979, Distributary channels, sand lobes and mesotopography of Navy submarine fan, California borderland. Sedimentology, v. 24, p. 749-774.

Normark, W.R., Piper, D.J.W., and Hiscott, R.N., in press, Sea level effects on the depositional architecture of the Hueneme and associated submarine fan systems, Santa Monica Basin, California. Sedimentology.

Normark, W.R., Posamentier, H., Mutti, E., 1993, Turbidite systems: state of the art and future. Reviews of Geophysics, v. 31, p. 91-116.

Ojakangas, R.W., 1968, Cretaceous sedimentation, Sacramento Valley, California. Geological Society of America Bulletin, v. 79, p. 973-1008.

Pfaffenberger, R.C., and Patterson, J.H., 1977, Statistical methods: for business and

economics. Richard D. Irwin, Inc., 750 p.

Pickering, K.T., 1981, Two types of outer fan lobe sequences, from the late Precambrian Kongsfjord Formation submarine fan, Finnmark, north Norway. Journal of Sedimentary Petrology, v. 51, p. 1277-1286.

Pickering, K.T., 1985, Kongsfjord turbidite system, Norway. In, A.H. Bouma, N.E. Barnes and W.R. Normark (editors), Submarine fans and related turbidite systems. New York, Springer, p. 237-244.

Pickering, K.T., and Hiscott, R.N., 1985, Contained (reflected) turbidity currents from the Middle Ordovician Cloridorme Formation, Quebec, Canada: an alternative to the antidune hypothesis. Sedimentology, v. 32, p. 373-394.

Pickering, K.T., Hiscott, R.N. & Hein, F.J., 1989, Deep-marine environments: clastic sedimentation and tectonics. Unwin Hyman Ltd, London, 416 p.

Pickering, K.T., Hiscott, R.N., Kenyon, N.H., Ricci Lucchi, F., and Smith, R.D.A. (editors), 1995, Atlas of deep water environments: Architectural style in turbidite systems. Chapman & Hall, London, 333 p.

Piper, D.J.W. and Normark, W.R., 1983, Turbidite depositional patterns and flow characteristics, Navy submarine fan, California borderland. Sedimentology, v.30, p. 681-694.

Pirmez, C., 1994, Growth of a submarine meandering channel-levee system on Amazon Fan. Ph.D. Thesis, Columbia University, New York.

Pirmez, C., Hiscott, R.N., and Kronen, J.D.Jr., in press, Sandy turbidite successions at the base of channel-levee systems of the Amazon Fan revealed by FMS logs and cores: unraveling the facies architecture of large submarine fans. In, R.D. Flood, D.J.W. Piper, A. Klaus, et al., (editors), Proceedings of the Ocean Drilling Program, Scientific Report volume 155: Ocean Drilling Program, College Station, TX.

Porebski, S.J., Meischner, D., and Görlich, K., 1991, Quaternary mud turbidites from the South Shetland Trench (West Antarctica): recognition and implications for turbidite facies modelling. Sedimentology, v. 38, p. 691-715.

Posamentier, H.W.,Jervey, M.T. and Vail, P.R., 1988, Eustatic controls on clastic deposition I--conceptual framework. In: C.k. Wilgus, b.S. Hastings, C.G.St.C. Kendall, H.W. Posamentier, C.A Ross and J.C. Van Wagoner (editors), Sea level changes: an integrated approach. S.E.P.M. Spec. Publ., No 42, p. 109-124.

Press, W.H., Flannery, B.P., Teukolsky, S.A., and Vetterling, W.T., 1986, Numerical Recipes: the art of scientific computing. Cambridge University Press, Cambridge, 818 p.

Pudsey, C. J. and Reading, H. G., 1982, Sedimentology and Structure of the Scotland Group, Barbados. In, J. Legget (editor), Trench-Forearc Geology: Sedimentation and Tectonics on Modern and Ancient Active Plate Margins. Geological Society Special Publication No. 10, Blackwell Scientific, Oxford, p. 291-308.

Quinlan, G., and Beaumont, C., 1984, Appalachian overthrusting, lithospheric flexure and the development of Paleozoic stratigraphy in the eastern interior region, U.S.A. Can. J. Earth Sci., v. 21, p. 973-996.

Radhakrishnan, S., Srikanth, G. and Mehta, C.H., 1991, Segmentation of well logs by maximum likelihood estimation: the algorithm and Fortran-77 implementation. Computers & Geosciences, v. 17, p. 1173-1196.

Reading, H.G., and Richards, M., 1994, Turbidite systems in deep-water basin margins classified by grain size and feeder system. AAPG, v. 78, p. 792-822.

Ricci Lucchi, F., 1973, Resedimented evaporites: indicators of slope instability and deep-basin conditions in Periadriatic Messinian (Apennines foredeep, Italy). In, C.W. Drooger (editor), Messinian events in the Mediterranean. North-Holland Publ. Co., Amsterdam, p. 142-149.

Ricci Lucchi, F., 1975, Depositional cycles in two turbidite formations of Northern Apennines (Italy). J. Sed. Petrol., v 45, p. 3-40.

Ricci Lucchi, F., 1978, Turbidite dispersal in a Miocene deep-sea plain. Geol. en Mijnbouw, v. 57, p. 559-576.

Ricci Lucchi, F., 1981, The Marnoso arenacea turbidites, Romagna and Umbria Apennines. In, F. Ricci Lucchi (editor), Excursion Guidebook, with Contribution on Sedimentology of some Italian Basins, International Association of Sedimentologists, 2nd European Meeting, Bologna, p. 229-303.

Ricci Lucchi, F., 1984, Deep-sea fan deposits on the Miocene Marnoso arenacea Formation, northern Apennines. Geo-Marine Letters, v. 3, p. 203-210.

Ricci Lucchi, F., 1986, The Oligocene to Recent foreland basins of the northern Apennines. In, P.A. Allen, and P. Homewood (editors), Foreland basins. International Association of Sedimentologists Special Publication No. 8, Oxford, Blackwell

Scientific, p. 105-139.

Ricci Lucchi, F., 1995. Contessa and associated megaturbidites: long distance (120 X 25 km) correlation of individual beds in a Miocene foredeep. In, K.T. Pickering, R.N. Hiscott, N.H. Kenyon, F. Ricci Lucchi, and R.D.A. Smith (editors), Atlas of deep-water environments: architectural style in turbidite systems. Chapman & Hall, London, p. 300-302.

Ricci Lucchi, F. and Valmori, E., 1980, Basin-wide turbidites in a Miocene "over-supplied" deep-sea plain: A geometrical analysis. Sedimentology, v. 27, p. 241-270.

Rock, N.M.S., 1988, Numerical geology. Springer-Verlag, Berlin Heidelberg, 427 p.

Rothman, D., Grotzinger, J., and Flemings, P., 1994, Scaling in turbidite deposition. Journal of Sedimentary Research, v. A64, p. 59-67.

SAS Institute, 1990, SAS user's guide: statistics, vers. 6 edition. SAS Institute, Cary, N. C.

Shanmugam, G. & Moiola, R.J., 1982, Eustatic control of turbidites and winnowed turbidites. Geology, v. 10, p. 231-235.

Shanmugam, G. & Moiola, R.J., 1988, Submarine fans: models, classification, and reservoir potential. Earth-Sci. Rev., v. 24, p. 382-428.

Shanmugam, G., and Moiola, R.J., 1991, Types of submarine fan lobs: models and implications. AAPG, v. 75, p. 156-179.

Shipboard Scientific Party, 1995, Site 934. In, Flood, R.D., Piper, D.J.W., Klaus, A., et al.(editors), Proceedings of the Ocean Drilling Program, initial reports, 155. College Station, TX (Ocean Drilling Program), 1233 p.

Siegel, S., 1956, Non-parametric statistics for the behavioral sciences. McGraw-Hill, New York, 312 p.

Simpson, G.G., Roe, A., and Lewontin, R.C., 1960, Quantitative zoology, revised edition. Harcourt, Brace and Company, New York, 440 p.

Smith, R.D.A., 1995, Sheet-like and channelized sediment bodies in a Silurian turbidite system, Welsh Basin, UK. In, K.T. Pickering, R.N. Hiscott, N.H. Kenyon, F. Ricci Lucchi, and R.D.A. Smith (editors), Atlas of deep water environments: Architectural style in turbidite systems. Chapman & Hall, p. 250-254.

Speed, R. C. and Larue, D. K., 1982, Barbados: Implications for accretion. Jour. Geophys. Res., v. 85, p. 3633-3643.

Srikanthan, R., McMahon, T.A., and Irish, J.L., 1983, Time series analyses of annual flows of Australian streams. Journal of Hydrology, v. 66, p. 213-226.

Stanley, D.J., and Kelling, G. (editors), 1978, Sedimentation in submarine canyons, fans, and trenches. Dowden, Hutchinson and Ross, Inc., Stroudsburg, Penn., 395 p.

Stow, D.A.V., Howell, D.G., and Nelson, C.H., 1985, Sedimentary, tectonic, and sea-level controls. In, A.H. Bouma, W.R. Normark and N.E.Barnes (editors), Submarine fans and related turbidite systems. Springer-Verlag, New York, N.Y., p. 23-28.

Stow, D.A.V., Reading, H.G., and Collinson, J.D., 1996, Deep seas. In, Reading, H.G. (editor), Sedimentary environments: processes, facies and stratigraphy, the third edition. Blackwell Science Ltd., p. 395-453.

Strong, P.G., and Walker, R.G., 1981, Deposition of the Cambrian continental rise: the St. Roch Formation near St. Jean-Port-Joli, Quebec. Canadian J. of Earth Sciences, v. 18, p. 1320-1335.

Sullwold, H.H. Jr., 1960, Tarzana fan, deep submarine fan of late Miocene age, Los Angeles County, California. AAPG, v. 44, p. 433-457.

Swart, R., 1990, The sedimentology of the Zerissene turbidite system, Damara Orogen, Namibia. Ph.D. thesis, Rhodes University, South Africa, 125 p.

Thomas, W.A., 1985, The Appalachian-Ouachita connection: Paleozoic orogenic belt in the southern margin of North America. Annual Review of Earth and Planetary Sciences, v. 13, p. 175-199.

Tillman, R.W., And Ali, S.A. (editors), 1982, Deep water canyons, fans and facies: Models for stratigraphic trap exploration. Am. Assoc. Pet. Geol., Reprint Ser., 26, 596 p.

Toro, G.A.E., 1995, Angel Formation turbidites in the Wanaea field area, Dampier Sub-basin, North-West shelf, Australia. In, K.T. Pickering, R.N. Hiscott, N.H. Kenyon, F. Ricci Lucchi, and R.D.A. Smith (editors), Atlas of deep water environments: Architectural style in turbidite systems. Chapman & Hall, p. 260-266.

Vail, P.R., Audemard, F., Bowman, S.A., Eisner, P.N. and Perez-Cruz, G., 1991, The stratigraphic signatures of tectonics, eustasy and sedimentology--an overview. In, G.

Einsele, W. Ricken & A. Seilacher (editors), Cycles and events in stratigraphy. Springer-Verlag Berlin Heidelberg, p. 617-659.

Velbel, M. A., 1980, Petrography of subduction zone sandstones - A discussion. Jour. Sediment. Petrol., v. 50, p. 303-304.

Wald, A., and Wolfowitz, J., 1944, An exact test for randomness in the non-parametric case based on serial correlation. Ann. Math. Statistics, v. 14, p. 378-388.

Waldron, J.W.F., 1986, Submarine ramp facies model for delta-fed, sand-rich turbidite systems - Discussion. AAPG Bulletin, v. 70, p. 174-176.

Waldron, J.W.F., 1987, A statistical test for significance of thinning- and thickening-upward cycles in turbidites. Sed. Geol., v. 54, p. 137-146.

Walker, R.G., 1978, Deep water sandstone facies and ancient submarine fans: models for exploration for stratigraphic traps. AAPG, v. 62, p. 932-966.

Walker, R.G., 1984, Turbidites and associated coarse clastic deposits. In, R.G. Walker (editor), Facies models, 2nd end. Geoscience Canada Reprint Series 1, Toronto, p. 171-188.

Walker, R.G., 1992, Turbidites and submarine fans. In, Walker, R.G., and James, N.P. (editors), Facies models: response to sea level change. Geological Association of Canada, p. 239-264.

Walker, R.G, and Mutti, E., 1973, Turbidite facies and facies associations. In, SEPM Pacific Section Short Course, Anaheim, Turbidite and deep water sedimentation, p. 119-158.

Wallis, J.R. and Matalas, N.C., 1970. Small sample properties of H and K--estimators of the Hurst coefficient h. Water Resources Research, v. 6, p. 1583-1594.

Wallis, J.R. and Matalas, N.C., 1971. Correlogram analysis revisited. Water Resources Research, v. 7, p. 1448-1459.

Watson, M.P., 1981, Submarine fan deposits of the Upper Ordovician-Lower Silurian Milliners Arm Formation, New World Island, Newfoundland. Ph.D. thesis, Oxford University.

Webster, R., 1973, Automatic soil-boundary location from transect data. Mathematical Geology, v. 5, p. 27-37.

Webster, R., 1980, Divide: a Fortran IV program for segmenting multivariate one-dimensional spatial series. Computers & geosciences, v. 6, p. 61-68.

Weimer, P., 1989, Sequence stratigraphy of the Mississippi Fan (Plio-Pleistocene), Gulf of Mexico. Geo-Marine Letters, v. 9, p. 185-272.

Weimer, P., and Link, M.H., 1991, Global petroleum occurrences in submarine fans and turbidite systems. In, Weimer, P., and Link, M.H. (editors), Seismic facies and sedimentary processes of modern and ancient submarine fans. New York, Springer-Verlag, p. 9-67.

Weimer, P., and Link, M.H. (editors), 1991, Seismic facies and sedimentary processes of modern and ancient submarine fans. New York, Springer-Verlag, 447 p.

Westbrook, G. K., 1982, The Barbados Ridge Complex: Tectonics of a mature forearc system. In, J.K. Legget (editor), Trench-forearc geology: Sedimentation and tectonics on modern and ancient active plate margins. Geological Society Special Publication No. 10, Blackwell Scientific, Oxford, p. 275-290.

Whitaker, J.H. McD., 1976, Submarine canyons and deep-sea fans. Dowden, Hutchinson and Ross, Inc., Stroudsburg, Penn., 460 p.

Williams, H., and Hatcher, R.D., Jr, 1983, Appalachian suspect terranes. In, R.D. Hatcher, Jr et al. (editors), Contributions to the tectonics and geophysics of mountain chains. Mem. Geol. Soc. Am., v. 158, p. 33-53.

Zelt, F.B., and Rossen, C., 1995, Geometry and continuity of deep-water sandstones and siltstones of the Brushy Canyon Formation (Permian), Delaware Mountains, Texas. In, K.T. Pickering, R.N. Hiscott, N.H. Kenyon, F. Ricci Lucchi, and R.D.A. Smith (editors), Atlas of deep-water environments: Architectural style in turbidite systems. Chapman & Hall, London, p. 167-183.

Appendix I
Data for Turbidite Sections

This appendix contains a full list of field data for turbidite sections measured for this thesis. In order to show how sandstone packets were statistically selected from individual sections, outputs of the Split-Moving Window procedure are attached. For sections measured in Italy, outputs of the Maximum Likelihood Estimation procedure are also attached. For computer programs of the Split-Moving Window and the Maximum Likelihood Estimation techniques, see Webster (1980) and Radhakrishnan et al. (1991).

The following abbreviations are used in spreadsheets:

Bed #: bed number
St: sandstone, siltstone and conglomerate thickness
Ct: cumulative thickness
S%: percentage of sandstone thickness (St) in a bed
Bt: bed thickness
G.Sco: grain size scores **
Str.Sco (or S.Sco): structure scores ***
T.G: grain size at the top of a sandy layer; for a mud bed, T.G = 8.5
Bas.G (or B.G): grain size at the base of a sandy layer; for a mud bed, B.G = 8.5
Seg.L: segmentation log (the Maximum Likelihood method)
Ev.Sq: event sequence -- value 1 is the possible segment boundary (the Maximum Likelihood method)
posi: position. For example, value 7.5 = between bed 7 and bed 8 (the Split-Moving Window method)
D.Sq: D square -- a peak value indicates a segment boundary (the Split-Moving Window method)
[50]: Sand packet number for bed thickness
[g30]: Sand packet number for grain size

****

Notes: ** Grain size scores(G.Sco) = -4 × (proportion of pebble & granule division + 0 × (proportion of coarse sand division) + 1.5 × (proportion of medium sand division) + 3 × (proportion of fine sand division) + 7 × (proportion of silt division)

Grain size score is set at 8.5 for mudstone beds

*** Structure scores (Str.Sco) = 0 × (proportion of massive division in a bed) + 1.5 × (proportion of graded division) + 3 × (proportion of T_b division) + 7 × (proportion of T_c division) + 8.5 × (proportion of T_d division)

The multiplies -4, 0, 1.5, 3, 7, and 8.5 are based on equivalent ϕ values of grain size.

Romagnano section 2
Savio Valley, northern Italian Apennines

								Maximum Likelihood Segmentation				Split Moving-Window Segmentation		
								Based on sst. thickness		Based on grain Size				
bed#	Ct (cm)	Bt (cm)	St (cm)	S%	G.Sco	Str.Sco	Bas.G	Seg.L	Ev.Sq	Seg.L	Ev.Sq			
1	100	100	92	92	1.7	2.8	0.75	1.05	0	-0.873	0			*****
2	155	55	50	91	2.58	2.9	0.75	-0.169	1	-0.873	0			
3	176	21	15	71.4	2.45	3.7	0.75	-0.169	0	-0.873	0			
4	192	16	9	56.3	4.3	5.2	1.5	-0.169	0	-0.873	0	POSI.	D.Sq	
5	315	123	96	78	3.6	3.2	0	-0.169	0	-0.873	0	5.5	0.0643	
6	331	16	9	56.3	3	5	1.5	-0.169	0	-0.722	1	6.5	0.9843	
7	427	96	83	86.5	2	1.9	0.75	-0.169	0	-0.722	0	7.5	0.4056	
8	465	38	33	86.8	1.5	2.25	0.75	-0.169	0	-0.722	0	8.5	0.2260	
9	628	163	153	93.9	2.4	3.6	0.75	-0.169	0	-0.722	0	9.5	0.5512	
10	672	44	35	79.5	2.8	3.5	2.25	-0.169	0	-0.722	0	10.5	0.3392	[1]
11	792	120	120	100	0.75	1	0.75	-0.169	0	-0.722	0	11.5	2.2010	[g35]
12	826	34	28	82.4	1.5	2.25	0.75	-0.169	0	-0.722	0	12.5	1.8855	
13	835	9	9	100	3.5	3.94	1.5	-0.666	1	-0.722	0	13.5	0.9924	
14	840	5	5	100	3.7	3.7	1.5	-0.666	0	-0.722	0	14.5	0.0129	
15	847	7	7	100	3.5	4.6	1.5	-0.666	0	-0.722	0	15.5	0.0726	
16	857	10	9	90	4.2	5.8	1.5	-0.666	0	-0.722	0	16.5	0.5126	
17	860	3	3	100	2.25	1.5	2.25	-0.666	0	-0.722	0	17.5	0.7878	
18	935	75	75	100	1.7	2.4	0	0.788	1	-0.722	0	18.5	1.0210	
19	1062	127	117	92	2.62	3.6	0	0.788	0	-0.722	0	19.5	2.8377	
20	1095	33	27	81.8	2.64	4.4	0.75	-0.614	1	-0.533	1	20.5	4.6885	*****
21	1116	21	5	23.8	7	7	7	-0.614	0	-0.533	0	21.5	3.7154	
22	1135	19	1.5	7.9	7	7	7	-0.614	0	0.953	1	22.5	2.6518	
23	1155	20	6	30	7	7	7	-0.614	0	0.953	0	23.5	1.1647	
24	1198	43	3	7	7	7	7	-0.614	0	0.953	0	24.5	0.2582	
25	1238	40	10	25	7	7	7	-0.614	0	0.953	0	25.5	0.0431	
26	1249	11	0	0	8.5	8.5	8.5	-0.614	0	0.953	0	26.5	0.1669	
27	1267	18	12	66.7	7	7	7	-0.614	0	0.953	0	27.5	0.1536	
28	1305	38	13	34.2	7	7	7	-0.614	0	0.953	0	28.5	0.1402	
29	1314	9	5	55.6	7	7	7	-0.614	0	0.953	0	29.5	0.1359	
30	1361	47	27	57.4	4.8	7.7	3	-0.614	0	0.953	0	30.5	0.0355	
31	1400	39	11	28.2	7	7	7	-0.614	0	0.953	0	31.5	0.0191	
32	1418	18	13	72	7	7	7	-0.614	0	0.953	0	32.5	0.2106	
33	1429	11	7	63.6	7	7	7	-0.614	0	0.953	0	33.5	0.8570	
34	1447	18	1	5.6	7	7	7	-0.614	0	0.953	0	34.5	1.4316	
35	1463	16	2	12.5	7	7	7	-0.614	0	0.92	1	35.5	2.1720	
36	1491	28	21	75	3.5	4.3	1.5	-0.614	0	0.92	0	36.5	0.5577	*****
37	1541	50	40	80	2.74	3.9	1.5	-0.614	0	-0.627	1	37.5	0.3389	
38	1585	44	29	66	3.36	4.86	0	-0.614	0	-0.627	0	38.5	0.2021	
39	1607	22	16	72.7	3	7	3	-0.614	0	-0.627	0	39.5	0.6867	
40	1612	5	3	60	7	7	7	-0.614	0	-0.627	0	40.5	1.0344	
41	1617	5	4	80	7	7	7	-0.614	0	-0.627	0	41.5	1.5252	
42	1762	145	132	91	2.73	2.6	1.5	0.463	1	-0.934	1	42.5	0.0997	
43	1813	51	43	84.3	3.3	5	0.75	0.463	0	-0.934	0	43.5	0.1941	
44	1937	124	124	100	1.2	1.5	0	0.463	0	-0.934	0	44.5	0.1595	[2]
45	1997	60	50	83.3	1.14	2.64	0	0.463	0	-0.934	0	45.5	0.3521	[g36]
46	2007	10	9	90	7	7	7	0.463	0	-0.934	0	46.5	0.0331	
47	2015	8	7	87.5	7	7	7	0.463	0	-0.934	0	47.5	2.7099	
48	2091	76	76	100	2.4	3.2	0	0.463	0	-0.934	0	48.5	1.0950	
49	2175	84	66	78.6	3.2	4.8	1.5	0.463	0	-0.934	0	49.5	0.9763	
50	2277	102	102	100	1.6	0.8	0.75	0.463	0	-0.934	0	50.5	0.2324	
51	2449	172	152	87.2	2.2	2.9	0	0.463	0	-0.934	0	51.5	2.1849	
52	2645	196	190	97	3	4.8	0	0.463	0	-0.934	0	52.5	9.9241	*****
53	2685	40	3	7.5	7	7	7	0.463	0	1.176	1	53.5	6.9064	
54	2752	67	5	7.5	7	7	7	-0.743	1	1.176	0	54.5	3.2294	
55	2765	13	1	7.5	7	7	7	-0.743	0	1.176	0			
56	2778	13	1	7.5	7	7	7	-0.743	0	1.176	0			

57	2858	80	6	7.5	7	7	7	-0.743	0	1.176	0
58	2885	27	2	7.5	7	7	7	-0.743	0	1.176	0
59	2945	60	60	100	2.1	3.1	0.75	-0.073	1	-0.154	1
60	3150	205	170	83	2.3	3.9	0.75	1.914	1	-0.154	0

Romagnano section 1
Savio Valley, northern Italian Apennines

								Maximum Likelihood Segmentation				Split Moving-Window Segmentation		
								Based on sst. thickness		Based on grain Size				
bed#	Ct (cm)	Bt (cm)	St (cm)	S%	G.Sco	Str.Sco	Bas.G	Seg.L	Ev.Sq	Seg.L	Ev.Sq			
1	20	20	20	100	2.5	5.1	1.5	-0.946	0	-0.115	0			*****
2	89	69	69	100	3.6	4.9	2.25	-0.268	1	-0.115	0			
3	182	93	93	100	0.75	3	0.75	-0.268	0	-0.483	1			
4	256	74	74	100	1.5	3	0.75	-0.268	0	-0.483	0	Posi.	D.Sq	
5	419	163	163	100	1.8	4	0.75	-0.268	0	-0.483	0	5.5	0.7358	
6	492	73	73	100	2.2	2.6	0	-0.268	0	-0.483	0	6.5	1.0565	
7	814	322	322	100	1.2	2	0	-0.268	0	-0.483	0	7.5	3.9505	
8	899	85	83	97.6	2.4	1.1	1.5	-0.268	0	-0.483	0	8.5	3.6659	
9	909	10	10	100	7	7	7	-0.268	0	-0.483	0	9.5	0.6726	
10	917	8	8	100	7	7	7	-0.268	0	-0.483	0	10.5	0.3244	[3]
11	969	52	45	88.5	3.1	4.1	0.75	-0.268	0	-0.483	0	11.5	0.2505	[g37]
12	1024	55	53	96.4	2	1.1	1.5	-0.268	0	-0.483	0	12.5	0.7278	
13	1115	91	87	95.6	2.5	1.3	1.5	-0.268	0	-0.483	0	13.5	0.9462	
14	1290	175	165	94.3	2.94	2.8	0	-0.268	0	-0.483	0	14.5	0.0126	
15	1298	8	5	62.5	7	7	7	-0.268	0	-0.483	0			
16	1355	57	57	100	2.5	3.7	1.5	-0.268	0	-0.483	0			
17	1455	100	100	100	1.4	3.4	0.75	-0.268	0	-0.483	0			
18	1558	103	103	100	1.4	3.5	0	-0.268	0	-0.699	1			
19	1618	60	60	100	1.6	3.5	0.75	-0.268	0	-0.699	0			
20	1798	180	180	100	1.2	2.4	0	1.626	1	-0.699	0			*****

Gesso Section
Santerno Valley, northern Italian Apennines

								Maximum Likelihood Segmentation				Split Moving-Window Segmentation		
								Based on sst. thickness		Based on grain Size				
bed#	Ct (cm)	Bt (cm)	St (cm)	S%	G.Sco	Str.Sco	Bas.G	Seg.L	Ev.Sq	Seg.L	Ev.Sq			
1	147	147	135	91.8	1.7	1.7	1.5	1.151	0	1.5	0	Posi.	D.Sq	*****
2	161	14	11	78.6	7	7	7	1.151	0	2.079	1	2.5	3.4696	
3	324	163	163	100	2.8	0.9	2.25	1.151	0	2.079	0	3.5	1.8968	[4]
4	494	170	167	98.2	2.5	0.4	2.25	0.768	1	2.079	0	4.5	0.2918	[g38]
5	600	105	98	93.3	3.7	2.14	2.25	0.768	0	2.079	0	5.5	0.3510	
6	774	174	170	97.7	2.25	0	2.25	0.768	0	2.079	0	6.5	5.5324	*****
7	809	35	27	77.1	2.25	0	2.25	0.457	1	2.079	0	7.5	2.6533	
8	815	6	4	66.7	7	8.5	7	0.457	0	2.079	0	8.5	2.3704	
9	856	41	41	100	1.5	1.5	1.5	-0.504	1	2.079	0	9.5	2.0015	
10	894	38	38	100	1.5	1.5	1.5	-0.504	0	2.079	0	10.5	0.2449	
11	974	80	70	87.5	2.25	1.5	1.5	-0.504	0	2.079	0	11.5	3.5364	[5]
12	1046	72	62	86.1	3.2	1.7	2.25	-0.504	0	2.079	0	12.5	3.2399	[g39]
13	1056	10	0	0	8.5	8.5	8.5	-0.504	0	2.079	0	13.5	2.7701	
14	1112	56	52	92.8	2.8	2.8	2.25	-0.504	0	2.079	0	14.5	2.0616	
15	1214	102	97	95	4.2	3.8	2.25	-0.504	0	2.079	0			
16	1252	38	24	63.2	3	0	3	-0.504	0	2.079	0			
17	1274	22	13	59.1	3	0	3	-0.504	0	2.079	0			*****

Casovona Section
Santerno Valley, northern Italian Apennines

								Maximum Likelihood Segmentation				Split Moving-Window Segmentation		
								Based on sst. thickness		Based on grain Size				
bed#	Ct (cm)	Bt (cm)	St (cm)	S%	G.Sco	Str.Sco	Bas.G	Seg.L	Ev.Sq	Seg.L	Ev.Sq			
1	183	183	136	74.3	1.5	2.25	1.5	2.063	0	-1.43	0			*****
2	336	153	123	80.4	1.64	2.44	1.5	2.063	0	-1.43	0			
3	363	27	1	3.7	7	7	7	0.016	1	-1.43	0			
4	377	14	0.5	3.7	7	7	7	0.016	0	-0.163	1	POSI.	D.Sq	
5	431	54	2	3.7	7	7	7	0.016	0	-0.163	0	5.5	0.3184	
6	458	27	1	3.7	7	7	7	0.016	0	-0.163	0	6.5	0.4336	
7	577	119	97	81.5	2.25	2.25	1.5	0.016	0	-0.163	0	7.5	0.0349	
8	597	20	8	40	7	7.5	7	0.016	0	-0.163	0	8.5	0.0327	
9	627	30	20	66.7	3	7	3	0.016	0	-0.163	0	9.5	0.1770	
10	707	80	0	0	8.5	8.5	8.5	0.016	0	-0.163	0	10.5	0.2821	
11	800	93	85	91.4	3.54	4.9	1.5	0.016	0	-0.163	0	11.5	0.2698	
12	815	15	1	7	7	7	7	0.016	0	-0.163	0	12.5	0.0334	[6]
13	852	37	2.5	7	7	7	7	0.016	0	-0.163	0	13.5	0.2544	[g59]
14	1032	180	146	81	0.93	3.3	0	0.016	0	-0.163	0	14.5	0.3940	
15	1054	22	1.5	7	7	7	7	0.016	0	-0.163	0	15.5	0.5024	
16	1068	14	1	7	7	7	7	0.016	0	-0.163	0	16.5	0.2213	
17	1169	101	7	7	7	7	7	0.016	0	-0.163	0	17.5	0.1359	
18	1245	76	54	71	2.25	3	1.5	0.016	0	-0.163	0	18.5	0.1117	
19	1254	9	9	100	5	5	3	0.016	0	-0.163	0	19.5	0.6701	
20	1391	137	0	0	8.5	8.5	8.5	0.016	0	-0.163	0	20.5	0.7360	
21	1538	147	76	51.7	2.2	3	1.5	0.716	1	-0.163	0	21.5	0.8199	
22	1623	85	0	0	8.5	8.5	8.5	0.716	0	-0.163	0	22.5	2.3550	
23	1833	210	210	100	1.15	2	0	0.716	0	-0.163	0	23.5	0.1521	*****
24	1855	22	1	5	7	7	7	0.716	0	-0.163	0	24.5	1.2564	
25	1887	32	1.5	5	7	7	7	0.716	0	-0.163	0	25.5	2.1332	*****
26	2077	190	170	89.5	1.05	1.76	0	2.248	1	-1.556	1	26.5	0.7502	
27	2204	127	127	100	2.34	3.26	0.75	2.248	0	-1.556	0	27.5	2.0728	[7]
28	2223	19	19	100	4.3	6.2	1.5	0.468	1	-1.556	0	28.5	0.8792	[g60]
29	2283	60	60	100	2.4	3.7	1.5	0.468	0	-1.556	0	29.5	3.2826	
30	2388	105	55	52.4	2.25	2.25	1.5	0.468	0	-1.264	1	30.5	7.2257	*****
31	2398	10	4	40	7	7	7	-0.452	1	-1.264	0	31.5	2.7369	
32	2406	8	1	12.5	7	7	7	-0.452	0	0.447	1	32.5	0.5555	
33	2415	9	1.5	16.7	7	7	7	-0.452	0	0.447	0	33.5	0.1044	
34	2420	5	1	20	7	7	7	-0.452	0	0.447	0	34.5	0.5789	
35	2474	54	1	2	7	7	7	-0.452	0	0.447	0	35.5	3.0567	
36	2502	28	12	42.9	5.7	5.7	3	-0.452	0	0.447	0	36.5	1.4602	*****
37	2531	29	13	44.8	5.5	7.9	3	-0.452	0	-0.83	1	37.5	0.8834	
38	2554	23	12	52.1	4.7	7.6	3	-0.452	0	-0.83	0	38.5	0.5708	
39	2574	20	11	55	5.2	7.8	3	-0.452	0	-0.83	0	39.5	0.2514	
40	2734	160	140	87.5	0.75	2.25	0.75	-0.452	0	-0.83	0	40.5	1.4993	
41	2764	30	6	20	7	7	7	-0.452	0	-0.83	0	41.5	0.2006	[8]
42	2792	28	11	39.3	5.5	7.9	3	-0.452	0	-0.83	0	42.5	0.5259	
43	2850	58	18	31	3.2	4.3	2.25	-0.452	0	-0.83	0	43.5	1.2775	
44	2865	15	4	26.7	7	7	7	-0.452	0	0.42	1	44.5	0.7210	
45	2893	28	0	0	8.5	8.5	8.5	-0.452	0	0.42	0	45.5	0.0738	
46	3026	133	95	71.4	2.5	2.5	1.5	-0.452	0	0.42	0	46.5	1.0291	*****
47	3042	16	2	12.5	7	7	7	-0.452	0	0.42	0	47.5	0.5458	
48	3054	12	1.5	12.5	7	7	7	-0.452	0	0.42	0	48.5	0.1840	
49	3074	20	2.5	12.5	7	7	7	-0.452	0	0.42	0	49.5	0.1852	
50	3082	8	1	12.5	7	7	7	-0.452	0	0.42	0	50.5	0.0598	
51	3160	78	10	12.5	7	7	7	-0.452	0	0.42	0	51.5	0.1210	
52	3191	31	4	12.5	7	7	7	-0.452	0	0.42	0	52.5	0.1194	
53	3207	16	2	12.5	7	7	7	-0.452	0	0.42	0	53.5	0.1194	
54	3211	4	0.5	12.5	7	7	7	-0.452	0	0.42	0	54.5	0.1202	
55	3234	23	23	100	3.5	3.5	2.25	-0.452	0	0.42	0	55.5	0.1289	
56	3283	49	2	4	7	7	7	-0.452	0	0.42	0	56.5	0.1229	

57	3320	37	1.5	4	7	7	7	-0.452	0	0.42	0	57.5	0.1221	
58	3382	62	2.5	4	7	7	7	-0.452	0	0.42	0	58.5	0.0029	
59	3407	25	1	4	7	7	7	-0.452	0	0.42	0	59.5	0.0029	
60	3527	120	5	4	7	7	7	-0.452	0	0.42	0	60.5	0.1616	
61	3601	74	3	4	7	7	7	-0.452	0	0.42	0	61.5	0.1608	
62	3613	12	0.5	4	7	7	7	-0.452	0	0.42	0	62.5	1.4528	
63	3653	40	20	50	3.4	4	1.5	-0.452	0	0.42	0	63.5	0.4451	
64	3660	7	1	14	7	7	7	-0.452	0	0.42	0	64.5	0.4477	
65	3679	19	3	14	7	7	7	-0.452	0	0.42	0	65.5	2.7548	
66	3693	14	2	14	7	7	7	-0.452	0	0.42	0	66.5	5.4870	*****
67	3888	195	195	100	1.86	2.9	0	-0.452	0	-0.032	1	67.5	0.3460	
68	3922	34	1	3	7	7	7	-0.452	0	-0.032	0	68.5	0.6996	
69	3972	50	1.5	3	7	7	7	-0.452	0	-0.032	0	69.5	0.7047	
70	4204	232	232	100	1.86	2.6	0	1.611	1	-0.032	0	70.5	1.4102	
71	4342	138	136	98.6	1.7	1.92	0	1.611	0	-0.032	0	71.5	3.5914	
72	4347	5	2	40	7	7	7	-0.47	1	-0.032	0	72.5	0.1337	
73	4360	13	5	40	7	7	7	-0.47	0	-0.032	0	73.5	0.3622	[9]
74	4368	8	3	40	7	7	7	-0.47	0	-0.032	0	74.5	0.8553	[g61]
75	4378	10	4	40	7	7	7	-0.47	0	-0.897	1	75.5	6.5275	
76	4534	156	141	90.4	2.3	2.9	0.75	1.603	1	-0.897	0	76.5	5.5218	
77	4684	150	128	85.3	1.5	3	0.75	1.603	0	-0.897	0	77.5	2.4797	
78	4939	255	230	90.2	1.5	2.25	0.75	1.603	0	-0.897	0	78.5	0.9190	
79	4959	20	20	100	3	3	1.5	1.603	0	-0.897	0	79.5	0.0573	
80	5090	131	131	100	1.5	2.25	0.75	1.603	0	-0.897	0	80.5	1.8512	
81	5170	80	56	70	3	3	0.75	1.603	0	-0.897	0	81.5	2.4612	
82	5240	70	54	77	1.1	1.9	0	1.603	0	-0.897	0	82.5	3.9549	
83	5510	270	235	87	0.7	0.7	0	1.603	0	-1.223	1	83.5	8.7356	*****
84	5522	11.5	1	8.7	7	7	7	-0.479	1	-1.223	0	84.5	6.7790	
85	5579	57.5	5	8.7	7	7	7	-0.479	0	-1.223	0	85.5	3.8071	
86	5614	34.5	3	8.7	7	7	7	-0.479	0	0.558	1	86.5	2.2241	
87	5625	11.5	1	8.7	7	7	7	-0.479	0	0.558	0	87.5	1.0266	
88	5671	46	4	8.7	7	7	7	-0.479	0	0.558	0	88.5	0.0000	
89	5694	23	2	8.7	7	7	7	-0.479	0	0.558	0	89.5	0.0000	
90	5729	34.5	3	8.7	7	7	7	-0.479	0	0.558	0	90.5	0.0000	
91	5740	11.5	1	8.7	7	7	7	-0.479	0	0.558	0	91.5	0.0003	
92	5798	57.5	5	8.7	7	7	7	-0.479	0	0.558	0	92.5	0.0001	
93	5821	23	2	8.7	7	7	7	-0.479	0	0.558	0	93.5	0.0000	
94	5867	46	4	8.7	7	7	7	-0.479	0	0.558	0	94.5	0.2573	
95	5884	17	1.5	8.7	7	7	7	-0.479	0	0.558	0	95.5	1.9202	
96	5918	34.5	3	8.7	7	7	7	-0.479	0	0.558	0	96.5	4.5544	
97	5936	17.5	1.5	8.7	7	7	7	-0.479	0	0.558	0	97.5	4.6120	
98	5970	34.5	3	8.7	7	7	7	-0.479	0	0.558	0	98.5	4.5773	
99	5985	15	15	100	0.75	1.5	0	-0.479	0	-0.98	1	99.5	2.2933	
100	6235	250	239	95.6	1.16	1.8	0	1.854	1	-0.98	0	100.5	0.4032	
101	6385	150	150	100	1.5	2	0	1.854	0	-0.98	0	101.5	4.5601	
102	6419	34	3	9.1	7	7	7	-0.406	1	-0.98	0	102.5	4.5946	
103	6430	11	1	9.1	7	7	7	-0.406	0	0.52	1	103.5	4.5601	
104	6488	58	5	9.1	7	7	7	-0.406	0	0.52	0	104.5	3.2057	
105	6511	23	2	9.1	7	7	7	-0.406	0	0.52	0	105.5	0.5708	
106	6557	46	4	9.1	7	7	7	-0.406	0	0.52	0	106.5	0.0002	
107	6575	17.5	1.5	9.1	7	7	7	-0.406	0	0.52	0	107.5	0.2252	
108	6599	24	2	9.1	7	7	7	-0.406	0	0.52	0	108.5	0.2252	
109	6616	17.5	1.5	9.1	7	7	7	-0.406	0	0.52	0	109.5	0.2286	
110	6674	58	5	9.1	7	7	7	-0.406	0	0.52	0	110.5	0.2220	
111	6685	11	1	9.1	7	7	7	-0.406	0	0.52	0	111.5	0.2257	
112	6727	42	42	100	1.93	4.4	0.75	-0.406	0	0.52	0	112.5	0.2286	
113	6776	49	3	6.1	7	7	7	-0.406	0	0.52	0	113.5	0.2324	
114	6792	16	1	6.1	7	7	7	-0.406	0	0.52	0	114.5	0.0095	
115	6824	32	2	6.1	7	7	7	-0.406	0	0.52	0	115.5	0.0110	
116	6848	24	1.5	6.1	7	7	7	-0.406	0	0.52	0	116.5	0.0118	
117	6897	49	3	6.1	7	7	7	-0.406	0	0.52	0	117.5	0.2676	
118	6913	16	1	6.1	7	7	7	-0.406	0	0.52	0	118.5	0.2735	
119	6983	70	70	100	2.3	2.9	0.75	-0.406	0	0.52	0	119.5	0.2735	
120	7000	17	1	6.3	7	7	7	-0.406	0	0.52	0	120.5	0.2676	
121	7047	47	3	6.3	7	7	7	-0.406	0	0.52	0	121.5	0.2745	
122	7072	25	1.5	6.3	7	7	7	-0.406	0	0.52	0	122.5	0.4165	
123	7104	32	2	6.3	7	7	7	-0.406	0	0.52	0	123.5	0.4019	

124	7120	16	1	6.3	7	7	7	-0.406	0	0.52	0	124.5	3.4288
125	7168	48	3	6.3	7	7	7	-0.406	0	0.52	0	125.5	3.4042
126	7183	15	1	6.3	7	7	7	-0.406	0	0.52	0	126.5	3.4288
127	7421	238	238	100	1.85	2.55	0	-0.406	0	0.092	1	127.5	0.0482
128	7581	160	0	0	8.5	8.5	8.5	-0.406	0	0.092	0	128.5	0.1665
129	7771	190	190	100	1.7	3.8	0	-0.406	0	0.092	0	129.5	2.8881
130	7855	84	3	3.6	7	7	7	-0.406	0	0.092	0	130.5	2.2472
131	7883	28	1	3.6	7	7	7	-0.406	0	0.092	0	131.5	2.3640
132	7911	28	1	3.6	7	7	7	-0.406	0	0.092	0	132.5	0.3582
133	7939	28	24	85.7	4.7	7.6	3	-0.406	0	0.092	0	133.5	0.6241
134	8155	216	0	0	8.5	8.5	8.5	-0.406	0	0.092	0	134.5	0.6470
135	8185	30	30	100	4.3	4.3	3	-0.406	0	0.092	0	135.5	0.4870
136	8535	350	0	0	8.5	8.5	8.5	-0.406	0	0.092	0	136.5	1.3331
137	8556	21	16	76.2	2.4	2.9	1.5	-0.406	0	0.092	0	137.5	0.1902
138	8630	74	0	0	8.5	8.5	8.5	-0.406	0	0.092	0	138.5	0.7983
139	8695	65	65	100	2.77	6.4	0.75	0.631	1	0.092	0	139.5	0.0579
140	8792	97	84	86.6	2.64	6	1.5	0.631	0	0.092	0	140.5	0.8617
141	8814	22	6	27.3	5	7.75	3	0.631	0	0.092	0	141.5	2.4000
142	8823	8.5	4.5	53	7	7	7	-0.473	1	0.404	1	142.5	0.4277
143	8830	7	2	28.6	7	8.5	7	-0.473	0	0.404	0	143.5	0.1210
144	8836	6	1	16.7	7	7	7	-0.473	0	0.404	0	144.5	0.1015
145	8843	7	5	71.4	7	7	7	-0.473	0	0.404	0	145.5	0.6174
146	8851	8	1	12.5	7	7	7	-0.473	0	0.404	0	146.5	1.0170
147	8964	113	107	94.7	2.44	5.5	1.5	1	1	0.404	0	147.5	0.0222
148	9031	67	62	92.5	1.94	3.3	1.5	1	0	0.404	0	148.5	0.9914
149	9038	7	1	14.3	7	7	7	-0.468	1	0.404	0	149.5	0.9823
150	9072	34	5	14.3	7	7	7	-0.468	0	0.404	0	150.5	0.9778
151	9079	7	1	14.3	7	7	7	-0.468	0	0.404	0	151.5	0.9733
152	9133	54	8	14.3	7	7	7	-0.468	0	0.404	0	152.5	0.2088
153	9161	28	4	14.3	7	7	7	-0.468	0	0.404	0	153.5	0.0001
154	9224	63	3	4.8	7	7	7	-0.468	0	0.404	0	154.5	0.0005
155	9349	125	6	4.8	7	7	7	-0.468	0	0.404	0	155.5	0.0018
156	9391	42	2	4.8	7	7	7	-0.468	0	0.404	0	156.5	0.0015
157	9454	63	3	4.8	7	7	7	-0.468	0	0.404	0	157.5	0.0007
158	9515	61	3	4.8	7	7	7	-0.468	0	0.404	0	158.5	0.0002
159	9536	21	1	4.8	7	7	7	-0.468	0	0.404	0	159.5	0.0001
160	9578	42	2	4.8	7	7	7	-0.468	0	0.404	0	160.5	0.0009
161	9662	84	4	4.8	7	7	7	-0.468	0	0.404	0	161.5	0.0005
162	9683	21	1	4.8	7	7	7	-0.468	0	0.404	0	162.5	0.1058
163	9788	105	5	4.8	7	7	7	-0.468	0	0.404	0	163.5	0.1069
164	9809	21	1	4.8	7	7	7	-0.468	0	0.404	0	164.5	0.1093
165	9977	168	8	4.8	7	7	7	-0.468	0	0.404	0	165.5	1.4449
166	10061	84	4	4.8	7	7	7	-0.468	0	0.404	0	166.5	1.4198
167	10093	32	32	100	4.9	7.7	3	0.04	1	0.404	0	167.5	0.5089
168	10311	218	8	3.6	7	7	7	0.04	0	0.404	0	168.5	0.4624
169	10393	82	3	3.6	7	7	7	0.04	0	0.404	0	169.5	1.1615
170	10693	300	220	73.3	2.68	5.2	0.75	0.04	0	0.404	0	170.5	0.6575
171	10725	32	0.5	1.6	7	7	7	0.04	0	0.404	0	171.5	0.6346
172	10757	32	0.5	1.6	7	7	7	0.04	0	0.404	0	172.5	0.3752
173	10889	132	2	1.6	7	7	7	0.04	0	0.404	0	173.5	0.3454
174	10993	104	64	61.5	1.92	4.1	0.75	0.04	0	0.404	0	174.5	1.9101
175	11011	18	1.5	8.3	7	7	7	-0.476	1	0.404	0	175.5	0.2482
176	11023	12	1	8.3	7	7	7	-0.476	0	0.404	0	176.5	0.0693
177	11059	36	3	8.3	7	7	7	-0.476	0	0.404	0	177.5	0.0824
178	11089	30	2.5	8.3	7	7	7	-0.476	0	0.404	0	178.5	0.0894
179	11149	60	5	8.3	7	7	7	-0.476	0	0.404	0	179.5	0.5713
180	11173	24	2	8.3	7	7	7	-0.476	0	0.404	0	180.5	0.5731
181	11327	154	124	80.5	3	6.5	1.5	-0.476	0	0.404	0	181.5	0.2498
182	11384	57	0	0	8.5	8.5	8.5	-0.476	0	0.404	0	182.5	0.1876
183	11396	12	12	100	5	5	3	-0.476	0	0.404	0	183.5	0.1559
184	11489	93	2.5	2.7	7	7	7	-0.476	0	0.404	0	184.5	0.1520
185	11601	112	3	2.7	7	7	7	-0.476	0	0.404	0	185.5	0.1061
186	11639	38	1	2.7	7	7	7	-0.476	0	0.404	0	186.5	2.2186
187	11696	57	1.5	2.7	7	7	7	-0.476	0	0.196	1	187.5	5.0055
188	11739	43	43	100	1.7	3.5	1.5	-0.476	0	0.196	0	188.5	5.4022

189	11851	112	1.5	1.3	7	7	7	-0.476	0	0.196	0	189.5	8.6162	*****
190	11941	90	90	100	1.5	1.5	0	1.294	1	0.196	0	190.5	6.2499	▲
191	12051	110	103	93.6	2.5	5.4	0	1.294	0	-1.839	1	191.5	3.2247	|
192	12236	185	185	100	0.75	1.5	0	1.294	0	-1.839	0	192.5	0.4121	|
193	12361	125	120	96	1.96	1.96	0.75	1.294	0	-1.839	0	193.5	0.0871	[10]
194	12476	115	109	95	1.5	1.5	0.75	1.294	0	-1.839	0	194.5	2.1382	[g62]
195	12627	151	151	100	1.79	1.79	0.75	1.294	0	-1.839	0	195.5	5.4859	|
196	12719	92	72	78.3	1.18	3.3	0	1.294	0	-1.793	1	196.5	7.7125	▼
197	12809	90	90	100	1.5	2.25	0	1.294	0	-1.793	0	197.5	9.7589	*****
198	12833	24	1.5	6.3	7	7	7	1.294	0	-1.793	0	198.5	6.1787	
199	12881	48	3	6.3	7	7	7	-0.497	1	0.337	1	199.5	2.2871	
200	12897	16	1	6.3	7	7	7	-0.497	0	0.337	0	200.5	0.7764	
201	12921	24	1.5	6.3	7	7	7	-0.497	0	0.337	0	201.5	0.0327	
202	12937	16	1	6.3	7	7	7	-0.497	0	0.337	0	202.5	0.5950	
203	12969	32	2	6.3	7	7	7	-0.497	0	0.337	0	203.5	0.5897	
204	13000	31	31	100	2	4.4	1.5	0.06	1	0.337	0	204.5	0.0276	
205	13030	30	0	0	8.5	8.5	8.5	0.06	0	0.337	0	205.5	0.5804	
206	13107	77	62	80.5	2.7	5.9	1.5	0.06	0	0.337	0	206.5	0.0327	
207	13187	80	5	6.3	7	7	7	-0.424	1	0.337	0	207.5	0.0331	
208	13195	8	0.5	6.3	7	7	7	-0.424	0	0.337	0	208.5	0.0329	
209	13227	32	2	6.3	7	7	7	-0.424	0	0.337	0	209.5	0.0593	
210	13331	104	84	80.7	1.4	3.4	0	-0.424	0	0.337	0	210.5	0.8224	
211	13339	8	4	50	7	7	7	-0.424	0	0.337	0	211.5	0.3049	
212	13362	23	4	17.4	7	8.5	7	-0.424	0	0.337	0	212.5	0.2843	
213	13364	2.5	0.5	20	7	8.5	7	-0.424	0	0.337	0	213.5	0.2707	
214	13372	8	6	75	7	7	7	-0.424	0	0.337	0	214.5	0.2698	
215	13384	12	9	75	6.3	8	5	-0.424	0	0.337	0	215.5	0.0675	
216	13391	7	0	0	8.5	8.5	8.5	-0.424	0	0.337	0	216.5	0.0074	
217	13428	37	13	35	7	7	7	-0.424	0	0.337	0	217.5	0.3539	
218	13430	20	8	40	7	7	7	-0.424	0	0.337	0	218.5	1.7296	
219	13446	16	10.5	65.6	7	7	7	-0.424	0	0.337	0	219.5	4.2130	
220	13459	13	7.5	57.7	7	7	7	-0.424	0	0.337	0	220.5	4.5677	
221	13466	7	1	14.3	7	7	7	-0.424	0	0.012	1	221.5	6.3619	*****
222	13596	130	113	87	1.54	2.3	0.75	1.615	1	0.012	0	222.5	1.7342	▲
223	13784	188	163	86.7	1.3	2.8	0.75	1.615	0	0.012	0	223.5	0.0615	[11]
224	13962	178	168	94.4	1.83	2.5	0.75	1.615	0	0.012	0	224.5	3.0262	[g63]
225	13992	30	2	6.7	7	8.5	7	-0.168	1	0.012	0	225.5	1.6585	▼
226	14057	65	55	84.6	1.9	5	0.75	-0.168	0	0.012	0	226.5	4.3944	*****
227	14075	18	3	16.7	7	7	7	-0.168	0	0.012	0	227.5	2.1450	
228	14087	12	2	16.7	7	7	7	-0.168	0	0.012	0	228.5	0.4618	
229	14101	14	1	7.1	7	7	7	-0.168	0	0.012	0	229.5	0.0168	
230	14174	73	70	95.9	2.9	6.1	0.75	-0.168	0	0.012	0	230.5	0.2667	
231	14209	35	6	17.1	7	7	7	-0.168	0	0.012	0	231.5	0.0068	
232	14251	42	10	23.8	7	7	7	-0.168	0	0.012	0	232.5	0.0029	
233	14315	64	10	15.6	7	7	7	-0.168	0	0.012	0	233.5	0.1193	
234	14346	31	1	3.2	7	7	7	-0.168	0	0.012	0	234.5	0.0563	
235	14433	87	77	88.5	2.5	5.75	1.5	-0.168	0	0.012	0	235.5	0.0890	
236	14439	6	0.2	3.4	7	7	7	-0.168	0	0.012	0	236.5	0.0845	
237	14483	44	1.5	3.4	7	7	7	-0.168	0	0.012	0	237.5	0.0839	
238	14526	43	27	63	3	5	1.5	-0.168	0	0.012	0	238.5	0.0443	
239	14596	70	0	0	8.5	8.5	8.5	-0.168	0	0.012	0	239.5	0.6686	
240	14652	56	56	100	3	5	1.5	-0.168	0	0.012	0	240.5	0.2588	
241	14703	51	6	11.8	7	7	7	-0.168	0	0.012	0	241.5	0.4103	
242	14745	42	5	11.8	7	7	7	-0.168	0	0.012	0	242.5	0.3512	
243	14838	93	87	93.5	1.7	3.14	1.5	1.13	1	0.012	0	243.5	0.1328	
244	14958	120	120	100	2.1	3.04	1.5	1.13	0	0.012	0	244.5	2.6439	
245	15168	210	0	0	8.5	8.5	8.5	-0.423	1	0.558	1	245.5	0.4902	
246	15210	42	42	100	5	7	5	-0.423	0	0.558	0	246.5	1.2370	
247	15352	142	0	0	8.5	8.5	8.5	-0.423	0	0.558	0	247.5	0.9181	
248	15356	4	4	100	7	7	7	-0.423	0	0.558	0	248.5	0.2558	
249	15483	127	0	0	8.5	8.5	8.5	-0.423	0	0.558	0	249.5	0.2210	
250	15519	36	36	100	5	7.75	3	-0.423	0	0.558	0	250.5	0.1752	
251	15561	42	1	2.4	7	8.5	7	-0.423	0	0.558	0	251.5	0.0404	
252	15602	41	1	2.4	7	8.5	7	-0.423	0	0.558	0	252.5	0.0924	
253	15644	42	1	2.4	7	8.5	7	-0.423	0	0.558	0	253.5	0.0897	

254	15654	10	10	100	7	7	7	-0.423	0	0.558	0	254.5	0.1808
255	15742	88	0	0	8.5	8.5	8.5	-0.423	0	0.558	0	255.5	0.0118
256	15748	6	6	100	7	8.5	7	-0.423	0	0.558	0	256.5	0.0121
257	15759	11	0.5	4.5	7	7	7	-0.423	0	0.558	0	257.5	0.0118
258	15803	44	2	4.5	7	7	7	-0.423	0	0.558	0	258.5	0.0118
259	15825	22	1	4.5	7	7	7	-0.423	0	0.558	0	259.5	0.0209
260	15858	33	1.5	4.5	7	7	7	-0.423	0	0.558	0	260.5	0.0188
261	15866	8	8	100	7	7	7	-0.423	0	0.558	0	261.5	0.1309
262	15938	72	6	8.3	7	7	7	-0.423	0	0.558	0	262.5	0.0628
263	15986	48	4	8.3	7	7	7	-0.423	0	0.558	0	263.5	0.0728
264	16001	15	15	100	7	7	7	-0.423	0	0.558	0	264.5	0.0133
265	16068	67	0	0	8.5	8.5	8.5	-0.423	0	0.558	0	265.5	0.9127
266	16113	45	45	100	2.25	2.25	1.5	0.255	1	0.558	0	266.5	0.1157
267	16248	135	0	0	8.5	8.5	8.5	0.255	0	0.558	0	267.5	0.1316
268	16261	13	13	100	7	7	7	0.255	0	0.558	0	268.5	0.1107
269	16319	58	0	0	8.5	8.5	8.5	0.255	0	0.558	0	269.5	0.1750
270	16487	168	133	79.2	2.45	3.07	0.75	0.255	0	0.558	0	270.5	0.1739
271	16499	12	12	100	7	7	7	-0.417	1	0.558	0	271.5	0.0240
272	16562	63	0	0	8.5	8.5	8.5	-0.417	0	0.558	0	272.5	0.0405
273	16576	14	14	100	7	7	7	-0.417	0	0.558	0	273.5	0.0509
274	16641	65	0	0	8.5	8.5	8.5	-0.417	0	0.558	0	274.5	0.0957
275	16776	135	103	76.3	2.03	2.03	0	-0.417	0	0.558	0	275.5	0.2631
276	16789	13	3	22.3	7	7	7	-0.417	0	0.558	0	276.5	0.2412
277	16821	32	7	22.3	7	7	7	-0.417	0	0.558	0	277.5	0.3376
278	16844	23	5	22.3	7	7	7	-0.417	0	0.558	0	278.5	0.2994
279	16853	9	2	22.3	7	7	7	-0.417	0	0.558	0	279.5	0.4061
280	16858	4.5	1	22.3	7	7	7	-0.417	0	0.558	0	280.5	0.0000
281	16862	4.5	1	22.3	7	7	7	-0.417	0	0.558	0	281.5	0.1786
282	16873	11	7	63.6	7	7	7	-0.417	0	0.558	0	282.5	1.0759
283	16885	12	8.5	70.8	7	7	7	-0.417	0	0.558	0	283.5	1.0459
284	16892	7	1	14.3	7	7	7	-0.417	0	0.558	0	284.5	1.1175
285	16901	9	2	22.2	7	7	7	-0.417	0	0.558	0	285.5	1.8997
286	16964	63	35	55.6	1.5	3	1.5	0.135	1	0.558	0	286.5	0.4014
287	17130	166	144	86.7	1.65	3.1	1.5	0.135	0	0.558	0	287.5	0.4716
288	17148	18	6	33.3	7	7	7	0.135	0	0.558	0	288.5	0.0806
289	17168	20	14	70	7	7	7	0.135	0	0.558	0	289.5	0.1721
290	17206	38	24	63	3.8	3.8	2.25	0.135	0	0.558	0	290.5	0.3589
291	17222	16	5	31.3	7	7	7	0.135	0	0.558	0	291.5	0.0977
292	17242	20	6	30	7	7	7	0.135	0	0.558	0	292.5	0.4007
293	17308	66	66	100	1.83	1.83	1.5	0.135	0	0.558	0	293.5	0.1599
294	17568	260	0	0	8.5	8.5	8.5	0.135	0	0.558	0	294.5	0.0161
295	17630	62	62	100	3.6	4.2	2.25	0.135	0	0.558	0	295.5	0.2574
296	17740	110	0	0	8.5	8.5	8.5	-0.414	1	0.558	0	296.5	0.0774
297	17760	20	20	100	3.2	3.8	2.25	-0.414	0	0.558	0	297.5	0.0031
298	17892	132	0	0	8.5	8.5	8.5	-0.414	0	0.558	0	298.5	0.2620
299	17909	17	17	100	5	5	3	-0.414	0	0.558	0	299.5	0.0775
300	18229	320	0	0	8.5	8.5	8.5	-0.414	0	0.558	0	300.5	0.3806
301	18306	77	58	75.3	2.5	2.5	2.25	0.618	1	0.558	0	301.5	0.1940
302	18393	87	70	80	3	2.25	1.5	0.618	0	0.558	0	302.5	0.9130
303	18465	72	0	0	8.5	8.5	8.5	-0.4	1	0.841	1	303.5	0.9130
304	18505	40	40	100	5	7	5	-0.4	0	0.841	0	304.5	1.0990
305	18765	260	0	0	8.5	8.5	8.5	-0.4	0	0.841	0	305.5	1.0990
306	18773	8	5	62.5	7	7	7	-0.4	0	0.841	0	306.5	0.1294
307	18779	6	6	100	7	7	7	-0.4	0	0.841	0	307.5	0.0025
308	18840	61	0	0	8.5	8.5	8.5	-0.4	0	0.841	0	308.5	0.1914
309	18850	10	10	100	7	7	7	-0.4	0	0.841	0	309.5	0.3534
310	18902	52	0	0	8.5	8.5	8.5	-0.4	0	0.841	0	310.5	0.4911
311	18934	32	32	100	5.75	6.3	3	-0.104	1	0.523	1	311.5	0.0179
312	19334	400	0	0	8.5	8.5	8.5	-0.104	0	0.523	0	312.5	0.1085
313	19358	24	24	100	4.7	7	3	-0.104	0	0.523	0	313.5	0.1805
314	19380	22	1	4.4	7	7	7	-0.505	1	0.523	0	314.5	0.1671
315	19391	11	0.5	4.4	7	7	7	-0.505	0	0.523	0	315.5	0.2565
316	19436	45	2	4.4	7	7	7	-0.505	0	0.523	0	316.5	0.0377
317	19459	23	1	4.4	7	7	7	-0.505	0	0.523	0	317.5	0.0883
318	19527	68	3	4.4	7	7	7	-0.505	0	0.523	0	318.5	0.0000

319	19538	11	0.5	4.4	7	7	7	-0.505	0	0.523	0	319.5	0.3215	
320	19572	34	1.5	4.4	7	7	7	-0.505	0	0.523	0	320.5	1.8459	
321	19640	68	3	4.4	7	7	7	-0.505	0	0.523	0	321.5	4.0134	
322	19696	56	2.5	4.4	7	7	7	-0.505	0	0.523	0	322.5	6.9109	
323	19718	22	1	4.4	7	7	7	-0.505	0	0.523	0	323.5	9.2421	*****
324	19818	100	66	66	2.8	3.1	0	-0.505	0	0.523	0	324.5	3.8126	
325	20007	189	173	91.5	1.96	4.8	0	0.913	1	-0.587	1	325.5	0.1597	[12]
326	20136	129	109	84.5	2	2.8	0	0.913	0	-0.587	0	326.5	0.9457	[g64]
327	20259	123	101	82.1	1.5	1.3	0	0.913	0	-0.587	0	327.5	4.9069	
328	20300	41	41	100	1.5	3	1.5	0.913	0	-0.587	0	328.5	9.0691	*****
329	20326	26	4	15	7	7	7	-0.361	1	-0.587	0	329.5	6.0123	
340	20333	7	1	15	7	7	7	-0.361	0	0.325	1	330.5	2.7313	
341	20379	46	7	15	7	7	7	-0.361	0	0.325	0	331.5	0.4815	
342	20399	20	3	15	7	7	7	-0.361	0	0.325	0	332.5	0.9148	
343	20439	40	6	15	7	7	7	-0.361	0	0.325	0	333.5	1.4143	
344	20505	66	10	15	7	7	7	-0.361	0	0.325	0	334.5	3.3184	
345	20530	25	4	15	7	7	7	-0.361	0	0.325	0	335.5	3.2596	
346	20825	295	280	95	2.14	2.4	0	-0.361	0	0.325	0	336.5	0.3350	
347	20855	30	5	16.7	7	7	7	-0.361	0	0.325	0	337.5	0.3642	
348	20877	22	4	18	7	7	7	-0.361	0	0.325	0	338.5	0.3551	
349	21017	140	140	100	2.6	3.3	0.75	-0.361	0	0.325	0	339.5	3.5236	
350	21055	38	2	5.2	7	7	7	-0.361	0	0.325	0	340.5	3.4868	
351	21074	19	1	5.2	7	7	7	-0.361	0	0.325	0	341.5	0.4937	
352	21084	10	0.5	5.2	7	7	7	-0.361	0	0.325	0	342.5	0.4579	
353	21161	77	4	5.2	7	7	7	-0.361	0	0.325	0	343.5	0.4716	
354	21209	48	2.5	5.2	7	7	7	-0.361	0	0.325	0	344.5	0.0001	
355	21266	57	3	5.2	7	7	7	-0.361	0	0.325	0	345.5	0.0000	
356	21285	19	1	5.2	7	7	7	-0.361	0	0.325	0			
357	21381	96	5	5.2	7	7	7	-0.361	0	0.325	0			
358	21391	10	0.5	5.2	7	7	7	-0.361	0	0.325	0			
359	21448	57	3	5.2	7	7	7	-0.361	0	0.325	0			
360	21477	29	1.5	5.2	7	7	7	-0.361	0	0.325	0			
361	21517	40	40	100	3.1	4.4	1.5	0.627	1	-1.988	1			

Coniale Section
Santerno Valley, northern Italian Apennines

								Maximum Likelihood Segmentation				Split Moving-Window Segmentation		
								Based on sst. thickness		Based on grain Size				
bed#	Ct (cm)	Bt (cm)	St (cm)	S%	G.Sco	Str.Sco	Bas.G	Seg.L	Ev.Sq	Seg.L	Ev.Sq			
1	15	15	4.0	26.7	7	7	7	-0.658	0	0.954	0			*****
2	23	8	1.0	12.5	7	7	7	-0.658	0	0.954	0			▲
3	96	73	65.0	89.0	2.6	1.9	2.25	0.412	1	0.027	1			[13]
4	110	14	7.0	50.0	7	7	7	0.412	0	0.027	0	POSI.	'D.Sq	[g52]
5	228	118	108.0	91.5	4.1	6	1.5	0.412	0	0.027	0	5.5	0.3229	▼
6	252	24	18.0	75.0	3.8	3.8	3	0.412	0	0.027	0	6.5	0.1472	
7	350	98	70.0	71.4	2.6	2.9	0.75	0.412	0	0.027	0	7.5	1.8281	*****
8	372	22	3.0	13.6	7	7	7	-0.571	1	0.027	0	8.5	0.2785	
9	396	24	15.0	62.5	3.65	3.8	2.25	-0.571	0	0.027	0	9.5	0.3417	
10	434	38	10.0	26.3	5.8	8.2	5	-0.571	0	0.027	0	10.5	0.1515	
11	452	18	8.0	44.4	7	7.75	7	-0.571	0	0.027	0	11.5	0.1786	
12	500.5	48.5	8.0	16.5	7	7.75	7	-0.571	0	0.027	0	12.5	0.8804	
13	576.5	76	50.0	65.8	1.74	1.74	1.5	0.215	1	0.027	0	13.5	0.0310	
14	585	8.5	1.0	11.8	7	7	7	0.215	0	0.027	0	14.5	0.4223	
15	694	109	57.0	52.3	3.4	3.9	1.5	0.215	0	0.027	0	15.5	0.0482	
16	715	21	8.0	38.1	7	7	7	0.215	0	0.027	0	16.5	0.3653	
17	732	17	7.0	41.2	7	8.5	7	-0.58	1	0.027	0	17.5	0.0405	
18	761	29	6.0	20.7	7	8.5	7	-0.58	0	0.027	0	18.5	0.7426	
19	785	24	14.0	58.3	5.9	5.9	3	-0.58	0	0.027	0	19.5	1.8771	*****
20	873	88	63.0	71.6	3	3.5	0.75	-0.58	0	0.027	0	20.5	1.1888	▲
21	950	77	45.0	58.4	2.8	5.4	1.5	0.523	1	-0.818	1	21.5	0.2878	[14]
22	1034	84	80.0	95.2	3.3	3.9	0	0.523	0	-0.818	0	22.5	0.1231	[g53]
23	1049	15	6.0	40.0	7	7	7	0.523	0	-0.818	0	23.5	2.3131	▼
24	1086	37	20.0	54.1	6	6	3	-0.535	1	0.029	1	24.5	2.3391	
25	1154	68	16.0	23.5	7	7	7	-0.535	0	0.029	0	25.5	3.3737	*****
26	1184	30	5.0	16.7	7	7	7	-0.535	0	0.029	0	26.5	1.8586	
27	1206	22	1.0	4.5	7	7	7	-0.535	0	0.029	0	27.5	0.8316	
28	1218	12	1.0	8.3	7	7	7	-0.535	0	0.029	0	28.5	0.0974	
29	1225	7	2.0	28.6	7	7	7	-0.535	0	0.029	0	29.5	0.0124	
30	1233	8	3.0	37.5	7	7	7	-0.535	0	0.029	0	30.5	1.0092	
31	1283	50	15.0	30.0	7	7	7	-0.535	0	0.029	0	31.5	2.1239	
32	1287	4	1.0	25.0	7	7	7	-0.535	0	0.029	0	32.5	2.0202	
33	1345	58	26.0	44.8	3.6	4.1	1.5	-0.535	0	-0.271	1	33.5	2.0413	
34	1479	134	81.0	60.4	3	3.6	0	-0.535	0	-0.271	0	34.5	0.3783	
35	1555	76	41.0	53.9	4.7	5.3	1.5	-0.535	0	-0.271	0	35.5	0.1207	
36	1567	12	2.0	16.7	7	7	7	-0.535	0	-0.271	0	36.5	1.3841	
37	1604	37	6.0	16.2	7	7	7	-0.535	0	0.2	1	37.5	1.3317	
38	1655	51	1.0	2.0	7	7	7	-0.535	0	0.2	0	38.5	0.3507	
39	1666	11	9.0	81.8	4.3	7.5	3	-0.535	0	0.2	0	39.5	0.0301	
40	1671	5	4.0	80.0	7	8.5	7	-0.535	0	0.2	0	40.5	0.1943	
41	1680	9	1.0	11.1	7	8.5	7	-0.535	0	0.2	0	41.5	1.6374	
42	1838	158	101.0	63.9	2.5	5.9	0.75	-0.535	0	0.2	0	42.5	2.8971	*****
43	1921	83	3.0	3.6	7	7	7	0.078	1	0.2	0	43.5	0.8980	▲
44	1986	65	52.0	80.0	3.8	5.6	1.5	0.078	0	0.2	0	44.5	2.1094	
45	2066	80	72.0	90.0	4	5.9	1.5	0.078	0	-1.065	1	45.5	0.7184	
46	2136	70	42.0	60.0	3.8	5.6	1.5	0.078	0	-1.065	0	46.5	0.0879	[15]
47	2233	97	44.0	45.4	2.3	3.9	1.5	0.078	0	-1.065	0	47.5	0.2076	[g54]
48	2300	67	57.0	85.1	3.3	3.5	0.75	0.078	0	-1.065	0	48.5	0.5285	
49	2323	23	9.0	39.1	7	7	7	0.078	0	-1.065	0	49.5	3.0195	▼
50	2349	26	3.0	11.5	7	7	7	-0.397	1	0.534	1	50.5	1.6966	
51	2445	96	84.0	87.5	2.5	2.9	0.75	-0.397	0	0.534	0	51.5	0.6933	
52	2475	30	10.0	33.3	7	7	7	-0.397	0	0.534	0	52.5	1.1828	*****
53	2488	13	3.0	23.1	7	8.5	7	-0.397	0	0.534	0	53.5	0.1393	
54	2506	18	6.0	33.3	7	8.5	7	-0.397	0	0.534	0	54.5	0.4984	
55	2525	19	3.0	15.8	7	7	7	-0.397	0	0.534	0	55.5	0.4930	

56	2561	36	30.0	83.3	3	3	1.5	-0.397	0	0.534	0	56.5	1.2419	*****
Covered 2m														
57	2602	41	32.0	78.0	3	1.5	1.5	-0.397	0	-0.188	0	58.5	0.0660	
58	2622	20	13.0	65.0	4.2	4.7	2.25	-0.397	0	-0.188	0	59.5	0.2125	
59	2640	18	11.0	61.1	7	7	7	-0.397	0	-0.188	0	60.5	0.0290	
60	2703	63	59.0	93.7	3.1	3.1	1.5	-0.397	0	-0.188	0	61.5	0.1776	
61	2723	20	11.0	55.0	5	5	3	-0.397	0	-0.188	0	62.5	0.1535	
62	2727.5	4.5	3.5	77.8	7	7	7	-0.397	0	-0.188	0	63.5	1.1154	
63	2741.5	14	8.0	57.1	7	7	7	-0.397	0	-0.188	0	64.5	3.9727	
64	2791.5	50	50.0	100.0	3.14	4.44	0.75	-0.397	0	-1.289	1	65.5	3.4469	
65	2928.5	137	102.0	74.5	3.44	3.93	1.5	1.004	1	-1.289	0	66.5	3.1761	[16]
66	2978.5	50	40.0	80.0	2.84	3.5	2.25	1.004	0	-1.289	0	67.5	5.1278	[g55]
67	3095.5	117	110.0	94.0	2.39	1.5	0.75	1.004	0	-1.289	0	68.5	3.4169	
68	3243.5	148	136.0	91.9	2.67	3.2	0.75	1.004	0	-1.289	0	69.5	5.1337	
69	3386.5	143	138.0	96.5	2.6	4.1	0.75	1.004	0	-1.289	0	70.5	3.0900	
70	3509.5	123	123.0	100.0	2.8	4.34	1.5	1.004	0	-1.289	0	71.5	1.5209	
71	3739.5	230	200.0	87.0	1.92	3	0.75	1.004	0	-1.289	0	72.5	0.3520	
72	3909.5	170	152.0	89.4	1.96	4.47	0.75	1.004	0	-1.289	0	73.5	0.7618	
73	4812.5	903	390.0	43.2	2.89	4.45	0.75	1.004	0	-1.289	0	74.5	9.3674	
74	4946.5	134	99.0	73.9	2.54	3.86	0.75	0.612	1	-1.289	0	75.5	11.5223	*****
75	4990.5	44	5.0	11.4	7	8.5	7	0.612	0	-1.289	0	76.5	7.8380	
76	5010.5	20	20.0	100.0	5.2	5.2	3	0.612	0	-1.289	0	77.5	4.9099	
77	5080.5	70	70.0	100.0	1.5	1.5	0.75	0.612	0	-1.289	0	78.5	5.6532	*****
78	5150.5	70	61.0	87.1	4.9	4.9	1.5	0.612	0	-1.289	0	79.5	2.1540	
79	5163.5	13	5.0	38.5	7	7	7	-0.588	1	-0.557	1	80.5	0.1878	
80	5186.5	23	12.0	52.2	7	7	7	-0.588	0	-0.557	0	81.5	0.0325	
81	5218.5	32	3.0	9.4	7	7	7	-0.588	0	-0.557	0	82.5	0.4235	
82	5251.5	33	1.0	3.0	7	7	7	-0.588	0	-0.557	0	83.5	2.7670	
83	5292.5	41	28.0	68.3	4.5	5.6	1.5	-0.588	0	-0.557	0	84.5	1.7327	
84	5366.5	74	53.0	71.6	3.6	4	1.5	0.249	1	-0.557	0	85.5	1.0603	
85	5431.5	65	38.0	58.5	4.1	5.6	2.25	0.249	0	-0.557	0	86.5	0.4773	[17]
86	5517.5	86	55.0	64.0	3.75	4.8	2.25	0.249	0	-0.557	0	87.5	0.0361	[g56]
87	5574.5	57	50.0	87.7	2.98	4.3	0.75	0.249	0	-0.557	0	88.5	1.3307	
88	5617.5	43	9.0	20.9	7	7	7	0.249	0	-0.557	0	89.5	0.0973	
89	5746.5	129	104.0	80.6	2.84	3.97	0.75	0.249	0	-0.557	0	90.5	0.0866	
90	5787.5	41	20.0	48.8	3	3	1.5	0.249	0	-0.557	0	91.5	0.5743	
91	5805.5	18	4.0	22.2	7	8.5	7	0.249	0	-0.557	0	92.5	0.2152	
92	5825.5	20	3.0	15.0	7	7	7	0.249	0	-0.557	0	93.5	0.5796	
93	5961.5	136	124.0	91.2	3.9	4.4	0.75	0.249	0	-0.557	0	94.5	0.3554	
94	6079.5	118	106.0	89.8	4.3	4.7	0.75	0.249	0	-0.557	0	95.5	1.4583	
95	6114.5	35	20.0	57.1	7	7	7	0.249	0	-0.557	0	96.5	0.9351	
96	6173.5	59	49.0	83.1	5.4	5.7	2.25	0.249	0	-0.557	0	97.5	2.8501	*****
97	6191.5	18	2.0	11.1	7	8.5	7	-0.67	1	0.841	1	98.5	2.8146	
98	6228.5	37	3.0	8.1	7	8.5	7	-0.67	0	0.841	0	99.5	0.2401	
99	6242.5	14	5.0	35.7	7	7	7	-0.67	0	0.841	0	100.5	0.4310	
100	6260.5	18	3.0	16.7	7	7.5	7	-0.67	0	0.841	0	101.5	1.6032	
101	6289.5	29	11.0	37.9	7	7	7	-0.67	0	0.841	0	102.5	2.5577	
102	6332.5	43	5.0	11.6	7	8.5	7							
103	6439.5	107	87.0	81.3	2.8	3.3	1.5	-0.67	0	0.841	0	103.5	2.5661	
104	6559.5	120	90.0	75.0	3.25	5	1.5	0.762	1	0.841	0	104.5	0.3024	
105	6710.5	151	100.0	66.2	4.15	4.15	1.5	0.762	0	-0.222	1	105.5	0.2446	
106	6790.5	80	2.0	2.5	7	7	7	0.762	0	-0.222	0	106.5	2.5411	
107	6822.5	32	9.0	28.1	7	7	7	0.762	0	-0.222	0	107.5	1.5802	
108	6843.5	21	3.0	14.3	7	7	7	-0.56	1	-0.222	0	108.5	0.7288	
109	6862.5	19	11.0	57.9	7	7	7	-0.56	0	-0.222	0	109.5	0.1123	
110	6882.5	20	10.0	50.0	7	7	7	-0.56	0	-0.222	0	110.5	0.0870	
111	6947.5	65	37.0	56.9	5.9	5.9	3	-0.56	0	-0.222	0	111.5	0.5835	
112	7014.5	67	57.0	85.1	4.5	4.95	1.5	0.064	1	-0.222	0	112.5	0.0130	
113	7086.5	72	10.0	13.9	7	7	7	0.064	0	-0.222	0	113.5	0.2357	
114	7112.5	26	6.0	23.1	7	7	7	-0.606	1	-0.222	0	114.5	0.0738	
115	7146.5	34	2.0	5.9	7	7	7	-0.606	0	-0.222	0	115.5	0.0579	
116	7163.5	17	2.0	11.8	7	7	7	-0.606	0	-0.222	0	116.5	0.0613	
117	7199.5	36	31.0	86.1	4.3	5.18	3	-0.606	0	-0.222	0	117.5	0.8578	
118	7311.5	112	22.0	19.6	5.2	5.2	3	-0.198	1	-0.222	0	118.5	1.5147	*****
119	7396.5	85	70.0	82.4	4.5	4.9	2.25	-0.198	0	-0.222	0	119.5	0.4763	
120	7423.5	27	3.0	11.1	7	7	7	-0.198	0	-0.222	0	120.5	0.0572	
121	7461.5	38	21.0	55.3	4.31	6.4	2.25	-0.198	0	0.177	1	121.5	0.0574	

122	7587.5	126	96.0	76.2	4.6	5	2.25	-0.198	0	0.177	0	122.5	0.9066	
123	7612.5	25	1.5	6.0	7	7	7	-0.198	0	0.177	0	123.5	2.4312	
124	7630.5	18	5.0	27.8	7	7	7	-0.198	0	0.177	0	124.5	0.6265	[18]
125	7643.5	13	1.0	7.7	7	7	7	-0.198	0	0.177	0	125.5	0.1162	[g57]
126	7668.5	25	2.5	10.0	7	7	7	-0.198	0	0.177	0	126.5	0.1110	
127	7693.5	25	4.0	16.0	7	7	7	-0.198	0	0.177	0	127.5	0.1244	
128	7794.5	101	64.0	63.4	2.7	4.3	1.5	-0.198	0	0.177	0	128.5	1.1631	
129	7830.5	36	12.0	33.3	7	7	7	-0.198	0	0.177	0	129.5	0.0377	
130	7842.5	12	3.0	25.0	7	7	7	-0.198	0	0.177	0	130.5	0.0460	
131	7860.5	18	11.0	61.1	5	7	3	-0.198	0	0.177	0	131.5	0.5793	
132	7910.5	50	29.0	58.0	4.8	7	3	-0.198	0	0.177	0	132.5	0.1906	
133	7924.5	14	6.0	42.9	7	7	7	-0.198	0	0.177	0	133.5	0.4080	
134	7950.5	26	7.0	26.9	7	7.5	7	-0.198	0	0.177	0	134.5	0.2765	
135	8208.5	258	153.0	59.3	3.23	4	1.5	-0.198	0	0.177	0	135.5	0.2765	
136	8240.5	32	8.0	25.0	7	7	7	-0.198	0	0.177	0	136.5	0.4100	*****
137	8277.5	37	7.0	18.9	7	7	7	-0.198	0	0.177	0	137.5	0.1523	
138	8314.5	37	9.0	24.3	7	7	7	-0.198	0	0.177	0	138.5	0.1074	
139	8328.5	14	2.0	14.3	7	7	7	-0.198	0	0.177	0	139.5	0.0992	
140	8476.5	148	117.0	79.1	4	4.96	1.5	-0.198	0	0.177	0	140.5	0.4683	*****
141	8526.5	50	4.0	8.0	7	7	7	-0.198	0	0.177	0	141.5	0.4366	
142	8629.5	103	85.0	82.5	4.8	5.65	3	-0.198	0	0.177	0	142.5	1.1508	
143	8648.5	19	4.0	21.1	7	7	7	-0.198	0	0.177	0	143.5	0.1313	
144	8722.5	74	27.0	36.5	4.5	4.5	2.25	-0.198	0	0.177	0	144.5	0.1223	
145	8830.5	108	98.0	90.7	3.7	3.7	2.25	-0.198	0	0.177	0	145.5	0.1689	
146	8905.5	75	55.0	73.3	3.98	4.45	2.25	-0.198	0	0.177	0	146.5	0.6896	[19]
147	8918.5	13	9.0	69.2	7	7	7	-0.198	0	0.177	0	147.5	1.2700	[g58]
148	8944.5	26	19.0	73.1	7	7	7	-0.557	1	0.177	0			
149	8955.5	11	2.0	18.2	7	7	7	-0.557	0	0.177	0			
150	9002.5	47	2.0	4.3	7	7	7	-0.557	0	0.177	0			
151	9137.5	135	104.0	77.0	4.4	4.4	2.25	-0.557	0	0.177	0			
152	9452.5	315	105.0	33.3	3.95	3.95	2.25	0.702	1	-0.413	1			

Castel del Rio Section
Santerno Valley, northern Italian Apennines

								Maximum Likelihood Segmentation				Split Moving-Window Segmentation		
								Based on sst. thickness		Based on grain Size				
bed#	Ct (cm)	Bt (cm)	St (cm)	S%	G.Sco	Str.Sco	Bas.G	Seg.L	Ev.Sq	Seg.L	Ev.Sq			
1	130	130	120	92.3	1.5	0	1.5	2.68	1	-1.982	0			*****
2	230	100	90	90	2.1	0.78	1.5	2.68	0	-1.982	0			
3	267	37	36	97.3	3.04	2.4	2.25	0.756	1	-1.982	0			
4	271	4	0.5	12.5	7	7	7	0.756	0	0.518	1	POSI.	'D.Sq	
5	279	8	1	12.5	7	7	7	0.756	0	0.518	0	5.5	0.6132	
6	291	12	1.5	12.5	7	7	7	-0.515	1	0.518	0	6.5	0.5055	
7	297	6	6	100	3	3	3	-0.515	0	0.518	0	7.5	0.3398	
8	335	38	32	84.2	2.25	0	2.25	0.216	1	-1.568	1	8.5	0.0945	[20]
9	340	5	2.5	50	3	7	3	0.216	0	-1.568	0	9.5	0.3415	[g40]
10	422	82	69	84.1	2.25	0	2.25	0.216	0	-1.568	0	10.5	0.2609	
11	431	9	3	33.3	7	7	7	0.216	0	0.583	1	11.5	0.2606	
12	438	7	2	28.6	7	7	7	0.216	0	0.583	0	12.5	0.0149	
13	448	10	7	70	5	7	5	0.216	0	0.583	0	13.5	0.0162	
14	514	66	66	100	2	2	1.5	0.216	0	-1.279	1	14.5	1.1350	
15	556	42	36	85.7	2.4	2.4	2.25	0.216	0	-1.279	0	15.5	2.1500	
16	567	11	1	9.1	7	7	7	-0.488	1	-1.279	0	16.5	2.1366	*****
17	573	6	0.5	9.1	7	7	7	-0.488	0	0.692	1	17.5	2.0980	
18	584	11	1	9.1	7	7	7	-0.488	0	0.692	0	18.5	1.5566	
19	587	3	0	0	8.5	8.5	8.5	-0.488	0	0.692	0	19.5	0.1144	
20	594	7	4	57.1	7	7	7	-0.488	0	0.692	0	20.5	0.0241	
21	599	5	1	20	7	7	7	-0.488	0	0.692	0	21.5	0.3325	
22	608	9	5	55.6	7	7	7	-0.488	0	0.692	0	22.5	1.0386	
23	615	7	5	71.4	7	7	7	-0.488	0	0.692	0	23.5	1.0275	
24	620	5	2	40	7	7	7	-0.488	0	0.692	0	24.5	0.7560	
25	628	8	3	37.5	7	7	7	-0.488	0	0.692	0	25.5	0.7560	
26	660	32	30	93.7	3.3	3.3	3	-0.488	0	-1.319	1	26.5	0.2214	
27	673	13	9	69.2	5.4	5.7	2.25	-0.488	0	-1.319	0	27.5	0.0138	
28	680	7	4	57.1	7	7	7	-0.488	0	0.552	1	28.5	0.3759	
29	686.5	6.5	3	46.2	7	7.75	7	-0.488	0	0.552	0	29.5	1.1423	
30	699.5	13	2	15.4	7	7	7	-0.488	0	0.552	0	30.5	2.0494	
31	716.5	17	11	64.7	3	7	3	-0.488	0	0.552	0	31.5	2.4678	*****
32	766.5	50	50	100	2.25	7	2.25	0.725	1	-1.543	1	32.5	1.7583	
33	820.5	54	54	100	2.25	3	2.25	0.725	0	-1.543	0	33.5	0.6232	[21]
34	852.5	32	28	87.5	3.5	5.6	2.25	0.725	0	-1.543	0	34.5	0.2944	[g41]
35	870.5	18	7	38.9	3	7	3	-0.352	1	-1.543	0	35.5	1.2219	
36	911.5	41	30	73.2	2.5	2.3	2.5	-0.352	0	-1.543	0	36.5	2.7209	*****
37	932.5	21	7	33.3	3	5	3	-0.352	0	-1.543	0	37.5	2.1699	
38	943.5	11	6	54.5	3	5	3	-0.352	0	-1.543	0	38.5	2.9136	
39	951.5	8	3	37.5	7	7	7	-0.352	0	0.692	1	39.5	0.5883	
40	959.5	8	2.5	31.5	7	7	7	-0.352	0	0.692	0	40.5	0.1242	
41	968.5	9	5	55.6	7	7	7	-0.352	0	0.692	0	41.5	1.8731	
42	991.5	23	9	39.1	5.4	7.75	3	-0.352	0	0.692	0	42.5	1.1872	
43	1003.5	12	2	16.7	7	7	7	-0.352	0	0.692	0	43.5	2.9079	*****
44	1085.5	82	60	73.2	2.34	2.5	2.25	0.485	1	-1.371	1	44.5	1.5922	
45	1125.5	40	33	82.5	4	3.5	2.25	0.485	0	-1.371	0	45.5	0.2950	
46	1219.5	94	87	92.6	3.2	4.7	2.25	0.485	0	-1.371	0	46.5	0.2195	
47	1231.5	12	5	41.7	7	7	7	0.485	0	-1.371	0	47.5	1.5474	[22]
48	1245.5	14	14	100	3	5	3	0.485	0	-1.371	0	48.5	1.3437	[g42]
49	1344.5	99	93	93.9	2.9	3.6	2.25	0.485	0	-1.371	0	49.5	0.8865	
50	1358.5	14	7	50	7	8.5	7	0.485	0	-1.371	0	50.5	0.4167	
51	1416.5	58	58	100	3.2	2.8	2.25	0.485	0	-1.371	0	51.5	0.8544	
52	1652.5	236	226	95.8	2.83	2.1	2.25	0.485	0	-1.371	0	52.5	7.6653	*****
53	1675.5	23	10	43.5	7	7	7	0.485	0	0.678	1	53.5	6.3650	
54	1705.5	30	3	10	7	7	7	-0.508	1	0.678	0	54.5	3.3914	
55	1715.5	10	1	10	7	7	7	-0.508	0	0.678	0	55.5	3.2507	
56	1730.5	15	1.5	10	7	7	7	-0.508	0	0.678	0	56.5	1.7036	

57	1740.5	10	3	30	7	7	7	-0.508	0	0.678	0	57.5	0.0011	
58	1751.5	11	9	81.8	7	7	7	-0.508	0	0.678	0	58.5	0.0000	
59	1759.5	8	5	62.5	7	7	7	-0.508	0	0.678	0	59.5	0.0001	
60	1765.5	6	3	50	7	7	7	-0.508	0	0.678	0	60.5	0.0009	
61	1770.5	5	3.5	70	7	7	7	-0.508	0	0.678	0	61.5	0.2563	
62	1775.5	5	4	80	7	7	7	-0.508	0	0.678	0	62.5	0.2540	
63	1782	6.5	3	46.2	7	7	7	-0.508	0	0.678	0	63.5	0.2768	
64	1795	13	4	30.8	7	7	7	-0.508	0	0.678	0	64.5	1.8163	
65	1800	5	1.5	30	7	7	7	-0.508	0	0.678	0	65.5	1.8575	
66	1858	58	48	82.8	3.4	5.3	2.25	0.064	1	0.678	0	66.5	0.1841	
67	1864	6	4	66.7	7	7	7	0.064	0	0.678	0	67.5	0.5364	
68	1876	12	6	50	7	7	7	0.064	0	0.678	0	68.5	0.5176	
69	2016	140	120	85.7	1.6	0.6	1.5	0.064	0	0.678	0	69.5	0.8791	
70	2021.5	5.5	4	72.7	7	7	7	0.064	0	0.678	0	70.5	0.9157	
71	2025.5	4	2	50	7	7	7	0.064	0	0.678	0	71.5	0.2452	
72	2070.5	45	30	66.7	3.7	7	3	0.064	0	0.678	0	72.5	0.7489	
73	2086.5	16	6	37.5	7	7	7	-0.432	1	0.678	0	73.5	0.7566	
74	2104.5	18	10	55.5	7	7	7	-0.432	0	0.678	0	74.5	0.0002	
75	2120.5	16	2	12.5	7	7	7	-0.432	0	0.678	0	75.5	0.0018	
76	2127.5	7	3.5	50	7	7	7	-0.432	0	0.678	0	76.5	0.0159	
77	2150.5	23	19	82.6	5.2	7	3	-0.432	0	0.678	0	77.5	0.1609	
78	2157.5	7	5	71.4	7	7	7	-0.432	0	0.678	0	78.5	0.1588	
79	2179.5	22	20	90.9	7	7	7	-0.073	1	0.678	0	79.5	0.1517	
80	2194.5	15	10	66.7	7	7	7	-0.073	0	0.678	0	80.5	0.1522	
81	2224.5	30	20	66.7	7	7	7	-0.073	0	0.678	0	81.5	0.1551	
82	2234.5	10	3	30	7	7	7	-0.52	1	0.678	0	82.5	0.0038	
83	2241.5	7	2	28.6	7	8.5	7	-0.52	0	0.678	0	83.5	0.0102	
84	2265.5	24	18	75	7	7	7	-0.062	1	0.678	0	84.5	0.0031	
85	2293.5	28	20	71.4	7	7	7	-0.062	0	0.678	0	85.5	0.0091	
86	2323.5	30	20	66.7	7	7	7	-0.062	0	0.678	0	86.5	0.0362	
87	2336.5	13	9	69.2	7	7	7	-0.416	1	0.678	0	87.5	0.0693	
88	2349.5	13	6	46.2	7	7	7	-0.416	0	0.678	0	88.5	0.1777	
89	2367.5	18	8	44.4	7	7	7	-0.416	0	0.678	0	89.5	0.3542	
90	2377.5	10	3	30	7	7	7	-0.416	0	0.678	0	90.5	0.6056	
91	2385.5	8	3	37.5	7	7	7	-0.416	0	0.678	0	91.5	1.4044	
92	2390.5	5	2	40	7	8.5	7	-0.416	0	0.678	0	92.5	3.0820	*****
93	2430.5	40	28	70	5.6	5.9	3	0.163	1	-0.57	1	93.5	1.2644	
94	2445.5	15	6	40	5	7	5	0.163	0	-0.57	0	94.5	0.6468	
95	2462.5	17	11	64.7	5	7	5	0.163	0	-0.57	0	95.5	1.5935	
96	2489.5	27	19	70.4	5.5	5.5	3	0.163	0	-1.359	1	96.5	0.7460	
97	2569.5	80	75	93.8	5.8	5.7	2.25	0.163	0	-1.359	0	97.5	0.2818	
98	2606.5	37	7	18.9	5	7	5	0.163	0	-1.359	0	98.5	0.0870	
99	2632.5	26	13	50	7	7	7	0.163	0	-1.359	0	99.5	0.5400	
100	2757.5	125	120	96	4.08	4.9	2.25	0.163	0	-1.359	0	100.5	0.5596	
101	2767.5	10	5	50	7	7	7	0.163	0	-1.359	0	101.5	1.2598	
102	2803.5	36	20	55.6	2.25	0.75	2.25	0.163	0	-1.359	0	102.5	0.9607	[23]
103	2819.5	16	8	50	3	7	3	0.163	0	-1.359	0	103.5	0.1777	[g43]
104	2895.5	76	62	81.6	2.8	1.4	2.25	0.163	0	-1.359	0	104.5	0.8746	
105	2940.5	45	10	22.2	3	7	3	0.163	0	-1.359	0	105.5	0.7580	
106	3000.5	60	47	78.3	3.3	1.5	2.25	0.163	0	-1.359	0	106.5	1.7327	
107	3025.5	25	16	64	3	7	3	0.163	0	-1.359	0	107.5	1.0951	
108	3035.5	10	2	20	7	7	7	-0.53	1	0.692	1	108.5	0.4336	
109	3043.5	8	3	37.5	7	7	7	-0.53	0	0.692	0	109.5	0.0631	
110	3050.5	7	4	57.1	7	7	7	-0.53	0	0.692	0	110.5	0.0896	
111	3100.5	50	43	86	2.5	5.6	1.5	0.632	1	-1.272	1	111.5	0.1519	
112	3156.5	56	50	89.3	3.7	3.7	1.5	0.632	0	-1.272	0	112.5	1.3373	
113	3166.5	10	4	40	7	7	7	-0.491	1	0.685	1	113.5	1.3422	*****
114	3181.5	15	10	66.7	7	7	7	-0.491	0	0.685	0	114.5	1.4182	
115	3185.5	4	1.5	37.5	7	7	7	-0.491	0	0.685	0	115.5	1.3981	
116	3199.5	14	7	50	7	7	7	-0.491	0	0.685	0	116.5	0.3915	
117	3208.5	9	1	11.1	7	7	7	-0.491	0	0.685	0	117.5	0.0023	
118	3226.5	18	5	27.8	7	7	7	-0.491	0	0.685	0	118.5	0.0049	
119	3242.5	16	3	18.8	7	7	7	-0.491	0	0.685	0	119.5	0.0009	
120	3252.5	10	2.5	25	7	7	7	-0.491	0	0.685	0	120.5	0.0389	
121	3270.5	18	3	16.7	7	7	7	-0.491	0	0.685	0	121.5	0.1638	
122	3277.5	7	1.5	21.4	7	7	7	-0.491	0	0.685	0	122.5	0.1693	
123	3283.5	6	2	33.3	7	7	7	-0.491	0	0.685	0	123.5	0.1759	

124	3306.5	23	3	13	7	7	7	-0.491	0	0.685	0	124.5	0.1741	
125	3328.5	22	15	68.2	6	8.1	5	-0.217	1	0.685	0	125.5	0.0049	
126	3349.5	21	13	61.9	6	8.2	5	-0.217	0	0.685	0	126.5	0.0385	
127	3360.5	11	6	54.5	7	7	7	-0.217	0	0.685	0	127.5	0.0416	
128	3372.5	12	3	25	7	7	7	-0.217	0	0.685	0	128.5	0.3605	
129	3389.5	17	2	11.8	7	7	7	-0.217	0	0.685	0	129.5	0.3978	
130	3412.5	23	13	56.5	7	7	7	-0.217	0	0.685	0	130.5	0.4963	
131	3422.5	10	6	60	5.7	7.5	5	-0.433	1	0.685	0	131.5	0.3914	
132	3429.5	7	4	57.1	7	7	7	-0.433	0	0.685	0	132.5	0.4172	
133	3556.5	127	111	87.4	3.3	4.4	2.25	-0.433	0	0.685	0	133.5	0.7965	
134	3578.5	22	7	33.3	7	7	7	-0.433	0	0.685	0	134.5	0.8527	
135	3590.5	12	4	33.3	7	7	7	-0.433	0	0.685	0	135.5	0.7831	
136	3606.5	16	5	33.3	7	7	7	-0.433	0	0.685	0	136.5	0.5723	
137	3624.5	18	6	33.3	7	7	7	-0.433	0	0.685	0	137.5	0.5928	
138	3642.5	18	6	33.3	7	7	7	-0.433	0	0.685	0	138.5	0.0011	
139	3655.5	13	4	33	7	7	7	-0.433	0	0.685	0	139.5	0.0008	
140	3670.5	15	5	33	7	7	7	-0.433	0	0.685	0	140.5	0.1516	
141	3680.5	10	3	33.3	7	7	7	-0.433	0	0.685	0	141.5	0.6052	
142	3696.5	16	5	33.3	7	7	7	-0.433	0	0.685	0	142.5	1.7583	
Covered 8m														
143	3706.5	10	5	50	7	7	7	-0.433	0	0.685	0	143.5	1.7531	
144	3716.5	10	2	20	7	7	7	-0.433	0	0.685	0	144.5	3.2614	*****
145	3754.5	38	8	21.1	3	7	3	-0.433	0	-1.265	1	145.5	1.2680	▲
146	3788.5	34	6	17.6	3	7	3	-0.433	0	-1.265	0	146.5	0.3523	[24]
147	3894.5	106	86	81.1	3.8	1.9	2.25	-0.433	0	-1.265	0	147.5	0.9588	▼
148	3907.5	13	3	23.1	7	7	7	-0.433	0	-1.265	0	148.5	0.9349	
149	3957.5	50	25	50	3.9	5.4	2.25	0.044	1	-1.265	0	149.5	3.6963	*****
150	3995.5	38	18	47.4	7	7	7	0.044	0	0.691	1	150.5	2.5865	
151	4007.5	12	0	0	8.5	8.5	8.5	-0.471	1	0.691	0	151.5	0.9985	
152	4025.5	18	3	16.7	7	7	7	-0.471	0	0.691	0	152.5	0.2454	
153	4051.5	26	8	30.8	7	7	7	-0.471	0	0.691	0	153.5	0.0506	
154	4071.5	20	4	20	7	7	7	-0.471	0	0.691	0	154.5	0.1583	
155	4076.5	5	2	40	7	7	7	-0.471	0	0.691	0	155.5	0.1524	
156	4085.5	9	3	33.3	7	7	7	-0.471	0	0.691	0	156.5	0.4040	
157	4091.5	6	0	0	8.5	8.5	8.5	-0.471	0	0.691	0	157.5	0.8659	
158	4101.5	10	7	70	4.2	4.2	3	-0.471	0	0.691	0	158.5	0.0338	
159	4112.5	11	6	54.5	7	7	7	-0.471	0	0.691	0	159.5	0.0409	
160	4124.5	12	7	58.3	7	8.5	7	-0.471	0	0.691	0	160.5	0.0314	
161	4139.5	15	12	80	4.3	4.3	3	-0.471	0	0.691	0	161.5	0.3995	
162	4155.5	16	5	31.5	7	7	7	-0.471	0	0.691	0	162.5	0.6056	
163	4179.5	24	6	25	7	7	7	-0.471	0	0.691	0	163.5	0.1518	
164	4229.5	50	13	25	7	7	7	-0.471	0	0.691	0	164.5	0.0001	
165	4249.5	20	5	25	7	7	7	-0.471	0	0.691	0	165.5	0.0000	
166	4265.5	16	4	25	7	7	7	-0.471	0	0.691	0	166.5	0.6113	
167	4285.5	20	5	25	7	7	7	-0.471	0	0.691	0	167.5	1.3897	
168	4301.5	20	5	25	7	7	7	-0.471	0	0.691	0	168.5	2.4611	
Covered 7.5 m														*****
169	4328.5	27	22	81.5	5	7	3	-0.081	1	-0.99	1	169.5	0.6089	▲
170	4363.5	35	5	14.3	7	7	7	-0.081	0	-0.99	0	170.5	2.3466	
171	4383.5	20	10	50	5.4	7.9	3	-0.081	0	-0.99	0	171.5	1.4679	
172	4411.5	28	21	75	5	7	3	-0.081	0	-0.99	0	172.5	0.5162	
173	4431.5	20	10	50	5	7	3	-0.081	0	-0.99	0	173.5	0.5177	
174	4466.5	35	6	17.1	7	7	7	-0.081	0	-0.99	0	174.5	0.9735	
175	4630.5	164	135	82.3	2.9	2.3	1.5	-0.081	0	-0.99	0	175.5	0.0431	
176	4650.5	20	15	75	4.3	4.3	3	-0.081	0	-0.99	0	176.5	0.3616	[25]
177	4676.5	26	10	38.5	5	7	5	-0.081	0	-0.123	1	177.5	0.3570	[g44]
178	4708.5	32	4	12.5	7	7	7	-0.081	0	-0.123	0	178.5	0.0449	
179	4766.5	58	48	82.5	2.8	3.5	2.25	-0.081	0	-0.123	0	179.5	0.5327	
180	4863.5	97	92	96.8	2.8	1.2	2.25	-0.081	0	-0.123	0	180.5	0.2606	
181	4881.5	18	7	38.9	7	7	7	-0.081	0	0.692	1	181.5	0.0179	
182	4885.5	4	2	50	7	7	7	-0.081	0	0.692	0	182.5	0.0166	
183	4894.5	9	6	66.7	7	7	7	-0.081	0	0.692	0	183.5	0.0179	
184	4946.5	52	48	92.3	3.1	3.75	2.25	-0.081	0	-1.68	1	184.5	0.0020	
185	5070.5	124	105	84.7	2.25	2.25	1.5	-0.081	0	-1.68	0	185.5	0.0848	▼
186	5090.5	20	10	50	7	8.5	7	-0.081	0	0.692	1	186.5	0.1028	*****

Covered 4 m														
187	5103.5	13	3	23.1	7	7	7	-0.081	0	0.692	0	187.5	0.0848	
188	5134.5	31	9	29	7	7	7	-0.081	0	0.692	0	188.5	0.1127	
189	5177.5	43	20	46.5	4	4	3	-0.081	0	-1.319	1	189.5	0.2635	*****
190	5280.5	103	81	78.6	3	1.6	2.25	-0.081	0	-1.319	0	190.5	0.1538	
191	5293.5	13	7	53.8	7	7	7	-0.081	0	0.068	1	191.5	0.0934	
192	5313.5	20	10	50	7	7	7	-0.081	0	0.068	0	192.5	0.0494	
193	5335.5	22	3	13.6	7	7	7	-0.081	0	0.068	0	193.5	0.0647	
194	5347.5	12	6	50	7	7	7	-0.081	0	0.068	0	194.5	0.8626	[26]
195	5447.5	100	88	88	2.25	0	2.25	-0.081	0	0.068	0	195.5	1.3731	[g45]
196	5535.5	88	66	75	3.5	4.5	2.25	-0.081	0	0.068	0	196.5	0.0586	
197	5540.5	5	1.5	30	7	7	7	-0.081	0	0.068	0	197.5	0.0834	
198	5553.5	13	3	23	7	8.5	7	-0.081	0	0.068	0	198.5	0.0862	
199	5573.5	20	15	75	4.3	4.3	3	-0.081	0	0.068	0	199.5	0.3133	
200	5784.5	211	185	87.7	3.15	2	3	-0.081	0	0.068	0	200.5	1.6293	******
201	5796.5	12	3	25	7	7	7	-0.081	0	0.692	1	201.5	0.7103	
202	5806.5	10	3	30	7	8.5	7	-0.081	0	0.692	0	202.5	0.7245	
203	5820.5	14	4	28.6	7	8.5	7	-0.081	0	0.692	0	203.5	0.7534	
204	5830.5	10	8	80	5.5	5.9	3	-0.081	0	0.692	0	204.5	0.8568	
205	5890.5	60	40	66.7	5	7	3	-0.081	0	0.692	0	205.5	0.1795	
206	5920.5	30	2	6.7	7	8.5	7	-0.454	1	0.692	0	206.5	0.1875	
207	5931.5	11	3	27.3	7	7	7	-0.454	0	0.692	0	207.5	0.1942	
208	5951.5	20	2	10	7	8.5	7	-0.454	0	0.692	0	208.5	0.1205	
209	5990.5	39	6	15.4	7	7	7	-0.454	0	0.692	0	209.5	0.3006	
210	6075.5	85	75	88.2	4.1	4.1	3	-0.454	0	0.692	0	210.5	0.1693	
211	6098.5	23	5	21.7	7	7	7	-0.454	0	0.692	0	211.5	0.1795	
212	6108.5	10	6	60	7	7	7	-0.454	0	0.692	0	212.5	0.1919	
213	6148.5	40	25	62.5	3	0	3	-0.068	1	0.692	0	213.5	0.3372	
214	6164.5	16	11	68.8	7	7	7	-0.068	0	0.692	0	214.5	0.1450	
215	6187.5	23	17	73.9	5.5	7.4	3	-0.068	0	0.692	0	215.5	0.1551	
216	6194.5	7	2	28.6	7	7	7	-0.521	1	0.692	0	216.5	0.1533	
217	6211.5	17	3	17.6	7	7	7	-0.521	0	0.692	0	217.5	0.1516	
218	6258.5	47	7	14.9	7	7	7	-0.521	0	0.692	0	218.5	0.0152	
219	6291.5	33	25	75.8	5.4	5.4	3	0.081	1	0.692	0	219.5	0.6089	
220	6309.5	18	16	88.9	7	7	7	0.081	0	0.692	0	220.5	0.1665	
221	6317.5	8	2	25	7	8.5	7	0.081	0	0.692	0	221.5	0.9116	
222	6339.5	22	11	50	7	7	7	0.081	0	0.692	0	222.5	0.7684	
Covered 6.5 m														
223	6371.5	32	8	25	7	7	7	0.081	0	0.692	0	223.5	0.7109	
224	6380.5	9	6	66.7	7	7	7	0.081	0	0.692	0	224.5	1.0567	
225	6392.5	12	4	33.3	7	7	7	0.081	0	0.692	0	225.5	2.3573	*****
226	6592.5	200	194	97	2.4	0.4	2.25	0.081	0	0.692	0	226.5	0.8306	
227	6604.5	12	5	41.7	7	7	7	0.081	0	0.692	0	227.5	0.8455	
228	6610.5	6	3	50	7	8.5	7	0.081	0	0.692	0	228.5	0.7635	
229	6615.5	5	1	20	7	7	7	0.081	0	0.692	0	229.5	0.7138	
230	6670.5	55	47	85.5	4.1	3.6	2.25	0.081	0	-1.329	1	230.5	1.1216	
231	6683.5	13	8	61.5	5	7	5	0.081	0	-1.329	0	231.5	0.0855	
232	6733.5	50	43	86	3.3	2.9	2.25	0.081	0	-1.329	0	232.5	0.1354	
233	6745.5	12	10	83.3	7	8.5	7	-0.416	1	0.692	1	233.5	0.0149	
234	6750.5	5	4	80	7	8.5	7	-0.416	0	0.692	0	234.5	0.0094	
235	6754.5	4	2	50	7	7	7	-0.416	0	0.692	0	235.5	2.0538	
236	6809.5	55	44	80	6	6	3	0.008	1	-1.238	1	236.5	1.1937	
237	6832.5	23	17	73.9	6	6	3	0.008	0	-1.238	0	237.5	2.1869	
238	6859.5	27	22	81.5	5	5.3	3	0.008	0	-1.238	0	238.5	1.8008	
239	6877.5	18	12	66.7	7	7	7	0.008	0	-1.238	0	239.5	1.6094	[27]
240	7042.5	165	160	97	3.3	3.1	2.25	0.527	1	-1.238	0	240.5	0.5084	[g46]
241	7071.5	29	29	100	4.4	3.4	3	0.527	0	-1.238	0	241.5	0.1897	
242	7141.5	70	70	100	4.9	4.1	3	0.527	0	-1.238	0	242.5	0.8951	
243	7199.5	58	43	74.1	4.5	4	3	0.527	0	-1.238	0	243.5	0.9119	
244	7219.5	20	6	30	7	7	7	0.527	0	-1.238	0	244.5	0.0762	
245	7231.5	12	10	83.3	7	8.5	7	0.527	0	-1.238	0	245.5	1.3585	
246	7311.5	80	76	95	4.2	4	2.25	0.527	0	-1.238	0	246.5	0.7350	
247	7342.5	31	25	80.6	5	3	5	0.527	0	-1.238	0	247.5	0.9290	
248	7414.5	72	62	86.1	3.8	3.8	3	1.141	1	-1.238	0	248.5	0.1598	
249	7534.5	120	100	83.3	3	0	3	1.141	0	-1.238	0	249.5	0.2574	
250	7606.5	72	67	93	4.2	4.2	3	1.141	0	-1.238	0	250.5	2.1200	
251	7686.5	80	74	92.5	3.8	3.2	3	1.141	0	-1.238	0	251.5	3.5410	*****

252	7700.5	14	3	21.4	7	7	7	1.141	0	0.67	1	252.5	2.6922	
253	7713.5	13	3	23.1	7	7	7	0.212	1	0.67	0	253.5	1.2827	
254	7768.5	55	49	89.1	4.1	2.4	3	0.212	0	0.67	0	254.5	1.9849	*****
255	7791.5	23	20	86.9	7	7	7	0.212	0	0.67	0	255.5	0.9508	
256	7818.5	27	21	77.8	7	7	7	0.212	0	0.67	0	256.5	0.0504	
257	7838.5	20	7	35	7	7	7	-0.422	1	0.67	0	257.5	0.0491	
258	7851.5	13	3	23.1	7	7	7	-0.422	0	0.67	0	258.5	0.0590	
259	7869.5	18	4	22.2	7	7	7	-0.422	0	0.67	0	259.5	0.5361	
260	7887.5	18	9	50	7	7	7	-0.422	0	0.67	0	260.5	1.6605	
261	7970.5	83	53	63.9	5	3	5	0.261	1	-0.48	1	261.5	1.5340	
262	8030.5	60	50	83.3	4.6	4.6	3	0.261	0	-0.48	0	262.5	0.2436	[28]
263	8049.5	19	10	52.6	7	7	7	0.261	0	-0.48	0	263.5	0.1959	[g47]
264	8074.5	25	12	48	7	7	7	0.261	0	-0.48	0	264.5	0.1470	
265	8164.5	90	70	77.8	3	0	3	1.184	1	-0.48	0	265.5	0.0410	
266	8254.5	90	71	78.9	4.2	2.1	3	1.184	0	-0.48	0	266.5	0.7722	
267	8324.5	70	37	52.9	7	7	7	1.184	0	0.684	1	267.5	0.4167	
268	8347.5	23	7	30.4	7	7	7	-0.152	1	0.684	0	268.5	0.0477	
269	8376.5	29	8	27.6	7	7	7	-0.152	0	0.684	0	269.5	0.0384	
270	8473.5	97	82	84.5	3.7	3.7	3	-0.152	0	0.684	0	270.5	0.6650	
271	8491.5	18	6	33.3	7	7	7	-0.152	0	0.684	0	271.5	0.1387	
272	8514.5	23	5	21.7	7	7	7	-0.152	0	0.684	0	272.5	0.0465	
273	8588.5	74	57	77	4.6	4.6	3	-0.152	0	0.684	0	273.5	1.2374	*****
274	8606.5	18	8	44.4	7	7	7	-0.152	0	0.684	0	274.5	1.2920	
275	8611	4.5	1	22.2	7	7	7	-0.152	0	0.684	0	275.5	0.2920	
276	8622.5	11.5	2.5	22.2	7	7	7	-0.152	0	0.684	0	276.5	0.1942	
277	8627	4.5	1	22.2	7	7	7	-0.152	0	0.684	0	277.5	0.1834	
278	8643	16	3.5	22.2	7	7	7	-0.152	0	0.684	0	278.5	0.0113	
279	8652	9	2	22.2	7	7	7	-0.152	0	0.684	0	279.5	0.0204	
280	8656.5	4.5	1	22.2	7	7	7	-0.152	0	0.684	0	280.5	0.0237	
281	8688.5	32	29	90.6	7	7	7	-0.152	0	0.684	0	281.5	0.0196	
282	8695.5	7	2	28.6	7	7	7	-0.387	1	0.684	0	282.5	0.0229	
283	8699	3.5	1	28.6	7	7	7	-0.387	0	0.684	0	283.5	0.1954	
284	8707.5	8.5	2.5	28.6	7	7	7	-0.387	0	0.684	0	284.5	0.1931	
285	8717.5	10	3	28.6	7	7	7	-0.387	0	0.684	0	285.5	0.1844	
286	8727.5	10	3	28.6	7	7	7	-0.387	0	0.684	0	286.5	0.2586	
287	8731	3.5	1	28.6	7	7	7	-0.387	0	0.684	0	287.5	0.2817	
288	8804	73	63	86.3	5.5	5.5	3	-0.387	0	0.684	0	288.5	0.2250	
289	8814	10	2	20	7	7	7	-0.387	0	0.684	0	289.5	0.2015	
290	8819	5	1	20	7	7	7	-0.387	0	0.684	0	290.5	0.1942	
291	8834	15	3	20	7	7	7	-0.387	0	0.684	0	291.5	0.0212	
292	8842	8	6	75	7	7	7	-0.387	0	0.684	0	292.5	0.2917	
293	8860	18	12	66.7	7	7	7	-0.387	0	0.684	0	293.5	2.4961	
294	8874	14	10	71.4	7	7	7	-0.387	0	0.684	0	294.5	2.3378	
295	8899	25	2	8	7	7	7	-0.387	0	0.684	0	295.5	2.3825	*****
296	8916	17	14	82.3	3	3	3	-0.387	0	-1.238	1	296.5	0.7451	
297	9013	97	87	89.7	4.2	4	2.25	-0.387	0	-1.238	0	297.5	0.2162	
298	9083	70	68	97	3.8	2.4	2.25	-0.387	0	-1.238	0	298.5	1.2828	
299	9090	7	1	14.3	7	8.5	7	-0.387	0	-1.238	0	299.5	1.3993	[29]
300	9103	13	8	61.5	7	7.75	7	-0.387	0	0.692	1	300.5	1.2655	[g48]
301	9109	6	1	16.7	7	8.5	7	-0.387	0	0.692	0	301.5	1.3242	
302	9116	7	1.5	21.4	7	8.5	7	-0.387	0	0.692	0	302.5	3.7277	
303	9444	328	303	92.4	2.4	2.4	2.25	-0.387	0	-1.004	1	303.5	1.6759	
304	9504	60	58	96.7	3.3	2.96	2.25	-0.387	0	-1.004	0	304.5	3.7112	*****
305	9515	11	3	27.3	7	8.5	7	-0.387	0	0.674	1	305.5	3.5677	
306	9535	20	5	25	7	7	7	-0.387	0	0.674	0	306.5	3.6699	
307	9575	40	20	50	4	4	3	-0.387	0	0.674	0	307.5	5.8097	
308	9598	23	8	34.8	7	7	7	-0.387	0	0.674	0	308.5	0.8294	
309	9605	7	5	71.4	7	7	7	-0.387	0	0.674	0	309.5	0.5715	
310	9612	7	5	71.4	7	7	7	-0.387	0	0.674	0	310.5	0.9540	
311	9629	17	4	23.5	7	7	7	-0.387	0	0.674	0	311.5	2.2495	
312	9645	16	6	37.5	7	7	7	-0.387	0	0.674	0	312.5	8.1055	
313	9674	29	16	55.2	7	7	7	-0.387	0	0.674	0	313.5	11.1801	*****
314	9829	155	145	93.5	4.6	4.6	3	-0.063	1	-1.269	1	314.5	2.8671	
315	9876	47	32	68.1	5.5	5.7	3	-0.063	0	-1.269	0	315.5	0.9006	[30]
316	9956	80	72	90	3	0	3	-0.063	0	-1.269	0	316.5	0.0599	[g49]
317	10146	190	180	94.7	2.9	1.6	2.25	-0.063	0	-1.269	0	317.5	4.0823	
318	10229	83	73	88	3.4	0.8	2.25	-0.063	0	-1.269	0	318.5	8.1865	*****
319	10246	17	10	58.8	7	7	7	-0.063	0	0.692	1	319.5	1.5655	

320	10271	25	8	32	7	7	7	-0.063	0	0.692	0	320.5	0.6391	
321	10299	28	5	17.9	7	7	7	-0.063	0	0.692	0	321.5	0.5575	*****
322	10325	26	16	61.5	6.3	6.3	3	-0.063	0	-0.872	1	322.5	0.2956	
323	10340	15	9	60	5.7	5.7	3	-0.063	0	-0.872	0	323.5	0.5800	[31]
324	10467	127	127	100	3.5	0.83	3	-0.063	0	-0.872	0	324.5	0.9443	
325	10522	55	50	91	3.4	0.7	3	-0.063	0	-0.872	0	325.5	3.5885	*****
326	10532	10	3	30	7	7	7	-0.063	0	0.692	1	326.5	3.5288	
327	10546	14	2	14.3	7	7	7	-0.063	0	0.692	0	327.5	2.2892	
328	10568	22	2	9.1	7	7	7	-0.063	0	0.692	0	328.5	1.4485	
329	10582	14	4	28.6	7	7	7	-0.063	0	0.692	0	329.5	0.2066	
330	10587	5	3	60	7	7	7	-0.063	0	0.692	0	330.5	0.0031	
331	10594	7	6	85.7	7	7	7	-0.063	0	0.692	0	331.5	0.0005	
332	10600	6	4	66.7	7	7	7	-0.063	0	0.692	0	332.5	0.0003	
333	10606	6	3	50	7	7	7	-0.063	0	0.692	0	333.5	0.0003	
334	10615	9	3	33.3	7	7	7	-0.063	0	0.692	0	334.5	0.0006	
335	10631	16	8	50	7	7	7	-0.063	0	0.692	0	335.5	0.0004	
336	10637	6	3	50	7	7	7	-0.063	0	0.692	0	336.5	0.0002	
337	10647	10	5	50	7	7	7	-0.063	0	0.692	0	337.5	0.0001	
338	10655	8	4	50	7	7	7	-0.063	0	0.692	0	338.5	0.0009	
339	10662	7	3.5	50	7	7	7	-0.063	0	0.692	0	339.5	0.0002	
340	10672	10	5	50	7	7	7	-0.063	0	0.692	0	340.5	0.0000	
341	10684	12	6	50	7	7	7	-0.063	0	0.692	0	341.5	0.1750	
342	10688	4	2	50	7	7	7	-0.063	0	0.692	0	342.5	0.7935	
343	10690	2	1	50	7	7	7	-0.063	0	0.692	0	343.5	0.8344	
344	10704	14	7	50	7	7	7	-0.063	0	0.692	0	344.5	0.8480	
345	10712	8	4	50	7	7	7	-0.063	0	0.692	0	345.5	0.8941	*****
346	10756	44	37	84.1	5	4.3	3	-0.063	0	0.406	1	346.5	0.0607	
347	10815	59	49	83	4.1	4.1	3	-0.063	0	0.406	0	347.5	0.6480	
348	10829	14	6	42.9	7	7	7	-0.063	0	0.406	0	348.5	0.6604	
349	10845	16	13	81.3	7	7	7	-0.063	0	0.406	0	349.5	0.6966	
350	10858	13	11	84.6	7	7	7	-0.063	0	0.406	0	350.5	0.7336	[32]
351	10878	20	16	80	7	7	7	-0.063	0	0.406	0	351.5	0.0384	[g50]
352	10898	20	15	75	7	7	7	-0.063	0	0.406	0	352.5	1.0344	
353	10907	9	6	66.7	7	7	7	-0.063	0	0.406	0	353.5	1.0540	
354	10918	11	7	63.6	7	7	7	-0.063	0	0.406	0	354.5	1.0799	
355	10930	12	8	66.7	7	7	7	-0.063	0	0.406	0	355.5	1.0961	
356	10954	24	24	100	3.8	2.6	3	-0.196	1	-1.338	1	356.5	0.1380	
357	11050	96	92	95.8	2.9	2.9	1.5	-0.196	0	-1.338	0	357.5	1.1925	
358	11064	14	10	71.4	7	7	7	-0.196	0	0.686	1	358.5	1.2467	*****
359	11073	9	6	66.7	7	7.75	7	-0.196	0	0.686	0	359.5	1.2467	
360	11091	18	8	44.4	7	7	7	-0.196	0	0.686	0	360.5	0.5572	
361	11101	10	5	50	7	7	7	-0.196	0	0.686	0	361.5	0.1838	
362	11108	7	4	57	7	7	7	-0.196	0	0.686	0	362.5	0.1574	
363	11115	7	6	85.7	7	7	7	-0.196	0	0.686	0	363.5	0.1679	
364	11122	7	5	71.4	7	7	7	-0.196	0	0.686	0	364.5	0.1814	
365	11155	33	27	81.8	6	6	3	-0.196	0	0.686	0	365.5	0.1551	
366	11164	9	7	77.8	7	7	7	-0.196	0	0.686	0	366.5	0.1533	
367	11168	4	2	50	7	7	7	-0.196	0	0.686	0	367.5	0.0282	
368	11185	17	11	64.7	7	7	7	-0.196	0	0.686	0	368.5	0.8575	
369	11203	18	12	66.7	7	7	7	-0.196	0	0.686	0	369.5	0.7918	
370	11210	7	4	57.1	7	7	7	-0.196	0	0.686	0	370.5	3.0401	
371	11228	18	12	66.7	7	7	7	-0.196	0	0.686	0	371.5	2.8585	******
372	11266	38	38	100	5	5	3	0.296	1	-1.235	1	372.5	0.6892	
373	11394	128	121	94.5	2.9	2.9	1.5	0.296	0	-1.235	0	373.5	0.6877	
374	11417	23	11	47.8	7	7	7	0.296	0	-1.235	0	374.5	0.7191	
375	11469	52	43	82.7	3.8	3.3	2.25	0.296	0	-1.235	0	375.5	2.1735	
376	11475	6	1	16.7	7	7	7	-0.462	1	0.622	1	376.5	0.9453	
377	11480	5	2	40	7	7	7	-0.462	0	0.622	0	377.5	0.2810	[33]
378	11492	12	7	58.3	7	7	7	-0.462	0	0.622	0	378.5	1.6389	[g51]
379	11499	7	6	85.7	7	7	7	-0.462	0	0.622	0	379.5	3.2283	
380	11519	20	15	75	4.9	4.9	3	-0.462	0	0.622	0	380.5	2.3640	
381	11569	50	39	78	3.7	3.2	2.25	0.295	1	-1.345	1	381.5	0.2797	
382	11604	35	35	100	4	3.5	2.25	0.295	0	-1.345	0	382.5	0.2186	
383	11630	26	26	100	4.5	4.5	3	0.295	0	-1.345	0	383.5	1.6154	
384	11687	57	47	82.5	5.3	5	2.25	0.295	0	-1.345	0	384.5	5.2523	******

385	11695	8	3	37.5	7	7	7	0.295	0	-1.345	0	385.5	3.6391
386	11713	18	4	22.2	7	7	7	-0.32	1	0.675	1	386.5	1.0642
387	11728	15	9	60	7	7	7	-0.32	0	0.675	0	387.5	0.3152
388	11744	16	8	50	7	7	7	-0.32	0	0.675	0	388.5	0.0482
389	11756	12	3	25	7	7	7	-0.32	0	0.675	0	389.5	0.1551
390	11761	5	1	20	7	7	7	-0.32	0	0.675	0	390.5	0.6393
391	11783	22	12	54.5	6	6	3	-0.32	0	0.675	0	391.5	0.2838
392	11805	22	8	36.4	7	7	7	-0.32	0	0.675	0	392.5	1.5367
393	11831	26	10	38.5	7	7	7	-0.32	0	0.675	0	393.5	1.4484
394	11848	17	7	41.2	7	7	7	-0.32	0	0.675	0	394.5	1.3832
395	11898	50	21	42	5.2	5.2	3	-0.009	1	-1.176	1	395.5	0.3577
396	11975	77	52	67.5	3	7	3	-0.009	0	-1.176	0		
397	12097	122	103	84.4	3.3	3.3	2.25	-0.009	0	-1.176	0		
398	12108	11	3	27.3	7	7	7	-0.511	1	-1.176	0		
399	12128	20	4	20	7	7	7	-0.511	0	0.692	1		
400	12137	9	2	22.2	7	7	7	-0.511	0	0.692	0		
401	12148	11	4	36.4	7	7	7	-0.511	0	0.692	0		

Monticello Dam Section, Great Valley, California

Note: data with ** symbols indicate a bed of interbedded siltstone and shale; in such a bed, sandstone thickness (St) is an estimated thickness of all siltstone in the bed.

bed#	Bt(cm)	St(cm)	S%	G.Sco	S.Sco	B.G	D.Sq	Split-Moving Window Segmentation Sq
1	927	927	100	-4	0	-4		*****
2	47	47	100	1.2	2.7	0		
3	150	150	100	-4	0.3	-4		[34]
4	59	59	100	0	0	0		[g1]
5	133	128	96	0.78	1.95	-4	0.015	
6	62	62	100	0.23	0.45	-2	0.000	
7	205	205	100	-4	0.1	-4	0.135	*****
8	21	21	100	0	0	0	0.015	
9	140	140	100	-0.6	0.45	-2	0.015	
10	36	36	100	0.3	0.3	-2	0.135	
11	41	41	100	0.3	0.3	-2	0.135	
12	30	30	100	0.38	1.5	-2	0.240	
13	690	690	100	-4	0	-4	0.000	[35]
14	25	25	100	-4	1.5	-4	0.135	[g2]
15	165	165	100	-0.1	0.54	-4	0.610	
16	140	140	100	-0.28	0.9	-2	0.817	
17	120	120	100	-0.63	0.75	-2	0.610	
18	65	65	100	0	1.5	0	0.085	
19	120	120	100	0.85	1.15	0	0.040	
20	44	44	100	0.75	0	1	0.434	
21	610	610	100	0.13	0.15	0	0.610	*****
22	120	120	100	-2.2	0.9	-4	0.053	
23	140	140	100	-1.2	0.6	-4	0.197	
24	84	84	100	-3.4	0.45	-4	1.053	
25	120	119	99	-1.2	0.6	-2	1.858	
26	220	217	99	1.3	1.7	0	1.986	
27	7	7	93	4.6	3	3	0.710	
28	7.5	6	80	4.6	3	3	0.011	
29	72	72	100	1.95	0.9	2	0.103	
30	145	145	100	1.2	0.6	1	0.287	
31	49	49	100	2.55	2.4	1	0.287	
32	240	240	100	1.2	0.6	1	0.124	[36]
33	130	130	100	0.55	1.05	-2	0.028	[g3]
34	96	96	100	0.45	0.9	0	0.068	
35	200	200	100	0.3	0.9	0	0.124	
36	20	18	90	3.9	3.9	2	0.046	
37	13	10	77	2.1	4.6	2	0.006	
38	25	12	48	2	4.2	2	0.053	
39	24	22	92	2.2	3	0	0.040	
40	70	70	100	0.98	1.73	1	0.287	
41	140	122	87	0.75	0.3	0	1.117	
42	107	52	49	0	0	0	2.489	
43	23	14	61	0.75	1.5	0	4.403	*****
44	**100	**60	60	7	7	7	2.787	
there are 20 thin siltstone beds (0.5-8 cm thick)								
45	100	100	100	0	1.5	0	0.271	
46	21	0	0	8.5	8.5	9	0.114	
47	7	3	43	7	7	7	0.046	
48	4.5	3	56	7	7	7	0.015	
49	9	4	44	7	7	7	0.015	
50	15	2	13	7	7	7	0.304	
51	7.5	4	47	7	7	7	0.634	
52	25	15	60	5	5	5	0.304	
53	22	12	55	2.6	3.2	2	0.015	
54	7	3	43	7	7	7	0.027	
55	13	3	23	7	7	7	0.027	
56	12	9	75	2.6	3.8	2	0.002	
57	9	1	11	7	7	7	0.514	
58	10.5	1.5	14	7	7	7	1.110	
59	18	14	78	4.7	4.3	2	0.822	
60	21	9	43	7	7	7	0.822	
61	23	16	70	2.4	3.9	3	0.020	
62	12	7.5	63	2.4	3.9	3	0.284	
63	6	2	33	7	7	7	0.023	
64	190	186	98	0.75	0	0	0.518	
65	5	3	60	7	7	7	0.518	
66	8	4	50	7	7	7	0.028	
67	52	42	81	0	0	0	0.225	
68	104	100	96	0.75	0	1	1.539	
69	**32	**16	50	7	7	7	0.659	
there are 8 thin siltstone beds (0.5-5 cm thick)								
70	100	93	93	1.3	1.35	0	0.019	
71	9	6	67	2.25	7	2	0.518	
72	**15	**9	60	7	7	7	0.518	
there are 6 thin siltstone beds (0.5-3 cm thick)								
73	6	6	100	1.5	7	2	0.240	
74	4.5	3.5	78	3	7	3	0.000	
75	3	2	67	3	7	3	0.240	
76	12	12	100	2.2	4.4	2	0.684	
77	8	6	75	7	7	7	0.684	
78	5	3.5	70	7	7	7	0.240	
79	2	1.5	75	7	7	7	0.060	
80	4	3	75	7	7	7	0.060	
81	17	12	71	2.3	5	2	0.008	
82	3	2	67	7	7	7	0.008	
83	3	2	67	7	7	7	0.008	
84	1	1	100	7	7	7	0.060	
85	7	3	43	6.1	7	3	0.060	
86	2.5	1.5	60	7	7	7	0.008	
87	5	2	40	7	7	7	0.008	
88	3	1	33	7	7	7	0.008	
89	11	8	73	2.3	5	2	0.339	
90	**21	**10.5	50	7	7	7	0.114	
there are 7 thin siltstone beds (0.5-5 cm thick)								
91	9	7	78	3.1	5	2	0.114	
92	**30	**12	40	7	7	7	0.114	
there are 10 thin siltstone beds (0.5-3 cm thick)								
93	6.5	5.5	85	4.2	7	3	0.144	
94	10	6	60	3.7	4.2	2	0.038	
95	37	36	97	1.5	0	2	0.066	
96	**12	**6	50	7	7	7	0.122	
there are 4 thin siltstone beds (1-2 cm thick)								
97	105	101	96	-3	0	-3	0.184	
98	4.5	3.5	78	7	7	9	1.655	
99	3	2	67	7	7	9	4.088	

bed#	Bt(cm)	St(cm)	S%	G.Sco	S.Sco	B.G	D.Sq	Sq
100	9	5	56	7	7	7	7.267	*****
101	300	300	100	-0.7	0	-4	3.607	
102	350	350	100	-2	0	-2	3.844	
103	255	255	100	-0.1	1.2	-4	1.150	
104	160	160	100	0.06	1.5	-2	0.184	
105	200	200	100	-1.04	1.5	-4	0.060	
106	154	154	100	-0.64	1.5	-2	0.000	
107	210	207	99	-0.77	1.6	-2	0.015	
108	110	110	100	-2	0	-2	0.000	[37]
109	210	210	100	-1.3	5	-2	0.069	[g4]
110	95	95	100	-2.5	0.95	-4	0.259	
111	188	183	97	0.01	1.98	-4	0.398	
112	80	80	100	0	1.5	0	0.259	
113	142	140	99	0.9	2.1	-2	0.398	
114	18	7	39	2.3	3	2	0.135	
115	100	100	100	0	0	0	0.015	
116	106	106	100	-2	1.5	-4	0.028	
117	69	69	100	0.9	1.2	0	0.046	
118	42	22	52	0	5	0	0.034	
119	30	30	100	3.8	4.3	2	0.008	
120	71	62	87	-3.4	1.7	-4	0.335	*****
121	70	70	100	0.86	1.7	1	0.083	
122	150	143	95	1.2	0.58	1	0.391	
123	39	35	90	1.5	1.5	2	0.237	
124	115	112	97	0.75	0	1	0.339	
125	440	436	99	0	0	0	0.114	
126	18	17	94	0.75	2.3	1	0.085	
127	10	10	100	7	7	7	0.225	
128	84	84	100	0.75	0	1	0.111	
129	18	18	100	2.5	3.6	1	0.111	[38]
130	250	250	100	0.2	0.2	0	0.059	[g5]
131	180	157	87	0.19	0.38	0	0.011	
132	86	86	100	1.65	3.8	1	0.105	
133	14	9	64	2.3	1.5	2	0.033	
134	100	93	93	1.66	0.5	1	0.051	
135	33	33	100	3.2	2.1	2	0.006	
136	113	113	100	2.5	1.2	2	0.149	
137	290	290	100	2.2	1.03	2	0.418	
138	218	218	100	2.3	1.25	2	0.659	
139	82	82	100	2.4	1.45	2	0.902	*****
140	210	210	100	-0.2	0.6	-2	0.271	
141	600	600	100	-0.1	0.12	-2	0.008	
142	317	317	100	-0.2	0	-2	0.060	
143	85	85	100	0.82	0.82	-2	0.394	
144	401	401	100	0.17	0.17	0	0.518	
145	34	24	71	3.3	3.3	2	0.211	
146	230	230	100	1.6	0.32	2	0.040	
147	37	32	86	0	2.1	0	0.015	[39]
148	115	115	100	0.75	0	1	0.002	[g6]
149	90	76	84	1.8	2.1	0	0.009	
150	23	18	78	2.5	4.1	1	0.056	
151	14	12	86	1.8	1.8	1	0.176	
152	653	647	99	0.8	0.1	1	0.107	
153	154	154	100	0.95	1.6	1	0.079	
154	46	38	83	4.4	4.8	2	0.184	
155	20	19	95	2.3	1.5	2	0.387	
156	24	24	100	5.2	5.2	3	0.532	
157	190	190	100	0	0	0	1.449	
158	185	175	95	1.3	2	0	2.818	*****
159	**192	**152	79	7	7	7	1.934	
there are 16 thin siltstone beds (1-20 cm thick)								
160	39	29	74	4.2	4.8	2	0.114	
161	**20	**15	75	7	7	7	0.008	
there are 5 thin siltstone beds (1-6 cm thick)								
162	31	17	55	3.4	4.3	0	0.008	
163	6	4.5	75	7	7	7	0.008	
164	7	5.5	79	7	7	7	0.008	
165	6	4.5	75	7	7	7	0.008	
166	59	42	71	2.8	3.4	2	0.228	
167	**28	**22	79	7	7	7	0.083	
there are 4 thin siltstone beds (1-10 cm thick)								
168	30	26	87	4.6	4.6	2	0.002	
169	35	28	80	4.8	4.8	2	0.391	
170	**240	**180	75	7	7	7	0.391	
there are 40 thin siltstone beds (0.5-15 cm thick)								
171	77	77	100	1.5	3	2	2.686	*****
172	13	8	62	1.5	3	2	2.686	
173	38	38	100	2.9	3.3	1	2.393	[40]
174	8	8	100	5.6	5.6	2	2.393	
175	11	11	100	5	3	3	2.207	*****
176	167	167	100	-4	0	-4	1.320	
177	120	120	100	-2	1.5	-4	0.659	
178	623	623	100	-0.5	1.5	-4	0.076	
179	135	135	100	0.6	1.5	-4	0.004	
180	55	55	100	0.75	1.5	0	0.000	
181	192	192	100	-0.8	1.5	-4	0.060	
182	153	153	100	-1.6	1.3	-4	0.060	
183	36	36	100	2.7	4.5	0	0.060	[41]
184	117	117	100	-0.4	1.2	-4	0.060	[g7]
185	758	758	100	-0.1	1.2	-4	0.000	
186	130	130	100	0	0	0	0.240	
187	120	120	100	-5	1.5	-4	0.240	
188	145	145	100	-0.8	1.5	-4	0.060	
189	122	122	100	-0.8	1.5	-4	0.060	
190	152	152	100	-1.2	1.1	-4	0.020	
191	125	125	100	-0.8	1.2	-4	0.523	
192	240	240	100	-0.2	1.4	-4	1.327	
193	140	140	100	-0.5	1.2	-4	2.499	
194	118	118	100	-0.4	1.5	-4	4.038	
195	300	300	100	2.3	0	2	3.654	
196	297	259	87	2.3	2.3	2	2.777	*****
197	20	15	75	5.6	5.6	3	2.198	
198	53	29	55	3	3	3	1.687	
199	19	16	84	5.5	5.5	3	1.243	
200	17	7	41	7	7	7	0.684	
201	76	73	96	3	3	3	0.541	
202	12	11	92	7	7	7	0.240	
203	15	13	87	7	7	7	0.060	
204	19	16	84	7	7	7	0.000	
205	6	4	67	7	7	7	0.000	
206	48	41	85	3.5	3.5	3	0.060	
207	**156	**117	75	7	7	7	0.060	
there are 13 thin siltstone beds (1-20 cm thick)								
208	85	79	93	4.3	4	3	2.003	*****
209	21	21	100	3.6	3.5	2	1.271	
210	85	80	94	2	2.7	-2	0.073	
211	16	15	94	3.4	3.2	2	0.094	
212	10	9	90	5.7	5.7	3	0.634	[42]
213	27	26	96	3.3	2	2	0.705	[g8]
214	27	11	41	5.7	5.5	2	0.625	
215	12	10	83	3	3	3	0.368	
216	11	6	55	7	7	7	0.038	
217	10	8.5	85	7	7	7	0.029	
218	22	12	55	5	4.7	2	0.014	
219	123	97	79	2.3	1.5	2	0.252	*****

bed#	Bt(cm)	St(cm)	S%	G.Sco	S.Sco	B.G	D.Sq	Sq
220	10	9	90	5	7	5	0.144	
221	10	7	70	5	7	5	0.391	
222	22	6	27	5	7	5	0.757	
223	9	5	56	7	7	7	0.339	
224	6	5	83	7	7	7	0.060	
225	36	28	78	5	7	5	0.135	
226	9	6	67	7	7	7	0.060	
227	12	6	50	7	7	7	0.015	
228	7	5	71	7	7	7	0.015	
229	5.5	4	64	7	7	7	0.027	
230	6	6	92	7	7	7	0.083	
231	17	4	24	7	7	7	0.083	
232	7	2	29	7	7	7	0.083	
233	4	3	63	7	7	7	0.083	
234	26	21	81	4.1	4.1	2	0.083	
235	13	9	69	7	7	7	0.083	
236	6	4	67	7	7	7	0.083	
237	5.5	2	36	7	7	7	0.009	
238	7	4	57	7	7	7	0.228	
239	5	3	60	7	7	7	1.216	
240	12	8	67	7	7	7	2.073	
241	5	5	100	7	7	7	3.157	*****
242	127	127	100	0.75	0	1	1.817	
243	330	326	99	1.6	0.71	1	0.845	
244	100	100	100	1.95	0.9	2	0.454	
245	198	196	99	1.8	0.4	2	0.147	
246	273	272	100	1.86	0.46	2	0.002	
247	30	30	100	1.5	0	2	0.002	[43]
248	70	65	93	2.7	1.6	2	0.000	[g9]
249	113	111	98	0.3	0.2	0	0.035	
250	77	75	97	1.65	1.5	1	0.379	
251	22	19	86	2.3	1.5	2	0.908	
252	26	21	81	5.4	5.6	2	1.420	
253	13	7	54	5.3	5.3	3	1.808	
254	26	21	81	5.6	5.3	2	2.528	******
255	**164	**123	75	7	7	7	1.457	
there are 41 thin siltstone beds (0.5-8 cm thick)								
256	21	20	95	1.5	0	2	2.839	******
257	4	4	100	3	0	3	0.271	[44]
258	231	231	100	1.8	1.5	2	0.023	[g10]
259	150	150	100	1.5	1.5	1	0.454	
260	22	22	100	0.75	3	1	2.073	******
261	38	2	5	7	7	7	1.216	
262	38	5	13	7	7	7	0.736	
263	38	2	5	7	7	7	0.271	
264	25	17	68	5.3	5.3	3	0.147	
265	4	1	25	7	7	7	0.060	
266	15	4	27	7	7	7	0.060	
267	4	1	25	7	7	7	0.060	
268	7	2	29	7	7	7	0.060	
269	15	13	87	4.5	7	3	0.000	
270	47	43	91	5	5	3	0.023	
271	4	1	25	7	7	7	0.008	
272	7	2	29	7	7	7	0.114	
273	10	3	30	7	7	7	0.339	
274	4	1	25	7	7	7	1.464	******
275	77	67	87	2.3	1.2	2	1.250	
276	8	8	100	5	5	3	0.394	[45]
277	10	6	60	5	5	3	0.019	[g11]
278	19	14	74	3	1.5	3	0.124	
279	118	103	87	0.75	0	1	1.250	
280	34	25	74	2.2	2	2	2.117	******
281	**610	**366	60	7	7	7	1.464	
there are 122 thin siltstone beds (0.5-15 cm thick)								
282	147	137	93	2.1	2.7	0	0.184	
283	**620	**372	60	7	7	7	0.184	
there are 124 thin siltstone beds (0.5-15 cm thick)								
284	100	99	99	0.7	0.5	0	0.023	
285	17	15	88	4.1	4.1	3	0.114	
286	3	2	67	7	7	7	0.114	
287	43	43	100	2.4	1.8	2	1.022	
288	**640	**384	60	7	7	7	1.022	
there are 128 thin siltstone beds (0.5-15 cm thick)								
289	25	16	64	2.3	1.5	2	2.537	******
290	17	12	71	2.3	1.5	2	0.757	
291	4	4	100	3	3	3	0.446	
292	30	30	100	1.65	1.65	2	0.079	
293	56	56	100	1.5	1.5	2	0.011	
294	46	43	93	2.4	1.2	2	0.023	
295	12	11	92	3.1	2.5	2	0.011	
296	7	7	100	2.3	1.5	2	0.010	
297	36	36	100	3.1	2.3	2	0.002	
298	3	3	100	3.8	3.3	2	0.009	[46]
299	6	6	100	4.6	5	2	0.037	[g12]
300	24	20	83	3	2.4	2	0.023	
301	76	76	100	1.5	1.5	2	0.056	
302	80	51	64	2.4	3.4	1	0.509	
303	23	12	52	4.2	4.5	2	0.573	
304	80	80	100	1.9	2.9	2	0.806	
305	22	18	82	3	2.3	3	0.730	
306	4	4	100	7	7	7	0.074	
307	4	4	100	7	7	7	0.012	
308	19	19	100	5.5	5	3	0.008	
309	10	10	100	4.2	4	3	0.060	
310	5	4	80	3	3	3	0.240	
311	8	8	100	3	3	3	0.961	******
312	**14	**4.2	30	7	7	7	0.961	
there are 7 thin siltstone beds (0.3-2 cm thick)								
313	71	70	99	3	0	3	1.022	******
314	11	6	55	3	2.3	3	0.736	
315	8	3	38	7	7	7	1.427	
316	77	77	100	2.2	3.1	2	0.271	
317	33	33	100	3.5	4	2	0.008	
318	55	55	100	2	2.8	2	0.008	[47]
319	197	190	96	1.8	2	2	0.034	[g13]
320	128	127	99	2.4	1.2	2	0.375	
321	9	6	67	7	7	7	0.001	
322	11	8	73	5	5	3	0.004	
323	7.5	3.5	47	5	5	3	0.008	
324	30	30	100	2.3	1.5	2	0.184	
325	6	6	100	3	3	3	0.339	
326	3	3	100	3	3	3	1.150	
327	10	9	90	3	3	3	1.735	******
328	**39	**7.8	20	7	7	7	1.150	
there are 13 thin siltstone beds (0.3-3 cm thick)								

bed#	Bt(cm)	St(cm)	S%	G.Sco	S.Sco	B.G	D.Sq	Sq
329	38	38	100	0.75	1.5	0	1.243	******
330	42	16	38	1.8	4	2	0.679	
331	38	37	97	2.6	3.3	2	0.342	
332	5	5	100	5.4	2.4	3	0.187	[48]
333	15	12	80	1.5	1.2	2	0.000	[g14]
334	126	126	100	1.5	0	2	0.000	
335	144	144	100	1.4	1.9	1	0.002	
336	33	33	100	1.5	2.3	2	0.034	
337	65	65	100	1.5	2.3	2	0.135	******
338	12	12	100	3	1.5	3	0.034	
339	6	6	100	5	5	3	0.000	
340	8	8	100	0.75	1.5	1	0.019	
341	12	5	42	5	5	3	0.002	
342	12	7	58	5	5	3	0.019	
343	11	11	100	2.3	1.5	2	0.085	
344	5	5	100	2.3	1.5	2	0.518	
345	2	2	100	3	1.5	3	0.684	
346	2	2	100	3	1.5	3	1.150	
347	68	65	96	2.3	1	2	2.253	
348	**18	**6	33	7	7	7	1.355	
there are 6 thin siltstone beds (0.5-3 cm thick)								
349	21	21	100	3.2	2.8	2	2.828	******
350	32	32	100	2.1	2.1	2	1.028	
351	100	97	97	1.5	0	2	0.458	
352	13	10	77	1.5	1.5	2	0.116	
353	248	248	100	1	0.4	1	0.008	
354	15	13	87	3	7	3	0.002	[49]
355	36	29	81	2.5	2.5	2	0.002	[g15]
356	30	30	100	1.5	1.5	2	0.008	
357	290	280	97	1.5	0.7	2	0.019	
358	13	12	92	1.5	1.5	2	0.271	
359	6	6	100	1.5	1.5	2	0.586	
360	45	45	100	1.5	0	2	1.216	
361	117	117	100	2	1.5	1	1.817	
362	105	105	100	1.2	0.5	1	2.537	******
363	43	43	100	-0.9	1	-4	1.577	
364	96	96	100	-0.4	1.5	-4	0.339	
365	94	94	100	-2.4	1.5	-4	0.015	
366	130	130	100	0.4	1.5	-4	0.085	
367	85	85	100	-0.9	1.5	-4	0.496	[50]
368	264	264	100	-0.3	1.4	-4	0.684	[g16]
369	95	91	96	1.75	0.3	2	0.287	
370	212	212	100	1	1.5	-2	0.710	
371	120	120	100	0.6	1.5	-2	1.320	
372	315	315	100	1.3	1.5	-2	2.117	
373	300	300	100	1.3	1.5	-2	3.103	
374	203	203	100	2.25	0	2	3.549	******
375	5	5	100	5	5	5	2.117	
376	10	10	95	5	5	5	1.053	
377	10	10	100	5	5	5	0.357	
378	2	2	100	5	5	5	0.028	
379	4	4	100	5	5	5	0.000	
380	2.5	3	100	5	5	5	0.000	
381	7	7	100	5	5	5	0.000	
382	**4	**3.5	80	5	5	5	0.046	
there are 4 thin siltstone beds (0.5-2 cm thick)								

bed#	Bt(cm)	St(cm)	S%	G.Sco	S.Sco	B.G	D.Sq	Sq
383	21	8	38	5	5	5	1.655	******
384	134	133	99	1.5	0	2	1.150	
385	203	203	100	1.5	0	2	0.736	
386	202	194	96	0.75	1.5	-2	0.046	
387	20	20	100	0.75	1.5	0	0.008	
388	5	4	80	3	1.5	3	0.015	
389	157	157	100	1.7	0.2	2	0.001	
390	110	110	100	1.5	0	2	0.001	
391	366	366	100	1.5	0	2	0.034	
392	231	231	100	1.5	1.5	0	0.000	
393	51	51	100	1.5	0	2	0.020	
394	350	350	100	0.9	1.7	0	0.105	
395	72	72	100	1.6	0.3	2	0.105	[51]
396	83	77	93	1.8	2.6	2	0.105	[g17]
397	7	7	100	3	1.5	3	0.002	
398	28	28	100	2.7	2.3	2	0.002	
399	64	64	100	1.9	0.4	2	0.002	
400	160	160	100	2	0.6	2	0.002	
401	61	59	97	1.6	0.4	2	0.002	
402	45	43	96	1.6	0.1	2	0.018	
403	9	6	67	3	1.5	3	0.002	
404	6	5	83	3	1.5	3	0.018	
405	180	174	97	1.8	1.7	2	0.018	
406	20	20	100	3.3	3.3	2	0.018	
407	20	20	100	3.7	4.3	2	0.006	
408	71	66	93	2.3	0.75	2	0.083	
409	60	60	100	1.5	1.5	2	0.353	
410	240	240	100	1.7	1.4	2	0.654	
411	49	46	94	2	2	2	1.047	******
412	17	12	71	5	5	5	0.654	
413	5	4	80	5	7	5	0.586	
414	6	4	67	5	5	5	0.304	
415	6	5	83	5	5	5	0.015	[52]
416	14	14	100	6	6	5	0.094	
417	12	12	100	6	6	5	0.034	
418	6	2	33	7	7	7	0.094	
419	9.5	5.5	58	5	5	5	0.034	
420	45	45	100	2.1	2.1	2	0.135	
421	58	58	100	2.5	2.1	2	0.845	******
422	**92	**57.5	63	7	7	7	0.634	
there are 23 thin siltstone beds (0.5-5 cm thick)								
423	22	22	100	3.9	4	3	0.000	
424	14	11	79	4	4	3	0.240	
425	**160	**96	60	7	7	7	0.240	
there are 32 thin siltstone beds (0.5-10 cm thick)								
426	30	20	67	3	1.5	2	2.839	******
427	204	204	100	2.3	0.4	2	0.757	
428	24	20	83	1.5	1.5	2	0.195	
429	14	14	100	1.5	1.5	2	0.011	[53]
430	265	262	99	1.7	0.3	2	0.020	[g18]
431	7	5	71	5.8	5.4	3	0.144	
432	23	23	100	3	2.6	2	0.664	
433	5	5	100	5.4	6.3	3	1.784	
434	280	280	100	1.5	0	2	2.797	
435	80	80	100	0.75	1.5	0	1.327	******
436	263	263	100	-1.6	1.5	-4	0.086	
437	224	218	97	-0.2	1.9	-4	0.147	[54]
438	85	85	100	-0.2	2	-4	2.207	
439	408	408	100	1.2	0.23	-4	5.069	******

bed#	Bt(cm)	St(cm)	S%	G.Sco	S.Sco	B.G	D.Sq	Sq
440	7	7	100	7	7	7	2.489	
441	18	18	100	5.4	5.4	3	1.320	
442	18	16	89	1.5	1.5	1	0.991	
443	2	2	100	7	7	7	0.006	
444	4	4	100	6	6.5	3	0.124	
445	14	14	100	5.2	5.2	3	0.011	
446	20	20	100	6.2	5.7	3	0.040	[55]
447	13	13	100	5	7.5	3	0.114	[g19]
448	9	5	56	5	5.5	3	0.018	
449	7	6	86	4.4	4.3	3	0.051	
450	5	4	80	5	1.5	3	0.133	
451	144	135	94	2.3	0.5	2	0.074	
452	19	10	53	5	4	3	0.074	
453	28	28	100	4.1	3.3	2	0.379	
454	17	17	100	2.3	1.5	2	0.325	
455	13	7	54	2	4.6	1	0.523	
456	21	21	100	2.6	2.6	2	1.123	
457	13	13	100	5	5	3	1.547	
458	48	48	100	-4	0	-4	0.375	
459	93	93	100	0.75	0	1	0.375	
460	66	66	100	-4	0	-4	0.006	
461	230	220	96	-4	0	-4	0.255	
462	13	4	31	0.75	1.5	0	0.475	
463	15	15	100	0.65	2.8	0	0.287	
464	13	6	46	0	3	0	0.454	
465	20	18	90	0	3	0	0.271	
466	14	6	43	0	0	0	0.135	
467	13	13	100	0.75	2.3	0	0.211	[56]
468	9	9	100	4.3	4.4	2	0.135	[g20]
469	5	5	100	1.5	3	2	0.076	
470	25	14	56	1.5	3	2	0.034	
471	74	64	86	2	2.3	2	0.008	
472	44	42	95	2	2.3	2	0.000	
473	19	18	95	1.5	0	2	0.000	
474	13	9	69	1.5	1.5	2	0.000	
475	24	12	50	1.5	1.5	2	0.000	
476	15	13	87	1.5	1.5	2		
477	29	26	90	1.5	1.5	2		
478	3	2	67	1.5	0	2		
479	3	2	67	1.5	0	2		
480	17	5	29	1.5	1.5	2		
481	19	14	74	1.5	2.3	2		

Cache Creek Section, Great Valley, California

Note: data with ** symbols indicate a bed of interbedded siltstone and shale; in such a bed, sandstone thickness (St) is an estimated thickness of all siltstone in the bed.

bed#	Bt(cm)	St(cm)	S%	G.Sco	S.Sco	B.G	D.Sq	Split-Moving Window Segmentation Sq
1	78	78	100	2.5	2.7	-2		*****
2	88	88	100	2.3	0	2.3		
3	144	144	100	2.1	0.04	2.3		
4	127	127	100	0.04	1.6	0		
5	250	250	100	2.3	0	2.3	0.432	
6	230	220	96	2.7	0.7	2.3	1.678	
7	40	20	50	4.6	3.7	3	0.621	
8	70	70	100	2.05	2.05	1.5	0.339	[57]
9	30	30	100	3.7	3.15	2.3	0.002	[g21]
10	240	240	100	3.9	2.5	2.3	0.057	
11	121	121	100	2.7	0.5	2.3	0.083	
12	120	87	73	2.3	0	2.3	0.864	
13	60	60	100	2.3	3	2.3	1.535	
14	94	93	99	2.4	1.6	2.3	3.022	
15	170	154	91	2.3	1.5	2.3	4.582	*****
16	11	10.5	95	3.2	3.2	1.5	3.301	
17	5	0.4	8	7	7	7	1.324	
18	4	2	50	7	7	7	0.075	
19	14	9	64	6.2	5.9	3	0.270	
20	5	0.4	8	7	7	7	3.618	
21	33	22	67	1.5	1.5	1.5	4.928	
22	5.5	2.5	45	5	5	3	7.687	*****
23	215	210	98	2.7	0.8	2.3	4.336	
24	41	37	90	4.8	4	2.3	6.193	
25	150	150	100	1.5	0	1.5	2.846	
26	140	140	100	1.5	0	1.5	1.087	
27	200	200	100	1.5	0	1.5	0.047	
28	250	250	100	1.5	0	1.5	0.245	
29	180	180	100	1.6	0.4	1.5	0.577	[58]
30	104	104	100	3.3	1	1.5	0.460	[g22]
31	140	80	57	3.1	1.6	1.5	0.000	
32	170	170	100	1.5	0	1.5	0.216	
33	110	110	100	1.5	0	1.5	1.035	
34	250	250	100	1.5	0	1.5	0.153	
35	80	80	100	1.5	0	1.5	0.919	
36	200	200	100	1.5	0	1.5	0.001	
37	270	270	100	1.5	0	1.5	0.544	
38	120	120	100	1.6	0.2	1.5	0.719	
39	150	150	100	1.7	0.4	1.5	0.425	*****
Covered 50 m								

bed#	Bt(cm)	St(cm)	S%	G.Sco	S.Sco	B.G	D.Sq	Split-Moving Window Segmentation Sq
40	140.6	140.6	100	1.5	1.5	1.5	2.148	*****
41	105.3	105.3	100	1.5	1.5	1.5	0.073	
42	157.9	157.9	100	1.5	1.5	1.5	0.046	
43	131.6	131.6	100	1.8	0.35	1.5	0.084	
44	104	104	100	3.7	2.1	2.3	0.340	
45	120	120	100	2.5	0.9	2.3	0.453	
46	270	265	98	2.2	1.6	0.8	0.744	
47	140	118	84	2.1	3	-2.0	1.108	
48	30	30	100	2.2	2.2	1.5	0.658	[59]
49	225	225	100	1.3	3	0.8	3.376	[g23]
50	47	47	100	5	4.8	2.3	2.697	
51	110	108	98	2.3	0	2.3	1.672	
52	29	27.5	95	4.2	3.7	2.3	0.424	
53	40	40	100	3.1	2.4	2.3	0.941	
54	77	77	100	3.4	0.9	3.0	0.797	
55	40	40	100	3.2	2.2	3.0	1.389	
56	50	50	100	4.5	4.1	3.0	1.957	
57	73	73	100	2.5	2.5	1.5	4.178	*****
Covered 7.6 m								
58	**150	**45	30	7	7	7.0	2.710	
there are 15 thin beds of siltstone (1-5 cm thick)								
59	140	130	93	1.9	0.6	1.5	0.417	
60	**300	**90	30	7	7	7.0	0.417	
there are 30 thin beds of siltstone (1-5 cm thick)								
61	170	166	98	2.9	1.8	1.5	10.006	*****
62	152	152	100	1.35	2.4	0.8	1.949	
63	94	84	89	1.35	2.4	0.8	0.776	
64	90	90	100	1.2	2	0.8	0.071	
65	80	80	100	3.7	3.7	1.5	0.061	
66	53	51	96	3.4	3.4	1.5	0.713	[60]
67	38	37	97	3.8	3.8	1.5	3.156	[g24]
68	231	231	100	1.7	0.3	1.5	0.253	
69	84	84	100	2	0.5	1.5	0.215	
70	130	124	95	2.1	0.8	1.5	0.650	
71	200	200	100	2.8	0.9	2.3	3.543	
72	210	180	86	2.7	0.8	2.3	9.359	
73	22	8	36	4.5	4	3.0	6.228	
74	70	63	90	3.7	3.2	2.3	7.906	*****
75	**80	**30	38	7	7	7.0	4.763	
there are 10 thin beds of siltstone (1-6 cm thick)								
76	240	237	99	2.1	0.7	1.5	2.567	
77	52	52	100	2	0	1.5	1.158	
Covered 10 m								
78	63	63	100	3.1	2.6	1.5	0.261	*****
79	46	46	100	3.4	3.5	2.3	0.088	
80	34	34	100	5.1	4.7	2.3	0.203	[61]
81	117	117	100	3.7	3.7	2.3	0.131	[g25]
82	45	45	100	3	1.5	2.3	0.120	
83	130	105	81	3.8	1.4	3.0	0.847	
84	39	39	100	2.8	2.8	1.5	1.693	*****

bed#	Bt(cm)	St(cm)	S%	G.Sco	S.Sco	B.G	D.Sq	Sq
85	31	23	74	3	0	3	2.316	debris
86	35	25	71	3	0	3	2.564	flow
87	33	31	94	2.7	0	2.3	3.879	depos.
88	**45	**3.5	8	7	7	7	1.332	
there are 5 thin beds of siltstone (0.2-2 cm thick)								
89	87	85	98	3	0	3	4.021	*****
90	71	66	93	3	0	3	0.509	
91	58	49	84	3	0	3	0.003	[62]
92	91	73	80	3	0	3	0.764	
93	58	52	90	3	0	3	2.606	
94	70	60	86	3	0	3	3.807	*****
95	**104	**10.5	10	7	7	7	2.399	
there are 13 thin beds of siltstone (0.3-3 cm thick)								
96	73	69	95	3.2	3.2	1.5	5.420	*****
97	33	21	64	2.8	1.2	1.5	1.090	
98	23	23	100	2.3	0	2.3	0.514	[63]
99	68	57	84	2.3	1.5	1.5	0.005	
100	70	70	100	2.3	1.5	1.5	0.974	
Covered 14 m								*****
101	55	52	95	0.75	1.5	0	2.728	
102	15	10	67	7	7	7	1.566	[64]
103	20	18	90	3.1	3.1	1.5	2.968	
104	12	11	92	4.4	4.4	3	3.476	*****
105	**60	**10	17	7	7	7	0.911	
there are 5 thin beds of siltstone (0.5-4 cm thick)								
106	93	78	84	2.7	0.7	2.3	0.181	
107	85	70	82	3.2	2.6	2.3	0.238	
108	62	40	65	3.2	2.6	2.3	1.651	
109	24	22	92	7	7	7	1.820	
110	5.5	5	91	7	7	7	1.096	
111	3	1	33	7	7	7	0.110	
112	4	3	75	7	7	7	0.073	
113	1.5	0.5	33	7	7	7	0.430	
114	9	7	78	7	7	7	0.438	
115	47	26	55	4.6	3.7	3	0.001	
116	27	17	63	6.2	6.9	3	0.441	
117	16	9	56	7	7	7	0.459	
118	**55	**5	9	7	7	7	0.041	
there are 5 thin beds of siltstone (0.5-3 cm thick)								
119	61	61	100	3	2.5	1.5	4.637	*****
120	66	36	55	2.3	1.5	1.5	0.358	
121	82	82	100	2.4	2.5	0.75	0.065	
122	95	85	89	2.4	2.5	0.75	1.224	
123	17	15.5	91	7	7	7	0.688	[65]
124	6	5	83	7	7	7	0.136	[g26]
125	21	21	100	3.5	2.2	3	0.072	
126	33	33	100	3.4	2.1	3	0.053	
127	28	28	100	3.2	2.2	3	0.076	
128	31	24	77	3.7	3.2	2.3	1.078	
129	41	37	90	3	3	3	2.964	*****
130	17	14	82	7	7	7	1.202	
131	10	4	40	7	7	7	0.072	
132	5	4	80	7	7	7	0.005	
133	12	11	92	7	7	7	0.956	
134	4	1	25	7	7	7	2.773	
135	26	12	46	3	1.5	3	2.104	
136	67	59	88	1.5	1.5	1.5	0.586	
137	18	8	44	7	7	7	3.241	
138	184	154	84	3	2.3	3	1.060	
139	52	39	75	3	1.5	3	0.797	
140	36	31	86	3	1.5	3	0.894	
141	19	6	32	3	1.5	3.0	1.941	*****
142	303	283	93	2.5	0.4	2.3	0.820	
143	94	94	100	3.9	2.5	2.3	0.625	
144	59	59	100	1.7	1.7	0.8	0.097	
145	43	43	100	1.6	1.7	1.5	0.090	
146	56	56	100	1.6	1.7	1.5	0.046	
147	65	65	100	1.5	1.5	1.5	0.956	
148	77	77	100	1.5	1.5	1.5	1.836	[66]
149	250	238	95	2.3	1.1	1.5	0.067	[g27]
150	112	112	100	1.6	0.3	1.5	0.118	
151	101	101	100	2.7	0.7	2.3	0.042	
152	53	52	98	2.5	1.7	2.3	0.301	
153	158	158	100	2.7	0.9	2.3	1.847	
154	56	56	100	3	2.2	2.3	1.675	
155	120	120	100	1.7	0.2	1.5	3.680	
156	200	190	95	2.3	0	2.3	8.294	*****
157	**130	**13	10	7	7	7.0	6.188	
there are 13 thin beds of siltstone (0.5-3 cm thick)								
158	13	6	46	7	7	7.0	5.188	*****
159	19	18	95	2.8	2.2	1.5	3.292	
160	71	61	86	3.1	2.4	1.5	1.466	
161	110	105	95	3.2	0.1	3.0	0.609	
162	25	23.5	94	2.7	2.1	1.5	0.226	
163	43	40	93	2.6	2.6	1.5	0.077	
164	39	33	85	2.3	1.5	2.3	0.082	
165	54	32	59	3.7	3.2	2.3	0.097	
166	25	15	60	3	0	3.0	0.377	
167	215	190	88	2.5	2.2	1.5	0.025	
168	44	44	100	2.3	1.7	1.5	0.021	
169	69	59	86	3.1	3.5	1.5	0.082	
170	11	10	91	5	5.7	3.0	0.035	
171	10	7	70	5	5.7	3.0	0.942	
172	287	230	80	2.3	0	2.3	0.289	[67]
173	29	29	100	2.5	2.5	2.3	0.294	[g28]
174	26	26	100	2.5	2.5	2.3	0.555	
175	85	60	71	2.3	1.5	2.3	0.595	
176	230	228	99	3	2	0.8	1.447	
177	155	145	94	2.1	2.1	1.5	1.696	
178	30	18	60	7	7	7.0	0.896	
179	52	52	100	2.3	0	2.3	0.945	
180	120	115	96	3.3	2.6	2.3	1.475	
181	9	4.5	50	7	7	7.0	0.463	
182	47.5	39.5	83	2.5	2.5	1.5	0.051	
183	14	14	100	4.7	3	3.0	0.220	
184	71	71	100	3	2.3	2.3	0.681	
185	106	106	100	3.5	1.3	3.0	0.590	
186	60	47	78	4.7	4.2	2.3	2.400	*****
187	28	18	64	7	7	7.0	1.191	
188	30	23	77	7	7	7.0	0.604	
189	125	45	36	7	7	7.0	0.189	
190	100	100	100	3.4	3.4	3.0	0.334	
191	29	23	79	7	7	7.0	0.183	
192	40	30	75	7	7	7.0	0.306	
193	66	23	35	7	7	7.0	0.251	
194	165	6	4	7	7	7.0	0.169	
195	42	33	79	3	1.5	3.0	0.206	
196	28	1	4	7	7	7.0	0.997	
197	18	8	44	7	7	7.0	1.765	

bed#	Bt(cm)	St(cm)	S%	G.Sco	S.Sco	B.G	D.Sq	Sq
198	38	37	97	7	7	7	2.632	*****
199	43	34	79	5.8	5.3	3	1.605	
200	70	60	86	2.3	2.3	1.5	0.958	
201	85	77	91	2.3	1.5	1.5	0.323	
202	15	10	67	5.8	6	3	0.125	
203	46	45	98	3	0	3	0.058	
204	38	20	53	3	0	3	0.015	
205	27	22	81	3.9	3.2	3	0.100	
206	29	29	100	2.8	2.7	2.3	0.158	
207	22	22	100	3	2.9	2.3	0.271	
208	87	71	82	2.8	2.3	2.3	0.027	[68]
209	40	37	93	3.1	3.1	1.5	0.159	[g29]
210	51	49	96	2.2	3.3	1.5	0.270	
211	24	18	75	4.3	3.3	3	0.183	
212	79	77	97	2.3	2.3	1.5	0.157	
213	16	10	63	7	7	7	0.201	
214	95	93	98	2.3	0	2.3	0.200	
215	50	47	94	2.6	0.4	2.3	0.257	
216	64	46	72	2.9	2.7	1.5	0.100	
217	37	35	95	3.1	2.1	1.5	0.017	
218	53	38	72	2.6	1.5	2.3	0.849	
219	59	55	93	2.6	1.5	2.3	1.703	
220	53	51	96	3	1.9	2.3	2.974	
221	87	87	100	2.8	1.8	2.3	4.806	*****
222	**200	**10	5	7	7	7	3.025	
there are 20 thin beds of siltstone (0.3-3 cm thick)								
223	75	73	97	4	1.5	3	0.669	
224	10	8	80	7	7	7	1.594	
225	3	1.5	50	7	7	7	2.931	
226	27	27	100	2.3	2.3	2.3	0.898	[69]
227	32	17	53	2.3	1.5	2.3	0.065	
228	14	11	79	2.3	1.5	2.3	0.063	
229	55	39	71	1.7	1.7	1.5	1.357	
230	37	27	73	1.5	1.5	1.5	4.304	*****
231	**75	**5	7	7	7	7	1.865	
there are 5 thin beds of siltstone (0.5-3 cm thick)								
232	17	3	18	3	1.5	3	6.128	*****
233	182	126	69	2.2	0	-2	0.484	
234	19	17	89	5	4	3	0.209	
235	24	21	88	0.75	0	0.75	0.262	
236	25	17	68	0.75	0	0.75	1.184	
237	5	5	100	7	7	7	0.200	
238	24	15	63	2.3	1.5	2.3	0.201	
239	19	7	37	3	1.5	3	0.264	
240	40	22	55	3	1.5	3	0.138	
241	59	44	75	3	0	3	0.007	
242	40	38	95	3	0	3	0.072	
243	8	6	75	7	7	7	0.252	[70]
244	38	35	92	3.4	0.7	3	0.365	[g30]
245	20	20	100	3	0	3	0.372	
246	15	10	67	3	1.5	3	0.077	
247	43	36	84	1.5	0	1.5	0.013	
248	16	11	69	2.7	1.9	2.3	0.132	
249	11	5	45	2.3	1.5	2.3	0.725	
250	14	14	100	3	1.5	3	1.099	
251	6	3	50	7	7	7	1.123	
252	78	73	94	3	2	1.5	0.535	
253	115	99	86	2.9	1.9	1.5	0.695	
254	122	113	93	2.5	0.3	2.3	2.160	
255	81	67	83	2.3	0	2.3	4.317	*****

bed#	Bt(cm)	St(cm)	S%	G.Sco	S.Sco	B.G	D.Sq	Sq
256	**78	**15	19	7	7	7.0	4.312	
there are 6 thin beds of siltstone (1-5 cm thick)								
257	25	13	52	3	0	3.0	2.751	*****
258	55	44	80	3	1.5	3.0	0.942	
259	20	18	90	3	1.5	3.0	0.119	[71]
260	20	16	80	3	1.5	3.0	0.043	
261	24	21	88	3	1.5	3.0	0.535	*****
262	5	4	80	3	1.5	3.0	0.511	
263	5	3	60	3	1.5	3.0	0.965	
264	4	3	75	7	7	7.0	0.107	
265	8	6.5	81	3	1.5	3.0	0.420	
266	4	3	75	7	7	7.0	0.927	
267	11	5	45	3	1.5	3.0	1.165	
268	8	3	38	7	7	7.0	2.006	
269	23	17	74	4.3	2	3.0	1.524	
270	4	1	25	7	7	7.0	3.637	*****
271	260	250	96	1.8	0	0.8	0.526	
272	43	38	88	4	1.8	3.0	0.669	
273	34	26	76	3.8	1.7	3.0	0.468	
274	35	25	71	3.8	1.7	3.0	0.557	
275	80	75	94	2.2	2.3	1.5	1.488	
276	24	21	88	2.5	2.1	2.3	0.043	
277	27	25	93	3.4	2.2	3.0	0.017	
278	23	22	96	3.9	2.9	3.0	0.002	
279	15	14	93	4.1	3.2	3.0	0.005	
280	16	8	50	3	0	3.0	0.222	
281	70	70	100	2.3	1.5	2.3	0.052	
282	33	27	82	2.3	1.5	2.3	0.013	
283	39	36	92	2.3	1.5	2.3	0.015	
284	33	30	91	2.8	2.2	2.3	0.018	
285	39	39	100	2.7	2.1	2.3	0.024	[72]
286	27	16	59	3	2.5	2.3	0.082	[g31]
287	13	13	100	3.9	1.6	3.0	0.127	
288	62	62	100	1.8	1.8	1.5	0.008	
289	31	31	100	1.5	3	1.5	0.015	
290	106	99	93	1.5	1.5	1.5	0.289	
291	13	11	85	2.3	1.5	2.3	0.321	
292	18	12	67	3	1.5	3.0	0.333	
293	34	24	71	2.3	1.5	2.3	0.262	
294	11	8	73	3	1.5	3.0	0.153	
295	45	37	82	2.3	1.5	2.3	0.061	
296	7	6	86	3	1.5	3.0	0.178	
297	7.5	7.5	100	3.5	1.8	3.0	0.527	
298	7	6	86	3	1.5	3.0	0.954	
299	3	3	100	3	0	3.0	1.681	
300	11	10	91	2.3	1.5	2.3	1.675	*****
301	12	11	92	7	7	7.0	0.349	
302	6	4	67	7	7	7.0	0.023	
303	8	7	88	7	7	7.0	0.682	
304	5	5	100	7	7	7.0	1.310	*****
305	10	9	90	2.8	2.2	2.3	0.583	
306	19	18	95	2.8	2.2	2.3	0.000	[73]
307	27	22	81	2.3	1.5	2.3	0.603	
308	26	14	54	2.3	1.5	2.3	2.366	*****
309	**56	**7	13	7	7	7.0	2.359	
there are 7 thin beds of siltstone (0.5-3 cm thick)								
310	23	0	0	8.5	8.5	8.5	0.219	
311	17	15	88	5	0	5.0	0.104	
312	27	25	93	5	0	5.0	0.081	
313	6	1	17	7	7	7.0	0.371	
314	6	1	17	7	7	7.0	0.372	

bed#	Bt(cm)	St(cm)	S%	G.Sco	S.Sco	B.G	D.Sq	Sq
315	6	1	17	7	7	7	0.694	
316	36	32	89	5	0	5	0.950	*****
317	16	14	88	3.8	2.6	3	2.021	
318	11	8	73	3	1.5	3	1.855	[74]
319	5	4	80	7	7	7	3.055	
320	49	39	80	3	0	3	1.828	
321	22	19	86	3	1.5	3	1.979	*****
322	180	180	100	0.7	2.3	-2	0.774	
323	45	42	93	2.2	3.1	0.75	1.289	
324	44	43	98	2.7	3.2	2.3	1.011	
325	30	15	50	3	0	3	1.089	
326	48	46	96	1.5	1.5	1.5	1.096	
327	49	38	78	1.1	1.5	-4	0.085	
328	24	23	96	1.1	1.5	-4	0.968	[75]
329	25	14	56	1.5	1.5	1.5	0.910	[g32]
330	15	15	100	1.5	1.5	1.5	0.904	
331	33	33	100	1.9	2.3	1.5	0.904	
332	20	20	100	3	7	3	0.084	
333	12	10	83	3	7	3	0.063	
334	35	35	100	1.3	1.5	0.75	0.078	
335	45	45	100	1.4	1.5	0	0.644	
336	20	20	100	1.5	1.5	1.5	0.833	
337	43	28	65	2	2	1.5	1.386	*****
338	30	20	67	5	1.5	5	1.030	
339	75	25	33	5	1.5	5	0.451	
340	40	10	25	5	1.5	5	0.100	
341	58	28	48	4	2.1	3	0.222	
342	53	45	85	4.4	2.8	3.3	0.422	
343	55	43	78	5.4	4	5	0.795	
344	16	15	94	5.6	3.7	5	0.751	
345	18	18	100	5.6	3.7	5	0.798	
346	10	1	10	7	7	7	0.172	
347	10	1	10	7	7	7	0.167	
348	10	1	10	7	7	7	1.454	
349	30	20	67	5	0	5	2.482	
350	43	10	23	5	0	5	5.543	
351	17	12	71	5	0	5	5.702	*****
352	84	76	90	2.8	2.2	2.3	4.586	
353	126	106	84	1.7	1.7	1.5	2.351	
354	90	90	100	1.5	1.5	1.5	1.098	[76]
355	237	229	97	1.7	1.7	1.5	0.586	[g33]
356	43	35	81	3	1.5	3	1.531	
357	162	145	90	2.8	2.1	2.3	4.301	
358	100	100	100	2.3	1.5	2.3	6.429	
359	56	56	100	2.3	1.5	2.3	7.830	*****
360	**60	**12	20	7	7	7	3.605	
there are 6 thin beds of siltstone (1-5 cm thick)								
361	24	20	83	3	3	1.5	1.775	
362	20	20	100	4.6	3.7	3	0.221	
363	57	30	53	3	0	3	1.310	
364	106	106	100	1.5	1.5	1.5	4.729	
365	87	77	89	2.6	0	1.5	3.049	
366	**150	**20	13	7	7	7	2.054	
there are 10 thin beds of siltstone (1-5 cm thick)								

bed#	Bt(cm)	St(cm)	S%	G.Sco	S.Sco	B.G	D.Sq	Sq
367	3	2	67	7	7	7.0	0.146	*****
368	11	9	82	7	7	7.0	0.149	
369	4	3	75	7	7	7.0	0.005	
370	35	23	66	5	7	5.0	0.067	
371	9	8	89	5	7	5.0	0.340	[77]
372	35	27	77	7	7	7.0	1.109	
373	14	11	79	7	7	7.0	2.217	
374	15	6	40	7	7	7.0	4.140	
375	33	7	21	7	7	7.0	2.739	*****
376	60	56	93	2	2	1.5	1.310	
377	37	28	76	2.3	2.3	1.5	0.129	
378	56	55	98	1.9	2.1	1.5	0.189	
379	15	14	93	2.5	2.6	1.5	0.659	[78]
380	16	11	69	3.5	3.1	2.3	0.630	[g34]
381	37	34	92	3.1	3	2.3	0.467	
382	21	21	100	3.3	3.1	2.3	0.024	
383	8	2	25	7	7	7.0	0.058	
384	25	11	44	3	1.5	3.0	0.083	
385	25	13	52	3	1.5	3.0	0.165	
386	26	20	77	3.4	2.2	3.0	0.095	
387	72	69	96	2.3	1.5	2.3	0.091	
388	10	3	30	3	1.5	3.0	0.060	
389	13	6	46	3	1.5	3.0	0.028	
390	25	13	52	3	1.5	3.0	0.091	
391	17	15	88	3.3	2.6	2.3	0.274	
392	13	7	54	5	0	5.0	0.285	
393	9	6	67	4.2	3.2	3.0	0.427	
394	35	20	57	3	1.5	3.0	0.750	
395	52	52	100	3.2	0.5	3.0	0.719	
396	64	55	86	4	2	3.0	1.081	
397	51	50	98	3	0	3.0	0.217	
398	6	2	33	7	7	7.0	0.064	
399	5	1	20	7	7	7.0	0.655	
400	6	1	17	7	7	7.0	1.240	
401	17	17	100	3.4	3.4	3.0	1.236	
402	69	61	88	3.1	0.5	3.0	0.840	
403	23	8	35	3	0	3.0	1.000	
404	30	20	67	5	0	5.0	0.621	
405	30	10	33	3	1.5	3.0	0.113	
406	152	138	91	3.9	3.9	1.5	0.176	
407	54	45	83	3.1	2.5	2.3	0.362	
408	39	29	74	3.7	3.2	2.3	0.762	
409	60	56	93	2.8	2.1	2.3	0.614	
410	19	11	58	2.3	1.5	2.3	0.228	
411	10	6	60	7	8.5	7.0	0.450	[78]
412	20	15	75	4.3	2.8	3.0	0.614	[g34]
413	15	10	67	3	6.7	3.0	0.529	
414	41	31	76	2.8	2.8	1.5	0.269	
415	39	39	100	3.2	3.2	1.5	0.054	
416	88	86	98	3.2	3.2	1.5	0.102	
417	45	45	100	4.1	3.7	2.3	0.356	
418	23	23	100	4.2	4.2	3.0	0.335	
419	23	23	100	3.2	2.6	2.3	0.358	
420	25	22	88	2.3	1.5	2.3	0.005	
421	130	128	98	2.2	2.2	1.5	0.286	
422	100	100	100	1.5	1.5	1.5	1.557	
423	114	112	98	1.5	1.5	1.5	1.396	
424	20	10	50	3	0	3.0	1.374	
425	20	10	50	3	0	3.0	0.103	
426	20	12	60	2.9	3.1	1.5	0.097	
427	15	7	47	1.5	1.5	1.5	0.358	

bed#	Bt(cm)	St(cm)	S%	G.Sco	S.Sco	B.G	D.Sq	Sq
428	10	9	90	1.5	1.5	1.5	0.294	
429	14	14	100	1.5	1.5	1.5	0.566	
430	18	7	39	1.5	1.5	1.5	0.054	
431	150	150	100	2.2	2.2	1.5	0.052	
432	24	24	100	2.1	2.1	1.5	0.197	
433	8	8	100	2.8	2.1	2.3	0.278	
434	54	10	19	2.5	1.8	2.3	0.129	
435	64	58	91	1.6	1.6	1.5	0.587	
436	35	35	100	1.5	1.5	1.5	0.025	
437	148	125	84	2.3	1.5	2.3	0.025	
438	110	90	82	2.3	1.5	2.3	0.031	
439	33	33	100	2.3	1.5	2.3	0.015	
440	68	58	85	2.3	1.5	2.3	0.055	
441	30	30	100	2.3	1.5	2.3	0.385	
442	50	50	100	4	3.5	2.3	0.050	
443	125	122	98	2.5	1.8	2.3	0.002	
444	37	37	100	3.7	3.7	1.5	0.029	
445	83	74	89	2.1	2.1	1.5	0.095	
446	89	89	100	1.5	1.5	1.5	1.019	
447	93	92	99	1.5	1.5	1.5	0.575	
448	29	27	93	3.8	2.6	3	0.201	[78]
449	33	26	79	4.2	3.2	3	0.487	[g34]
450	88	80	91	3.8	2.9	3	1.571	
451	98	93	95	2.4	2.4	1.5	0.506	
452	4	3	75	7	7	7	1.112	
453	34	30	88	4.3	3.3	3	3.727	
454	116	116	100	1.5	1.5	1.5	0.853	
455	**25	**5	20	7	7	7	0.133	
there are 5 thin beds of siltstone (0.5-3 cm thick)								
456	102	100	98	1.5	1.5	1.5		
457	**20	**8	40	7	7	7		
there are 4 thin beds of siltstone (1-5 cm thick)								*****

Cap Ste-Anne Section 1, Gaspe, Quebec

Split-Moving Window Segmentation

bed#	Bt(cm)	St(cm)	S%	T.G	B.G	Posi.	D.Sq	Sq
234	89	57	64	7	7			*****
233	147	54	37	7	1.5			
232	24	24	100	7	1.5			
231	55	45	82	3	1.5	Posi.	D.Sq	
230	42	42	100	3	1.5	5.5	0.004	
229	90	90	100	3	1.5	6.5	0.241	
228	85	35	41	7	3	7.5	0.421	
227	76	76	100	7	3	8.5	0.492	
226	13	13	100	7	3	9.5	0.293	
225	24	24	100	7	3	10.5	0.193	
224	36	36	100	7	1.5	11.5	0.215	
223	30	30	100	7	7	12.5	0.077	
222	41	27	66	7	3	13.5	0.037	
221	20	20	100	7	3	14.5	0.092	
220	21	17	81	7	3	15.5	0.289	
219	21	15	71	7	3	16.5	1.227	[79]
218	53	31	58	7	3	17.5	1.240	
217	56	30	54	7	3	18.5	1.800	
216	80	68	85	3	1.5	19.5	1.770	
215	37	37	100	3	0	20.5	1.532	
214	200	180	90	7	0	21.5	0.100	
213	112	92	82	7	1.5	22.5	0.028	
212	100	100	100	3	1.5	23.5	0.015	
211	135	135	100	3	1.5	24.5	0.100	
210	70	70	100	3	1.5	25.5	0.305	
209	54	54	100	7	1.5	26.5	0.201	
208	127	90	71	7	1.5	27.5	0.196	
207	110	110	100	4	0	28.5	0.182	
206	115	115	100	4	0	29.5	0.262	
205	40	40	100	4	0	30.5	0.281	
204	120	120	100	4	0	31.5	1.742	
203	58	58	100	7	1.5	32.5	2.673	
202	37	37	100	7	0	33.5	3.893	
201	14	14	100	3	3	34.5	3.688	
200	20	20	100	3	1.5	35.5	4.756	****
199	25	10	40	7	7	36.5	1.485	
198	25	13	52	7	7	37.5	0.695	
197	22	22	100	7	7	38.5	0.118	
196	23	23	100	7	7	39.5	0.007	
195	35	35	100	7	7	40.5	0.167	
194	80	75	94	7	1.5	41.5	0.377	
193	6	4	67	7	7	42.5	0.361	
192	0.7	0.2	29	7	7	43.5	0.307	
191	3.3	2.5	76	7	7	44.5	0.267	
190	6.5	5	77	7	7	45.5	0.224	
189	3	3	100	7	7	46.5	0.001	
188	3	1	33	7	7	47.5	0.001	
187	2.2	0.2	9	7	7	48.5	0.000	
186	6	1	17	7	7	49.5	0.000	
185	1.2	0.5	42	7	7	50.5	0.001	

Split-Moving Window Segmentation

bed#	Bt(cm)	St(cm)	S%	T.G	B.G	Posi.	D.Sq	Sq
184	3	1.5	50	7	7	51.5	0.005	
183	9.3	0.8	9	7	7	52.5	0.010	
182	1.3	0.5	38	7	7	53.5	0.014	
181	3.3	2.5	76	7	7	54.5	0.013	
180	11	10	91	7	7	55.5	0.006	
179	26	15	58	7	7	56.5	0.000	
178	12.5	10	80	7	7	57.5	0.001	
177	13.6	6	44	7	7	58.5	0.004	
176	3.5	3	86	7	7	59.5	0.003	
175	13	6	46	7	7	60.5	0.003	
174	12	10	83	7	7	61.5	0.001	
173	2.5	1.5	60	7	7	62.5	0.000	
172	2	1	50	7	7	63.5	0.000	
171	11	7	64	7	7	64.5	0.000	
170	3	1.5	50	7	7	65.5	0.012	
169	22.5	12	53	7	7	66.5	0.005	
168	2.5	1	40	7	7	67.5	0.005	
167	11	1	9	7	7	68.5	0.006	
166	173	15	9	7	7	69.5	0.000	
165	103	28	27	7	7	70.5	0.016	
164	13.5	1.5	11	7	7	71.5	0.007	
163	12.5	1.5	12	7	7	72.5	0.007	
162	2	1.5	75	7	7	73.5	0.008	
161	14	4	29	7	7	74.5	0.004	
160	16	6	38	7	7	75.5	0.000	
159	9	5	56	7	7	76.5	0.000	
158	30	2	7	7	7	77.5	0.000	
157	11.5	1.5	13	7	7	78.5	0.001	
156	6.5	1.5	23	7	7	79.5	0.002	
155	14	4	29	7	7	80.5	0.003	
154	6	2	33	7	7	81.5	0.022	
153	18	5	28	7	7	82.5	0.018	
152	22	15	68	7	7	83.5	0.187	
151	21	5	24	7	7	84.5	0.529	
150	13	5	38	7	7	85.5	1.286	
149	36	30	83	7	7	86.5	2.678	
148	4	4	100	7	7	87.5	3.736	*****
147	37	34	92	3	1.5	88.5	1.985	
146	24	24	100	7	3	89.5	0.716	
145	58	25	43	7	1.5	90.5	0.017	[80]
144	49	49	100	7	0	91.5	1.067	
143	45	14	31	7	3	92.5	2.636	
142	36	20	56	7	3	93.5	3.270	*****
141	118	70	59	7	7	94.5	2.484	
140	28	7	25	7	7	95.5	1.374	
139	12	5	42	7	7	96.5	0.413	
138	12	11	92	7	7	97.5	0.135	
137	6	1	17	7	7	98.5	0.422	
136	4.7	4	85	7	7	99.5	5.483	
135	10	9	90	7	7	100.5	8.900	

bed#	Bt(cm)	St(cm)	S%	T.G	B.G	Posi.	D.Sq	Sq
134	16	6	38	7	7	101.5	11.19	*****
133	24	20	83	7	7	102.5	10.80	
132	193	186	96	7	0	103.5	3.23	[81]
131	505	505	100	7	0	104.5	2.18	
130	160	160	100	3	0	105.5	7.10	
129	62	62	100	7	1.5	106.5	11.44	*****
128	5	5	100	7	7	107.5	9.982	
127	10	5	50	7	7	108.5	5.813	
126	18	5	28	7	7	109.5	0.288	
125	14.4	0.4	3	7	7	110.5	0.044	
124	5.5	0.5	9	7	7	111.5	1.196	
123	28	14	50	7	3	112.5	0.337	
122	30	12	40	7	7	113.5	0.352	
121	85	70	82	7	3	114.5	0.037	
120	23	15	65	7	7	115.5	0.034	
119	79	56	71	7	1.5	116.5	1.083	
118	10	10	100	7	7	117.5	0.560	
117	123	25	20	7	7	118.5	0.201	
116	112	10	9	7	7	119.5	0.090	
115	15	10	67	7	7	120.5	0.123	
114	15	10	67	7	7	121.5	0.631	
113	110	20	18	7	7	122.5	0.655	
112	124	62	50	3	3	123.5	0.028	
111	34	34	100	3	1.5	124.5	0.113	
110	53	48	91	7	7	125.5	1.025	
109	89	26	29	7	7	126.5	1.459	
108	40	40	100	7	7	127.5	1.958	
107	62	6	10	7	7	128.5	4.412	*****
106	102	70	69	7	1.5	129.5	4.076	
105	360	360	100	3	0	130.5	2.059	
104	57	57	100	3	1.5	131.5	1.459	
103	31	31	100	3	1.5	132.5	1.791	
102	31	31	100	3	1.5	133.5	3.719	
101	81	56	69	7	1.5	134.5	5.319	
100	23	23	100	1.5	1.5	135.5	4.434	
99	40	3	8	7	7	136.5	2.796	
98	6	1	17	7	7	137.5	0.668	
97	7	1	14	7	7	138.5	0.035	
96	1.5	1	67	7	7	139.5	0.357	[82]
95	1.5	1	67	7	7	140.5	1.805	
94	4	3	75	7	7	141.5	3.347	
93	95	72	76	3	1.5	142.5	1.736	
92	69	69	100	3	1.5	143.5	0.693	
91	30	30	100	7	7	144.5	1.800	
90	60	23	38	3	1.5	145.5	0.873	
89	158	95	60	3	1.5	146.5	0.120	
88	30	30	100	1.5	1.5	147.5	0.138	
87	51	31	61	3	1.5	148.5	0.529	
86	97	64	66	3	0	149.5	3.238	
85	30	30	100	3	1.5	150.5	4.923	*****
84	60	25	42	7	7	151.5	3.207	
83	72	22	31	7	7	152.5	2.003	
82	13.5	2	15	7	7	153.5	1.015	
81	5.7	0.7	12	7	7	154.5	0.211	
80	5	1	20	7	7	155.5	0.013	
79	8	2	25	7	7	156.5	0.002	
78	4	2	50	7	7	157.5	0.000	
77	9.5	1.5	16	7	7	158.5	0.000	
76	7.5	1.5	20	7	7	159.5	0.000	
75	23	6	26	7	7	160.5	0.000	

bed#	Bt(cm)	St(cm)	S%	T.G	B.G	Posi.	D.Sq	Sq
74	12.5	0.5	4	7	7	161.5	0.000	
73	19	3	16	7	7	162.5	0.000	
72	18	3	17	7	7	163.5	0.001	
71	15.7	0.7	4	7	7	164.5	0.001	
70	10.5	0.5	5	7	7	165.5	0.000	
69	26.5	1.5	6	7	7	166.5	0.000	
68	2.5	0.5	20	7	7	167.5	0.000	
67	8.5	1.5	18	7	7	168.5	0.000	
66	13	1	8	7	7	169.5	0.000	
65	5.5	0.5	9	7	7	170.5	0.000	
64	39.3	0.3	1	7	7	171.5	0.000	
63	4	1	25	7	7	172.5	0.001	
62	4.5	1.5	33	7	7	173.5	0.001	
61	27.5	4	15	7	7	174.5	0.000	
60	13.5	1.5	11	7	7	175.5	0.000	
59	5.5	3	55	7	7	176.5	0.000	
58	18.5	2.5	14	7	7	177.5	0.000	
57	5	2	40	7	7	178.5	0.000	
56	16	1	6	7	7	179.5	0.000	
55	23.5	1.5	6	7	7	180.5	0.008	
54	17	3	18	7	7	181.5	0.007	
53	4	3	75	7	7	182.5	0.006	
52	5	2	40	7	7	183.5	0.099	
51	2.7	2	74	7	7	184.5	0.373	
50	47	30	64	7	7	185.5	0.347	
49	12.8	0.8	6	7	7	186.5	0.347	
48	12	2	17	7	7	187.5	0.349	
47	17	13	76	3	3	188.5	0.109	
46	19	19	100	7	3	189.5	0.290	
45	11.5	0.5	4	7	7	190.5	0.470	
44	17	6	35	7	7	191.5	0.486	
43	15	12	80	7	7	192.5	0.520	
42	63	60	95	7	3	193.5	0.258	
41	165	165	100	7	3	194.5	0.516	
40	36	20	56	7	7	195.5	0.612	
39	35	15	43	7	7	196.5	0.648	
38	35	30	86	7	7	197.5	0.071	
37	19	5	26	7	7	198.5	0.473	
36	57	37	65	7	7	199.5	1.210	
35	19	5	26	7	7	200.5	1.279	
34	27	13	48	7	7	201.5	1.242	
33	337	315	93	3	0	202.5	1.116	
32	16	16	100	7	3	203.5	1.872	
31	11	5	45	7	7	204.5	1.684	
30	15	5	33	7	7	205.5	1.677	
29	13	3	23	7	7	206.5	1.612	
28	7	3	43	7	7	207.5	0.088	
27	11	4	36	7	7	208.5	0.169	
26	3.5	2.5	71	7	7	209.5	0.956	
25	9	6	67	7	7	210.5	2.594	
24	6	4	67	7	7	211.5	8.091	

bed#	Bt(cm)	St(cm)	S%	T.G	B.G	Posi.	D.Sq	Sq
23	7.6	6.5	86	7	7	212.5	14.64	*****
22	55	25	45	3	1.5	213.5	15.80	
21	85	85	100	7	0	214.5	16.93	
20	140	140	100	3	0	215.5	10.34	[83]
19	450	450	100	3	0	216.5	0.568	
18	344	294	85	7	0	217.5	1.105	
17	180	180	100	3	0	218.5	3.811	
16	313	313	100	3	0	219.5	12.337	*****
15	35	35	100	3	1.5	220.5	10.138	
14	87	67	77	3	0	221.5	4.897	
13	70	50	71	3	0	222.5	2.726	
12	59	40	68	7	1.5	223.5	1.504	
11	48	28	58	7	3	224.5	0.196	
10	49	40	82	7	3	225.5	0.120	[84]
9	48	30	63	7	3	226.5	0.096	
8	54	44	81	3	3	227.5	0.248	
7	67	47	70	3	1.5	228.5	0.190	
6	75	65	87	3	1.5			
5	78	73	94	7	3			
4	65	55	85	7	3			
3	90	90	100	7	1.5			
2	54	46	85	7	3			
1	143	97	68	7	3			*****

Cap Ste-Anne Section 2, Gaspé, Quebec

Split-Moving Window Segmentation

bed#	Bt(cm)	St(cm)	S%	T.G	B.G	Posi.	D.Sq	Sq
289	55	55	100	3	1.5			*****
288	98	98	100	3	0			
287	378	378	100	3	1.5			
286	240	240	100	7	1.5			
285	40	40	100	3	1.5	5.5	6.101	
284	57	21	37	3	1.5	6.5	5.249	
283	49	49	100	7	3	7.5	5.584	
282	14	14	100	7	7	8.5	1.795	[85]
281	14	14	100	7	3	9.5	2.139	
280	10	10	100	7	7	10.5	0.145	
279	158	85	54	7	1.5	11.5	0.411	
278	7	5	71	7	7	12.5	1.786	
277	16	12	75	7	7	13.5	1.812	
276	12	6	50	7	7	14.5	4.953	
275	106	104	98	7	1.5	15.5	0.917	
274	333	290	87	7	0	16.5	0.372	
273	166	92	55	7	1.5	17.5	2.450	
272	38	15	39	7	7	18.5	2.495	
271	39	34	87	7	1.5	19.5	7.174	*****
270	8	8	100	7	7	20.5	4.137	
269	114	40	35	7	7	21.5	1.424	
268	132	102	77	7	7	22.5	0.383	
267	7	7	100	7	7	23.5	0.372	
266	121	53	44	7	7	24.5	0.091	
265	20	11	55	7	7	25.5	0.082	
264	45	45	100	7	7	26.5	0.121	

Split-Moving Window Segmentation

bed#	Bt(cm)	St(cm)	S%	T.G	B.G	Posi.	D.Sq	Sq
263	38	18	47	7	7	27.5	0.023	
262	45	13	29	7	7	28.5	0.031	
261	6	6	100	7	7	29.5	0.004	
260	20	20	100	7	7	30.5	0.019	
259	26	26	100	7	7	31.5	0.019	
258	10	10	100	7	7	32.5	0.019	
257	10	10	100	7	7	33.5	0.015	
256	14	2	14	7	7	34.5	0.005	
255	5	1	20	7	7	35.5	0.004	
254	6	6	100	7	7	36.5	0.020	
253	6	2	33	7	7	37.5	0.046	
252	71	13	18	7	7	38.5	0.047	
251	40	19	48	7	7	39.5	0.025	
250	75	35	47	7	7	40.5	0.026	
249	32	15	47	7	7	41.5	0.030	
248	118	22	19	7	7	42.5	0.017	
247	42	17	40	7	7	43.5	0.013	
246	13	13	100	7	7	44.5	0.010	
245	103	70	68	7	7	45.5	0.020	
244	52	29	56	7	7	46.5	0.041	
243	32	26	81	7	7	47.5	0.071	
242	44	15	34	7	7	48.5	0.068	
241	35.5	1.5	4	7	7	49.5	0.044	
240	15	10	67	7	7	50.5	0.004	
239	30	20	67	7	7	51.5	0.007	
238	25	5	20	7	7	52.5	0.000	

bed#	Bt(cm)	St(cm)	S%	T.G	B.G	Posi.	D.Sq	Sq	bed#	Bt(cm)	St(cm)	S%	T.G	B.G	Posi.	D.Sq	Sq
237	23	15	65	7	7	53.5	0.000		177	13	3	23	7	7	113.5	0.013	
236	19	10	53	7	7	54.5	0.002		176	7	3	43	7	7	114.5	0.001	
235	10	8	80	7	7	55.5	0.003		175	8.5	2	24	7	7	115.5	0.002	
234	3	2	67	7	7	56.5	0.000		174	9	3	33	7	7	116.5	0.032	
233	9.5	8	84	7	7	57.5	0.000		173	22	13	59	7	7	117.5	0.026	
232	16	15	94	7	7	58.5	0.001		172	15	8	53	7	7	118.5	0.020	
231	13	10	77	7	7	59.5	0.001		171	25	21	84	7	7	119.5	0.004	
230	7	3	43	7	7	60.5	0.001		170	21	21	100	7	7	120.5	0.000	
229	9	4	44	7	7	61.5	0.001		169	39	28	72	7	7	121.5	0.004	
228	10.7	10	93	7	7	62.5	0.002		168	22	8	36	7	7	122.5	0.001	
227	3.5	3	86	7	7	63.5	0.000		167	22	6	27	7	7	123.5	0.005	
226	12	8	67	7	7	64.5	0.001		166	14	10	71	7	7	124.5	0.019	
225	5	2	40	7	7	65.5	0.001		165	32	16	50	7	7	125.5	0.026	
224	8	5	63	7	7	66.5	0.003		164	32	26	81	7	7	126.5	0.093	
223	17	5	29	7	7	67.5	0.017		163	54	42	78	7	7	127.5	0.028	
222	5.5	1.5	27	7	7	68.5	0.020		162	46	18	39	7	7	128.5	0.043	
221	17.5	2.5	14	7	7	69.5	0.033		161	25	25	100	7	7	129.5	0.018	
220	5	3	60	7	7	70.5	0.031		160	44	19	43	7	7	130.5	0.008	
219	40	36	90	7	7	71.5	0.000		159	80	80	100	7	7	131.5	0.048	
218	54	30	56	7	7	72.5	0.006		158	97	23	24	7	7	132.5	0.039	
217	81	5	6	7	7	73.5	0.005		157	125	45	36	7	7	133.5	0.127	
216	12	12	100	7	7	74.5	0.012		156	179	12	7	7	7	134.5	0.107	
215	2	2	100	7	7	75.5	0.007		155	107	5	5	7	7	135.5	0.038	
214	5	4	80	7	7	76.5	0.000		154	59	14	24	7	7	136.5	0.001	
213	35	20	57	7	7	77.5	0.000		153	45	12	27	7	7	137.5	0.000	
212	15	12	80	7	7	78.5	0.000		152	24	11	46	7	7	138.5	0.004	
211	13	5	38	7	7	79.5	0.000		151	38	10	26	7	7	139.5	0.004	
210	18	12	67	7	7	80.5	0.002		150	55	42	76	7	7	140.5	0.012	
209	13	8	62	7	7	81.5	0.004		149	66	10	15	7	7	141.5	0.010	
208	15	13	87	7	7	82.5	0.005		148	25	7	28	7	7	142.5	0.010	
207	8	5	63	7	7	83.5	0.001		147	315	8	3	7	7	143.5	0.011	
206	9	4	44	7	7	84.5	0.001		146	10	8	80	7	7	144.5	0.013	
205	11	7	64	7	7	85.5	0.000		145	31	13	42	7	7	145.5	0.005	
204	8	3	38	7	7	86.5	0.000		144	30	10	33	7	7	146.5	0.008	
203	13	3	23	7	7	87.5	0.008		143	6	2	33	7	7	147.5	0.006	
202	19	15	79	7	7	88.5	0.001		142	6	3	50	7	7	148.5	0.004	
201	4.5	3	67	7	7	89.5	0.001		141	2.4	2	83	7	7	149.5	0.003	
200	8	5	63	7	7	90.5	0.001		140	5.5	1.5	27	7	7	150.5	0.000	
199	14	8	57	7	7	91.5	0.000		139	6	2	33	7	7	151.5	0.001	
198	29	25	86	7	7	92.5	0.009		138	5	3	60	7	7	152.5	0.001	
197	2.5	0.5	20	7	7	93.5	0.003		137	13.5	1.5	11	7	7	153.5	0.002	
196	5	5	100	7	7	94.5	0.005		136	12.5	2.5	20	7	7	154.5	0.004	
195	3	2	67	7	7	95.5	0.001		135	14	4	29	7	7	155.5	0.004	
194	3.5	0.5	14	7	7	96.5	0.000		134	17	9	53	7	7	156.5	0.006	
193	22	12	55	7	7	97.5	0.000		133	8	7	88	7	7	157.5	0.011	
192	4	1	25	7	7	98.5	0.001		132	15	4	27	7	7	158.5	0.010	
191	4	1	25	7	7	99.5	0.005		131	14	12	86	7	7	159.5	0.003	
190	16	12	75	7	7	100.5	0.002		130	17	4	24	7	7	160.5	0.003	
189	2	1	50	7	7	101.5	0.005		129	32	24	75	7	7	161.5	0.001	
188	8	4	50	7	7	102.5	0.018		128	21	21	100	7	7	162.5	0.010	
187	18	15	83	7	7	103.5	0.012		127	15	5	33	7	7	163.5	0.011	
186	20	13	65	7	7	104.5	0.007		126	16	3	19	7	7	164.5	0.006	
185	59	11	19	7	7	105.5	0.008		125	5	3	60	7	7	165.5	0.002	
184	40	12	30	7	7	106.5	0.012		124	11	10	91	7	7	166.5	0.000	
183	71	20	28	7	7	107.5	0.002		123	17	5	29	7	7	167.5	0.002	
182	52	19	37	7	7	108.5	0.000		122	9	5	56	7	7	168.5	0.001	
181	26	15	58	7	7	109.5	0.002		121	9	5	56	7	7	169.5	0.001	
180	30	13	43	7	7	110.5	0.006		120	32	12	38	7	7	170.5	0.001	
179	64	31	48	7	7	111.5	0.038		119	12	10	83	7	7	171.5	0.002	
178	15	11	73	7	7	112.5	0.028		118	15	10	67	7	7	172.5	0.005	

bed#	Bt(cm)	St(cm)	S%	T.G	B.G	Posi.	D.Sq	Sq
117	3.5	1.5	43	7	7	173.5	0.004	
116	17	4	24	7	7	174.5	0.004	
115	33.5	2.5	7	7	7	175.5	0.001	
114	5.5	1.5	27	7	7	176.5	0.000	
113	28	4	14	7	7	177.5	0.000	
112	4	3	75	7	7	178.5	0.001	
111	7	2	29	7	7	179.5	0.003	
110	49	4	8	7	7	180.5	0.004	
109	22	10	45	7	7	181.5	0.001	
108	6	3	50	7	7	182.5	0.001	
107	14	10	71	7	7	183.5	0.000	
106	18	8	44	7	7	184.5	0.000	
105	7	7	100	7	7	185.5	0.001	
104	18.5	6	32	7	7	186.5	0.001	
103	7	6	86	7	7	187.5	0.002	
102	5	2	40	7	7	188.5	0.584	
101	13	10	77	7	7	189.5	2.560	
100	5	3	60	7	7	190.5	5.664	
99	12	2	17	7	7	191.5	12.11	
98	13	3	23	7	7	192.5	18.52	*****
97	103	49	48	1.5	0	193.5	13.41	
96	183	173	95	1.5	0	194.5	7.18	
95	73	73	100	1.5	0	195.5	3.85	
94	217	210	97	1.5	-2	196.5	0.56	
93	125	125	100	1.5	0	197.5	5.01	
92	142	142	100	1.5	0	198.5	11.49	[86]
91	65	65	100	1.5	0	199.5	14.06	
90	126	115	91	1.5	0	200.5	12.70	
89	262	262	100	1.5	0	201.5	9.48	
88	910	910	100	1.5	0	202.5	9.00	
87	683	683	100	1.5	0	203.5	34.09	
86	141	92	65	7	1.5	204.5	36.92	*****
85	20	20	100	7	7	205.5	26.69	
84	9	5	56	7	7	206.5	18.49	
83	35	15	43	7	7	207.5	2.740	
82	25	7	28	7	7	208.5	0.367	[87]
81	10	10	100	3	3	209.5	0.209	
80	35	35	100	7	0	210.5	1.472	
79	22	14	64	7	7	211.5	1.485	
78	170	110	65	7	7	212.5	1.489	
77	23	13	57	7	7	213.5	1.509	*****
76	23.7	10	42	7	7	214.5	0.678	
75	15	15	100	7	7	215.5	0.075	
74	33	33	100	7	7	216.5	0.140	
73	5	2	40	7	7	217.5	0.005	
72	5	5	100	7	7	218.5	0.004	
71	10	2	20	7	7	219.5	0.000	
70	33	14	42	7	7	220.5	0.012	
69	14	13	93	7	7	221.5	0.033	
68	12	11	92	7	7	222.5	0.026	
67	16.5	2	12	7	7	223.5	0.039	
66	25	23	92	7	7	224.5	0.009	
65	49	49	100	7	7	225.5	0.013	
64	21	21	100	7	7	226.5	0.022	
63	19	13	68	7	7	227.5	0.031	
62	17	13	76	7	7	228.5	0.053	
61	4	3	75	7	7	229.5	0.031	
60	5.5	4	73	7	7	230.5	0.004	
59	35	15	43	7	7	231.5	0.006	
58	5.3	5	94	7	7	232.5	0.001	

bed#	Bt(cm)	St(cm)	S%	T.G	B.G	Posi.	D.Sq	Sq
57	4	3	75	7	7	233.5	0.001	
56	5.5	4	73	7	7	234.5	0.001	
55	6.5	4	62	7	7	235.5	0.001	
54	3.6	3	83	7	7	236.5	0.004	
53	13	11	85	7	7	237.5	0.001	
52	21.5	20	93	7	7	238.5	0.004	
51	4.5	3	67	7	7	239.5	0.003	
50	5.5	5	91	7	7	240.5	0.004	
49	5	4	80	7	7	241.5	0.005	
48	4	2	50	7	7	242.5	0.001	
47	8	5	63	7	7	243.5	0.000	
46	5.5	2.5	45	7	7	244.5	0.000	
45	3.7	3	81	7	7	245.5	0.001	
44	3.5	2.5	71	7	7	246.5	0.002	
43	6.5	6	92	7	7	247.5	0.001	
42	7	3	43	7	7	248.5	0.003	
41	4	2	50	7	7	249.5	0.003	
40	25	15	60	7	7	250.5	0.000	
39	7	6	86	7	7	251.5	0.001	
38	6	4	67	7	7	252.5	0.001	
37	18	12	67	7	7	253.5	0.007	
36	3.5	1.5	43	7	7	254.5	0.003	
35	2	1	50	7	7	255.5	0.000	
34	2.6	0.6	23	7	7	256.5	0.001	
33	6	2	33	7	7	257.5	0.003	
32	2.5	2	80	7	7	258.5	0.006	
31	14	10	71	7	7	259.5	0.001	
30	13	12	92	7	7	260.5	0.001	
29	6	3	50	7	7	261.5	0.001	
28	11	10	91	7	7	262.5	0.004	
27	2.5	1.5	60	7	7	263.5	0.004	
26	1	0.5	50	7	7	264.5	0.001	
25	2.5	1.5	60	7	7	265.5	0.002	
24	3.5	2	57	7	7	266.5	0.005	
23	6.5	6	92	7	7	267.5	0.005	
22	2	1.5	75	7	7	268.5	0.005	
21	17.5	2.5	14	7	7	269.5	0.005	
20	30	20	67	7	7	270.5	0.001	
19	23	13	57	7	7	271.5	0.008	
18	48	3	6	7	7	272.5	0.005	
17	11	1	9	7	7	273.5	0.004	
16	19	3	16	7	7	274.5	0.004	
15	3	1	33	7	7	275.5	0.000	
14	2	1	50	7	7	276.5	0.000	
13	22	6	27	7	7	277.5	0.000	
12	22	5	23	7	7	278.5	0.188	
11	2.5	2	80	7	7	279.5	0.188	
10	2.5	0.5	20	7	7	280.5	0.188	
9	6	1	17	7	7	281.5	0.188	
8	2	1	50	7	7	282.5	0.191	
7	14	5	36	7	3	283.5	0.192	
6	5	0.5	10	7	7			
5	5	3	60	7	7			
4	7	6	86	7	7			
3	19	17	89	7	7			
2	22.5	7.5	33	7	7			
1	106	70	66	7	7			

Petite Vallee Section, Gaspe, Quebec

bed#	Bt(cm)	St(cm)	S%	T.G	B.G	Split-Moving Window Segmentation Posi.	D.Sq	Sq
2893	12.5	1.5	12	7	7			
2892	5	2	40	7	7			
2891	5	1	20	7	7			
2890	7	4.5	64	7	7	Posi.	D.Sq	
2889	1.7	0.5	29	7	7	2888.5	2.770	
2888	6	3	50	7	7	2887.5	3.254	
2887	5	3	60	7	7	2886.5	4.522	
2886	25.5	23	90	7	7	2885.5	5.318	*****
2885	58	50	86	7	1.5	2884.5	2.510	
2884	74	30	41	3	3	2883.5	0.475	
2883	18	15	83	7	7	2882.5	0.491	[88]
2882	19	17	89	3	3	2881.5	0.319	
2881	75	30	40	7	0	2880.5	2.414	
2880	45	45	100	7	0	2879.5	5.938	*****
2879	35	5	14	7	7	2878.5	3.911	
2878	17	15	88	7	7	2877.5	3.154	
2877	4.5	2	44	7	7	2876.5	1.648	
2876	3	0.5	17	7	7	2875.5	0.301	
2875	4.3	2.3	53	7	7	2874.5	0.123	
2874	4	2	50	7	7	2873.5	0.195	
2873	93.5	13	14	7	3	2872.5	0.280	
2872	39	12	31	7	7	2871.5	0.132	
2871	9.5	5	53	7	7	2870.5	0.104	
2870	6	2	33	7	7	2869.5	0.225	
2869	16	10	63	7	7	2868.5	0.071	
2868	20.5	19	93	7	7	2867.5	0.421	
2867	8	5	63	7	7	2866.5	0.421	
2866	22	20	91	7	3	2865.5	0.173	
2865	12	12	100	7	7	2864.5	0.457	
2864	4	4	100	7	7	2863.5	0.419	
2863	4	4	100	3	3	2862.5	0.260	
2862	4	4	100	7	7	2861.5	0.260	
2861	4	4	100	7	7	2860.5	0.030	
2860	10	10	100	3	3	2859.5	0.480	
2859	1.2	0.2	17	7	7	2858.5	0.113	
2858	1.2	0.2	17	7	7	2857.5	1.263	
2857	3	3	100	7	7	2856.5	4.208	
2856	3	3	100	7	7	2855.5	4.584	
2855	3	3	100	7	7	2854.5	5.982	
2854	37	35	95	3	0	2853.5	0.958	
2853	27	27	100	7	0	2852.5	0.590	
2852	57	52	91	7	0	2851.5	3.035	
2851	15	10	67	7	7	2850.5	2.924	
2850	8	4	50	7	7	2849.5	2.918	
2849	7	5	71	7	7	2848.5	1.325	
2848	40	35	88	7	7	2847.5	0.460	
2847	50	40	80	7	7	2846.5	0.555	
2846	50	30	60	7	7	2845.5	2.184	
2845	10	6	60	7	7	2844.5	2.413	
2844	3.3	0.8	24	7	7	2843.5	2.213	
2843	9	4	44	7	7	2842.5	1.292	
2842	6	3	50	7	7	2841.5	0.601	

bed#	Bt(cm)	St(cm)	S%	T.G	B.G	Split-Moving Window Segmentation Posi.	D.Sq	Sq
2841	8	3	38	7	3	2840.5	0.002	
2840	10	10	100	7	3	2839.5	0.105	
2839	2.5	1.5	60	7	7	2838.5	0.108	
2838	0.8	0.3	38	7	7	2837.5	0.105	
2837	0.4	0.2	50	7	7	2836.5	0.106	
2836	3	2	67	7	7	2835.5	0.001	
2835	17.3	15	87	3	3	2834.5	0.019	
2834	1.2	0.2	17	7	7	2833.5	0.007	
2833	5.6	0.1	2	7	7	2832.5	0.004	
2832	1	0.2	20	7	7	2831.5	0.004	
2831	1.3	0.3	23	7	7	2830.5	0.002	
2830	10.2	9	88	3	3	2829.5	0.108	
2829	4.5	2.5	56	7	7	2828.5	0.059	
2828	4.5	1	22	7	7	2827.5	0.075	
2827	7.3	0.3	4	7	7	2826.5	0.117	
2826	0.9	0.2	22	7	7	2825.5	0.119	
2825	4.5	2	44	7	7	2824.5	0.932	
2824	25.5	25	98	7	3	2823.5	0.467	
2823	6	4	67	7	7	2822.5	1.354	
2822	10	5	50	7	7	2821.5	2.776	
2821	1.8	0.3	17	7	7	2820.5	5.279	*****
2820	34	20	59	3	3	2819.5	4.491	
2819	25	25	100	3	0	2818.5	2.972	
2818	20	20	100	1.5	1.5	2817.5	2.073	
2817	7	7	100	0	0	2816.5	1.094	
2816	20	20	100	3	0	2815.5	0.050	
2815	15	15	100	3	0	2814.5	0.672	
2814	15	12	80	1.5	1.5	2813.5	1.315	
2813	51	45	88	7	0	2812.5	4.034	
2812	37	25	68	7	0	2811.5	5.266	
2811	12	10	83	7	3	2810.5	2.994	
2810	9	4	44	7	7	2809.5	0.046	
2809	13	2	15	7	7	2808.5	0.296	[89]
2808	4	0.8	20	7	7	2807.5	2.918	
2807	7	6	86	7	0	2806.5	6.182	
2806	20	20	100	3	0	2805.5	4.756	
2805	85	72	85	7	0	2804.5	0.123	
2804	22	20	91	7	7	2803.5	0.840	
2803	10	10	100	7	3	2802.5	0.781	
2802	50	50	100	7	0	2801.5	3.174	
2801	17	15	88	7	0	2800.5	2.984	
2800	15	15	100	7	0	2799.5	1.003	
2799	21	14	67	3	0	2798.5	2.521	
2798	10	10	100	0	0	2797.5	5.286	
2797	12	11	92	7	0	2796.5	4.742	
2796	7	7	100	7	3	2795.5	5.003	*****
2795	8.5	0.5	6	7	7	2794.5	2.673	
2794	3	0.5	17	7	7	2793.5	1.044	
2793	17	2	12	7	7	2792.5	0.200	
2792	8	8	100	7	1.5	2791.5	0.591	
2791	9.5	3	32	7	7	2790.5	0.201	
2790	0.6	0.1	17	7	7	2789.5	0.206	

bed#	Bt(cm)	St(cm)	S%	T.G	B.G	Posi.	D.Sq	Sq
2789	6.3	6	95	7	7	2788.5	0.203	
2788	1.7	0.7	41	7	7	2787.5	0.090	
2787	19	8	42	7	7	2786.5	0.263	
2786	5	3	60	7	7	2785.5	0.720	
2785	4.5	2	44	7	7	2784.5	1.965	
2784	20.5	10	49	7	7	2783.5	3.126	*****
2783	18	15	83	3	1.5	2782.5	1.698	
2782	12.5	5	40	7	7	2781.5	1.698	
2781	51	10	20	7	3	2780.5	0.880	
2780	52	27	52	7	1.5	2779.5	0.241	
2779	15	8	53	7	1.5	2778.5	0.008	
2778	27	20	74	7	1.5	2777.5	0.175	
2777	12	2	17	7	7	2776.5	0.063	
2776	10	5	50	7	3	2775.5	0.049	[90]
2775	26	18	69	7	1.5	2774.5	0.050	
2774	16	14	88	7	1.5	2773.5	0.138	
2773	28	4	14	3	3	2772.5	0.123	
2772	32	16	50	7	3	2771.5	0.819	
2771	19	16	84	7	3	2770.5	0.739	
2770	17	17	100	7	3	2769.5	1.220	
2769	4	1	25	7	7	2768.5	0.397	
2768	55	10	18	3	3	2767.5	1.062	
2767	35	2	6	7	7	2766.5	0.439	
2766	19	12	63	7	1.5	2765.5	1.464	*****
2765	8.5	6.5	76	7	7	2764.5	0.790	
2764	3.1	0.1	3	7	7	2763.5	0.767	
2763	1.3	0.1	8	7	7	2762.5	0.273	
2762	1.1	0.1	9	7	7	2761.5	0.255	
2761	1.1	0.1	9	7	7	2760.5	0.002	
2760	11	1	9	7	7	2759.5	0.000	
2759	2.5	1	40	7	7	2758.5	0.000	
2758	8.1	0.1	1	7	7	2757.5	0.000	
2757	6.5	0.5	8	7	7	2756.5	0.000	
2756	9	1	11	7	7	2755.5	0.002	
2755	6.6	0.1	2	7	7	2754.5	0.000	
2754	3.1	0.1	3	7	7	2753.5	0.000	
2753	3.1	0.1	3	7	7	2752.5	0.000	
2752	4.1	0.1	2	7	7	2751.5	0.000	
2751	15.5	0.5	3	7	7	2750.5	0.000	
2750	5	1	20	7	7	2749.5	0.000	
2749	10.5	0.5	5	7	7	2748.5	0.000	
2748	8.3	0.3	4	7	7	2747.5	0.000	
2747	3.3	0.3	9	7	7	2746.5	0.000	
2746	4.2	0.2	5	7	7	2745.5	0.008	
2745	2.2	0.2	9	7	7	2744.5	0.024	
2744	5.3	0.3	6	7	7	2743.5	0.025	
2743	0.7	0.2	29	7	7	2742.5	0.026	
2742	15	1	7	7	7	2741.5	0.022	
2741	7.5	6.5	87	7	7	2740.5	0.001	
2740	12	4	33	7	7	2739.5	0.021	
2739	6.3	0.3	5	7	7	2738.5	0.022	
2738	2.2	0.2	9	7	7	2737.5	0.020	
2737	9	1	11	7	7	2736.5	0.023	
2736	3.2	0.2	6	7	7	2735.5	0.001	
2735	5.5	0.5	9	7	7	2734.5	0.000	
2734	19.2	0.2	1	7	7	2733.5	0.001	
2733	15.5	0.5	3	7	7	2732.5	0.001	
2732	9.8	0.3	3	7	7	2731.5	0.002	
2731	8	2	25	7	7	2730.5	0.000	
2730	0.7	0.5	71	7	7	2729.5	0.000	
2729	0.8	0.5	63	7	7	2728.5	0.000	

bed#	Bt(cm)	St(cm)	S%	T.G	B.G	Posi.	D.Sq	Sq
2728	3.5	1	29	7	7	2727.5	0.000	
2727	1.7	0.7	41	7	7	2726.5	0.000	
2726	0.6	0.3	50	7	7	2725.5	0.008	
2725	3	2	67	7	7	2724.5	0.004	
2724	3.5	1	29	7	7	2723.5	0.014	
2723	3.5	1	29	7	7	2722.5	0.018	
2722	3	1	33	7	7	2721.5	0.019	
2721	4.5	4	89	7	7	2720.5	0.001	
2720	5	2	40	7	7	2719.5	0.000	
2719	7	5	71	7	7	2718.5	0.012	
2718	3.5	2	57	7	7	2717.5	0.017	
2717	3	1.5	50	7	7	2716.5	0.021	
2716	13.5	0.5	4	7	7	2715.5	0.009	
2715	1.2	0.2	17	7	7	2714.5	0.004	
2714	2.5	1.5	60	7	7	2713.5	0.001	
2713	3	1.5	50	7	7	2712.5	0.002	
2712	2	1	50	7	7	2711.5	0.003	
2711	3	0.5	17	7	7	2710.5	0.003	
2710	1.2	0.2	17	7	7	2709.5	0.003	
2709	0.3	0.1	33	7	7	2708.5	0.000	
2708	0.3	0.1	33	7	7	2707.5	0.001	
2707	0.5	0.3	60	7	7	2706.5	0.002	
2706	1.5	0.5	33	7	7	2705.5	0.001	
2705	0.6	0.3	50	7	7	2704.5	0.002	
2704	2	1	50	7	7	2703.5	0.000	
2703	4.8	2	42	7	7	2702.5	0.000	
2702	1.2	0.2	17	7	7	2701.5	0.000	
2701	3.2	0.2	6	7	7	2700.5	0.000	
2700	4	1	25	7	7	2699.5	0.000	
2699	2.2	0.2	9	7	7	2698.5	0.000	
2698	3	1	33	7	7	2697.5	0.000	
2697	6.5	1	15	7	7	2696.5	0.000	
2696	2.5	0.5	20	7	7	2695.5	0.000	
2695	2.3	0.3	13	7	7	2694.5	0.001	
2694	3.5	1	29	7	7	2693.5	0.000	
2693	10.3	0.3	3	7	7	2692.5	0.001	
2692	3.2	0.7	22	7	7	2691.5	0.001	
2691	9	1	11	7	7	2690.5	0.002	
2690	3	2	67	7	7	2689.5	0.000	
2689	11	1	9	7	7	2688.5	0.000	
2688	1.8	0.3	17	7	7	2687.5	0.001	
2687	3	1	33	7	7	2686.5	0.002	
2686	9.5	2	21	7	7	2685.5	0.002	
2685	61.5	1.5	2	7	7	2684.5	0.013	
2684	23	1	4	7	7	2683.5	0.010	
2683	34	2	6	7	7	2682.5	0.002	
2682	25	2	8	7	7	2681.5	0.000	
2681	4.5	2.5	56	7	7	2680.5	0.216	
2680	37	6	16	7	7	2679.5	0.161	
2679	1.2	0.2	17	7	7	2678.5	0.177	
2678	4.6	0.1	2	7	7	2677.5	0.196	
2677	0.9	0.2	22	7	7	2676.5	0.214	
2676	33	25	76	3	3	2675.5	0.223	
2675	4.2	4	95	7	7	2674.5	0.186	
2674	2.7	1.5	56	7	7	2673.5	0.188	
2673	2.5	0.5	20	7	7	2672.5	0.154	
2672	0.7	0.3	43	7	7	2671.5	0.717	
2671	3.5	2	57	7	7	2670.5	5.158	
2670	8.5	6	71	7	7	2669.5	4.816	
2669	3.5	2.5	71	7	7	2668.5	4.705	
2668	8.5	5.5	65	7	7	2667.5	4.163	

bed#	Bt(cm)	St(cm)	S%	T.G	B.G	Posi.	D.Sq	Sq
2667	70	70	100	7	0	2666.5	0.140	
2666	64	57	89	7	0	2665.5	5.420	
2665	9	2	22	7	7	2664.5	5.288	
2664	4.5	1.5	33	7	7	2663.5	5.312	
2663	1.2	0.2	17	7	7	2662.5	4.991	
2662	0.4	0.1	25	7	7	2661.5	1.108	
2661	0.4	0.1	25	7	7	2660.5	0.001	
2660	0.5	0.2	40	7	7	2659.5	0.000	
2659	0.3	0.1	33	7	7	2658.5	0.002	
2658	1.2	0.4	33	7	7	2657.5	0.007	
2657	0.5	0.2	40	7	7	2656.5	0.014	
2656	1.7	1.2	71	7	7	2655.5	0.013	
2655	0.5	0.2	40	7	7	2654.5	0.026	
2654	2.2	1.5	68	7	7	2653.5	0.071	
2653	4.3	3.5	81	7	7	2652.5	0.040	
2652	4.5	2.5	56	7	7	2651.5	0.025	
2651	2.5	2	80	7	7	2650.5	0.070	
2650	5	3.5	70	7	7	2649.5	0.231	
2649	12	10	83	7	7	2648.5	0.117	
2648	3	2	67	7	7	2647.5	0.131	
2647	3	2	67	7	7	2646.5	0.134	
2646	10	10	100	7	7	2645.5	0.105	
2645	15	13	87	7	3	2644.5	0.210	
2644	4	2	50	7	7	2643.5	0.150	
2643	5	4	80	7	7	2642.5	0.160	
2642	3	2	67	7	7	2641.5	0.611	
2641	8	7	88	7	7	2640.5	5.482	
2640	0.9	0.1	11	7	7	2639.5	12.956	
2639	2.5	1.5	60	7	7	2638.5	17.069	
2638	5.5	4.5	82	7	7	2637.5	16.663	*****
2637	72	68	94	7	0	2636.5	3.328	
2636	110	102	93	7	0	2635.5	0.520	[91]
2635	65	53	82	7	0	2634.5	5.566	
2634	20	20	100	3	0	2633.5	10.979	*****
2633	11	1	9	7	7	2632.5	10.317	
2632	19	1.5	8	7	7	2631.5	2.112	
2631	53.5	52	97	7	7	2630.5	0.991	
2630	25	15	60	7	7	2629.5	0.068	
2629	19	15	79	7	7	2628.5	0.282	
2628	11	7	64	7	7	2627.5	0.377	
2627	42	39	93	1.5	1.5	2626.5	2.578	
2626	3	3	100	7	7	2625.5	0.008	
2625	11.5	10	87	7	7	2624.5	0.383	
2624	8	6	75	7	7	2623.5	1.870	
2623	6	4	67	7	7	2622.5	3.645	
2622	3	1	33	7	7	2621.5	8.961	*****
2621	54	52	96	7	1.5	2620.5	2.052	
2620	40	40	100	7	1.5	2619.5	0.423	
2619	41	38	93	7	1.5	2618.5	2.184	
2618	23	23	100	1.5	1.5	2617.5	2.458	
2617	9	6	67	7	1.5	2616.5	3.460	
2616	5	1	20	7	7	2615.5	1.044	
2615	6	3	50	7	7	2614.5	4.033	[92]
2614	15	7	47	7	7	2613.5	10.237	
2613	62.5	50	80	1.5	1.5	2612.5	7.004	
2612	20	20	100	7	3	2611.5	4.725	
2611	90	90	100	7	0	2610.5	0.230	
2610	36	36	100	7	1.5	2609.5	1.751	
2609	48	40	83	3	1.5	2608.5	5.166	
2608	51	49	96	7	7	2607.5	7.288	*****
2607	8	5	63	7	7	2606.5	6.061	

bed#	Bt(cm)	St(cm)	S%	T.G	B.G	Posi.	D.Sq	Sq
2606	30	28	93	7	7	2605.5	3.411	
2605	15	15	100	3	1.5	2604.5	3.236	
2604	15	15	100	3	1.5	2603.5	3.312	
2603	1.2	0.2	17	7	7	2602.5	1.467	
2602	1.8	0.3	17	7	7	2601.5	1.127	
2601	25	3	12	7	7	2600.5	0.826	
2600	20	1	5	7	7	2599.5	0.201	
2599	8.5	0.5	6	7	7	2598.5	0.111	
2598	5	3	60	7	7	2597.5	0.069	
2597	14	12	86	7	7	2596.5	0.006	
2596	7.5	4.5	60	7	7	2595.5	0.215	
2595	5	3	60	7	7	2594.5	0.604	
2594	9.5	5	53	7	7	2593.5	0.636	
2593	3.5	1	29	7	7	2592.5	1.208	
2592	2.7	0.7	26	7	7	2591.5	2.396	*****
2591	5.5	2.5	45	7	1.5	2590.5	1.297	
2590	6	6	100	3	3	2589.5	1.001	
2589	3	3	100	7	7	2588.5	2.148	
2588	10	5	50	3	3	2587.5	1.667	
2587	16.5	10	61	3	1.5	2586.5	0.475	
2586	29	10	34	3	1.5	2585.5	0.046	
2585	23	18	78	3	1.5	2584.5	0.230	
2584	15	11	73	7	1.5	2583.5	0.792	
2583	18	10	56	7	1.5	2582.5	1.301	
2582	5	4	80	7	3	2581.5	1.411	
2581	6.5	3	46	7	7	2580.5	1.432	[93]
2580	7	6	86	7	7	2579.5	1.784	
2579	32	30	94	3	1.5	2578.5	0.472	
2578	25	25	100	7	3	2577.5	0.516	
2577	31	31	100	7	3	2576.5	0.094	
2576	33	33	100	7	3	2575.5	1.685	
2575	18	4	22	7	7	2574.5	0.880	
2574	9	6	67	7	3	2573.5	0.187	
2573	52	32	62	7	0	2572.5	1.238	
2572	14	1	7	7	7	2571.5	0.303	
2571	17	2	12	7	7	2570.5	0.286	
2570	34	19	56	1.5	1.5	2569.5	0.230	
2569	20	18	90	7	1.5	2568.5	1.357	*****
2568	21	5	24	7	7	2567.5	0.018	
2567	16	2	13	7	7	2566.5	0.018	
2566	21	21	100	7	1.5	2565.5	0.860	
2565	2	2	100	7	7	2564.5	0.184	
2564	5.5	3	55	7	7	2563.5	0.358	
2563	25	21	84	3	0	2562.5	0.001	
2562	40	3	8	7	7	2561.5	0.209	
2561	62	1	2	7	7	2560.5	1.727	
2560	35	1	3	7	7	2559.5	2.672	*****
2559	81	20	25	7	1.5	2558.5	1.222	
2558	29	26	90	3	0	2557.5	0.947	
2557	12	9	75	1.5	1.5	2556.5	0.011	[94]
2556	10	8	80	7	3	2555.5	0.341	
2555	5	3.5	70	7	3	2554.5	0.443	
2554	15	11	73	7	1.5	2553.5	1.219	
2553	25	24	96	7	1.5	2552.5	2.230	*****
2552	15	15	100	7	7	2551.5	1.538	
2551	30	1	3	7	7	2550.5	0.789	
2550	42	5	12	7	0	2549.5	2.597	
2549	12.5	1.5	12	7	7	2548.5	1.332	
2548	2	1	50	7	7	2547.5	0.367	
2547	42	1	2	7	7	2546.5	0.321	
2546	20	5	25	7	7	2545.5	0.321	

bed#	Bt(cm)	St(cm)	S%	T.G	B.G	Posi.	D.Sq	Sq
2545	24	1	4	7	7	2544.5	0.003	
2544	54	1	2	7	7	2543.5	0.507	
2543	37	1	3	7	7	2542.5	0.518	
2542	2	1	50	7	7	2541.5	0.518	
2541	10	8	80	7	7	2540.5	0.326	
2540	3.5	2	57	7	7	2539.5	1.930	
2539	66	45	68	7	7	2538.5	0.322	
2538	29.8	1.5	5	7	7	2537.5	1.309	
2537	6	1	17	7	7	2536.5	1.326	
2536	2	1	50	7	7	2535.5	1.552	
2535	86	50	58	7	0	2534.5	0.792	
2534	44.5	1.5	3	7	7	2533.5	0.329	
2533	78	15	19	3	0	2532.5	0.004	
2532	209	4	2	7	7	2531.5	0.012	
2531	20	15	75	7	7	2530.5	0.060	
2530	6	3	50	7	7	2529.5	0.583	
2529	17	12	71	3	0	2528.5	0.213	
2528	52	30	58	3	0	2527.5	0.505	
2527	6	4	67	7	7	2526.5	0.510	
2526	28	20	71	7	7	2525.5	0.141	
2525	27	7	26	7	7	2524.5	0.230	
2524	21	18	86	3	1.5	2523.5	0.347	
2523	7	3	43	7	7	2522.5	2.503	
2522	8	3	38	7	7	2521.5	4.794	*****
2521	22	14	64	7	0	2520.5	2.743	
2520	39	23	59	3	0	2519.5	0.199	
2519	10	10	100	7	3	2518.5	0.115	[95]
2518	18	10	56	3	0	2517.5	0.810	
2517	37	24	65	3	0	2516.5	2.147	
2516	20	12	60	3	0	2515.5	2.122	*****
2515	44	3	7	7	7	2514.5	0.612	
2514	25	20	80	7	7	2513.5	0.088	
2513	23	10	43	7	7	2512.5	0.447	*****
2512	55	25	45	7	0	2511.5	0.220	
2511	33	23	70	7	0	2510.5	0.202	
2510	34	29	85	7	0	2509.5	1.163	
2509	12	2	17	7	7	2508.5	0.331	
2508	18	14	78	7	7	2507.5	0.239	
2507	12	12	100	7	1.5	2506.5	0.216	[96]
2506	25	20	80	7	0	2505.5	0.114	
2505	4	3	75	7	7	2504.5	2.576	
2504	20	10	50	3	3	2503.5	2.594	
2503	22	18	82	7	0	2502.5	0.402	
2502	33	20	61	3	0	2501.5	0.232	
2501	22.5	19.5	87	7	1.5	2500.5	0.596	
2500	29	29	100	7	0	2499.5	2.406	
2499	29	29	100	7	0	2498.5	3.845	*****
2498	20	5	25	7	7	2497.5	0.691	
2497	6	1	17	7	7	2496.5	0.119	
2496	6.5	1.5	23	7	7	2495.5	0.745	
2495	25	24	96	3	1.5	2494.5	1.085	
2494	19	18	95	7	0	2493.5	0.884	
2493	40	17	43	3	0	2492.5	0.152	
2492	20	15	75	3	3	2491.5	1.090	[97]
2491	26	18	69	7	7	2490.5	0.427	
2490	29	29	100	7	1.5	2489.5	0.606	
2489	27	7	26	1.5	1.5	2488.5	0.241	
2488	12	2	17	7	7	2487.5	0.506	
2487	42	2	5	7	7	2486.5	1.918	*****

bed#	Bt(cm)	St(cm)	S%	T.G	B.G	Posi.	D.Sq	Sq
2486	37	30	81	7	1.5	2485.5	0.456	
2485	90	20	22	3	1.5	2484.5	0.579	
2484	28	18	64	3	1.5	2483.5	0.291	
2483	40	30	75	1.5	1.5	2482.5	0.205	
2482	15	5	33	3	3	2481.5	0.231	[98]
2481	20	10	50	3	3	2480.5	0.203	
2480	34	25	74	7	1.5	2479.5	0.930	
2479	35	10	29	3	3	2478.5	1.236	
2478	35	20	57	1.5	1.5	2477.5	1.529	
2477	35	10	29	3	3	2476.5	2.365	*****
2476	26	13	50	7	7	2475.5	1.475	
2475	13	10	77	7	7	2474.5	0.201	
2474	14	13	93	7	7	2473.5	0.300	
2473	68	40	59	7	3	2472.5	0.113	
2472	5	2	40	7	7	2471.5	0.108	
2471	15	10	67	7	7	2470.5	0.147	
2470	35	25	71	7	0	2469.5	0.452	
2469	35	25	71	7	7	2468.5	1.276	
2468	44	2	5	7	7	2467.5	0.254	
2467	13	1	8	7	7	2466.5	0.176	
2466	28	2	7	7	7	2465.5	0.129	
2465	58	26	45	7	1.5	2464.5	0.277	
2464	89	1	1	7	7	2463.5	0.024	
2463	7	1	14	7	7	2462.5	0.244	
2462	19	15	79	7	1.5	2461.5	0.000	
2461	6.5	1.5	23	7	7	2460.5	0.227	
2460	45	2	4	7	7	2459.5	2.300	
2459	14.5	2	14	7	7	2458.5	2.300	*****
2458	38	25	66	7	1.5	2457.5	0.971	
2457	20	15	75	7	1.5	2456.5	0.248	
2456	28	12	43	7	1.5	2455.5	0.206	[99]
2455	28	15	54	7	1.5	2454.5	2.014	
2454	27	3	11	7	7	2453.5	2.052	
2453	29	29	100	7	1.5	2452.5	4.127	*****
2452	47.5	1.5	3	7	7	2451.5	2.377	
2451	17.5	1.5	9	7	7	2450.5	1.171	
2450	81.5	1.5	2	7	7	2449.5	0.353	
2449	40.5	1.5	4	7	7	2448.5	0.336	
2448	22	2	9	7	7	2447.5	0.001	
2447	15	2	13	7	7	2446.5	0.000	
2446	5	1.5	30	7	7	2445.5	0.000	
2445	6	3	50	7	7	2444.5	0.001	
2444	5	1.5	30	7	7	2443.5	0.001	
2443	6	2	33	7	7	2442.5	0.002	
2442	13.5	2	15	7	7	2441.5	0.002	
2441	4	1.5	38	7	7	2440.5	0.001	
2440	4.7	1.2	26	7	7	2439.5	0.000	
2439	3	1	33	7	7	2438.5	0.002	
2438	17	1.5	9	7	7	2437.5	0.003	
2437	4	1.5	38	7	7	2436.5	0.005	
2436	7	3	43	7	7	2435.5	0.001	
2435	10	2	20	7	7	2434.5	0.000	
2434	35	3	9	7	7	2433.5	0.172	
2433	4	1.5	38	7	7	2432.5	0.172	
2432	17.5	2	11	7	7	2431.5	0.158	
2431	10	2	20	7	7	2430.5	0.158	
2430	4	1	25	7	7	2429.5	0.795	
2429	26	22	85	7	3	2428.5	0.341	
2428	4	1.5	38	7	7	2427.5	1.160	
2427	1.7	0.5	29	7	7	2426.5	6.927	

bed#	Bt(cm)	St(cm)	S%	T.G	B.G	Posi.	D.Sq	Sq
2426	3	1	33	7	7	2425.5	15.443	*****
2425	22	15	68	3	1.5	2424.5	9.813	
2424	28	20	71	1.5	1.5	2423.5	10.577	
2423	30	17	57	1.5	1.5	2422.5	6.684	[100]
2422	122	116	95	7	0	2421.5	1.495	
2421	83	80	96	7	0	2420.5	14.217	
2420	6	0.5	8	7	7	2419.5	9.145	
2419	36.5	30	82	7	1.5	2418.5	10.332	*****
2418	23.5	0.5	2	7	7	2417.5	4.397	
2417	43.5	1.5	3	7	7	2416.5	0.137	
2416	22	1	5	7	7	2415.5	1.089	
2415	16	15	94	7	3	2414.5	0.148	
2414	78	26	33	3	1.5	2413.5	0.079	
2413	67	46	69	7	3	2412.5	0.697	
2412	4.2	0.2	5	7	7	2411.5	0.664	
2411	4.5	1.5	33	7	7	2410.5	0.699	
2410	5.2	0.2	4	7	7	2409.5	0.351	
2409	16	15	94	3	1.5	2408.5	0.095	
2408	28	18	64	7	1.5	2407.5	0.148	[101]
2407	5.3	0.3	6	7	7	2406.5	0.460	
2406	4.5	0.5	11	7	7	2405.5	1.584	
2405	4	1	25	7	7	2404.5	1.563	
2404	24.8	24	97	7	1.5	2403.5	1.622	
2403	41	35	85	3	1.5	2402.5	1.484	
2402	10.5	9	86	1.5	1.5	2401.5	0.948	
2401	34	25	74	7	1.5	2400.5	0.024	
2400	7	1	14	7	7	2399.5	0.024	
2399	29.5	26	88	7	0	2398.5	0.142	
2398	58	30	52	7	0	2397.5	0.475	
2397	67	24	36	7	0	2396.5	2.131	
2396	22	4	18	7	7	2395.5	0.921	
2395	26	1	4	7	7	2394.5	0.926	
2394	92	50	54	1.5	1.5	2393.5	3.371	
2393	41	15	37	7	3	2392.5	3.573	*****
2392	41	3	7	7	7	2391.5	1.706	
2391	1.2	0.2	17	7	7	2390.5	1.582	
2390	1.2	0.2	17	7	7	2389.5	1.506	
2389	0.9	0.2	22	7	7	2388.5	0.106	
2388	1.4	0.2	14	7	7	2387.5	0.157	
2387	2	1	50	7	7	2386.5	0.184	
2386	1.5	0.5	33	7	7	2385.5	0.189	
2385	5.7	2	35	7	7	2384.5	0.179	
2384	20.7	17	82	7	7	2383.5	0.001	
2383	11.5	10	87	7	7	2382.5	0.089	
2382	2.2	1.2	55	7	7	2381.5	0.100	
2381	2.2	1.2	55	7	7	2380.5	0.028	
2380	4	3	75	7	7	2379.5	0.033	
2379	4	3	75	7	7	2378.5	0.000	
2378	9	2	22	7	7	2377.5	0.015	
2377	1.2	0.2	17	7	7	2376.5	0.022	
2376	16	12	75	7	7	2375.5	0.025	
2375	5	3	60	7	7	2374.5	0.013	
2374	6	2	33	7	7	2373.5	0.010	
2373	4.5	1.5	33	7	7	2372.5	0.550	
2372	3.5	1	29	7	7	2371.5	1.701	
2371	12	2	17	7	7	2370.5	4.136	

bed#	Bt(cm)	St(cm)	S%	T.G	B.G	Posi.	D.Sq	Sq
2370	8	6	75	7	7	2369.5	7.382	*****
2369	33	2	6	7	7	2368.5	7.431	
2368	47	40	85	7	0	2367.5	2.134	[102]
2367	50	25	50	7	1.5	2366.5	0.209	
2366	110	23	21	7	0	2365.5	0.843	
2365	37	35	95	7	0	2364.5	5.300	*****
2364	15	3	20	7	7	2363.5	5.384	
2363	34	5	15	3	3	2362.5	4.544	
2362	53	2	4	7	7	2361.5	2.306	
2361	20	10	50	7	7	2360.5	0.919	
2360	12	10	83	7	7	2359.5	0.117	
2359	25	2	8	7	7	2358.5	0.117	
2358	14	2	14	7	7	2357.5	0.008	
2357	17	15	88	7	7	2356.5	0.247	
2356	4	2	50	7	7	2355.5	0.163	
2355	3.5	1.5	43	7	7	2354.5	0.085	
2354	4	1	25	7	7	2353.5	0.077	
2353	2.5	0.5	20	7	7	2352.5	0.067	
2352	3	0.5	17	7	7	2351.5	0.002	
2351	14.3	0.3	2	7	7	2350.5	0.000	
2350	2.5	0.5	20	7	7	2349.5	0.000	
2349	4	1	25	7	7	2348.5	0.000	
2348	6.2	0.2	3	7	7	2347.5	0.002	
2347	5.2	0.2	4	7	7	2346.5	0.038	
2346	3	1	33	7	7	2345.5	0.059	
2345	2.1	0.1	5	7	7	2344.5	0.134	
2344	1.7	0.2	12	7	7	2343.5	0.143	
2343	14	4	29	7	7	2342.5	0.081	
2342	11	10	91	7	7	2341.5	0.000	
2341	5	5	100	7	7	2340.5	0.108	
2340	8	8	100	7	7	2339.5	0.448	
2339	2.2	0.2	9	7	7	2338.5	0.444	
2338	3.5	1.5	43	7	7	2337.5	0.438	
2337	8	2	25	7	7	2336.5	0.420	
2336	6.5	4	62	7	3	2335.5	0.005	
2335	8	8	100	7	3	2334.5	0.452	
2334	15	1	7	7	7	2333.5	0.459	
2333	2.5	0.5	20	7	7	2332.5	0.453	
2332	3	1	33	7	7	2331.5	0.452	
2331	4.5	0.5	11	7	7	2330.5	0.120	
2330	12.5	0.5	4	7	7	2329.5	0.000	
2329	2.5	0.5	20	7	7	2328.5	0.000	
2328	2.5	0.5	20	7	7	2327.5	0.106	
2327	14.2	0.2	1	7	7	2326.5	0.615	
2326	8	1	13	7	7	2325.5	0.697	
2325	1.8	1	56	7	7	2324.5	2.343	
2324	1.5	0.7	47	7	7	2323.5	3.898	*****
2323	2.7	2	74	7	3	2322.5	3.393	
2322	18	8	44	7	1.5	2321.5	1.980	
2321	17.5	13	74	7	7	2320.5	3.299	
2320	51	30	59	3	0	2319.5	0.372	[103]
2319	8	8	100	1.5	1.5	2318.5	0.296	
2318	18	10	56	1.5	1.5	2317.5	1.248	
2317	20	8	40	1.5	1.5	2316.5	2.377	
2316	17	12	71	3	0	2315.5	6.943	*****
2315	4.5	0.5	11	7	7	2314.5	3.856	
2314	5	1	20	7	7	2313.5	2.280	
2313	5.5	2	36	7	7	2312.5	1.106	
2312	3	1.5	50	7	7	2311.5	0.363	
2311	2.7	0.7	26	7	7	2310.5	0.000	
2310	3.4	0.2	6	7	7	2309.5	0.106	

bed#	Bt(cm)	St(cm)	S%	T.G	B.G	Posi.	D.Sq	Sq
2309	2.2	0.2	9	7	7	2308.5	0.447	
2308	2.8	1.5	54	7	7	2307.5	0.444	
2307	12	0.5	4	7	7	2306.5	1.243	
2306	4.5	2	44	7	7	2305.5	1.235	
2305	7.5	4	53	3	3	2304.5	1.308	
2304	10	8	80	3	3	2303.5	0.224	
2303	17.2	0.2	1	7	7	2302.5	0.236	
2302	29	4	14	7	1.5	2301.5	0.322	
2301	3	2	67	7	7	2300.5	0.311	
2300	59	30	51	7	0	2299.5	2.193	
2299	6.7	0.2	3	7	7	2298.5	1.298	
2298	3.2	0.2	6	7	7	2297.5	1.294	
2297	7.2	0.2	3	7	7	2296.5	0.536	
2296	10.2	0.2	2	7	7	2295.5	0.490	
2295	2.7	0.2	7	7	7	2294.5	0.126	
2294	8.2	0.2	2	7	7	2293.5	0.488	
2293	6	0.5	8	7	7	2292.5	0.506	
2292	15.2	0.2	1	7	7	2291.5	0.527	
2291	16	2	13	7	7	2290.5	1.039	
2290	8	8	100	7	3	2289.5	1.344	
2289	8	8	100	7	3	2288.5	0.325	
2288	9	3	33	7	7	2287.5	0.779	
2287	6.5	2.5	38	7	7	2286.5	1.644	*****
2286	5.5	2.5	45	3	3	2285.5	1.593	
2285	45	45	100	7	0	2284.5	0.341	
2284	13	0.5	4	7	7	2283.5	1.782	
2283	9	8	89	1.5	1.5	2282.5	0.804	
2282	20	8	40	1.5	1.5	2281.5	0.199	
2281	21	20	95	1.5	1.5	2280.5	0.158	
2280	33	15	45	7	1.5	2279.5	0.125	
2279	25	3	12	7	1.5	2278.5	0.079	
2278	26	20	77	3	1.5	2277.5	0.027	
2277	10	8	80	7	1.5	2276.5	0.046	[104]
2276	25	20	80	1.5	1.5	2275.5	0.014	
2275	13	10	77	7	3	2274.5	0.045	
2274	17	15	88	3	0	2273.5	0.232	
2273	12	2	17	1.5	1.5	2272.5	1.231	
2272	17	7	41	7	3	2271.5	2.319	
2271	52	40	77	3	0	2270.5	1.198	
2270	9.5	1.5	16	7	7	2269.5	4.756	
2269	16	10	63	1.5	1.5	2268.5	4.126	
2268	83	65	78	1.5	1.5	2267.5	0.018	
2267	55	40	73	7	0	2266.5	1.730	
2266	30	30	100	3	0	2265.5	3.685	
2265	60	60	100	3	0	2264.5	15.691	*****
2264	30.2	0.2	1	7	7	2263.5	12.709	
2263	25.5	0.5	2	7	7	2262.5	6.380	
2262	1.5	0.5	33	7	7	2261.5	2.873	
2261	3	1	33	7	7	2260.5	0.999	
2260	1.7	0.7	41	7	7	2259.5	0.002	
2259	1.7	0.5	29	7	7	2258.5	0.002	
2258	5.5	2	36	7	7	2257.5	0.000	
2257	2.5	2	80	7	7	2256.5	0.001	
2256	1.7	1.5	88	7	7	2255.5	0.107	
2255	2.2	0.2	9	7	7	2254.5	0.494	
2254	1	0.2	20	7	7	2253.5	0.522	
2253	2.7	0.2	7	7	7	2252.5	0.570	
2252	20.3	2.3	11	7	7	2251.5	1.191	
2251	14	7	50	3	3	2250.5	1.323	
2250	16.5	15	91	3	3	2249.5	9.396	
2249	4	3	75	7	7	2248.5	13.891	

bed#	Bt(cm)	St(cm)	S%	T.G	B.G	Posi.	D.Sq	Sq
2248	5	3	60	7	7	2247.5	13.453	*****
2247	11.5	10	87	7	3	2246.5	10.496	
2246	28	28	100	7	0	2245.5	5.984	[105]
2245	180	180	100	7	0	2244.5	7.153	
2244	50	40	80	7	0	2243.5	16.985	
2243	6.7	1.5	22	7	7	2242.5	16.962	*****
2242	4.8	1.3	27	7	7	2241.5	14.994	
2241	7.5	1	13	7	7	2240.5	10.828	
2240	6.5	4	62	3	3	2239.5	1.110	
2239	0.9	0.1	11	7	7	2238.5	0.107	
2238	4.2	0.2	5	7	7	2237.5	0.109	
2237	1.8	1.5	83	7	7	2236.5	0.107	
2236	14	3	21	7	7	2235.5	0.105	
2235	6.5	5	77	7	7	2234.5	0.010	
2234	3.8	1.5	39	7	7	2233.5	0.014	
2233	3.2	0.2	6	7	7	2232.5	0.007	
2232	4.2	0.2	5	7	7	2231.5	0.004	
2231	4.5	1	22	7	7	2230.5	0.002	
2230	6.2	0.2	3	7	7	2229.5	0.001	
2229	3	1.5	50	7	7	2228.5	0.002	
2228	3.8	2.5	66	7	7	2227.5	0.001	
2227	0.5	0.2	40	7	7	2226.5	0.001	
2226	1.8	0.3	17	7	7	2225.5	0.008	
2225	0.7	0.2	29	7	7	2224.5	0.010	
2224	4.2	3	71	7	7	2223.5	0.002	
2223	4.5	4	89	7	7	2222.5	0.170	
2222	6.5	0.5	8	7	7	2221.5	0.211	
2221	7	3	43	7	7	2220.5	0.152	
2220	2	0.8	40	7	7	2219.5	0.184	
2219	2.4	1.2	50	7	7	2218.5	0.218	
2218	32.5	30	92	7	7	2217.5	0.172	
2217	13	4	31	7	7	2216.5	0.202	
2216	4	1	25	7	7	2215.5	0.720	
2215	9	4	44	7	7	2214.5	0.641	
2214	5	2	40	7	7	2213.5	0.617	
2213	11.5	7	61	7	3	2212.5	0.528	
2212	9.5	4	42	7	7	2211.5	0.456	
2211	74	57	77	7	3	2210.5	1.416	
2210	4.5	2	44	7	7	2209.5	0.879	
2209	10.5	1	10	7	7	2208.5	0.257	
2208	12	3	25	7	7	2207.5	0.039	
2207	4.5	0.5	11	7	7	2206.5	0.022	
2206	2.7	0.2	7	7	7	2205.5	0.937	
2205	8.5	8	94	7	3	2204.5	0.688	
2204	35	33	94	7	7	2203.5	0.111	
2203	23	12	52	7	7	2202.5	0.165	
2202	3.8	0.2	5	7	7	2201.5	0.114	
2201	19	15	79	7	7	2200.5	0.370	
2200	7.5	4	53	7	7	2199.5	0.134	
2199	10	8	80	7	7	2198.5	0.028	
2198	15.5	10	65	7	7	2197.5	0.307	
2197	24	10	42	7	7	2196.5	0.560	
2196	3	1.5	50	7	7	2195.5	3.143	
2195	17	10	59	7	7	2194.5	3.882	
2194	19	19	100	7	7	2193.5	6.844	
2193	28	27	96	7	3	2192.5	4.777	
2192	42	35	83	7	7	2191.5	4.346	

bed#	Bt(cm)	St(cm)	S%	T.G	B.G	Posi.	D.Sq	Sq
2191	62	60	97	7	7	2190.5	5.371	*****
2190	35	17	49	3	0	2189.5	2.807	
2189	68	58	85	7	0	2188.5	4.407	
2188	17.5	12	69	3	0	2187.5	3.237	
2187	16	14	88	3	1.5	2186.5	3.234	
2186	19	17	89	1.5	1.5	2185.5	3.794	
2185	20.5	19	93	1.5	1.5	2184.5	3.674	
2184	21	11	52	3	0	2183.5	2.422	
2183	12.5	0.5	4	7	7	2182.5	0.930	
2182	5	1.5	30	7	7	2181.5	0.235	
2181	11	9	82	7	7	2180.5	0.042	
2180	17.5	14	80	7	1.5	2179.5	0.015	
2179	109	11	10	3	0	2178.5	0.223	
2178	18	1	6	7	7	2177.5	0.220	
2177	22	1	5	7	7	2176.5	0.054	
2176	2.2	0.2	9	7	7	2175.5	1.001	
2175	25.8	23	89	3	0	2174.5	0.231	
2174	3.2	0.2	6	7	7	2173.5	2.438	[106]
2173	2.5	2	80	7	7	2172.5	3.613	
2172	25	24	96	3	0	2171.5	1.462	
2171	34	27	79	3	0	2170.5	0.122	
2170	15	7	47	7	3	2169.5	0.166	
2169	25.5	20	78	3	1.5	2168.5	0.500	
2168	42	11	26	7	3	2167.5	1.987	
2167	33.5	33	99	7	1.5	2166.5	1.470	
2166	19	19	100	7	1.5	2165.5	2.478	
2165	19	1	5	7	7	2164.5	1.568	
2164	23	5	22	7	7	2163.5	0.041	
2163	30.5	0.5	2	7	7	2162.5	0.490	
2162	63	37	59	3	0	2161.5	0.033	
2161	5.6	0.1	2	7	7	2160.5	0.694	
2160	1.1	0.1	9	7	7	2159.5	1.766	
2159	47	30	64	7	1.5	2158.5	0.597	
2158	19	19	100	7	1.5	2157.5	0.253	
2157	5.2	4.2	81	7	7	2156.5	1.520	
2156	19	12	63	7	1.5	2155.5	0.809	
2155	22	14	64	7	1.5	2154.5	0.324	
2154	35	13	37	7	1.5	2153.5	0.040	
2153	42	17	40	7	1.5	2152.5	0.107	
2152	17	12	71	3	3	2151.5	0.441	
2151	58	18	31	7	0	2150.5	2.032	
2150	25	23	92	7	0	2149.5	5.012	*****
2149	43	3	7	7	7	2148.5	3.196	
2148	2	1	50	7	7	2147.5	0.444	
2147	145	13	9	7	3	2146.5	1.072	
2146	8.8	0.3	3	7	7	2145.5	0.065	
2145	18	1	6	7	7	2144.5	2.099	

bed#	Bt(cm)	St(cm)	S%	T.G	B.G	Posi.	D.Sq	Sq
2144	8	1	13	7	7	2143.5	3.326	*****
2143	26	18	69	7	0	2142.5	1.368	
2142	4	2	50	7	7	2141.5	2.356	
2141	36	13	36	3	0	2140.5	0.919	
2140	15	15	100	3	0	2139.5	0.062	
2139	16	13	81	3	3	2138.5	0.958	
2138	15	10	67	3	0	2137.5	2.311	
2137	6.1	4	66	7	7	2136.5	2.352	
2136	25	17	68	3	0	2135.5	2.338	
2135	8.5	1	12	7	7	2134.5	0.851	
2134	4.5	1.5	33	7	7	2133.5	0.323	
2133	5.4	0.1	2	7	7	2132.5	0.019	
2132	5.5	3	55	7	7	2131.5	0.024	
2131	29	22	76	3	0	2130.5	0.015	
2130	9	2	22	7	7	2129.5	0.019	[107]
2129	4.5	3	67	7	7	2128.5	0.584	
2128	5	3	60	7	7	2127.5	1.218	
2127	4	3	75	7	7	2126.5	1.238	
2126	20.5	15	73	7	1.5	2125.5	1.949	
2125	12	9	75	7	7	2124.5	3.577	
2124	44.5	42	94	7	0	2123.5	2.926	
2123	24	8	33	3	1.5	2122.5	2.478	
2122	15.5	4	26	7	7	2121.5	2.294	
2121	26	18	69	3	0	2120.5	2.037	
2120	18	17	94	3	0	2119.5	1.708	
2119	139	118	85	1.5	1.5	2118.5	4.656	
2118	30	19	63	3	1.5	2117.5	6.315	
2117	11.2	0.7	6	7	7	2116.5	4.206	
2116	20	20	100	3	1.5	2115.5	6.086	*****
2115	2.5	0.5	20	7	7	2114.5	3.978	
2114	6	1	17	7	7	2113.5	0.030	
2113	72	7	10	7	3	2112.5	0.334	
2112	70	21	30	3	3	2111.5	0.113	
2111	53	2	4	7	7	2110.5	0.164	
2110	2	1	50	7	7	2109.5	0.152	
2109	38.5	20.5	53	3	3	2108.5	0.320	
2108	30	17	57	1.5	1.5	2107.5	1.536	
2107	13.5	3	22	7	7	2106.5	0.717	
2106	24	16	67	7	7	2105.5	0.475	
2105	30.5	0.5	2	7	7	2104.5	0.185	
2104	2	1	50	7	7	2103.5	0.125	
2103	4.5	1.5	33	7	7	2102.5	0.595	[108]
2102	3.5	0.5	14	7	7	2101.5	0.603	
2101	39	13	33	7	1.5	2100.5	0.102	
2100	35.5	12	34	3	3	2099.5	0.202	
2099	53	1	2	7	7	2098.5	0.201	
2098	3.6	0.1	3	7	7	2097.5	0.205	
2097	5.5	1	18	7	7	2096.5	0.204	
2096	26	19	73	3	3	2095.5	0.046	
2095	11	11	100	7	7	2094.5	0.323	
2094	55	0.5	1	7	7	2093.5	0.842	
2093	4.2	0.7	17	7	7	2092.5	0.835	
2092	6	1	17	7	7	2091.5	0.830	
2091	17.5	15	86	3	1.5	2090.5	0.503	
2090	19	18	95	7	1.5	2089.5	0.061	
2089	13.5	12	89	7	3	2088.5	0.940	
2088	14.7	0.2	1	7	7	2087.5	0.895	
2087	2.6	0.1	4	7	7	2086.5	0.885	
2086	18.5	17.5	95	3	3	2085.5	1.538	*****
2085	4	2	50	7	7	2084.5	0.552	
2084	29	1	3	7	7	2083.5	0.129	

bed#	Bt(cm)	St(cm)	S%	T.G	B.G	Posi.	D.Sq	Sq
2083	27	4	15	7	7	2082.5	0.164	
2082	14.2	0.2	1	7	7	2081.5	0.165	
2081	10.5	1	10	7	7	2080.5	0.022	
2080	87	1	1	7	7	2079.5	0.023	
2079	14	4	29	7	7	2078.5	0.003	
2078	24	2	8	7	7	2077.5	0.004	
2077	18.7	0.2	1	7	7	2076.5	0.004	
2076	19	11	58	7	7	2075.5	0.058	
2075	3.7	0.2	5	7	7	2074.5	0.013	
2074	1.2	0.2	17	7	7	2073.5	0.001	
2073	22	1	5	7	7	2072.5	0.001	
2072	1.5	0.3	20	7	7	2071.5	0.001	
2071	1.2	0.2	17	7	7	2070.5	0.017	
2070	12.4	8	65	7	7	2069.5	0.010	
2069	6.8	2.3	34	7	7	2068.5	0.025	
2068	0.9	0.1	11	7	7	2067.5	0.019	
2067	2.7	0.2	7	7	7	2066.5	0.017	
2066	1.4	0.1	7	7	7	2065.5	0.016	
2065	6.7	0.2	3	7	7	2064.5	0.000	
2064	5	0.5	10	7	7	2063.5	0.000	
2063	4.2	0.5	12	7	7	2062.5	0.000	
2062	3.9	0.7	18	7	7	2061.5	0.000	
2061	2	0.3	15	7	7	2060.5	0.000	
2060	1.6	0.1	6	7	7	2059.5	0.001	
2059	1.7	0.1	6	7	7	2058.5	0.005	
2058	3.3	0.6	18	7	7	2057.5	0.008	
2057	1.3	0.3	23	7	7	2056.5	0.011	
2056	3	2	67	7	7	2055.5	0.124	
2055	2.7	1	37	7	7	2054.5	0.129	
2054	15.5	2.5	16	7	7	2053.5	0.116	
2053	13.3	2	15	7	7	2052.5	0.112	
2052	3	1	33	7	7	2051.5	0.123	
2051	9	6	67	7	3	2050.5	0.105	
2050	8.5	3	35	7	7	2049.5	0.107	
2049	3.2	1.5	47	7	7	2048.5	0.105	
2048	3.2	2	63	7	7	2047.5	0.105	
2047	7	5	71	7	7	2046.5	0.105	
2046	0.9	0.2	22	7	7	2045.5	0.014	
2045	5.3	2.3	43	7	7	2044.5	0.024	
2044	5.2	4	77	7	7	2043.5	0.009	
2043	3.5	2.5	71	7	7	2042.5	0.009	
2042	12	9	75	7	7	2041.5	0.001	
2041	4	2	50	7	7	2040.5	0.000	
2040	5	4	80	7	7	2039.5	0.008	
2039	3	2.3	77	7	7	2038.5	0.007	
2038	7	3	43	7	7	2037.5	0.011	
2037	7	5	71	7	7	2036.5	0.006	
2036	6	5	83	7	7	2035.5	0.035	
2035	3.2	0.2	6	7	7	2034.5	0.017	
2034	4.9	1	20	7	7	2033.5	0.014	
2033	4.2	2	48	7	7	2032.5	0.113	
2032	6.5	3	46	7	7	2031.5	0.127	
2031	3.7	0.5	14	7	7	2030.5	0.158	
2030	4.2	0.2	5	7	7	2029.5	0.158	
2029	2.2	0.5	23	7	7	2028.5	0.168	
2028	20.5	15	73	7	3	2027.5	0.130	
2027	8	5	63	7	7	2026.5	0.171	
2026	2.5	1.5	60	7	7	2025.5	0.189	
2025	1.4	0.2	14	7	7	2024.5	0.188	
2024	2.7	1.5	56	7	7	2023.5	0.184	
2023	0.7	0.2	29	7	7	2022.5	0.003	

bed#	Bt(cm)	St(cm)	S%	T.G	B.G	Posi.	D.Sq	Sq
2022	0.9	0.5	56	7	7	2021.5	0.000	
2021	2.7	0.2	7	7	7	2020.5	0.002	
2020	1	0.3	30	7	7	2019.5	0.003	
2019	4	3	75	7	7	2018.5	0.001	
2018	2.2	0.7	32	7	7	2017.5	0.000	
2017	3.2	1.2	38	7	7	2016.5	0.000	
2016	4.2	0.7	17	7	7	2015.5	0.001	
2015	7.2	0.5	7	7	7	2014.5	0.001	
2014	2.8	2.8	100	7	7	2013.5	0.005	
2013	1.5	0.2	13	7	7	2012.5	0.002	
2012	1.6	0.1	6	7	7	2011.5	0.001	
2011	2.8	0.3	11	7	7	2010.5	0.000	
2010	1.4	0.2	14	7	7	2009.5	0.000	
2009	3.5	0.5	14	7	7	2008.5	0.000	
2008	1.5	1	67	7	7	2007.5	0.000	
2007	1.5	0.7	47	7	7	2006.5	0.000	
2006	5	0.2	4	7	7	2005.5	0.000	
2005	4.8	0.3	6	7	7	2004.5	0.000	
2004	2.3	0.1	4	7	7	2003.5	0.006	
2003	1.3	1	77	7	7	2002.5	0.005	
2002	4.2	0.2	5	7	7	2001.5	0.007	
2001	6.5	1	15	7	7	2000.5	0.005	
2000	2.5	1	40	7	7	1999.5	0.004	
1999	9	4.5	50	7	7	1998.5	0.003	
1998	10.3	0.3	3	7	7	1997.5	0.000	
1997	4.5	0.5	11	7	7	1996.5	0.001	
1996	13	1	8	7	7	1995.5	0.001	
1995	8.2	1.2	15	7	7	1994.5	0.000	
1994	9.5	1	11	7	7	1993.5	0.002	
1993	5.5	2	36	7	7	1992.5	0.001	
1992	0.8	0.3	38	7	7	1991.5	0.004	
1991	3.5	0.5	14	7	7	1990.5	0.007	
1990	6	3	50	7	7	1989.5	0.000	
1989	2.7	1.5	56	7	7	1988.5	0.001	
1988	26.5	3	11	7	7	1987.5	0.000	
1987	5.5	2	36	7	7	1986.5	0.001	
1986	28.5	1	4	7	7	1985.5	0.000	
1985	4.4	0.8	18	7	7	1984.5	0.000	
1984	3.7	3	81	7	7	1983.5	0.002	
1983	2.5	1.5	60	7	7	1982.5	0.002	
1982	4.3	2	47	7	7	1981.5	0.004	
1981	4.3	2	47	7	7	1980.5	0.007	
1980	2	0.5	25	7	7	1979.5	0.002	
1979	13	0.5	4	7	7	1978.5	0.000	
1978	5.3	0.2	4	7	7	1977.5	0.000	
1977	2.3	1	43	7	7	1976.5	0.000	
1976	2.5	1.5	60	7	7	1975.5	0.000	
1975	3.5	3	86	7	7	1974.5	0.001	
1974	0.8	0.1	13	7	7	1973.5	0.000	
1973	0.8	0.2	25	7	7	1972.5	0.000	
1972	1.5	0.5	33	7	7	1971.5	0.000	
1971	5.1	0.3	6	7	7	1970.5	0.000	
1970	8.8	3	34	7	7	1969.5	0.001	
1969	4	1.5	38	7	7	1968.5	0.005	
1968	1.9	0.1	5	7	7	1967.5	0.003	
1967	5.5	0.2	4	7	7	1966.5	0.002	
1966	1.9	0.1	5	7	7	1965.5	0.002	
1965	8.4	0.1	1	7	7	1964.5	0.002	
1964	2.7	0.2	7	7	7	1963.5	0.008	
1963	3.2	1	31	7	7	1962.5	0.004	
1962	1.7	0.5	29	7	7	1961.5	0.003	

bed#	Bt(cm)	St(cm)	S%	T.G	B.G	Posi.	D.Sq	Sq
1961	1.1	0.1	9	7	7	1960.5	0.005	
1960	4.5	3	67	7	7	1959.5	0.000	
1959	3	2	67	7	7	1958.5	0.004	
1958	15.2	0.2	1	7	7	1957.5	0.003	
1957	25.1	0.1	0	7	7	1956.5	0.002	
1956	4.5	1.5	33	7	7	1955.5	0.007	
1955	1.2	0.2	17	7	7	1954.5	0.002	
1954	3.4	0.1	3	7	7	1953.5	0.000	
1953	2.4	0.4	17	7	7	1952.5	0.000	
1952	5.1	0.1	2	7	7	1951.5	0.000	
1951	6.7	0.2	3	7	7	1950.5	0.001	
1950	5.7	0.2	4	7	7	1949.5	0.001	
1949	8.8	0.3	3	7	7	1948.5	0.003	
1948	10.8	0.3	3	7	7	1947.5	0.008	
1947	5.3	1.8	34	7	7	1946.5	0.007	
1946	2.4	0.4	17	7	7	1945.5	0.006	
1945	9.4	0.4	4	7	7	1944.5	0.010	
1944	6.2	1.7	27	7	7	1943.5	0.032	
1943	6.3	3	48	7	7	1942.5	0.010	
1942	3.8	3	79	7	7	1941.5	0.003	
1941	2.8	0.1	4	7	7	1940.5	0.005	
1940	6	2	33	7	7	1939.5	0.006	
1939	9.5	8.5	89	7	7	1938.5	0.016	
1938	1.5	0.3	20	7	7	1937.5	0.002	
1937	1.5	1.2	80	7	7	1936.5	0.000	
1936	1.8	1	56	7	7	1935.5	0.000	
1935	5.2	4	77	7	7	1934.5	0.002	
1934	4.5	1.5	33	7	7	1933.5	0.002	
1933	7.7	3.5	45	7	7	1932.5	0.002	
1932	4.5	2.5	56	7	7	1931.5	0.010	
1931	6	3	50	7	7	1930.5	0.017	
1930	6	1.5	25	7	7	1929.5	0.012	
1929	3.2	0.7	22	7	7	1928.5	0.001	
1928	1.5	0.3	20	7	7	1927.5	0.001	
1927	1.1	0.1	9	7	7	1926.5	0.006	
1926	4	3	75	7	7	1925.5	0.002	
1925	1.7	0.5	29	7	7	1924.5	0.004	
1924	6.2	5.5	89	7	7	1923.5	0.007	
1923	27	1	4	7	7	1922.5	0.002	
1922	4	1	25	7	7	1921.5	0.105	
1921	3	0.5	17	7	7	1920.5	0.109	
1920	5	1	20	7	7	1919.5	0.107	
1919	1.3	0.3	23	7	7	1918.5	0.132	
1918	4.7	4	85	7	7	1917.5	0.123	
1917	7.5	5.5	73	7	3	1916.5	0.106	
1916	5	2	40	7	7	1915.5	0.106	
1915	2.6	0.6	23	7	7	1914.5	0.110	
1914	4.3	2.8	65	7	7	1913.5	0.105	
1913	7.5	5	67	7	7	1912.5	0.109	
1912	4.2	3	71	7	7	1911.5	0.001	
1911	6.5	3.5	54	7	7	1910.5	0.007	
1910	6	3	50	7	7	1909.5	0.022	
1909	1.1	0.1	9	7	7	1908.5	0.003	
1908	2.8	2	71	7	7	1907.5	0.007	
1907	4	3	75	7	7	1906.5	0.003	
1906	2.2	1	45	7	7	1905.5	0.016	
1905	2.5	1.3	52	7	7	1904.5	0.025	
1904	12	11	92	7	7	1903.5	0.017	
1903	2.3	1.1	48	7	7	1902.5	0.017	
1902	2.3	1.1	48	7	7	1901.5	0.008	
1901	4.2	3	71	7	7	1900.5	0.014	

bed#	Bt(cm)	St(cm)	S%	T.G	B.G	Posi.	D.Sq	Sq
1900	3.8	1.8	47	7	7	1899.5	0.013	
1899	3.8	2.5	66	7	7	1898.5	0.000	
1898	1.2	0.2	17	7	7	1897.5	0.008	
1897	3.4	2	59	7	7	1896.5	0.009	
1896	8	3	38	7	7	1895.5	0.007	
1895	4.2	2.5	60	7	7	1894.5	0.004	
1894	2	0.3	15	7	7	1893.5	0.012	
1893	17	7	41	7	7	1892.5	0.002	
1892	6	3	50	7	7	1891.5	0.007	
1891	4.5	2.5	56	7	7	1890.5	0.013	
1890	5.5	1.5	27	7	7	1889.5	0.013	
1889	15.5	1.5	10	7	7	1888.5	0.013	
1888	21.5	3.5	16	7	7	1887.5	0.010	
1887	6	1	17	7	7	1886.5	0.007	
1886	74.2	0.2	0	7	7	1885.5	0.002	
1885	3.7	0.5	14	7	7	1884.5	0.001	
1884	17.5	2.5	14	7	7	1883.5	0.007	
1883	6	1	17	7	7	1882.5	0.001	
1882	2.6	0.1	4	7	7	1881.5	0.002	
1881	4.6	0.3	7	7	7	1880.5	0.003	
1880	10.2	0.2	2	7	7	1879.5	0.008	
1879	5	0.5	10	7	7	1878.5	0.024	
1878	9	1.5	17	7	7	1877.5	0.016	
1877	10	5	50	7	7	1876.5	0.000	
1876	2	1	50	7	7	1875.5	0.000	
1875	10	2	20	7	7	1874.5	0.001	
1874	35	3	9	7	7	1873.5	0.010	
1873	20.2	0.2	1	7	7	1872.5	0.004	
1872	9	1	11	7	7	1871.5	0.000	
1871	6	2.5	42	7	7	1870.5	0.001	
1870	4	1	25	7	7	1869.5	0.002	
1869	3.7	1.2	32	7	7	1868.5	0.004	
1868	4.1	1.2	29	7	7	1867.5	0.005	
1867	5.5	2.5	45	7	7	1866.5	0.000	
1866	2.5	0.5	20	7	7	1865.5	0.433	
1865	12	5.5	46	7	7	1864.5	0.361	
1864	3.2	0.2	6	7	7	1863.5	0.387	
1863	4.5	3	67	7	7	1862.5	0.357	
1862	3.3	0.3	9	7	7	1861.5	0.372	
1861	25.3	20	79	3	0	1860.5	0.403	
1860	12	1	8	7	7	1859.5	0.363	
1859	12.5	3	24	7	7	1858.5	0.385	
1858	0.4	0.2	50	7	7	1857.5	0.333	
1857	1.7	0.5	29	7	7	1856.5	0.321	
1856	6.5	5	77	7	7	1855.5	0.293	
1855	4	2	50	7	7	1854.5	0.333	
1854	5	2.5	50	7	7	1853.5	1.029	
1853	12	7	58	7	7	1852.5	0.873	
1852	11	9	82	7	7	1851.5	1.812	*****
1851	10	10	100	7	1.5	1850.5	0.827	
1850	7.5	7	93	7	7	1849.5	1.876	
1849	16	10	63	7	1.5	1848.5	0.730	
1848	1.2	0.2	17	7	7	1847.5	1.783	
1847	10.8	10	93	7	1.5	1846.5	1.461	[109]
1846	19	16	84	7	1.5	1845.5	0.890	
1845	32	20	63	7	1.5	1844.5	0.221	
1844	32	22	69	7	3	1843.5	0.362	
1843	22	20	91	7	3	1842.5	2.079	
1842	31	28	90	1.5	1.5	1841.5	4.877	
1841	11.5	6	52	7	3	1840.5	5.358	*****
1840	3.7	0.2	5	7	7	1839.5	3.180	

bed#	Bt(cm)	St(cm)	S%	T.G	B.G	Posi.	D.Sq	Sq
1839	1.3	0.3	23	7	7	1838.5	1.759	
1838	2	1	50	7	7	1837.5	0.823	
1837	0.9	0.2	22	7	7	1836.5	0.109	
1836	2.4	1.5	63	7	7	1835.5	0.000	
1835	1.3	0.1	8	7	7	1834.5	0.000	
1834	1.5	1	67	7	7	1833.5	0.000	
1833	3	0.2	7	7	7	1832.5	0.245	
1832	2.3	0.3	13	7	7	1831.5	0.900	
1831	1.9	1.5	79	7	7	1830.5	0.926	
1830	1	0.3	30	7	7	1829.5	0.924	
1829	5	1.5	30	7	7	1828.5	0.905	
1828	18	14	78	7	1.5	1827.5	0.004	
1827	8	8	100	7	1.5	1826.5	0.877	
1826	17	4	24	7	7	1825.5	0.846	
1825	3.8	0.3	8	7	7	1824.5	0.846	
1824	14.2	0.2	1	7	7	1823.5	0.796	
1823	4	1	25	7	7	1822.5	0.523	
1822	21.2	0.2	1	7	7	1821.5	0.819	
1821	27.5	10.5	38	7	7	1820.5	0.428	
1820	1.2	0.2	17	7	7	1819.5	0.430	
1819	55	19	35	7	7	1818.5	0.010	
1818	57	22	39	7	7	1817.5	0.285	
1817	20	15	75	7	7	1816.5	0.685	
1816	54.1	0.1	0	7	7	1815.5	0.361	
1815	1.2	0.2	17	7	7	1814.5	0.338	
1814	1.2	0.4	33	7	7	1813.5	0.018	
1813	7.7	0.2	3	7	7	1812.5	0.061	
1812	11	10	91	7	7	1811.5	0.061	
1811	10	5	50	7	7	1810.5	0.030	
1810	10.5	1.5	14	7	7	1809.5	0.026	
1809	15.5	12	77	7	7	1808.5	0.025	
1808	6	4	67	7	7	1807.5	0.074	
1807	14.5	5	34	7	7	1806.5	0.062	
1806	16.5	5	30	7	7	1805.5	0.115	
1805	7	2	29	7	7	1804.5	0.120	
1804	12.5	2	16	7	7	1803.5	0.105	
1803	10.2	0.2	2	7	7	1802.5	0.110	
1802	24.5	1.5	6	7	7	1801.5	0.115	
1801	19	15	79	7	3	1800.5	0.172	
1800	4	1	25	7	7	1799.5	0.158	
1799	0.7	0.2	29	7	7	1798.5	0.133	
1798	1.8	1.3	72	7	7	1797.5	0.133	
1797	1.1	0.1	9	7	7	1796.5	0.119	
1796	0.8	0.6	75	7	7	1795.5	0.009	
1795	2.2	2	91	7	7	1794.5	0.004	
1794	9	2.5	28	7	7	1793.5	0.000	
1793	5	2.5	50	7	7	1792.5	0.001	
1792	4	2	50	7	7	1791.5	0.001	
1791	1.9	0.7	37	7	7	1790.5	0.000	
1790	1.5	0.5	33	7	7	1789.5	0.001	
1789	0.7	0.3	43	7	7	1788.5	0.004	
1788	2.3	2	87	7	7	1787.5	0.034	
1787	4.5	3.5	78	7	7	1786.5	0.027	
1786	5.5	2	36	7	7	1785.5	0.061	
1785	4	2	50	7	7	1784.5	0.061	
1784	4.5	0.5	11	7	7	1783.5	0.149	
1783	13.5	10	74	7	7	1782.5	0.027	
1782	8	3.5	44	7	7	1781.5	0.273	
1781	11	9	82	7	7	1780.5	0.867	
1780	7.5	3.5	47	7	7	1779.5	1.857	
1779	12.5	10	80	7	7	1778.5	1.782	

bed#	Bt(cm)	St(cm)	S%	T.G	B.G	Posi.	D.Sq	Sq
1778	23	3	13	7	7	1777.5	1.785	*****
1777	16	11	69	7	1.5	1776.5	0.221	
1776	25	16	64	1.5	1.5	1775.5	0.439	
1775	6.5	5	77	7	1.5	1774.5	1.167	
1774	6.7	0.5	7	7	7	1773.5	1.081	
1773	5.7	0.2	4	7	7	1772.5	1.048	
1772	5.2	4.5	87	7	7	1771.5	0.017	
1771	15.7	0.2	1	7	7	1770.5	0.230	
1770	49	14	29	3	3	1769.5	0.016	
1769	5.3	0.3	6	7	7	1768.5	0.017	
1768	15	3	20	7	7	1767.5	0.015	
1767	14	12	86	7	1.5	1766.5	0.681	
1766	16	5	31	7	7	1765.5	0.739	
1765	2.2	1	45	7	7	1764.5	0.203	[110]
1764	4.5	1.5	33	7	7	1763.5	0.198	
1763	2.5	1.5	60	7	7	1762.5	0.198	
1762	7.3	0.3	4	7	7	1761.5	0.312	
1761	14	4	29	7	7	1760.5	0.903	
1760	9	9	100	7	7	1759.5	0.686	
1759	9	7	78	7	7	1758.5	0.610	
1758	6	1	17	7	7	1757.5	1.271	
1757	24	19	79	3	3	1756.5	0.275	
1756	12	10	83	3	1.5	1755.5	0.460	
1755	1.1	0.1	9	7	7	1754.5	0.048	
1754	27	1	4	7	7	1753.5	0.019	
1753	34	10	29	3	3	1752.5	0.591	
1752	5.2	0.2	4	7	7	1751.5	0.143	
1751	0.5	0.2	40	7	7	1750.5	1.571	
1750	23	11	48	7	1.5	1749.5	0.105	
1749	3.5	0.5	14	7	7	1748.5	0.106	
1748	2.2	0.2	9	7	7	1747.5	0.453	
1747	29.7	29	98	3	0	1746.5	0.557	
1746	9	7	78	7	1.5	1745.5	2.539	*****
1745	3.7	0.2	5	7	7	1744.5	1.248	
1744	4.7	0.2	4	7	7	1743.5	1.233	
1743	22.2	0.2	1	7	7	1742.5	0.220	
1742	3	0.5	17	7	7	1741.5	0.093	
1741	5	3	60	7	7	1740.5	0.989	
1740	2	1	50	7	7	1739.5	0.968	
1739	6	1	17	7	7	1738.5	0.958	
1738	43	21	49	7	0	1737.5	0.041	
1737	62	1	2	7	7	1736.5	0.042	
1736	44	10	23	7	3	1735.5	0.273	
1735	15.2	0.2	1	7	7	1734.5	0.006	
1734	17	1	6	7	7	1733.5	0.011	
1733	17.5	14	80	3	1.5	1732.5	0.105	
1732	9.1	0.1	1	7	7	1731.5	0.108	
1731	0.5	0.2	40	7	7	1730.5	0.103	
1730	24	23	96	7	1.5	1729.5	0.386	
1729	15.5	3	19	7	7	1728.5	0.406	
1728	2.6	0.1	4	7	7	1727.5	0.020	
1727	5	3	60	7	7	1726.5	0.038	
1726	19	8	42	7	7	1725.5	0.161	
1725	9	7	78	7	3	1724.5	0.163	
1724	24.5	2.5	10	7	7	1723.5	0.171	
1723	9	1	11	7	7	1722.5	0.184	
1722	2.5	0.5	20	7	7	1721.5	0.166	
1721	1.8	0.3	17	7	7	1720.5	0.123	
1720	3.5	0.5	14	7	7	1719.5	0.001	
1719	4.5	1	22	7	7	1718.5	0.000	
1718	1.7	0.2	12	7	7	1717.5	0.000	

bed#	Bt(cm)	St(cm)	S%	T.G	B.G	Posi.	D.Sq	Sq
1717	2	0.3	15	7	7	1716.5	0.000	
1716	5.8	0.3	5	7	7	1715.5	0.000	
1715	4	1	25	7	7	1714.5	0.000	
1714	1.9	0.1	5	7	7	1713.5	0.000	
1713	4.5	2	44	7	7	1712.5	0.002	
1712	3.7	0.2	5	7	7	1711.5	0.002	
1711	1.1	0.1	9	7	7	1710.5	0.001	
1710	5.8	0.3	5	7	7	1709.5	0.001	
1709	7.2	0.2	3	7	7	1708.5	0.000	
1708	1.2	0.2	17	7	7	1707.5	0.000	
1707	5.1	0.1	2	7	7	1706.5	0.000	
1706	12.2	0.2	2	7	7	1705.5	0.001	
1705	1.3	0.3	23	7	7	1704.5	0.001	
1704	23	1	4	7	7	1703.5	0.000	
1703	1.4	0.4	29	7	7	1702.5	0.007	
1702	5.3	0.3	6	7	7	1701.5	0.014	
1701	5	1	20	7	7	1700.5	0.081	
1700	7.3	0.1	1	7	7	1699.5	0.109	
1699	1.3	0.1	8	7	7	1698.5	0.119	
1698	10	6	60	7	7	1697.5	0.035	
1697	9	3	33	7	7	1696.5	0.018	
1696	13	13	100	7	7	1695.5	0.043	
1695	5	3	60	7	7	1694.5	0.086	
1694	1.4	0.2	14	7	7	1693.5	0.076	
1693	3.5	1	29	7	7	1692.5	0.035	
1692	3.5	2	57	7	7	1691.5	0.035	
1691	7	2	29	7	7	1690.5	0.001	
1690	2.1	0.1	5	7	7	1689.5	0.000	
1689	2	1.5	75	7	7	1688.5	0.000	
1688	3	2	67	7	7	1687.5	0.002	
1687	1.3	1	77	7	7	1686.5	0.002	
1686	2	1	50	7	7	1685.5	0.001	
1685	2.3	1	43	7	7	1684.5	0.003	
1684	10.7	0.7	7	7	7	1683.5	0.001	
1683	5.7	0.7	12	7	7	1682.5	0.000	
1682	3.1	0.1	3	7	7	1681.5	0.000	
1681	3	0.5	17	7	7	1680.5	0.000	
1680	7	1	14	7	7	1679.5	0.000	
1679	2	1	50	7	7	1678.5	0.000	
1678	2	0.5	25	7	7	1677.5	0.000	
1677	4	1	25	7	7	1676.5	0.001	
1676	2.2	1	45	7	7	1675.5	0.002	
1675	3.3	0.3	9	7	7	1674.5	0.001	
1674	5.1	0.1	2	7	7	1673.5	0.000	
1673	1.6	0.1	6	7	7	1672.5	0.000	
1672	5.1	0.1	2	7	7	1671.5	0.000	
1671	1.7	0.7	41	7	7	1670.5	0.000	
1670	3	1	33	7	7	1669.5	0.000	
1669	2.6	0.1	4	7	7	1668.5	0.000	
1668	2.7	0.7	26	7	7	1667.5	0.000	
1667	1.1	0.3	27	7	7	1666.5	0.000	
1666	2	0.2	10	7	7	1665.5	0.000	
1665	2.3	0.3	13	7	7	1664.5	0.000	
1664	1.9	0.4	21	7	7	1663.5	0.000	
1663	4.3	0.1	2	7	7	1662.5	0.000	
1662	2.8	1	36	7	7	1661.5	0.001	
1661	8.8	0.3	3	7	7	1660.5	0.001	
1660	5.8	0.3	5	7	7	1659.5	0.001	
1659	2.9	0.2	7	7	7	1658.5	0.001	
1658	3.6	0.4	11	7	7	1657.5	0.002	
1657	12.5	3	24	7	7	1656.5	0.001	
1656	3.6	0.1	3	7	7	1655.5	0.001	
1655	3.4	0.7	21	7	7	1654.5	0.402	
1654	2.8	0.3	11	7	7	1653.5	0.411	
1653	21.6	0.8	4	7	7	1652.5	0.410	
1652	40.9	0.2	0	7	7	1651.5	0.455	
1651	19.3	0.3	2	7	7	1650.5	0.453	
1650	25.2	22	87	7	0	1649.5	0.387	
1649	17.5	1.5	9	7	7	1648.5	0.406	
1648	9.5	1	11	7	7	1647.5	0.399	
1647	8	2	25	7	7	1646.5	0.406	
1646	1.1	0.3	27	7	7	1645.5	0.396	
1645	14.5	1.5	10	7	7	1644.5	0.000	
1644	2.6	0.3	12	7	7	1643.5	0.003	
1643	12	2	17	7	7	1642.5	0.000	
1642	8.5	3	35	7	7	1641.5	0.001	
1641	3.5	1.5	43	7	7	1640.5	0.005	
1640	1.5	0.5	33	7	7	1639.5	0.007	
1639	2.5	1.5	60	7	7	1638.5	0.008	
1638	4.9	1	20	7	7	1637.5	0.014	
1637	0.5	0.2	40	7	7	1636.5	0.262	
1636	13.5	10	74	7	7	1635.5	0.149	
1635	2.7	0.2	7	7	7	1634.5	1.064	
1634	5.4	3	56	7	7	1633.5	2.643	
1633	3	2	67	7	7	1632.5	2.713	
1632	26.4	24	91	7	7	1631.5	2.911	
1631	11	10	91	7	7	1630.5	2.771	
1630	37	32	86	3	0	1629.5	0.314	
1629	35	25	71	3	0	1628.5	1.521	
1628	5	5	100	7	7	1627.5	1.068	
1627	12.2	11	90	7	1.5	1626.5	2.965	
1626	3	2	67	7	7	1625.5	1.819	
1625	25.5	5	20	7	7	1624.5	0.133	
1624	3.5	1	29	7	7	1623.5	0.495	
1623	28	25	89	7	7	1622.5	0.289	
1622	7	3.5	50	7	7	1621.5	0.944	
1621	13.5	7	52	7	3	1620.5	0.105	
1620	13	13	100	0	3	1619.5	0.168	
1619	11.5	7	61	7	3	1618.5	1.103	
1618	9	6	67	7	7	1617.5	0.164	
1617	6.5	1	15	7	7	1616.5	0.165	
1616	17	14	82	7	7	1615.5	0.079	
1615	6.5	4.5	69	7	7	1614.5	0.101	
1614	6	3	50	7	7	1613.5	0.331	
1613	19	14	74	7	0	1612.5	0.161	
1612	29	1	3	7	7	1611.5	0.276	
1611	12.3	0.3	2	7	7	1610.5	0.591	
1610	2.4	0.4	17	7	7	1609.5	0.595	
1609	8	6	75	7	7	1608.5	0.594	
1608	7	3	43	3	1.5	1607.5	0.204	
1607	9.5	8	84	3	0	1606.5	0.492	
1606	26.3	4	15	7	3	1605.5	1.843	
1605	4.5	2	44	7	7	1604.5	1.829	
1604	15	1	7	7	7	1603.5	1.805	
1603	6	1	17	7	7	1602.5	0.806	
1602	7.5	0.5	7	7	7	1601.5	0.105	
1601	4.8	0.3	6	7	7	1600.5	0.005	
1600	8.5	5.5	65	7	7	1599.5	0.003	
1599	6.5	0.5	8	7	7	1598.5	0.003	
1598	6	1.2	20	7	7	1597.5	0.005	
1597	2	1	50	7	7	1596.5	0.004	
1596	10.5	1.5	14	7	7	1595.5	0.010	

bed#	Bt(cm)	St(cm)	S%	T.G	B.G	Posi.	D.Sq	Sq
1595	9.7	0.2	2	7	7	1594.5	0.000	
1594	80.2	0.2	0	7	7	1593.5	0.000	
1593	9.3	0.3	3	7	7	1592.5	0.000	
1592	3.6	1.8	50	7	7	1591.5	0.001	
1591	43.3	0.3	1	7	7	1590.5	0.003	
1590	60	1	2	7	7	1589.5	0.001	
1589	6.5	1	15	7	7	1588.5	0.000	
1588	5	0.5	10	7	7	1587.5	0.000	
1587	23	3	13	7	7	1586.5	0.003	
1586	9	1	11	7	7	1585.5	0.006	
1585	3	0.5	17	7	7	1584.5	0.006	
1584	79.2	0.2	0	7	7	1583.5	0.004	
1583	55.1	0.1	0	7	7	1582.5	0.001	
1582	1.4	0.2	14	7	7	1581.5	0.001	
1581	10.2	0.2	2	7	7	1580.5	0.242	
1580	1.2	0.2	17	7	7	1579.5	0.917	
1579	2.2	0.2	9	7	7	1578.5	0.948	
1578	22	2	9	7	7	1577.5	0.916	
1577	71	2	3	7	7	1576.5	0.888	
1576	78	11	14	7	1.5	1575.5	0.000	
1575	27	9.5	35	7	1.5	1574.5	0.865	
1574	9.5	3	32	7	7	1573.5	0.880	
1573	12.5	1	8	7	7	1572.5	0.856	
1572	6	1	17	7	7	1571.5	0.841	
1571	1.7	0.5	29	7	7	1570.5	0.202	
1570	4	1	25	7	7	1569.5	0.007	
1569	14.8	4	27	7	7	1568.5	0.248	
1568	4.5	3	67	7	7	1567.5	1.422	
1567	21.5	2	9	7	7	1566.5	1.495	
1566	4.5	1	22	7	7	1565.5	2.200	
1565	12	2	17	7	7	1564.5	4.410	*****
1564	40	25	63	7	3	1563.5	1.352	
1563	39.8	33	83	3	0	1562.5	0.112	
1562	9	6	67	7	7	1561.5	0.156	
1561	30	25	83	7	7	1560.5	0.929	
1560	28	25	89	3	0	1559.5	4.603	
1559	5	0.3	6	7	7	1558.5	2.720	
1558	2	1	50	7	7	1557.5	0.782	
1557	0.8	0.5	63	7	7	1556.5	0.661	
1556	4.9	3	61	7	7	1555.5	0.366	
1555	5	3	60	7	7	1554.5	0.017	
1554	2.2	1	45	7	7	1553.5	0.314	
1553	12.7	4	31	7	7	1552.5	0.255	[111]
1552	3.5	1.5	43	7	7	1551.5	0.259	
1551	16.7	6	36	7	7	1550.5	1.116	
1550	7.5	4	53	7	7	1549.5	1.095	
1549	17	16	94	7	1.5	1548.5	0.049	
1548	4.3	0.1	2	7	7	1547.5	0.015	
1547	9.7	3	31	7	7	1546.5	0.017	
1546	14.2	13	92	7	0	1545.5	1.103	
1545	3.2	2.5	78	7	7	1544.5	1.066	
1544	2.5	0.5	20	7	7	1543.5	0.376	
1543	11	8.5	77	7	7	1542.5	0.285	
1542	2.5	1.5	60	7	7	1541.5	0.416	
1541	6.5	4	62	7	7	1540.5	0.871	
1540	18	6	33	7	7	1539.5	2.129	
1539	16	15	94	7	7	1538.5	3.470	
1538	38.5	37	96	7	0	1537.5	0.352	
1537	10.5	7.5	71	7	7	1536.5	0.458	
1536	3	1.5	50	7	7	1535.5	0.427	
1535	30.5	21.5	70	7	0	1534.5	1.036	

bed#	Bt(cm)	St(cm)	S%	T.G	B.G	Posi.	D.Sq	Sq
1534	40	19	48	7	0	1533.5	4.288	*****
1533	2	2	100	7	7	1532.5	1.759	
1532	8.5	0.5	6	7	7	1531.5	1.584	
1531	18	2	11	7	7	1530.5	1.618	
1530	6.8	2	29	7	7	1529.5	0.409	
1529	7.2	0.2	3	7	7	1528.5	0.000	
1528	25.3	0.3	1	7	7	1527.5	0.000	
1527	8.5	3	35	7	7	1526.5	0.005	
1526	28.5	0.5	2	7	7	1525.5	0.003	
1525	65.5	1.5	2	7	7	1524.5	0.004	
1524	3.2	0.2	6	7	7	1523.5	0.003	
1523	3.7	0.2	5	7	7	1522.5	0.001	
1522	6.2	0.2	3	7	7	1521.5	0.000	
1521	8.7	0.2	2	7	7	1520.5	0.001	
1520	1.9	0.4	21	7	7	1519.5	0.002	
1519	1.6	1	63	7	7	1518.5	0.357	
1518	2	1	50	7	7	1517.5	0.342	
1517	3.2	0.7	22	7	7	1516.5	0.346	
1516	5	1	20	7	7	1515.5	0.348	
1515	6.2	0.2	3	7	7	1514.5	0.927	
1514	30.3	26	86	7	1.5	1513.5	0.040	
1513	3	0.5	17	7	7	1512.5	0.035	
1512	4	1.5	38	7	7	1511.5	0.044	
1511	7	2	29	7	7	1510.5	0.058	
1510	21	13	62	3	3	1509.5	0.934	
1509	8.7	1.2	14	7	7	1508.5	1.080	
1508	5	1	20	7	7	1507.5	2.028	
1507	1.5	0.5	33	7	7	1506.5	2.177	
1506	1.5	0.5	33	7	7	1505.5	4.266	
1505	5.3	0.3	6	7	7	1504.5	10.759	*****
1504	84.5	84	99	3	0	1503.5	0.708	
1503	34	28	82	7	7	1502.5	0.478	
1502	17.5	3	17	7	7	1501.5	0.450	[112]
1501	33	29	88	7	0	1500.5	0.523	
1500	69	67	97	7	7	1499.5	5.990	
1499	34	16	47	7	7	1498.5	2.558	
1498	27	25	93	7	0	1497.5	4.629	*****
1497	3	3	100	7	7	1496.5	4.683	
1496	8	3	38	7	7	1495.5	2.535	
1495	4.2	3.5	83	7	7	1494.5	0.639	
1494	1.2	0.7	58	7	7	1493.5	0.074	
1493	6.7	6.5	97	7	7	1492.5	0.684	
1492	2.5	2	80	7	7	1491.5	0.724	
1491	2	1	50	7	7	1490.5	0.737	
1490	3.8	2.3	61	7	7	1489.5	0.748	
1489	17.5	15	86	7	3	1488.5	0.198	
1488	35.5	17	48	3	1.5	1487.5	0.331	
1487	7	5	71	7	7	1486.5	0.418	
1486	7.2	0.2	3	7	7	1485.5	0.396	
1485	4	2	50	7	7	1484.5	0.415	
1484	16.5	4	24	7	3	1483.5	0.720	
1483	11.5	1.5	13	7	7	1482.5	0.127	
1482	25	1	4	7	7	1481.5	0.115	
1481	5.5	1	18	7	7	1480.5	0.120	
1480	14.3	0.3	2	7	7	1479.5	0.115	
1479	0.7	0.2	29	7	7	1478.5	0.001	
1478	28.2	0.2	1	7	7	1477.5	0.000	
1477	12.2	0.2	2	7	7	1476.5	0.000	
1476	7.2	0.2	3	7	7	1475.5	0.001	
1475	30.7	0.2	1	7	7	1474.5	0.002	
1474	6	1	17	7	7	1473.5	0.003	

bed#	Bt(cm)	St(cm)	S%	T.G	B.G	Posi.	D.Sq	Sq
1473	1.2	0.5	42	7	7	1472.5	0.830	
1472	8	1	13	7	7	1471.5	2.278	
1471	7.7	0.2	3	7	7	1470.5	3.086	
1470	3.5	1	29	7	7	1469.5	4.231	
1469	3.5	3	86	7	7	1468.5	6.703	*****
1468	53	45	85	3	0	1467.5	2.056	
1467	51	48	94	7	7	1466.5	0.321	[113]
1466	21	18	86	7	7	1465.5	0.560	
1465	26	23	88	7	7	1464.5	1.399	
1464	86	42	49	7	7	1463.5	5.141	*****
1463	21	8	38	7	7	1462.5	3.106	
1462	9.5	7	74	7	7	1461.5	1.545	
1461	2.3	2	87	7	7	1460.5	1.087	
1460	25	8	32	7	7	1459.5	0.886	
1459	11	3	27	7	7	1458.5	0.224	
1458	0.7	0.2	29	7	7	1457.5	0.157	
1457	12	1	8	7	7	1456.5	0.128	
1456	4	3	75	7	3	1455.5	0.148	
1455	1.2	0.2	17	7	7	1454.5	0.112	
1454	2.3	0.3	13	7	7	1453.5	0.107	
1453	4.3	0.3	7	7	7	1452.5	0.093	
1452	5.2	0.2	4	7	7	1451.5	0.100	
1451	1.2	0.2	17	7	7	1450.5	1.175	
1450	18.6	0.6	3	7	7	1449.5	2.395	
1449	21.2	0.2	1	7	7	1448.5	4.645	*****
1448	23	16	70	3	0	1447.5	1.914	
1447	8.7	0.7	8	7	7	1446.5	3.357	
1446	19	10	53	3	1.5	1445.5	1.835	
1445	10	10	100	3	1.5	1444.5	0.201	
1444	15	15	100	3	0	1443.5	0.708	
1443	8	6	75	7	1.5	1442.5	0.382	[114]
1442	7.5	6	80	7	1.5	1441.5	1.094	
1441	7.5	6	80	7	1.5	1440.5	1.033	
1440	7.5	0.5	7	7	7	1439.5	0.323	
1439	2	0.5	25	7	7	1438.5	0.071	
1438	13	12	92	3	1.5	1437.5	0.199	
1437	11	10	91	3	1.5	1436.5	0.823	
1436	16	13	81	3	1.5	1435.5	2.002	*****
1435	7	1.5	21	7	7	1434.5	2.030	
1434	10.5	0.5	5	7	7	1433.5	2.035	
1433	4.5	2	44	7	7	1432.5	0.431	
1432	1	0.2	20	7	7	1431.5	0.043	
1431	1.2	0.2	17	7	7	1430.5	0.107	
1430	16.5	0.5	3	7	7	1429.5	0.110	
1429	4.2	0.2	5	7	7	1428.5	0.112	
1428	21.5	3.5	16	7	3	1427.5	0.105	
1427	3	1.5	50	7	7	1426.5	0.105	
1426	14	2	14	7	7	1425.5	0.111	
1425	5	1	20	7	7	1424.5	0.114	
1424	4	1	25	7	7	1423.5	0.118	
1423	12.1	0.1	1	7	7	1422.5	0.003	
1422	1.1	0.1	9	7	7	1421.5	0.368	
1421	1.1	0.1	9	7	7	1420.5	0.388	
1420	1	0.5	50	7	7	1419.5	0.409	
1419	12.3	0.3	2	7	7	1418.5	0.422	
1418	9	1	11	7	7	1417.5	0.409	
1417	60.5	17	28	3	0	1416.5	0.363	
1416	3	1	33	7	7	1415.5	0.368	
1415	64.5	2.5	4	7	7	1414.5	0.399	
1414	24	1	4	7	7	1413.5	0.006	
1413	15.5	0.5	3	7	7	1412.5	0.265	

bed#	Bt(cm)	St(cm)	S%	T.G	B.G	Posi.	D.Sq	Sq
1412	1.1	0.1	9	7	7	1411.5	3.028	
1411	19	1	5	7	7	1410.5	3.056	
1410	2.3	0.3	13	7	7	1409.5	3.218	*****
1409	52.5	26	50	3	0	1408.5	1.191	
1408	15	12	80	3	1.5	1407.5	0.091	
1407	44	30	68	3	1.5	1406.5	0.117	
1406	25	2	8	7	7	1405.5	0.212	
1405	9.5	3.5	37	7	7	1404.5	1.548	
1404	25	23	92	3	0	1403.5	0.509	[115]
1403	5	1.2	24	7	7	1402.5	2.555	
1402	34	32	94	3	0	1401.5	1.851	
1401	38	37	97	3	0	1400.5	0.058	
1400	46.5	44	95	1.5	0	1399.5	3.427	
1399	3.5	1.5	43	7	7	1398.5	1.667	
1398	22	12	55	3	0	1397.5	5.000	
1397	23	18	78	3	0	1396.5	7.118	*****
1396	14	5	36	7	7	1395.5	1.671	
1395	31.5	2	6	7	7	1394.5	0.321	
1394	6.5	0.5	8	7	7	1393.5	0.321	
1393	7.5	3	40	7	7	1392.5	0.006	
1392	10	7	70	7	7	1391.5	0.345	
1391	27.5	26	95	3	0	1390.5	0.143	
1390	5.3	0.3	6	7	7	1389.5	0.130	
1389	5.3	0.3	6	7	7	1388.5	0.116	
1388	1.3	0.3	23	7	7	1387.5	0.010	
1387	4	1	25	7	7	1386.5	0.011	
1386	19	17	89	3	3	1385.5	0.595	
1385	0.7	0.2	29	7	7	1384.5	3.492	
1384	8	2	25	7	7	1383.5	4.478	
1383	15	10	67	3	3	1382.5	3.136	
1382	6	3	50	7	7	1381.5	4.051	*****
1381	53	39	74	3	0	1380.5	1.998	
1380	71.5	65	91	3	0	1379.5	0.715	
1379	25.5	24	94	7	7	1378.5	2.025	[116]
1378	19	14	74	2	7	1377.5	2.522	
1377	14.5	10.5	72	1.5	1.5	1376.5	4.645	
1376	30	28	93	1.5	1.5	1375.5	4.892	*****
1375	4.2	0.2	5	7	7	1374.5	0.737	
1374	1.3	0.3	23	7	7	1373.5	0.130	
1373	2.2	0.2	9	7	7	1372.5	0.448	
1372	2.7	0.2	7	7	7	1371.5	2.658	
1371	9	8	89	7	1.5	1370.5	4.076	*****
1370	15	12.5	83	7	4.5	1369.5	4.355	
1369	13	12	92	1.5	1.5	1368.5	3.035	
1368	22.5	18	80	1.5	1.5	1367.5	1.558	
1367	21.5	15	70	1.5	1.5	1366.5	0.856	
1366	34	29	85	3	0	1365.5	0.030	
1365	18	16	89	3	0	1364.5	0.154	
1364	17	15	88	3	0	1363.5	0.212	
1363	23	21	91	1.5	1.5	1362.5	0.476	
1362	24	23	96	3	0	1361.5	0.993	
1361	13.1	0.1	1	7	7	1360.5	2.895	
1360	17	16	94	3	0	1359.5	2.391	
1359	27	25	93	3	0	1358.5	1.400	
1358	73	73	100	3	0	1357.5	0.482	
1357	52	50	96	3	0	1356.5	2.269	
1356	16	16	100	3	0	1355.5	3.484	
1355	26.5	15	57	7	7	1354.5	1.666	[117]
1354	7.5	5	67	7	7	1353.5	1.998	
1353	25	24	96	3	0	1352.5	1.286	
1352	17	10	59	3	0	1351.5	1.729	

bed#	Bt(cm)	St(cm)	S%	T.G	B.G	Posi.	D.Sq	Sq
1351	26	26	100	3	0	1350.5	0.347	
1350	27	27	100	3	0	1349.5	0.088	
1349	15	15	100	3	0	1348.5	1.690	
1348	28	28	100	3	0	1347.5	4.101	
1347	21	19	90	3	0	1346.5	4.564	
1346	5	2	40	7	7	1345.5	0.813	
1345	9.4	8	85	3	0	1344.5	0.501	[117]
1344	4	2	50	7	7	1343.5	0.283	
1343	1.7	0.7	41	7	7	1342.5	3.211	
1342	19	15	79	3	0	1341.5	2.839	
1341	21	18	86	3	0	1340.5	1.940	
1340	29	25	86	1.5	1.5	1339.5	1.672	
1339	22	20	91	3	0	1338.5	0.074	
1338	15	11	73	3	0	1337.5	1.576	
1337	31	23	74	3	3	1336.5	1.918	
1336	44	43	98	3	0	1335.5	5.393	
1335	19	18	95	7	0	1334.5	8.855	*****
1334	1.1	0.1	9	7	7	1333.5	5.365	
1333	2.5	1	40	7	7	1332.5	3.048	
1332	44	10	23	7	7	1331.5	1.747	
1331	53	3	6	7	7	1330.5	1.433	
1330	4	2	50	7	7	1329.5	7.298	
1329	24	3	13	7	7	1328.5	6.848	
1328	13.2	2.2	17	7	7	1327.5	6.602	
1327	23	16	70	7	7	1326.5	5.045	
1326	81	80	99	7	7	1325.5	0.092	
1325	99	97	98	7	7	1324.5	5.536	
1324	1.2	0.2	17	7	7	1323.5	3.489	
1323	0.7	0.2	29	7	7	1322.5	3.025	
1322	0.4	0.2	50	7	7	1321.5	2.244	
1321	32	26	81	7	7	1320.5	0.810	
1320	15	13	87	7	7	1319.5	0.225	
1319	33.5	32	96	7	3	1318.5	0.455	
1318	38	7	18	7	7	1317.5	0.693	
1317	8.5	1	12	7	7	1316.5	0.341	
1316	19.5	14	72	7	7	1315.5	0.372	
1315	10.5	9	86	7	7	1314.5	0.390	
1314	1.2	0.5	42	7	7	1313.5	0.220	
1313	3	2	67	7	7	1312.5	0.202	
1312	92	15	16	1.5	1.5	1311.5	0.348	
1311	6.7	0.2	3	7	7	1310.5	0.012	
1310	6.5	4	62	7	7	1309.5	1.058	
1309	5.2	0.2	4	7	7	1308.5	2.294	
1308	7	3	43	7	7	1307.5	2.842	
1307	10	7	70	7	7	1306.5	3.607	
1306	21	20	95	7	1.5	1305.5	1.384	
1305	54	54	100	7	1.5	1304.5	0.921	
1304	35	35	100	7	7	1303.5	2.716	
1303	18	16	89	7	7	1302.5	3.104	
1302	3.5	2.5	71	7	7	1301.5	1.261	
1301	23	6	26	7	7	1300.5	0.695	
1300	1.5	0.5	33	7	7	1299.5	0.804	
1299	1.5	0.5	33	7	7	1298.5	2.460	

bed#	Bt(cm)	St(cm)	S%	T.G	B.G	Posi.	D.Sq	Sq
1298	43	20	47	7	7	1297.5	3.822	*****
1297	59	31	53	7	1.5	1296.5	0.795	
1296	21	14	67	3	1.5	1295.5	0.232	
1295	4.5	2	44	7	7	1294.5	0.814	
1294	38	14	37	3	1.5	1293.5	0.300	
1293	38	23	61	1.5	1.5	1292.5	0.361	
1292	7.5	1.5	20	7	7	1291.5	0.795	[118]
1291	19	13	68	1.5	1.5	1290.5	0.595	
1290	9.5	6	63	1.5	1.5	1289.5	0.057	
1289	18	16	89	1.5	1.5	1288.5	0.130	
1288	7	7	100	7	1.5	1287.5	0.477	
1287	9	9	100	1.5	1.5	1286.5	2.568	
1286	16	11	69	3	3	1285.5	2.200	
1285	19	6	32	3	3	1284.5	1.195	*****
1284	8.5	8.5	100	7	7	1283.5	0.420	
1283	4.5	4.5	100	7	7	1282.5	0.041	
1282	7.5	2	27	7	7	1281.5	0.074	
1281	12	9	75	3	3	1280.5	0.150	
1280	30.5	28	92	3	0	1279.5	0.112	
1279	15.2	0.2	1	7	7	1278.5	0.007	
1278	1.7	0.2	12	7	7	1277.5	0.008	
1277	7	3	43	7	7	1276.5	0.007	
1276	21	19	90	3	3	1275.5	0.253	
1275	26	14	54	3	3	1274.5	0.100	
1274	54	6	11	3	3	1273.5	0.468	
1273	17.7	0.2	1	7	7	1272.5	0.416	
1272	16.2	0.2	1	7	7	1271.5	0.353	
1271	5.8	0.3	5	7	7	1270.5	0.018	
1270	13	10	77	7	1.5	1269.5	0.025	
1269	16	2	13	7	7	1268.5	0.318	
1268	5.7	4.5	79	7	7	1267.5	0.738	
1267	9	4	44	7	7	1266.5	1.381	*****
1266	6.5	4	62	3	3	1265.5	0.283	
1265	18	9	50	3	3	1264.5	0.435	
1264	6	5	83	3	3	1263.5	0.000	[119]
1263	14.5	3.5	24	3	3	1262.5	0.419	
1262	8	4	50	3	3	1261.5	1.682	
1261	20	8.5	43	7	7	1260.5	1.008	
1260	21	11	52	3	3	1259.5	1.862	*****
1259	4.2	0.2	5	7	7	1258.5	1.059	
1258	2.3	0.3	13	7	7	1257.5	0.483	
1257	2	0.2	10	7	7	1256.5	0.141	
1256	4.5	1	22	7	7	1255.5	0.112	
1255	12.7	1.2	9	7	7	1254.5	0.003	
1254	5.5	1.5	27	7	7	1253.5	0.000	
1253	6.5	3	46	7	7	1252.5	0.004	
1252	0.7	0.7	100	7	7	1251.5	0.006	
1251	0.7	0.7	100	7	7	1250.5	0.105	
1250	0.7	0.7	100	7	7	1249.5	0.438	
1249	6.3	0.3	5	7	7	1248.5	0.446	
1248	2.3	0.3	13	7	7	1247.5	0.464	
1247	0.9	0.2	22	7	7	1246.5	0.475	
1246	6.5	6	92	3	3	1245.5	0.006	
1245	29	9	31	3	3	1244.5	0.446	
1244	12	1	8	7	7	1243.5	0.454	
1243	4.8	0.8	17	7	7	1242.5	0.460	
1242	5.3	1.3	25	7	7	1241.5	0.468	
1241	24.4	0.4	2	7	7	1240.5	0.125	
1240	19.2	1.2	6	7	7	1239.5	0.001	
1239	2.2	0.2	9	7	7	1238.5	0.000	
1238	21.3	0.3	1	7	7	1237.5	0.000	

bed#	Bt(cm)	St(cm)	S%	T.G	B.G	Posi.	D.Sq	Sq
1237	8.5	1	12	7	7	1236.5	0.000	
1236	5.2	0.2	4	7	7	1235.5	0.403	
1235	19	1	5	7	7	1234.5	0.393	
1234	11.7	0.2	2	7	7	1233.5	0.404	
1233	20	2	10	7	7	1232.5	1.034	
1232	27.2	1.2	4	7	7	1231.5	1.030	
1231	37	29	78	7	1.5	1230.5	0.022	
1230	21.1	0.1	0	7	7	1229.5	0.166	
1229	4	1	25	7	7	1228.5	1.160	
1228	19	18	95	3	3	1227.5	0.823	
1227	5.2	1.2	23	7	7	1226.5	0.913	
1226	29	19	66	7	7	1225.5	2.853	*****
1225	21	10	48	7	1.5	1224.5	2.495	
1224	29	26	90	1.5	0	1223.5	0.226	
1223	35	33	94	1.5	1.5	1222.5	0.059	
1222	19	6	32	7	7	1221.5	0.041	[120]
1221	24	22	92	3	3	1220.5	0.000	
1220	70	44	63	1.5	1.5	1219.5	1.496	
1219	32.2	0.2	1	7	7	1218.5	0.547	
1218	94	17	18	3	1.5	1217.5	0.627	
1217	23	10	43	7	1.5	1216.5	2.297	
1216	36	25	69	1.5	1.5	1215.5	4.728	*****
1215	18.5	2	11	7	7	1214.5	0.820	
1214	17	2	12	7	7	1213.5	0.468	
1213	8.5	1.5	18	7	7	1212.5	0.740	
1212	14.5	1.5	10	7	7	1211.5	1.142	
1211	14	5	36	7	7	1210.5	2.236	
1210	52	33	63	1.5	1.5	1209.5	0.066	
1209	53	50	94	1.5	1.5	1208.5	2.200	
1208	41	9	22	7	7	1207.5	2.812	
1207	5.5	0.5	9	7	7	1206.5	2.283	
1206	6.5	0.5	8	7	7	1205.5	2.131	
1205	3.3	0.3	9	7	7	1204.5	0.640	
1204	3.7	0.7	19	7	7	1203.5	0.005	
1203	3.2	0.7	22	7	7	1202.5	0.040	
1202	15	13	87	7	7	1201.5	0.030	
1201	2.3	0.3	13	7	7	1200.5	0.029	
1200	1.1	0.8	73	7	7	1199.5	0.034	
1199	4	1	25	7	7	1198.5	0.039	
1198	4	1	25	7	7	1197.5	0.431	
1197	7	0.5	7	7	7	1196.5	0.662	
1196	1.3	0.3	23	7	7	1195.5	0.664	
1195	3.8	0.3	8	7	7	1194.5	0.676	
1194	2.4	0.4	17	7	7	1193.5	0.698	
1193	62	37	60	7	0	1192.5	0.536	
1192	57	5	9	7	7	1191.5	0.678	
1191	14.4	0.4	3	7	7	1190.5	0.669	
1190	3.5	0.5	14	7	7	1189.5	0.675	
1189	2	1	50	7	7	1188.5	0.700	
1188	1	0.3	30	7	7	1187.5	0.003	
1187	1.5	0.5	33	7	7	1186.5	0.000	
1186	4	1	25	7	7	1185.5	0.000	
1185	1.9	0.4	21	7	7	1184.5	0.000	
1184	3.7	0.2	5	7	7	1183.5	0.000	
1183	3.5	1.5	43	7	7	1182.5	0.000	
1182	1.5	0.2	13	7	7	1181.5	0.001	
1181	7	0.5	7	7	7	1180.5	0.001	
1180	0.4	0.2	50	7	7	1179.5	0.256	
1179	3.8	0.8	21	7	7	1178.5	0.248	
1178	15	1	7	7	7	1177.5	0.884	
1177	10.5	2.5	24	7	7	1176.5	0.886	

bed#	Bt(cm)	St(cm)	S%	T.G	B.G	Posi.	D.Sq	Sq
1176	3	0.5	17	7	7	1175.5	0.891	
1175	40	14	35	7	1.5	1174.5	0.007	
1174	12.2	0.2	2	7	7	1173.5	0.004	
1173	16	6	38	7	1.5	1172.5	0.830	
1172	12.5	5	40	7	7	1171.5	0.877	
1171	21	1	5	7	7	1170.5	0.886	
1170	30	1	3	7	7	1169.5	0.209	
1169	2.5	1	40	7	7	1168.5	0.213	
1168	18	2	11	7	7	1167.5	0.007	
1167	2	1	50	7	7	1166.5	0.002	
1166	23.5	0.5	2	7	7	1165.5	0.001	
1165	7.5	1.5	20	7	7	1164.5	0.003	
1164	7.7	0.7	9	7	7	1163.5	0.014	
1163	3.5	0.5	14	7	7	1162.5	0.022	
1162	34.1	0.1	0	7	7	1161.5	0.028	
1161	53	1	2	7	7	1160.5	0.031	
1160	7.6	0.1	1	7	7	1159.5	0.044	
1159	22.5	12	53	7	7	1158.5	0.002	
1158	7	1	14	7	7	1157.5	0.003	
1157	6.5	0.5	8	7	7	1156.5	0.202	
1156	4	2	50	7	7	1155.5	0.844	
1155	20	1	5	7	7	1154.5	2.383	
1154	10.5	6	57	7	7	1153.5	2.547	
1153	3.5	1	29	7	7	1152.5	2.556	*****
1152	26	9	35	1.5	1.5	1151.5	0.493	
1151	22.5	14	62	3	1.5	1150.5	0.086	
1150	41	21	51	3	0	1149.5	1.138	
1149	10	9.5	95	7	7	1148.5	0.417	
1148	2.5	1.5	60	7	7	1147.5	0.020	
1147	10.5	1	10	7	7	1146.5	0.671	
1146	19	16	84	1.5	1.5	1145.5	0.689	[121]
1145	1.6	0.1	6	7	7	1144.5	3.807	
1144	25	15	60	1.5	1.5	1143.5	1.988	
1143	24.5	18	73	7	1.5	1142.5	1.236	
1142	31	17	55	7	1.5	1141.5	0.334	
1141	21	20	95	7	1.5	1140.5	0.001	
1140	12.5	12	96	7	1.5	1139.5	0.889	
1139	17	15	88	7	3	1138.5	1.475	
1138	34	31	91	7	0	1137.5	4.466	
1137	14.5	13	90	7	1.5	1136.5	6.316	*****
1136	67	1	1	7	7	1135.5	3.976	
1135	10	1	10	7	7	1134.5	2.339	
1134	13.2	0.2	2	7	7	1133.5	1.288	
1133	33	3	9	7	7	1132.5	0.217	
1132	9	7	78	7	7	1131.5	0.021	
1131	24.2	0.2	1	7	7	1130.5	0.001	
1130	5.3	0.3	6	7	7	1129.5	0.243	
1129	12	1	8	7	7	1128.5	0.234	
1128	11.3	0.3	3	7	7	1127.5	2.107	

bed#	Bt(cm)	St(cm)	S%	T.G	B.G	Posi.	D.Sq	Sq
1127	1.7	0.7	41	7	7	1126.5	2.321	*****
1126	25	7	28	7	7	1125.5	2.040	
1125	19	16	84	7	1.5	1124.5	1.025	
1124	8.3	0.3	4	7	7	1123.5	1.063	
1123	85	55	65	7	0	1122.5	0.929	
1122	22	1	5	7	7	1121.5	0.905	
1121	8	5	63	7	7	1120.5	0.961	[122]
1120	29	25	86	3	3	1119.5	1.219	
1119	2	1	50	7	7	1118.5	1.210	
1118	7	1.5	21	7	7	1117.5	0.321	
1117	4.5	2.5	56	7	7	1116.5	0.323	
1116	0.7	0.2	29	7	7	1115.5	0.321	
1115	22.5	13	58	7	1.5	1114.5	0.000	
1114	12	2	17	7	7	1113.5	0.000	
1113	29	16	55	7	1.5	1112.5	1.002	*****
1112	36.5	0.5	1	7	7	1111.5	0.957	
1111	21.5	0.5	2	7	7	1110.5	0.327	
1110	4.3	0.3	7	7	7	1109.5	0.053	
1109	1.2	0.5	42	7	7	1108.5	0.096	
1108	3.5	1	29	7	7	1107.5	0.478	
1107	10	2	20	7	7	1106.5	0.487	
1106	61	23	38	3	3	1105.5	0.105	
1105	11.2	6	54	7	7	1104.5	0.107	
1104	10.5	5	48	7	7	1103.5	0.123	
1103	9	8	89	7	7	1102.5	0.211	
1102	4.7	4	85	7	7	1101.5	0.259	
1101	4.5	4	89	7	7	1100.5	0.018	
1100	8.7	8	92	7	7	1099.5	0.056	
1099	4.5	4	89	7	7	1098.5	0.002	
1098	8.5	2	24	7	7	1097.5	0.013	
1097	4	1.5	38	7	7	1096.5	0.158	
1096	3.5	2.5	71	7	7	1095.5	0.149	
1095	5	3	60	7	7	1094.5	0.179	
1094	23.5	22	94	7	7	1093.5	0.027	
1093	1.8	0.8	44	7	7	1092.5	0.020	
1092	18.7	18	96	7	7	1091.5	0.360	
1091	5.2	0.2	4	7	7	1090.5	0.856	
1090	1.3	0.5	38	7	7	1089.5	1.899	
1089	4	0.5	13	7	7	1088.5	4.737	
1088	1.5	1	67	7	7	1087.5	4.943	*****
1087	18.2	17	93	7	1.5	1086.5	2.249	
1086	47	42	89	1.5	1.5	1085.5	0.023	
1085	29	25	86	7	3	1084.5	0.237	
1084	31	30	97	3	1.5	1083.5	0.845	
1083	7	6	86	7	7	1082.5	0.311	
1082	7	3	43	7	7	1081.5	0.476	
1081	8	3	38	7	7	1080.5	3.079	
1080	20	19	95	7	1.5	1079.5	2.431	
1079	40	40	100	7	0	1078.5	0.348	[123]
1078	20	20	100	7	1.5	1077.5	0.021	
1077	23.5	20	85	3	1.5	1076.5	0.285	
1076	35	34	97	7	3	1075.5	1.100	
1075	55	13	24	3	3	1074.5	0.919	
1074	19	2	11	7	7	1073.5	0.084	
1073	34	24	71	3	1.5	1072.5	0.014	
1072	62	44	71	7	3	1071.5	0.807	
1071	9.5	5	53	7	3	1070.5	0.200	
1070	10	7	70	7	3	1069.5	0.358	
1069	25	23	92	7	3	1068.5	2.226	
1068	12	8	67	3	3	1067.5	2.282	
1067	17	15	88	7	3	1066.5	2.810	*****

bed#	Bt(cm)	St(cm)	S%	T.G	B.G	Posi.	D.Sq	Sq
1066	7	6	86	7	7	1065.5	1.961	
1065	4	3	75	7	7	1064.5	1.154	
1064	32.5	2.5	8	7	7	1063.5	0.446	
1063	29	8	28	7	7	1062.5	0.176	
1062	10	9	90	7	7	1061.5	0.088	
1061	52.5	0.5	1	7	7	1060.5	0.032	
1060	12	4	33	7	7	1059.5	0.050	
1059	9	2	22	7	7	1058.5	0.055	
1058	101	1	1	7	7	1057.5	0.017	
1057	44	1	2	7	7	1056.5	0.090	
1056	11	3	27	7	7	1055.5	0.051	
1055	3	2	67	7	7	1054.5	0.052	
1054	33.7	0.7	2	7	7	1053.5	0.061	
1053	11	1	9	7	7	1052.5	0.057	
1052	24.5	22	90	7	7	1051.5	0.136	
1051	39.5	0.5	1	7	7	1050.5	0.110	
1050	34.2	0.2	1	7	7	1049.5	0.091	
1049	3.6	0.6	17	7	7	1048.5	0.093	
1048	17.5	0.5	3	7	7	1047.5	0.087	
1047	2.7	2	74	7	7	1046.5	0.000	
1046	2.5	0.5	20	7	7	1045.5	0.000	
1045	13.5	0.5	4	7	7	1044.5	0.000	
1044	10.7	0.2	2	7	7	1043.5	0.005	
1043	6.7	0.7	10	7	7	1042.5	0.013	
1042	11	1	9	7	7	1041.5	0.014	
1041	2.1	0.1	5	7	7	1040.5	0.017	
1040	5.5	1.5	27	7	7	1039.5	0.011	
1039	9	5	56	7	7	1038.5	0.001	
1038	4.5	4	89	7	7	1037.5	0.017	
1037	6.7	0.2	3	7	7	1036.5	0.002	
1036	2.3	0.5	22	7	7	1035.5	0.002	
1035	9	1	11	7	7	1034.5	0.001	
1034	5.5	0.3	5	7	7	1033.5	0.006	
1033	4.7	0.7	15	7	7	1032.5	0.026	
1032	10	5	50	7	7	1031.5	0.018	
1031	6	1	17	7	7	1030.5	0.013	
1030	3.5	2	57	7	7	1029.5	0.006	
1029	5	2.5	50	7	7	1028.5	0.000	
1028	6.5	3	46	7	7	1027.5	0.003	
1027	10.5	8	76	7	7	1026.5	0.029	
1026	0.6	0.3	50	7	7	1025.5	0.025	
1025	2.4	0.4	17	7	7	1024.5	0.018	
1024	2.9	0.4	14	7	7	1023.5	0.010	
1023	5.5	0.5	9	7	7	1022.5	0.005	
1022	12	3.5	29	7	7	1021.5	0.001	
1021	3.3	0.3	9	7	7	1020.5	0.032	
1020	2.5	0.5	20	7	7	1019.5	0.040	
1019	6.7	0.4	6	7	7	1018.5	0.040	
1018	3.3	0.3	9	7	7	1017.5	0.042	
1017	10	1	10	7	7	1016.5	0.058	
1016	17	15	88	7	7	1015.5	0.024	
1015	6.5	2	31	7	7	1014.5	0.037	
1014	10.3	0.3	3	7	7	1013.5	0.014	
1013	2	0.5	25	7	7	1012.5	0.016	
1012	22	1	5	7	7	1011.5	0.009	
1011	30	3	10	7	7	1010.5	0.004	
1010	8	1	13	7	7	1009.5	0.006	
1009	16	5	31	7	7	1008.5	0.004	
1008	22.3	0.3	1	7	7	1007.5	0.004	
1007	10	3	30	7	7	1006.5	0.012	
1006	40	1.5	4	7	7	1005.5	0.006	

bed#	Bt(cm)	St(cm)	S%	T.G	B.G	Posi.	D.Sq	Sq
1005	53	1	2	7	7	1004.5	0.003	
1004	11.7	0.2	2	7	7	1003.5	0.001	
1003	4.2	0.2	5	7	7	1002.5	0.003	
1002	18	2	11	7	7	1001.5	0.006	
1001	5	2	40	7	7	1000.5	0.010	
1000	7	2.5	36	7	7	999.5	0.007	
999	4	1.5	38	7	7	998.5	0.003	
998	3.5	1.5	43	7	7	997.5	0.116	
997	4	2.5	63	7	7	996.5	0.107	
996	4.5	4	89	7	7	995.5	1.128	
995	5	3	60	7	7	994.5	2.326	
994	5	1	20	7	7	993.5	2.420	
993	25	22	88	7	7	992.5	2.412	
992	5	2	40	7	7	991.5	2.412	*****
991	56	49	88	7	1.5	990.5	0.460	
990	55	22	40	7	1.5	989.5	1.323	
989	4.5	3	67	7	7	988.5	1.419	
988	20	10	50	7	1.5	987.5	1.221	
987	7.5	1.5	20	7	7	986.5	0.323	[124]
986	8	6	75	7	7	985.5	0.026	
985	6	4	67	7	7	984.5	0.447	
984	3	2	67	7	7	983.5	0.447	
983	40	19	48	7	0	982.5	0.016	
982	27	23	85	7	1.5	981.5	1.494	*****
981	5.5	1.5	27	7	7	980.5	1.430	
980	9.5	3	32	7	7	979.5	1.459	
979	8	1	13	7	7	978.5	1.453	
978	2.7	1.2	44	7	7	977.5	0.363	
977	43	1	2	7	7	976.5	0.003	
976	30.3	0.3	1	7	7	975.5	0.000	
975	6	0.5	8	7	7	974.5	0.000	
974	2.3	0.3	13	7	7	973.5	0.001	
973	1.2	0.2	17	7	7	972.5	0.003	
972	4	3	75	7	7	971.5	0.121	
971	16	1	6	7	7	970.5	0.940	
970	17	1	6	7	7	969.5	0.951	
969	4.2	0.7	17	7	7	968.5	0.968	
968	16.7	0.2	1	7	7	967.5	1.048	*****
967	14	10	71	3	3	966.5	0.125	
966	22	19	86	3	0	965.5	0.795	
965	3.7	2.5	68	7	7	964.5	0.207	
964	3.5	2.5	71	7	7	963.5	0.446	
963	8.5	6	71	7	7	962.5	0.401	[125]
962	2.2	0.2	9	7	7	961.5	0.730	
961	17.5	16	91	7	7	960.5	1.162	
960	14	14	100	1.5	1.5	959.5	0.132	
959	43	43	100	1.5	1.5	958.5	1.482	
958	13.5	9.5	70	7	7	957.5	1.722	*****
957	2	1	50	7	7	956.5	1.754	
956	1	0.7	70	7	7	955.5	1.310	
955	11	9	82	7	7	954.5	0.793	
954	14.5	3	21	7	7	953.5	0.034	
953	9	4	44	7	7	952.5	0.008	
952	13.7	0.7	5	7	7	951.5	0.003	
951	5	3	60	7	7	950.5	0.007	
950	1.5	0.5	33	7	7	949.5	0.195	
949	10	2.5	25	7	7	948.5	0.191	
948	11.5	5	43	7	7	947.5	0.156	
947	4.5	3	67	7	7	946.5	0.128	
946	4.5	3	67	7	7	945.5	0.118	
945	24	18	75	7	3	944.5	0.251	

bed#	Bt(cm)	St(cm)	S%	T.G	B.G	Posi.	D.Sq	Sq
944	2	1.5	75	7	7	943.5	0.224	
943	3	1.5	50	7	7	942.5	0.187	
942	1.2	0.2	17	7	7	941.5	0.156	
941	3.8	0.5	13	7	7	940.5	0.116	
940	5	2	40	7	7	939.5	0.012	
939	4	3	75	7	7	938.5	0.078	
938	4	2	50	7	7	937.5	0.082	
937	2	1.5	75	7	7	936.5	0.132	
936	6.3	6	95	7	7	935.5	0.043	
935	1.5	0.5	33	7	7	934.5	0.064	
934	17.5	16	91	7	7	933.5	0.018	
933	7.5	3	40	7	7	932.5	0.027	
932	15.5	8	52	7	7	931.5	0.122	
931	8	1	13	7	7	930.5	0.071	
930	7	2	29	7	7	929.5	0.092	
929	4	3	75	7	7	928.5	0.016	
928	36	2	6	7	7	927.5	0.009	
927	52	2	4	7	7	926.5	0.004	
926	15.5	1.5	10	7	7	925.5	0.134	
925	6.5	1	15	7	7	924.5	0.135	
924	9	2	22	7	7	923.5	0.131	
923	14.5	3	21	7	7	922.5	0.116	
922	8.5	7	82	7	7	921.5	0.109	
921	34	9	26	7	3	920.5	0.187	
920	17.2	0.2	1	7	7	919.5	0.178	
919	9.2	0.2	2	7	7	918.5	0.145	
918	3.3	0.3	9	7	7	917.5	0.121	
917	5.5	0.5	9	7	7	916.5	0.106	
916	11.5	1.5	13	7	7	915.5	0.004	
915	8	0.5	6	7	7	914.5	0.006	
914	22	3	14	7	7	913.5	0.004	
913	2.8	2.5	89	7	7	912.5	0.002	
912	1.7	0.2	12	7	7	911.5	0.003	
911	10	1	10	7	7	910.5	0.003	
910	4	1.5	38	7	7	909.5	0.001	
909	11	5	45	7	7	908.5	0.003	
908	13	3	23	7	7	907.5	0.007	
907	13	1	8	7	7	906.5	0.012	
906	1.5	0.5	33	7	7	905.5	0.011	
905	4	0.5	13	7	7	904.5	0.258	
904	3	1.5	50	7	7	903.5	0.285	
903	2.5	1.5	60	7	7	902.5	0.291	
902	4.7	0.2	4	7	7	901.5	0.309	
901	2.2	0.2	9	7	7	900.5	0.313	
900	34	33	97	3	3	899.5	0.367	
899	1.2	0.2	17	7	7	898.5	0.210	
898	2	0.5	25	7	7	897.5	0.179	
897	1.3	0.8	62	7	7	896.5	0.147	
896	0.7	0.2	29	7	7	895.5	0.131	
895	0.4	0.2	50	7	7	894.5	0.144	
894	12	11.5	96	7	7	893.5	0.007	
893	10	3	30	7	7	892.5	0.235	
892	7	6	86	7	7	891.5	0.148	
891	3.7	3	81	7	7	890.5	0.133	
890	5	4	80	7	7	889.5	0.816	

bed#	Bt(cm)	St(cm)	S%	T.G	B.G	Posi.	D.Sq	Sq
889	8	3	38	7	7	888.5	1.037	*****
888	26	24	92	3	3	887.5	0.154	
887	5	1	20	7	7	886.5	0.265	
886	6	3	50	7	7	885.5	0.720	
885	41	39	95	3	3	884.5	0.211	
884	9	5	56	7	7	883.5	0.792	
883	9	7	78	7	3	882.5	1.093	
882	10	8	80	7	7	881.5	7.139	[126]
881	14	13	93	7	3	880.5	4.846	
880	17	15	88	7	3	879.5	5.660	
879	32	30	94	3	0	878.5	4.444	
878	26	26	100	3	3	877.5	2.277	
877	131	129	98	7	0	876.5	7.434	
876	13	10	77	7	7	875.5	6.988	
875	13	10	77	7	7	874.5	6.632	
874	45	40	89	7	0	873.5	10.083	*****
873	20.5	1	5	7	7	872.5	7.477	
872	3.7	0.2	5	7	7	871.5	0.554	
871	3	0.5	17	7	7	870.5	0.369	
870	0.9	0.4	44	7	7	869.5	0.199	
869	12	10	83	7	1.5	868.5	0.203	
868	1	0.5	50	7	7	867.5	0.203	
867	5.3	0.3	6	7	7	866.5	0.200	
866	1.9	0.4	21	7	7	865.5	0.199	
865	5	2	40	7	7	864.5	0.016	
864	12	4	33	7	7	863.5	0.456	
863	4.2	0.2	5	7	7	862.5	1.672	
862	2.2	2	91	7	7	861.5	2.722	
861	2	1	50	7	7	860.5	3.924	*****
860	5.5	4	73	3	3	859.5	1.835	
859	21	13	62	3	3	858.5	0.401	
858	21	17	81	7	0	857.5	0.365	
857	17.5	14	80	3	3	856.5	0.910	
856	19	7	37	7	3	855.5	1.602	
855	11.8	0.8	7	7	7	854.5	0.895	
854	8.5	0.5	6	7	7	853.5	0.067	
853	4.5	0.5	11	7	7	852.5	0.458	
852	24	17	71	3	3	851.5	0.098	[127]
851	17	12	71	3	3	850.5	0.047	
850	11.2	0.2	2	7	7	849.5	0.051	
849	27	25	93	7	1.5	848.5	0.419	
848	6	3	50	7	7	847.5	0.240	
847	6.5	5	77	7	7	846.5	0.224	
846	9	3	33	7	7	845.5	0.424	
845	4	1	25	7	7	844.5	1.193	
844	64	43	67	7	1.5	843.5	0.041	
843	30	30	100	3	3	842.5	0.833	
842	1.1	0.1	9	7	7	841.5	0.382	
841	1.2	0.2	17	7	7	840.5	0.348	
840	24	23	96	3	3	839.5	2.296	*****
839	2	1	50	7	7	838.5	0.608	
838	5	4	80	7	7	837.5	0.116	
837	20.5	20	98	7	7	836.5	0.585	
836	11.2	0.2	2	7	7	835.5	0.587	
835	8.3	0.3	4	7	7	834.5	0.207	
834	2.5	0.5	20	7	7	833.5	0.206	
833	35.3	0.3	1	7	7	832.5	0.200	
832	25.2	0.2	1	7	7	831.5	1.408	
831	1.1	0.1	9	7	7	830.5	1.962	
830	20	18	90	3	1.5	829.5	0.308	
829	55.2	0.2	0	7	7	828.5	0.436	

bed#	Bt(cm)	St(cm)	S%	T.G	B.G	Posi.	D.Sq	Sq
828	1.6	0.1	6	7	7	827.5	0.442	
827	39	36	92	1.5	1.5	826.5	0.930	
826	23	20	87	7	7	825.5	1.340	
825	14.2	0.2	1	7	7	824.5	0.200	
824	9	7	78	7	7	823.5	0.093	
823	1.7	0.2	12	7	7	822.5	0.876	
822	3	2	67	7	7	821.5	2.873	
821	17	15	88	7	7	820.5	3.397	
820	38	35	92	7	7	819.5	3.337	*****
819	33	30	91	3	3	818.5	0.857	
818	47	43	91	7	3	817.5	0.480	
817	14	12	86	7	7	816.5	0.916	
816	13	10	77	3	3	815.5	0.719	
815	44	42	95	7	1.5	814.5	3.273	
814	14	10	71	7	7	813.5	2.081	
813	7	5	71	7	7	812.5	0.101	[128]
812	19	16	84	7	1.5	811.5	0.657	
811	4.1	0.1	2	7	7	810.5	0.064	
810	3.5	3	86	7	7	809.5	1.608	
809	11	6	55	7	7	808.5	1.837	
808	62	40	65	7	0	807.5	0.059	
807	6	1	17	7	7	806.5	0.156	
806	43	38	88	3	1.5	805.5	0.774	
805	10.5	10	95	3	3	804.5	2.310	
804	22	10	45	7	7	803.5	2.601	*****
803	25	5	20	7	7	802.5	0.628	
802	14	10	71	7	7	801.5	0.751	
801	22	16	73	7	7	800.5	0.020	
800	8	5	63	7	7	799.5	0.203	
799	3.5	2	57	7	7	798.5	0.200	
798	20	18	90	7	7	797.5	0.323	
797	5	5	100	7	7	796.5	0.320	
796	21	16	76	7	1.5	795.5	0.533	
795	24.2	0.2	1	7	7	794.5	0.281	
794	14	2	14	7	7	793.5	0.273	
793	7	4	57	7	7	792.5	0.198	
792	26.3	0.3	1	7	7	791.5	0.203	
791	1	0.5	50	7	7	790.5	0.102	
790	19.5	15	77	7	7	789.5	0.012	
789	7	3	43	7	7	788.5	0.027	
788	13	8	62	7	7	787.5	0.225	
787	2	1	50	7	7	786.5	0.803	
786	4	1.5	38	7	7	785.5	0.813	
785	15	1	7	7	7	784.5	0.937	
784	5.2	0.2	4	7	7	783.5	2.407	*****
783	22	12	55	7	1.5	782.5	0.823	
782	30	20	67	3	1.5	781.5	0.124	
781	10	5	50	7	7	780.5	0.292	
780	13	3	23	7	7	779.5	0.608	
779	29	25	86	7	1.5	778.5	0.158	
778	16.5	16	97	7	7	777.5	0.165	
777	8	8	100	3	3	776.5	0.042	[129]
776	24	20	83	3	3	775.5	0.052	
775	32	10	31	3	3	774.5	0.270	
774	33.2	0.2	1	7	7	773.5	0.010	
773	35	28	80	3	3	772.5	0.132	
772	6.7	0.7	10	7	7	771.5	0.001	
771	22	20	91	3	3	770.5	0.203	
770	12	12	100	3	3	769.5	0.667	
769	3.3	0.3	9	7	7	768.5	0.669	
768	27	22	81	3	3	767.5	1.480	*****

bed#	Bt(cm)	St(cm)	S%	T.G	B.G	Posi.	D.Sq	Sq
767	4	3	75	7	7	766.5	1.582	
766	3.5	0.5	14	7	7	765.5	0.657	
765	4.5	1.5	33	7	7	764.5	0.225	
764	7.3	0.3	4	7	7	763.5	0.225	
763	5.3	0.3	6	7	7	762.5	0.000	
762	5.8	0.8	14	7	7	761.5	0.000	
761	11.5	2	17	7	7	760.5	0.001	
760	4.5	0.5	11	7	7	759.5	0.000	
759	19.3	0.3	2	7	7	758.5	0.178	
758	13	1	8	7	7	757.5	0.730	
757	1.3	0.3	23	7	7	756.5	0.745	
756	6.6	0.6	9	7	7	755.5	0.775	
755	9.3	0.3	3	7	7	754.5	0.776	*****
754	32	20	63	3	3	753.5	0.000	
753	42	21	50	3	3	752.5	0.749	
752	3.7	0.7	19	7	7	751.5	0.764	
751	4.9	0.9	18	7	7	750.5	0.287	
750	24.2	0.2	1	7	7	749.5	0.276	
749	1.2	0.9	75	7	7	748.5	0.019	
748	4.8	0.8	17	7	7	747.5	0.131	[130]
747	24.2	0.2	1	7	7	746.5	0.793	
746	19	12	63	7	3	745.5	0.027	
745	7	1	14	7	7	744.5	0.024	
744	18.8	0.3	2	7	7	743.5	0.424	
743	4	1	25	7	7	742.5	0.422	
742	29	19	66	7	1.5	741.5	0.161	
741	5.3	0.3	6	7	7	740.5	0.004	
740	7.7	0.7	9	7	7	739.5	0.004	
739	16	15	94	1.5	1.5	738.5	1.024	*****
738	1.7	1	59	7	7	737.5	1.024	
737	12.3	0.3	2	7	7	736.5	0.241	
736	19.5	0.5	3	7	7	735.5	0.243	
735	65.5	0.5	1	7	7	734.5	0.242	
734	12.2	1.2	10	7	7	733.5	0.244	
733	19	1	5	7	7	732.5	0.917	
732	20.2	0.2	1	7	7	731.5	0.927	
731	10.2	0.3	3	7	7	730.5	2.213	
730	21.5	0.5	2	7	7	729.5	2.388	*****
729	17	16	94	7	1.5	728.5	1.570	
728	41	25	61	3	3	727.5	0.760	
727	19.7	0.7	4	7	7	726.5	0.838	[131]
726	20	19	95	1.5	1.5	725.5	0.132	
725	81	7	9	7	7	724.5	0.105	
724	33	33	100	3	1.5	723.5	1.150	
723	36	27	75	3	1.5	722.5	3.117	*****
722	15	5	33	7	7	721.5	3.448	
721	33.4	0.4	1	7	7	720.5	1.828	
720	26.7	0.7	3	7	7	719.5	1.646	
719	6.2	1.2	19	7	7	718.5	0.415	
718	2.5	1.5	60	7	7	717.5	0.011	
717	1.2	0.2	17	7	7	716.5	0.001	
716	5.7	0.2	4	7	7	715.5	0.001	
715	2.7	0.7	26	7	7	714.5	0.001	
714	1.3	0.3	23	7	7	713.5	0.000	
713	1.2	0.2	17	7	7	712.5	0.000	
712	1.7	0.2	12	7	7	711.5	0.000	
711	3.2	0.2	6	7	7	710.5	0.000	
710	1.8	0.5	28	7	7	709.5	0.000	
709	3.3	0.3	9	7	7	708.5	0.000	
708	13.3	0.3	2	7	7	707.5	0.000	
707	1.1	0.1	9	7	7	706.5	0.000	

bed#	Bt(cm)	St(cm)	S%	T.G	B.G	Posi.	D.Sq	Sq
706	4.6	0.6	13	7	7	705.5	0.000	
705	2.9	0.4	14	7	7	704.5	0.000	
704	1.7	0.2	12	7	7	703.5	0.000	
703	2.3	0.3	13	7	7	702.5	0.000	
702	3.4	0.4	12	7	7	701.5	0.000	
701	2.8	0.3	11	7	7	700.5	0.000	
700	45.3	0.3	1	7	7	699.5	0.000	
699	19.1	0.1	1	7	7	698.5	0.204	
698	13.7	0.2	1	7	7	697.5	0.206	
697	6	2	33	7	7	696.5	0.201	
696	4.2	0.2	5	7	7	695.5	0.201	
695	2.7	0.2	7	7	7	694.5	0.202	
694	22	4	18	3	1.5	693.5	0.200	
693	5	1	20	7	7	692.5	0.203	
692	4	1	25	7	7	691.5	0.198	
691	1.7	0.2	12	7	7	690.5	0.203	
690	2.1	0.6	29	7	7	689.5	0.275	
689	16	0.5	3	7	7	688.5	0.194	
688	5.5	0.5	9	7	7	687.5	1.503	
687	17	4	24	7	7	686.5	1.503	
686	9.5	5.5	58	7	7	685.5	1.621	
685	19	15	79	7	7	684.5	1.482	
684	13	8	62	7	7	683.5	1.608	*****
683	59	50	85	7	3	682.5	0.562	
682	9.5	7	74	7	7	681.5	1.200	
681	6.5	5	77	3	3	680.5	1.238	
680	6.5	5	77	7	3	679.5	2.459	
679	23	21	91	7	7	678.5	3.269	
678	20	19	95	3	3	677.5	5.524	[132]
677	38	30	79	7	1.5	676.5	2.812	
676	55	55	100	7	1.5	675.5	0.478	
675	45	45	100	7	1.5	674.5	0.990	
674	39	34	87	1.5	1.5	673.5	2.708	
673	27	27	100	1.5	1.5	672.5	5.435	
672	26	18	69	1.5	1.5	671.5	6.596	
671	12	11	92	1.5	1.5	670.5	6.244	
670	20	20	100	3	3	669.5	4.577	*****
669	15.2	0.2	1	7	7	668.5	0.941	
668	4.2	0.2	5	7	7	667.5	0.183	
667	29	5	17	7	7	666.5	2.336	
666	0.8	0.3	38	7	7	665.5	6.966	
665	14.5	4	28	3	0	664.5	7.656	*****
664	20	18	90	1.5	1.5	663.5	6.314	
663	12.5	7	56	3	0	662.5	4.714	
662	69	66	96	3	1.5	661.5	0.276	
661	52	45	87	3	3	660.5	0.539	
660	27	23	85	7	1.5	659.5	0.277	
659	30	30	100	3	0	658.5	0.436	[133]
658	10.5	10	95	1.5	1.5	657.5	0.666	
657	39.5	20	51	1.5	1.5	656.5	0.048	
656	20.5	7.5	37	1.5	1.5	655.5	1.261	
655	65	60	92	1.5	0	654.5	0.670	
654	32	29	91	1.5	1.5	653.5	0.781	
653	17	7	41	7	7	652.5	0.081	
652	22	19	86	3	0	651.5	0.133	

bed#	Bt(cm)	St(cm)	S%	T.G	B.G	Posi.	D.Sq	Sq
651	51	45	88	7	3	650.5	2.422	*****
650	32	19	59	3	3	649.5	1.063	
649	37.5	12.5	33	3	3	648.5	0.878	
648	10	9	90	3	3	647.5	0.799	
647	19	15	79	3	0	646.5	0.845	
646	9.5	2.5	26	7	7	645.5	0.107	[134]
645	11.5	11	96	7	0	644.5	0.048	
644	5	4	80	7	3	643.5	0.292	
643	14	12	86	3	3	642.5	0.658	
642	15.5	13	84	3	3	641.5	0.799	
641	17	15	88	3	3	640.5	1.031	
640	16	16	100	3	3	639.5	1.441	*****
639	3.5	1.5	43	7	7	638.5	0.823	
638	7	3	43	7	7	637.5	0.318	
637	5	1.5	30	7	7	636.5	0.050	
636	21.5	13	60	3	0	635.5	0.908	
635	5	2	40	7	7	634.5	0.077	
634	14	1.5	11	7	7	633.5	0.079	
633	6.5	4	62	7	7	632.5	0.067	
632	6.5	2.5	38	7	7	631.5	0.062	
631	9	2	22	7	7	630.5	0.884	
630	20	20	100	7	3	629.5	0.123	
629	5	2	40	7	7	628.5	0.485	
628	5	1.5	30	7	7	627.5	0.481	
627	5	1	20	7	7	626.5	0.479	
626	11.5	8	70	3	0	625.5	0.270	
625	2.5	0.5	20	7	7	624.5	0.017	
624	13	12	92	1.5	1.5	623.5	1.093	
623	1.7	0.5	29	7	7	622.5	1.086	
622	1.2	0.2	17	7	7	621.5	1.057	
621	11.2	1.2	11	7	7	620.5	0.208	
620	39.5	2	5	7	7	619.5	0.219	
619	2.2	1.2	55	7	7	618.5	0.000	
618	1.4	0.4	29	7	7	617.5	0.000	
617	9.5	4	42	7	7	616.5	0.008	
616	5.7	0.2	4	7	7	615.5	0.006	
615	1.4	0.4	29	7	7	614.5	0.003	
614	0.4	0.2	50	7	7	613.5	0.000	
613	16.6	0.6	4	7	7	612.5	0.003	
612	8.7	1.2	14	7	7	611.5	0.015	
611	11.2	0.2	2	7	7	610.5	0.255	
610	9.2	0.2	2	7	7	609.5	0.256	
609	5	3.5	70	7	7	608.5	0.230	
608	16	4	25	7	7	607.5	0.203	
607	7	3	43	7	7	606.5	0.613	
606	13	8	62	3	1.5	605.5	0.042	
605	3.2	0.2	6	7	7	604.5	0.295	
604	3.5	2.5	71	7	7	603.5	0.762	
603	1.3	0.3	23	7	7	602.5	1.537	*****
602	13	10	77	7	3	601.5	1.040	
601	12	8	67	7	3	600.5	1.599	
600	10	7	70	7	3	599.5	0.351	[135]
599	29	6	21	3	3	598.5	0.021	
598	10	10	100	3	3	597.5	0.556	
597	16	11	69	1.5	1.5	596.5	1.771	
596	14.5	11	76	3	1.5	595.5	3.685	*****
595	5.5	1.5	27	7	7	594.5	2.530	
594	13.5	6	44	7	7	593.5	0.541	
593	9.7	0.7	7	7	7	592.5	0.061	
592	3.5	2	57	7	7	591.5	1.346	
591	26	3	12	7	7	590.5	5.287	
590	4.7	0.2	4	7	7	589.5	8.366	*****
589	11.5	10	87	3	0	588.5	4.045	
588	13.5	12	89	7	0	587.5	1.094	
587	14	13	93	1.5	1.5	586.5	0.462	
586	39	34	87	3	0	585.5	1.283	[136]
585	21	11	52	3	0	584.5	5.238	
584	30	30	100	7	7	583.5	2.943	
583	12	3	25	7	7	582.5	1.315	
582	6	6	100	1.5	1.5	581.5	2.714	*****
581	20	18	90	7	7	580.5	2.101	
580	48	45	94	7	7	579.5	0.000	
579	13	12	92	7	7	578.5	0.084	
578	23	22	96	7	7	577.5	0.214	
577	20	19	95	7	7	576.5	1.149	
576	44	40	91	7	7	575.5	3.348	*****
575	8.5	7.5	88	3	1.5	574.5	1.193	
574	17	15	88	7	7	573.5	1.881	
573	15.5	13	84	7	1.5	572.5	0.776	
572	12.7	0.2	2	7	7	571.5	1.270	
571	18.5	10	54	7	3	570.5	1.252	
570	8	3	38	3	3	569.5	2.097	
569	15	12	80	3	3	568.5	0.720	[137]
568	32	29	91	7	0	567.5	0.009	
567	3	3	100	1.5	1.5	566.5	0.167	
566	31	31	100	3	0	565.5	1.098	
565	19.5	15	77	1.5	1.5	564.5	1.640	
564	0.7	0.2	29	7	7	563.5	0.830	
563	3	1.5	50	7	7	562.5	0.007	
562	38	13	34	3	0	561.5	0.433	
561	33	11	33	3	3	560.5	0.480	
560	37	24	65	3	3	559.5	0.999	
559	13.5	0.5	4	7	7	558.5	0.952	
558	21	4	19	7	3	557.5	2.572	*****
557	8	4	50	7	7	556.5	0.650	
556	4.5	2.5	56	7	7	555.5	0.735	
555	12	8	67	7	7	554.5	3.228	
554	9	4.5	50	7	7	553.5	4.241	
553	19.7	2.7	14	7	7	552.5	7.505	*****
552	104	67	64	7	1.5	551.5	2.833	
551	11	10	91	3	3	550.5	2.142	
550	41	40	98	7	1.5	549.5	1.669	
549	11	9	82	7	1.5	548.5	0.936	
548	19	14	74	1.5	1.5	547.5	2.342	
547	42	31	74	3	1.5	546.5	1.971	
546	12	8	67	1.5	1.5	545.5	2.080	[138]
545	12	8	67	1.5	1.5	544.5	1.434	
544	3	3	100	7	7	543.5	0.110	
543	31.8	0.8	3	7	7	542.5	0.421	
542	37	11	30	3	3	541.5	0.232	
541	24.5	19	78	3	3	540.5	0.109	
540	13	10	77	1.5	1.5	539.5	0.197	
539	8	8	100	1.5	1.5	538.5	0.854	
538	12.5	6	48	1.5	1.5	537.5	3.135	*****
537	5.7	0.2	4	7	7	536.5	1.993	
536	6.5	2.5	38	7	7	535.5	1.076	
535	4.5	0.5	11	7	7	534.5	0.329	
534	5.7	5	88	7	3	533.5	0.107	
533	5.5	4	73	7	7	532.5	0.015	
532	4.2	0.2	5	7	7	531.5	0.015	
531	17.5	1.5	9	7	7	530.5	0.037	
530	4.2	0.2	5	7	7	529.5	0.058	

bed#	Bt(cm)	St(cm)	S%	T.G	B.G	528.5	D.Sq	Sq
529	24.5	5	20	3	1.5	527.5	0.225	
528	5.2	4	77	7	7	526.5	0.212	
527	10	1.5	15	7	7	525.5	0.237	
526	19.5	10.5	54	7	7	524.5	0.200	
525	5	4	80	7	7	523.5	0.014	
524	5.2	2	38	7	7	522.5	0.241	
523	43	1	2	7	7	521.5	0.277	
522	12.5	8	64	7	7	520.5	0.816	
521	4	3	75	7	7	519.5	1.199	*****
520	20	19	95	7	1.5	518.5	0.032	
519	5.5	5	91	7	7	517.5	0.027	
518	3.5	3	86	7	7	516.5	0.027	
517	6.5	6	92	7	1.5	515.5	0.816	
516	29	28	97	7	7	514.5	0.525	
515	4	3	75	7	7	513.5	0.058	[139]
514	9	7	78	7	7	512.5	0.103	
513	6	5	83	7	7	511.5	0.178	
512	4.5	3.5	78	7	7	510.5	1.504	
511	17.2	12	70	3	3	509.5	0.325	
510	4.5	3.5	78	7	7	508.5	0.336	
509	5.5	3	55	7	7	507.5	0.331	
508	14	2	14	3	3	506.5	0.014	
507	33	14	42	7	0	505.5	1.669	*****
506	5	3.5	70	7	7	504.5	0.898	
505	44.2	0.2	0	7	7	503.5	0.858	
504	1.3	0.3	23	7	7	502.5	0.834	
503	10.3	0.3	3	7	7	501.5	0.337	
502	11.8	0.3	3	7	7	500.5	0.037	
501	18	3	17	7	7	499.5	0.034	
500	11.5	1.5	13	7	7	498.5	0.027	
499	4	1	25	7	7	497.5	0.034	
498	6	4	67	7	7	496.5	0.007	
497	9	8	89	7	7	495.5	0.018	
496	3.5	2	57	7	7	494.5	0.014	
495	2.8	1.5	54	7	7	493.5	0.014	
494	4	3	75	7	7	492.5	0.127	
493	40	1	3	7	7	491.5	0.116	
492	57	1	2	7	7	490.5	0.105	
491	5	2	40	7	7	489.5	0.106	
490	4.5	1.5	33	7	7	488.5	0.106	
489	4	3	75	7	3	487.5	0.106	
488	22	1	5	7	7	486.5	0.004	
487	39.2	0.2	1	7	7	485.5	0.006	
486	15.2	0.2	1	7	7	484.5	0.013	
485	5	2	40	7	7	483.5	0.009	
484	41	3	7	7	7	482.5	0.447	
483	8.5	7.5	88	7	3	481.5	0.001	
482	10.7	0.2	2	7	7	480.5	0.020	
481	43	1	2	7	7	479.5	0.017	
480	52	1	2	7	7	478.5	0.021	
479	28	8	29	7	3	477.5	0.421	
478	3	0.5	17	7	7	476.5	0.108	
477	17	12	71	7	7	475.5	0.191	
476	29	1	3	7	7	474.5	0.195	
475	11	1	9	7	7	473.5	0.202	
474	31.3	0.3	1	7	7	472.5	0.108	
473	4.2	0.2	5	7	7	471.5	0.107	
472	4.2	0.2	5	7	7	470.5	0.120	
471	6.6	0.6	9	7	7	469.5	0.122	
470	45.2	0.2	0	7	7	468.5	0.502	
469	45	10	22	3	3		0.000	

bed#	Bt(cm)	St(cm)	S%	T.G	B.G	Posi.	D.Sq	Sq
468	40.1	0.1	0	7	7	467.5	0.001	
467	1.7	0.2	12	7	7	466.5	0.001	
466	18.6	0.6	3	7	7	465.5	0.001	
465	66	10	15	3	3	464.5	0.488	
464	11	1	9	7	7	463.5	0.120	
463	5	1	20	7	7	462.5	0.126	
462	1.3	0.3	23	7	7	461.5	0.127	
461	2.7	0.7	26	7	7	460.5	0.129	
460	2.2	0.2	9	7	7	459.5	0.000	
459	3.3	1.5	45	7	7	458.5	0.000	
458	1.7	0.2	12	7	7	457.5	0.000	
457	2.2	0.2	9	7	7	456.5	0.001	
456	4.3	0.3	7	7	7	455.5	0.001	
455	5.9	0.9	15	7	7	454.5	0.001	
454	3.5	1	29	7	7	453.5	0.001	
453	2	1.5	75	7	7	452.5	0.000	
452	4	1	25	7	7	451.5	0.000	
451	1.8	0.3	17	7	7	450.5	0.000	
450	7.5	1.5	20	7	7	449.5	0.001	
449	4.3	0.3	7	7	7	448.5	0.000	
448	2.3	0.3	13	7	7	447.5	0.000	
447	6.3	1.3	21	7	7	446.5	0.001	
446	2.5	0.5	20	7	7	445.5	0.001	
445	1.8	0.3	17	7	7	444.5	0.000	
444	1.7	0.7	41	7	7	443.5	0.000	
443	2.2	0.2	9	7	7	442.5	0.000	
442	1.1	0.3	27	7	7	441.5	0.000	
441	1.3	0.3	23	7	7	440.5	0.000	
440	1.3	0.3	23	7	7	439.5	0.003	
439	1.8	0.6	33	7	7	438.5	0.004	
438	3.3	1.3	39	7	7	437.5	0.002	
437	1.3	0.3	23	7	7	436.5	0.002	
436	1.4	0.4	29	7	7	435.5	0.137	
435	7	3	43	7	7	434.5	0.114	
434	11.2	1.2	11	7	7	433.5	0.111	
433	1.6	0.6	38	7	7	432.5	0.112	
432	2.25	0.25	11	7	7	431.5	0.113	
431	15	10	67	7	3	430.5	0.139	
430	2.2	0.2	9	7	7	429.5	0.118	
429	2.3	0.3	13	7	7	428.5	0.115	
428	18.6	0.6	3	7	7	427.5	0.116	
427	5.6	0.6	11	7	7	426.5	0.115	
426	5.9	0.9	15	7	7	425.5	0.000	
425	8	2	25	7	7	424.5	0.001	
424	1.3	0.5	38	7	7	423.5	0.001	
423	0.7	0.3	43	7	7	422.5	0.000	
422	6.7	1.2	18	7	7	421.5	0.000	
421	1.3	0.1	8	7	7	420.5	0.000	
420	2.2	0.2	9	7	7	419.5	0.001	
419	1.3	0.8	62	7	7	418.5	0.000	
418	7	2	29	7	7	417.5	0.001	
417	3.5	0.5	14	7	7	416.5	0.001	
416	1.2	0.2	17	7	7	415.5	0.000	
415	1.3	0.5	38	7	7	414.5	0.000	
414	0.9	0.1	11	7	7	413.5	0.000	
413	1.7	0.7	41	7	7	412.5	0.000	
412	0.8	0.3	38	7	7	411.5	0.000	
411	8.5	1.5	18	7	7	410.5	0.000	
410	11.3	0.3	3	7	7	409.5	0.000	
409	0.5	0.2	40	7	7	408.5	0.000	
408	2.2	0.7	32	7	7	407.5	0.000	

bed#	Bt(cm)	St(cm)	S%	T.G	B.G	Posi.	D.Sq	Sq
407	1.2	0.2	17	7	7	406.5	0.000	
406	2.4	0.9	38	7	7	405.5	0.000	
405	2.2	0.7	32	7	7	404.5	0.000	
404	4.3	0.3	7	7	7	403.5	0.000	
403	2.3	0.3	13	7	7	402.5	0.000	
402	4.2	0.2	5	7	7	401.5	0.000	
401	1.45	0.25	17	7	7	400.5	0.000	
400	1.7	0.2	12	7	7	399.5	0.001	
399	2.2	1	45	7	7	398.5	0.000	
398	2.2	0.2	9	7	7	397.5	0.024	
397	5.7	0.7	12	7	7	396.5	0.024	
396	3.6	0.6	17	7	7	395.5	0.021	
395	1.3	0.3	23	7	7	394.5	0.022	
394	7.7	0.7	9	7	7	393.5	0.024	
393	15	10	67	7	7	392.5	0.010	
392	4.2	1.2	29	7	7	391.5	0.016	
391	3.3	0.3	9	7	7	390.5	0.015	
390	2.5	0.5	20	7	7	389.5	0.017	
389	3.4	0.9	26	7	7	388.5	0.021	
388	8.5	2.5	29	7	7	387.5	0.023	
387	2.7	0.2	7	7	7	386.5	0.035	
386	8.25	0.25	3	7	7	385.5	0.049	
385	4.1	0.1	2	7	7	384.5	0.053	
384	9.1	0.1	1	7	7	383.5	0.069	
383	21	15	71	7	7	382.5	0.015	
382	34.5	1.5	4	7	7	381.5	0.015	
381	5.5	2.5	45	7	7	380.5	0.034	
380	11.8	0.3	3	7	7	379.5	0.000	
379	24.5	1.5	6	7	7	378.5	0.426	
378	23.5	1.5	6	7	7	377.5	1.388	
377	15	3	20	7	7	376.5	2.004	
376	11.5	0.5	4	7	7	375.5	3.216	*****
375	44	12	27	7	7	374.5	2.707	
374	46	36	78	1.5	1.5	373.5	0.318	[140]
373	26	16	62	3	3	372.5	0.399	
372	46	5	11	3	3	371.5	1.111	
371	26	12	46	3	3	370.5	3.142	*****
370	12	6	50	7	7	369.5	3.095	
369	6.2	0.2	3	7	7	368.5	1.204	
368	9	2.5	28	7	7	367.5	0.537	
367	5.2	0.2	4	7	7	366.5	0.179	
366	1.2	0.2	17	7	7	365.5	0.010	
365	5.5	1.5	27	7	7	364.5	0.003	
364	6.3	0.3	5	7	7	363.5	0.003	
363	9.3	0.3	3	7	7	362.5	0.000	
362	2.2	0.2	9	7	7	361.5	0.000	
361	3.2	0.2	6	7	7	360.5	0.000	
360	0.6	0.2	33	7	7	359.5	0.000	
359	0.9	0.2	22	7	7	358.5	0.000	
358	4.8	0.8	17	7	7	357.5	0.000	
357	1.4	0.2	14	7	7	356.5	0.000	
356	2.4	0.4	17	7	7	355.5	0.000	
355	2.7	0.2	7	7	7	354.5	0.000	
354	1.3	0.3	23	7	7	353.5	0.000	
353	4.7	0.7	15	7	7	352.5	0.000	
352	1.1	0.3	27	7	7	351.5	0.010	
351	5.4	0.4	7	7	7	350.5	0.012	
350	0.8	0.3	38	7	7	349.5	0.012	
349	2.8	0.3	11	7	7	348.5	0.022	
348	4.3	0.3	7	7	7	347.5	0.025	
347	8	7.5	94	7	7	346.5	0.003	

bed#	Bt(cm)	St(cm)	S%	T.G	B.G	Posi.	D.Sq	Sq
346	2	1	50	7	7	345.5	0.004	
345	1.1	0.3	27	7	7	344.5	0.109	
344	3.6	3	83	7	7	343.5	0.105	
343	4.5	0.5	11	7	7	342.5	0.593	
342	13.4	0.4	3	7	7	341.5	0.614	
341	2.5	1	40	7	7	340.5	1.312	*****
340	10	9	90	3	3	339.5	0.214	
339	1.2	0.2	17	7	7	338.5	0.943	
338	8	5	63	3	1.5	337.5	0.355	
337	0.8	0.3	38	7	7	336.5	0.390	
336	14	14	100	3	3	335.5	0.262	
335	3	3	100	7	7	334.5	1.495	
334	17	15	88	1.5	1.5	333.5	0.581	
333	10.5	10	95	1.5	1.5	332.5	0.801	
332	5	3	60	7	7	331.5	0.705	
331	31	31	100	3	3	330.5	0.480	
330	20	20	100	1.5	1.5	329.5	0.078	[141]
329	15	15	100	1.5	1.5	328.5	0.096	
328	20	20	100	3	0	327.5	0.838	
327	2.3	0.8	35	7	7	326.5	0.241	
326	13.5	12	89	1.5	1.5	325.5	0.205	
325	22	22	100	3	1.5	324.5	0.388	
324	6.5	5	77	3	3	323.5	0.482	
323	1.7	0.7	41	7	7	322.5	0.198	
322	20	15	75	3	1.5	321.5	0.062	
321	11	7	64	3	3	320.5	0.135	
320	9	8	89	7	1.5	319.5	0.318	
319	22	2	9	7	7	318.5	0.747	
318	11	8	73	1.5	1.5	317.5	0.272	
317	16	15	94	7	0	316.5	0.143	
316	30	20	67	3	1.5	315.5	0.871	
315	13	10	77	3	0	314.5	1.652	*****
314	9.2	0.2	2	7	7	313.5	0.473	
313	59	20	34	1.5	1.5	312.5	1.482	
312	18	3	17	7	7	311.5	0.416	
311	5.8	0.8	14	7	7	310.5	0.015	
310	14	12	86	3	3	309.5	0.063	
309	52	19	37	3	0	308.5	1.586	
308	4.3	0.3	7	7	7	307.5	0.527	
307	2.8	0.3	11	7	7	306.5	0.484	
306	1.7	0.9	53	7	7	305.5	0.490	
305	5.2	0.7	13	7	3	304.5	0.332	
304	6.5	2	31	7	7	303.5	0.277	
303	1.1	0.6	55	7	7	302.5	0.990	
302	3	1	33	7	7	301.5	1.675	
301	1.5	0.5	33	7	7	300.5	2.591	
300	22	10	45	3	3	299.5	6.492	
299	11	11	100	1.5	1.5	298.5	7.266	
298	17	12	71	1.5	1.5	297.5	4.627	
297	8	2	25	3	3	296.5	6.079	
296	6	2	33	3	3	295.5	8.942	*****
295	111	110	99	7	0	294.5	0.236	
294	50	50	100	3	0	293.5	1.792	
293	2.5	2.5	100	3	3	292.5	0.722	
292	38	28	74	3	0	291.5	2.184	[142]
291	42	42	100	3	0	290.5	7.487	
290	15	14	93	3	0	289.5	2.593	
289	1.3	0.3	23	7	7	288.5	0.444	
288	30	25	83	7	1.5	287.5	1.132	
287	17	14	82	3	1.5	286.5	1.500	*****
286	8	3	38	3	3	285.5	1.288	

bed#	Bt(cm)	St(cm)	S%	T.G	B.G	Posi.	D.Sq	Sq
285	21	12	57	7	3	284.5	0.797	
284	18	2	11	7	7	283.5	0.437	
283	31	26	84	7	3	282.5	0.168	
282	14	10	71	7	7	281.5	0.394	
281	11	11	100	7	7	280.5	4.722	*****
280	11.5	10	87	7	3	279.5	6.079	
279	23.5	22	94	7	3	278.5	3.405	
278	30.5	28	92	3	0	277.5	2.678	
277	22.5	21	93	7	7	276.5	1.714	
276	111	105	95	7	0	275.5	0.480	
275	48	40	83	7	7	274.5	2.069	
274	5	5	100	3	3	273.5	0.049	[143]
273	20	20	100	7	1.5	272.5	0.231	
272	5	5	100	3	3	271.5	1.188	
271	70	70	100	3	0	270.5	0.618	
270	20	20	100	7	7	269.5	5.473	
269	90	90	100	3	3	268.5	0.347	
268	30	30	100	3	1.5	267.5	0.568	
267	38	38	100	1.5	1.5	266.5	2.766	
266	15	15	100	1.5	1.5	265.5	1.307	
265	100	100	100	3	0	264.5	16.321	*****
264	20	11	55	3	3	263.5	10.913	
263	14	10	71	3	3	262.5	10.905	
262	1	0.2	20	7	7	261.5	6.667	
261	1.3	0.8	62	7	7	260.5	4.631	
260	1.3	0.3	23	7	7	259.5	0.509	
259	21.6	0.6	3	7	7	258.5	0.128	
258	14.5	0.5	3	7	7	257.5	0.000	
257	20.1	0.6	3	7	7	256.5	0.000	
256	1.7	0.2	12	7	7	255.5	0.004	
255	7.2	0.2	3	7	7	254.5	0.027	
254	3.2	0.2	6	7	7	253.5	0.030	
253	3	1	33	7	7	252.5	0.038	
252	3.2	2.5	78	7	7	251.5	0.017	
251	4.5	2.5	56	7	7	250.5	0.006	
250	9	7	78	7	7	249.5	0.016	
249	5.3	0.3	6	7	7	248.5	0.010	
248	10	3	30	7	7	247.5	0.013	
247	5.2	0.2	4	7	7	246.5	0.002	
246	14.2	1	7	7	7	245.5	0.001	
245	1.8	0.3	17	7	7	244.5	0.007	
244	4	2	50	7	7	243.5	0.005	
243	14	4	29	7	7	242.5	0.000	
242	4.5	3	67	7	7	241.5	0.005	
241	1.1	0.1	9	7	7	240.5	0.002	
240	5.5	1.5	27	7	7	239.5	0.007	
239	5.5	2.5	45	7	7	238.5	0.015	
238	3.5	0.5	14	7	7	237.5	0.006	
237	2	1	50	7	7	236.5	0.003	
236	1.4	0.7	50	7	7	235.5	0.002	
235	1.2	0.3	25	7	7	234.5	0.119	
234	63.3	0.3	0	7	7	233.5	0.590	
233	4.2	0.2	5	7	7	232.5	1.349	
232	5	0.5	10	7	7	231.5	1.365	

bed#	Bt(cm)	St(cm)	S%	T.G	B.G	Posi.	D.Sq	Sq
231	12	2	17	7	7	230.5	1.322	*****
230	64	10	16	3	3	229.5	0.768	
229	30	18	60	3	3	228.5	0.006	
228	18	15	83	3	3	227.5	0.551	
227	4.8	0.8	17	7	7	226.5	0.536	
226	1.5	1	67	7	7	225.5	0.526	
225	18.5	18	97	7	3	224.5	0.722	[144]
224	2	1	50	7	7	223.5	0.177	
223	2.2	0.2	9	7	7	222.5	0.003	
222	9.5	2.5	26	7	7	221.5	0.023	
221	3	1	33	7	7	220.5	0.457	
220	26	11	42	3	3	219.5	0.390	
219	5	3	60	7	7	218.5	0.529	
218	10	7	70	7	7	217.5	1.521	
217	12.5	11	88	7	7	216.5	1.396	*****
216	29	25	86	7	1.5	215.5	0.521	
215	11	11	100	7	7	214.5	1.847	
214	3	2.5	83	3	3	213.5	2.114	
213	40	40	100	3	3	212.5	0.088	[145]
212	16	15	94	7	7	211.5	0.060	
211	35	32	91	3	1.5	210.5	0.259	
210	22	22	100	3	1.5	209.5	1.998	
209	25	25	100	3	1.5	208.5	3.255	*****
208	19	7	37	7	7	207.5	1.044	
207	14	10	71	7	7	206.5	0.037	
206	6	5	83	7	7	205.5	1.144	
205	7	4	57	7	7	204.5	3.908	*****
204	22	18	82	3	1.5	203.5	3.883	
203	8	2	25	1.5	1.5	202.5	3.199	
202	80	80	100	3	1.5	201.5	2.114	
201	5	5	100	3	1.5	200.5	1.384	
200	4	4	100	1.5	1.5	199.5	0.761	[146]
199	12.5	10	80	1.5	1.5	198.5	0.598	
198	10	10	100	3	0	197.5	0.572	
197	5	2.5	50	3	3	196.5	0.174	
196	15	13	87	3	0	195.5	0.798	
195	17	17	100	3	0	194.5	1.639	
194	12.5	12.5	100	3	0	193.5	2.685	*****
193	14	13	93	7	3	192.5	2.045	
192	1.6	0.6	38	7	7	191.5	1.186	
191	4	1.5	38	7	7	190.5	0.252	
190	8	7.5	94	3	3	189.5	0.323	
189	23	15	65	7	3	188.5	0.108	
188	17	7	41	3	3	187.5	0.421	
187	18	6	33	7	7	186.5	0.456	
186	3.5	0.5	14	7	7	185.5	0.441	
185	12	10	83	7	7	184.5	0.188	
184	18	10	56	3	3	183.5	0.535	
183	3	2	67	7	7	182.5	0.000	
182	3.5	1.5	43	7	7	181.5	0.004	
181	10.5	2.5	24	7	7	180.5	0.129	
180	12	3	25	7	7	179.5	0.161	
179	4.5	1.5	33	7	7	178.5	0.541	
178	47	20	43	3	3	177.5	0.239	
177	49	1	2	7	7	176.5	0.242	
176	24	11	46	3	3	175.5	0.106	
175	12.5	1.5	12	7	7	174.5	0.152	
174	1.6	0.6	38	7	7	173.5	0.169	
173	29.5	28	95	7	1.5	172.5	0.133	
172	1.5	1	67	7	7	171.5	0.212	
171	32	20	63	3	1.5	170.5	0.290	

bed#	Bt(cm)	St(cm)	S%	T.G	B.G	Posi.	D.Sq	Sq
170	20	6	30	7	7	169.5	0.937	
169	4.5	1.5	33	7	7	168.5	2.080	
168	30	25	83	7	7	167.5	2.876	*****
167	17	16	94	3	0	166.5	0.438	
166	52	35	67	3	0	165.5	0.029	
165	31	31	100	3	3	164.5	1.194	
164	27	26	96	7	3	163.5	4.234	
163	17	16	94	7	7	162.5	2.656	
162	5	3	60	7	7	161.5	0.799	[147]
161	23	11	48	7	3	160.5	0.086	
160	7	3	43	7	7	159.5	2.063	
159	5	2	40	7	7	158.5	4.283	
158	30	26	87	7	3	157.5	2.064	
157	11	11	100	7	3	156.5	1.539	
156	38	34	89	7	0	155.5	0.469	
155	62	62	100	7	3	154.5	3.438	*****
154	18	15	83	7	7	153.5	3.204	
153	14	12	86	7	7	152.5	1.861	
152	29	12	41	3	3	151.5	1.627	
151	26	1	4	7	7	150.5	2.473	
150	1.2	0.5	42	7	7	149.5	6.022	*****
149	17.5	10	57	3	0	148.5	2.782	
148	25	20	80	3	0	147.5	0.823	
147	24.5	24	98	7	0	146.5	0.002	[148]
146	15	15	100	3	1.5	145.5	0.421	
145	16	10	63	3	0	144.5	1.802	
144	14	3	21	3	3	143.5	1.975	
143	54	24	44	7	3	142.5	2.611	*****
142	54.5	2	4	7	7	141.5	0.878	
141	27	15	56	3	3	140.5	2.117	
140	20	11	55	1.5	1.5	139.5	1.590	
139	3	0.5	17	7	7	138.5	1.207	
138	0.8	0.3	38	7	7	137.5	2.137	
137	50	47	94	7	7	136.5	0.030	
136	71	60	85	7	7	135.5	2.326	*****
135	12	10	83	3	0	134.5	2.142	
134	56	8	14	3	3	133.5	1.835	
133	6	2	33	7	7	132.5	1.707	
132	3	2	67	7	7	131.5	0.617	[149]
131	13	8	62	3	3	130.5	0.730	
130	8	3	38	3	3	129.5	0.861	
129	36	20	56	1.5	1.5	128.5	0.638	
128	12	7	58	7	7	127.5	0.570	
127	58	55	95	3	0	126.5	3.869	*****
126	5	2	40	7	7	125.5	1.602	
125	5.5	1.5	27	7	7	124.5	0.455	
124	16	10	63	7	7	123.5	0.308	
123	20	8	40	7	7	122.5	0.456	
122	1.2	0.2	17	7	7	121.5	0.443	
121	46	16	35	3	3	120.5	0.076	
120	14	13	93	3	3	119.5	0.813	
119	16.3	1.3	8	7	7	118.5	0.672	
118	6.8	0.8	12	7	7	117.5	0.551	
117	8	1	13	7	7	116.5	0.452	
116	2	1	50	7	7	115.5	0.108	
115	5.8	0.8	14	7	7	114.5	0.080	
114	2.2	1	45	7	7	113.5	0.215	
113	6	3	50	7	7	112.5	0.493	
112	23	14	61	7	7	111.5	1.195	
111	13	2	15	7	7	110.5	2.391	

bed#	Bt(cm)	St(cm)	S%	T.G	B.G	Posi.	D.Sq	Sq
110	20	4	20	7	7	109.5	4.490	*****
109	14	4	29	3	3	108.5	4.172	
108	20.2	1.2	6	3	3	107.5	3.979	
107	13	12	92	1.5	1.5	106.5	2.206	
106	25	11	44	1.5	1.5	105.5	0.750	
105	64	13	20	7	0	104.5	0.057	
104	24	9	38	7	0	103.5	0.138	
103	27	11	41	7	0	102.5	0.730	[150]
102	22	17	77	3	3	101.5	0.662	
101	4.5	3	67	3	3	100.5	0.133	
100	16	15	94	1.5	1.5	99.5	0.139	
99	6	5	83	3	3	98.5	0.207	
98	57	10	18	3	3	97.5	0.089	
97	18.5	3.5	19	3	3	96.5	0.281	
96	44	18	41	7	0	95.5	0.948	
95	14	13	93	7	3	94.5	1.488	*****
94	36.1	0.1	0	7	7	93.5	0.809	
93	8.6	0.6	7	7	3	92.5	0.645	
92	1.2	0.2	17	7	7	91.5	0.232	
91	17	11	65	3	1.5	90.5	0.625	
90	1.2	1	83	7	7	89.5	0.322	
89	0.5	0.3	60	7	7	88.5	0.190	
88	13.5	7	52	3	3	87.5	0.150	
87	30	25	83	7	7	86.5	0.150	
86	24	4	17	7	7	85.5	0.191	
85	23.3	0.3	1	7	7	84.5	0.438	
84	24	5	21	3	3	83.5	0.079	
83	56	10	18	7	3	82.5	0.329	
82	3.2	0.2	6	7	7	81.5	0.112	
81	9.5	2	21	7	7	80.5	0.166	
80	24	10	42	3	3	79.5	0.287	
79	7.1	0.1	1	7	7	78.5	0.076	
78	1.1	0.1	9	7	7	77.5	0.131	
77	5.5	1.5	27	7	7	76.5	0.105	
76	156	32	21	7	1.5	75.5	0.959	
75	97.5	0.5	1	7	7	74.5	0.419	
74	25.9	0.9	3	7	7	73.5	0.435	
73	8.5	0.5	6	7	7	72.5	0.435	
72	2.1	0.1	5	7	7	71.5	0.403	
71	1.8	0.8	44	7	7	70.5	0.000	
70	19.2	0.2	1	7	7	69.5	0.136	
69	4.6	0.6	13	7	7	68.5	2.060	
68	12	0.9	8	7	7	67.5	4.155	
67	94	1	1	7	7	66.5	5.585	
66	5	1	20	7	7	65.5	7.919	*****
65	33	11	33	3	3	64.5	4.708	
64	84	70	83	3	1.5	63.5	0.155	[151]
63	30	30	100	3	1.5	62.5	1.514	
62	13	12.5	96	3	3	61.5	3.495	
61	26.5	22.5	85	3	3	60.5	6.612	*****
60	5.75	0.75	13	7	7	59.5	4.451	
59	7	3	43	7	7	58.5	1.098	
58	6.6	0.6	9	7	7	57.5	0.227	
57	5.8	1.8	31	7	7	56.5	1.089	
56	9.9	0.9	9	3	3	55.5	5.749	
55	4	0.5	13	3	3	54.5	5.888	
54	12	1	8	7	7	53.5	19.793	

bed#	Bt(cm)	St(cm)	S%	T.G	B.G	Posi.	D.Sq	Sq
53	7.5	3	40	7	7	52.5	19.134	*****
52	64	60	94	7	0	51.5	5.828	
51	85	85	100	3	0	50.5	0.329	[152]
50	12	12	100	3	3	49.5	0.952	
49	131	130	99	3	0	48.5	21.779	*****
48	4.6	0.1	2	7	7	47.5	20.941	
47	6.2	0.2	3	7	7	46.5	12.351	
46	6.7	1.2	18	7	7	45.5	3.206	
45	11.5	2.5	22	7	7	44.5	0.143	
44	7	2.5	36	7	7	43.5	5.234	
43	13	4	31	7	7	42.5	6.232	
42	2.5	1.5	60	7	7	41.5	7.076	*****
41	20.5	18.5	90	3	3	40.5	4.309	
40	88	86	98	3	1.5	39.5	0.752	
39	47	32	68	3	3	38.5	2.395	
38	23	11	48	7	3	37.5	2.744	[153]
37	16	16	100	7	7	36.5	4.235	
36	8	3	38	3	3	35.5	3.776	
35	6	4	67	3	3	34.5	1.173	
34	5.5	4	73	7	7	33.5	0.363	
33	22.5	12.5	56	1.5	1.5	32.5	1.339	*****
32	4	3	75	7	7	31.5	0.656	
31	8	1	13	7	7	30.5	0.275	
30	3.2	0.2	6	7	7	29.5	0.243	
29	41.5	1.5	4	7	7	28.5	0.521	
28	16	8	50	7	7	27.5	2.544	
27	45	33	73	3	3	26.5	1.078	
26	33.5	0.5	1	7	7	25.5	1.113	
25	53	8	15	3	3	24.5	0.221	
24	42	2	5	3	3	23.5	0.231	
23	60	33	55	3	3	22.5	1.168	
22	29	25	86	3	3	21.5	2.195	
21	60	3	5	7	7	20.5	2.284	
20	31	11	35	7	7	19.5	1.227	
19	186.5	3.5	2	7	7	18.5	1.023	
18	8	2	25	7	7	17.5	0.276	
17	2.4	0.4	17	7	7	16.5	0.601	
16	5.5	1.5	27	7	7	15.5	1.388	
15	19	6	32	3	3	14.5	0.583	
14	13	1	8	7	7	13.5	0.823	
13	10.2	0.2	2	7	7	12.5	1.760	*****
12	30	18	60	3	1.5	11.5	0.772	
11	23	23	100	3	3	10.5	0.205	
10	15	13	87	7	7	9.5	3.028	
9	11	10	91	7	7	8.5	3.936	
8	7	3	43	0	0	7.5	3.883	[154]
7	23	23	100	1.5	1.5	6.5	3.895	
6	31	25	81	7	3			
5	100	95	95	7	3			
4	29	24	83	7	3			
3	32	30	94	7	3			
2	35	31	89	7	7			
1	28	24	86	7	7			******

Appendix II-1

ASYMRAN.FOR--A FORTRAN 77 PROGRAM USED TO TEST FOR ASYMMETRIC TRENDS AND RANDOMNESS

```
C     ------------------------------------------------------
C     ASYMRAN.FOR
C     ------------------------------------------------------
C     PURPOSE:
C
C  This program is written to statistically test for asymmetric trends and
C   randomness in a set of sequences. It includes the most powerful methods for
C   trend tests (i.e., correlation tests): Kendall's rank correlation, Spearman's rank
C   correlation, and Pearson's linear correlation tests. Four tests for randomness
C   (the Rank Difference test, Turning Point test, Median Crossing test, and
C   Length-of-Runs test) are also incorporated into this program.
C
C    INPUT:
C       NBLOCK = the number of sequences (or sand packets) to be analysed
C       NB(L) = a list of bed number (or sample size) of individual sequences
C       A(K,2) = two dimensional matrix; the first column is the ordered
C                   number of events in a sequence, for instance, bed
C                   number 1 2 3 4...; the second column is measurements
C                   of a sequence, for example, bed thickness. Note: put
C                   10 stars, **********, between each of two or more sequences.
C
C    OUTPUT:
C       N = number of beds in individual sequences
C       Tau = coefficient of Kendall's rank correlation
C       Ztau = value of Z test for Tau
C       SP = coefficient of Spearman's rank correlation test
C       Tsp = value of student's t test for SP
C       R = coefficient of Pearson's linear correlation test
C       Tr = value of student's t test for R
C       Zt = value of Z test for the Turning Point test
C       Zr = value of Z test for the Rank Difference test
C       Zc = value of Z test for the Median Crossing test
C       FLR = value of F test for the Length-of-Runs test
C       Pztau, Ptsp, Ptr, Pzt, Pzr, Pzc, Pflr are the significance levels at which a
```

```
C     sequence passed Kendall's, Spearman's and Pearson's correlation tests,
C     the Turning Point, Rank Difference, Median Crossing, and Length-of-Runs
C     tests respectively.
C
C     NOTE: Parametric dimensions of this program are adjustable, so
C        that they can meet the requirements of longer sequences and
C        a larger number of sequences.
C
C     Author: C. Chen      Date: June 1995
C     ---------------------------------------------------

      DIMENSION X(100),Y(100),A(100,2),NB(400)
      DIMENSION WKSP1(100),WKSP2(100)
      DIMENSION C(2),INDX(100),IRANK(100),RSL(400,24)
      INTEGER   N,NB,NBLOCK,INDX,IRANK,IS
      REAL X,Y,A,WKSP1,WKSP2,XM,TAU,ZK,PROBK,D,ZD,RS
      REAL TS,PROBD,PROBRS,ZT,ZR,ZC,QR,R,ZP,PPROB,C
      REAL  RL2,RL,FRL,PROBZT,PROBZC,PROBZR,PROBQR
      REAL      PROBRL,TL
      CHARACTER STAR*10
      CHARACTER*60 INPFIL, OUTFIL
      WRITE(*,*) 'Enter input file name (maxm. 60
     *            characters):'
      READ(*,999) INPFIL
999   FORMAT (A60)
      WRITE(*,*) 'Enter output file name (maxm. 60
     *            characters):'
      READ(*,999) OUTFIL
      OPEN (UNIT=7, FILE=INPFIL, STATUS='OLD')
      OPEN (UNIT=8, FILE=OUTFIL, STATUS='NEW')
C     ------------------------------------------------
C     Read input data
C     ------------------------------------------------
      read(7,*) NBLOCK
      read(7,*) (NB(L), L=1,NBLOCK)
C     ------------------------------------------------
C     Read sequence 1 and start to analyze sequence 1,
C     then turn to the next sequence
C     ------------------------------------------------
      DO 100 I=1,NBLOCK
      DO 110 K=1,NB(I)
      READ(7,*) (A(K,J),J=1,2)
```

```
      X(K)=A(K,1)
      Y(K)=A(K,2)
110   CONTINUE
      READ(7,120) STA
120   FORMAT(10A)
      N=NB(I)
C     ------------------------------------------------
C     Calculating median of a sequence
C     ------------------------------------------------
      CALL MEDIAN(Y,N,XM)
      DO 200 J=1,N
      Y(J)=A(J,2)
200   CONTINUE
      CALL INDEX(N,Y,INDX)
      CALL RANK(N,INDX,IRANK)
C     ------------------------------------------------
C     Running Kendall's Rank Correlation test
C     ------------------------------------------------
      CALL KENDAL(X,Y,N,TAU,ZK,PROBK)
      NKK=N
      RSL(I,1)=FLOAT(NKK)
      RSL(I,2)=TAU
      RSL(I,3)=ZK
      RSL(I,4)=PROBK
C
      DO 400 II=1,N
      WKSP1(II)=0.0
      WKSP2(II)=0.0
400   CONTINUE
C     ------------------------------------------------
C     Running Spearman's rank correlation test
C     ----------------------------------------
      CALL SPEARM(X,Y,N,WKSP1,WKSP2,D,ZD,RS,TS,PROBD
     *            PROBRS)
      RSL(I,5)=RS
      RSL(I,6)=TS
      RSL(I,7)=PROBRS
C     ------------------------------------------------
C     Running Turning Point test
C     ------------------------------------------------
      CALL TURNP(Y,N,ZT,PROBZT)
      RSL(I,8)=ZT
```

```
      RSL(I,9)=PROBZT
C     ------------------------------------------------
C     Running Rank Difference test
C     ------------------------------------------------
      CALL RANKD(IRANK,N,ZR,PROBZR)
      RSL(I,10)=ZR
      RSL(I,11)=PROBZR
C     ------------------------------------------------
C     Running Median Crossing test
C     ------------------------------------------------
      CALL MCROS(Y,N,XM,ZC,PROBZC)
     RSL(I,12)=ZC
     RSL(I,13)=PROBZC
C     ------------------------------------------------
C     Running Length-of-Runs test
C     ------------------------------------------------
      CALL LRUN(Y,N,XM,QR,IS,PROBQR)
      RSL(I,14)=QR
      RSL(I,15)=PROBQR
C     ------------------------------------------------
C     Running Pearson's linear correlation test
C     ------------------------------------------------
      CALL PEARSN(X,Y,N,R,TP,PROB)
      RSL(I,16)=R
      RSL(I,17)=TP
      RSL(I,18)=PROB
C     ---------------------------------
C     Finishing the test of a sequence and going to test
C     the next sequence
C     ------------------------------------------------
100   CONTINUE
C     ---------------------------------------
C     Write outputs as a matrix with 18 columns and
C     Nblock (number of sequences) of rows
C     ------------------------------------------------
      Write(8,801) 'N      Tau    Ztau   Pztau  Sp
     *Tsp    Ptsp    Zt     Pzt    Zr     Pzr    Zc
     *Pzc    Flr     Pflr   R      Tr     Ptr    '
801   Format(1X,A168)
      DO 902 IK=1,NBLOCK
      write(8,903)(RSL(IK,IJ),IJ=1,18)
903   FORMAT(1X,18(1X,F7.3))
```

```
902   CONTINUE
      STOP
      END
C     ---------------------------------------------
C     Subroutine Median
C     Given an array X of N numbers, returns their
C     median value Xm.The array X is modified and
C     returned sorted into ascending order
C     ---------------------------------------------
      SUBROUTINE MEDIAN(X,N,XM)
      DIMENSION X(N)
      CALL SORT(N,X)
      N2=N/2
      IF(2*N2 .EQ. N) THEN
        XM=0.5*(X(N2)+X(N2+1))
         ELSE
           XM=X(N2+1)
         ENDIF
         RETURN
         END
C     ---------------------------------------------
C     Subroutine Sort (from Press et al., 1986)
C     Sort an array RA of length N into ascending
C     numerical order.
C     ---------------------------------------------
      SUBROUTINE SORT(N,RA)
      DIMENSION RA(N)
      L=N/2+1
      IR=N
10    CONTINUE
      IF(L .GT. 1) THEN
           L=L-1
           RRA=RA(L)
       ELSE
          RRA=RA(IR)
          RA(IR)=RA(1)
          IR=IR-1
         IF(IR .EQ. 1) THEN
             RA(1)=RRA
             RETURN
         ENDIF
       ENDIF
```

```
            I=L
            J=L+L
20       IF(J .LE. IR) THEN
            IF(J .LT. IR) THEN
               IF(RA(J) .LT. RA(J+1)) J=J+1
            ENDIF
            IF(RRA .LT. RA(J)) THEN
               RA(I)=RA(J)
               I=J
               J=J+J
            ELSE
               J=IR+1
            ENDIF
          GOTO 20
          ENDIF
          RA(I)=RRA
         GOTO 10
         END
C        ------------------------------------------
C        SUBROUTINE INDEX (adapted from Press et al.,
C        1986)
C        To output the array INDX in which ARRIN(INDX(J))
C        is in ascending order for J=1,2,...,N. The input
C        N and ARRIN are not changed.
C        ------------------------------------------------
         SUBROUTINE INDEX(N,ARRIN,INDX)
         DIMENSION ARRIN(N),INDX(N)
         DO 11 J=1,N
            INDX(J)=J
11       CONTINUE
         L=N/2+1
         IR=N
10       CONTINUE
           IF(L .GT. 1) THEN
               L=L-1
               INDXT=INDX(L)
               Q=ARRIN(INDXT)
           ELSE
               INDXT=INDX(IR)
               Q=ARRIN(INDXT)
               INDX(IR)=INDX(1)
               IR=IR-1
```

```
            IF(IR .EQ. 1) THEN
               INDX(1)=INDXT
               RETURN
            ENDIF
         ENDIF
         I=L
         J=L+L
20     IF(J .LE. IR)THEN
        IF(J .LT. IR) THEN
         IF(ARRIN(INDX(J)) .LT. ARRIN(INDX(J+1))) J=J+1
         ENDIF
          IF(Q .LT. ARRIN(INDX(J))) THEN
             INDX(I)=INDX(J)
             I=J
             J=J+J
          ELSE
             J=IR+1
          ENDIF
       GOTO 20
       ENDIF
       INDX(I)=INDXT
       GOTO 10
       END
C      ------------------------------------------------
C      SUBROUTINE RANK
C      This routine outputs corresponding ranks of
C      INDX(N).
C      ------------------------------------------------
       SUBROUTINE RANK(N,INDX,IRANK)
       DIMENSION INDX(N),IRANK(N)
       DO 11 J=1,N
          IRANK(INDX(J))=J
11     CONTINUE
       RETURN
       END
C      ------------------------------------------------
C      SUBROUTINE KENDAL (adapted from Press et al.,
C      1986)
C      This routine runs Kendall's rank correlation
C      test. It returns Kendall's correlation
C      coefficient (TAU), Z test of TAU (ZK), and the
C      significance level (PROBK) at which a sequence
```

```
C     passed the test. Smaller values of PROBK
C     indicate a significant correlation (when Tau is
C     positive) or anti-correlation (when Tau is
C     negative).
C     ---------------------------------------------
      SUBROUTINE KENDAL(DATA1,DATA2,N,TAU,ZK,PROBK)
      DIMENSION DATA1(N),DATA2(N)
      N1=0
      N2=0
      IS=0
      DO 12 J=1,N-1
      DO 11 K=J+1,N
         A1=DATA1(J)-DATA1(K)
         A2=DATA2(J)-DATA2(K)
         AA=A1*A2
         IF(AA .NE. 0.) THEN
           N1=N1+1
           N2=N2+1
           IF(AA .GT. 0.) THEN
              IS=IS+1
           ELSE
              IS=IS-1
           ENDIF
         ELSE
           IF(A1 .NE. 0.) N1=N1+1
             IF(A2 .NE. 0.) N2=N2+1
           ENDIF
11       CONTINUE
12     CONTINUE
      TAU=FLOAT(IS)/SQRT(FLOAT(N1)*FLOAT(N2))
      VAR=(4.*N+10.)/(9.*N*(N-1.))
      ZK=TAU/SQRT(VAR)
      PROBK=ERFCC(ABS(ZK)/1.4142136)
      RETURN
      END
C
      FUNCTION ERFCC(X)
      Z=ABS(X)
      T=1./(1.+0.5*Z)
      ERFCC=T*EXP(-Z*Z-1.26551223+T*(1.00002368+
     &T*(.37409196+T*(.09678418+T*(-.18628806+
     &T*(.27886807+T*(-1.13520398+T*(1.48851587+
```

```
     &T*(-.82215223+T*.17087277)))))))))
      IF(X .LT. 0.) ERFCC=2.-ERFCC
      RETURN
      END
C     ---------------------------------------------
C     SUBROUTINE SPEARM (adapted from Press et al.,
C     1987)
C     This routine runs Spearman's rank correlation
C     test. It returns Spearman's correlation
C     coefficient (RS), student t test of RS (TS), and
C     the significance level (PROBRS) at which a
C     sequence passed the test. A small value of PROBRS
C     indicates a significant correlation for a
C     positive RS or a significant anti-correlation for
C     a negative RS.
C     ---------------------------------------------
C     SUBROUTINE SPEARM(DATA1,DATA2,N,WKSP1
     &  WKSP2,D,ZD,RS,TS,PROBD,PROBRS)
      DIMENSION DATA1(N),DATA2(N),WKSP1(N),WKSP2(N)
      parameter(TINY = 1.E-20)
      DO 11 J=1,N
        WKSP1(J)=DATA1(J)
        WKSP2(J)=DATA2(J)
11    CONTINUE
      CALL SORT2(N,WKSP1,WKSP2)
      CALL CRANK(N,WKSP1,SF)
      CALL SORT2(N,WKSP2,WKSP1)
      CALL CRANK(N,WKSP2,SG)
      D=0.
      DO 12 J=1,N
      D=D+(WKSP1(J)-WKSP2(J))**2
12    CONTINUE
      EN=N
      EN3N=EN**3-EN
      AVED=EN3N/6.-(SF+SG)/12.
      FAC=(1.-SF/EN3N)*(1.-SG/EN3N)
      VARD=((EN-1.0)*EN**2*(EN+1.)**2/36.)*FAC
      ZD=(D-AVED)/SQRT(VARD)
      PROBD=ERFCC(ABS(ZD)/1.4142136)
      RS=(1.-(6./EN3N)*(D+0.5*(SF+SG)))/FAC
      TS=RS*SQRT((EN-2.)/(((1.+RS)+
     &   TINY)*((1.-RS)+TINY)))
```

```
      DF=EN-2.
      PROBRS=BETAI(0.5*DF,0.5,DF/(DF+TS**2))
      RETURN
      END
C
      SUBROUTINE SORT2(N,RA,RB)
      DIMENSION RA(N),RB(N)
      L=N/2+1
      IR=N
10    CONTINUE
        IF(L .GT. 1) THEN
         L=L-1
         RRA=RA(L)
         RRB=RB(L)
        ELSE
         RRA=RA(IR)
         RRB=RB(IR)
          RA(IR)=RA(1)
          RB(IR)=RB(1)
          IR=IR-1
           IF(IR .EQ. 1) THEN
           RA(1)=RRA
           RB(1)=RRB
          RETURN
          ENDIF
        ENDIF
        I=L
        J=L+L
20    IF(J .LE. IR) THEN
        IF(J .LT. IR) THEN
          IF(RA(J) .LT. RA(J+1)) J=J+1
        ENDIF
        IF(RRA .LT. RA(J)) THEN
          RA(I)=RA(J)
          RB(I)=RB(J)
          I=J
          J=J+J
        ELSE
          J=IR+1
        ENDIF
      GOTO 20
      ENDIF
```

```
      RA(I)=RRA
      RB(I)=RRB
      GOTO 10
C     RETURN
      END
C
      SUBROUTINE CRANK(N,W,S)
      DIMENSION W(N)
      S=0.
      J=1
1     IF(J .LT. N) THEN
        IF(W(J+1) .NE. W(J)) THEN
          W(J)=J
          J=J+1
        ELSE
          DO 11 JT=J+1,N
            IF(W(JT) .NE. W(J)) GOTO 2
11        CONTINUE
          JT=N+1
2         RANK=0.5*(J+JT-1)
          DO 12 JI=J,JT-1
             W(JI)=RANK
12        CONTINUE
          T=JT-J
          S=S+T**3-T
          J=JT
       ENDIF
      GOTO 1
      ENDIF
      IF(J .EQ. N) W(N)=N
      RETURN
      END
C
      FUNCTION BETAI(A,B,X)
      IF(X .LT. 0. .OR. X .GT. 1.) X=1.E-20
      IF(X .EQ. 0. .OR. X .EQ. 1.) THEN
         BT=0.
      ELSE
       BT=EXP(GAMMLN(A+B)-GAMMLN(A)-GAMMLN(B)
     &     +A*ALOG(X)+B*ALOG(1.-X))
      ENDIF
      IF(X .LT. (A+1.)/(A+B+2.)) THEN
```

```
      BETAI=BT*BETACF(A,B,X)/A
         RETURN
        ELSE
         BETAI=1.-BT*BETACF(B,A,1.-X)/B
         RETURN
        ENDIF
        END
C
        FUNCTION BETACF(A,B,X)
        PARAMETER (ITMAX=100,EPS=3.E-7)
        AM=1.
        BM=1.
        AZ=1.
        QAB=A+B
        QAP=A+1.
        QAM=A-1.
        BZ=1.-QAB*X/QAP
        DO 11 M=1,ITMAX
        EM=M
        TEM=EM+EM
        D=EM*(B-M)*X/((QAM+TEM)*(A+TEM))
        AP=AZ+D*AM
        BP=BZ+D*BM
        D=-(A+EM)*(QAB+EM)*X/((A+TEM)*(QAP+TEM))
        APP=AP+D*AZ
        BPP=BP+D*BZ
        AOLD=AZ
        AM=AP/BPP
        BM=BP/BPP
        AZ=APP/BPP
        BZ=1.
        IF(ABS(AZ-AOLD) .LT. EPS*ABS(AZ)) GOTO 1
11      CONTINUE
1       BETACF=AZ
        RETURN
        END
C
        FUNCTION GAMMLN(XX)
        REAL*8 COF(6),STP,HALF,ONE,FPF,X,TMP,SER
        DATA COF,STP/76.18009173D0,-86.50532033D0,
     &  24.01409822D0,-1.231739516D0,.120858003D-2,
     &  -.536382D-5,2.50662827465D0/
```

```
      DATA HALF,ONE,FPF/0.5D0,1.0D0,5.5D0/
      X=XX-ONE
      TMP=X+FPF
      TMP=(X+HALF)*LOG(TMP)-TMP
      SER=ONE
      DO 11 J=1,6
      X=X+ONE
      SER=SER+COF(J)/X
11    CONTINUE
      GAMMLN=TMP+LOG(STP*SER)
      RETURN
      END
C     ---------------------------------------------
C     SUBROUTINE TURNP runs Turning Point test and
C     returns Z test value (ZT) and the significance
C     level (PROBZT) at which a sequence passed the
C     test. A small PROBZT indicates a non-random
C     sequence.
C     ---------------------------------------------
      SUBROUTINE TURNP(X,N,ZT,PROBZT)
      DIMENSION X(N)
      T=0.
      DO 10 I=1,N-2
      IF((X(I) .LT. X(I+1) .AND. X(I+1) .GT. X(I+2))
     &   .OR.(X(I) .GT. X(I+1) .AND. X(I+1) .LT.
     &   X(I+2))) THEN
      T=T+1.
      ENDIF
10    CONTINUE
      ET=(N-2.)*2./3.
      VT=(16.*N-29.)/90.
      ZT=(T-ET)/SQRT(VT)
      PROBZT=ERFCC(ABS(ZT)/1.4142136)
      RETURN
      END
C     -----------------------------------------------
C     SUBROUTINE RANKD runs Rank Difference test. It
C     returns Z test value (ZR) and the significance
C     level (PROBZR) at which a sequence passed the
C     test.
C     ---------------------------------------------
      SUBROUTINE RANKD(IRANK,N,ZR,PROBZR)
```

```
      DIMENSION IRANK(N)
      R=0.
      DO 30 I=2,N
      R=R+ABS(IRANK(I)-IRANK(I-1))
30    CONTINUE
      ER=(N+1.)*(N-1.)/3.
      VR=(N-2.)*(N+1.)*(4.*N-7.)/90.
      ZR=(R-ER)/SQRT(VR)
      PROBZR=ERFCC(ABS(ZR)/1.4142136)
      RETURN
      END
C     ------------------------------------------------
C     SUBROUTINE MCROS runs Median Crossing test. It
C     returns Z test value (ZC) and the significance
C     level (PROBZC) at which a sequence passed the
C     test.
C     ------------------------------------------------
      SUBROUTINE MCROS(X,N,XM,ZC,PROBZC)
      DIMENSION X(N),X1(100),X2(100)
      L=0
      DO 20 I=1,N
      IF(X(I) .NE. XM) THEN
      L=L+1
      X1(L)=X(I)
      ENDIF
20    CONTINUE
      DO 30 J=1,L
      IF(X1(J) .LT. XM) THEN
      X2(J)=0.
      ELSE
      X2(J)=1.
      ENDIF
30    CONTINUE
      CR=0.
      DO 40 I=1,L-1
      IF(X2(I) .NE. X2(I+1)) THEN
      CR=CR+1.
      ENDIF
40    CONTINUE
      EC=(L-1.)/2.
      VC=(L-1.)/4.
      ZC=(CR-EC)/SQRT(VC)
```

```
      PROBZC=ERFCC(ABS(ZC)/1.4142136)
      RETURN
      END
C     ------------------------------------------------
C     SUBROUTINE LRUN runs Length-of-Runs test. It
C     returns the statistic of this test (QR), degrees
C     of freedom (IS) (both QR and IS are used for the
C     Chi-Square test), and the significance level
C     (PROBQR) at which a sequence passed the test.
C     ------------------------------------------------
      SUBROUTINE LRUN(X,N,XM,QR,IS,PROBQR)
      DIMENSION X(N),X1(100),M(100)
      INTEGER X1,M,IP,IM,IS,ISS
      DO 21 I=1,N
      M(I)=0
21    CONTINUE
      J=0
      DO 10 I=1,N
      IF(X(I) .LT. XM) THEN
        J=J+1
        X1(J)=-1
      ELSE IF(X(I) .GT. XM) THEN
        J=J+1
        X1(J)=1
      ENDIF
10    CONTINUE
      IP=0
      IM=0
      IS=1
      ISS=1
      DO 150 I=1,N
      IF(X1(I) .EQ. 1) THEN
        IF(IM .EQ. 0) THEN
           IP=IP+1
           IF(IP .GT. IS) THEN
             IS=IP
           ENDIF
        ELSE
           M(IM)=M(IM)+1
           IP=IP+1
           IM=0
        ENDIF
```

```
      ELSE
        IF(IP .EQ. 0) THEN
           IM=IM+1
           IF(IM .GT. ISS) THEN
             ISS=IM
           ENDIF
        ELSE
           M(IP)=M(IP)+1
           IM=IM+1
           IP=0
        ENDIF
      ENDIF
150   CONTINUE
      IF(IM .EQ. 0) THEN
        M(IP)=M(IP)+1
      ELSE
        M(IM)=M(IM)+1
      ENDIF
      IF(IS .LT. ISS) THEN
         IS=ISS
      ENDIF
      QR=0.
      DO 250 I=1,IS
      L=I+1
      ER=FLOAT(J+3-I)/FLOAT(2**L)
      QR=QR+(M(I)-ER)*(M(I)-ER)/ER
250   CONTINUE
      IS=IS-1
      PROBQR=GAMMQ(0.5*IS,0.5*QR)
      RETURN
      END
C
      FUNCTION GAMMQ(A,X)
      IF(X .LT. 0.) X=1.E-20
      IF(A .LE. 0.) A=1.E-20
      IF(X .LT. A+1.) THEN
        CALL GSER(GAMSER,A,X,GLN)
        GAMMQ=1.-GAMSER
      ELSE
        CALL GCF(GAMMQ,A,X,GLN)
      ENDIF
      RETURN
```

```
      END
C
      SUBROUTINE GSER(GAMSER,A,X,GLN)
      PARAMETER (ITMAX=100,EPS=3.E-7)
      GLN=GAMMLN(A)
      IF(X .LE. 0.) THEN
        IF(X .LT. 0.) X=1.E-20
        GAMSER=0.
        RETURN
      ENDIF
      AP=A
      SUM=1./A
      DEL=SUM
      DO 11 N=1,ITMAX
        AP=AP+1.
        DEL=DEL*X/AP
        SUM=SUM+DEL
        IF(ABS(DEL) .LT. ABS(SUM)*EPS) GOTO 1
11    CONTINUE
1     GAMSER=SUM*EXP(-X+A*LOG(X)-GLN)
      RETURN
      END
C
      SUBROUTINE GCF(GAMMCF,A,X,GLN)
      PARAMETER (ITMAX=100,EPS=3.E-7)
      GLN=GAMMLN(A)
      GOLD=0.
      A0=1.
      A1=X
      B0=0.
      B1=1.
      FAC=1.
      DO 11 N=1,ITMAX
      AN=FLOAT(N)
      ANA=AN-A
      A0=(A1+A0*ANA)*FAC
      B0=(B1+B0*ANA)*FAC
      ANF=AN*FAC
      A1=X*A0+ANF*A1
      B1=X*B0+ANF*B1
      IF(A1 .NE. 0.) THEN
        FAC=1./A1
```

```
          G=B1*FAC
          IF(ABS((G-GOLD)/G) .LT. EPS) GOTO 1
          GOLD=G
        ENDIF
11      CONTINUE
1       GAMMCF=EXP(-X+A*ALOG(X)-GLN)*G
        RETURN
        END
C       ------------------------------------------------
C   SUBROUTINE PEARSN (adapted from Press et al., 1986). This routine runs
C   Pearson's linear correlation test. It returns Pearson's correlation
C   coefficient (R), student t test value, and the significance level (PROB) at which a
C   sequence passed the correlation test.
C       ------------------------------------------------
        SUBROUTINE PEARSN (X,Y,N,R,TP,PROB)
        PARAMETER (TINY=1.E-20)
        DIMENSION X(N),Y(N)
        AX=0.
        AY=0.
        DO 11 J=1,N
        AX=AX+X(J)
        AY=AY+Y(J)
11      CONTINUE
        AX=AX/N
        AY=AY/N
        SXX=0.
        SYY=0.
        SXY=0.
        DO 12 J=1,N
          XT=X(J)-AX
          YT=Y(J)-AY
          SXX=SXX+XT**2
          SYY=SYY+YT**2
          SXY=SXY+XT*YT
12      CONTINUE
        R=SXY/SQRT(SXX*SYY)
        DF=N-2
        TP=R*SQRT(DF/(((1.-R)+TINY)*((1.+R)+TINY)))
        PROB=BETAI(0.5*DF,0.5,DF/(DF+TP**2))
        RETURN
        END
C            --------------End of the program.
```

APPENDIX II-2

RANSHUF.FOR, A FORTRAN 77 PROGRAM USED TO RANDOMLY SHUFFLE N SEQUENCES

```
C-----------------------------------------
C    RANSHUF
C-----------------------------------------
C    Purpose:
C       This program is designed for Monte Carlo simulation. It randomly shuffles
C       original data to generate random sequences.
C    Input:
C      NBLOCK = the number of the original sequences (or sand packets)
C      Seed = any random value, chosen by users
C      NB(L)= a list of bed numbers (or sample size) of individual sequences
C      A(K,2)= two dimension matrix; the first column is the ordered number of
C      events in a sequence,for instance, bed number 1 2 3 4...; the second column
C      is measurements of a sequence, for example, bed thickness.
C      Note: put 10 stars, **********, between each of two or more sequences.
C  Output:
C    N blocks of random sequences
C  ---------------------------------------
C   Author: C. Chen         Date: June, 1995
C  ---------------------------------------
      DIMENSION X(100),Y(100),A(100,2),NB(400),
     &         YT(100),YY(100,2), RANDNU(2)
      INTEGER  N,NB,NBLOCK,SEED
      REAL     X,Y,A,YT,YY,RANDNU
      CHARACTER STAR*10
      CHARACTER*60 INPFIL, OUTFIL
      WRITE(*,*) 'Enter input file name (maxm. 60 characters) :'
      READ(*,999) INPFIL
999   FORMAT (A60)
      WRITE(*,*) 'Enter output file name (maxm. 60 characters) :'
      READ(*,999) OUTFIL
```

```
      OPEN (UNIT=7, FILE=INPFIL, STATUS='OLD')
      OPEN (UNIT=8, FILE=OUTFIL, STATUS='NEW')
C     ------------------------------------
C     Read input data
C     ------------------------------------
      read(7,*) NBLOCK
      read(7,*) SEED
      read(7,*) (NB(L), L=1,NBLOCK)
      DO 100 I=1,NBLOCK
      DO 110 K=1,NB(I)
      READ(7,*) (A(K,J),J=1,2)
      X(K)=A(K,1)
      Y(K)=A(K,2)
110   CONTINUE
      READ(7,120) STAR
120   FORMAT(10A)
      N=NB(I)
      DO 10 J=1,N
      YT(J)=Y(J)
10    CONTINUE
C     ------------------------------------------
C     To shuffle the first sequence and generate a
C       random sequence
C     ------------------------------------
      CALL SHUFFLE(YT,N,SEED)
      DO 20 L=1,N
      YY(L,1)=FLOAT(L)
      YY(L,2)=YT(L)
20    CONTINUE
      DO 30 LL=1,N
      WRITE(8,101) (YY(LL,IJ), IJ=1,2)
101   FORMAT(1X, 2F6.1)
30    CONTINUE
      WRITE(8,102) STAR
102   FORMAT(1X, 60A)
C     ------------------------------------------
C     To turn to the next sequence and shuffle it
C     ------------------------------------------
100   CONTINUE
      STOP
      END
```

```
C     ----------------------------------------
C     SUBROUTINE SHUFFLE (adapted from Murray, 1992)
C     This routine randomly shuffles an original
C     sequence 20,000 times to generate a random
C     sequence.
C     ----------------------------------------
      SUBROUTINE SHUFFLE(X,N,SEED)
      REAL X(N), RANDNU(2)
      INTEGER SEED
      MAXSHUF=20000
      DO 10 I=1, MAXSHUF
      CALL RAND(SEED,2,RANDNU)
      INDEX1=1+INT(RANDNU(1)*N)
      INDEX2=1+INT(RANDNU(2)*N)
      TEMP=X(INDEX1)
      X(INDEX1)=X(INDEX2)
      X(INDEX2)=TEMP
10    CONTINUE
      RETURN
      END
C
      SUBROUTINE RAND(SEED,N,VECTOR)
      DIMENSION VECTOR(*)
      COMMON /UNUSUAL/ITAB(55),N1,N2,NSEED
      INTEGER M1, SEED
      IF((SEED .GT. 0) .OR. (NSEED .LT. 1)) THEN
      NSEED=SEED
      IF(SEED .LE. 0) NSEED=7931
      DO 10 I=1, 55
      M1=MOD(NSEED*9069,32768)
        IF(MOD(M1,2) .EQ. 0) M1=M1-1
          ITAB(I)=M1
          NSEED=M1
10        CONTINUE
          N1=0
          N2=24
        ENDIF
      DO 30 I=1,N
      ITAB(55-N1)=MOD(ITAB(55-N2)*ITAB(55-N1),32768)
      NSEED=ITAB(55-N1)/2
      VECTOR(I)=ABS(FLOAT(NSEED)/FLOAT(16384))
```

```
      N1=MOD(N1+1,55)
      N2=MOD(N2+1,55)
30    CONTINUE
      IF(SEED .GT. 0) SEED=NSEED
      RETURN
      END
C----------the end of the program
```

APPENDIX II-3
HURST.FOR—A FORTRAN 77 PROGRAM USED TO TEST FOR LONG-TERM PERSISTENCE IN A TIME-SERIES SEQUENCE

```
C     ------------------------------------------
C     HURST.FOR
C     ------------------------------------------
C     PURPOSE:
C     This program is written to statistically test for long-term persistence or clustering
C     patterns in a time-series sequence, using the Hurst statistic which has been
C     demonstrated to be the most powerful method for this purpose. The Monte Carlo
C     simulation technique that randomly shuffles an analyzed sequence to generate 300
C     random sequences is used to estimate the significance level at which the analyzed
C     sequence passes the Hurst test (i.e., the null hypothesis is rejected).
C
C     INPUT:
C     N = the number of beds in the analyzed section
C     Seed = any integer number chosen by users for generating randomly shuffled
C            sections
C     A(J) = the measurement, i. e., bed thickness or grain size, to be tested
C
C     OUTPUT*:
C     Hurst K for the original sequence (or turbidite section) and 300 randomly shuffled
C            sequences
C     Hurst H, the slope of the regression line of values of R/S against log values of
C            subseries lengths for the analyzed section and 300 randomly shuffled
C            sections
C     R/S: the mean ranges of cumulated departures from the mean over subseries with
C            the chosen lengths (R) divided by the standard deviation of the subseries
C            (S)
C     * For calculation of K, H, and R/S, see text.
C
C     Author: C. Chen        Date: September 1996
C     ------------------------------------------
      Dimension M(37), Z(500,100), RS(38,2), A(3000)
      Dimension Y(3000),MQ(37), R2(500), B(3000),tr(301,37)
```

```
      INTEGER SEED
      REAL INTCPT
      DATA M(1),M(2),M(3),M(4),M(5),M(6),M(7),M(8),M(9),M(10),M(11),
     &M(12),M(13),M(14),M(15),M(16),M(17),M(18),M(19),M(20),M(21),
     &M(22),M(23),M(24),M(25),M(26),M(27),M(28),M(29),M(30),M(31),
     &M(32),M(33),M(34),M(35),M(36),M(37)/16,20,24,30,36,
     &40,50,60,70,80,90,100,120,140,160,180,200,
     &240,280,320,360,400,450,500,550,600,700,800,900,1000,1200,
     &1400,1600,1800,2000,2400,3000/
      CHARACTER*60 INPFIL,OUTFIL
      WRITE(*,*) 'ENTER INPUT FILE NAME (MAX. 60 CHARACTERS):'
      READ(*,10) INPFIL
10    FORMAT(A60)
      WRITE(*,*)'ENTER OUTPUT FILE NAME (MAX. 60 CHARACTERS):'
      READ(*,10) OUTFIL
      OPEN (UNIT=7, FILE=INPFIL, STATUS='OLD')
      OPEN (UNIT=8, FILE=OUTFIL, STATUS='NEW')
      READ(7,*) N
      READ(7,*) SEED
      READ(7,*) (A(J),J=1,N)
      DO 101 J=1,N
      IF(A(J) .EQ. 0.) A(J)=0.5
      A(J)=ALOG10(A(J))
101   CONTINUE
      DO 100 NA=1,301
C     ----------------------------------------
C     TO DETERMINE THE NUMBER OF SUBSERIES LENGTHS, NN, AND
C     MAKE THE LONGEST SUBSERIES LENGTH EQUAL TO N
C     ----------------------------------------
      NT=37
      DO 555 LP=1,NT
      MQ(LP)=M(LP)
555   CONTINUE
      I=0
15    I=I+1
      IF(MQ(I) .LT. N)GOTO 15
      MQ(I)=N
C     ----------------------------------------
C     CALCULATE THE MEAN VALUES OF THE RANGES OF CUMULATIVE
C     DEPARTURES FROM THE MEAN OF A(NN) OVER NN DATA POINTS
C     ----------------------------------------
```

```
      DO 20 K=1,I
      II=1
      NB=0
      NN=MQ(K)
      NG=MQ(K)
40    NB=NB+1
       JX=0
      DO 30 L=II,NN
       JX=JX+1
      Y(JX)=A(L)
30    CONTINUE
      CALL HURSTRS(Y,NG,R1)
      R2(NB)=R1
      NN=NN+NG/2
      II=II+NG/2
      IF(NN .LE. N) GOTO 40
      SUM=0.0
      IF(NB .EQ. 1) then
       SUM=SUM+R2(NB)
      ELSE
       DO 60 NC=1,NB
       SUM=SUM+R2(NC)
60     CONTINUE
      ENDIF
       IF(SUM .LE. 0.) SUM = 1.0
      RS(K,1)=ALOG10(FLOAT(MQ(K)))
      RS(K,2)=ALOG10(SUM/FLOAT(NB))
20    CONTINUE
C     ----------------------------------------
C     TO CALCULATE THE SLOPE OF THE REGRESSION LINE
C     ----------------------------------------
      CALL REGRESSION(RS,I,SLOPE,INTCPT,POINT1,POINT2)
      Z(NA,1)=RS(I,2)/ALOG10(FLOAT(N)/2.)
      Z(NA,2)=SLOPE
      Z(NA,3)=INTCPT
      IK=3
      DO 80 KW=1,I
       IK=IK+1
      Z(NA,IK)=RS(KW,2)
80    CONTINUE
       WRITE (8,333) (Z(NA,KQ),KQ=1,IK)
```

```
333   FORMAT (1x,35(F10.4))
C     ---------------------------------
C     SHUFFLE THE SECTION THE DESIRED NUMBER OF TIMES, AND
C     ANALYZE EACH ONE
C     ---------------------------------------------
      CALL SHUFFLE(A,N,SEED)
100   CONTINUE
C     ---------------------------------------------
C     THE OUTPUTS IS A MATRIX: THE FIRST AND SECOND COLUMNS
C     CONTAIN HURST K AND H VALUES FOR THE ORIGINAL SECTION (THE
C     FIRST ROW) AND FOR 300 RANDOMLY SHUFFLED SECTIONS (2 TO 301
C     ROWS), THE THIRD COLUMN CONTAINS REGRESSION INTERCEPTS,
C     THE SUCCESSIVE COLUMNS CONTAIN THE MEAN RANGES OF
C     CUMULATIVE DEPARTURES FROM THE MEAN OF EACH SUBSERIES
C     LENGTH.
C     ---------------------------------------------
      STOP
      END
C     ---------------------------------------------
C     SUBROUTINE HURSTRS IS WRITTEN FOR CALCULATING THE MAIN
C     PARAMETER OF HURST TEST----THE RANGE OF CUMULATIVE
C     DEPARTURE FROM THE MEAN OVER THE ANALYZED SUBSERIES,
C     DIVIDED BY THE STANDARD DEVIATION----R/S
C     ---------------------------------------------
      SUBROUTINE HURSTRS(Y,N,RS)
      DIMENSION Y(3000),B(3000)
      SUM1=0.0
      DO 101 I=1,N
      SUM1=SUM1+Y(I)
101   CONTINUE
      AM=SUM1/FLOAT(N)
       IF(AM) 20,30,20
30     RS=0.
       GO TO 99
20    SUM2=0.0
      SUM3=0.0
      DO 102 K=1,N
      D=Y(K)-AM
      SUM2=SUM2+D
      B(K)=SUM2
      SUM3=SUM3+D**2
```

```
102  CONTINUE
       IF(SUM2) 40,30,40
40     IF(SUM3) 50,30,50
50   XXA=B(1)
     XXI=B(1)
     DO 500 KD=2,N
     IF(XXA .LT. B(KD)) XXA=B(KD)
     IF(XXI .GT. B(KD)) XXI=B(KD)
500  CONTINUE
     R=XXA-XXI
     S=SQRT(SUM3/FLOAT(N-1))
     RS=R/S
99   RETURN
     END
C    ------------------------------------------
C    Subroutine regression runs linear regression analysis.
C    It returns constants of the regression line, i.e., slope
C    and intercept of the regression line.
C    ------------------------------------------
     SUBROUTINE REGRESSION(RS,I,SLOPE,INTCPT,POINT1,POINT2)
     DIMENSION RS(38,2)
     REAL INTCPT
     SUMX=0.
     SUMY=0.
      DO 10 K=1,I
        SUMX=SUMX+RS(K,1)
        SUMY=SUMY+RS(K,2)
10    CONTINUE
     AVGX=SUMX/FLOAT(I)
     AVGY=SUMY/FLOAT(I)
     SUMXX=0.
     SUMYY=0.
     SUMXY=0.
      DO 20 J=1,I
        XD=RS(J,1)-AVGX
        YD=RS(J,2)-AVGY
        SUMXX=SUMXX+XD*XD
        SUMYY=SUMYY+YD*YD
        SUMXY=SUMXY+XD*YD
20    CONTINUE
     SLOPE=SUMXY/SUMXX
```

```
      INTCPT=AVGY-SLOPE*AVGX
      POINT1=INTCPT+SLOPE*RS(1,1)
      POINT2=INTCPT+SLOPE*RS(I,1)
      RETURN
      END
C     ------------------------------------------
      SUBROUTINE SHUFFLE(X,N,SEED)
      DIMENSION X(3000),RANDNU(2)
      INTEGER SEED
      MAXSHUF=20000
      DO 10 I=1, MAXSHUF
      CALL RAND(SEED,2,RANDNU)
      INDEX1=1+INT(RANDNU(1)*N)
      INDEX2=1+INT(RANDNU(2)*N)
      TEMP=X(INDEX1)
      X(INDEX1)=X(INDEX2)
      X(INDEX2)=TEMP
10    CONTINUE
      RETURN
      END
C
      SUBROUTINE RAND(SEED,N,VECTOR)
      DIMENSION VECTOR(*)
      COMMON /UNUSUAL/ITAB(55),N1,N2,NSEED
      INTEGER M1, SEED
      IF((SEED .GT. 0) .OR. (NSEED .LT. 1)) THEN
      NSEED=SEED
      IF(SEED .LE. 0) NSEED=7931
      DO 10 I=1, 55
      M1=MOD(NSEED*9069,32768)
      IF(MOD(M1,2) .EQ. 0) M1=M1-1
      ITAB(I)=M1
      NSEED=M1
10    CONTINUE
      N1=0
      N2=24
      ENDIF
      DO 30 I=1,N
      ITAB(55-N1)=MOD(ITAB(55-N2)*ITAB(55-N1),32768)
      NSEED=ITAB(55-N1)/2
      VECTOR(I)=ABS(FLOAT(NSEED)/FLOAT(16384))
```

```
      N1=MOD(N1+1,55)
      N2=MOD(N2+1,55)
30    CONTINUE
      IF(SEED .GT. 0) SEED=NSEED
      RETURN
      END
C     ------------------------------------------
C     End of the program
C     ------------------------------------------
```

Appendix III

Sandstone Packets Statistically Selected From Turbidite Sections

This appendix gives a straightforward view of the selected sandstone packets and statistical results of tests for trends and randomness. The 286 sandstone packets are statistically selected from turbidite sections involved in this study and are plotted using bed thickness (horizontal) versus bed number (vertical). The significance levels at which a sandstone packet (or sequence) passed individual tests are attached. The null hypothesis of individual tests (i.e. non asymmetric trends for correlation tests and non order for tests for randomness) is rejected if a sandstone packet passed a test at the 0.1 significance level which is taken as the limited value of tests by this study. For instance, if a sandstone packet passed Kendall's rank correlation test at the significance level $(\alpha\tau) \leq 0.1$, the sandstone packet is identified by this statistical test as an asymmetric sequence (for details see Appendix IV-1: a negative τ indicates a thinning-upward sequence, whereas a positive τ indicates a thickening-upward sequence).

****

Note:

(1) The sequence (or sandstone packet) number (i.e., No: 5) corresponds to those in Appendix I, in Appendix IV-1, and in lithofacies logs of chapter 2, that is, if a sandstone packet, for example, is marked as sequence 35 in Appendix III, it is still sequence 35 in Appendix I, in Appendix IV-1 and in lithofacies logs of chapter 2.

(2)$\alpha\tau$, $\alpha\rho$, $\alpha\gamma$, αT, αR, αm, and αL represent significance levels at which a sequence passed Kendall's, Spearman's and Pearson's correlation tests, the Turning Point, Rank Difference, Median Crossing and Length-of-Runs tests, respectively.

Sections of the northern Italian Apennines

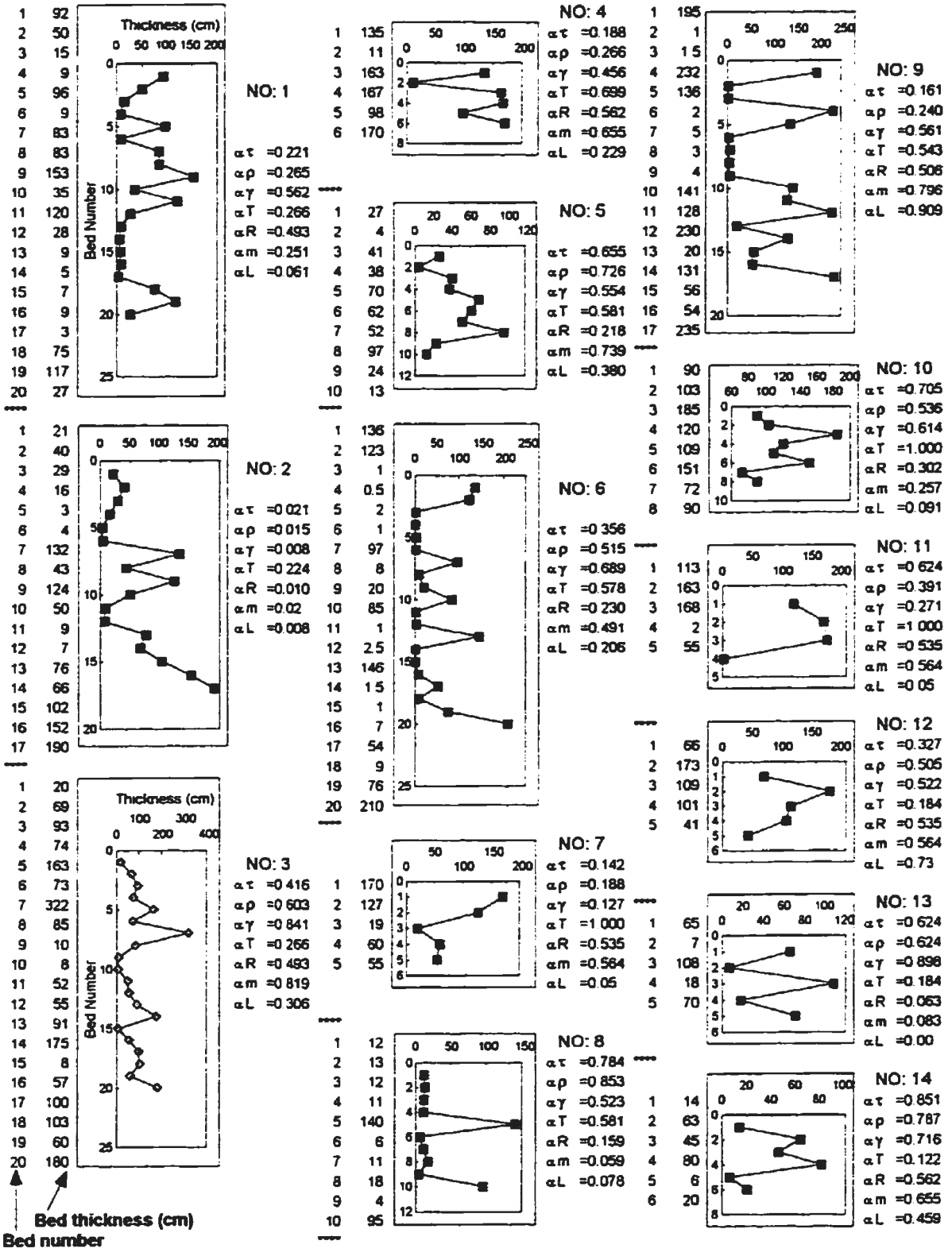

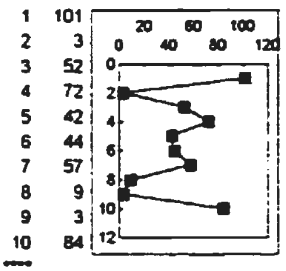

NO: 15
ατ =0.587
αρ =0.631
αγ =0.538
αT =0.782
αR =0.725
αm =0.317
αL =0.133

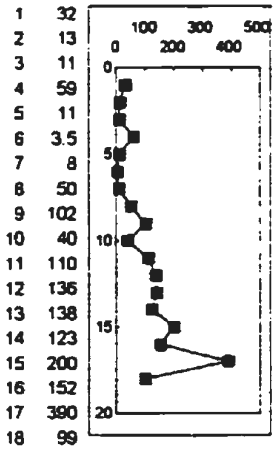

NO: 16
ατ =0.001
αρ =0.000
αγ =0.000
αT =0.694
αR =0.000
αm =0.008
αL =0.000

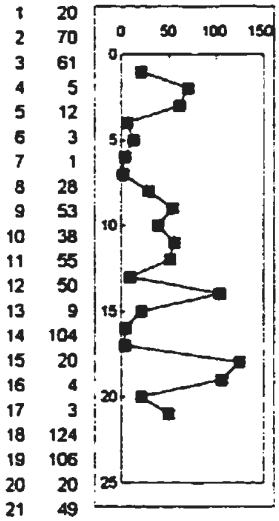

NO: 17
ατ =0.583
αρ =0.538
αγ =0.247
αT =0.718
αR =0.274
αm =0.819
αL =0.334

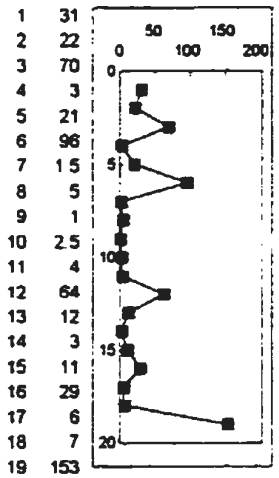

NO: 18
ατ =1.000
αρ =0.902
αγ =0.678
αT =0.849
αR =0.620
αm =0.808
αL =0.554

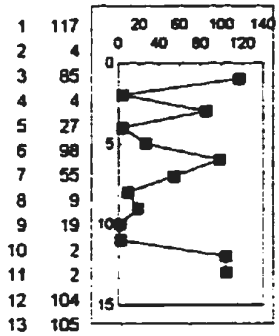

NO: 19
ατ =0.805
αρ =0.802
αγ =0.982
αT =0.344
αR =0.425
αm =0.763
αL =0.592

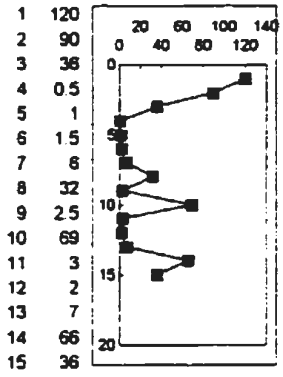

NO: 20
ατ =0.921
αρ =0.847
αγ =0.267
αT =0.082
αR =0.041
αm =0.782
αL =0.778

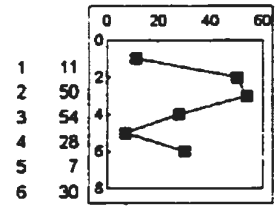

NO: 21
ατ =0.851
αρ =0.787
αγ =0.754
αT =0.440
αR =0.885
αm =0.655
αL =0.229

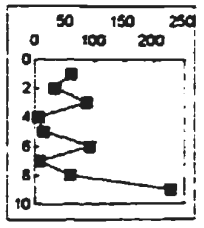

NO: 22
ατ =0.532
αρ =0.606
αγ =0.233
αT =0.768
αR =0.362
αm =0.059
αL =0.049

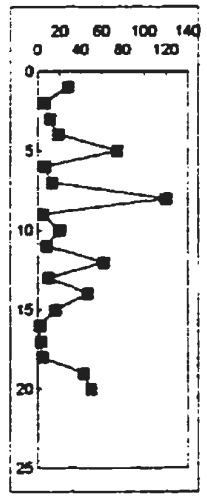

NO: 23
ατ =0.746
αρ =0.686
αγ =0.932
αT =0.578
αR =0.648
αm =0.251
αL =0.271

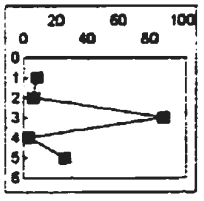

NO: 24
ατ =1.000
αρ =0.873
αγ =0.821
αT =0.184
αR =0.063
αm =0.083
αL =0.00

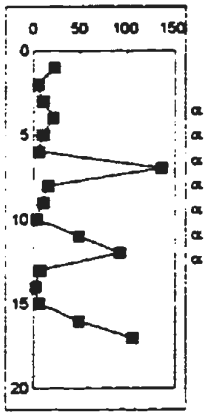

NO: 25
ατ =0.769
αρ =0.738
αγ =0.283
αT =0.068
αR =0.767
αm =0.405
αL =0.875

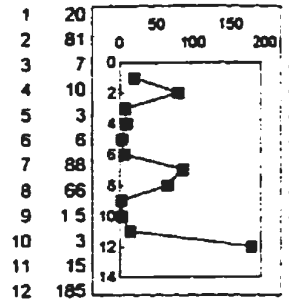

NO: 26
ατ =0.945
αρ =0.987
αγ =0.307
αT =0.620
αR =0.319
αm =0.366
αL =0.030

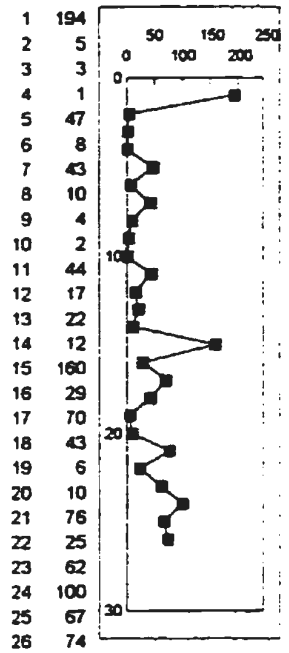

NO: 27
ατ =0.016
αρ =0.020
αγ =0.435
αT =0.630
αR =0.185
αm =0.841
αL =0.192

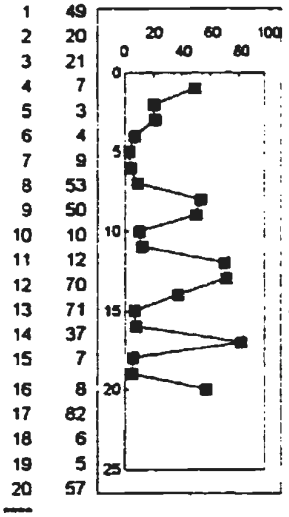

NO: 28
ατ =0.672
αρ =0.648
αγ =0.449
αT =0.095
αR =0.110
αm =0.491
αL =0.299

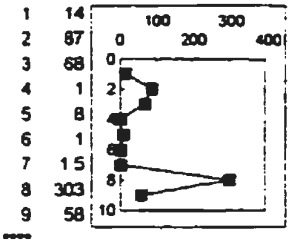

NO: 29
ατ =0.916
αρ =0.923
αγ =0.392
αT =0.768
αR =0.726
αm =0.257
αL =0.111

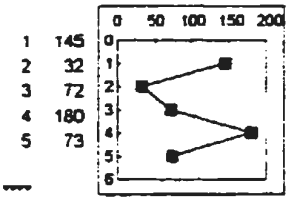

NO: 30
ατ =0.624
αρ =0.747
αγ =0.987
αT =1.000
αR =0.535
αm =0.564
αL =0.73

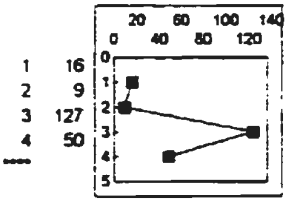

NO: 31
ατ =0.497
αρ =0.400
αγ =0.475
αT =0.285
αR =1.000
αm =0.564
αL =0.033

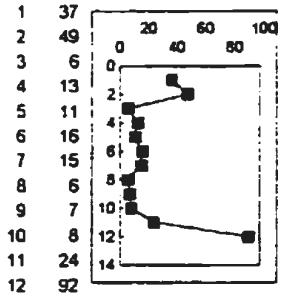

NO: 32
ατ =0.945
αρ =0.935
αγ =0.590
αT =0.620
αR =0.130
αm =0.366
αL =0.034

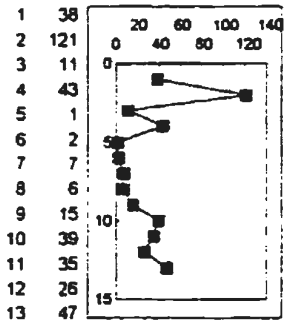

NO: 33
ατ =0.625
αρ =0.887
αγ =0.503
αT =0.636
αR =0.305
αm =0.366
αL =0.236

Monticello Dam Section, California

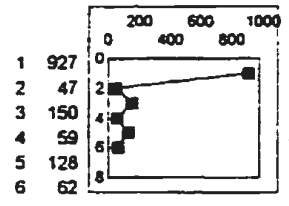

NO: 34
ατ =0.573
αρ =0.623
αγ =0.165
αT =0.122
αR =0.147
αm =0.025
αL =0.000

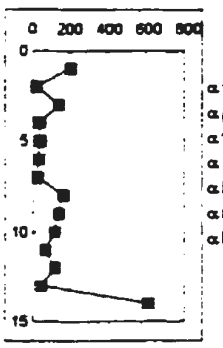

NO: 35
ατ =0.472
αρ =0.377
αγ =0.170
αT =0.497
αR =0.419
αm =0.405
αL =0.171

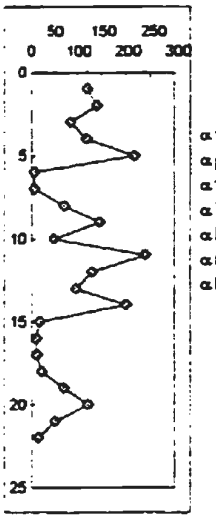

No: 36
ατ =0.204
αρ =0.172
αγ =0.129
αT =0.218
αR =0.258
αm =0.035
αL =0.015

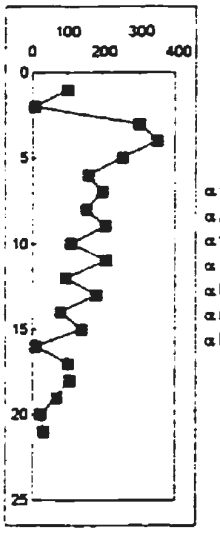

NO: 37
ατ =0.005
αρ =0.016
αγ =0.011
αT =0.206
αR =0.117
αm =0.108
αL =0.000

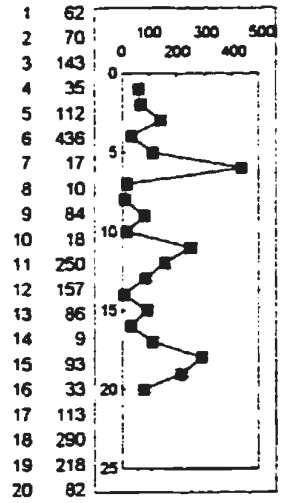

NO: 38
ατ =0 436
αρ =0.413
αγ =0 617
αT =0 578
αR =0.864
αm =0.819
αL =0 820

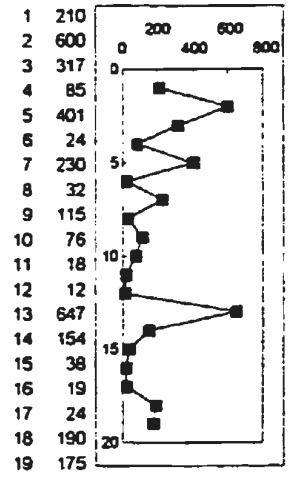

NO: 39
ατ =0.141
αρ =0 129
αγ =0.181
αT =0 849
αR =0 620
αm =0 808
αL =0.731

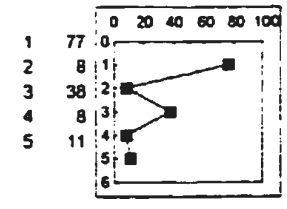

NO: 40
ατ =0 439
αρ =0.334
αγ =0.191
αT =0 184
αR =0 215
αm =0 083
αL =0 00

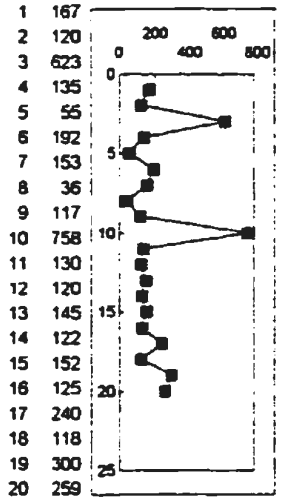

NO: 41
ατ =0 537
αρ =0 605
αγ =0 894
αT =0 266
αR =0 253
αm =0 039
αL =0 016

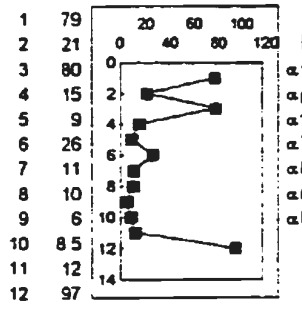

NO: 42
ατ =0 217
αρ =0.319
αγ =0.605
αT =0 216
αR =0.209
αm =0 366
αL =0 083

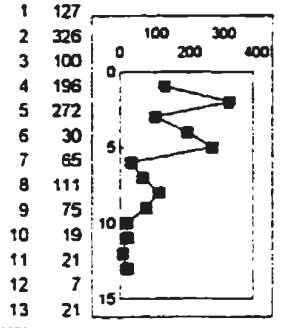

NO: 43
ατ =0 004
αρ =0 000
αγ =0 006
αT =0 636
αR =0 030
αm =0.132
αL =0.085

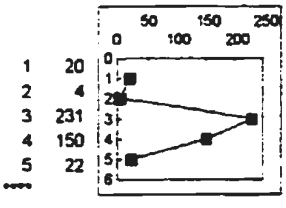

NO: 44
ατ =0.624
αρ =0 391
αγ =0 702
αT =1 000
αR =0 535
αm =0.564
αL =0.05

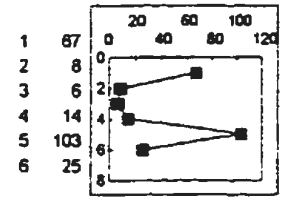

NO: 45
ατ =0.573
αρ =0 623
αγ =0.831
αT =0 440
αR =0.772
αm =0.655
αL =0.459

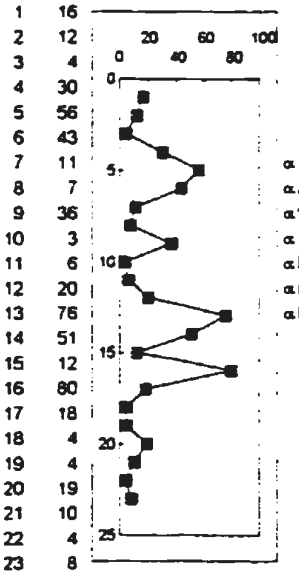

NO: 46
ατ =0 362
αρ =0 334
αγ =0 619
αT =0 039
αR =0 436
αm =0.655
αL =0 542

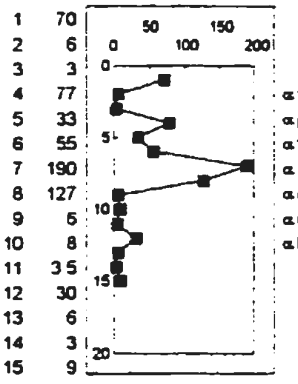

NO: 47
ατ =0 246
αρ =0 223
αγ =0 301
αT =0.828
αR =0 547
αm =0 405
αL =0 313

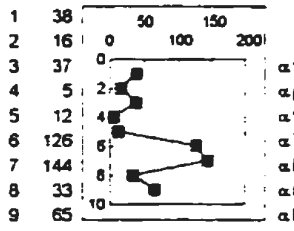

NO: 48
ατ =0.404
αρ =0 332
αγ =0 223
αT =0 768
αR =0 726
αm =0 705
αL =0 813

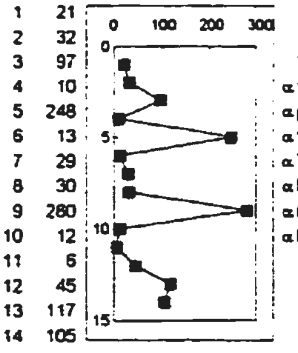

NO: 49
ατ =0.477
αρ =0 513
αγ =0 683
αT =0 497
αR =0.762
αm =0.782
αL =0 483

Cache Creek Section, California

1	43
2	96
3	94
4	130
5	85
6	264
7	91
8	212
9	120
10	315
11	300
12	203

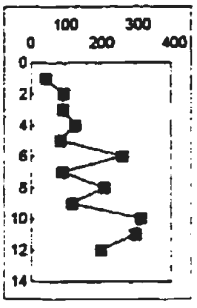

NO: 50

ατ =0.028
αρ =0.014
αγ =0.008
αT =0.083
αR =0.931
αm =0.366
αL =0.064

1	133
2	203
3	194
4	20
5	4
6	157
7	110
8	366
9	231
10	51
11	350
12	72
13	77
14	7
15	28
16	64
17	160
18	59
19	43
20	6
21	5
22	174
23	20
24	20
25	66
26	60
27	240
28	46

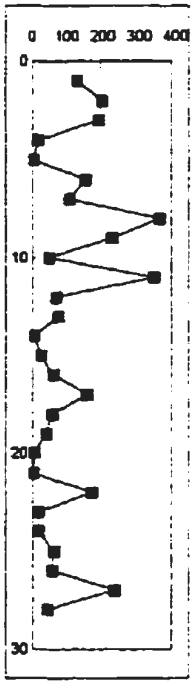

NO: 51

ατ =0.137
αρ =0.154
αγ =0.122
αT =0.537
αR =0.312
αm =0.847
αL =0.356

1	12
2	4
3	4
4	5
5	14
6	12
7	2
8	55
9	45
10	58

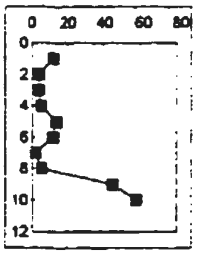

NO: 52

ατ =0.120
αρ =0.188
αγ =0.037
αT =0.006
αR =0.291
αm =0.739
αL =0.176

1	20
2	204
3	20
4	14
5	262
6	5
7	23
8	5
9	280
10	80

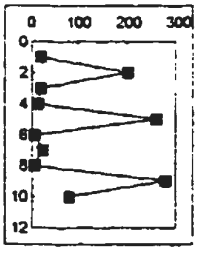

NO: 53

ατ =0.784
αρ =0.761
αγ =0.730
αT =0.167
αR =0.113
αm =0.096
αL =0.070

1	263
2	218
3	85
4	408

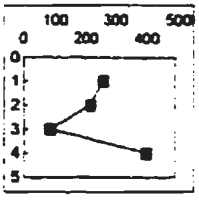

NO:54

ατ =1.000
αρ =0.800
αγ =0.707
αT =0.583
αR =1.000
αm =0.564
αL =0.531

1	7
2	18
3	16
4	2
5	4
6	14
7	20
8	13
9	5
10	6
11	4
12	135
13	10
14	28
15	17
16	7
17	21
18	13

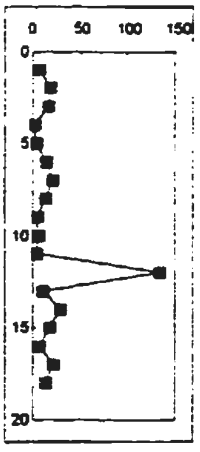

NO: 55

ατ =0.359
αρ =0.323
αγ =0.495
αT =0.844
αR =0.928
αm =0.439
αL =0.57

1	48
2	93
3	66
4	220
5	4
6	15
7	6
8	18
9	6
10	13
11	9
12	5
13	14
14	64
15	42
16	18
17	9
18	12
19	13
20	26
21	2
22	2
23	5
24	14

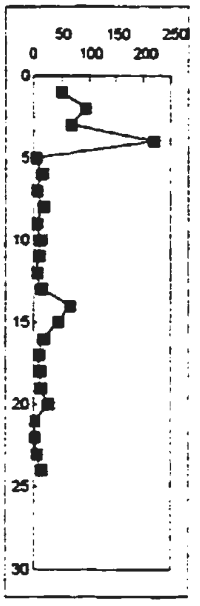

NO: 56

ατ =0.053
αρ =0.028
αγ =0.027
αT =0.401
αR =0.050
αm =0.532
αL =0.014

1	78
2	88
3	144
4	127
5	250
6	220
7	20
8	70
9	30
10	240
11	121
12	87
13	60
14	93
15	154

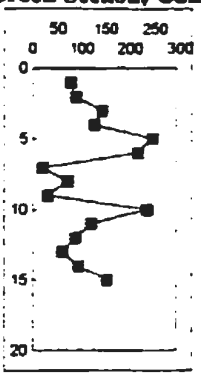

NO: 57

ατ =0.961
αρ =0.840
αγ =0.779
αT =0.663
αR =0.292
αm =0.405
αL =0.294

1	210
2	37
3	150
4	140
5	200
6	250
7	180
8	104
9	80
10	170
11	110
12	250
13	80
14	200
15	270
16	120
17	150

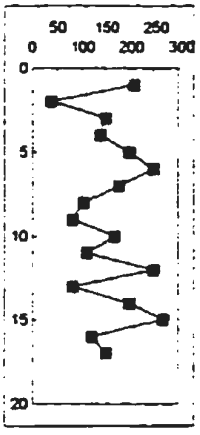

NO: 58

ατ =0.802
αρ =0.862
αγ =0.686
αT =0.543
αR =0.416
αm =0.285
αL =0.747

1	141
2	105
3	158
4	132
5	104
6	120
7	265
8	118
9	30
10	225
11	47
12	108
13	27 5
14	40
15	77
16	40
17	50
18	73

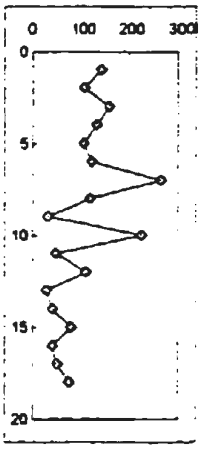

NO: 59

ατ =0.018
αρ =0.006
αγ =0.029
αT =0.844
αR =0.605
αm =0.467
αL =0.084

1	166
2	152
3	84
4	90
5	80
6	51
7	37
8	231
9	84
10	124
11	200
12	180
13	8
14	63

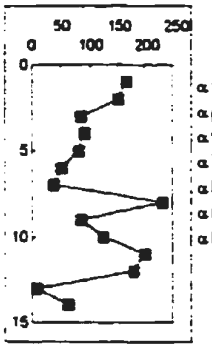

NO: 60
ατ =0.441
αρ =0.623
αγ =0.713
αT =0.497
αR =0.225
αm =0.782
αL =0.483

1	63
2	46
3	34
4	117
5	45
6	105
7	39

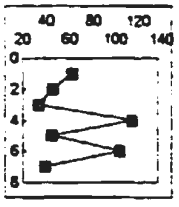

NO: 61
ατ =0.652
αρ =0.819
αγ =0.779
αT =0.488
αR =0.102
αm =0.025
αL =0.00

1	85
2	66
3	49
4	73
5	52
6	60

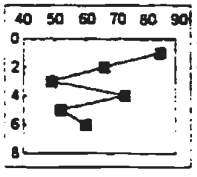

NO: 62
ατ =0.348
αρ =0.329
αγ =0.241
αT =0.699
αR =0.562
αm =0.655
αL =0.229

1	69
2	21
3	23
4	57
5	70

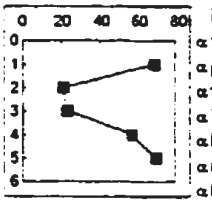

NO: 63
ατ =0.327
αρ =0.505
αγ =0.688
αT =0.184
αR =0.535
αm =0.564
αL =0.73

1	52
2	10
3	18
4	11

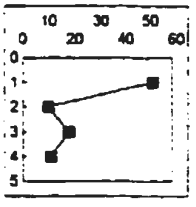

NO: 64
ατ =0.497
αρ =0.600
αγ =0.251
αT =0.285
αR =0.317
αm =0.083
αL =0.000

1	61
2	36
3	82
4	85
5	15.5
6	5
7	21
8	33
9	28
10	24
11	37

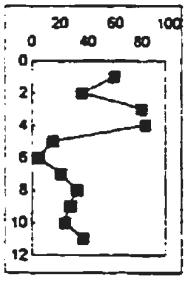

NO: 65
ατ =0.484
αρ =0.259
αγ =0.124
αT =0.434
αR =0.051
αm =0.096
αL =0.033

1	283
2	94
3	59
4	43
5	56
6	65
7	77
8	238
9	112
10	101
11	52
12	158
13	56
14	120
15	190

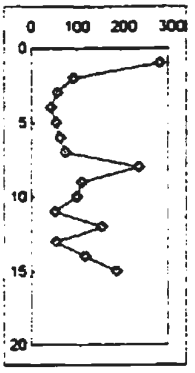

NO: 66
ατ =0.426
αρ =0.577
αγ =0.972
αT =0.017
αR =0.547
αm =0.782
αL =0.395

1	18
2	61
3	105
4	23.5
5	40
6	33
7	32
8	15
9	190
10	44
11	59
12	10
13	7
14	230
15	29
16	26
17	60
18	228
19	145
20	18
21	52
22	115
23	4.5
24	39.5
25	14
26	71
27	106
28	47

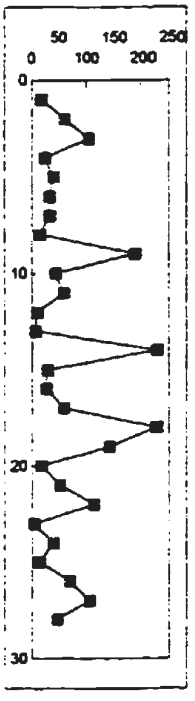

NO: 67
ατ =0.707
αρ =0.590
αγ =0.660
αT =0.877
αR =0.840
αm =0.336
αL =0.119

1	34
2	60
3	77
4	10
5	45
6	20
7	22
8	29
9	22
10	71
11	37
12	49
13	18
14	77
15	10
16	93
17	47
18	46
19	35
20	38
21	55
22	51
23	87

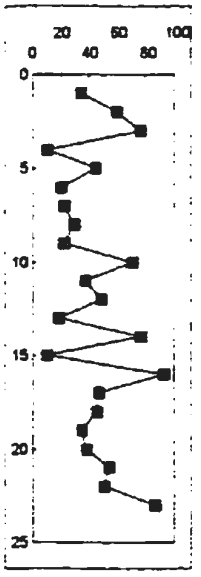

NO: 68
ατ =0.151
αρ =0.172
αγ =0.224
αT =0.303
αR =0.855
αm =0.827
αL =0.608

1	73
2	8
3	15
4	27
5	17
6	11
7	39
8	27

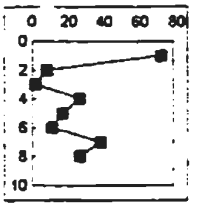

NO: 69
ατ =0.705
αρ =0.787
αγ =0.651
αT =1.000
αR =1.000
αm =0.705
αL =0.073

1	126
2	17
3	21
4	17
5	5
6	15
7	7
8	22
9	44
10	38
11	6
12	35
13	20
14	10
15	36
16	11
17	5
18	14
19	3
20	73
21	99
22	113
23	67

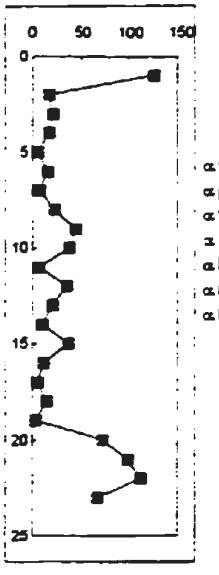

NO: 70
ατ =0.542
αρ =0.53
αγ =0.26
αT =0.78
αR =0.142
αm =0.827
αL =0.012

1	13
2	44
3	18
4	16
5	21

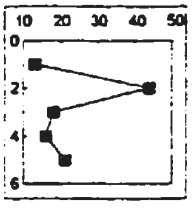

NO: 71
ατ =0.624
αρ =0.624
αγ =0.806
αT =1
αR =0.535
αm =0.083
αL =0.00

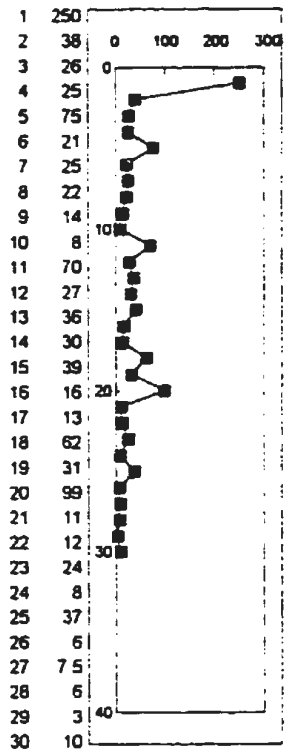

NO: 72

ατ =0.002
αρ =0.002
αγ =0.022
αT =0.297
αR =0.017
αm =0.041
αL =0.000

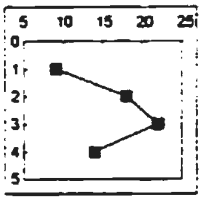

NO: 73

ατ =0.497
αρ =0.600
αγ =0.559
αT =0.593
αR =1.000
αm =0.564
αL =0.531

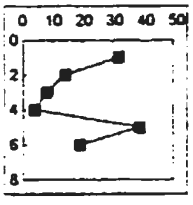

NO: 74

ατ =0.851
αρ =0.872
αγ =0.965
αT =0.440
αR =0.772
αm =0.655
αL =0.459

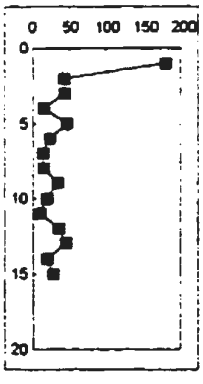

NO: 75

ατ =0.294
αρ =0.249
αγ =0.073
αT =0.828
αR =0.88
αm =0.782
αL =0.544

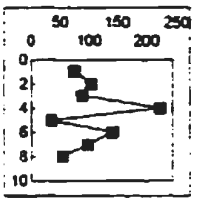

NO: 76

ατ =0.805
αρ =0.779
αγ =0.820
αT =0.340
αR =0.121
αm =0.059
αL =0.027

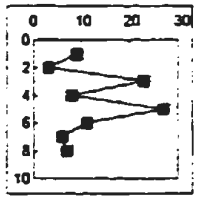

NO: 77

ατ =0.805
αρ =0.823
αγ =0.898
αT =0.340
αR =0.439
αm =0.257
αL =0.209

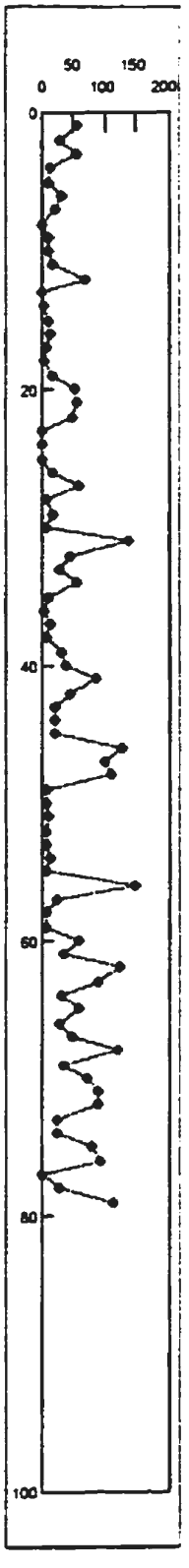

NO: 78

ατ =0.003
αρ =0.002
αγ =0.001
αT =0.024
αR =0.000
αm =0.000
αL =0.000

Cap Ste-Anne Sections, Quebec

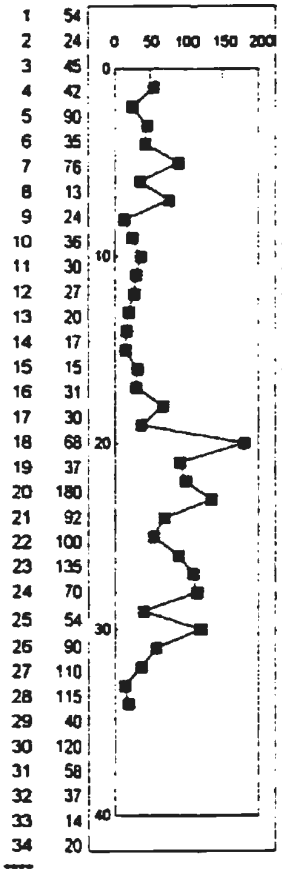

NO: 79
ατ =0 175
αρ =0.150
αγ =0 108
αT =0 889
αR =0 001
αm =0 056
αL =0 000

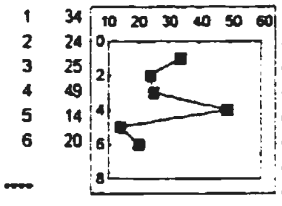

NO: 80
ατ =0 348
αρ =0.266
αγ =0 524
αT =0 699
αR =0 772
αm =0 655
αL =0 229

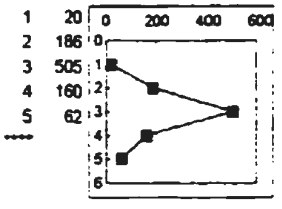

NO: 81
ατ =1 000
αρ =0 873
αγ =0 939
αT =0 184
αR =0 535
αm =0 564
αL =0.73

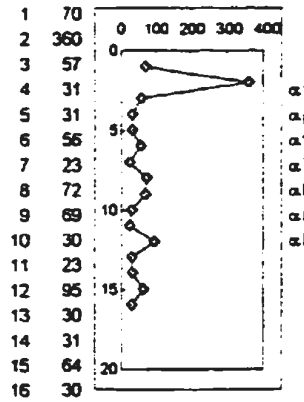

NO: 82
ατ =0 178
αρ =0 23
αγ =0 143
αT =0 401
αR =0 935
αm =0 439
αL =0 425

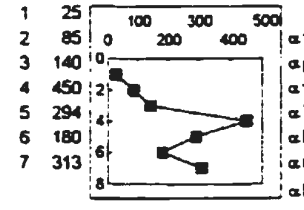

NO: 83
ατ =0.051
αρ =0.052
αγ =0 129
αT =0 165
αR =0.102
αm =0.180
αL =0 012

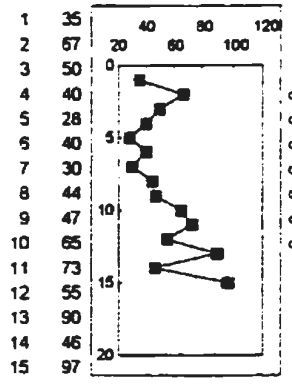

NO: 84
ατ =0 022
αρ =0.032
αγ =0.020
αT =0 663
αR =0.132
αm =0 405
αL =0.226

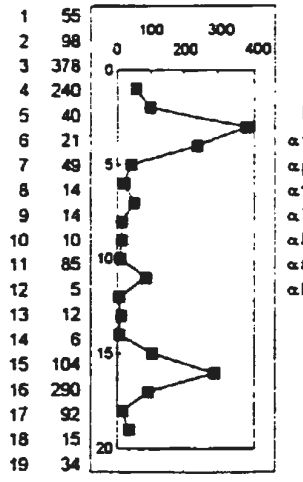

NO: 85
ατ =0.233
αρ =0 318
αγ =0.367
αT =0.446
αR =0.030
αm =0.467
αL =0.174

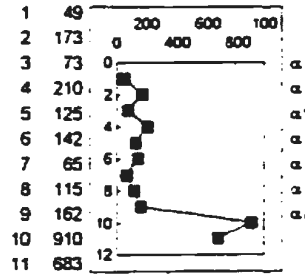

NO: 86
ατ =0 102
αρ =0 110
αγ =0.028
αT =0 434
αR =0 653
αm =0 739
αL =0.124

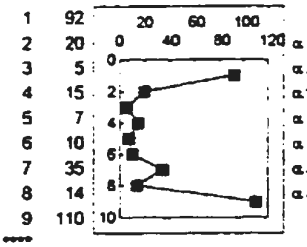

NO: 87
ατ =0.677
αρ =0.732
αγ =0.744
αT =0 768
αR =0 944
αm =0.705
αL =0.813

Petite-Vallee Section, Quebec

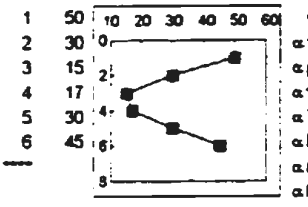

NO: 88
ατ =1 000
αρ =0.717
αγ =0.871
αT =0 053
αR =0 246
αm =0.564
αL =0.894

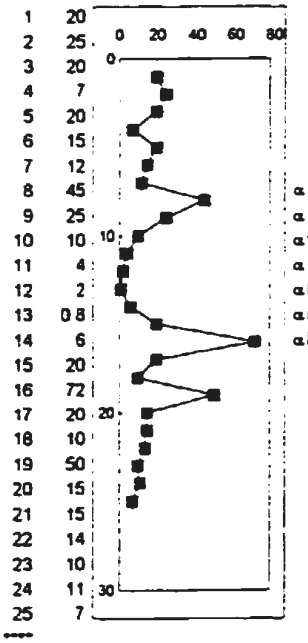

NO: 89
ατ =0 210
αρ =0 237
αγ =0.826
αT =0 033
αR =0 024
αm =0 513
αL =0 5

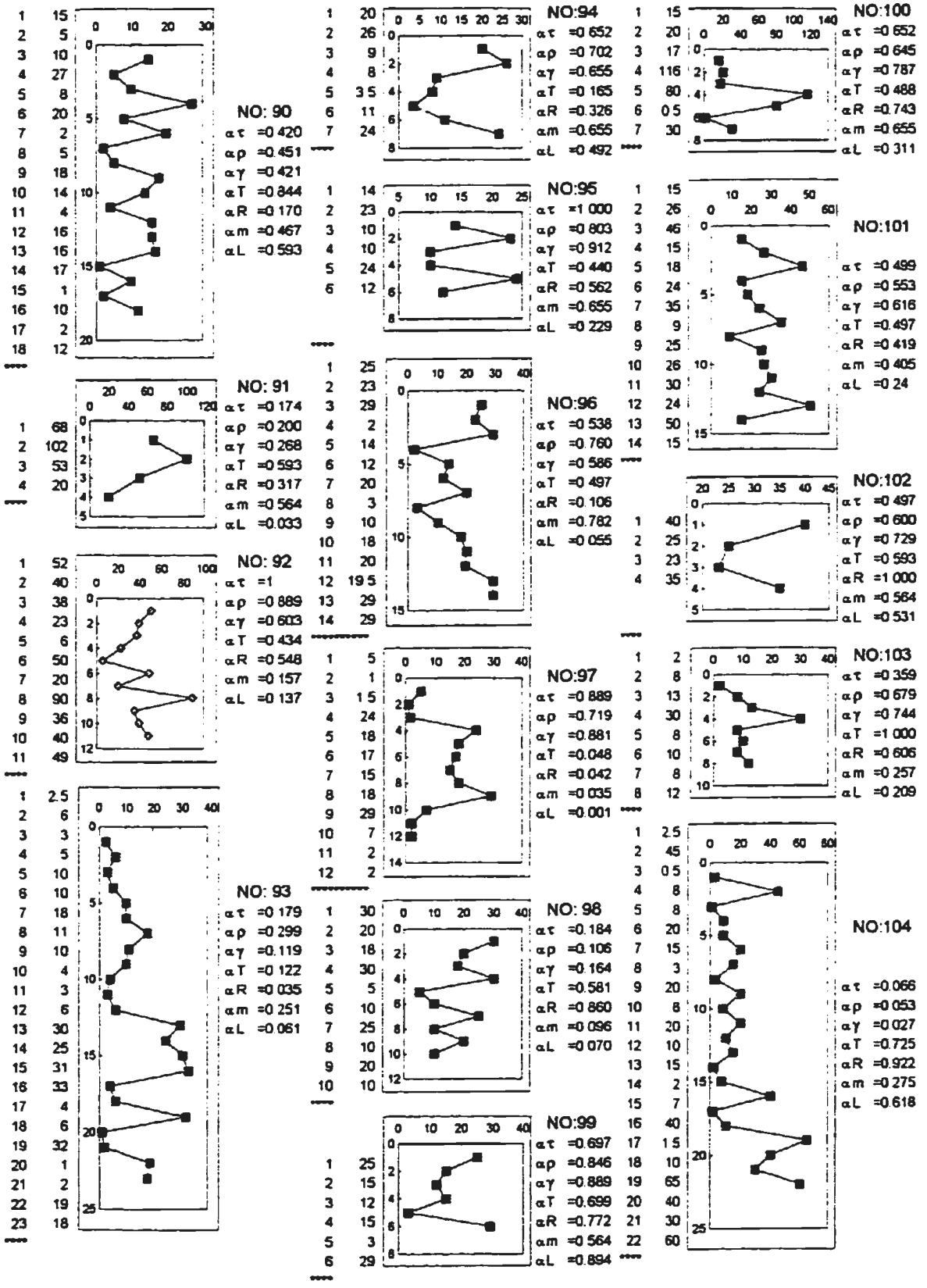
NO: 90
ατ =0 420
αρ =0.451
αγ =0 421
αT =0 844
αR =0 170
αm =0 467
αL =0 593
NO: 91
ατ =0 174
αρ =0 200
αγ =0 268
αT =0 593
αR =0 317
αm =0 564
αL =0.033
NO: 92
ατ =1
αρ =0 889
αγ =0 603
αT =0 434
αR =0 548
αm =0 157
αL =0 137
NO: 93
ατ =0 179
αρ =0 299
αγ =0.119
αT =0 122
αR =0 035
αm =0 251
αL =0 061
NO:94
ατ =0 652
αρ =0 702
αγ =0.655
αT =0 165
αR =0.326
αm =0.655
αL =0 492
NO:95
ατ =1 000
αρ =0 803
αγ =0 912
αT =0 440
αR =0 562
αm =0.655
αL =0 229
NO:96
ατ =0 538
αρ =0.760
αγ =0 586
αT =0 497
αR =0 106
αm =0.782
αL =0 055
NO:97
ατ =0 889
αρ =0.719
αγ =0.881
αT =0.048
αR =0.042
αm =0 035
αL =0.001
NO: 98
ατ =0.184
αρ =0 106
αγ =0.164
αT =0.581
αR =0 860
αm =0 096
αL =0 070
NO:99
ατ =0.697
αρ =0.846
αγ =0.889
αT =0.699
αR =0.772
αm =0 564
αL =0.894
NO:100
ατ =0 652
αρ =0 645
αγ =0 787
αT =0 488
αR =0.743
αm =0 655
αL =0 311
NO:101
ατ =0 499
αρ =0 553
αγ =0 616
αT =0 497
αR =0 419
αm =0 405
αL =0 24
NO:102
ατ =0 497
αρ =0 600
αγ =0 729
αT =0 593
αR =1 000
αm =0 564
αL =0 531
NO:103
ατ =0 359
αρ =0 679
αγ =0 744
αT =1 000
αR =0 606
αm =0 257
αL =0 209
NO:104
ατ =0 066
αρ =0 053
αγ =0 027
αT =0.725
αR =0.922
αm =0 275
αL =0.618

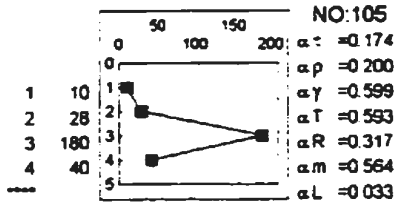

NO:105

ατ =0.174
αρ =0.200
αγ =0.599
αT =0.593
αR =0.317
αm =0.564
αL =0.033

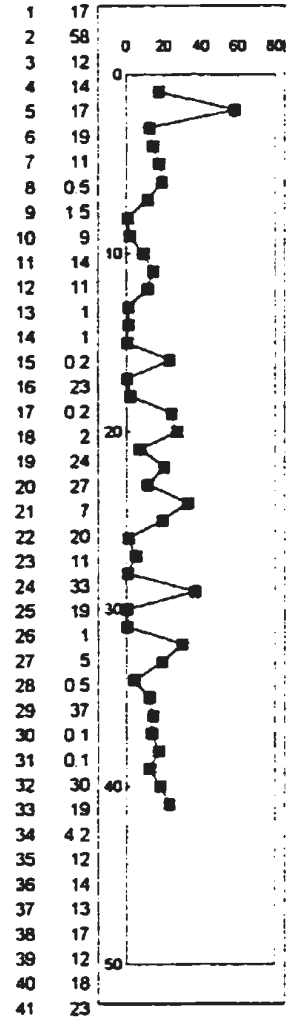

NO:106

ατ =0.802
αρ =0.716
αγ =0.895
αT =0.256
αR =0.331
αm =0.411
αL =0.207

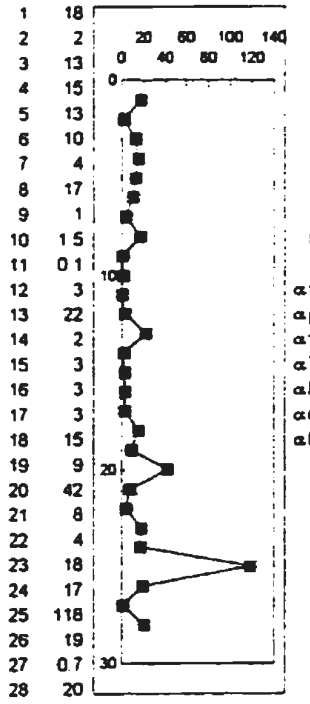

NO:107

ατ =0.185
αρ =0.234
αγ =0.121
αT =0.877
αR =0.345
αm =0.847
αL =0.001

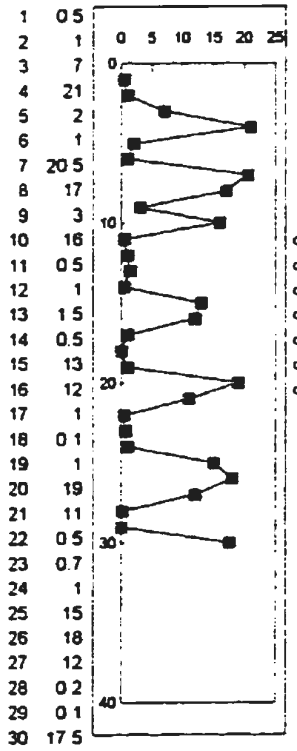

NO:108

ατ =0.533
αρ =0.521
αγ =0.801
αT =0.037
αR =0.455
αm =0.194
αL =0.041

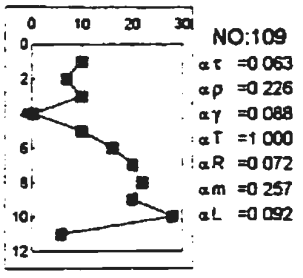

NO:109

ατ =0.063
αρ =0.226
αγ =0.088
αT =1.000
αR =0.072
αm =0.257
αL =0.092

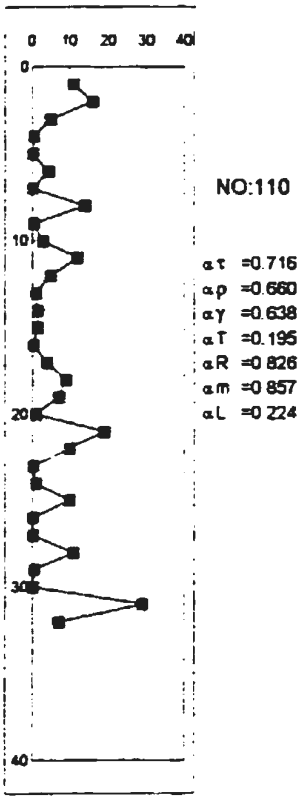

NO:110

ατ =0.716
αρ =0.660
αγ =0.638
αT =0.195
αR =0.826
αm =0.857
αL =0.224

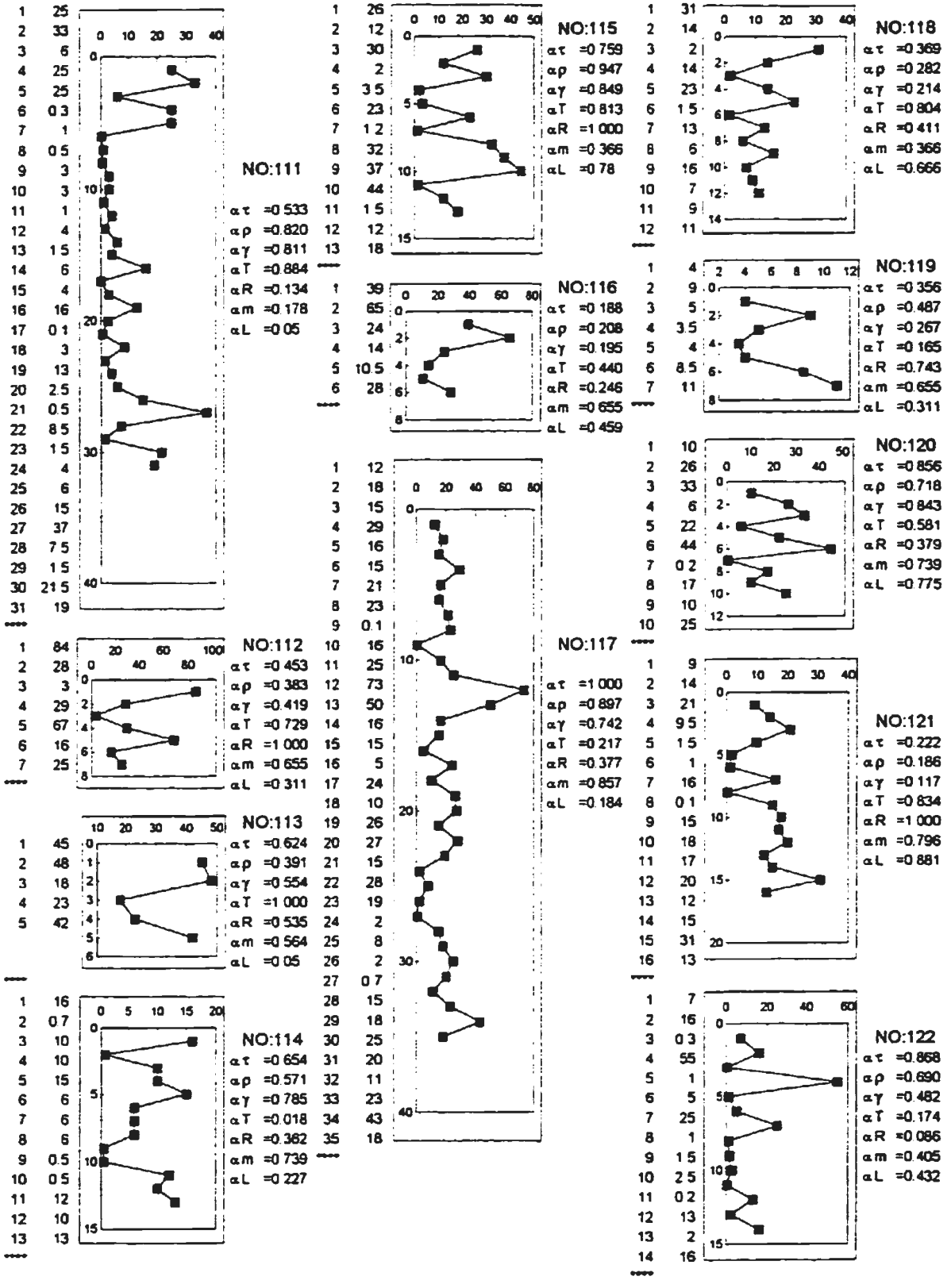
NO:111
ατ =0 533
αρ =0.820
αγ =0.811
αT =0.884
αR =0.134
αm =0.178
αL =0 05
NO:112
ατ =0 453
αρ =0 383
αγ =0.419
αT =0 729
αR =1 000
αm =0 655
αL =0 311
NO:113
ατ =0.624
αρ =0 391
αγ =0 554
αT =1 000
αR =0 535
αm =0 564
αL =0 05
NO:114
ατ =0 654
αρ =0.571
αγ =0 785
αT =0.018
αR =0.362
αm =0 739
αL =0 227
NO:115
ατ =0 759
αρ =0 947
αγ =0 849
αT =0 813
αR =1 000
αm =0 366
αL =0 78
NO:116
ατ =0 188
αρ =0 208
αγ =0.195
αT =0 440
αR =0.246
αm =0 655
αL =0 459
NO:117
ατ =1 000
αρ =0 897
αγ =0.742
αT =0 217
αR =0.377
αm =0 857
αL =0.184
NO:118
ατ =0 369
αρ =0 282
αγ =0 214
αT =0 804
αR =0 411
αm =0 366
αL =0.666
NO:119
ατ =0 356
αρ =0.487
αγ =0 267
αT =0 165
αR =0.743
αm =0.655
αL =0.311
NO:120
ατ =0 856
αρ =0.718
αγ =0 843
αT =0.581
αR =0 379
αm =0 739
αL =0 775
NO:121
ατ =0.222
αρ =0.186
αγ =0 117
αT =0 834
αR =1 000
αm =0.796
αL =0 881
NO:122
ατ =0.868
αρ =0.690
αγ =0.482
αT =0.174
αR =0 086
αm =0.405
αL =0.432

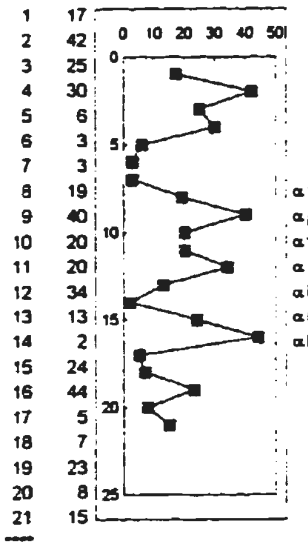

NO:123
ατ =0.544
αρ =0.455
αγ =0.411
αT =0.149
αR =0.470
αm =0.491
αL =0.308

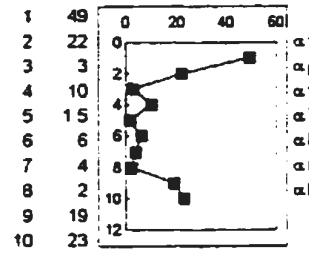

NO:124
ατ =0.655
αρ =0.701
αγ =0.341
αT =0.782
αR =0.481
αm =0.739
αL =0.380

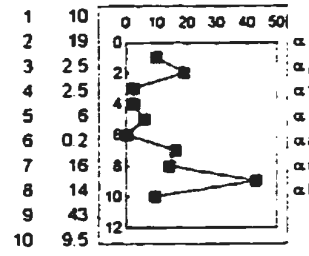

NO:125
ατ =0.587
αρ =0.595
αγ =0.283
αT =0.581
αR =0.725
αm =0.317
αL =0.321

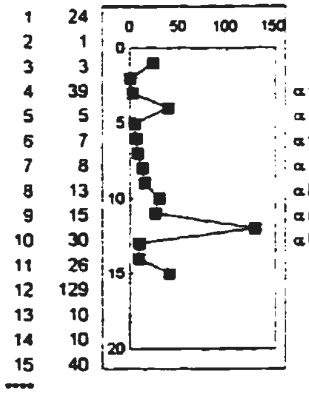

NO:126
ατ =0.029
αρ =0.070
αγ =0.213
αT =0.082
αR =0.252
αm =0.782
αL =0.778

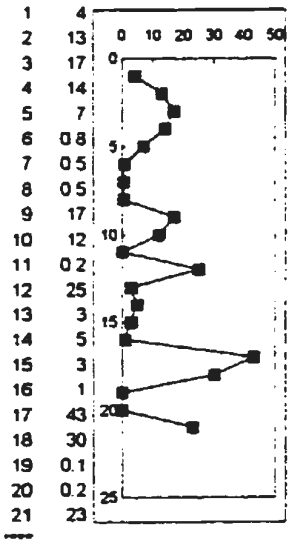

NO:127
ατ =0.714
αρ =0.853
αγ =0.413
αT =0.047
αR =0.324
αm =0.819
αL =0.767

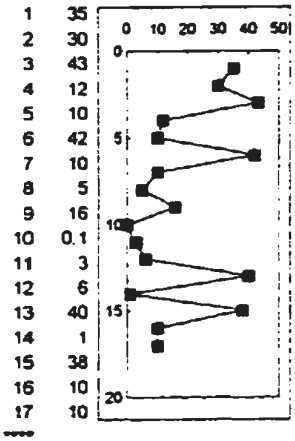

NO:128
ατ =0.109
αρ =0.112
αγ =0.182
αT =1.000
αR =0.882
αm =1
αL =0.261

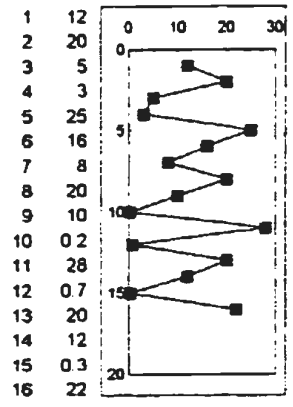

NO:129
ατ =0.927
αρ =0.898
αγ =0.956
αT =0.675
αR =0.073
αm =0.052
αL =0.079

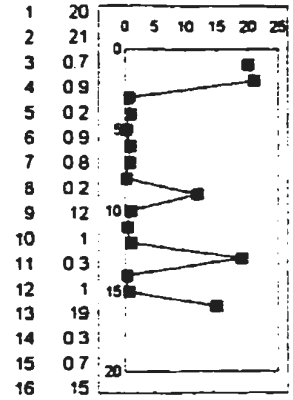

NO:130
ατ =0.818
αρ =0.613
αγ =0.605
αT =0.675
αR =0.935
αm =0.782
αL =0.2

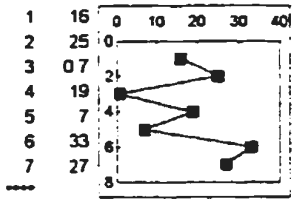

NO:131
ατ =0.293
αρ =0.253
αγ =0.408
αT =0.083
αR =0.743
αm =0.655
αL =0.311

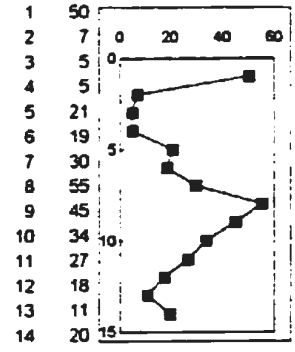

NO:132
ατ =0.826
αρ =0.699
αγ =0.859
αT =0.007
αR =0.020
αm =0.405
αL =0.112

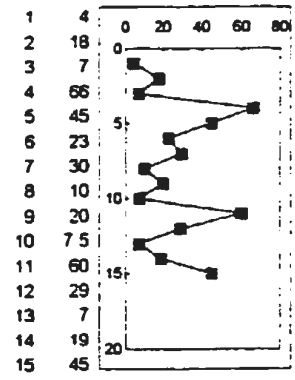

NO:133
ατ =0.583
αρ =0.477
αγ =0.669
αT =0.384
αR =0.880
αm =0.405
αL =0.294

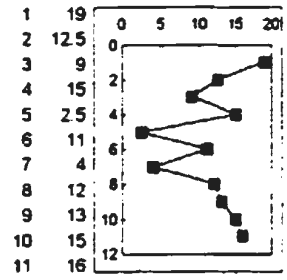

NO:134
ατ =0.530
αρ =0.795
αγ =0.965
αT =0.434
αR =0.453
αm =0.739
αL =0.366

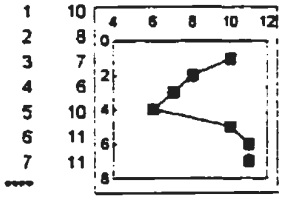

NO:135
ατ =0.269
αρ =0.274
αγ =0.296
αT =0.015
αR =0.050
αm =0.317
αL =0.226

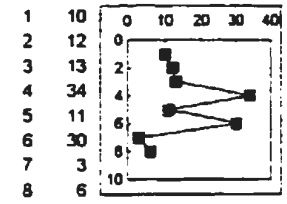

NO:136
ατ =0.621
αρ =0.420
αγ =0.781
αT =1.000
αR =0.606
αm =0.705
αL =0.736

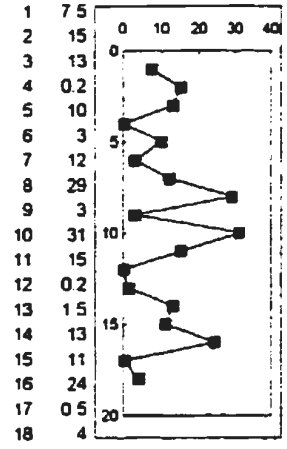

NO:137
ατ =0.788
αρ =0.737
αγ =0.871
αT =0.432
αR =0.444
αm =0.808
αL =0.068

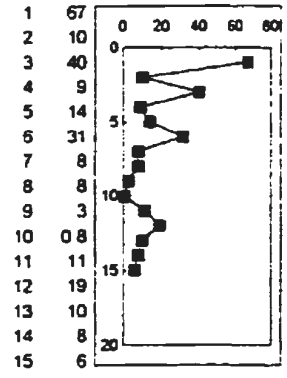

NO:138
ατ =0.030
αρ =0.039
αγ =0.026
αT =0.082
αR =0.092
αm =0.565
αL =0.105

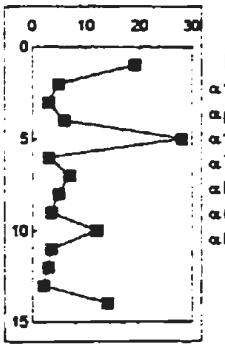

NO:139
ατ =0.311
αρ =0.300
αγ =0.413
αT =0.497
αR =0.686
αm =0.132
αL =0.262

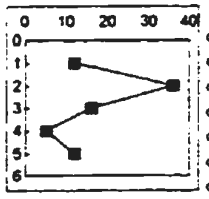

NO:140
ατ =0.439
αρ =0.334
αγ =0.485
αT =1.000
αR =0.535
αm =1
αL =0.525

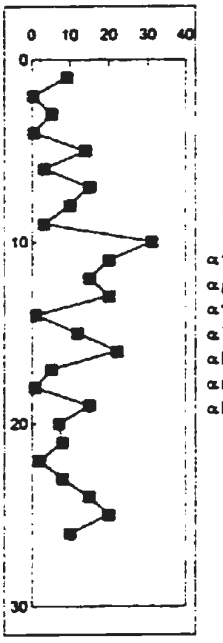

NO:141
ατ =0.280
αρ =0.364
αγ =0.484
αT =0.335
αR =0.940
αm =0.549
αL =0.067

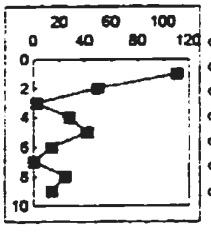

NO:142
ατ =0.072
αρ =0.076
αγ =0.060
αT =0.555
αR =0.440
αm =0.705
αL =0.386

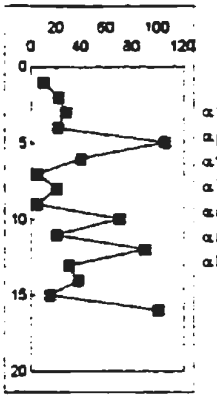

NO:143
ατ =0.364
αρ =0.391
αγ =0.264
αT =0.093
αR =0.569
αm =0.439
αL =0.471

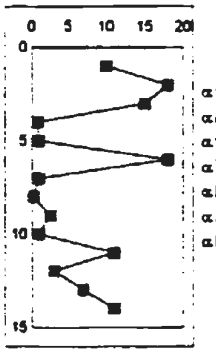

NO:144
ατ =1.000
αρ =0.611
αγ =0.360
αT =1.000
αR =0.686
αm =0.782
αL =0.766

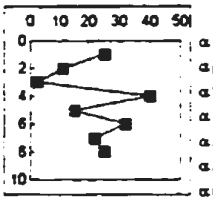

NO:145
ατ =0.529
αρ =0.555
αγ =0.485
αT =0.340
αR =0.302
αm =0.059
αL =0.027

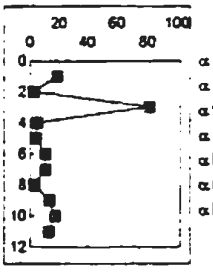

NO:146
ατ =0.637
αρ =0.889
αγ =0.497
αT =0.434
αR =0.653
αm =1
αL =0.134

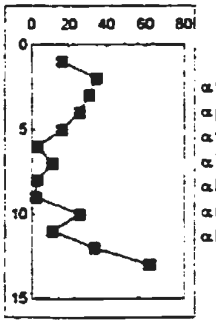

NO:147
ατ =0.802
αρ =0.943
αγ =0.500
αT =0.344
αR =0.030
αm =0.527
αL =0.527

1	10
2	20
3	24
4	15
5	10
6	3
7	24

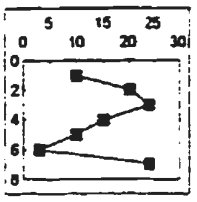

NO:148
ατ =0 875
αρ =0 843
αγ =0 902
αT =0.165
αR =1 000
αm =0 655
αL =0 311

1	10
2	8
3	2
4	2
5	8
6	3
7	20
8	7
9	55

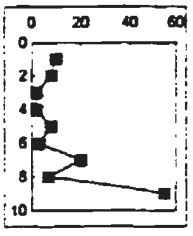

NO:149
ατ =0 391
αρ =0 495
αγ =0 100
αT =0.555
αR =0.888
αm =0.414
αL =0 34

1	4
2	1 2
3	12
4	11
5	13
6	9
7	11
8	17
9	3
10	15
11	5
12	10
13	3 5
14	18
15	13

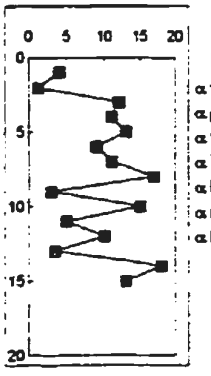

NO:150
ατ =0.294
αρ =0.294
αγ =0.288
αT =0 029
αR =0 451
αm =0.564
αL =0.771

1	11
2	70
3	30
4	12.5
5	22.5

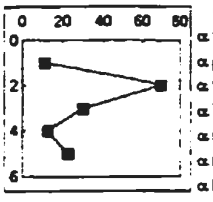

NO:151
ατ =1 000
αρ =0 873
αγ =0 714
αT =1 000
αR =1 000
αm =0 564
αL =0.73

1	60
2	85
3	12
4	130

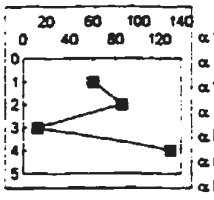

NO:152
ατ =0.497
αρ =0 600
αγ =0.641
αT =0 285
αR =0 317
αm =0 083
αL =0 000

1	18 5
2	86
3	32
4	11
5	16
6	3
7	4
8	4
9	12 5

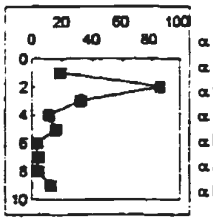

NO:153
ατ =0 072
αρ =0 029
αγ =0.099
αT =0.555
αR =0.160
αm =0.705
αL =0 077

1	18
2	23
3	13
4	10
5	3
6	23
7	25
8	95
9	24
10	30
11	31
12	24

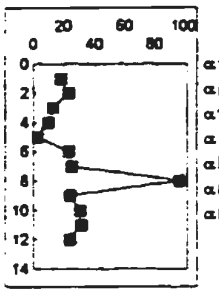

NO:154
ατ =0.037
αρ =0 013
αγ =0 293
αT =0 216
αR =0.015
αm =0 007
αL =0.000

Amazon Fan Sections

1	1170
2	417
3	100
4	255
5	44
6	513
7	67
8	17
9	63
10	395
11	93
12	28

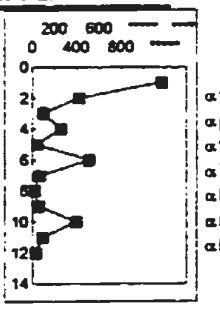

NO:155
ατ =0 055
αρ =0 051
αγ =0 057
αT =0 620
αR =0 634
αm =0 763
αL =0 649

1	105
2	10
3	35
4	6
5	4
6	4
7	2
8	4
9	213
10	10
11	13
12	47

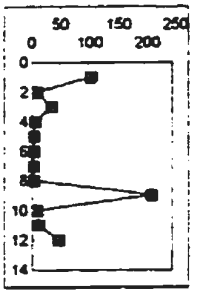

NO: 156
ατ =1
αρ =0 952
αγ =0 878
αT =0 216
αR =0.1
αm =0.096
αL =0 068

1	258
2	75
3	82
4	205
5	212

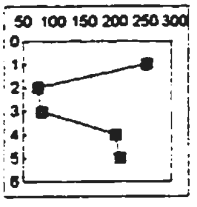

NO: 157
ατ =0 624
αρ =1
αγ =0 908
αT =0.184
αR =0 535
αm =0.564
αL =0.73

1	887
2	59
3	130
4	5
5	155
6	3
7	18
8	16
9	82
10	6
11	2
12	5
13	55
14	68
15	42
16	50
17	185

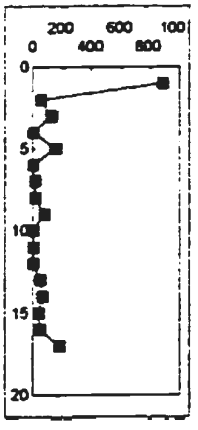

NO:158
ατ =0.710
αρ =0 671
αγ =0 139
αT =0 543
αR =0 824
αm =0.796
αL =0 12

1	100
2	5
3	8
4	17
5	18
6	5
7	302
8	17
9	5
10	32
11	70
12	7
13	14
14	132
15	23
16	117

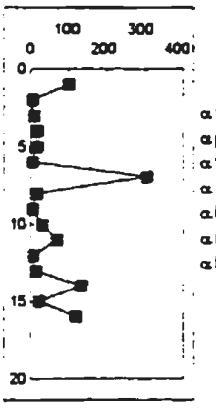

NO:159
ατ =0.200
αρ =0 271
αγ =0 681
αT =0 834
αR =0 625
αm =0.796
αL =0 493

1	37
2	8
3	325
4	57
5	5
6	3
7	16
8	5
9	53
10	2
11	6
12	112
13	85
14	87
15	112

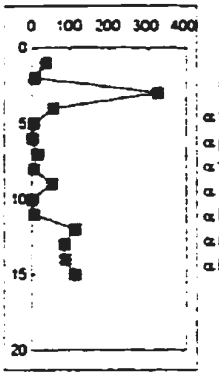

NO:160
ατ =0.342
αρ =0.364
αγ =0 969
αT =0 828
αR =0 292
αm =0 405
αL =0.052

1	953
2	5
3	4
4	3
5	3
6	3
7	2
8	2
9	3
10	5
11	440
12	6
13	4
14	3
15	2
16	2
17	42
18	138
19	40
20	15
21	36

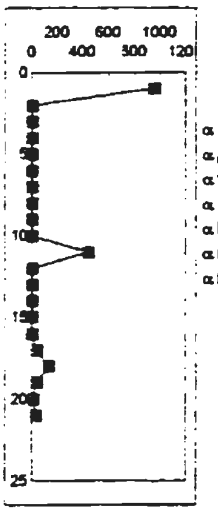

NO:161
ατ =0 487
αρ =0 441
αγ =0.226
αT =0 000
αR =0.000
αm =0 018
αL =0 011

1	90
2	85
3	3
4	157
5	70
6	63
7	18
8	37
9	45
10	35

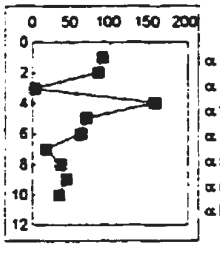

NO:162
ατ =0 089
αρ =0 128
αγ =0.216
αT =0.269
αR =0.597
αm =0.317
αL =0 321

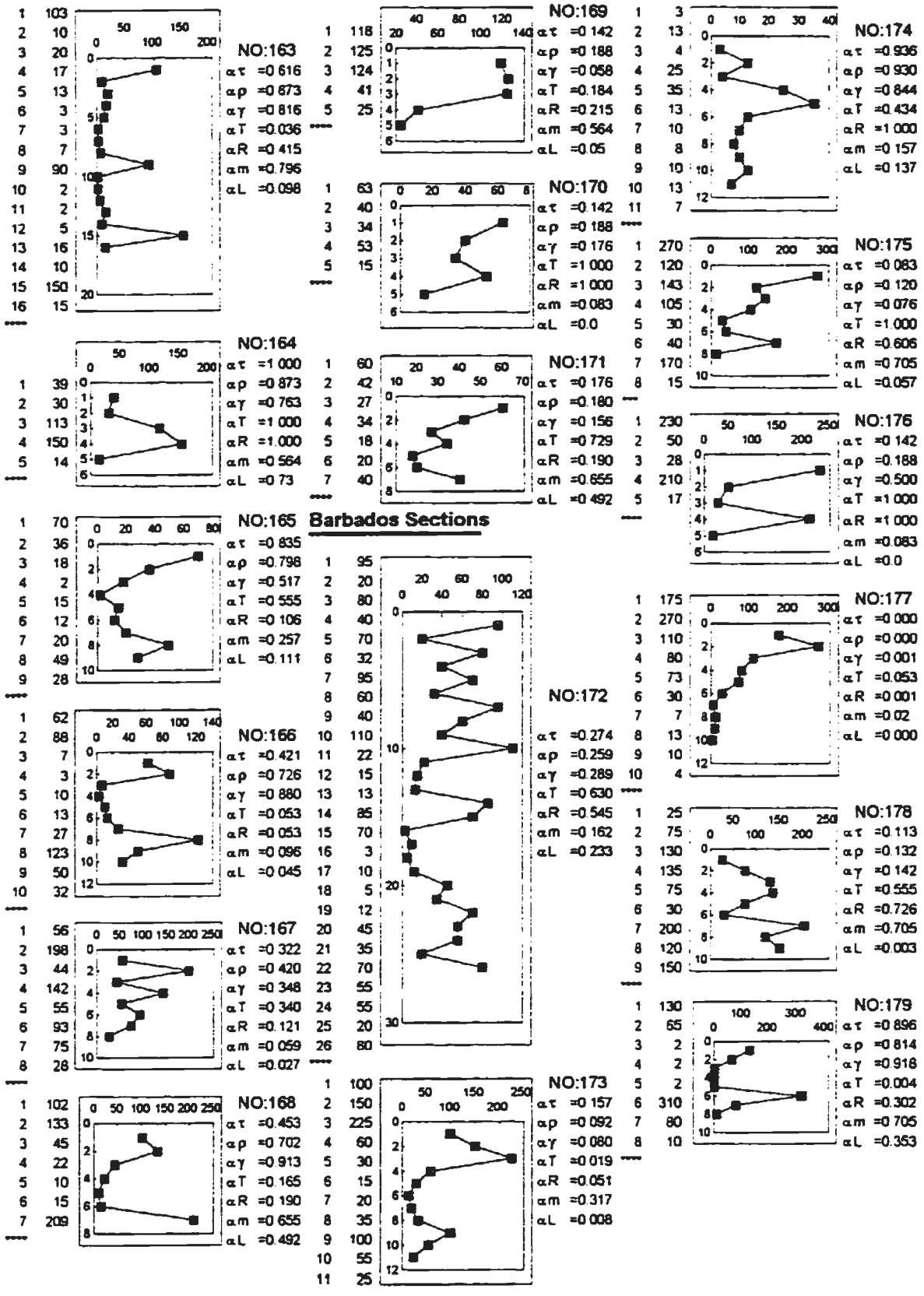
Barbados Sections
NO:163
ατ =0 616
αρ =0 673
αγ =0 816
αT =0.036
αR =0 415
αm =0.796
αL =0.098
NO:164
ατ =1 000
αρ =0 873
αγ =0 763
αT =1 000
αR =1.000
αm =0 564
αL =0 73
NO:165
ατ =0 835
αρ =0.798
αγ =0 517
αT =0 555
αR =0 106
αm =0 257
αL =0.111
NO:166
ατ =0.421
αρ =0 726
αγ =0 880
αT =0 053
αR =0 053
αm =0 096
αL =0 045
NO:167
ατ =0 322
αρ =0 420
αγ =0 348
αT =0 340
αR =0.121
αm =0 059
αL =0.027
NO:168
ατ =0.453
αρ =0 702
αγ =0 913
αT =0.165
αR =0 190
αm =0 655
αL =0.492
NO:169
ατ =0 142
αρ =0 188
αγ =0 058
αT =0.184
αR =0 215
αm =0 564
αL =0.05
NO:170
ατ =0.142
αρ =0 188
αγ =0 176
αT =1 000
αR =1 000
αm =0 083
αL =0.0
NO:171
ατ =0 176
αρ =0.180
αγ =0 156
αT =0 729
αR =0.190
αm =0.655
αL =0 492
NO:172
ατ =0.274
αρ =0.259
αγ =0.289
αT =0 630
αR =0.545
αm =0 162
αL =0 233
NO:173
ατ =0 157
αρ =0 092
αγ =0 080
αT =0 019
αR =0.051
αm =0.317
αL =0 008
NO:174
ατ =0.936
αρ =0 930
αγ =0 844
αT =0.434
αR =1 000
αm =0 157
αL =0 137
NO:175
ατ =0 083
αρ =0 120
αγ =0 076
αT =1.000
αR =0.606
αm =0 705
αL =0.057
NO:176
ατ =0 142
αρ =0.188
αγ =0.500
αT =1 000
αR =1 000
αm =0.083
αL =0.0
NO:177
ατ =0 000
αρ =0 000
αγ =0 001
αT =0.053
αR =0 001
αm =0.02
αL =0 000
NO:178
ατ =0.113
αρ =0.132
αγ =0 142
αT =0.555
αR =0.726
αm =0.705
αL =0.003
NO:179
ατ =0 896
αρ =0 814
αγ =0 918
αT =0.004
αR =0.302
αm =0 705
αL =0.353

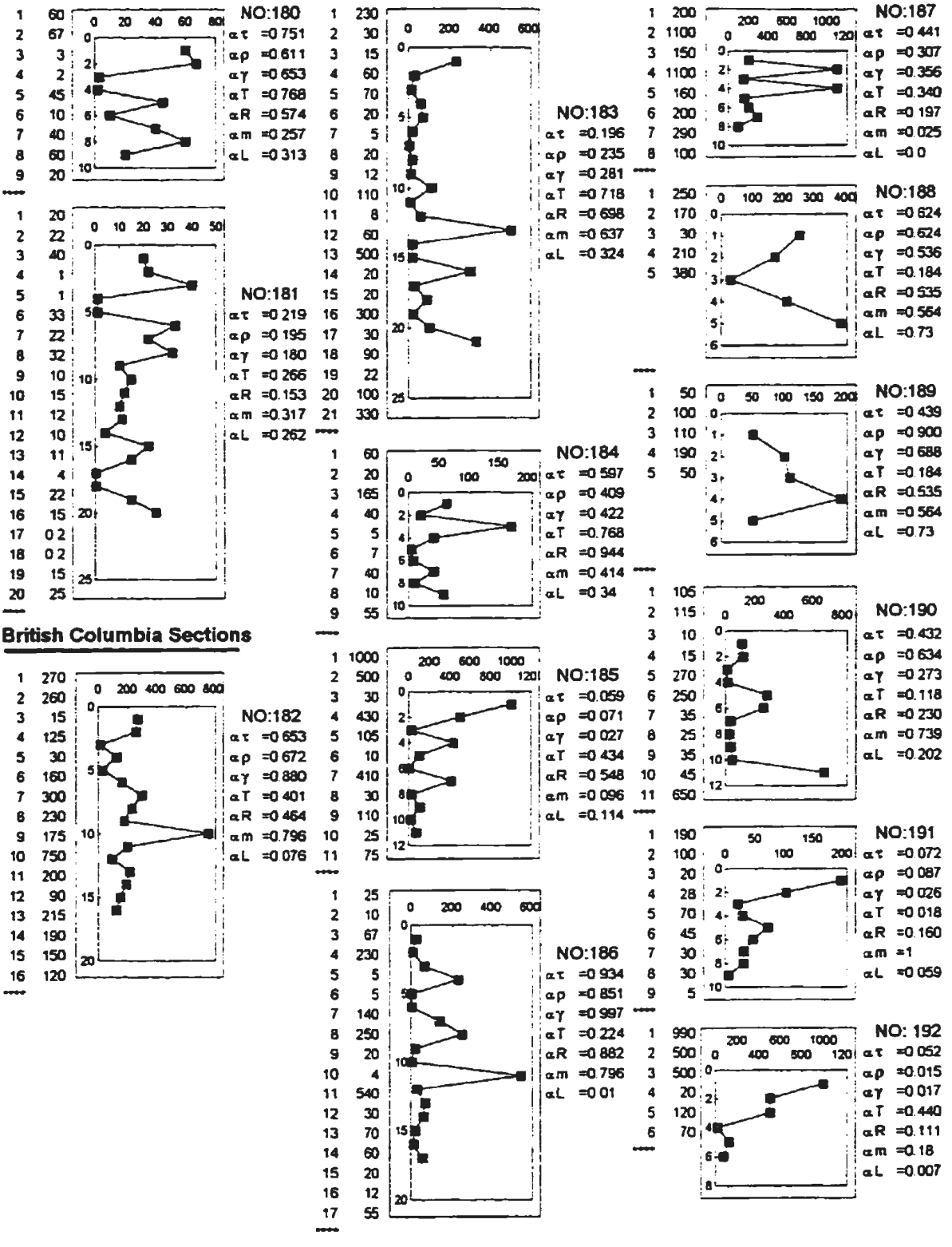
NO:180
ατ =0 751
αρ =0.611
αγ =0 653
αT =0768
αR =0 574
αm =0 257
αL =0 313
NO:181
ατ =0 219
αρ =0 195
αγ =0 180
αT =0 266
αR =0.153
αm =0.317
αL =0 262
British Columbia Sections
NO:182
ατ =0 653
αρ =0 672
αγ =0 880
αT =0 401
αR =0 464
αm =0.796
αL =0 076
NO:183
ατ =0.196
αρ =0 235
αγ =0 281
αT =0 718
αR =0 698
αm =0 637
αL =0 324
NO:184
ατ =0 597
αρ =0 409
αγ =0 422
αT =0.768
αR =0 944
αm =0 414
αL =0 34
NO:185
ατ =0.059
αρ =0 071
αγ =0 027
αT =0 434
αR =0 548
αm =0 096
αL =0.114
NO:186
ατ =0 934
αρ =0 851
αγ =0 997
αT =0 224
αR =0 882
αm =0.796
αL =0 01
NO:187
ατ =0 441
αρ =0 307
αγ =0.356
αT =0.340
αR =0 197
αm =0.025
αL =0 0
NO:188
ατ =0 624
αρ =0.624
αγ =0 536
αT =0.184
αR =0 535
αm =0 564
αL =0.73
NO:189
ατ =0 439
αρ =0 900
αγ =0 688
αT =0 184
αR =0.535
αm =0 564
αL =0.73
NO:190
ατ =0.432
αρ =0 634
αγ =0 273
αT =0.118
αR =0 230
αm =0 739
αL =0.202
NO:191
ατ =0 072
αρ =0 087
αγ =0 026
αT =0 018
αR =0.160
αm =1
αL =0 059
NO: 192
ατ =0 052
αρ =0.015
αγ =0 017
αT =0.440
αR =0.111
αm =0.18
αL =0.007

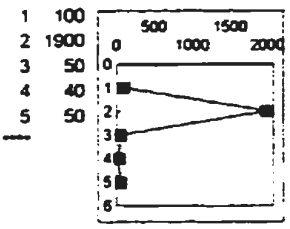

NO:193

ατ	=0 197
αρ	=0.056
αγ	=0 532
αT	=1 000
αR	=0 535
αm	=1
αL	=0 525

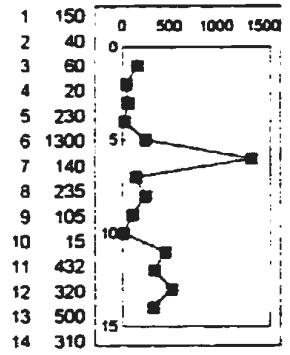

NO:194

ατ	=0.112
αρ	=0.075
αγ	=0 458
αT	=0 174
αR	=0.312
αm	=0.405
αL	=0 043

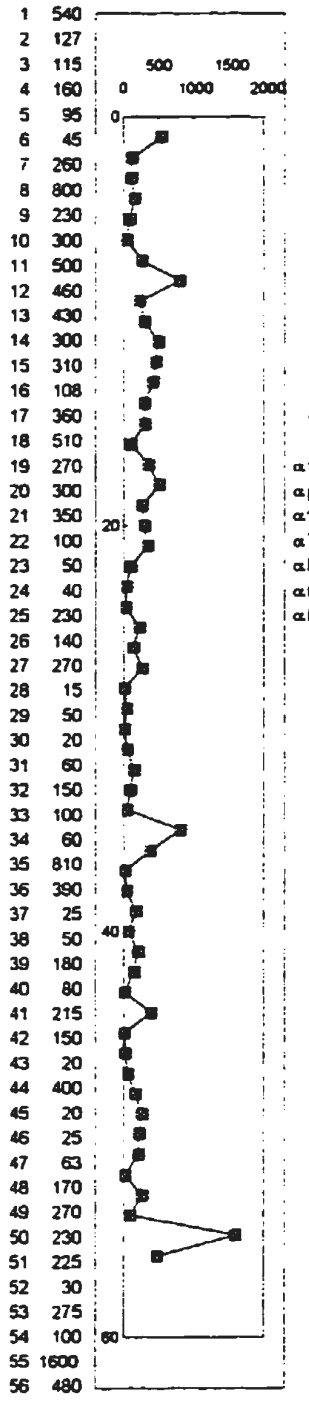

NO:195

ατ	=0 161
αρ	=0 144
αγ	=0 942
αT	=0 519
αR	=0 006
αm	=0 138
αL	=0 001

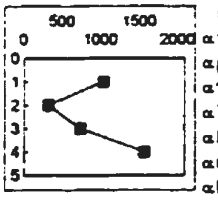

NO:196

ατ	=0.497
αρ	=0 600
αγ	=0 515
αT	=0 583
αR	=1.000
αm	=0 564
αL	=0.531

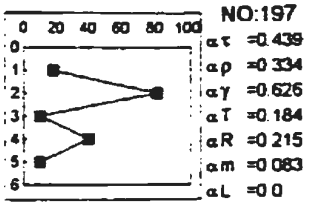

NO:197

ατ	=0 439
αρ	=0 334
αγ	=0.626
αT	=0.184
αR	=0 215
αm	=0 083
αL	=0 0

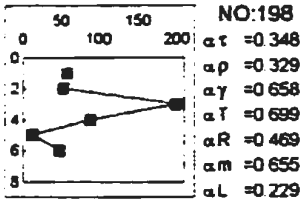

NO:198

ατ	=0 348
αρ	=0 329
αγ	=0 658
αT	=0 699
αR	=0 469
αm	=0 655
αL	=0 229

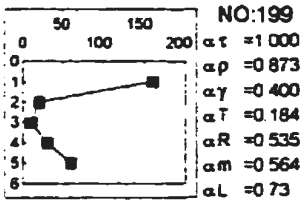

NO:199

ατ	=1 000
αρ	=0 873
αγ	=0 400
αT	=0.184
αR	=0 535
αm	=0 564
αL	=0 73

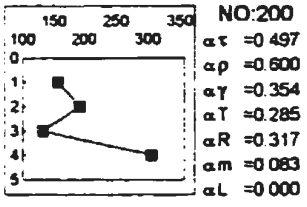

NO:200

ατ	=0 497
αρ	=0 600
αγ	=0.354
αT	=0.285
αR	=0.317
αm	=0 083
αL	=0 000

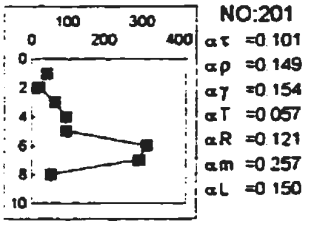

NO:201

ατ	=0 101
αρ	=0 149
αγ	=0 154
αT	=0 057
αR	=0 121
αm	=0 257
αL	=0 150

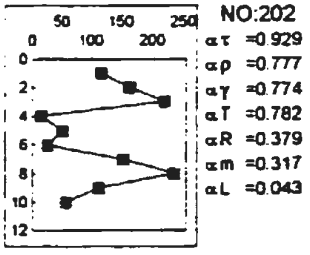

NO:202

ατ	=0.929
αρ	=0.777
αγ	=0.774
αT	=0.782
αR	=0.379
αm	=0.317
αL	=0.043

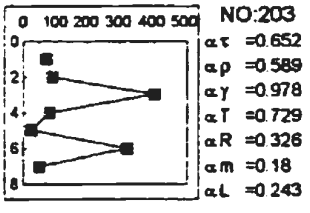

NO:203

ατ	=0.652
αρ	=0.589
αγ	=0.978
αT	=0.729
αR	=0.326
αm	=0.18
αL	=0 243

1	225
2	70
3	150
4	160
5	330

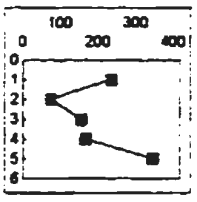

NO:204

ατ =0 327
αρ =0 505
αγ =0 403
αT =0 184
αR =0 535
αm =0 564
αL =0 73

1	250
2	10
3	90
4	160
5	340
6	115
7	80
8	80
9	225
10	270

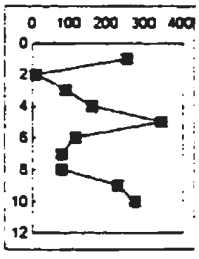

NO:205

ατ =0 587
αρ =0 668
αγ =0 571
αT =0 006
αR =0 725
αm =0 739
αL =0 176

1	130
2	250
3	255
4	180
5	125
6	60
7	360

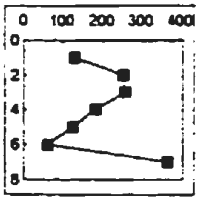

NO:206

ατ =0 881
αρ =1
αγ =0 769
αT =0 165
αR =0 513
αm =0 655
αL =0 687

1	65
2	160
3	100
4	450

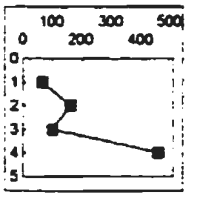

NO:207

ατ =0 174
αρ =0 200
αγ =0 193
αT =0 285
αR =1 000
αm =0 083
αL =0 000

Arkansas DeDray Lake Sections

1	11
2	14
3	58
4	4
5	3
6	15
7	22
8	4
9	8
10	11

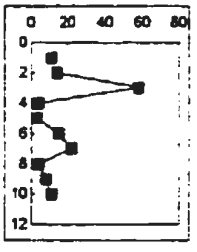

NO:208

ατ =0 784
αρ =0 528
αγ =0 436
αT =0 269
αR =1 000
αm =0 705
αL =0 005

1	37
2	27
3	4
4	5
5	1
6	3
7	0.5
8	22.4

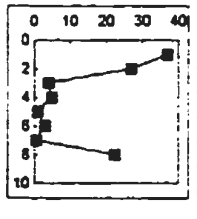

NO:209

ατ =0.083
αρ =0 120
αγ =0.209
αT =0.340
αR =0 197
αm =0 705
αL =0.736

1	32
2	0 5
3	23
4	2
5	2 8
6	64 8

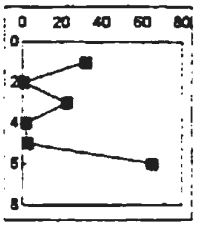

NO:210

ατ =0 573
αρ =0 623
αγ =0 538
αT =0 699
αR =0 562
αm =0 18
αL =0 155

1	17
2	0 8
3	16 3
4	0 3
5	23 6
6	3 6
7	34 3
8	12.2
9	1
10	13.7

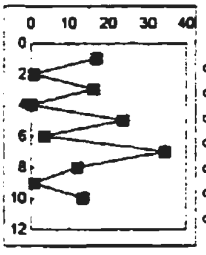

NO:211

ατ =0.929
αρ =0 987
αγ =0.881
αT =0.167
αR =0.022
αm =0 02
αL =0.004

1	45.7
2	0 8
3	1 3
4	8 9
5	182
6	0 8
7	146

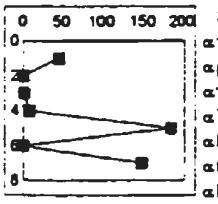

NO:212

ατ =0 538
αρ =0 653
αγ =0 271
αT =0 729
αR =0 326
αm =0 18
αL =0 243

1	26.7
2	71
3	444
4	310

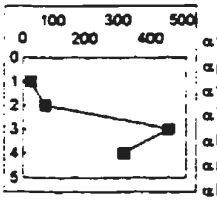

NO:213

ατ =0 174
αρ =0 200
αγ =0 203
αT =0 593
αR =0 317
αm =0 564
αL =0 033

1	15
2	57
3	60.5
4	52
5	2 6
6	1 3
7	142
8	7 6
9	6 6
10	5 6
11	3.3
12	30 5

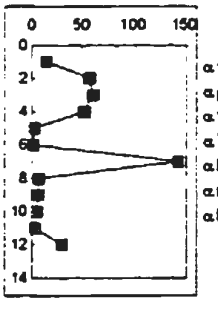

NO:214

ατ =0 273
αρ =0 276
αγ =0 463
αT =0 048
αR =0 260
αm =0 366
αL =0 022

1	1 5
2	0 8
3	1 5
4	5
5	1
6	1 3
7	3
8	1.3
9	4
10	5
11	4.6
12	1 5
13	3.8

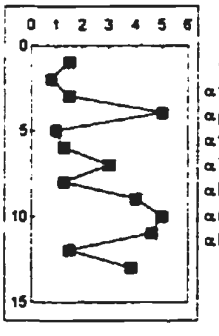

NO:215

ατ =0 115
αρ =0 094
αγ =0 106
αT =0 813
αR =0 732
αm =0 739
αL =0 533

1	8
2	23
3	2 5
4	18
5	1
6	1
7	10 5
8	99
9	2 5
10	27
11	1 8
12	0 8
13	0 8
14	0 8
15	82 5
16	2 5
17	2 5
18	1 3
19	166
20	2
21	20
22	7
23	1 8
24	0 8
25	5 6
26	20

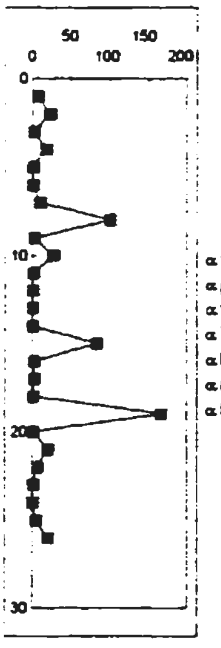

NO:216

ατ =0 718
αρ =0 653
αγ =0 833
αT =0 054
αR =0 880
αm =0 827
αL =0 671

1	28 7
2	0 3
3	3
4	29 2
5	16 5
6	0 5
7	1 3
8	21
9	2 5

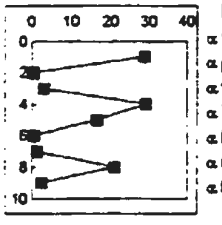

NO:217

ατ =0.835
αρ =0 700
αγ =0 473
αT =0 555
αR =0 483
αm =0 257
αL =0 313

1	26
2	40
3	59
4	43
5	4 5

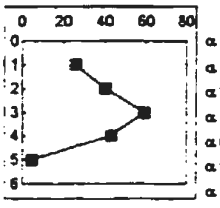

NO:218

ατ =1 000
αρ =0 873
αγ =0 613
αT =0 184
αR =0 535
αm =0 564
αL =0 73

1	21
2	5 6
3	2 8
4	46 5
5	1 8
6	6 1

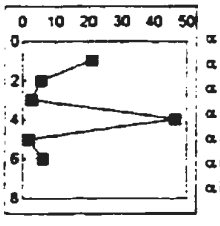

NO:219

ατ =0 573
αρ =0 704
αγ =0 807
αT =0 699
αR =0 147
αm =0 18
αL =0 155

1	18
2	15
3	6 6
4	16
5	25 4

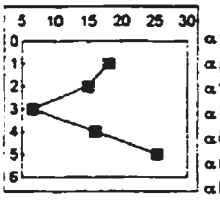

NO:220

ατ =0 624
αρ =0 624
αγ =0 539
αT =0 184
αR =0 535
αm =0 564
αL =0 73

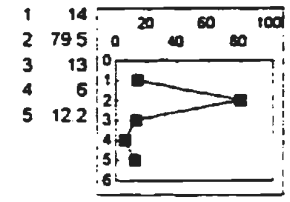

NO:221
ατ =0.142
αρ =0.104
αγ =0.507
αT =1.000
αR =0.215
αm =0.564
αL =0.05

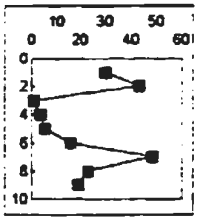

NO:222
ατ =0.532
αρ =0.865
αγ =0.962
αT =0.140
αR =0.160
αm =0.257
αL =0.111

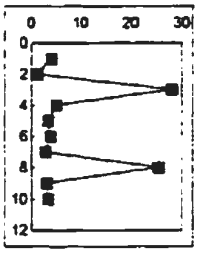

NO:223
ατ =0.587
αρ =0.583
αγ =0.954
αT =0.167
αR =0.113
αm =0.096
αL =0.070

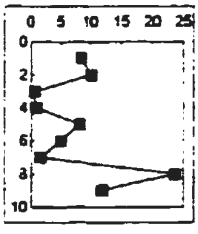

NO:224
ατ =0.404
αρ =0.381
αγ =0.311
αT =0.768
αR =0.160
αm =0.257
αL =0.111

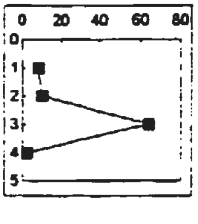

NO:225
ατ =1.000
αρ =0.800
αγ =0.835
αT =0.593
αR =1.000
αm =0.564
αL =0.531

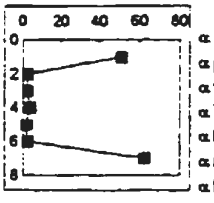

NO:226
ατ =1.000
αρ =0.742
αγ =0.834
αT =0.165
αR =0.743
αm =0.564
αL =0.868

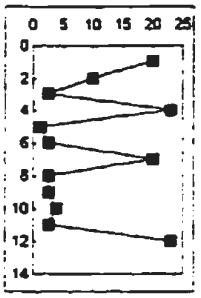

NO:227
ατ =0.879
αρ =0.398
αγ =0.650
αT =0.620
αR =0.225
αm =0.132
αL =0.086

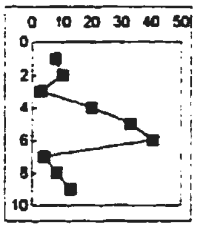

NO:228
ατ =0.404
αρ =0.576
αγ =0.741
αT =0.555
αR =0.726
αm =0.705
αL =0.386

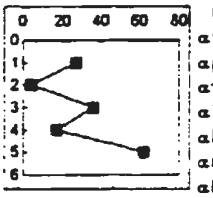

NO:229
ατ =0.327
αρ =0.391
αγ =0.284
αT =0.184
αR =0.215
αm =0.083
αL =0.0

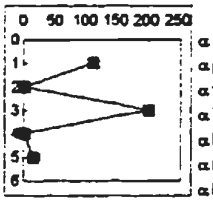

NO:230
ατ =0.624
αρ =0.624
αγ =0.568
αT =0.184
αR =0.063
αm =0.083
αL =0.0

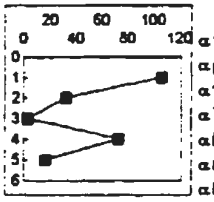

NO:231
ατ =0.327
αρ =0.391
αγ =0.371
αT =1.000
αR =0.535
αm =0.083
αL =0.0

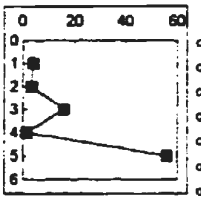

NO:232
ατ =0.624
αρ =0.624
αγ =0.186
αT =0.184
αR =0.215
αm =0.083
αL =0.0

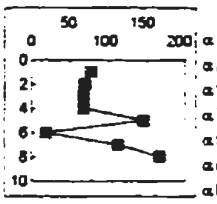

NO:233
ατ =0.529
αρ =0.405
αγ =0.246
αT =0.057
αR =1.000
αm =0.705
αL =0.736

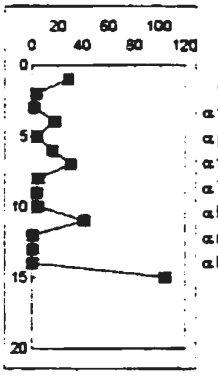

NO:234
ατ =0.616
αρ =0.627
αγ =0.290
αT =0.082
αR =0.609
αm =0.405
αL =0.297

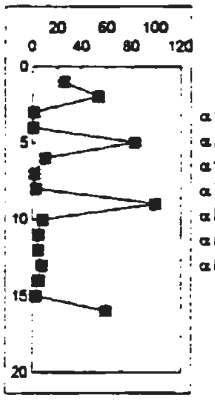

NO:235
ατ =0.964
αρ =0.981
αγ =0.682
αT =0.401
αR =0.684
αm =0.796
αL =0.000

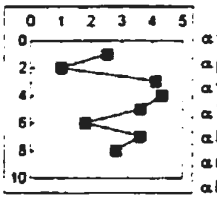

NO:236
ατ =0.900
αρ =0.787
αγ =0.653
αT =1.000
αR =0.606
αm =0.705
αL =0.736

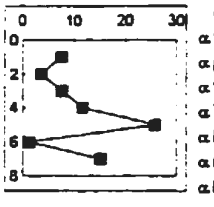

NO:237
ατ =0.356
αρ =0.41
αγ =0.453
αT =0.729
αR =0.513
αm =0.317
αL =0.617

1	94 5
2	2
3	6 4
4	5
5	41 4
6	43 2
7	3 8
8	10.7
9	4 1
10	16.8
11	7 6

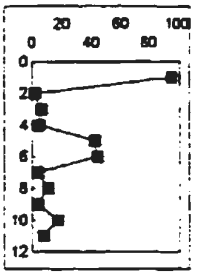

NO:238

ατ =0.938
αρ =0.915
αγ =0.182
αT =0.118
αR =0 453
αm =0 317
αL =0 535

1	30.5
2	5
3	4
4	21 6
5	11 4
6	8
7	0 8
8	17 8
9	0 5
10	2 3
11	0 8
12	2 5
13	2
14	29 8

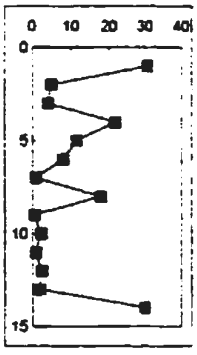

NO:239

ατ =0 186
αρ =0.172
αγ =0.461
αT =0 497
αR =0.686
αm =0.782
αL =0.360

1	11.4
2	58.4
3	39.4
4	4 8
5	2 5

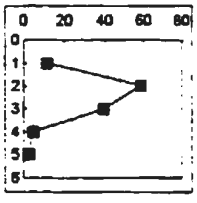

NO:240

ατ =0 142
αρ =0 188
αγ =0.436
αT =0 184
αR =0 215
αm =0 564
αL =0 05

1	70
2	11
3	35 6
4	4.6
5	2 5
6	12.5
7	11 4

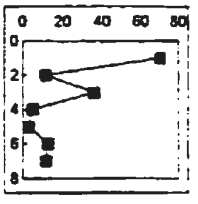

NO:241

ατ =0.293
αρ =0.432
αγ =0.108
αT =0 488
αR =0 743
αm =0 18
αL =0.243

1	5 3
2	4 6
3	61
4	0 8
5	5
6	4.6

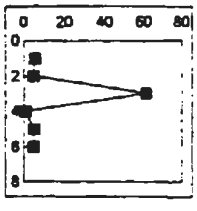

NO:242

ατ =0.437
αρ =0.364
αγ =0.786
αT =0.122
αR =0.147
αm =0.025
αL =0 000

1	3.8
2	23 6
3	8 4
4	13.7
5	20.3
6	29.8

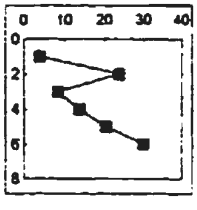

NO:243

ατ =0 091
αρ =0.156
αγ =0.132
αT =0.440
αR =0.772
αm =0.655
αL =0 229

1	16 5
2	4 3
3	2 3
4	4
5	6 4
6	44.5

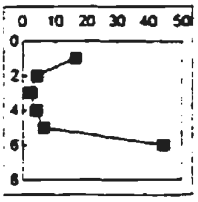

NO:244

ατ =0.573
αρ =0.623
αγ =0 327
αT =0 053
αR =0 246
αm =0.655
αL =0 459

1	5.6
2	5 3
3	1 3
4	17
5	6.9

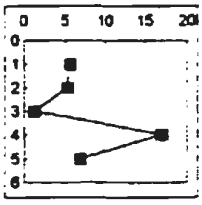

NO:245

ατ =0 624
αρ =0.391
αγ =0.521
αT =1 000
αR =0.535
αm =0 564
αL =0.05

1	10
2	11
3	127
4	1
5	12
6	3.3
7	10
8	10 6
9	9
10	0.5
11	16.5
12	5
13	2
14	0 8
15	18.3
16	9

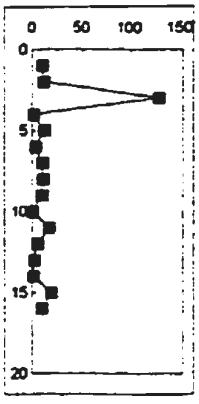

NO:246

ατ =0 364
αρ =0.337
αγ =0.253
αT =0 834
αR =0.290
αm =0 439
αL =0.471

1	3
2	41
3	1
4	109
5	1
6	1 8
7	1
8	1 3
9	46
10	0 8
11	0.5
12	1 8
13	4.8
14	5
15	2.5
16	2
17	86
18	1
19	3.8
20	3.8
21	1 5
22	3 3
23	2.3
24	4.6
25	2.3

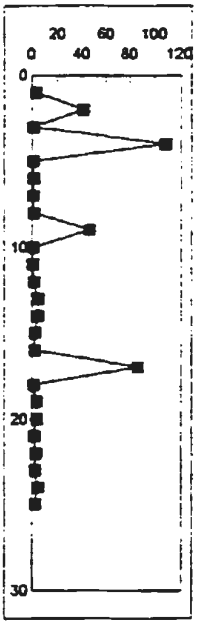

NO:247

ατ
αρ =0 585
αγ =0 612
αT =0.267
αR =0 743
αm =0 469
αL =0.67
=0 972

1	44 5
2	1 5
3	2 8
4	17 8
5	16 5
6	1 3
7	3
8	3 3
9	1 8
10	49 5

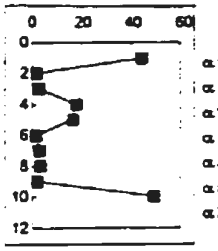

NO:248

ατ =0 929
αρ =0 855
αγ =0.978
αT =0.782
αR =0 725
αm =0 317
αL =0 133

1	24
2	16
3	1
4	47
5	0 8
6	3 8
7	10.2

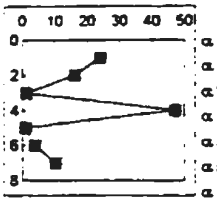

NO:249

ατ =0 453
αρ =0 383
αγ =0.503
αT =0.729
αR =0 513
αm =0 655
αL =0 311

Northern Norway Sections

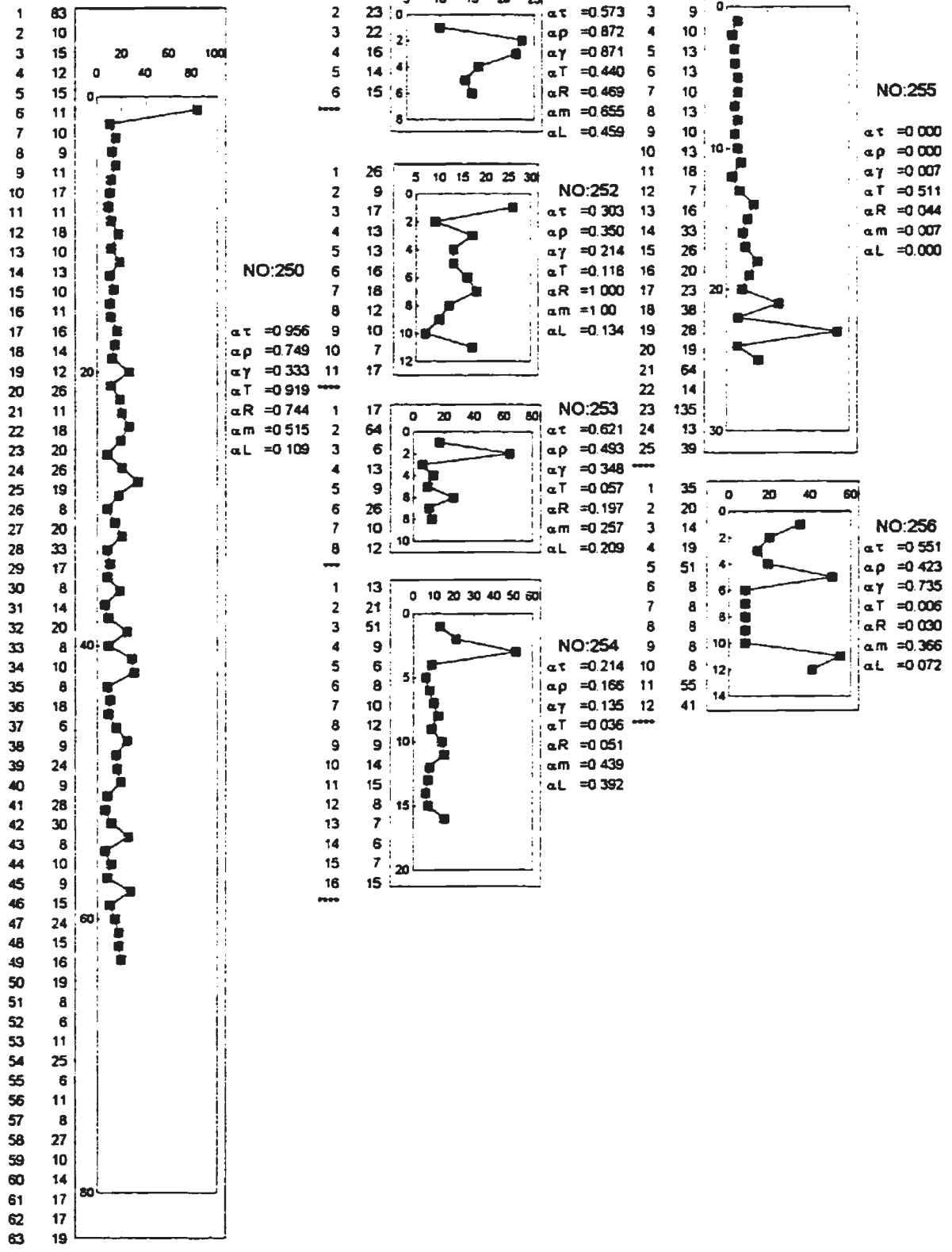

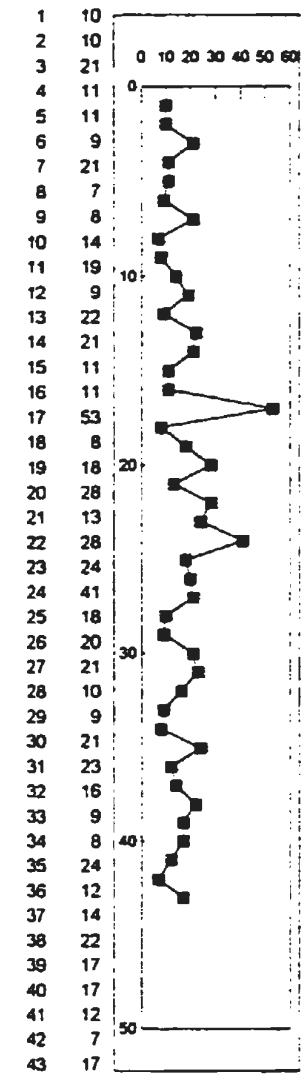

NO:257

ατ =0 487
αρ =0 470
αγ =0.681
αT =0 109
αR =0.781
αm =0.876
αL =0 289

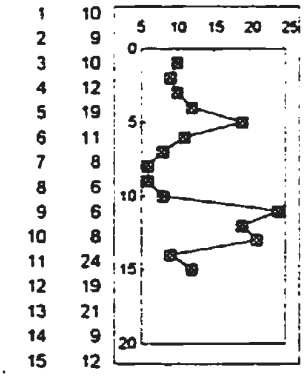

NO: 258

ατ =0 508
αρ =0 533
αγ =0 291
αT =0 082
αR =0.05
αm =0 564
αL =0.231

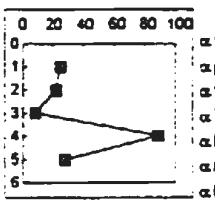

NO: 259

ατ =0 624
αρ =0 391
αγ =0.544
αT =1
αR =0 535
αm =0 564
αL =0 05

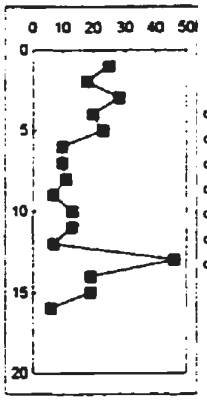

NO:260

ατ =0.170
αρ =0 155
αγ =0 562
αT =0 401
αR =0 254
αm =0.02
αL =0 000

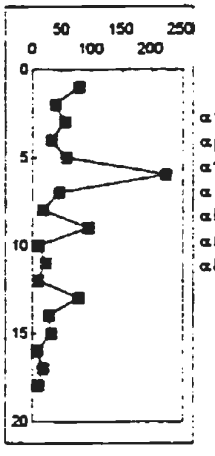

NO:261

ατ =0 015
αρ =0 008
αγ =0.104
αT =0 049
αR =0.857
αm =0.197
αL =0.062

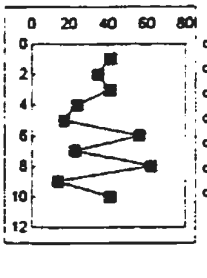

NO:262

ατ =0.711
αρ =0.745
αγ =0 985
αT =0.167
αR =0 078
αm =0 02
αL =0 004

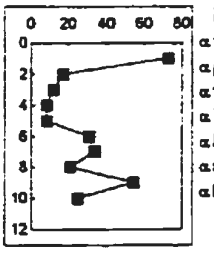

NO:263

ατ =0.587
αρ =0 595
αγ =0.948
αT =0 053
αR =0.218
αm =0 739
αL =0 380

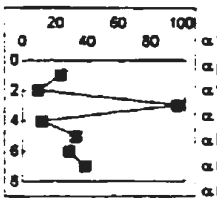

NO:264

ατ =0 293
αρ =0 294
αγ =0 910
αT =0 083
αR =0 326
αm =0 655
αL =0 311

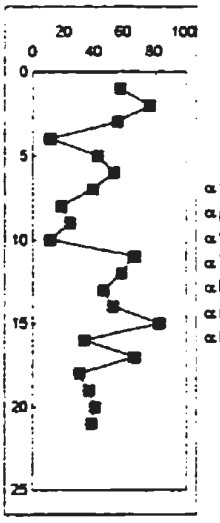

NO:265

ατ =0.585
αρ =0 584
αγ =0 827
αT =0 857
αR =0 378
αm =0 251
αL =0 09

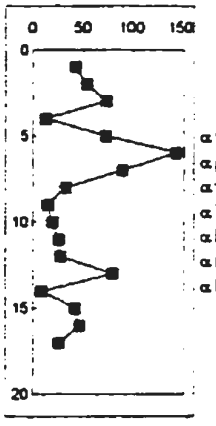

NO:266

ατ =0 385
αρ =0 226
αγ =0 235
αT =0 068
αR =0 460
αm =0 796
αL =0 192

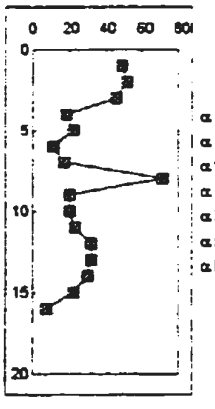

NO:267

ατ =0 338
αρ =0 253
αγ =0 122
αT =0 006
αR =0 073
αm =0 197
αL =0 052

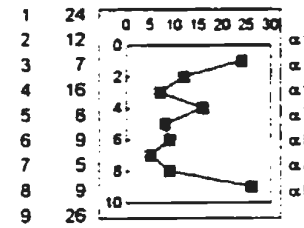

NO:268
ατ =0 751
αρ =0.788
αγ =0.853
αT =0.768
αR =0 944
αm =0.414
αL =0.492

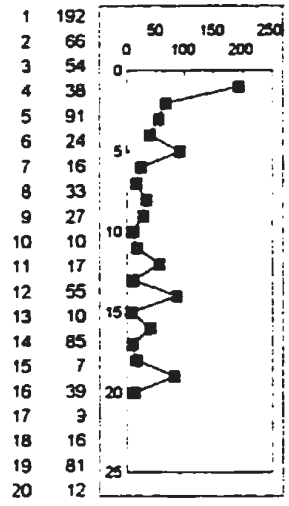

NO:269
ατ =0.031
αρ =0 049
αγ =0 051
αT =1 000
αR =0 493
αm =0 491
αL =0 439

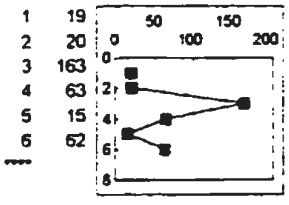

NO:270
ατ =0 851
αρ =0.872
αγ =0 858
αT =0 440
αR =0.885
αm =0 655
αL =0 229

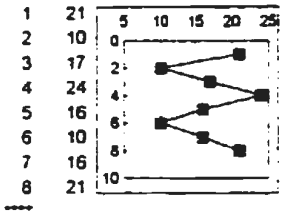

NO:271
ατ =0 896
αρ =0.715
αγ =0 989
αT =0 340
αR =0 606
αm =0 705
αL =0 736

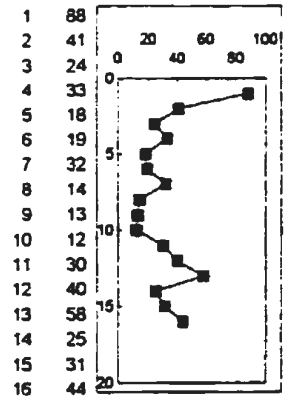

NO:272
ατ =0.857
αρ =0 966
αγ =0 589
αT =0.142
αR =0.122
αm =0 796
αL =0 346

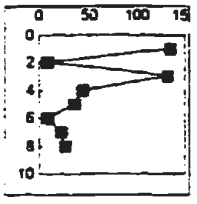

NO:273
ατ =0 166
αρ =0 220
αγ =0.117
αT =0 340
αR =0 796
αm =0 705
αL =0 057

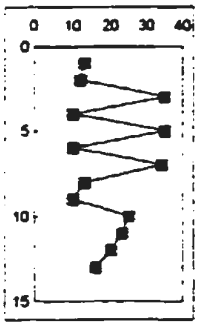

NO:274
ατ =0 950
αρ =0 800
αγ =0 955
αT =0 636
αR =0.111
αm =0 366
αL =0 78

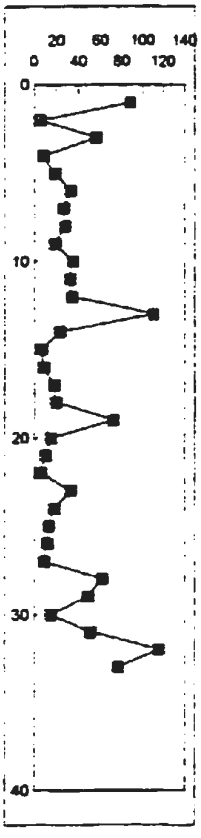

NO:275
ατ =0.755
αρ =0 694
αγ =0 462
αT =0 257
αR =0.213
αm =0 59
αL =0 113

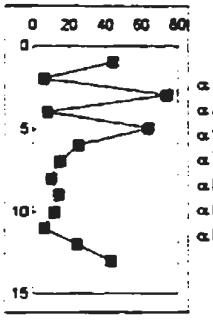

NO:276
ατ =0 581
αρ =0.568
αγ =0 365
αT =0 813
αR =0.425
αm =0 763
αL =0 592

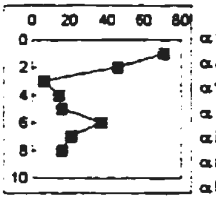

NO:277
ατ =0 529
αρ =0.423
αγ =0.149
αT =0.057
αR =0 121
αm =0.705
αL =0.353

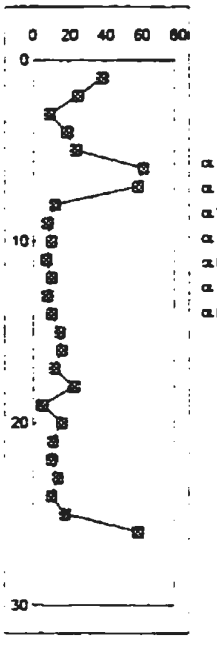

NO: 278
ατ =0 513
αρ =0 358
αγ =0 368
αT =0 63
αR =0 064
αm =0 841
αL =0.06

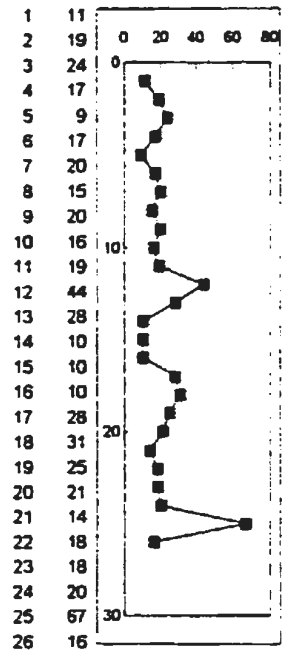

NO: 279

ατ =0 302
αρ =0 296
αγ =0 13
αT =0 004
αR =0 289
αm =0.841
αL =0 237

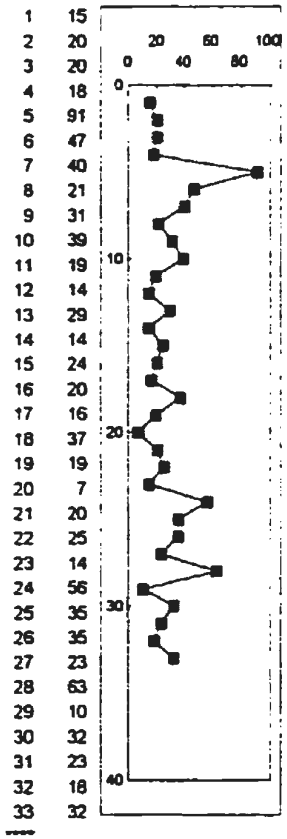

NO:280

ατ =0 950
αρ =0 853
αγ =0 794
αT =0 479
αR =0.848
αm =0 465
αL =0 583

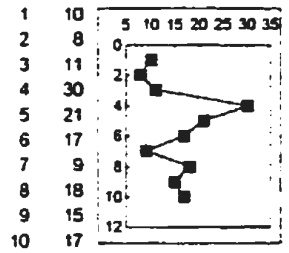

NO:281

ατ =0 469
αρ =0 387
αγ =0 541
αT =0.782
αR =0 597
αm =0 739
αL =0 094

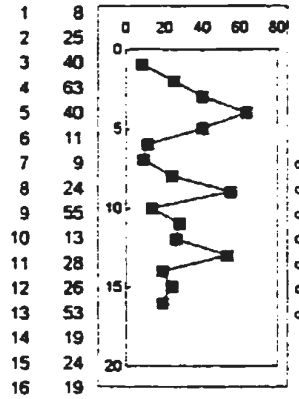

NO:282

ατ =0 964
αρ =0.92
αγ =0 833
αT =0.834
αR =0.464
αm =0 439
αL =0 065

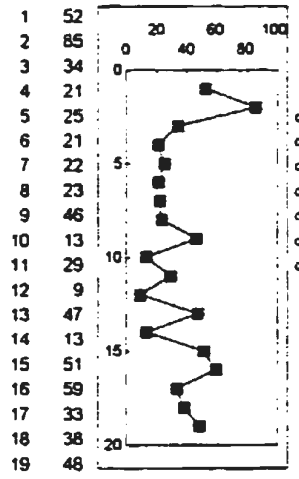

NO:283

ατ =0.699
αρ =0 789
αγ =0 895
αT =0.703
αR =0 536
αm =0 225
αL =0.172

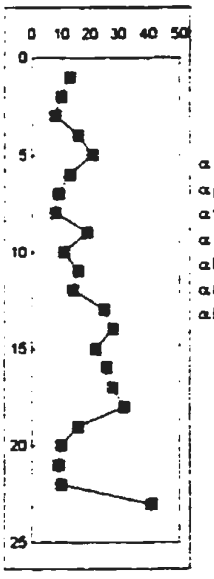

NO:284

ατ =0 056
αρ =0 114
αγ =0 042
αT =0 122
αR =0 012
αm =0 251
αL =0 067

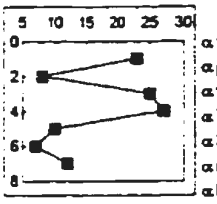

NO:285

ατ =0 652
αρ =0 535
αγ =0 315
αT =0 729
αR =0.743
αm =0 655
αL =0 311

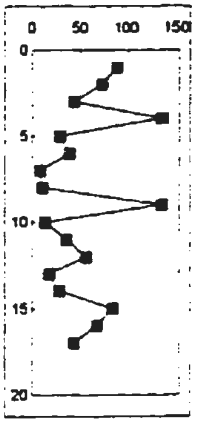

NO:286

ατ =0 591
αρ =0 475
αγ =0 442
αT =1 000
αR =0 657
αm =0 439
αL =0 06

Appendix IV-1, IV-2, IV-3

Results of statistical tests for asymmetric trends and randomness using respectively bed thickness, grain size, and sedimentary structure data of sandstone packets selected from turbidite sections involved in this study.

Abbreviations:

No: Sandstone packet number N: The munber of beds in a packet

Asy: statistically recognized asymmetric sequences
****: upward thickening (in Appendix IV-1), upward coarsening (in Appendix IV-2), upward decrease in upper Bouma divisions (in Appendix IV-3)
** : upward thinning (in Appendix IV-1), upward fining (in Appendix IV-2), upward increase in upper Bouma divisions (in Appendix IV-3)

τ: Kendall's rank correlation coefficient $Z\tau$: the value of Z test for τ
$\alpha\tau$: the significantce level at which a sequence would pass Kendall's correlation test

ρ: Spearman's rank correlation coefficient $t\rho$: the value of student t test for ρ
$\alpha\rho$: the significance level at which a sequence would pass Spearman's correlation test

γ: Pearson's linear correlation coefficient $t\gamma$: the value of student t test for γ
$\alpha\gamma$: the significance level at which a sequence would pass Pearson's correlation test

ZT: the value of Z test for the Turning Point test
αT: the significance level at which a sequence would pass the Turning Point test

ZR: the value of Z test for the Rank difference test
αR: the significance level at which a sequence would pass the Rank Difference test

Zm: the value of Z test for the Median Crossing test
αm: the significance level at which a sequence would pass the Median Crossing test

FL: the value of F test for the Length-of-runs test
αL: the significance level at which a sequence would pass the Length-of-runs test

****

Note:

An upward thinning sequence has negative values of τ, ρ, and γ (i.e., a negative correlation); upward thickening sequences have positive values of these parameters (i.e., a positive correlation). Since grain size and sedimentary structure were scored with larger values for fine grain size and for upper Bouma divisions, and smaller values for coarse grain size and for lower Bouma diviaions, sequences which coarsen up or decrease upward in upper Bouma divisions would have negative values of τ, ρ, and γ (i.e., a negative correlation), and sequences which fine up or increase upward in upper Bouma divisions would have positive values of τ, ρ, and γ (i.e., a positive correlation).

Appendix IV-1

Results of tests for asymmetric trends and randomness using bed-thickness data of 286 turbidite sandstone packets

Sections of northern Italian Apennines

No	N	τ	Zτ	ατ	ρ	ιρ	αρ	γ	ιγ	αγ	ZT	αT	ZR	αR	Zm	αm	FL	αL	ASY
1	20	-0.198	-1.223	0.221	-0.262	-1.152	0.265	-0.138	-0.59	0.562	-1.112	0.266	-0.685	0.493	-1.147	0.251	10.533	0.061	
2	17	0.412	2.307	0.021	0.578	2.746	0.015	0.617	3.038	0.008	-1.217	0.224	-2.587	0.01	-2.324	0.02	15.701	0.008	****
3	20	0.132	0.813	0.416	0.124	0.529	0.603	0.048	0.204	0.841	-1.112	0.266	-0.685	0.493	-0.229	0.819	3.613	0.306	
4	6	0.467	1.315	0.188	0.543	1.293	0.266	0.381	0.824	0.456	0.386	0.699	0.58	0.562	0.447	0.655	1.446	0.229	
5	10	0.111	0.447	0.655	0.127	0.363	0.726	0.213	0.618	0.554	0.553	0.581	-1.232	0.218	-0.333	0.739	3.079	0.38	
6	20	0.15	0.923	0.356	0.155	0.664	0.515	0.095	0.406	0.689	-0.556	0.578	-1.199	0.23	-0.688	0.491	4.571	0.206	
7	5	-0.6	-1.47	0.142	-0.7	-1.698	0.188	-0.77	-2.093	0.127	0	1	-0.62	0.535	-0.577	0.564	3.833	0.05	
8	10	-0.068	-0.274	0.784	-0.067	-0.191	0.853	0.23	0.667	0.523	0.553	0.581	1.408	0.159	1.89	0.059	3.102	0.078	
9	17	0.25	1.401	0.161	0.301	1.225	0.24	0.152	0.595	0.561	0.609	0.543	-0.665	0.506	0.258	0.796	0.545	0.909	
10	8	-0.109	-0.378	0.705	-0.259	-0.657	0.536	-0.212	-0.532	0.614	0	1	-1.033	0.302	-1.134	0.257	6.471	0.091	
11	5	-0.2	-0.49	0.624	-0.5	-1	0.391	-0.613	-1.345	0.271	0	1	-0.62	0.535	-0.577	0.564	3.833	0.05	
12	5	-0.4	-0.98	0.327	-0.4	-0.756	0.505	-0.385	-0.723	0.522	-1.328	0.184	-0.62	0.535	0.577	0.564	0.119	0.73	
13	5	0.2	0.49	0.624	0.3	0.545	0.624	0.081	0.14	0.898	1.328	0.184	1.861	0.063	1.732	0.083	2.893	0	
14	6	-0.067	-0.188	0.851	-0.143	-0.289	0.787	-0.192	-0.391	0.716	1.545	0.122	0.58	0.562	-0.447	0.655	1.56	0.459	
15	10	-0.135	-0.543	0.587	-0.174	-0.499	0.631	-0.222	-0.644	0.538	-0.276	0.782	0.352	0.725	1	0.317	2.254	0.133	
16	18	0.59	3.42	0.001	0.788	5.115	0	0.748	4.514	0	-0.393	0.694	-3.487	0	-2.668	0.008	159.8	0	****
17	21	0.087	0.549	0.583	0.142	0.627	0.538	0.264	1.195	0.247	-0.361	0.718	-1.093	0.274	-0.229	0.819	3.402	0.334	
18	19	0	0	1	-0.03	-0.125	0.902	0.102	0.422	0.678	-0.191	0.849	-0.496	0.62	-0.243	0.808	3.02	0.554	
19	13	-0.052	-0.247	0.805	-0.077	-0.257	0.802	-0.007	-0.023	0.982	-0.945	0.344	-0.798	0.425	0.302	0.763	1.907	0.592	
20	15	0.019	0.099	0.921	-0.055	-0.197	0.847	-0.306	-1.161	0.267	-1.742	0.082	-2.048	0.041	-0.277	0.782	1.095	0.778	
21	6	-0.067	-0.188	0.851	-0.143	-0.289	0.787	-0.166	-0.336	0.754	-0.773	0.44	0.145	0.885	0.447	0.655	1.446	0.229	
22	9	0.167	0.626	0.532	0.2	0.54	0.606	0.443	1.306	0.233	0.295	0.768	0.912	0.362	1.89	0.059	3.891	0.049	
23	20	-0.053	-0.324	0.746	-0.096	-0.41	0.686	-0.021	-0.087	0.932	-0.556	0.578	0.457	0.648	1.147	0.251	2.608	0.271	
24	5	0	0	1	0.1	0.174	0.873	0.141	0.246	0.821	1.328	0.184	1.861	0.063	1.732	0.083	2.893	0	

No	N	τ	Zτ	ατ	ρ	tρ	αρ	γ	tγ	αγ	ZT	αT	ZR	αR	Zm	αm	FL	αL	ASY
25	17	0.052	0.294	0.769	0.088	0.341	0.738	0.276	1.114	0.283	-1.826	0.068	-0.296	0.767	0.832	0.405	0.267	0.875	
26	12	-0.015	-0.069	0.945	-0.005	-0.017	0.987	0.322	1.075	0.307	-0.495	0.62	-0.996	0.319	-0.905	0.366	8.974	0.03	
27	26	0.336	2.41	0.016	0.452	2.482	0.02	0.16	0.793	0.435	0.482	0.63	-1.324	0.185	-0.2	0.841	4.736	0.192	****
28	20	0.069	0.423	0.672	0.109	0.464	0.648	0.18	0.774	0.449	-1.668	0.095	-1.599	0.11	-0.688	0.491	3.675	0.299	
29	9	-0.028	-0.106	0.916	-0.038	-0.1	0.923	0.326	0.911	0.392	0.295	0.768	-0.351	0.726	-1.134	0.257	6.012	0.111	
30	5	0.2	0.49	0.624	0.2	0.354	0.747	0.01	0.018	0.987	0	1	0.62	0.535	0.577	0.564	0.119	0.73	
31	4	0.333	0.679	0.497	0.6	1.061	0.4	0.525	0.873	0.475	1.069	0.285	0	1	-0.577	0.564	4.525	0.033	
32	12	0.015	0.069	0.945	-0.026	-0.083	0.935	0.173	0.557	0.59	-0.495	0.62	-1.516	0.13	-0.905	0.366	6.747	0.034	
33	13	0.103	0.488	0.625	0.044	0.146	0.887	-0.204	-0.692	0.503	0.473	0.636	-1.026	0.305	-0.905	0.366	5.546	0.236	
Monticello Dam Section, California																			
34	6	-0.2	-0.564	0.573	-0.257	-0.532	0.623	-0.647	-1.699	0.165	1.545	0.122	1.449	0.147	2.236	0.025	8	0	
35	14	0.144	0.72	0.472	0.256	0.918	0.377	0.389	1.461	0.17	0.679	0.497	-0.808	0.419	0.832	0.405	5.011	0.171	
36	22	-0.195	-1.269	0.204	-0.302	-1.417	0.172	-0.334	-1.585	0.129	-1.232	0.218	-1.13	0.258	2.111	0.035	5.872	0.015	
37	21	-0.438	-2.778	0.005	-0.519	-2.65	0.016	-0.544	-2.826	0.011	1.263	0.206	-1.569	0.117	-1.606	0.108	39.23	0	
38	20	0.126	0.779	0.436	0.194	0.839	0.413	0.119	0.509	0.617	-0.556	0.578	0.171	0.864	0.229	0.819	0.922	0.82	
39	19	-0.246	-1.474	0.141	-0.361	-1.598	0.129	-0.321	-1.395	0.181	-0.191	0.849	-0.496	0.62	-0.243	0.808	1.294	0.731	
40	5	-0.316	-0.775	0.439	-0.553	-1.148	0.334	-0.697	-1.682	0.191	1.328	0.184	1.24	0.215	1.732	0.083	2.893	0	
41	20	0.1	0.618	0.537	0.123	0.526	0.605	-0.032	-0.135	0.894	1.112	0.266	1.142	0.253	2.065	0.039	5.831	0.016	
42	12	-0.273	-1.234	0.217	-0.315	-1.048	0.319	-0.166	-0.533	0.605	-1.238	0.216	-1.256	0.209	-0.905	0.366	8.256	0.083	
43	13	-0.606	-2.886	0.004	-0.833	-5	0	-0.712	-3.359	0.006	0.473	0.636	-2.165	0.03	-1.508	0.132	8.182	0.085	
44	5	0.2	0.49	0.624	0.5	1	0.391	0.236	0.421	0.702	0	1	-0.62	0.535	-0.577	0.564	3.833	0.05	
45	6	0.2	0.564	0.573	0.257	0.532	0.623	0.113	0.227	0.831	-0.773	0.44	-0.29	0.772	-0.447	0.655	1.56	0.459	
46	23	-0.136	-0.911	0.362	-0.211	-0.989	0.334	-0.11	-0.505	0.619	-2.061	0.039	-0.779	0.436	-0.447	0.655	3.093	0.542	
47	15	-0.223	-1.161	0.246	-0.334	-1.279	0.223	-0.286	-1.078	0.301	0.218	0.828	-0.602	0.547	-0.832	0.405	4.759	0.313	
48	9	0.222	0.834	0.404	0.367	1.043	0.332	0.451	1.337	0.223	0.295	0.768	-0.351	0.726	0.378	0.705	0.413	0.813	
49	14	0.143	0.712	0.477	0.191	0.675	0.513	0.12	0.418	0.683	-0.679	0.497	0.303	0.762	0.277	0.782	1.455	0.483	
50	12	0.485	2.194	0.028	0.685	2.976	0.014	0.723	3.311	0.008	1.734	0.083	-0.087	0.931	0.905	0.366	5.494	0.064	

No	N	τ	Zτ	ατ	ρ	tρ	αρ	γ	tγ	αγ	ZT	αT	ZR	αR	Zm	αm	FL	αL	ASY
51	28	-0.199	-1.488	0.137	-0.277	-1.468	0.154	-0.299	-1.596	0.122	-0.618	0.537	-1.011	0.312	-0.192	0.847	3.239	0.356	
52	10	0.386	1.555	0.12	0.454	1.441	0.188	0.663	2.504	0.037	-2.763	0.006	-1.056	0.291	-0.333	0.739	3.479	0.176	
53	10	0.068	0.274	0.784	0.11	0.314	0.761	0.125	0.358	0.73	1.381	0.167	1.584	0.113	1.667	0.096	3.284	0.07	
54	4	0	0	1	0.2	0.289	0.8	0.293	0.433	0.707	-0.535	0.593	0	1	0.577	0.564	0.392	0.531	
55	18	0.158	0.918	0.359	0.247	1.019	0.323	0.172	0.699	0.495	0.196	0.844	0.09	0.928	0.775	0.439	1.126	0.57	
56	24	-0.283	-1.935	0.053	-0.448	-2.351	0.028	-0.45	-2.365	0.027	-0.839	0.401	-1.958	0.05	-0.626	0.532	10.571	0.014	**
Cache Creek Section, California																			
57	15	-0.01	-0.049	0.961	-0.057	-0.206	0.84	-0.079	-0.286	0.779	-0.435	0.663	-1.054	0.292	-0.832	0.405	3.713	0.294	
58	17	0.045	0.251	0.802	0.046	0.177	0.862	0.106	0.413	0.686	0.609	0.543	0.813	0.416	1.069	0.285	0.583	0.747	
59	18	-0.407	-2.356	0.018	-0.621	-3.172	0.006	-0.515	-2.401	0.029	0.196	0.844	-0.517	0.605	-0.728	0.467	9.703	0.084	**
60	14	-0.155	-0.771	0.441	-0.144	-0.505	0.623	-0.108	-0.376	0.713	-0.679	0.497	-1.212	0.225	0.277	0.782	1.455	0.483	
61	7	-0.143	-0.451	0.652	-0.107	-0.241	0.819	0.132	0.297	0.779	0.694	0.488	1.637	0.102	2.236	0.025	6.25	0	
62	6	-0.333	-0.939	0.348	-0.486	-1.111	0.329	-0.566	-1.374	0.241	0.386	0.699	0.58	0.562	0.447	0.655	1.446	0.229	
63	5	0.4	0.98	0.327	0.4	0.756	0.505	0.247	0.442	0.688	-1.328	0.184	-0.62	0.535	0.577	0.564	0.119	0.73	
64	4	-0.333	-0.679	0.497	-0.4	-0.617	0.6	-0.749	-1.599	0.251	1.069	0.285	1	0.317	1.732	0.083	4.167	0	
65	11	-0.164	-0.701	0.484	-0.373	-1.205	0.259	-0.493	-1.699	0.124	-0.782	0.434	-1.951	0.051	-1.667	0.096	10.509	0.033	
66	15	0.153	0.796	0.426	0.157	0.571	0.577	0.01	0.035	0.972	-2.395	0.017	-0.602	0.547	-0.277	0.782	4.083	0.395	
67	28	0.05	0.376	0.707	0.106	0.545	0.59	0.087	0.445	0.66	-0.154	0.877	0.202	0.84	-0.962	0.336	7.343	0.119	
68	23	0.215	1.435	0.151	0.295	1.416	0.172	0.264	1.253	0.224	1.031	0.303	0.183	0.855	0.218	0.827	2.707	0.608	
69	8	0.109	0.378	0.705	0.114	0.282	0.787	-0.191	-0.476	0.651	0	1	0	1	0.378	0.705	3.225	0.073	
70	23	0.091	0.61	0.542	0.138	0.638	0.53	0.245	1.158	0.26	0	1	-1.467	0.142	-0.218	0.827	11.002	0.012	
71	5	0.2	0.49	0.624	0.3	0.545	0.624	-0.153	-0.268	0.806	0	1	0.62	0.535	1.732	0.083	2.893	0	
72	30	-0.406	-3.151	0.002	-0.552	-3.499	0.002	-0.415	-2.415	0.022	1.042	0.297	-2.383	0.017	-2.043	0.041	20.285	0	**
73	4	0.333	0.679	0.497	0.4	0.617	0.6	0.441	0.695	0.559	-0.535	0.593	0	1	0.577	0.564	0.392	0.531	
74	6	-0.067	-0.188	0.851	0.086	0.172	0.872	0.023	0.047	0.965	-0.773	0.44	-0.29	0.772	-0.447	0.655	1.56	0.459	
75	15	-0.202	-1.049	0.294	-0.317	-1.206	0.249	-0.475	-1.948	0.073	0.218	0.828	-0.151	0.88	0.277	0.782	1.219	0.544	
76	8	-0.071	-0.247	0.805	-0.119	-0.294	0.779	-0.096	-0.237	0.82	0.953	0.34	1.549	0.121	1.89	0.059	4.914	0.027	

No	N	τ	Zτ	ατ	ρ	ιρ	αρ	γ	ιγ	αγ	ZT	αT	ZR	αR	Zm	αm	FL	αL	ASY
77	8	-0.071	-0.247	0.805	-0.095	-0.234	0.823	-0.054	-0.134	0.898	0.953	0.34	0.775	0.439	1.134	0.257	1.581	0.209	
78	79	0.226	2.951	0.003	0.342	3.194	0.002	0.358	3.367	0.001	-2.25	0.024	-3.734	0	-4.217	0	*****	0	****
Cap Ste-Anne Sections, Quebec																			
79	34	-0.163	-1.356	0.175	-0.257	-1.504	0.142	-0.281	-1.656	0.108	-0.139	0.889	-3.22	0.001	-1.915	0.056	113.466	0	
80	6	0.333	0.939	0.348	0.543	1.293	0.266	0.329	0.697	0.524	0.386	0.699	-0.29	0.772	0.447	0.655	1.446	0.229	
81	5	0	0	1	-0.1	-0.174	0.873	-0.048	-0.083	0.939	-1.328	0.184	-0.62	0.535	0.577	0.564	0.119	0.73	
82	16	0.249	1.345	0.178	0.318	1.256	0.23	0.383	1.553	0.143	-0.84	0.401	-0.081	0.935	0.775	0.439	1.71	0.425	
83	7	-0.619	-1.952	0.051	-0.75	-2.535	0.052	-0.631	-1.819	0.129	-1.388	0.165	-1.637	0.102	-1.342	0.18	8.83	0.012	****
84	15	-0.44	-2.287	0.022	-0.563	-2.454	0.029	-0.593	-2.652	0.02	-0.435	0.663	-1.506	0.132	-0.832	0.405	5.655	0.226	****
85	19	0.199	1.193	0.233	0.237	1.008	0.328	0.219	0.927	0.367	-0.763	0.446	-2.168	0.03	-0.728	0.467	4.971	0.174	
86	11	-0.382	-1.635	0.102	-0.509	-1.774	0.11	-0.658	-2.623	0.028	0.782	0.434	-0.45	0.653	0.333	0.739	4.179	0.124	
87	9	-0.111	-0.417	0.677	-0.133	-0.356	0.732	-0.127	-0.339	0.744	0.295	0.768	0.07	0.944	0.378	0.705	0.413	0.813	
Petite Valley Section, Quebec																			
88	6	0	0	1	0.044	0.088	0.934	0.086	0.174	0.871	-1.932	0.053	-1.16	0.246	0.577	0.564	0.018	0.894	
89	25	0.179	1.253	0.21	0.187	0.914	0.37	0.046	0.223	0.826	-2.134	0.033	-2.253	0.024	-0.655	0.513	3.359	0.5	
90	18	0.139	0.806	0.42	0.169	0.685	0.503	0.202	0.827	0.421	0.196	0.844	1.372	0.17	0.728	0.467	1.045	0.593	
91	4	0.667	1.359	0.174	0.8	1.886	0.2	0.732	1.52	0.268	-0.535	0.593	-1	0.317	-0.577	0.564	4.525	0.033	
92	11	0	0	1	-0.048	-0.144	0.889	-0.177	-0.539	0.603	-0.782	0.434	0.6	0.548	1.414	0.157	3.969	0.137	
93	23	-0.201	-1.345	0.179	-0.254	-1.201	0.243	-0.334	-1.623	0.119	-1.546	0.122	-2.108	0.035	-1.147	0.251	7.382	0.061	
94	7	0.143	0.451	0.652	0.179	0.406	0.702	0.207	0.474	0.655	-1.388	0.165	-0.982	0.326	-0.447	0.655	1.418	0.492	
95	6	0	0	1	-0.015	-0.029	0.978	0.059	0.118	0.912	-0.773	0.44	0.58	0.562	0.447	0.655	1.446	0.229	
96	14	-0.124	-0.616	0.538	-0.146	-0.51	0.62	-0.16	-0.56	0.586	0.679	0.497	-1.616	0.106	-0.277	0.782	5.819	0.055	
97	12	-0.031	-0.139	0.889	-0.151	-0.484	0.639	-0.049	-0.154	0.881	-1.982	0.048	-2.036	0.042	-2.111	0.035	20.001	0.001	
98	10	0.33	1.328	0.184	0.352	1.064	0.318	0.477	1.534	0.164	0.553	0.581	0.176	0.86	1.667	0.096	3.284	0.07	
99	6	0.138	0.389	0.697	-0.044	-0.088	0.934	0.074	0.149	0.889	0.386	0.699	-0.29	0.772	0.577	0.564	0.018	0.894	
100	7	-0.143	-0.451	0.652	-0.214	-0.491	0.645	-0.127	-0.286	0.787	0.694	0.488	0.327	0.743	0.447	0.655	1.028	0.311	

No	N	τ	Zτ	ατ	ρ	ιρ	αρ	γ	ιγ	αγ	ZT	αT	ZR	αR	Zm	αm	FL	αL	ASY
101	14	-0.136	-0.676	0.499	-0.174	-0.611	0.553	-0.147	-0.515	0.616	-0.679	0.497	0.808	0.419	0.832	0.405	2.855	0.24	
102	4	0.333	0.679	0.497	0.4	0.617	0.6	0.271	0.398	0.729	-0.535	0.593	0	1	0.577	0.564	0.392	0.531	
103	8	-0.265	-0.917	0.359	-0.425	-1.15	0.294	-0.138	-0.342	0.744	0	1	-0.516	0.606	1.134	0.257	1.581	0.209	
104	22	-0.283	-1.841	0.066	-0.417	-2.054	0.053	-0.47	-2.382	0.027	0.352	0.725	0.098	0.922	1.091	0.275	1.788	0.618	**
105	4	-0.667	-1.359	0.174	-0.8	-1.886	0.2	-0.401	-0.618	0.599	-0.535	0.593	-1	0.317	-0.577	0.564	4.525	0.033	
106	41	-0.027	-0.25	0.802	-0.071	-0.443	0.66	0.021	0.133	0.895	-1.137	0.256	-0.973	0.331	-0.822	0.411	5.896	0.207	
107	28	-0.177	-1.325	0.185	-0.254	-1.341	0.192	-0.3	-1.605	0.121	-0.154	0.877	-0.944	0.345	0.192	0.847	16.291	0.001	
108	30	0.08	0.623	0.533	0.069	0.367	0.717	-0.048	-0.255	0.801	-2.085	0.037	-0.747	0.455	-1.3	0.194	8.232	0.041	
109	11	-0.434	-1.859	0.063	-0.514	-1.797	0.106	-0.538	-1.913	0.088	0	1	-1.801	0.072	-1.134	0.257	7.976	0.092	**
110	32	0.045	0.364	0.716	0.052	0.287	0.776	-0.086	-0.475	0.638	-1.295	0.195	0.219	0.826	0.18	0.857	4.376	0.224	
111	31	-0.079	-0.623	0.533	-0.065	-0.35	0.729	0.045	0.242	0.811	-0.146	0.884	-1.497	0.134	-1.347	0.178	12.597	0.05	
112	7	0.238	0.751	0.453	0.393	0.955	0.383	0.367	0.881	0.419	-0.347	0.729	0	1	0.447	0.655	1.028	0.311	
113	5	0.2	0.49	0.624	0.5	1	0.391	0.358	0.664	0.554	0	1	-0.62	0.535	-0.577	0.564	3.833	0.05	
114	13	0.094	0.448	0.654	0.046	0.154	0.88	0.084	0.28	0.785	-2.364	0.018	-0.912	0.362	-0.333	0.739	5.649	0.227	
115	13	-0.065	-0.307	0.759	-0.034	-0.114	0.911	-0.059	-0.195	0.849	-0.236	0.813	0	1	0.905	0.366	0.496	0.78	
116	6	0.467	1.315	0.188	0.6	1.5	0.208	0.613	1.553	0.195	-0.773	0.44	-1.16	0.246	-0.447	0.655	1.56	0.459	
117	35	0	0	1	0.001	0.005	0.996	0.058	0.332	0.742	-1.235	0.217	-0.883	0.377	-0.18	0.857	6.209	0.184	
118	12	0.198	0.898	0.369	0.321	1.072	0.309	0.387	1.326	0.214	0.248	0.804	0.823	0.411	0.905	0.366	0.813	0.666	
119	7	-0.293	-0.923	0.356	-0.409	-1.002	0.362	-0.488	-1.249	0.267	-1.388	0.165	-0.327	0.743	0.447	0.655	1.028	0.311	
120	10	0.045	0.181	0.856	0.101	0.286	0.782	0.072	0.204	0.843	0.553	0.581	0.88	0.379	0.333	0.739	0.509	0.775	
121	16	-0.226	-1.221	0.222	-0.356	-1.424	0.176	-0.408	-1.673	0.117	-0.21	0.834	0	1	0.258	0.796	0.665	0.881	
122	14	0.033	0.166	0.868	0.095	0.33	0.747	0.205	0.725	0.482	1.359	0.174	1.717	0.086	0.832	0.405	2.751	0.432	
123	21	0.096	0.607	0.544	0.166	0.733	0.473	0.189	0.84	0.411	-1.444	0.149	-0.723	0.47	-0.688	0.491	3.599	0.308	
124	10	0.111	0.447	0.655	0.139	0.398	0.701	0.337	1.012	0.341	-0.276	0.782	-0.704	0.481	-0.333	0.739	3.079	0.38	
125	10	-0.135	-0.543	0.587	-0.223	-0.646	0.537	-0.377	-1.151	0.283	0.553	0.581	-0.352	0.725	-1	0.317	3.497	0.321	
126	15	-0.421	-2.188	0.029	-0.489	-2.023	0.064	-0.342	-1.311	0.213	-1.742	0.082	-1.144	0.252	-0.277	0.782	1.095	0.778	**
127	21	0.058	0.366	0.714	0.03	0.131	0.897	-0.188	-0.836	0.413	-1.985	0.047	-0.987	0.324	-0.229	0.819	1.14	0.767	
128	17	0.286	1.601	0.109	0.337	1.388	0.185	0.34	1.399	0.182	0	1	0.148	0.882	0	1	5.268	0.261	

No	N	τ	Zτ	ατ	ρ	ιρ	αρ	γ	ιγ	αγ	ZT	αT	ZR	αR	Zm	αm	FL	αL	ASY
129	16	0.017	0.092	0.927	-0.002	-0.008	0.994	0.015	0.056	0.956	0.42	0.675	1.792	0.073	1.941	0.052	3.083	0.079	
130	16	0.043	0.23	0.818	0.1	0.376	0.713	0.14	0.53	0.605	0.42	0.675	-0.081	0.935	-0.277	0.782	4.645	0.2	
131	7	-0.333	-1.051	0.293	-0.5	-1.291	0.253	-0.374	-0.902	0.408	1.736	0.083	0.327	0.743	0.447	0.655	1.028	0.311	
132	14	-0.044	-0.22	0.826	-0.124	-0.434	0.672	-0.052	-0.181	0.859	-2.717	0.007	-2.323	0.02	-0.832	0.405	7.499	0.112	
133	15	-0.106	-0.55	0.583	-0.217	-0.801	0.438	-0.12	-0.437	0.669	0.871	0.384	-0.151	0.88	-0.832	0.405	3.713	0.294	
134	11	-0.147	-0.629	0.53	-0.112	-0.338	0.743	-0.015	-0.045	0.965	-0.782	0.434	-0.75	0.453	-0.333	0.739	3.174	0.366	
135	7	-0.35	-1.105	0.269	-0.667	-2	0.102	-0.463	-1.168	0.296	-2.43	0.015	-1.964	0.05	-1	0.317	2.973	0.226	
136	8	0.143	0.495	0.621	0.333	0.866	0.42	0.118	0.291	0.781	0	1	-0.516	0.606	0.378	0.705	0.614	0.736	
137	18	0.046	0.269	0.788	0.064	0.258	0.8	0.041	0.165	0.871	0.786	0.432	0.765	0.444	-0.243	0.808	5.382	0.068	
138	15	0.418	2.17	0.03	0.491	2.032	0.063	0.571	2.51	0.026	-1.742	0.082	-1.687	0.092	-0.577	0.564	6.146	0.105	****
139	14	0.203	1.014	0.311	0.232	0.825	0.426	0.238	0.848	0.413	-0.679	0.497	0.404	0.686	1.508	0.132	2.676	0.262	
140	5	0.316	0.775	0.439	0.289	0.524	0.637	0.417	0.795	0.485	0	1	-0.62	0.535	0	1	0.405	0.525	
141	26	-0.151	-1.08	0.28	-0.216	-1.086	0.288	-0.143	-0.71	0.484	0.964	0.335	-0.076	0.94	-0.6	0.549	7.155	0.067	
142	9	0.479	1.798	0.072	0.576	1.862	0.105	0.646	2.24	0.06	-0.59	0.555	-0.772	0.44	-0.378	0.705	1.904	0.386	****
143	16	-0.168	-0.908	0.364	-0.245	-0.945	0.361	-0.297	-1.165	0.264	1.679	0.093	0.57	0.569	0.775	0.439	1.507	0.471	
144	14	0	0	1	0.082	0.286	0.779	0.265	0.952	0.36	0	1	-0.404	0.686	-0.277	0.782	1.144	0.766	
145	8	-0.182	-0.63	0.529	-0.307	-0.791	0.459	-0.29	-0.744	0.485	0.953	0.34	1.033	0.302	1.89	0.059	4.914	0.027	
146	11	-0.11	-0.471	0.637	-0.071	-0.213	0.836	0.23	0.708	0.497	-0.782	0.434	0.45	0.653	0	1	4.025	0.134	
147	13	0.053	0.251	0.802	-0.033	-0.111	0.914	-0.206	-0.697	0.5	-0.945	0.344	-2.165	0.03	-0.632	0.527	2.223	0.527	
148	7	0.05	0.158	0.875	-0.093	-0.208	0.843	0.058	0.13	0.902	-1.388	0.165	0	1	0.447	0.655	1.028	0.311	
149	9	-0.229	-0.858	0.391	-0.347	-0.98	0.36	-0.582	-1.896	0.1	-0.59	0.555	-0.14	0.888	0.816	0.414	2.158	0.34	
150	15	-0.202	-1.049	0.294	-0.308	-1.168	0.264	-0.294	-1.109	0.288	2.177	0.029	0.753	0.451	0.577	0.564	0.519	0.771	
151	5	0	0	1	-0.1	-0.174	0.873	0.226	0.403	0.714	0	1	0	1	0.577	0.564	0.119	0.73	
152	4	-0.333	-0.679	0.497	-0.4	-0.617	0.6	-0.359	-0.544	0.641	1.069	0.285	1	0.317	1.732	0.083	4.167	0	
153	9	0.479	1.798	0.072	0.676	2.43	0.045	0.584	1.904	0.099	-0.59	0.555	-1.404	0.16	-0.378	0.705	5.128	0.077	****
154	12	-0.462	-2.089	0.037	-0.725	-3.332	0.008	-0.331	-1.109	0.293	-1.238	0.216	-2.426	0.015	-2.714	0.007	59.334	0	**

Amazon Fan Sections																			
No	N	τ	Zτ	ατ	ρ	ιρ	αρ	γ	ιγ	αγ	ZT	αT	ZR	αR	Zm	αm	FL	αL	ASY
155	12	-0.424	-1.92	0.055	-0.573	-2.213	0.051	-0.563	-2.155	0.057	-0.495	0.62	-0.476	0.634	-0.302	0.763	1.648	0.649	**
156	12	0	0	1	0.02	0.062	0.952	0.05	0.157	0.878	-1.238	0.216	-1.646	0.1	-1.667	0.096	8.724	0.068	
157	5	0.2	0.49	0.624	0	0	1	0.073	0.126	0.908	-1.328	0.184	-0.62	0.535	0.577	0.564	0.119	0.73	
158	17	-0.066	-0.372	0.71	-0.111	-0.433	0.671	-0.374	-1.563	0.139	0.609	0.543	-0.222	0.824	0.258	0.796	4.241	0.12	
159	16	0.237	1.282	0.2	0.293	1.145	0.271	0.112	0.42	0.681	-0.21	0.834	0.489	0.625	0.258	0.796	1.416	0.493	
160	15	0.183	0.949	0.342	0.253	0.942	0.364	0.011	0.039	0.969	0.218	0.828	-1.054	0.292	-0.832	0.405	7.709	0.052	
161	21	0.11	0.695	0.487	0.178	0.787	0.441	-0.276	-1.253	0.226	-5.234	0	-3.578	0	-2.357	0.018	14.766	0.011	
162	10	-0.422	-1.699	0.089	-0.515	-1.7	0.128	-0.429	-1.343	0.216	-1.105	0.269	-0.528	0.597	-1	0.317	3.497	0.321	**
163	16	-0.093	-0.502	0.616	-0.114	-0.431	0.673	0.063	0.238	0.816	-2.099	0.036	-0.815	0.415	0.258	0.796	4.651	0.098	
164	5	0	0	1	-0.1	-0.174	0.873	0.187	0.331	0.763	0	1	0	1	0.577	0.564	0.119	0.73	
165	9	-0.056	-0.209	0.835	-0.1	-0.266	0.798	-0.25	-0.682	0.517	-0.59	0.555	-1.614	0.106	-1.134	0.257	6.012	0.111	
166	10	0.2	0.805	0.421	0.127	0.363	0.726	0.055	0.156	0.88	-1.934	0.053	-1.936	0.053	-1.667	0.096	9.734	0.045	
167	8	-0.286	-0.99	0.322	-0.333	-0.866	0.42	-0.383	-1.017	0.348	0.953	0.34	1.549	0.121	1.89	0.059	4.914	0.027	
168	7	-0.238	-0.751	0.453	-0.179	-0.406	0.702	0.052	0.115	0.913	-1.388	0.165	-1.309	0.19	-0.447	0.655	1.418	0.492	
169	5	-0.6	-1.47	0.142	-0.7	-1.698	0.188	-0.865	-2.992	0.058	-1.328	0.184	-1.24	0.215	-0.577	0.564	3.833	0.05	
170	5	-0.6	-1.47	0.142	-0.7	-1.698	0.188	-0.713	-1.763	0.176	0	1	0	1	1.732	0.083	2.893	0	
171	7	-0.429	-1.352	0.176	-0.571	-1.557	0.18	-0.598	-1.668	0.156	-0.347	0.729	-1.309	0.19	-0.447	0.655	1.418	0.492	
Barbados Sections																			
172	26	-0.153	-1.094	0.274	-0.23	-1.156	0.259	-0.216	-1.085	0.289	0.482	0.63	-0.605	0.545	1.4	0.162	4.279	0.233	
173	11	-0.33	-1.414	0.157	-0.532	-1.885	0.092	-0.549	-1.97	0.08	-2.347	0.019	-1.951	0.051	-1	0.317	11.781	0.008	
174	11	-0.019	-0.081	0.936	-0.03	-0.091	0.93	-0.067	-0.202	0.844	-0.782	0.434	0	1	1.414	0.157	3.969	0.137	
175	8	-0.5	-1.732	0.083	-0.595	-1.814	0.12	-0.657	-2.137	0.076	0	1	-0.516	0.606	-0.378	0.705	5.725	0.057	**
176	5	-0.6	-1.47	0.142	-0.7	-1.698	0.188	-0.404	-0.765	0.5	0	1	0	1	1.732	0.083	2.893	0	
177	10	-0.867	-3.488	0	-0.952	-8.749	0	-0.861	-4.778	0.001	-1.934	0.053	-3.345	0.001	-2.333	0.02	33.406	0	**
178	9	0.423	1.586	0.113	0.542	1.706	0.132	0.53	1.654	0.142	-0.59	0.555	-0.351	0.726	-0.378	0.705	8.8	0.003	

No	N	τ	Zτ	ατ	ρ	ιρ	αρ	γ	ιγ	αγ	ZT	αT	ZR	αR	Zm	αm	FL	αL	ASY
179	8	-0.038	-0.131	0.896	-0.1	-0.246	0.814	0.044	0.107	0.918	-2.86	0.004	-1.033	0.302	-0.378	0.705	2.081	0.353	
180	9	-0.085	-0.317	0.751	-0.197	-0.533	0.611	-0.175	-0.469	0.653	0.295	0.768	-0.561	0.574	1.134	0.257	1.018	0.313	
181	20	-0.2	-1.23	0.219	-0.302	-1.345	0.195	-0.312	-1.395	0.18	-1.112	0.266	-1.428	0.153	-1	0.317	5.257	0.262	
British Columbia Section																			
182	16	-0.083	-0.45	0.653	-0.115	-0.432	0.672	0.041	0.153	0.88	-0.84	0.401	-0.733	0.464	-0.258	0.796	6.881	0.076	
183	21	0.204	1.293	0.196	0.271	1.227	0.235	0.247	1.111	0.281	-0.361	0.718	0.388	0.698	0.471	0.637	3.476	0.324	
184	9	-0.141	-0.529	0.597	-0.315	-0.879	0.409	-0.307	-0.852	0.422	0.295	0.768	0.07	0.944	0.816	0.414	2.158	0.34	
185	11	-0.44	-1.886	0.059	-0.564	-2.049	0.071	-0.66	-2.636	0.027	0.782	0.434	0.6	0.548	1.667	0.096	2.494	0.114	**
186	17	0.015	0.083	0.934	0.049	0.191	0.851	0.001	0.004	0.997	-1.217	0.224	0.148	0.882	-0.258	0.796	9.214	0.01	
187	8	-0.222	-0.77	0.441	-0.415	-1.116	0.307	-0.378	-0.999	0.356	0.953	0.34	1.291	0.197	2.236	0.025	4.9	0	
188	5	0.2	0.49	0.624	0.3	0.545	0.624	0.374	0.698	0.536	-1.328	0.184	-0.62	0.535	0.577	0.564	0.119	0.73	
189	5	0.316	0.775	0.439	0.079	0.137	0.9	0.248	0.443	0.688	-1.328	0.184	-0.62	0.535	0.577	0.564	0.119	0.73	
190	11	0.183	0.786	0.432	0.162	0.493	0.634	0.362	1.167	0.273	-1.565	0.118	-1.201	0.23	-0.333	0.739	3.2	0.202	
191	9	-0.479	-1.798	0.072	-0.601	-1.989	0.087	-0.728	-2.809	0.026	-2.359	0.018	-1.404	0.16	0	1	3.564	0.059	**
192	6	-0.69	-1.945	0.052	-0.897	-4.06	0.015	-0.893	-3.968	0.017	-0.773	0.44	-1.594	0.111	-1.342	0.18	9.917	0.007	**
193	5	-0.527	-1.291	0.197	-0.868	-3.034	0.056	-0.376	-0.704	0.532	0	1	-0.62	0.535	0	1	0.405	0.525	
194	14	0.319	1.588	0.112	0.49	1.948	0.075	0.216	0.767	0.458	1.359	0.174	-1.01	0.312	-0.832	0.405	8.136	0.043	****
195	56	-0.129	-1.402	0.161	-0.198	-1.482	0.144	-0.01	-0.074	0.942	-0.644	0.519	-2.763	0.006	-1.483	0.138	26.498	0.001	
196	4	0.333	0.679	0.497	0.4	0.617	0.6	0.485	0.784	0.515	-0.535	0.593	0	1	0.577	0.564	0.392	0.531	
197	5	-0.316	-0.775	0.439	-0.553	-1.148	0.334	-0.298	-0.541	0.626	1.328	0.184	1.24	0.215	1.732	0.083	2.893	0	
198	6	-0.333	-0.939	0.348	-0.486	-1.111	0.329	-0.232	-0.477	0.658	0.386	0.699	-0.725	0.469	0.447	0.655	1.446	0.229	
199	5	0	0	1	-0.1	-0.174	0.873	-0.492	-0.979	0.4	-1.328	0.184	-0.62	0.535	0.577	0.564	0.119	0.73	
200	4	0.333	0.679	0.497	0.4	0.617	0.6	0.646	1.196	0.354	1.069	0.285	1	0.317	1.732	0.083	4.167	0	
201	8	0.473	1.638	0.101	0.56	1.657	0.149	0.554	1.632	0.154	-1.907	0.057	-1.549	0.121	-1.134	0.257	5.315	0.15	
202	10	-0.022	-0.089	0.929	-0.103	-0.293	0.777	-0.105	-0.298	0.774	-0.276	0.782	-0.88	0.379	-1	0.317	6.309	0.043	
203	7	-0.143	-0.451	0.652	-0.25	-0.577	0.589	0.013	0.029	0.978	-0.347	0.729	0.982	0.326	1.342	0.18	1.361	0.243	
204	5	0.4	0.98	0.327	0.4	0.756	0.505	0.489	0.97	0.403	-1.328	0.184	-0.62	0.535	0.577	0.564	0.119	0.73	

No	N	τ	Zτ	ατ	ρ	tρ	αρ	γ	tγ	αγ	ZT	αT	ZR	αR	Zm	αm	FL	αL	ASY
205	10	0.135	0.543	0.587	0.155	0.445	0.668	0.205	0.591	0.571	-2.763	0.006	-0.352	0.725	-0.333	0.739	3.479	0.176	
206	7	-0.048	-0.15	0.881	0	0	1	0.137	0.31	0.769	-1.388	0.165	-0.65	0.513	-1	0.317	11.781	0.008	
207	4	0.667	1.359	0.174	0.8	1.886	0.2	0.807	1.929	0.193	1.069	0.285	0	1	1.732	0.083	4.167	0	
Arkansas DeDray Lake Sections																			
208	10	0.068	0.274	0.784	0.166	0.475	0.647	0.278	0.82	0.436	-1.105	0.269	0	1	-0.378	0.705	8.011	0.005	
209	8	0.5	1.732	0.083	0.595	1.814	0.12	0.498	1.406	0.209	0.953	0.34	-1.291	0.197	0.378	0.705	0.614	0.736	****
210	6	-0.2	-0.564	0.573	-0.257	-0.532	0.623	-0.319	-0.673	0.538	0.386	0.699	0.58	0.562	1.342	0.18	2.018	0.155	
211	10	-0.022	-0.089	0.929	-0.006	-0.017	0.987	-0.054	-0.154	0.881	1.381	0.167	2.289	0.022	2.333	0.02	8.436	0.004	
212	7	-0.195	-0.616	0.538	-0.3	-0.703	0.513	-0.484	-1.237	0.271	-0.347	0.729	0.982	0.326	1.342	0.18	1.361	0.243	
213	4	-0.667	-1.359	0.174	-0.8	-1.886	0.2	-0.797	-1.869	0.203	-0.535	0.593	-1	0.317	-0.577	0.564	4.525	0.033	
214	12	0.242	1.097	0.273	0.343	1.153	0.276	0.235	0.764	0.463	-1.982	0.048	-1.126	0.26	-0.905	0.366	9.613	0.022	
215	13	-0.331	-1.577	0.115	-0.483	-1.831	0.094	-0.469	-1.76	0.106	-0.236	0.813	-0.342	0.732	0.333	0.739	2.192	0.533	**
216	26	0.05	0.361	0.718	0.053	0.259	0.797	-0.044	-0.213	0.833	-1.929	0.054	0.151	0.88	-0.218	0.827	1.549	0.671	
217	9	0.056	0.209	0.835	0.15	0.401	0.7	0.276	0.758	0.473	-0.59	0.555	0.702	0.483	1.134	0.257	1.018	0.313	
218	5	0	0	1	0.1	0.174	0.873	0.309	0.563	0.613	-1.328	0.184	-0.62	0.535	0.577	0.564	0.119	0.73	
219	6	0.2	0.564	0.573	0.2	0.408	0.704	0.13	0.262	0.807	0.386	0.699	1.449	0.147	1.342	0.18	2.018	0.155	
220	5	-0.2	-0.49	0.624	-0.3	-0.545	0.624	-0.371	-0.692	0.539	-1.328	0.184	-0.62	0.535	0.577	0.564	0.119	0.73	
221	5	0.6	1.47	0.142	0.8	2.309	0.104	0.398	0.751	0.507	0	1	-1.24	0.215	-0.577	0.564	3.833	0.05	
222	9	-0.167	-0.626	0.532	-0.067	-0.177	0.865	-0.009	-0.023	0.982	-1.474	0.14	-1.404	0.16	-1.134	0.257	6.012	0.111	
223	10	0.135	0.543	0.587	0.168	0.481	0.643	0.021	0.059	0.954	1.381	0.167	1.584	0.113	1.667	0.096	3.284	0.07	
224	9	-0.222	-0.834	0.404	-0.333	-0.935	0.381	-0.381	-1.092	0.311	0.295	0.768	-1.404	0.16	-1.134	0.257	6.012	0.111	
225	4	0	0	1	0.2	0.289	0.8	-0.165	-0.237	0.835	-0.535	0.593	0	1	0.577	0.564	0.392	0.531	
226	7	0	0	1	-0.231	-0.53	0.619	-0.098	-0.221	0.834	-1.388	0.165	0.327	0.743	0.577	0.564	0.028	0.868	
227	12	0.034	0.152	0.879	-0.148	-0.472	0.647	0.146	0.468	0.65	-0.495	0.62	1.213	0.225	1.508	0.132	2.949	0.086	
228	9	-0.222	-0.834	0.404	-0.217	-0.587	0.576	-0.129	-0.344	0.741	-0.59	0.555	-0.351	0.726	-0.378	0.705	1.904	0.386	
229	5	-0.4	-0.98	0.327	-0.5	-1	0.391	-0.6	-1.301	0.284	1.328	0.184	1.24	0.215	1.732	0.083	2.893	0	
230	5	0.2	0.49	0.624	0.3	0.545	0.624	0.346	0.64	0.568	1.328	0.184	1.861	0.06	1.732	0.083	2.893	0	

No	N	τ	Zτ	ατ	ρ	tρ	αρ	γ	tγ	αγ	ZT	αT	ZR	αR	Zm	αm	FL	αL	ASY
231	5	0.4	0.98	0.327	0.5	1	0.391	0.518	1.049	0.371	0	1	0.62	0.535	1.732	0.083	2.893	0	
232	5	-0.2	-0.49	0.624	-0.3	-0.545	0.624	-0.702	-1.708	0.186	1.328	0.184	1.24	0.215	1.732	0.083	2.893	0	
233	8	-0.182	-0.63	0.529	-0.404	-1.081	0.321	-0.465	-1.286	0.246	-1.907	0.057	0	1	0.378	0.705	0.614	0.736	
234	15	0.097	0.502	0.616	0.101	0.365	0.721	-0.293	-1.104	0.29	-1.742	0.082	-0.512	0.609	0.832	0.405	2.425	0.297	
235	16	-0.008	-0.045	0.964	-0.014	-0.052	0.959	0.111	0.418	0.682	-0.84	0.401	-0.407	0.684	0.258	0.796	12.573	0	
236	8	-0.036	-0.126	0.9	-0.175	-0.435	0.679	-0.189	-0.472	0.653	0	1	-0.516	0.606	0.378	0.705	0.614	0.736	
237	7	-0.293	-0.923	0.356	-0.373	-0.898	0.41	-0.341	-0.812	0.453	-0.347	0.729	0.655	0.513	1	0.317	0.25	0.617	
238	11	0.018	0.078	0.938	0.036	0.109	0.915	0.435	1.448	0.182	1.565	0.118	0.75	0.453	1	0.317	1.251	0.535	
239	14	0.265	1.321	0.186	0.376	1.404	0.186	0.215	0.762	0.461	0.679	0.497	-0.404	0.686	-0.277	0.782	4.353	0.36	
240	5	0.6	1.47	0.142	0.7	1.698	0.188	0.46	0.898	0.436	-1.328	0.184	-1.24	0.215	-0.577	0.564	3.833	0.05	
241	7	0.333	1.051	0.293	0.357	0.855	0.432	0.659	1.958	0.108	0.694	0.488	0.327	0.743	1.342	0.18	1.361	0.243	
242	6	0.276	0.778	0.437	0.309	0.649	0.551	0.143	0.29	0.786	1.545	0.122	1.449	0.147	2.236	0.025	8	0	
243	6	-0.6	-1.691	0.091	-0.657	-1.744	0.156	-0.687	-1.889	0.132	-0.773	0.44	-0.29	0.772	0.447	0.655	1.446	0.229	**
244	6	-0.2	-0.564	0.573	-0.257	-0.532	0.623	-0.487	-1.115	0.327	-1.932	0.053	-1.16	0.246	-0.447	0.655	1.56	0.459	
245	5	-0.2	-0.49	0.624	-0.5	-1	0.391	-0.386	-0.725	0.521	0	1	-0.62	0.535	-0.577	0.564	3.833	0.05	
246	16	0.168	0.908	0.364	0.242	0.933	0.367	0.304	1.192	0.253	-0.21	0.834	1.059	0.29	0.775	0.439	1.507	0.471	
247	25	-0.078	-0.545	0.585	-0.132	-0.637	0.531	0.231	1.137	0.267	0.328	0.743	0.724	0.469	0.426	0.67	0.234	0.972	
248	10	-0.022	-0.089	0.929	-0.067	-0.189	0.855	0.01	0.028	0.978	-0.276	0.782	0.352	0.725	1	0.317	2.254	0.133	
249	7	0.238	0.751	0.453	0.393	0.955	0.383	0.307	0.721	0.503	-0.347	0.729	0.655	0.513	0.447	0.655	1.028	0.311	
Northern Norway Nalneset Sections																			
250	63	-0.005	-0.055	0.956	-0.041	-0.322	0.749	-0.124	-0.977	0.333	0.101	0.919	-0.327	0.744	0.651	0.515	7.554	0.109	
251	6	-0.2	-0.564	0.573	-0.086	-0.172	0.872	-0.086	-0.173	0.871	-0.773	0.44	-0.725	0.469	-0.447	0.655	1.56	0.459	
252	11	-0.241	-1.031	0.303	-0.312	-0.985	0.35	-0.407	-1.337	0.214	-1.565	0.118	0	1	0	1	4.025	0.134	
253	8	-0.143	-0.495	0.621	-0.286	-0.73	0.493	-0.383	-1.017	0.348	1.907	0.057	1.291	0.197	1.134	0.257	1.581	0.209	
254	16	-0.23	-1.242	0.214	-0.364	-1.461	0.166	-0.39	-1.586	0.135	-2.099	0.036	-1.955	0.051	-0.775	0.439	2.998	0.392	
255	25	0.568	3.982	0	0.709	4.827	0	0.529	2.989	0.007	-0.657	0.511	-2.011	0.044	-2.711	0.007	458.5	0	****
256	12	-0.132	-0.596	0.551	-0.256	-0.836	0.423	0.109	0.348	0.735	-2.725	0.006	-2.166	0.03	-0.905	0.366	8.599	0.072	

No	N	τ	Zτ	ατ	ρ	ιρ	αρ	γ	ιγ	αγ	ZT	αT	ZR	αR	Zm	αm	FL	αL	ASY
257	43	0.074	0.695	0.487	0.113	0.73	0.47	0.064	0.414	0.681	-1.601	0.109	-0.278	0.781	0.156	0.876	6.179	0.289	
258	15	0.128	0.663	0.508	0.175	0.641	0.533	0.292	1.101	0.291	-1.742	0.082	-1.958	0.05	-0.577	0.564	4.295	0.231	
259	5	0.2	0.49	0.624	0.5	1	0.391	0.367	0.683	0.544	0	1	-0.62	0.535	-0.577	0.564	3.833	0.05	
260	16	-0.254	-1.374	0.17	-0.373	-1.503	0.155	-0.157	-0.594	0.562	-0.84	0.401	-1.14	0.254	-2.324	0.02	27.588	0	
261	18	-0.42	-2.432	0.015	-0.606	-3.046	0.008	-0.396	-1.726	0.104	1.965	0.049	-0.18	0.857	-1.291	0.197	10.503	0.062	**
262	10	-0.092	-0.37	0.711	-0.118	-0.336	0.745	-0.007	-0.019	0.985	1.381	0.167	1.76	0.078	2.333	0.02	8.436	0.004	
263	10	0.135	0.543	0.587	0.192	0.554	0.595	-0.024	-0.067	0.948	-1.934	0.053	-1.232	0.218	-0.333	0.739	3.079	0.38	
264	7	0.333	1.051	0.293	0.464	1.172	0.294	0.053	0.119	0.91	1.736	0.083	0.982	0.326	0.447	0.655	1.028	0.311	
265	21	-0.086	-0.546	0.585	-0.127	-0.557	0.584	-0.051	-0.221	0.827	0.18	0.857	-0.881	0.378	-1.147	0.251	8.047	0.09	
266	17	-0.155	-0.868	0.385	-0.31	-1.262	0.226	-0.304	-1.238	0.235	-1.826	0.068	-0.739	0.46	-0.258	0.796	6.091	0.192	
267	16	-0.177	-0.958	0.338	-0.304	-1.192	0.253	-0.403	-1.648	0.122	-2.729	0.006	-1.792	0.073	-1.291	0.197	7.732	0.052	
268	9	-0.085	-0.317	0.751	-0.105	-0.279	0.788	-0.072	-0.192	0.853	0.295	0.768	0.07	0.944	0.816	0.414	0.473	0.492	
269	20	-0.349	-2.153	0.031	-0.445	-2.108	0.049	-0.442	-2.088	0.051	0	1	0.685	0.493	0.688	0.491	3.766	0.439	**
270	6	0.067	0.188	0.851	0.086	0.172	0.872	0.095	0.191	0.858	-0.773	0.44	0.145	0.885	0.447	0.655	1.446	0.229	
271	8	-0.038	-0.131	0.896	-0.154	-0.383	0.715	0.006	0.014	0.989	-0.953	0.34	0.516	0.606	0.378	0.705	0.614	0.736	
272	16	-0.033	-0.18	0.857	0.012	0.044	0.966	-0.146	-0.553	0.589	-1.469	0.142	-1.548	0.122	0.258	0.796	3.312	0.346	
273	8	-0.4	-1.386	0.166	-0.488	-1.369	0.22	-0.599	-1.832	0.117	-0.953	0.34	-0.258	0.796	-0.378	0.705	5.725	0.057	
274	13	-0.013	-0.063	0.95	0.078	0.26	0.8	0.017	0.058	0.955	0.473	0.636	1.595	0.111	0.905	0.366	0.496	0.78	
275	33	0.038	0.312	0.755	0.071	0.398	0.694	0.132	0.744	0.462	-1.133	0.257	-1.246	0.213	-0.539	0.59	5.967	0.113	
276	13	-0.116	-0.553	0.581	-0.175	-0.589	0.568	-0.274	-0.944	0.365	-0.236	0.813	0.798	0.425	0.302	0.763	1.907	0.592	
277	8	-0.182	-0.63	0.529	-0.331	-0.86	0.423	-0.56	-1.655	0.149	-1.907	0.057	-1.549	0.121	-0.378	0.705	2.081	0.353	
278	26	-0.091	-0.653	0.513	-0.188	-0.937	0.358	-0.184	-0.917	0.368	-0.482	0.63	-1.854	0.064	-0.2	0.841	12.079	0.06	
279	26	0.144	1.032	0.302	0.213	1.068	0.296	0.305	1.568	0.13	-2.893	0.004	-1.06	0.289	-0.2	0.841	4.235	0.237	
280	33	0.008	0.063	0.95	0.034	0.187	0.853	-0.047	-0.263	0.794	-0.708	0.479	0.192	0.848	0.73	0.465	1.948	0.583	
281	10	0.18	0.724	0.469	0.308	0.915	0.387	0.22	0.638	0.541	-0.276	0.782	-0.528	0.597	0.333	0.739	4.733	0.094	
282	16	-0.008	-0.046	0.964	-0.027	-0.102	0.92	-0.057	-0.214	0.833	-0.21	0.834	-0.733	0.464	-0.775	0.439	7.227	0.065	
283	19	0.065	0.387	0.699	0.066	0.272	0.789	-0.033	-0.134	0.895	0.381	0.703	-0.619	0.536	-1.213	0.225	6.391	0.172	
284	23	0.286	1.913	0.056	0.338	1.648	0.114	0.427	2.165	0.042	-1.546	0.122	-2.521	0.012	-1.147	0.251	10.294	0.067	****

No	N	τ	Zτ	ατ	ρ	ιρ	αρ	γ	ιγ	αγ	ZT	αT	ZR	αR	Zm	αm	FL	αL	ASY
285	7	-0.143	-0.451	0.652	-0.286	-0.667	0.535	-0.446	-1.116	0.315	-0.347	0.729	0.327	0.743	0.447	0.655	1.028	0.311	
286	17	-0.096	-0.537	0.591	-0.186	-0.733	0.475	-0.2	-0.789	0.442	0	1	-0.444	0.657	-0.775	0.439	7.405	0.06	

Appendix IV-2

Results of tests for asymmetric trends and randomness using grain-size data of 86 turbidite sandstone packets

Sections of northern Italian Apennines

No	N	τ	Zτ	ατ	ρ	tρ	αρ	γ	tγ	αγ	ZT	αT	ZR	αR	Zm	αm	FL	αL	ASY
1	20	0.037	0.229	0.819	0.054	0.229	0.822	0.041	0.175	0.863	-1.112	0.266	-1.77	0.077	-1.147	0.251	6.463	0.091	
2	13	-0.348	-1.658	0.097	-0.478	-1.805	0.099	-0.395	-1.427	0.181	-0.236	0.813	-0.342	0.732	0.302	0.763	2.074	0.355	****
3	17	-0.127	-0.714	0.476	-0.232	-0.924	0.37	-0.22	-0.874	0.396	-1.217	0.224	-1.183	0.237	-1.291	0.197	5.291	0.259	
4	6	-0.067	-0.188	0.851	0.029	0.057	0.957	-0.208	-0.424	0.693	0.386	0.699	0.58	0.562	1.342	0.18	2.018	0.155	
5	9	0.551	2.069	0.039	0.679	2.45	0.044	0.713	2.688	0.031	-1.474	0.14	-1.404	0.16	-1.89	0.059	16.813	0.001	**
6	10	0.09	0.362	0.717	0.003	0.009	0.993	0.144	0.412	0.691	-1.934	0.053	-0.352	0.725	-0.333	0.739	3.479	0.176	
7	5	0.2	0.49	0.624	0.3	0.545	0.624	0.334	0.613	0.583	-1.328	0.184	-0.62	0.535	0.577	0.564	0.119	0.73	
9	11	-0.343	-1.47	0.142	-0.486	-1.668	0.13	-0.213	-0.652	0.53	-0.782	0.434	-0.15	0.881	0.333	0.739	0.328	0.849	
10	8	-0.189	-0.655	0.513	-0.35	-0.915	0.395	-0.22	-0.553	0.6	1.907	0.057	2.324	0.02	1	0.317	0.114	0.736	
11	4	0.667	1.359	0.174	0.8	1.886	0.2	0.752	1.613	0.248	-0.535	0.593	-1	0.317	-0.577	0.564	4.525	0.033	
12	5	-0.6	-1.47	0.142	-0.8	-2.309	0.104	-0.89	-3.374	0.043	1.328	0.184	-0.62	0.535	-0.577	0.564	3.833	0.05	
13	4	-0.183	-0.372	0.71	-0.389	-0.597	0.611	-0.049	-0.07	0.951	-0.535	0.593	0	1	0.577	0.564	0.392	0.531	
14	5	0.2	0.49	0.624	0.3	0.545	0.624	0.049	0.085	0.937	-1.328	0.184	-0.62	0.535	0.577	0.564	0.119	0.73	
15	7	-0.25	-0.789	0.43	-0.426	-1.053	0.341	-0.287	-0.671	0.532	-0.347	0.729	-0.327	0.743	-0.447	0.655	1.418	0.492	
16	16	-0.533	-2.881	0.004	-0.759	-4.359	0.001	-0.613	-2.9	0.012	1.049	0.294	-2.525	0.012	-2.324	0.02	86.683	0	****
17	15	0.019	0.099	0.921	0.064	0.229	0.822	0.127	0.46	0.653	-1.742	0.082	-1.596	0.11	-1.387	0.166	13.796	0.017	
18	10	0.022	0.089	0.929	0.03	0.086	0.934	-0.06	-0.169	0.87	-0.276	0.782	0.352	0.725	1	0.317	1.661	0.436	
19	8	-0.143	-0.495	0.621	-0.19	-0.475	0.651	0.15	0.372	0.723	-0.953	0.34	0.258	0.796	0.378	0.705	3.225	0.073	
20	10	0.159	0.64	0.522	0.196	0.566	0.587	0.299	0.887	0.401	0.553	0.581	0.352	0.725	1.667	0.096	3.284	0.07	
21	6	0.072	0.202	0.84	0.03	0.061	0.955	0.107	0.215	0.84	-1.932	0.053	0.145	0.885	0.447	0.655	1.446	0.229	
22	7	-0.195	-0.616	0.538	-0.136	-0.308	0.771	-0.066	-0.148	0.888	-0.347	0.729	-0.327	0.743	1.342	0.18	1.361	0.243	
23	9	0.087	0.327	0.744	-0.034	-0.091	0.93	-0.022	-0.058	0.956	0.295	0.768	0.07	0.944	1.342	0.18	0.618	0.432	
25	7	-0.39	-1.231	0.218	-0.609	-1.717	0.147	-0.519	-1.357	0.233	-1.388	0.165	-0.327	0.743	0.447	0.655	1.028	0.311	
26	6	0.067	0.188	0.851	0.143	0.289	0.787	0.065	0.131	0.902	-0.773	0.44	0.145	0.885	0.447	0.655	1.446	0.229	

No	N	τ	Zτ	ατ	ρ	lρ	αρ	γ	lγ	αγ	ZT	αT	ZR	αR	Zm	αm	FL	αL	ASY
27	18	-0.134	-0.776	0.438	-0.166	-0.675	0.509	-0.117	-0.473	0.643	-0.393	0.694	-0.585	0.559	-0.243	0.808	4.871	0.182	
28	12	-0.183	-0.826	0.409	-0.474	-1.7	0.12	-0.271	-0.889	0.395	-1.982	0.048	0.433	0.665	0.302	0.763	1.318	0.517	
29	5	-0.2	-0.49	0.624	-0.2	-0.354	0.747	-0.272	-0.489	0.658	0	1	0.62	0.535	0.577	0.564	0.119	0.73	
30	5	-0.4	-0.98	0.327	-0.6	-1.299	0.285	-0.7	-1.696	0.188	0	1	-0.62	0.535	-0.577	0.564	3.833	0.05	
32	8	-0.242	-0.837	0.402	-0.689	-2.33	0.059	-0.274	-0.697	0.512	-2.86	0.004	-2.066	0.039	-1.134	0.257	6.471	0.091	
33	9	0.111	0.417	0.677	0.083	0.221	0.831	-0.004	-0.01	0.992	0.295	0.768	1.334	0.182	1.89	0.059	3.891	0.049	
Monticello Dam Section, California																			
34	6	0.276	0.778	0.437	0.25	0.516	0.633	0.535	1.266	0.274	0.386	0.699	1.015	0.31	0.447	0.655	1.446	0.229	
35	15	0.273	1.42	0.156	0.318	1.208	0.249	0.36	1.389	0.188	-1.742	0.082	-1.596	0.11	-1.732	0.083	9.518	0.049	
36	22	0.074	0.484	0.629	0.196	0.893	0.382	0.279	1.297	0.209	-2.287	0.022	-3.539	0	-2.837	0.005	30.101	0	
37	20	0.381	2.347	0.019	0.53	2.648	0.016	0.575	2.979	0.008	1.112	0.266	-1.142	0.253	-2.065	0.039	13.231	0.021	**
38	20	0.4	2.466	0.014	0.576	2.992	0.008	0.429	2.016	0.059	-1.112	0.266	-1.599	0.11	-2.065	0.039	50.625	0	**
39	19	0.413	2.471	0.013	0.526	2.553	0.021	0.48	2.258	0.037	0.381	0.703	-1.61	0.107	-0.728	0.467	4.213	0.378	**
41	21	0.219	1.389	0.165	0.253	1.14	0.268	0.33	1.526	0.143	-1.985	0.047	-2.098	0.036	-1.886	0.059	11.776	0.019	
42	12	0.092	0.418	0.676	0.176	0.566	0.584	0.279	0.919	0.38	-1.238	0.216	0.433	0.665	0.905	0.366	5.494	0.064	
43	13	0.513	2.44	0.015	0.659	2.909	0.014	0.741	3.66	0.004	0.473	0.636	-1.481	0.138	-0.302	0.763	3.564	0.313	**
44	5	-0.527	-1.291	0.197	-0.711	-1.749	0.179	-0.579	-1.231	0.306	-1.328	0.184	-0.62	0.535	0	1	0.405	0.525	
45	6	-0.414	-1.167	0.243	-0.662	-1.765	0.152	-0.484	-1.106	0.331	-1.932	0.053	-1.16	0.246	-0.447	0.655	1.56	0.459	
46	23	0.357	2.384	0.017	0.472	2.456	0.023	0.513	2.736	0.012	-3.092	0.002	-2.246	0.025	-0.728	0.467	3.794	0.435	**
47	15	0.01	0.053	0.958	-0.063	-0.228	0.823	-0.037	-0.133	0.896	-1.742	0.082	-0.873	0.382	0.333	0.739	3.219	0.2	
48	19	0.227	1.36	0.174	0.304	1.315	0.206	0.256	1.094	0.289	-4.195	0	-1.301	0.193	-1.291	0.197	7.099	0.131	
49	14	-0.326	-1.623	0.105	-0.774	-4.24	0.001	-0.42	-1.603	0.135	-3.397	0.001	-0.707	0.48	0	1	1.426	0.49	****
50	12	0.677	3.064	0.002	0.831	4.724	0.001	0.801	4.227	0.002	-0.495	0.62	-2.036	0.042	-2.714	0.007	59.334	0	**
51	28	0.422	3.148	0.002	0.521	3.112	0.004	0.461	2.645	0.014	-4.326	0	-3.507	0	-2.2	0.028	23.923	0	**
53	10	-0.163	-0.656	0.512	-0.272	-0.799	0.447	0.024	0.068	0.947	-1.934	0.053	-1.056	0.291	-1	0.317	6.309	0.043	
55	17	-0.453	-2.535	0.011	-0.596	-2.872	0.012	-0.437	-1.882	0.079	-0.609	0.543	-0.813	0.416	-1.508	0.132	12.891	0.024	****
56	24	0.51	3.489	0	0.47	2.501	0.02	0.622	3.723	0.001	-5.874	0	-4.745	0	-2.887	0.004	129.63	0	**

Cache Creek Section, California

No	N	τ	Zτ	ατ	ρ	tρ	αρ	γ	tγ	αγ	ZT	αT	ZR	αR	Zm	αm	FL	αL	ASY
57	15	0.081	0.418	0.676	0.068	0.245	0.81	0.188	0.688	0.503	-2.395	0.017	-0.873	0.382	-0.333	0.739	2.852	0.415	
58	17	-0.108	-0.608	0.543	-0.851	-6.27	0	-0.427	-1.827	0.088	-4.869	0	-2.587	0.01	-2.449	0.014	26.649	0	
59	18	0.465	2.696	0.007	0.623	3.186	0.006	0.579	2.843	0.012	0.196	0.844	-1.8	0.072	-1.698	0.09	14.682	0.012	**
60	14	0.344	1.716	0.086	0.424	1.621	0.131	0.468	1.833	0.092	0	1	-1.717	0.086	-0.277	0.782	5.819	0.055	**
61	7	-0.143	-0.451	0.652	-0.25	-0.577	0.589	-0.22	-0.504	0.636	-0.347	0.729	0.655	0.513	1.342	0.18	1.361	0.243	
65	11	0.224	0.961	0.337	0.417	1.377	0.202	0.116	0.351	0.734	-2.347	0.019	-1.951	0.051	-1.667	0.096	10.509	0.033	
66	15	0.129	0.669	0.503	0.142	0.519	0.613	0.034	0.124	0.903	-1.089	0.276	-1.596	0.11	-1.732	0.083	13.61	0.018	
67	26	0.041	0.297	0.767	0.047	0.23	0.82	0.201	1.003	0.326	-1.929	0.054	-0.643	0.52	-0.6	0.549	3.389	0.335	
68	23	-0.103	-0.688	0.491	-0.204	-0.955	0.35	-0.238	-1.121	0.275	-0.515	0.606	1.604	0.109	1.964	0.05	6.87	0.076	
70	23	-0.017	-0.114	0.909	-0.092	-0.425	0.675	0.017	0.079	0.938	-3.092	0.002	-0.963	0.336	0.535	0.593	0.803	0.669	
72	30	-0.109	-0.849	0.396	-0.247	-1.351	0.188	-0.238	-1.295	0.206	-3.425	0.001	-2.05	0.04	-0.928	0.353	7.376	0.117	
75	16	0.104	0.564	0.573	0.007	0.025	0.98	0.03	0.113	0.912	-4.618	0	-1.873	0.061	-0.302	0.763	2.396	0.302	
76	8	0.113	0.393	0.694	0.13	0.32	0.76	0.237	0.598	0.572	-1.907	0.057	-0.775	0.439	-0.447	0.655	1.414	0.493	
78	79	-0.186	-2.429	0.015	-0.285	-2.609	0.011	-0.218	-1.963	0.053	-5.489	0	-5.253	0	-4.185	0	*****	0	****

Barbados Sections

172	25	0.103	0.723	0.47	0.116	0.56	0.581	0.19	0.927	0.364	-2.134	0.033	-0.282	0.778	-0.626	0.532	3.662	0.3	
173	11	-0.208	-0.889	0.374	-0.356	-1.142	0.283	-0.264	-0.822	0.433	-0.782	0.434	0.15	0.881	0.707	0.48	1.519	0.218	
174	11	-0.443	-1.897	0.058	-0.594	-2.217	0.054	-0.441	-1.473	0.175	-3.13	0.002	-2.101	0.036	-0.333	0.739	2.847	0.416	****
175	10	0.736	2.963	0.003	0.781	3.535	0.008	0.883	5.316	0.001	-2.763	0.006	-2.641	0.008	-1	0.317	3.497	0.321	**
176	5	0.2	0.49	0.624	0.2	0.354	0.747	0.04	0.069	0.949	0	1	1.24	0.215	1.732	0.083	2.893	0	
177	10	0.828	3.333	0.001	0.873	5.074	0.001	0.881	5.254	0.001	-2.763	0.006	-2.641	0.008	-2.333	0.02	33.406	0	**
178	9	0.857	3.218	0.001	0.907	5.69	0.001	0.94	7.266	0	-3.244	0.001	-2.667	0.008	-1.633	0.102	6.59	0.086	**
179	5	0.105	0.258	0.796	-0.079	-0.137	0.9	0.252	0.451	0.683	0	1	0.62	0.535	0.577	0.564	0.119	0.73	
180	7	0.586	1.847	0.065	0.664	1.984	0.104	0.667	2.001	0.102	-1.388	0.165	-0.982	0.326	0.447	0.655	1.028	0.311	**
181	16	0.039	0.21	0.833	-0.319	-1.259	0.229	0.068	0.254	0.803	-0.21	0.834	1.629	0.103	2.324	0.02	7.083	0.008	

British Columbia Sections																		
No	N	τ	Zτ	ατ	ρ	lρ	αρ	γ	lγ	αγ	ZT	αT	ZR	αR	Zm	αm	FL	αL	ASY
182	18	-0.094	-0.545	0.586	-0.288	-1.202	0.247	-0.129	-0.519	0.611	-0.982	0.326	-0.99	0.322	0.728	0.467	1.045	0.593	
183	18	0.063	0.363	0.717	-0.053	-0.214	0.833	-0.038	-0.152	0.881	-2.751	0.006	-1.192	0.233	-1.213	0.225	7.337	0.062	
184	9	0.21	0.786	0.432	0.14	0.375	0.719	0.337	0.946	0.375	-1.474	0.14	-0.983	0.326	-0.816	0.414	3.976	0.264	
185	10	0.184	0.741	0.459	0.155	0.445	0.668	0.165	0.474	0.648	-1.934	0.053	-0.528	0.597	-0.333	0.739	3.461	0.177	
186	12	-0.097	-0.439	0.661	-0.259	-0.848	0.416	-0.428	-1.497	0.165	-2.725	0.006	-0.347	0.729	0.302	0.763	1.318	0.517	
187	9	0.629	2.36	0.018	0.729	2.816	0.026	0.801	3.534	0.01	-1.474	0.14	-2.035	0.042	-1.633	0.102	6.59	0.086	**
189	6	0.333	0.939	0.348	0.486	1.111	0.329	0.511	1.191	0.3	0.386	0.699	0.58	0.562	0.447	0.655	1.446	0.229	
190	11	-0.411	-1.761	0.078	-0.537	-1.91	0.088	-0.399	-1.304	0.225	0	1	-1.201	0.23	-1	0.317	5.922	0.052	****
191	9	0.203	0.762	0.446	0.138	0.368	0.723	0.46	1.372	0.213	-0.59	0.555	0.702	0.483	1.134	0.257	1.018	0.313	
192	6	0.6	1.691	0.091	0.771	2.425	0.072	0.765	2.375	0.076	0.386	0.699	-1.16	0.246	-1.342	0.18	9.917	0.007	**
194	14	0.189	0.941	0.347	0.309	1.126	0.282	0.338	1.246	0.237	0.679	0.497	0	1	0.277	0.782	1.544	0.672	
195	55	0.405	4.364	0	0.57	5.053	0	0.557	4.884	0	-3.035	0.002	-4.128	0	-3.592	0	86.591	0	**

Appendix IV-3

Results of tests for asymmetric trends and randomness using structure score data of 69 sandstone packets

Sections of northern Italian Apennines

No	N	τ	Zτ	ατ	ρ	τρ	αρ	γ	τγ	αγ	ZT	αT	ZR	αR	Zm	αm	FL	αL	ASY
1	20	0.090	0.556	0.578	0.073	0.313	0.758	0.050	0.212	0.835	-1.112	0.266	-0.685	0.493	-0.229	0.819	3.613	0.306	
2	17	-0.161	-0.902	0.367	-0.342	-1.407	0.180	-0.287	-1.159	0.265	-1.826	0.068	-0.739	0.460	-0.535	0.593	2.346	0.504	
3	20	-0.118	-0.725	0.468	-0.136	-0.581	0.568	-0.098	-0.417	0.682	-3.893	0.000	-1.999	0.046	-0.229	0.819	4.307	0.116	
4	6	-0.467	-1.315	0.188	-0.543	-1.293	0.266	-0.492	-1.129	0.322	0.386	0.699	0.580	0.562	0.447	0.655	1.446	0.229	
5	11	0.000	0.000	1.000	-0.206	-0.632	0.543	-0.171	-0.519	0.616	-1.565	0.118	-0.750	0.453	-1.134	0.257	7.976	0.092	
6	23	0.040	0.265	0.791	-0.161	-0.748	0.463	0.027	0.126	0.901	-2.061	0.039	0.046	0.963	0	1	2.419	0.49	
7	5	0.200	0.490	0.624	0.300	0.545	0.624	0.130	0.227	0.835	-1.328	0.184	-0.620	0.535	0.577	0.564	0.119	0.73	
9	17	-0.398	-2.230	0.026	-0.628	-3.123	0.007	-0.536	-2.460	0.027	-1.826	0.068	-1.109	0.268	-1.387	0.166	7.052	0.133	****
10	8	0.265	0.917	0.359	0.200	0.500	0.635	-0.104	-0.257	0.806	0.953	0.340	0.516	0.606	1.134	0.257	1.581	0.209	
11	5	0.600	1.470	0.142	0.800	2.309	0.104	0.668	1.556	0.218	1.328	0.184	-0.620	0.535	-0.577	0.564	3.833	0.05	
12	5	-0.400	-0.980	0.327	-0.600	-1.299	0.285	-0.471	-0.924	0.424	0.000	1.000	-0.620	0.535	-0.577	0.564	3.833	0.05	
13	5	-0.200	-0.490	0.624	0.000	0.000	1.000	-0.089	-0.155	0.887	-1.328	0.184	-0.620	0.535	0.577	0.564	0.119	0.73	
14	9	0.145	0.544	0.586	0.207	0.560	0.593	0.187	0.505	0.629	-1.474	0.140	-0.772	0.440	-0.378	0.705	5.128	0.077	
15	16	-0.091	-0.493	0.622	-0.250	-0.964	0.351	-0.157	-0.593	0.562	2.309	0.021	1.385	0.166	1.155	0.248	0.507	0.776	
16	23	-0.110	-0.734	0.463	-0.186	-0.867	0.396	-0.133	-0.614	0.546	0.000	1.000	0.229	0.819	-0.218	0.827	2.424	0.489	
17	32	0.067	0.536	0.592	-0.087	-0.478	0.636	0.103	0.570	0.573	-2.158	0.031	-0.603	0.546	0.816	0.414	3.124	0.21	
18	35	0.168	1.420	0.156	-0.137	-0.792	0.434	0.202	1.183	0.245	-0.412	0.681	1.527	0.127	-1.46	0.144	40.605	0	
19	22	-0.137	-0.894	0.371	-0.443	-2.208	0.039	-0.172	-0.779	0.445	0.352	0.725	1.130	0.258	1.291	0.197	0.274	0.872	
20	15	0.153	0.794	0.427	-0.109	-0.396	0.698	0.193	0.711	0.490	-3.048	0.002	-0.241	0.810	-0.277	0.782	5.405	0.067	
21	6	-0.447	-1.260	0.208	-0.935	-5.295	0.006	-0.520	-1.219	0.290	-0.773	0.440	-1.160	0.246	0.447	0.655	1.446	0.229	
22	9	0.000	0.000	1.000	-0.067	-0.177	0.865	0.011	0.028	0.978	-1.474	0.140	-1.193	0.233	-1.134	0.257	6.012	0.111	
23	20	-0.056	-0.346	0.729	-0.582	-3.036	0.007	-0.149	-0.640	0.531	-2.225	0.026	0.457	0.648	-2.828	0.005	81.631	0	
25	11	-0.020	-0.086	0.931	-0.290	-0.909	0.387	0.014	0.041	0.968	-3.912	0.000	-0.750	0.453	-0.333	0.739	3.2	0.202	
26	12	0.033	0.149	0.882	-0.113	-0.359	0.727	-0.008	-0.025	0.980	-2.725	0.006	-0.866	0.386	-0.905	0.366	8.974	0.03	

No	N	τ	Zτ	ατ	ρ	ιρ	αρ	γ	ιγ	αγ	ZT	αT	ZR	αR	Zm	αm	FL	αL	ASY
27	26	-0.275	-1.966	0.049	-0.377	-1.995	0.058	-0.340	-1.769	0.090	-0.964	0.335	-1.551	0.121	-0.905	0.366	8.974	0.03	****
29	9	0.059	0.221	0.825	-0.135	-0.360	0.730	0.115	0.306	0.768	0.295	0.768	-0.351	0.726	-1.134	0.257	6.012	0.111	
30	5	-0.400	-0.980	0.327	-0.600	-1.299	0.285	-0.746	-1.941	0.148	1.328	0.184	0.000	1.000	-0.577	0.564	3.833	0.05	
33	13	-0.069	-0.329	0.742	-0.276	-0.951	0.362	-0.136	-0.456	0.657	-2.364	0.018	0.114	0.909	-0.632	0.527	9.754	0.021	
Monticello Dam Section, California																			
34	6	0.138	0.389	0.697	0.162	0.328	0.759	-0.014	-0.028	0.979	0.386	0.699	1.015	0.310	0.447	0.655	1.446	0.229	
35	15	0.197	1.024	0.306	0.208	0.766	0.457	0.261	0.974	0.348	0.871	0.384	-0.512	0.609	-1.387	0.166	12.315	0.031	
36	22	0.134	0.875	0.382	0.146	0.660	0.517	0.210	0.963	0.347	-3.343	0.001	-2.261	0.024	-0.655	0.513	2.467	0.651	
37	20	0.437	2.691	0.007	0.452	2.149	0.045	0.545	2.761	0.013	-0.556	0.578	-0.286	0.775	0	1	0.886	0.829	**
38	20	0.027	0.164	0.869	-0.030	-0.128	0.899	-0.016	-0.066	0.948	-1.112	0.266	0.571	0.568	1.147	0.251	2.608	0.271	
39	19	0.231	1.381	0.167	0.319	1.385	0.184	0.420	1.911	0.073	0.953	0.340	1.425	0.154	0.243	0.808	6.232	0.182	
41	21	-0.102	-0.647	0.517	-0.354	-1.651	0.115	-0.032	-0.139	0.891	-2.527	0.012	-0.723	0.470	-1.508	0.132	36.032	0	
42	12	0.046	0.207	0.836	0.107	0.340	0.741	0.191	0.614	0.553	-1.238	0.216	0.303	0.762	0.905	0.366	5.494	0.064	
43	13	0.536	2.551	0.011	0.719	3.429	0.006	0.799	4.400	0.001	-0.236	0.813	-1.595	0.111	-1.508	0.132	23.199	0	**
45	6	-0.138	-0.389	0.697	-0.250	-0.516	0.633	-0.372	-0.802	0.467	-1.932	0.053	0.145	0.885	0.447	0.655	1.446	0.229	
46	23	0.453	3.029	0.002	0.616	3.585	0.002	0.596	3.406	0.003	-3.092	0.002	-2.475	0.013	-1.528	0.127	27.433	0	**
47	15	0.059	0.304	0.761	0.097	0.353	0.730	0.090	0.325	0.750	-1.742	0.082	-1.325	0.185	-0.905	0.366	7.523	0.023	
48	9	-0.197	-0.740	0.459	-0.265	-0.726	0.491	-0.278	-0.767	0.468	-2.359	0.018	-1.404	0.160	-0.816	0.414	6.037	0.049	
49	14	-0.281	-1.401	0.161	-0.480	-1.898	0.082	-0.266	-0.956	0.358	-0.679	0.497	0.000	1.000	-0.707	0.48	4.693	0.096	
51	28	0.347	2.591	0.010	0.385	2.127	0.043	0.444	2.524	0.018	-1.545	0.122	-1.349	0.177	-1.147	0.251	7.5	0.186	**
53	10	0.119	0.480	0.631	-0.013	-0.036	0.972	0.255	0.747	0.477	0.553	0.581	0.176	0.860	-0.447	0.655	1.661	0.436	
55	18	-0.378	-2.188	0.029	-0.542	-2.580	0.020	-0.461	-2.077	0.054	-0.982	0.326	-1.800	0.072	-2.183	0.029	48.618	0	****
56	24	0.004	0.028	0.978	-0.113	-0.534	0.599	0.073	0.344	0.734	-5.874	0.000	-3.287	0.001	-1.698	0.09	11.12	0.049	
Cache Creek Section, California																			
57	15	0.087	0.454	0.650	0.125	0.455	0.657	0.176	0.645	0.530	-0.435	0.663	0.030	0.976	-0.577	0.564	7.386	0.061	
58	17	-0.108	-0.608	0.543	-0.877	-7.066	0.000	-0.386	-1.622	0.126	-4.869	0.000	-2.587	0.010	-2.449	0.014	26.649	0	

No	N	τ	Zτ	ατ	ρ	tρ	αρ	γ	tγ	αγ	ZT	αT	ZR	αR	Zm	αm	FL	αL	ASY
59	18	0.353	2.048	0.041	0.453	2.031	0.059	0.398	1.734	0.102	-0.393	0.694	-0.180	0.857	-1.698	0.09	19.731	0.003	**
60	14	0.033	0.166	0.868	-0.073	-0.253	0.805	-0.090	-0.314	0.759	0.000	1.000	-2.121	0.034	-0.832	0.405	4.953	0.292	
61	7	-0.238	-0.751	0.453	-0.357	-0.855	0.432	-0.440	-1.094	0.324	-1.388	0.165	-0.982	0.326	-0.447	0.655	1.418	0.492	
65	11	0.114	0.490	0.624	0.112	0.339	0.743	0.044	0.133	0.897	-2.347	0.019	-1.201	0.230	-0.378	0.705	1.866	0.393	
66	15	-0.394	-2.049	0.040	-0.491	-2.032	0.063	-0.422	-1.677	0.117	-2.395	0.017	-1.054	0.292	0	1	1.242	0.743	****
67	28	0.151	1.124	0.261	0.201	1.047	0.305	0.236	1.239	0.226	-0.618	0.537	0.843	0.399	0.577	0.564	1.33	0.722	
68	23	-0.178	-1.188	0.235	-0.283	-1.350	0.191	-0.225	-1.059	0.302	-1.546	0.122	-1.238	0.216	-1.147	0.251	16.348	0.012	
70	23	0.105	0.702	0.482	-0.016	-0.075	0.941	-0.018	-0.084	0.934	-3.092	0.002	0.092	0.927	0	1	1.085	0.781	
72	30	-0.248	-1.922	0.055	-0.547	-3.456	0.002	-0.166	-0.893	0.379	-2.978	0.003	-2.837	0.005	-3.157	0.002	38.659	0	****
75	15	0.000	0.000	1.000	-0.382	-1.492	0.159	0.114	0.413	0.687	-4.354	0.000	-1.596	0.110	-1.134	0.257	5.213	0.157	
76	8	-0.454	-1.571	0.116	-0.966	-9.117	0.000	-0.440	-1.200	0.275	0.000	1.000	-0.258	0.796	1.134	0.257	1.581	0.209	
78	79	-0.014	-0.185	0.853	-0.102	-0.901	0.371	-0.047	-0.411	0.682	-5.489	0.000	-3.748	0.000	-2.458	0.014	38.665	0	
Barbados Sections																			
172	25	-0.098	-0.687	0.492	-0.166	-0.807	0.428	0.004	0.020	0.984	-4.104	0.000	-1.810	0.070	-1.043	0.297	7.224	0.204	
174	11	0.019	0.082	0.934	-0.068	-0.205	0.842	-0.023	-0.069	0.947	-0.782	0.434	1.201	0.230	1.414	0.157	1.109	0.292	
175	10	0.580	2.333	0.020	0.434	1.364	0.210	0.832	4.242	0.003	-2.763	0.006	-0.880	0.379	-1	0.317	3.327	0.189	**
176	5	0.200	0.490	0.624	0.200	0.354	0.747	0.043	0.074	0.946	0.000	1.000	1.240	0.215	1.732	0.083	2.893	0	
177	10	0.337	1.358	0.175	0.076	0.215	0.835	0.305	0.905	0.392	-3.592	0.000	-1.408	0.159	-0.447	0.655	1.661	0.436	
178	9	0.149	0.560	0.576	-0.786	-3.361	0.012	0.159	0.426	0.683	-4.128	0.000	-0.772	0.440	-1.414	0.157	4.34	0.114	
179	5	0.400	0.980	0.327	0.400	0.756	0.505	0.620	1.369	0.264	0.000	1.000	0.620	0.535	1.732	0.083	2.893	0	
180	7	0.350	1.105	0.269	0.389	0.944	0.389	0.446	1.115	0.316	0.694	0.488	0.982	0.326	2.236	0.025	6.25	0	
181	16	0.186	1.007	0.314	0.034	0.128	0.900	0.230	0.883	0.392	-0.210	0.834	1.466	0.143	2.324	0.02	7.083	0.008	